Kentville Post Box 604

GEORGIA INSTITUTE OF TECHNOLOGY

OFFICE OF RESEARCH ADMINISTRATION

RESEARCH PROJECT INITIATION

Date: January 26, 1972

Project Title: The Study of Hazards from Burning Apparel and the Relation of Hazards to Test Methods

Project No.: E-25-625 (Renewal of E-25-618)

Principal Investigator: Dr. Wolfgang Wulff and Dr. Novak Zuber

Sponsor: National Science Foundation

Agreement Period: From November 1, 1971 Until April 30, 1973*

Type Agreement: Grant No. GI-31882

Amount: $79,000 NSF (E-25-625)
6,649 GIT (E-25-322)
$85,649 Total Budget

Reports Required: Interim Technical Reports; Final Technical Report

*All commitments to be met by this date unless formal extension obtained in advance. Basic Work Period (12 months) ends October 31, 1972

Sponsor Contact Person (s):

Technical Matters
Dr. Ralph H. Long, Jr.
Division of Advanced Technology Applications
National Science Foundation
Washington, D. C. 20550

Administrative Matters (thru ORA)
Mr. Wilbur W. Bolton, Jr.
Grants Officer
National Science Foundation
Washington, D. C. 20550

Assigned to: School of Mechanical Engineering

COPIES TO:

- Principal Investigator
- School Director
- Dean of the College
- Director, Research Administration
- Director, Financial Affairs (2)
- Security-Reports-Property Office
- Patent Coordinator
- Library
- Rich Electronic Computer Center
- Photographic Laboratory
- Project File
- Other

RA-3 (6-71)

GEORGIA INSTITUTE OF TECHNOLOGY
OFFICE OF CONTRACT ADMINISTRATION

SPONSORED PROJECT TERMINATION

Date: July 20, 1977

Project Title: The Study of Hazards from Burning Apparel and the Relation of Hazards to Test Methods

Project No: E-25-625

Project Director: Dr. P. Durbetaki

Sponsor: National Science Foundation

No Actions — OAH

Effective Termination Date: 2/28/77

Clearance of Accounting Charges: 2/28/77

Grant/Contract Closeout Actions Remaining:

None

_ Final Invoice and Closing Documents
_ Final Fiscal Report
_ Final Report of Inventions
_ Govt. Property Inventory & Related Certificate
_ Classified Material Certificate
_ Other _____

NOTE: Sub-project is E-27-632/Freeston/TE

Assigned to: Mechanical Engineering (School/Laboratory)

COPIES TO:

Project Director
Division Chief (EES)
School/Laboratory Director
Dean/Director—EES
Accounting Office
Procurement Office
Security Coordinator (OCA)
Reports Coordinator (OCA)
Library, Technical Reports Section
Office of Computing Services
Director, Physical Plant
EES Information Office
Project File (OCA)
Project Code (GTRI)
Other _____

CA—4 (3/76)

GEORGIA INSTITUTE OF TECHNOLOGY

SCHOOL OF MECHANICAL ENGINEERING

ATLANTA, GEORGIA

STUDY OF HAZARDS FROM BURNING APPAREL AND THE RELATION OF HAZARDS TO TEST METHODS

PROGRESS REPORT NO. [redacted]

by

A. Alkidas
E. Champion
W. Giddens
R. W. Hess
P. Durbetaki
W. Wulff

For The

GOVERNMENT-INDUSTRY RESEARCH COMMITTEE
ON FABRIC FLAMMABILITY

Office of Flammable Fabrics

National Bureau of Standards

Washington, D. C. 20234

NSF Grant No. GI-31882

July 1, 1972

STUDY OF HAZARDS FROM BURNING APPAREL

AND THE RELATION OF HAZARDS TO TEST METHODS

PROGRESS REPORT NO. 5

By

A. Alkidas
E. R. Champion
W. E. Giddens
R. W. Hess
P. Durbetaki
W. Wulff

School of Mechanical Engineering
Georgia Institute of Technology
Atlanta, Georgia 30332

July 1, 1972

Monitored by

GOVERNMENT-INDUSTRY RESEARCH COMMITTEE
ON FABRIC FLAMMABILITY

Office of Flammable Fabrics

National Bureau of Standards

Washington, D. C. 20234

NSF Grant No. GI-31882

W. [illegible] Investigator

N. Zuber, Principal Investigator

Stothe P. Kezios
Director
School of Mechanical Engineering

FOREWORD

This project is being carried out in the Fire Hazard and Combustion Research Laboratory of the School of Mechanical Engineering at Georgia Institute of Technology under the Principal Investigators Dr. Wolfgang Wulff and Dr. Novak Zuber. For the program period covered by this report, from April 1, 1972 through June 30, 1972, Graduate Research Assistants Dr. Alexandrox Alkidas (ignition temperature and enthalpy measurements), Messrs. Richard W. Hess (ignition time measurements) and William E. Giddens (thermal conductance and reaction kinetics) have directly participated in this work. Their participation has been supported in part by the School of Mechanical Engineering under the matching-fund provision of the grant.

Dr. P. Durbetaki, Associate Professor of Mechanical Engineering performed the flame ignition studies, assisted by Graduate Research Assistant Mr. Edward R. Champion.

SUMMARY

The work reported herein was carried out at the Georgia Institute of Technology during the second reporting period from April 1, 1972 through June 30, 1972, sponsored by the National Science Foundation under the RANN program (Research Applied to National Needs) and monitored by the Government-Industry Research Committee on Fabric Flammability (GIRCFF). The work constitutes a continuation of the research carried out under the previous NSF Grant GK-27189 and under the same GIRCFF program during the contract period from November 1, 1970 through November 30, 1971 [1]*. The GIRCFF program involves, besides the Georgia Institute of Technology, the Massachusetts Institute of Technology [2], the Factory Mutual Research Institute [3] and the Gillette Company Research Institute [4,5].

The purpose of the experimental and analytical research performed at the Georgia Institute of Technology is to provide the modeling rules and the fabric characteristics needed for determining the fabric ignition probability for given exposure to a heat source.

The Experimental Program consists of four tasks: (1) the fabric property measurements, (2) the measurement of the moisture effects on fabric ignition time, (3) the assessment of the heating mode on ignition time, and (4) the collection of statistical fabric ignition data.

1. The fabric properties relevant to the description of the ignition process are the fabric ignition or melting temperatures, the specific heat, the thermal conductance, the radiative absorptance and the parameters of chemical reaction kinetics, namely activation energy, pre-exponential factor and reaction enthalpy.

During this second reporting period the Setchkin furnace modification was completed, the furnace core temperature distribution rechecked and the furnace temperature calibrated against furnace and air preheater power settings. The total of 32 auto ignitions and 26 pilot ignitions has been carried out. This completes the ignition temperature measurements on the GIRCFF Fabrics.

*Numbers in square brackets refer to the Bibliography of this report.

Thirty-three additional enthalpy measurements were completed on the ten Secondary GIRCFF Fabrics. Except for additional data verification on two fabrics, the enthalpy measurements on the Secondary GIRCFF Fabrics is completed. Specific heat data are presented.

Ten additional thermal conductance measurements were carried out on the Secondary GIRCFF Fabrics, all at the intermediate contact pressure of 866 N/m^2 and in the temperature range between 88 and 95°C.

The fabric mass per unit area and fabric thickness was measured on all ten Secondary GIRCFF Fabrics.

Precharring of all GIRCFF Fabrics, for the purpose of measuring the optical properties on thermally decomposed samples, has been completed.

The supplementary equipment to be used with the METTLER thermo-analyzer 2 of the School of Chemistry at Georgia Institute of Technology, for the measurement of reaction parameters of the fabrics has been received. Four preliminary DTA/TGA measurements were performed on GIRCFF Fabric No. 2.

2. The measurement of moisture effects on fabric ignition time consists of (a) measuring the fabric ignition times on desiccated samples of the ten Secondary GIRCFF Fabrics with the Ignition Time Apparatus, in accordance with the methods described in Reference [1], and (b) repeating the above task in a psychrometrically controlled environment, at three different humidity levels, but on the Primary GIRCFF Fabrics.

During this second reporting period the measurement of ignition time on the ten desiccated Secondary GIRCFF Fabrics has been completed by performing the total of 94 single-shutter experiments at six heating intensities between 0.25 and 16 Wcm^2.

The delivery of the psychrometrically controlled enclosure was six weeks late. The enclosure has been assembled and checked out at extreme temperature and humidity levels. Final connections between Ignition Time Apparatus and instrumentation, through the enclosure walls, are in preparation.

3. The effect of heating source on ignition time. While the ignition analysis developed in Reference [1] provides for due consideration of all possible heating modes, it must be verified experimentally. The verification of the radiative heating mode has been in progress for considerable time [1,3 (and others)]. The third task has the objective to verify

the present mathematical ignition model under convective heating conditions or to provide the necessary experimental information to modify the ignition model.

During the second reporting period the design of the Convective Ignition Time Apparatus in the "static" test mode was completed and construction was carried out to near completion. The design was modified to use air cylinders for the actuation of the shutters instead of the springs that were originally considered.

The design of the transport system for the "transient" tests has been initiated.

A third burner, Fisher blast type has been selected and with some minor modifications will be used for the early tests. This burner provides usable fuel heat release rates from 140 watts to 2800 watts. The fabric will be exposed to flame through an aperture of one inch diameter in the fabric holder.

4. The collection of statistical fabric ignition data for the purpose of obtaining statistical confidence measures, such as ignition time frequency distribution and variance, consists of measuring, in the Ignition Time Apparatus [1] and in the controlled environment, the frequency with which ignition occurs under square-pulse heating exposure. The timing circuit needed for activating the shutter of the Ignition Time Apparatus under dual shutter mode operation is being assembled and checked out.

The Analytical Program is proposed to verify and modify as necessary the complete and partial modeling analyses developed during the last year's program, specifically by including the experimentally obtained reaction kinetics of pyrolysis, and convective heating in the gas flame. The analysis is scheduled to be continued after reaction kinetics have been measured. No work was performed on the analysis during the second reporting period.

TABLE OF CONTENTS

LIST OF FIGURES

LIST OF TABLES

I. PROGRAM OBJECTIVES AND PREVIOUS WORK

A. Objective

The Government-Industry Research Committee on Fabric Flammability (GIRCFF) is monitoring a research program to provide the necessary scientific foundation for legislation required to reduce the hazard of fabric-originated burn injuries. As one of four participating laboratories, the Fire Hazard and Combustion Research Laboratory in the School of Mechanical Engineering at Georgia Institute of Technology, is performing an analytical and experimental study with the objective of predicting the fabric ignition probability for prescribed exposure time as a function of measured fabric properties and exposure conditions. This effort is funded by the National Science Foundation under its second one-year grant and as part of the RANN program.

The achievements attained during the first year contract period are reported in Reference [1]. Thermophysical properties were measured on the first ten of twenty fabrics selected by GIRCFF and referred to as the Primary GIRCFF Fabrics*. Ignition times were measured under radiative heating on desiccated samples of the Primary GIRCFF Fabrics. Complete and partial modeling analyses were performed for the fabric ignition process. The comparison of analytical with experimental ignition data indicated a significant influence of pyrolysis on ignition time.

The objectives of the current contract period are (a) to extend the experimental program over the remaining ten fabrics, i.e. the Secondary GIRCFF Fabrics listed in Table 2, (b) to include into both the experimental and analytical efforts the consideration of fabric moisture content and thermal decomposition, (c) to predict ignition or melting time under convective heating in the gas flame, and (d) to determine the fabric ignition probability as a function of exposure time, heating intensity and fabric properties.

The Experimental Program serves to provide the fabric characteristics relevant to the ignition process, to verify the analytical ignition models

* For their identification, see Table 1.

TABLE 1. THE TEN PRIMARY GIRCFF FABRICS

GIRCFF No.	Classification	Fiber Composition	Color	Chemical Finish	Weight oz/sq.yd.
2	Textured Woven Blouse	100% Polyester	Yellow	---	2.19
5	T-Shirt, Jersey	100% Cotton	White	---	3.97
8	T-Shirt, Jersey	65/35% PE/C	White	---	4.82
10	Batiste	100% Cotton	Purple	---	2.04
11	Tricot	80/20% Acet./Nylon	White	---	2.67
12	Tricot	100% Nylon	White	---	2.47
13	Tricot	100% Acetate	White	---	2.44
17	Batiste	65/35% PE/C	White	---	2.53
18	Flannel	100% Cotton	White	---	3.69
19	Flannel	100% Cotton	White	Fire Rtd	4.21

TABLE 2. LIST OF TEN SECONDARY GIRCFF FABRICS

GIRCFF NO.	Classification	Fiber Composition	Color	Chemical Finish	Weight oz/sq.yd.
1	Durable Press Slack	65/35% P.E./Cotton	White	DP treated	7.07
3	Double Knit	100% Polyester	White	---	5.83
4	Denim	100% Cotton	Navy	---	8.66
6	Untreated Slack	65/35% P.E./Cotton	White	---	6.99
7	Jersey Tube Knit	100% Acrylic	Gold	---	2.64
9	Terry Cloth	100% Cotton	White	---	7.42
14	Taffeta	100% Nylon	White	---	1.67
15	Durable Press Slack	65/35% P.E./Rayon	Brown	DP treated	6.62
16	Shirting	50/50% P.E./Cotton	White	---	3.91
20	Flannel	100% Wool	Navy Blue	---	6.48

and to establish statistically the confidence to be expected of the ignition data. The relevant fabric characteristics are the ignition or melting temperatures, density, specific heat, thermal conductance, radiative absorptance, activation energy, order of reaction, pre-exponential factor and reaction enthalpy. In order to verify the analytical ignition models, the fabric ignition time is measured under carefully controlled, radiative and convective (gas flame) heating conditions. The statistical confidence of the experimental ignition data under radiative heating is obtained by measuring the ignition frequency as a function of heating intensity, fabric moisture content and exposure time.

The specific objectives and the achievements attained during the second reporting period are presented in Chapter II.

The Analytical Program has the purpose of advancing, under inclusion of fabric humidity and pyrolysis effects, the complete and partial model analyses developed during the previous contract period with the objective to predict the fabric ignition time in terms of fabric properties and process parameters. The program is designed further to assess the expected error of partially modeling the ignition process. For fabrics which melt prior to ignition, the melting time is substituted for ignition time.

As there was no analytical work scheduled during the second reporting period, pending the development of experimental data on reaction kinetics, no discussion of the analysis is included in this report.

B. Achievements During First Reporting Period

Details of the accomplishments during the first reporting period, together with experimental results obtained during that period, are given in the fourth quarterly report [6]. A brief summary is given below.

1. Experimental Program

a. Fabric Property Measurements

Task 1: Fabric Ignition and Melting Temperatures. The modified Setchkin Furnace was reconverted from enthalpy to ignition temperature measurements and an air preheater for purge air conditioning designed,

constructed and installed.

Task 3: Specific Heat. Eighteen fabric enthalpy measurements were performed on GIRCFF Fabrics No. 1, 4, 9 and 15, in the temperature range between 100 and 300°C. Previously obtained enthalpy data were reevaluated.

Task 4: Thermal Conductance. Thirty conductance measurements were carried out in the temperature range from 60 to 180°C. One anomalous fabric of the Primary GIRCFF Fabric Set, Fabric No. 12, was remeasured and its previously obtained conductance data was confirmed.

Task 5: Optical Fabric Properties reflectance and transmittance were measured successfully on eight Secondary GIRCFF Fabrics in their original states.

Task 6: Reaction Kinetic Parameters. Supplementary equipment to be used with the METTLER Thermoanalyzer 2 of the School of Chemistry at Georgia Tech was selected and ordered.

b. Fabric Ignition Time Measurements and Moisture Effects. The Ignition Time Apparatus was recalibrated after completion of the second shutter assembly. The failure of the heat flux meter interrupted fabric testing. The thermostatically and psychrometrically controlled enclosure was selected and ordered from Environair Systems, Inc. East Longmeadow, Mass. Its delivery had been scheduled for May 3, 1972. Ignition data previously obtained were reevaluated with mean values of specific heat.

c. Effect of Heating Mode on Fabric Ignition Time. The Convective Ignition Time Apparatus was designed in overall concept and operational procedures were established. Techniques for flame characterization were developed.

d. Ignition Time Statistics. The electronic timing circuit required for operating the Radiative Ignition Time Apparatus under dual shutter mode was designed, and the necessary components were ordered. A shutter position sensing circuit was completed.

II. EXPERIMENTAL PROGRAM

The basic objectives of the experimental program are outlined in Chapter I. The entire experimental program is divided into four major parts: the property measurements consisting of six subtasks, the measurement of fabric ignition time and of moisture effects on ignition time, the investigation of the effect of heating modes on fabric ignition time and the measurement of fabric ignition time frequency under radiative heating. Specific objectives and accomplishments during the first reporting period, of these four major program phases, are presented in the following four sections, Sections A through D.

A. Fabric Property Measurements

1. Purpose

The property measurement program is designed to provide (a) for the Secondary GIRCFF Fabrics, listed in Table 2, the following thermophysical properties: fabric ignition or melting temperature, fabric density, specific heat, thermal conductance and radiative absorptance and (b) for the Primary GIRCFF Fabrics, listed in Table 1 below, the reaction kinetics parameters, namely activation energy, pre-exponential frequency factor, order of reaction and reaction enthalpy, all averaged over the pre-ignition processes. These properties are necessary to describe the ignition processes via the ignition models presented in Reference [1].

The objectives listed under (a) above are carried out, in five tasks, in accordance with the test specifications, test procedures and with the instrumentation discussed in Reference [1], Appendix B, as follows:

Task 1. Fabric Ignition or Melting Temperature, measured as discussed in Appendix B.4, pg. 142 [1].

Task 2. Fabric Mass Per Unit Area, simply obtained by weighing square samples of approximately 160 cm^2 area, after desiccation, on an analytical balance.

Task 3. Specific Heat of Fabrics, obtained as discussed in Appendix B.2, pg. 126 [1].

Task 4. Thermal Conductance (or product of fabric density and thermal

conductivity), measured in accordance with Appendix B.3, pg. 136 [1].

Task 5. Radiative Absorptance, derived from measurements of reflectance and transmittance, as presented in Appendix B.5, pg. 153 [1].

The parameters of reaction kinetics listed under item (b) above are to be obtained simultaneously, in Task 6, through thermogravimetric and differential thermal analyses in the TG/DTG/DTA METTLER Thermoanalyzer 2 [6]. The thermal decomposition is scheduled to be performed in air at 1 atm and at two selected heating rates in the range between 5 and 60°C/min. N_2-environment can be provided.

Listed below are first the achievements attained during the second reporting period, then the development details and experimental results.

2. Achievements During Second Reporting Period: Fabric Property Measurements

Task 1. The fabric ignition or melting temperature was measured in a modified Setchkin Furnace (Appendix B.4 in Reference [1]). The furnace had been considerably modified during the first reporting period. During the second period final wiring and furnace calibrations were completed. The calibrations consist of verifying temperature uniformity within the furnace core and of balancing the power supplies to air preheater and furnace, for maximum temperature uniformity within that furnace. Thirty-two auto ignition and 26 pilot ignition temperature tests were carried out. This completes the basic ignition temperature measurements on the GIRCFF Fabrics. Results are reported in Section 3 below, under Task 1.

Task 2. The mass per unit area was obtained for all ten Secondary GIRCFF Fabrics by weighing square, desiccated samples of 5 in. by 5 in. size on an analytical balance. Fabric thickness was measured on the same fabrics with a micrometer. Results are given in Section 3 under Task 4.

Task 3. The specific heat of fabrics as a function of temperature is

obtained from enthalpy measurements (Appendix B.2 in Reference [1]). During the second reporting period the total of 33 enthalpy measurements was performed on the eight GIRCFF Fabrics No. 3, 6, 7, 9, 14, 15, 16 and 20, in the temperature range between 100°C and 300°C. Apparent discrepancies in the results of two GIRCFF Fabrics No. 3 and 7 require further enthalpy measurements.

Task 4. The thermal conductance is measured in a guarded hot plate apparatus (Appendix B.3 in Reference [1]). During the second reporting period the total of 10 conductance measurements was performed on the Secondary GIRCFF Fabric Set at a contact pressure of 866 N/m^2 and in the temperature range of 88°C to 95°C. The results of the thermal conductance measurements are presented in Section 3 below.

Task 5. Optical fabric properties reflectance and transmittance are measured in an integrating sphere reflectometer (Appendix B.5 in Reference [1]). All twenty GIRCFF Fabrics were charred in a furnace at the mean temperature between 24°C (room temperature) and ignition or melting temperature, for the purpose of measuring optical properties at the state associated with that mean temperature.

Task 6. The supplementary equipment ordered during the first reporting period for use on the METTLER Thermoanalyzer 2, of the School of Chemistry at Georgia Tech, was received and consists of 1 Middle Range Furnace, 3 different Sample Holders, and 2 Platinum crucibles. An extensive literature survey was performed dealing specifically with the techniques of DTA and TGA. Several articles [7, 8, 9] were most helpful in preparing the sample, choosing a reference material, and analyzing the results. A search of textiles, polymer, and plastics literature was also made for the purpose of finding quantitative data on the activation energy, pre-exponential factor, order of reaction and the heat of reaction of textiles. Incomplete data was found for cellulose and nylon only. Experimental data on thermal decomposition of all GIRCFF

Fabrics, taken by Dr. R. J. McCarter of the National Bureau of Standards were received and their evaluation is being prepared. Familiarization with the Mettler Thermoanalyzer 2 was accomplished with the assistance of Dr. Pierre Claudy, who is currently with the School of Chemistry at Georgia Tech. Under Dr. Claudy's guidance four familiarization tests were performed on GIRCFF Fabrics No. 2 and the results qualitatively analyzed.

3. Development Details and Test Results: Fabric Property Measurements

Task 1. Ignition or Melting Temperature Measurements

The basic procedure of measuring ignition or melting temperatues was retained as described in Appendix B.4 of Reference [1]. Two improvements in the design of the test apparatus were made to achieve uniform furnace core temperatures [6, pg. 9].

Auto and pilot ignition data taken during the second reporting period are presented in Tables 3 and 4, respectively. The auto ignition and melting temperatures of all GIRCFF Fabrics are presented graphically in Figure 1, the pilot ignition temperatures of all GIRCFF Fabrics which ignite without prior melting are presented in Figure 2. A complete summary of ignition and melting temperatures is given in Table 5.

Ignition of molten fabrics has not been investigated since the present interest lies essentially in the occurrence of thermal fabric destruction rather than in the interaction between skin tissue and burning fabric or molten fabric.

Preliminary conclusions are that thermoplastics melt between 235 and 265°C, cotton fabrics self-ignite generally between 290 and 330°C and that polyester/cotton blends have higher auto ignition temperatures than both cotton and polyester. Wool ignited at 480°C without pilot.

Exceptional results were obtained for the fire retardant Cotton Flannel, GIRCFF Fabric No. 19, which ignited without pilot between 480 and 497°C, and for the Cotton Batiste, GIRCFF Fabric No. 10, with its self-ignition interval of 429 to 439°C. Cotton Batiste has a relatively low mass per unit area and may have to be heated to a relatively high temperature before the rate of volatile evolution becomes sufficiently

Table 3. SELF IGNITION AND MELTING TEMPERATURE DATA OF THE FABRICS MEASURED DURING THE SECOND REPORTING PERIOD

Ignition ● Melting ■
No Ignition ○ Flash ◇

	GIRCFF FABRIC				
Air Temp. °C	# 3	# 7	# 14	# 15	# 16
209	○	○	○	○	
226	○	○	○	○	
236		○	○		
246	○	■	■	○	
255	■				
261	■			○	
300				○	○
333				○	○
372				○	○
400				○	○
419				○	○
426				●	
454				●	○
466					○
473					●

Table 4. PILOT IGNITION TEMPERATURE DATA OF THE FABRICS MEASURED DURING THE SECOND REPORTING PERIOD

Ignition ● Flash ◇

No Ignition ○

	GIRCFF FABRIC					
Air Temp °C	# 1	# 4	# 6	# 9	# 15	# 16
280		○		○		
290		●		○		
297		●		●		
312		●		●		
324	○	●	○	●	○	○
331	○				○	
337	●		○		●	
345			●			
353	●		●		●	○
360						●
364						●

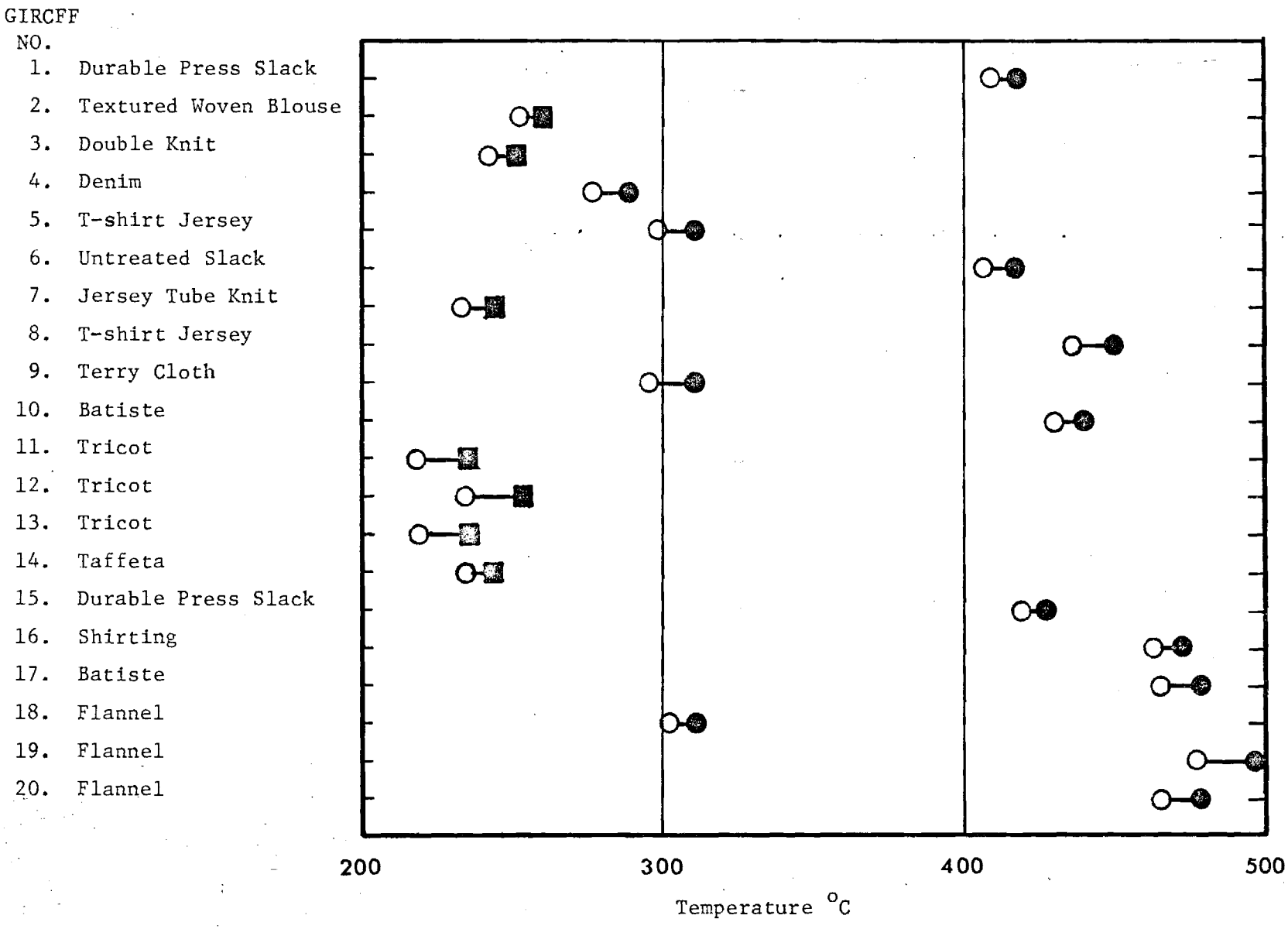

Figure 1. Self-Ignition and Melting Temperature

GIRCFF
NO.

1. Durable Press Slack
4. Denim
5. T-shirt Jersey
6. Untreated Slack
8. T-shirt Jersey
9. Terry Cloth
10. Batiste
15. Durable Press Slack
16. Shirting
17. Batiste
18. Flannel
19. Flannel
20. Flannel

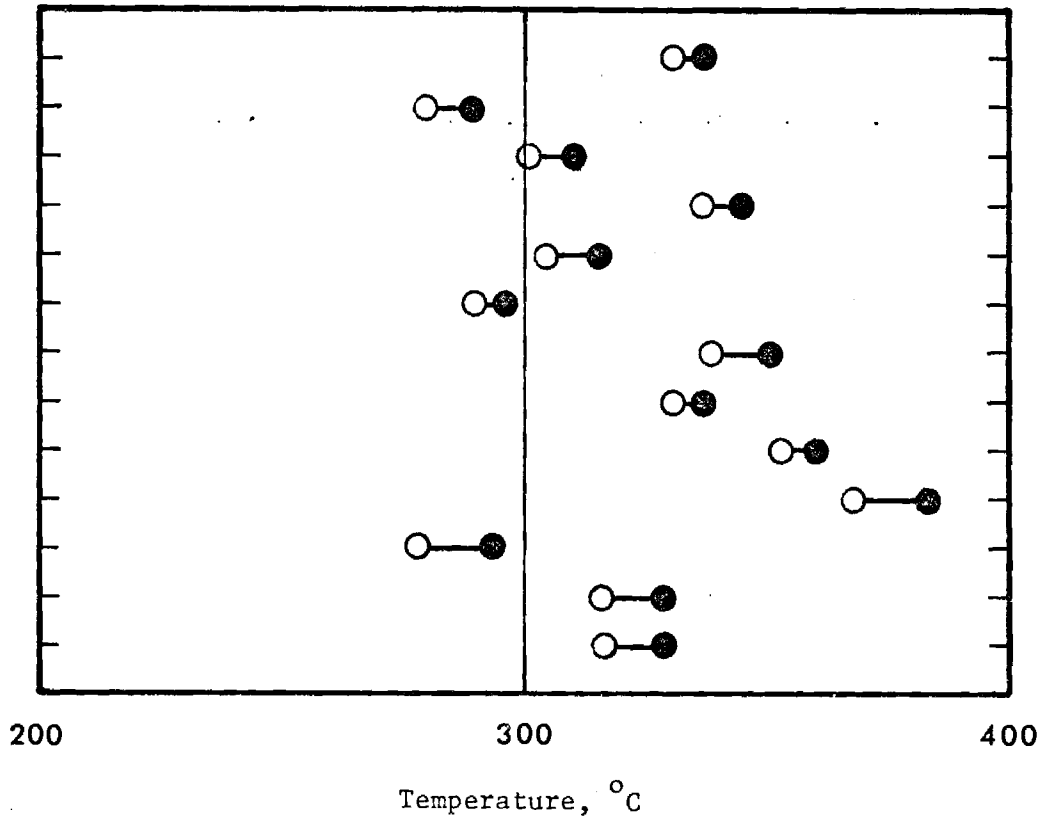

Figure 2. Pilot-Ignition Temperatures

Table 5. SUMMARY OF SELF AND PILOT IGNITION AND MELTING TEMPERATURES

GIRCFF Fabric No.	Temperature, °C Self-Ignition, Melting	Pilot-Ignition
1	416-409	337-331
2	262-255 M**	
3	255-246 M	
4	297-287 290-280 *	290-280
5	311-301 327-318	311-301
6	416-409	345-337
7	246-236 M	
8	450-439 443-416	316-304
9	308-297	297-290
10	439-429 443-434	351-339
11	237-218 M	
12	255-237 M	
13	237-218 M	
14	246-236 M	
15	426-419	337-331
16	473-466	360-353
17	480-463	384-368
18	311-301	294-278
19	497-480	329-316
20	480-463	329-316

* check on reproducibility

** M represents melting

high to produce an ignitable volatile-air mixture.

Task 2. Fabric Density Measurements

Square fabric samples with sides of 5 x 5 in. were desiccated and weighed on an analytical balance. The fabric thickness was obtained by averaging four thicknesses as measured with a micrometer, the fabric being placed between plane-parallel plates under the net contact pressure of 528 N/m^2.

Results are shown in Table 7 for the Second Primary GIRCFF Fabrics.

Task 3. Specific Heat Determination

The operating procedure for the enthalpy measurements was slightly changed from the procedure described in Appendix B.2 of Reference [1], in that larger fabric samples of approximately 150 g were tightly wrapped in aluminum foil and heated in a Cole-Parker Type 1400 Furnace rather than in the Setchkin Furnace. Use of the new furnace freed the Setchkin Furnace for ignition temperature measurements, and the larger sample mass is necessary to compensate for mass losses particularly above 200°C.

Care is taken to heat all samples equally long, namely 20 hours, prior to the transfer into the calorimeter, by means of thermally insulated prongs.

The results are shown in Figures 3 through 10 for the eight GIRCFF Fabrics tested during the second reporting period. Fabrics GIRCFF Nos. 1 and 4 were reported in Reference [6].

Specific Heat Data for the ten Secondary GIRCFF Fabrics are summarized as a function of temperature in Table 6.

Task 4. Thermal Conductance of Fabrics

The thermal conductance, that is the ratio of thermal conductivity to density, is obtained in a guarded hot plate apparatus described in Appendix B.3 of Reference [1]. A preliminary summary of test results, all obtained for the Secondary GIRCFF Fabrics, at the contact pressure

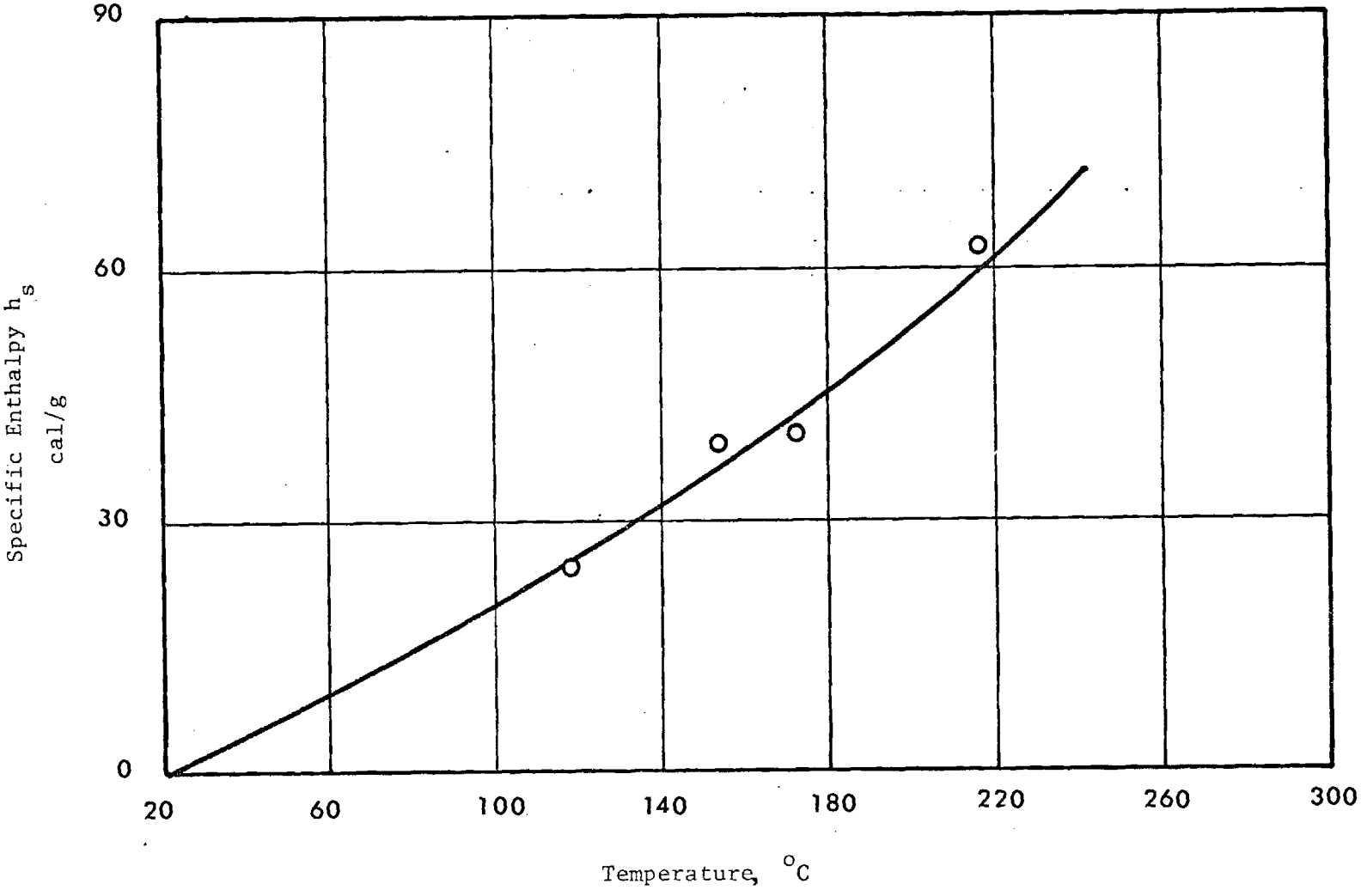

Figure 3. Enthalpy vs Temperature For
100% Polyester; GIRCFF No. 3

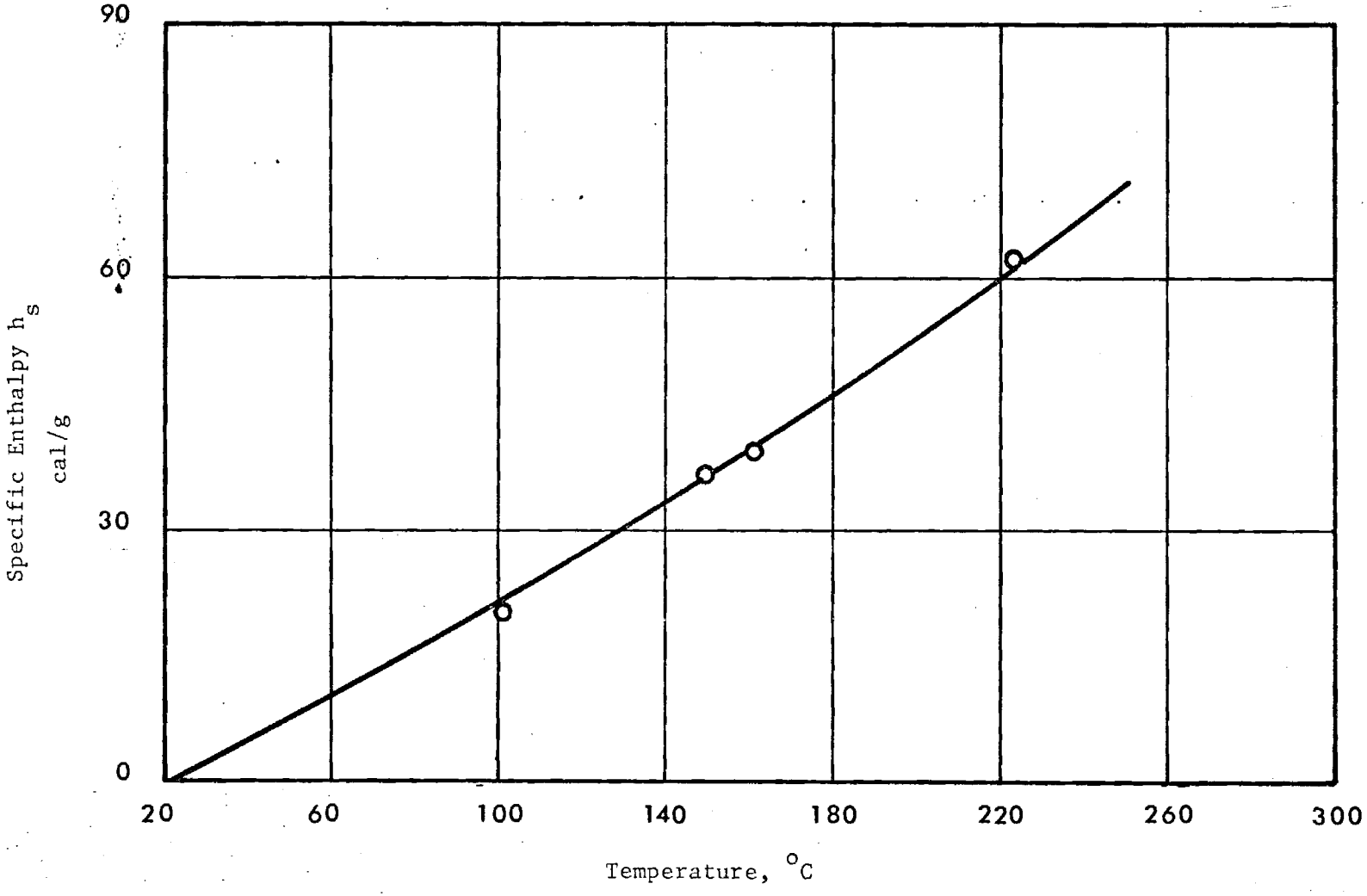

Figure 4. Enthalpy vs Temperature For
65/35% Polyester/Cotton; GIRCFF No. 6

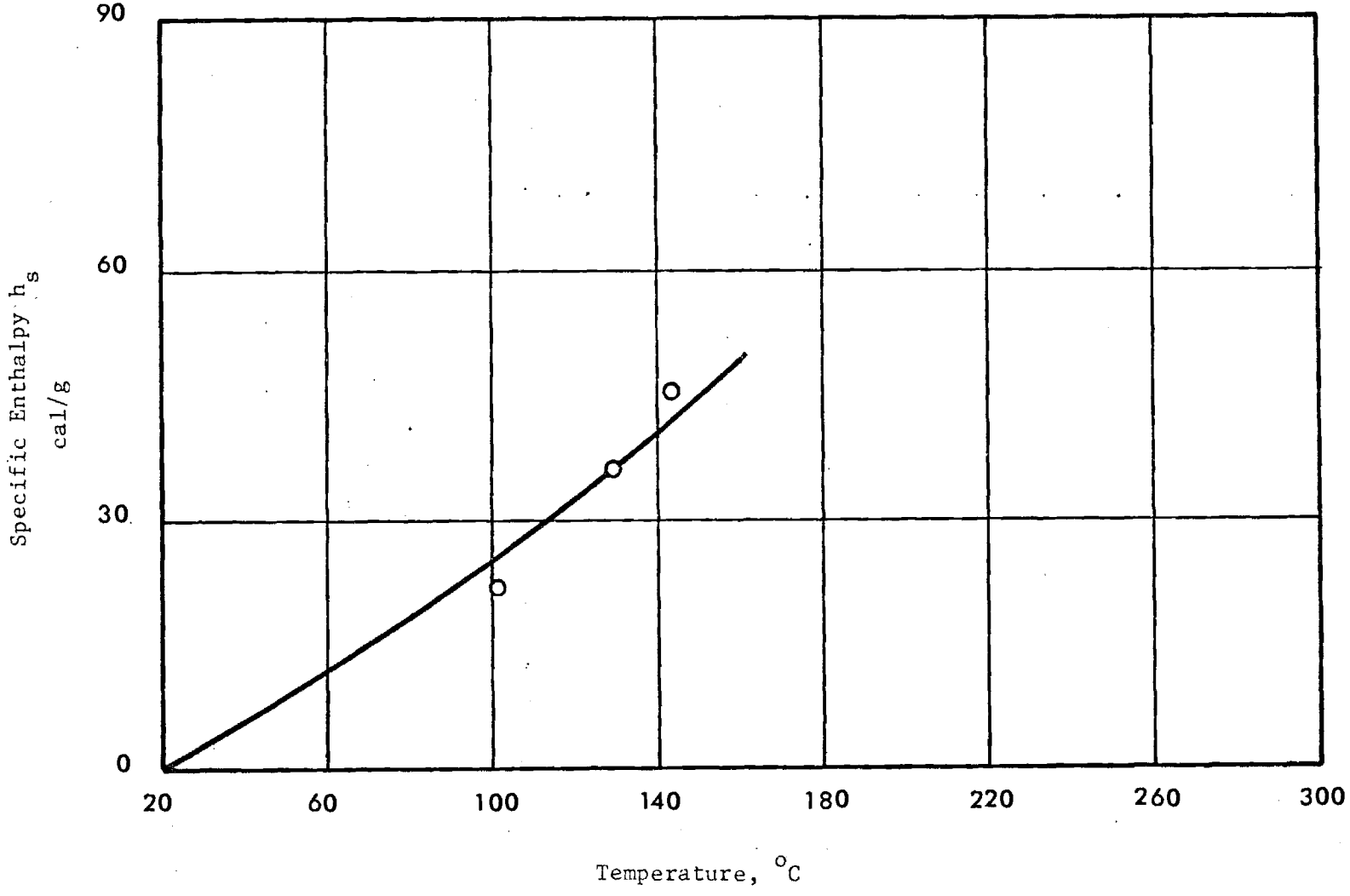

Figure 5. Enthalpy vs Temperature For
100% Acrylic; GIRCFF No. 7

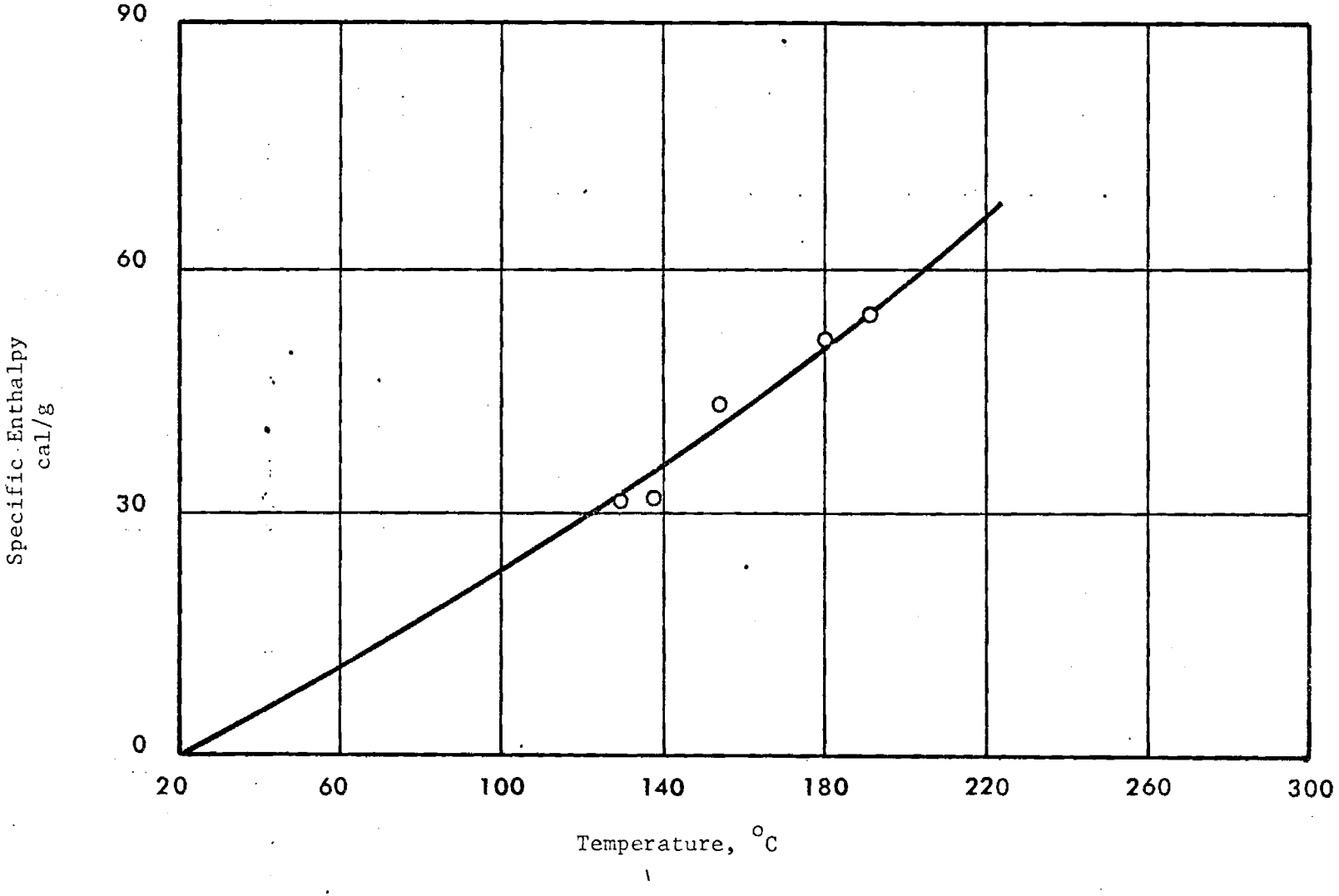

Figure 6. Enthalpy vs Temperature For
100% Cotton; GIRCFF No. 9

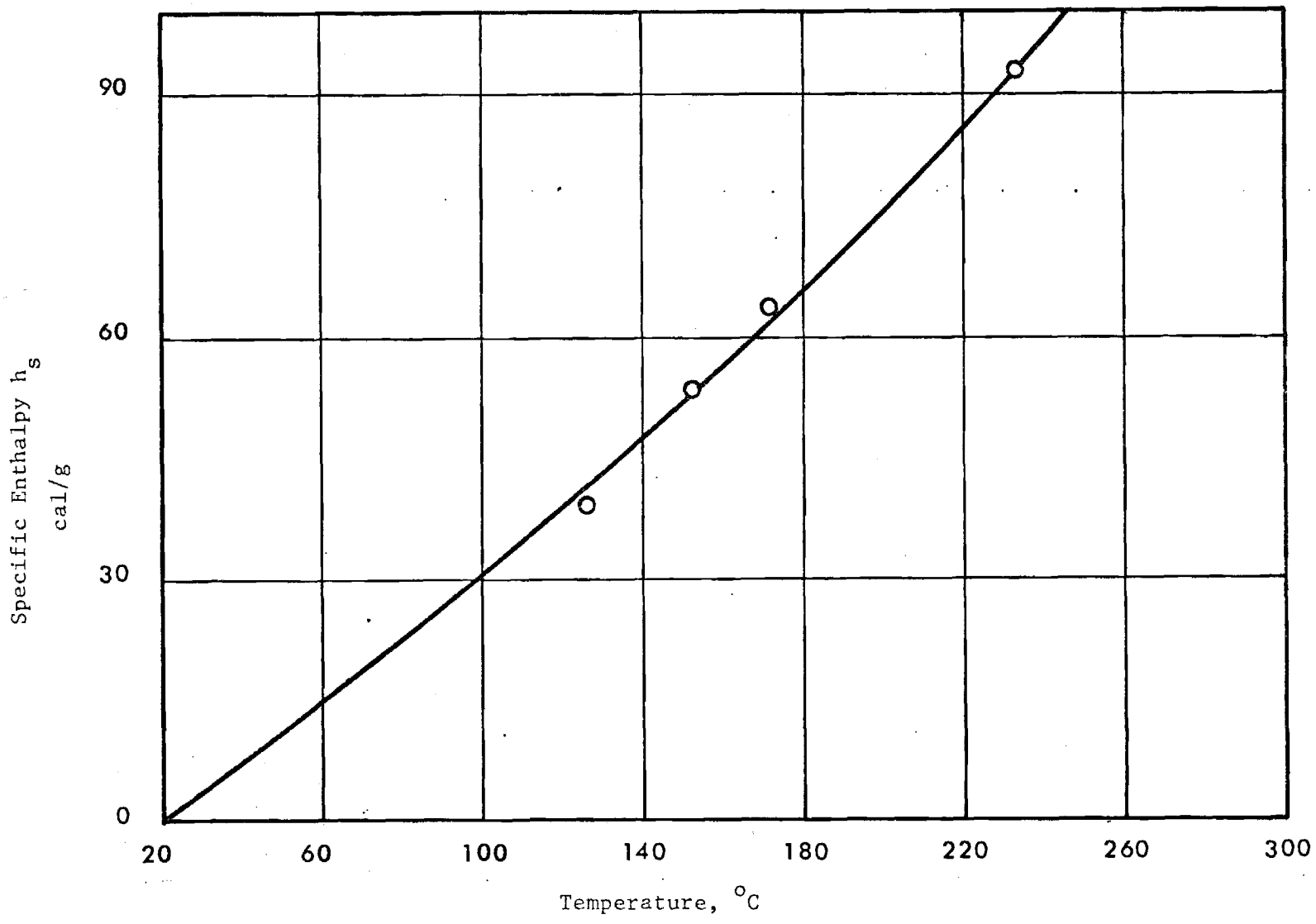

Figure 7. Enthalpy vs Temperature For
100 Nylon; GIRCFF No. 14

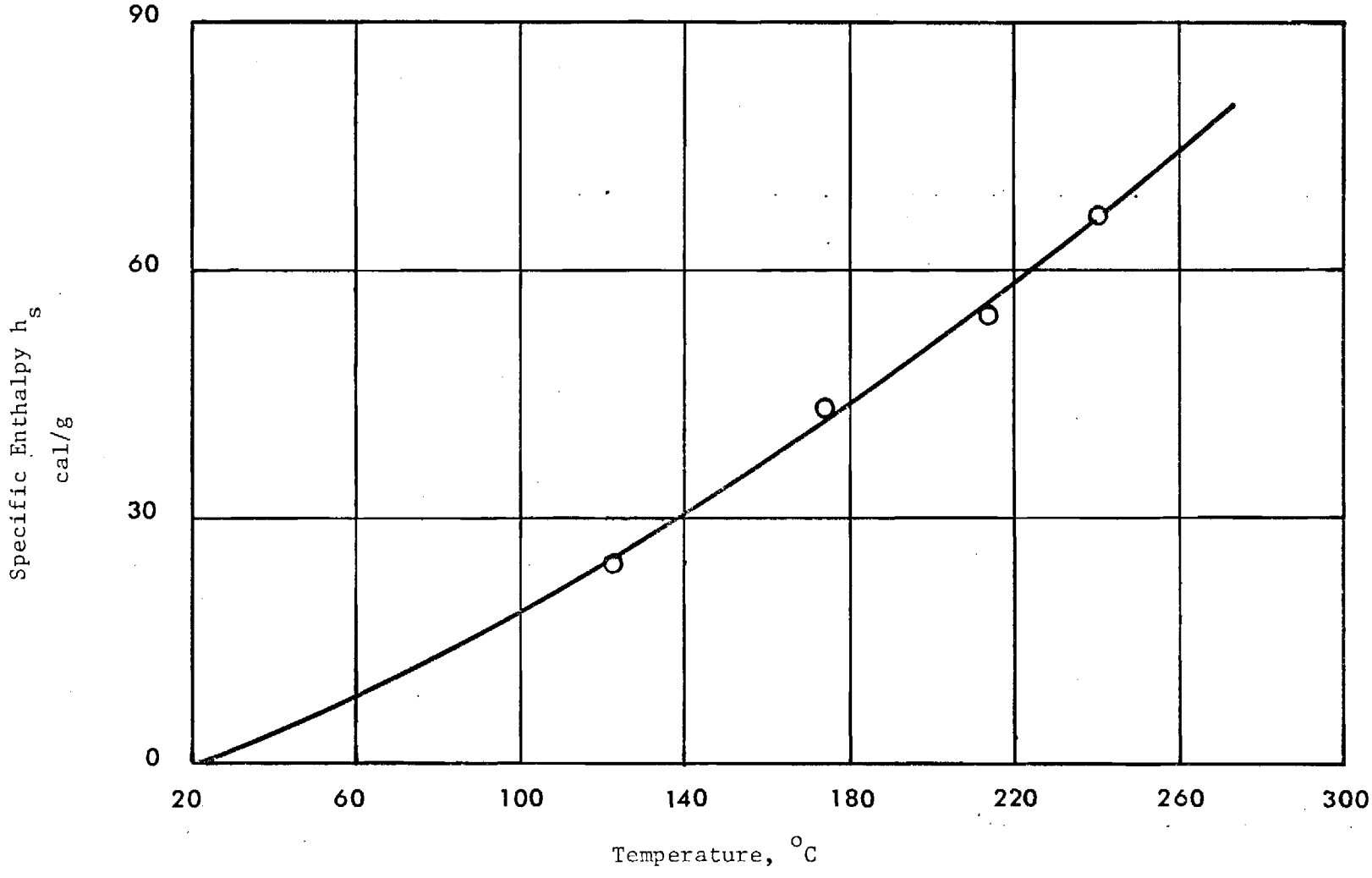

Figure 8.Enthalpy vs Temperature For
65/35% Ployester/Rayon; GIRCFF No. 15

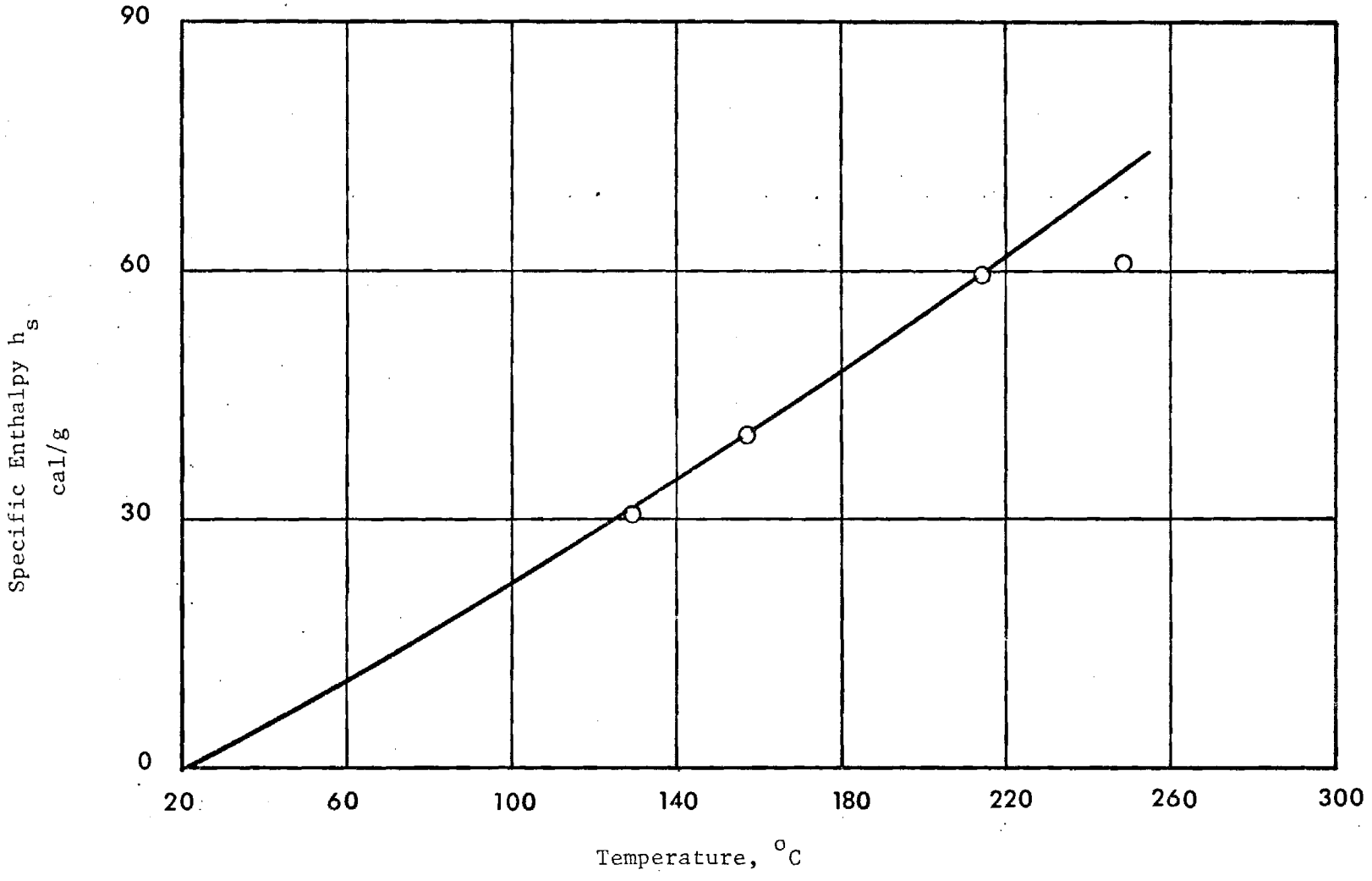

Figure 9. Enthalpy vs Temperature For
50/50% Polyester/Cotton; GIRCFF No. 16

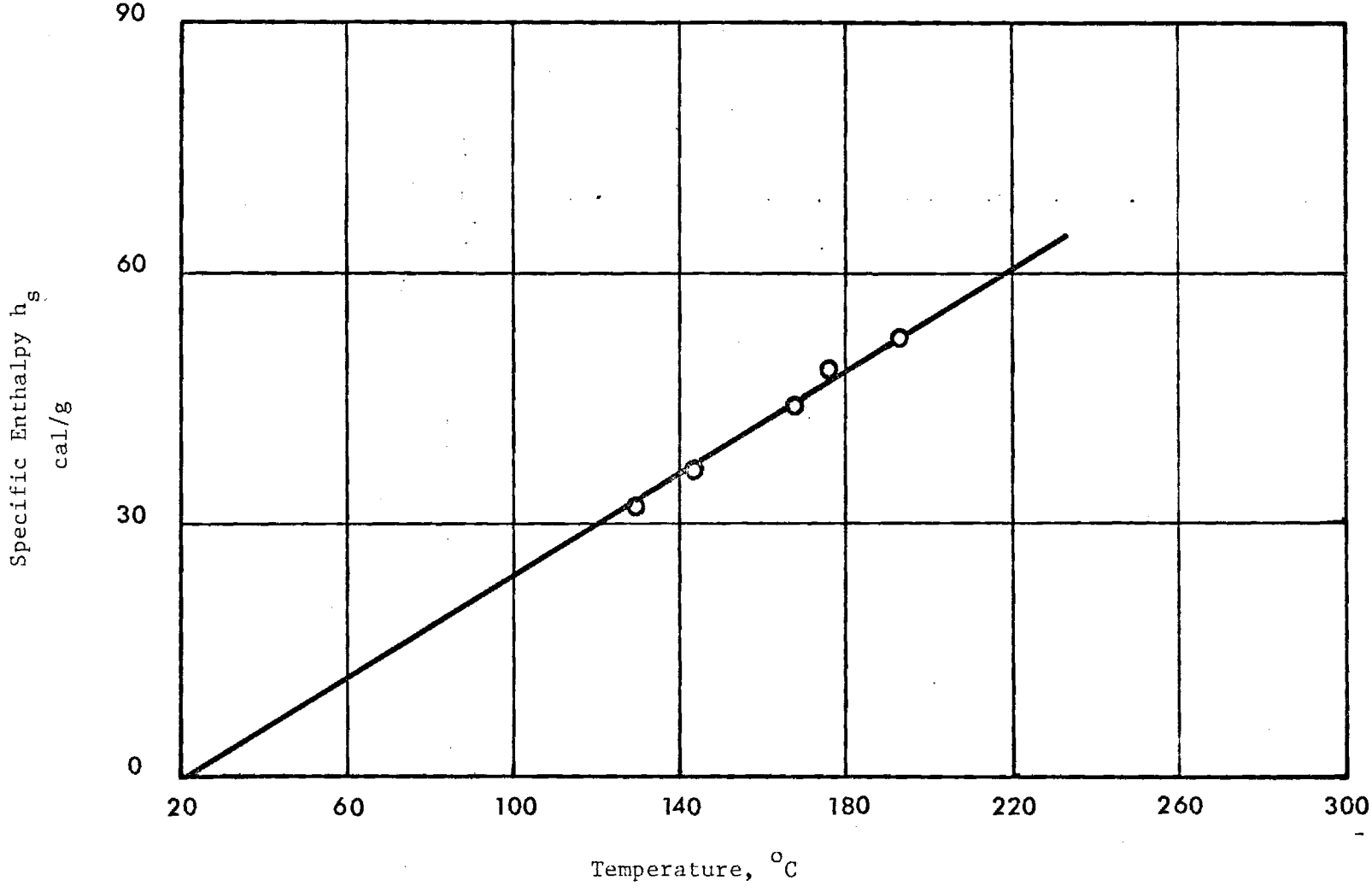

Figure 10 Enthalpy vs Temperature For
100% Wool; GIRCFF No. 20

Table 6. SPECIFIC HEAT OF FABRICS

GIRCFF Fabric No.	Fabric Temperature in °C							
	75	100	150	175	200	225	250	275
	Specific Heat in Ws/ (gC)							
1	1.24	1.29	1.38	1.43	1.47	1.50	1.53	1.56
3	1.10	1.17	1.36	1.50	1.67	1.89	2.16	---
4	1.23	1.29	1.40	1.46	1.50	1.53	1.55	---
6	1.16	1.21	1.32	1.39	1.48	1.59	---	---
7*	1.40	1.53	1.92	2.23	---	---	---	---
9	1.21	1.32	1.53	1.61	1.64	---	---	---
14	1.66	1.73	1.86	1.96	2.13	2.39		
15	1.03	1.15	1.37	1.47	1.55	1.62	1.66	---
16	1.21	1.26	1.37	1.41	1.44	1.45	---	---
20	1.27	1.27	1.27	1.27	1.27	---	---	

*Preliminary Results

Table 7. THERMAL CONDUCTANCE AND DENSITY OF TEN SECONDARY GIRCFF FABRICS.

GIRCFF Fabric Number	Mass Per Unit Area mg/cm^2		Original Fabric Thickness cm	Mean Temperature ^oC	Specific* Conductance $mW\ cm^{-2}\ C^{-1}$
	N.B.S.	G.T.			
1	24.04	23.49	0.0464	88.7	15.71
3	19.82	20.91	0.0953	92.0	5.46
4	29.44	29.63	0.0575	90.2	13.05
6	23.77	23.57	0.0476	88.9	14.53
7	8.98	15.13	0.0791	88.3	7.93
9	25.23	26.48	0.2080	15.3	2.98
14	5.68	5.66	0.0110	88.2	27.80
15	22.51	22.82	0.0421	89.0	15.37
16	13.29	13.14	0.0321	90.7	19.72
20	22.03	19.93	0.0721	91.7	7.00

*Contact Pressure of 866 N/m^2.

of $p = 528\ N/m^2$, were presented in Table 4 of Reference [6].

Results obtained during the second reporting period are listed, together with density and mass per unit area, in Table 7 below. They are the conductance under intermediate contact pressure $p = 866\ N/m^2$.

B. Fabric Ignition Time And Moisture Effects (Radiative Heating)

1. Purpose

The objective is to measure the ignition time defined as the time span between instantaneous fabric exposure to a well known, uniform and time-invariant heat flux, and the fabric destruction either through complete melting or ignition. The ignition time is the central parameter in the definition of ignition probability and must be measured for the verification of its analytical prediction.

The schedule calls for the determination of ignition time on the ten Secondary GIRCFF Fabrics, after desiccation of these fabrics, in the heating intensity range between 0.25 and 16 W/cm^2 and for the ignition time measurement on both the Primary and Secondary GIRCFF Fabrics at three levels of relative humidity between 5% and 95% relative humidity.

2. Achievements During Second Reporting Period

The ignition time under radiative heating is measured in the Radiative Ignition Time Apparatus in accordance with the procedures described in Reference [1], Appendix B1.

During the second reporting period a new radiative heat flux meter was modified and calibrated for specific use in the Radiative Ignition Time Apparatus.

The total of 94 ignition times was measured on all ten Secondary GIRCFF Fabrics at six different power flux levels between 0.25 and 16 W/cm^2.

For the purpose of efficient updating of ignition time data evaluation a computer code was written which also plots the results in final form.

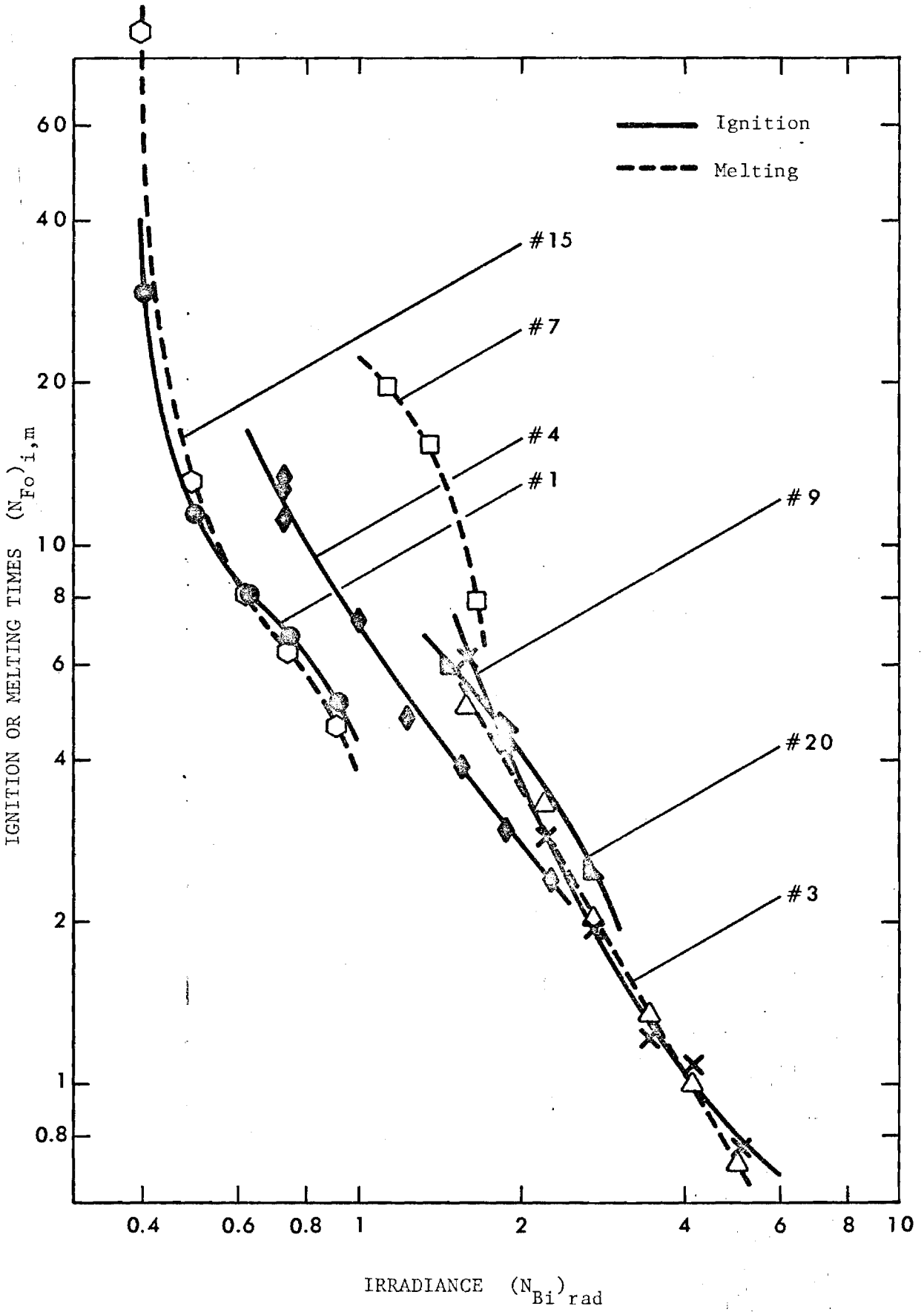

Figure 11. Summary of Ignition and Melting Times for Secondary GIRCFF Fabrics.

The thermostatically and psychrometrically controlled enclosure described in Progress Report No. 4 [6], was delivered, assembled, and tested by representatives of Environair Systems, Inc. The enclosure was turned over the Georgia Tech on June 16, 1972 and preparations are being made to transfer the Ignition Time Apparatus into the enclosure.

3. Results

Figure 11 presents a summary of the ignition and melting times, in non-dimensional forms, for the Secondary GIRCFF Fabrics No. 1, 3, 4, 7, 9, 15 and 20. GIRCFF Fabrics No. 6, 14 and 16 have not yet been evaluated pending the verification of some property data.

Presented in Fig. 11 are the non-dimensional destruction time $(N_{Fo})_{i,m}$ (i for ignition, m for melting) versus the normalized radiant heating intensity $(N_{Bi})_{rad}$, namely

$$(N_{Fo})_{i,m} = \frac{(\frac{k}{\delta})\ t_{i,m}}{c(\rho\delta)}$$

$$(N_{Bi})_{rad} = \frac{(1-\tilde{\rho})\ W_o}{(\frac{k}{\delta})\ (T_{i,m}-T_o)}$$

where

(k/δ)	thermal conductance (W/cm^2c), or ratio of thermal conductivity k over thickness δ
$t_{i,m}$	ignition time (s), or melting time
$(\rho\delta)$	mass per unit of fabric area, (g/cm^2), ρ is fabric density
c	specific heat of fabric, (Ws/g K)
$T_{i,m}$	ignition temperature (self ignition) (K), or melting temperature
T_o	initial fabric temperature, equal to environmental temperature, (K)
$\tilde{\rho}$	radiative fabric reflectance, (-)

C. Effect of Heating Mode on Fabric Ignition Time

1. Objective

The purpose is to provide a well defined convective heat source in the form of a gas flame and to measure fabric ignition time under two conditions: (i) the stationary ignition test, where the fabric is suddenly exposed to a time-invariant convective heat source, and (ii) the transient ignition test, where the fabric is moved into the convective heat source at a predetermined velocity. In the first case one measures the time from initial exposure of the fabric to the heat source, to ignition. In the second case one measures the time from initial start of the motion, from the flame boundary, to ignition, for different rates of motion.

The Convection Ignition Time Apparatus is being designed to meet the following conditions:

(a) Specimen heating by a gaseous fuel-air flame, provided by a variable fuel rate burner.

(b) Specimen exposure to the flame, for the static tests, through a shutter providing full exposure of the sample in five-hundredths of a second or less.

(c) Specimen side of shutter not to exceed 150°F, to avoid preheating of the sample.

(d) Specimen transport for the transient tests at different speeds between 2 in/sec and near zero.

The major components of the Convection Ignition Time Apparatus are the shutter system, the gas burner, the sample transport system, and instrumentation for flame characterization, ignition detection and timing.

2. Achievements During the Second Reporting Period: Convective Ignition Time Apparatus

During the second reporting period the design of the "static" test apparatus was completed. Construction was started and at this reporting time the construction is in the final stages of completion.

The design of the sample transport system for the transient tests has been initiated and is expected to be completed by mid-July.

Two air cylinders were selected and purchased for the supply of compressed air used to activate the shutter system.

A third burner was selected for use with the Convective Ignition Time Apparatus.

3. Development Details and Results: Convective Ignition Time Apparatus

The operating principle and the major components of the Convective Ignition Time Apparatus are described in detail in the fourth Progress Report [6]. New developments are summarized below.

All components are designed to be mounted onto a one inch thick base plate made of aluminum tooling plate which form a table for the apparatus. A six inch diameter opening in the plate exposes the sample to the burner flame either through use of the shutter system in the static test or through employment of the sample transport system in the transient test.

Shutter Design Details

During the second reporting period the concept of spring-operated shutter plates was discarded in favor of shutter activation by two compressed-air operated cylinders. Each of the two shutter plates is an eight inch by eight inch by one-eight inch copper plate. One plate has a 1/4 inch by 1/8 inch by 7 3/8 inch stop for the other shutter plate which is constructed such that it has a 2 1/2 inch by 1/8 inch by 7 3/8 inch portion and overlaps the stop of the first plate to shield the center portion of the flame. The overlap of the plates allows acceleration of the plate before exposure to make possible a short time interval for total exposure of the sample to the flame.

Each shutter is positioned below and adjacent to the base plate and is supported by a shutter support (2) and a shutter support rod (3) (See Fig. 12). The support rod is mounted on an air operated cylinder (Parker-Hannifin Model CC-2A 14C 1.5). Initially the air cylinder

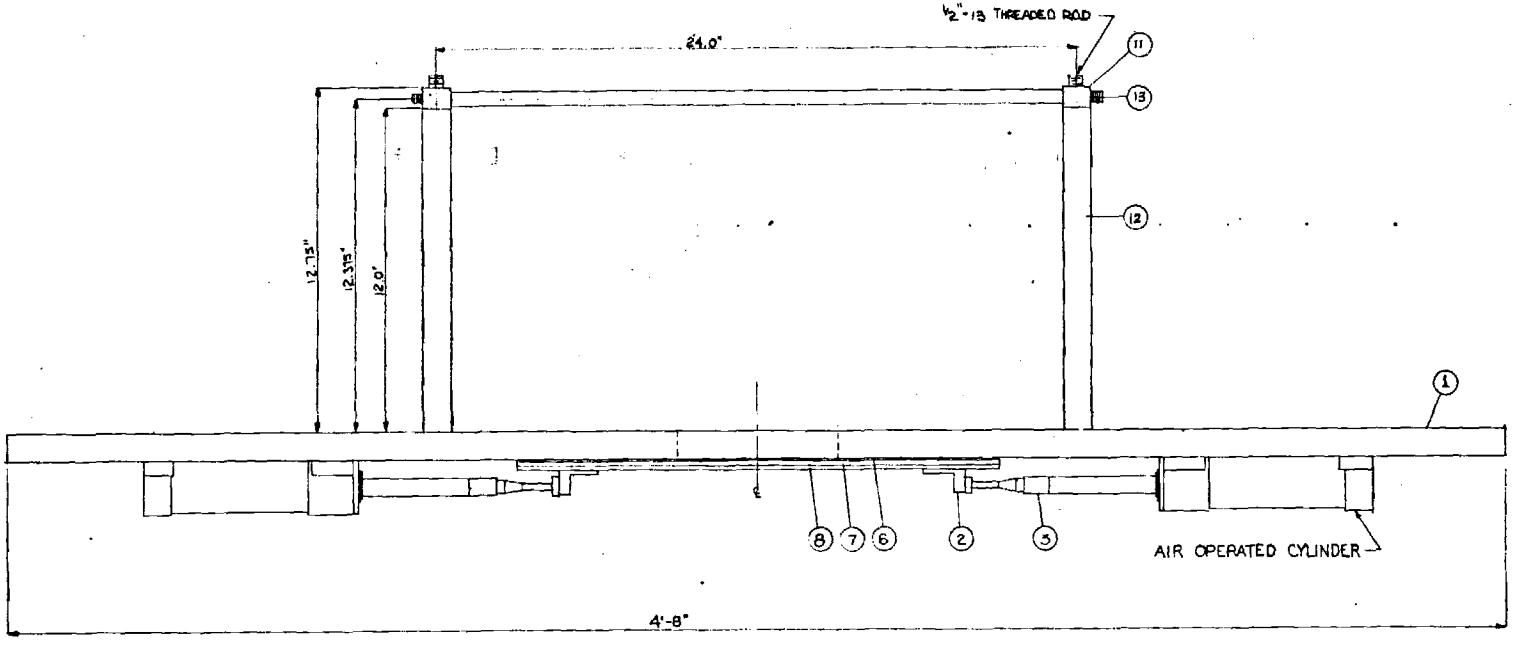

DRAWING NO.		DRAWING NO.	
4	SHUTTER PLATE (1)	1	BASE PLATE
5	SHUTTER PLATE (2)	2	SHUTTER SUPPORT
		3	SUPPORT ROD
		6	TRACK - A
		7	TRACK - B
		8	TRACK - C
		11	END BAR SUPPORT
		12	SUPPORT TUBE
		13	SUPERSTRUCTURE ROD

GEORGIA INSTITUTE OF TECHNOLOGY - MECHANICAL ENGINEERING

SIDE VIEW OF ASSEMBLY	FABRIC FLAMMABILITY
SCALE: 1/4" = 1"	DRAWN BY: ERC

Figure 12. Side View of Convective Ignition Time Apparatus

rod is extended as shown in Figs. 12 and 13. A solenoid value is then actuated to pressurize the cylinder and thus retracts the shutter, which in turn exposes the fabric sample to the flame.

To cool the plates during exposure to the flame a 1/8 inch diameter copper tube will be soldered to the lower side of the plates. Before the burner is ignited, water will be passed through the tubes. Flexible hoses will connect the cooling coils to the water source and the drain.

The shutter plates will be guided by a track consisting of two sets of three pieces of retangular brass bar with thickness of 1/32 inch (6), 1/8 inch (7) and 3/16 inch (8) (See Fig. 12).

Superstructure and Sample Carrier

The superstructure consists of (i) four 1/2 inch diameter by fourteen inch long rods threaded into the base plate, (ii) four, one inch O.D. by twelve inch long brass tubes surrounding the threaded rods (12), (iii) two brass end supports (11), (iv) two, 1/2 inch diameter by twenty-six inch long Thompson 60 Case Hardenedard Ground shafts (13), (v) four No. A-81420 Thompson Ball Bushings, and (vi) a sample carrier.

The sample carrier consists of the sample holder, the supporting vertical adjusting rod and a cradle to support various sample holders.

A first sample holder is designed to expose a one inch diameter fabric sample to the flame for the blast type burner (Fisher Scientific No. 3-910-5). Another sample holder has also been designed to provide a two and one half inch aperture for the Fletcher Burner (New York Laboratory Supply Company No. 19338) which delivers a 4 1/2 inch diameter solid flame. The holders will be made of stainless steel and are designed large enough to prevent the flame from engulfing the entire fabric holder. A 3/8 inch diameter rod will be used to adjust the vertical position of the holder.

The cradle supports the sample holder through the vertical support rod. The vertical height of the rod and sample holder is maintained by the aluminum clamp. The cradle is mounted by four aluminum blocks, which house the Thompson linear ball bushings, allowing horizontal movement of the sample.

Two 28V DC, 0.01 hp, 450 rpm motors are to be used for the "transient" tests to move the cradle with the sample over the flame. The gearing

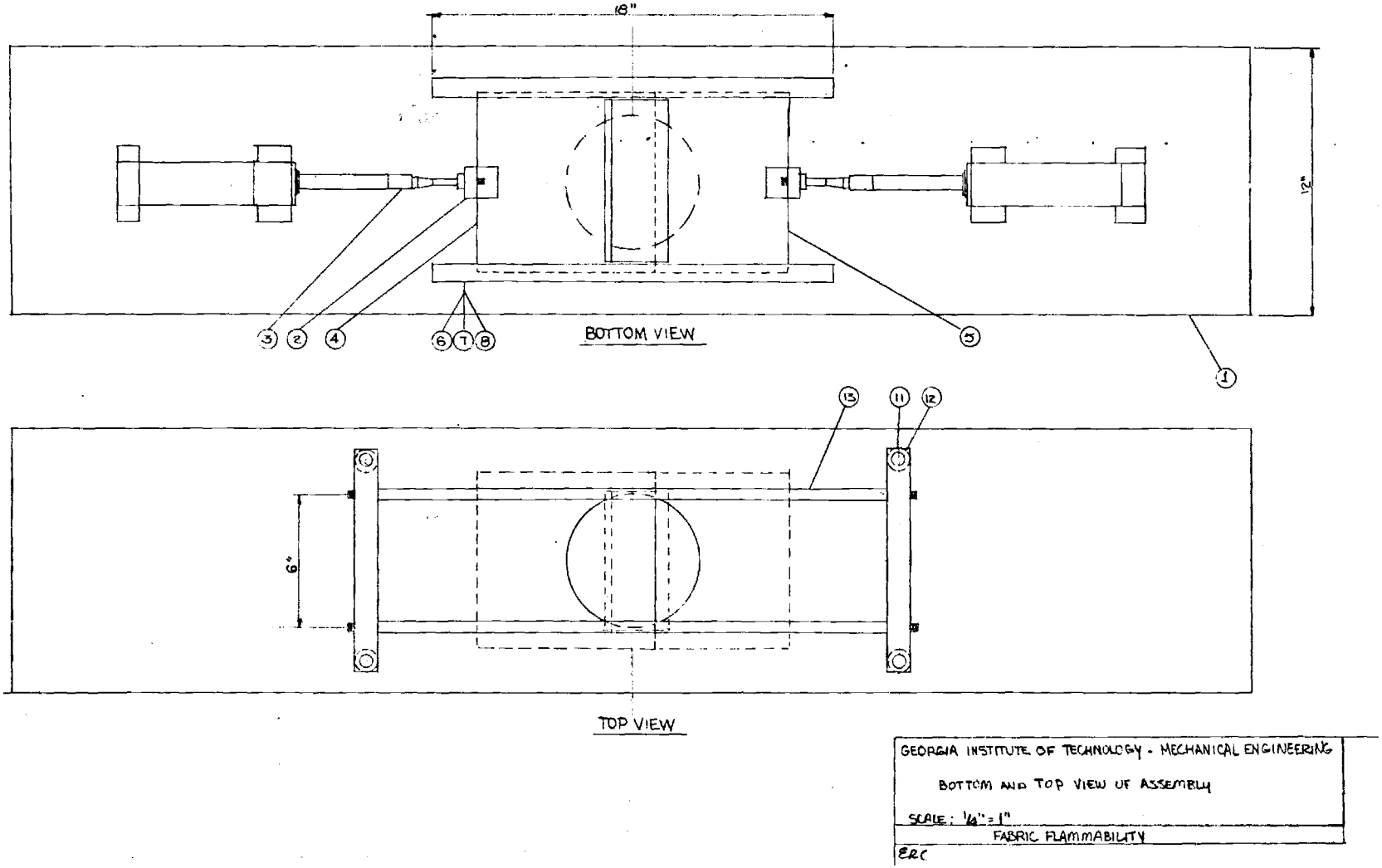

Figure 13. Top and Bottom Views of Convective Ignition Time Apparatus

mechanism is in the design stage and is expected to be completed by mid July.

The Burner

In order to provide adjustment for the flow rates of both the fuel and the air, a third burner was selected with such a capability. This is the blast type burner of Fisher Scientific No. 3-910-5. The ports of the air are totally blocked and all air to the burner is provided from the compressed air supply in the laboratory. The air is first filtered and the moisture is removed by a desicant. It is then metered through a pressure regulator and monitored by a variable-area flow meter.

Preliminary tests of the three burners, (i) Boiling Type, Preiser Scientific No. 10-9215, (ii) Fletcher Burner, New York Laboratory Supply Co. No. 19338, and (iii) Blast Type, Fisher Scientific Co. No. 3-910-5, have shown the desirability to use initially the blast type burner in the modified manner discussed above. During the next reporting period more extensive modifications will be carried out with either or both of the other burners before they are used with the Convective Ignition Time Apparatus.

The blast type Fisher burner provides a usable flame, for the proposed ignition tests, with a minimum methane fuel rate of 10 g/hr and a maximum fuel rate of 200 g/hr. This represents a heat release rate by the fuel from 140 watts to 2800 watts.

Temperature profiles at 3/8 inches above the top surface of the burner, at three fuel rates are shown on Figure 14. One inch is scaled on the graph to show the aperture in the fabric holder through which the material will be exposed to the convective heat source.

The temperature profiles, with a fixed fuel rate, at four heights above the top surface of the burner are shown on Figure 15. Again a one-inch scale is included for reference.

D. Measurement of Ignition Time Statistics

1. Purpose

The purpose of this fourth phase is to determine the extent to which

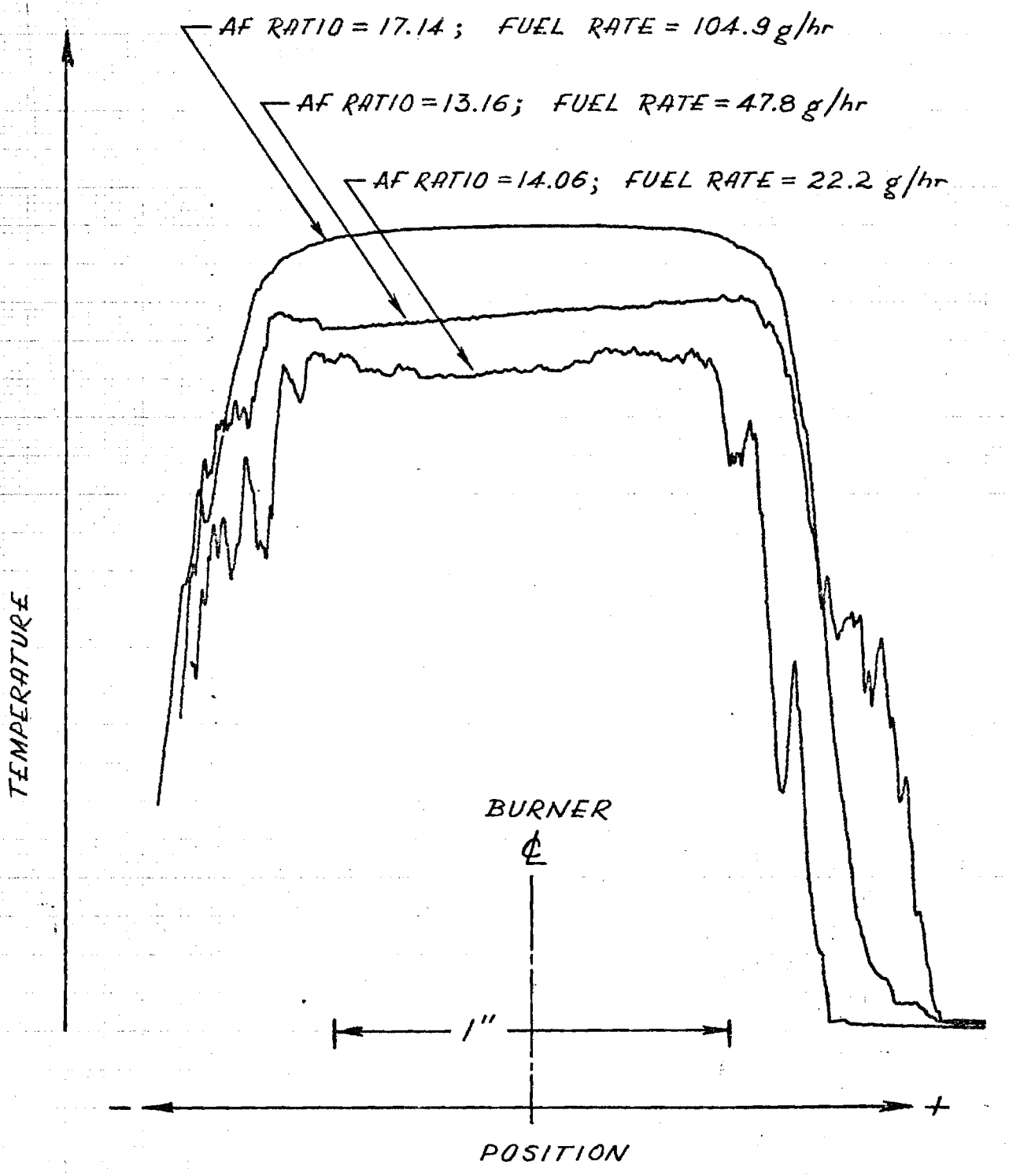

Figure 14. Flame Temperature Profiles, 3/8" above the Burner at Three Fuel Rates.

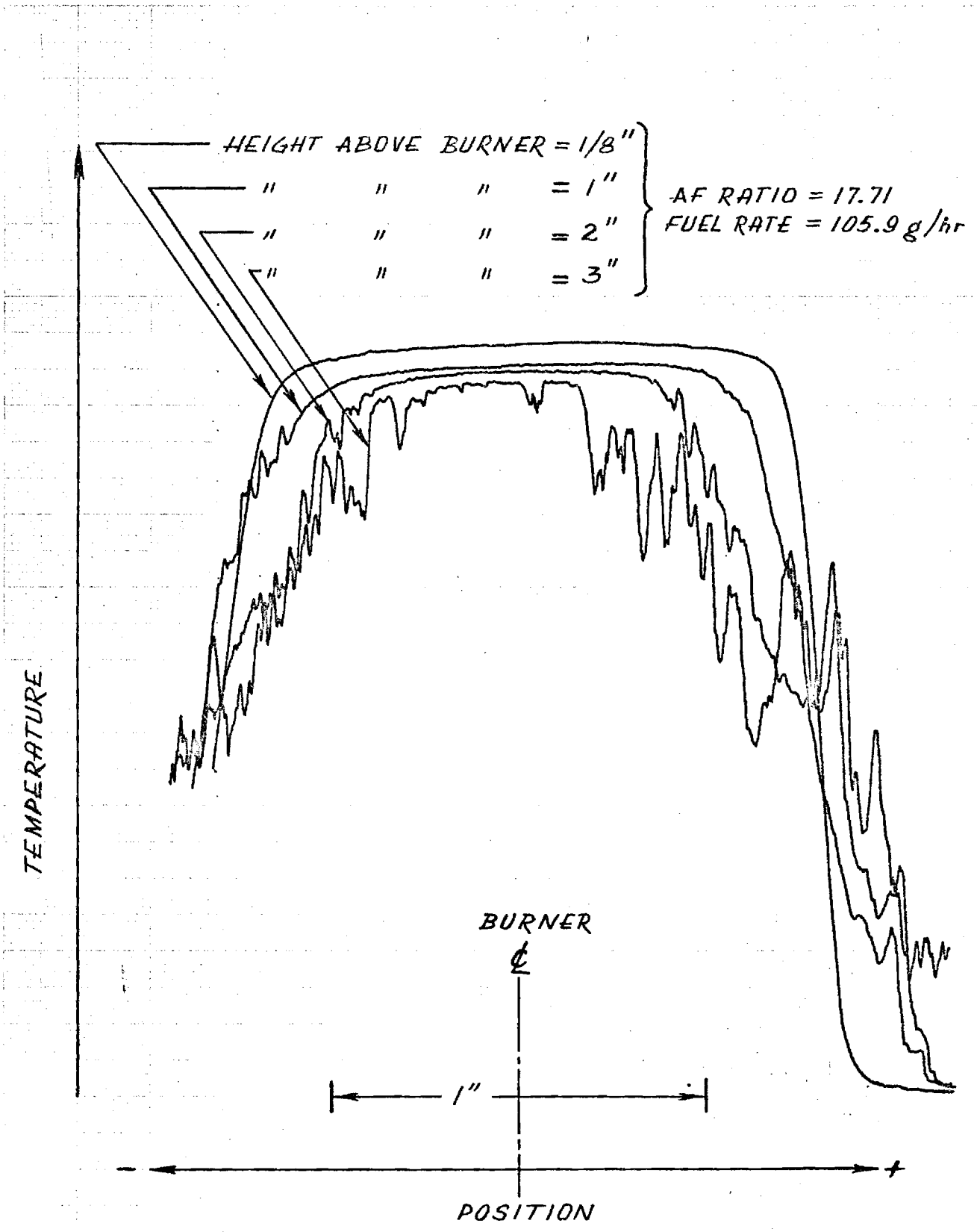

Figure 15. Flame Temperature Profiles with Fixed Fuel Supply Rate at Three Different Heights Above Burner.

the measured ignition time is a unique function of heating intensity for fixed fabric properties and conditions. More specifically, there are to be obtained

the statistical distribution function of fabric ignition time vs. heating intensity

the expected ignition time

the variance of ignition time

for determining a confidence measure associated with ignition experiments on fabrics.

The exposure time, heating intensity and humidity level are carefully controlled as independent variables; the dependent variable is the frequency with which ignition occurs. The frequency thus obtained leads to the probability of ignition under experimental exposure. The real-life fabric ignition probability is then related to the laboratory ignition probability via the stochastic behavior of people, that is the exposure frequency.

The application of the Radiative Ignition Time Apparatus to achieve this objective and the operating procedures are described in the fourth Progress Report [6], Chapter I.D.

2. Achievements During First Reporting Period

(Ignition Time Statistics)

Developments concerning the environmental enclosure controls have been discussed in Section B.2 of this chapter. The wiring of the timing circuit required for activating the shutter release mechanisms of the Radiation Ignition Time Apparatus is being assembled and tested.

III. EFFORTS PLANNED FOR THE SECOND REPORTING PERIOD

Below are listed the advances planned for the third reporting period ending September 30, 1972.

A. Experimental Program

1. Property Measurement Program

Task 1. Ignition Temperature Measurement

The auto and pilot ignition temperature measurements are completed. Supplementary experiments are planned to monitor fabric temperature during the ignition process.

Task 2. Fabric Density Measurements

Complete.

Task 3. Specific Heat Measurements

Verification of two enthalpy measurements will be completed.

Task 4. Thermal Conductance Measurements

Will be continued. By the end of the second reporting period will be measured the thermal conductance at the third contact pressure of 1370 N/m^2, on all ten Secondary GIRCFF Fabrics.

Task 5. Radiative Property Measurements

Reflectance and Transmittance will be measured on fabrics charred at the arithmetic mean temperature between 24°C, the most frequent initial temperature in ignition time measurements, and the ignition or melting temperature. These measurements will be completed on the primary GIRCFF Fabrics early during the third reporting period.

Task 6. Reaction Kinetics Measurements

During the third reporting period the DTA/TGA measurements will be completed and evaluated.

2. Fabric Ignition Time Measurements and Measurements of Moisture Effects on Ignition Time

During the third reporting period the Radiative Ignition Time Apparatus will be installed into the psychrometrically and thermally controlled enclosure and ignition times will be measured on the ten primary GIRCFF Fabrics at 60% and 90% relative humidity at 75°F initial fabric temperature.

3. Effect of Heating Mode on Fabric Ignition Time

During the early part of the third reporting period construction of the Convective Ignition Time Apparatus for the "static" tests will be completed and shake-down tests will be carried out. The design of the apparatus for the "transient" tests will be finalized during the first part of this reporting period and built during the middle part of the reporting period.

Tests for the flame characterization of the blast type burner will be carried out during the early part of the third reporting period as well as needed during the remainder part of the period. One or both of the other two burners will be modified to yield a usable flame to expose the fabric to a 2 1/2 inch constant temperature convective source of ignition.

Tests with fabrics in the static mode will be initiated during the last half of the third reporting period.

4. Measurement of Ignition Time Statistics

During the third reporting period the electronic timing circuit for the dual shutter operation will be completed and the repetitive, dural shutter mode operation will be started during the third month of the third reporting period.

B. Analytical Program

The computer code developed during the last year contract period

will be utilized in conjunction with the measured reaction kinetics papameters to predict ignition time.

BIBLIOGRAPHY

1. Alkidas, A., Hess, R.W., Wulff, W. and Zuber, N., "Study of Hazards from Burning Apparel and the Relation of Hazards to Test Methods", Final Report, NSF Grant No. GK-27189, Georgia Institute of Technology, Atlanta, Ga., December 1971.

2. Mehta, A.K., Franklin, W., Williams, G.C., "Measurement of Flammability and Burn Potential of Fabrics", Summary Report, Fuels Research Laboratory, Massachusetts Institute of Technology, Cambridge, Mass., Project No. DSR 72894, February, 1972.

3. Heskestad, G., Kalelkar, A.S., and Kung, H.C., "A Study of Pre-Ignition Heat Transfer Through A Fabric-Skin System Subjected to a (Radiant) Heat Source", Annual Report, Factory Mutual Research Corporation, Norwood, Mass. FMC Ser. No. 19967, December 1971.

4. Krasny, J.F. and Fisher, A.L. "Study of Hazards from Burning Apparel and the Delation of Hazards to Test Methods; Flammability of Clothing Assemblies"., First Annual Review Report, Gillette Company Research Institute, Rockville, Maryland, January 1972.

5. Fourt, L., "Study of Ignition and Exposure", Final Report, Gillette Company Research Institute, Rockville, Maryland, December 1971.

6. Wulff,W., Zuber, N. et al, "Study of Hazards from Burning Apparel and the Relation of Hazards to Test Methods", Progress Report No. 4, NSF Grant No. GI-31882 (RANN), submitted to GIRCFF, Office of Flammable Fabrics, National Bureau of standards, Washington, D.C. 20234, July 1, 1972.

7. Scwenker, R.F., Beck, L.R., and Zuccarelle, R.K. American Dyesluff Reporter, September 14, 1964, pp. 30-40.

8. Akita, K. and Kase, M., Journal of Polymer Sciences, Part A-1, Vol. 5, 833-848 (1967).

BIBLIOGRAPHY (CONTINUED)

9. Tang, W.K. and Neill, W.K., Journal of Polymer Science, Part C No. 6 pp. 65-81 (1964).

E-25-625

GEORGIA INSTITUTE OF TECHNOLOGY
School of Mechanical Engineering
Atlanta, Georgia

FABRIC IGNITION

Semiannual Progress Report
No. 1

prepared by

R. L. Acree
E. R. Champion
C. Lee
O. A. A. Naveda
P. Durbetaki
G. L. Wedel
P. T. Williams
W. Wulff

For The

National Science Foundation,

RANN Program

NSF Grant No. GI-31882

July 31, 1973

FABRIC IGNITION

Semiannual Progress Report No. 1

By

R. L. Acree

E. R. Champion

P. Durbetaki

C. Lee

O. A. A. Naveda

G. L. Wedel

P. T. Williams

W. Wulff

School of Mechanical Engineering

Georgia Institute of Technology

Atlanta, Georgia 30332

July 31, 1973

Research Sponsored By The

National Science Foundation

Under the RANN Program
(Research Applied to National Needs)

NSF Grant No. GI-31882A#1

P. Durbetaki, Principal Investigator

W. Wulff, Principal Investigator

Stothe P. Kezios, Director
School of Mechanical Engineering

FOREWORD

The research described herein is being funded and supported by the National Science Foundation under the RANN Program (Research Applied to National Needs). The work originated in November of 1970, [1] from the need for fabric flammability standards as formulated by the Government-Industry Research Committee on Fabric Flammability (GIRCFF) in an effort to provide the technical background for satisfying the Flammable Fabrics Act of 1953 as amended in 1967.

The project is being performed in the Fire Hazard and Combustion Research Laboratory of the School of Mechanical Engineering at the Georgia Institute of Technology under the Principal Investigators, Dr. Wolfgang Wulff and Dr. Pandeli Durbetaki. Participating in the research are Research Associate, Dr. Calvin Lee, Ph. D. candidate Edward R. Champion, M. S. candidates Oscar A. A. Naveda, Craig L. Wedel, Paul T. Williams and Robert L. Acree.

The research is being supported in part by the School of Mechanical Engineering under the matching fund provision of the grant. The interest in, and the support of, this research by the National Science Foundation is greatly appreciated.

ABSTRACT

This semiannual report covers the research performed during the time from February 1, 1973 through July 31, 1973. Research performed previously during the period from Nov. 1, 1970 through December 31, 1972 is described in detail in the annual reports [1, 2] submitted to the Government-Industry Research Committee on Fabric Flammability. The results have been published [3, 4] and presented [5, 6] in technical conferences on material flammability characteristics and fire research.

A quantitative measure of a material's potential fire hazard, suitable for the purpose of defining flammability standards, has been established in terms of the probability that such material contribute to a fire-related loss. This probability depends on, among other factors, the probability of ignition after given exposure which in turn is a function of the material's ignition time [2, 5]. Experimental and analytical research has been performed to predict fabric ignition time as functions of fabric properties and heating intensity. Ignition probabilities have been derived from experimental ignition statistics.

The objectives of the current program period are (i) to develop ignition criteria which are applicable to thermally thin and thick materials, (ii) to investigate the dynamic interaction between the heated surface and its boundary layer during the evolution of pyrolysates, (iii) to establish the relationship between laboratory experiments and actual heating conditions, and (iv) to expand previous experiments so as to assess the effects of geometry and materal combinations. The program is subdivided into seven tasks and the accomplishments are:

Task 1: Ignition Temperature Measurement on Pyrolysate Air Mixture. A furnace has been designed and is under construction to decompose combustible materials in the absence of air. A test cell, in which to mix air with the decomposition products and to subsequently monitor the mixture temperature during heating until ignition occurs, is being designed.

Task 2: Measurement of Convective Film Coefficient Under Simulated Pyrolysate Evolution. An air injection test cell has been designed and constructed to accommodate stainless steel wire cloths. The wire cloth is selected to simulate the fabric geometry and serves as part of a thermocouple circuit to measure its thermal response during heating in the existing Radiative Ignition Time Apparatus and Convective Ignition Time Apparatus. Installation of the test cell is under way.

Task 3: Characterization of Actual Ignition Sources. A heat flux and temperature scanning apparatus is being designed to determine the heating conditions of household ignition sources for the purpose of relating their heating conditions to laboratory heating conditions.

Task 4: Ignition Time Measurement on Fabric Assemblies Under Various Geometric Configurations. This task has been rescheduled to commence with the Fall Quarter on September 19. 1973, since it involves the least effort in instrument modification.

Task 5: Measurement of Ignition Time Under Flame Heating on Ten Secondary GIRCFF Fabrics. The total of 232 ignition time measurements was performed during the reporting period on both sets of fabrics originally selected by the Government-Industry Research Committee on Fabric Flammability (GIRCFF), to supplement the data from 139 tests performed previously. Measurements performed so far essentially complete the testing of sixteen out of twenty fabrics. The results, obtained with both stationary and moving fabric specimen, under five different heating intensities, indicate that ignition or melting times under gas flame heating range between 1 and 15 seconds.

Task 6: Ignition Time Statistics. The total of 606 ignition tests have been performed during the reporting period and the ignition probability under given laboratory conditions has been established for two additional fabrics, at three different environmental humidity levels and three different heating intensities.

Task 7: Modeling Analysis for Composite Systems Ignited by Radiant and Convective Heating Sources. Governing field equations have been formulated for porous, semitransparent media and gaseous boundary layers. These equations are being transformed into integral forms. The purpose is to predict ignition time form an ignition criterion imposed on the reacting boundary layer, form material properties and from exposure conditions.

There are currently three faculty members, namely two Principal Investigators and one Research Associate, five Graduate Research Assistants, namely one Ph. D. and four M. S. students and two senior undergraduate students involved in the research program. The anticipated date of completion for this research is March 31, 1974, twelve months after the first Academic Quarter commencement following the renewal of the contract.

TABLE OF CONTENTS

LIST OF FIGURES AND TABLES

Figure

Table

NOMENCLATURE

Symbol

b	Width of impinging flame jet
c, c_p	Specific heat, specific heat at constant pressure
$D/D\tau$	Substantial derivative
$\mathscr{D}$	Mass diffusivity
E	Activation energy
$\underset{\sim}{g}$	Gravitational body force
$\bar{h}_c$	Convective film coefficient
Δh_f^o	Enthalpy of formation
i	Counting index
k	Thermal conductivity
k_o	Frequency factor
n	Reaction order
N_{Fo}	Fourier number, Eq.2.1
p	Gas Pressure
P (I/E)	Ignition probability for given exposure
$\underset{\sim}{q}_{rad}$	Radiative heat flux
q_c^*	Normalized time-averaged heating intensity, Eq.2.2
$\dot{r}$	Volumetric mass generation rate
R	Universal gas constant
T	Temperature
U_m	Maximum axial jet velocity component
$\underset{\sim}{v}$	Gas velocity
V_m	Maximum tangential boundary layer velocity component
x	Mole Fraction

Greek symbols

β	Isobaric thermal expansion coefficient

δ	Fabric thickness, boundary layer thickness
$\zeta = \frac{-1}{\rho}\left(\frac{\partial \rho}{\partial x}\right)_T$	Relative density variation with respect to mole concentration, at constant temperature
Θ	Normalized temperature, Eq. 2.3
λ	Degree of decomposition
μ	Dynamic viscosity
ρ	Density
$\Delta\rho$	Decomposible mass per unit volume
σ	Standard deviation
τ	Time
$<\tau>$	Median time
ψ	Porosity
ω	Mass fraction of pyrolysate

Subscripts

e	exposure
f	fluid, flame
i	ignition
m	melting
s	solid
∞	free stream

superscripted	dot	derivative with respect to time
	bar	average

1. INTRODUCTION

Acceptable flammability standards for materials or final products must rationally relate suitable laboratory and field test results to the potential fire loss that could be related to such materials or products. The necessary relationships require a quantitative measure of hazard and must account for, firstly, the stochastic events which lead from product certification to all conceivable hazardous situations and, secondly, the combination of stochastic human behavior in fire with deterministic material response to fire. Unfortunately, the majority of currently employed flammability tests are applied without conceptual relation between hazard and test results but frequently with indefensible generalization.

The concepts developed in connection with the study of fabric flammability garment fires and burn injury apply in principle to the assessment of fire hazard and the loss from building fires.

The fire hazard of a material is defined and measured in terms of the probability with which such material might contribute to a specified, fire-related loss. Particularly, the burn injury hazard of any material equals the probability with which such material might contribute to a burn injury as specified by the relative area of the burn injury and the depth of tissue destruction. The burn injury probability is computed, via the construction of a decision tree, from partial probabilities associated with the events leading from material production to burn injury. These events fall into two classes, the class of selection events and the class of physicochemical events. Partial probabilities for selection events are computed from the relative frequency with which the material is selected for specific end uses and is likely to encounter accident-prone circumstances. Physicochemical processes, such as material ignition, extinguishment, flame spread and attendant tissue destruction, are transient in nature and the associated probabilities are functions of the ratio of characteristic times, namely the time during which the process is allowed to proceed over the time which the process requires for its completion.

The first physicochemical process in the chain of events is ignition after given exposure to a heat source. The probability P(I/E) of ignition after given exposure under specified conditions is, in the case of normally distributed (Gaussian) ignition frequency

$$P(I/E) = 1/\sqrt{2\pi} \int_{-\infty}^{X} \exp(-Z^2/2)dZ, \qquad (1.1)$$

where X depends on the ratio of exposure time, τ_e over a median ignition time $\langle\tau_i\rangle$

$$X = (\tau_e/\langle\tau_i\rangle - 1)/\sigma \qquad (1.2)$$

and σ represents the standard deviation of ignition time. The exposure time τ_e reflects the stochastic response of the potential burn victim, while the median ignition time depends primarily on material properties, geometry and exposure conditions.

An experimental and analytical program is being carried out to predict fabric ignition time $\langle\tau_i\rangle$ as a function of exposure parameters and material properties.

2. OVERVIEW OF PROGRESS

2.1. Previous Accomplishments

Accomplishments and results of research performed at the Georgia Institute of Technology during the period from November 1970 through December 1972 are detailed in previously published reports [1, 2] and briefly summarized here.

Thermophysical fabric properties which characterize the ignition process have been measured, namely thermal conductance, specific heat, specific mass, ignition or melting temperature, optical properties, reaction kinetic parameters and reaction enthalpy, on cotton nylon, polyester, acetate and wool fabrics and blends.

Ignition or melting times have been measured on the same fabrics under radiative and convective (gas flame) heating. The median ignition time $<\tau_m>$, as well as the standard deviations σ have been evaluated through probit analysis of ignition statistics for an igniting cotton fabric and a melting nylon fabric, respectively, as functions of radiative heating intensity and fabric moisture content. Ignition times have been measured on fabrics while these were either held stationary over the flame or moved through the flame at selected velocities. Ignition probabilities have been evaluated. Figure 1 represents a typical relation between ignition probability, exposure time and heating intensity for cotton fabrics.

An analytical ignition model has been developed on the basis of energy conservation which accounts for thermal energy storage in the fabric, moisture desorption and endothermic phrolysis within the condensed phase, and exothermic reaction in the gaseous phase, that is, in the fabric boundary layer. The analysis resulted in an initial value problem with three coupled, non-linear, first-order, ordinary differential equations. Scaling laws were derived from the differential equations, and the numerical solution was used to elucidate the significance of the above processes on the prediction of ignition time (partial modeling).

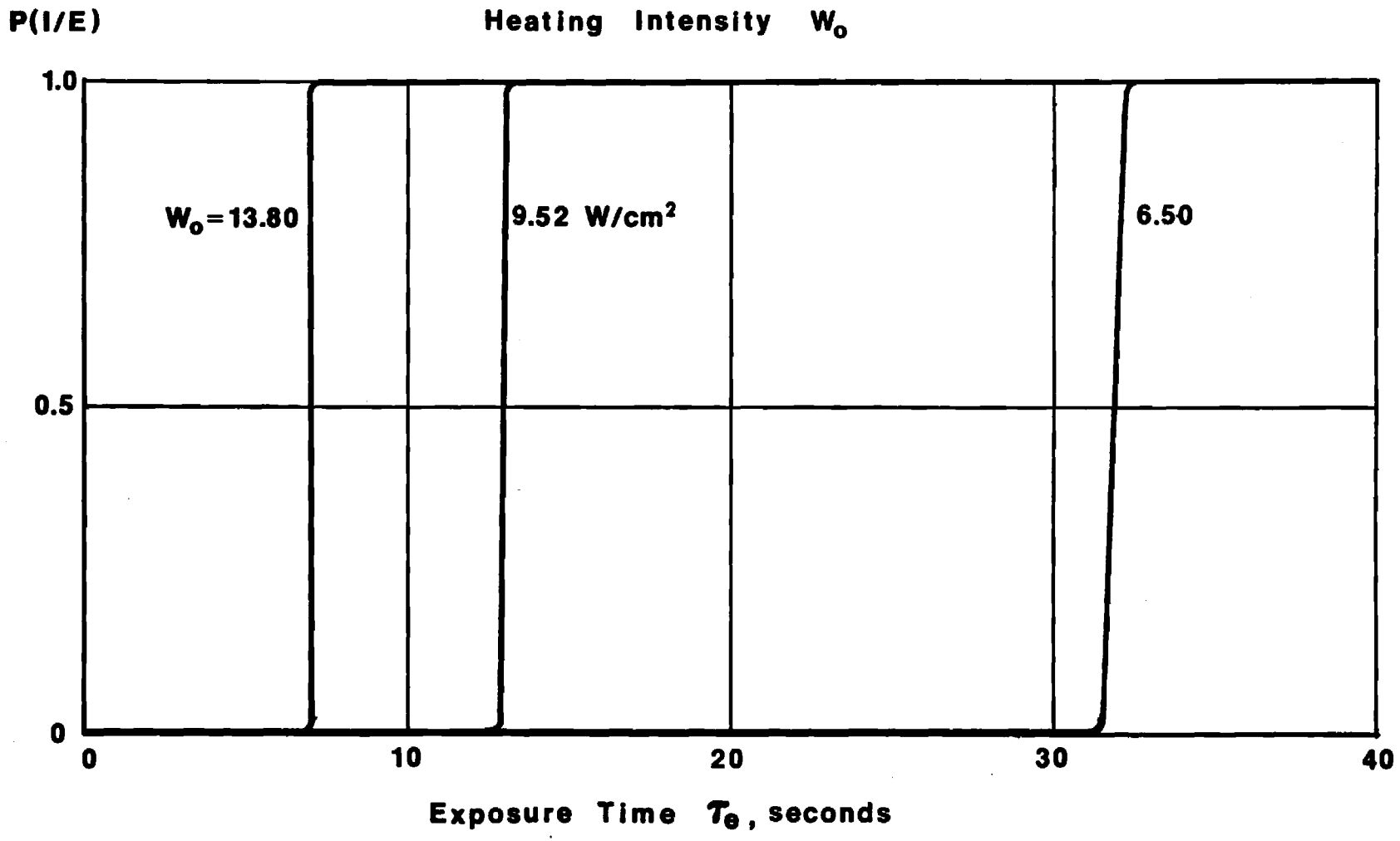

Figure 1. Ignition Probability As Function of Exposure Time And Heating Intensity.

2.2. Progress During Reporting Period

An overview of current progress is listed here for each of the seven tasks to be performed. Additional details are presented in the Appendix.

2.2.1. Task 1. Ignition Temperature Measurements of Pyrolysate-Air Mixtures.

Ignition occurs in the gaseous phase near the heated surface of a thermally degrading material. The ignition process must be described in terms of the reactions taking place in the boundary layer near the heated surface, either in terms of fundamental reaction kinetics or in terms of critical local pyrolysate concentrations and mixture temperatures. The latter approach is taken here.

The fabric is thermally decomposed in an initially evacuated furnace. The decomposition product is mixed with dry air at known concentrations. The mixture is subsequently heated until ignition occurs while passing over an inert platinum resistance thermometer which monitors the gas temperature prior to and during ignition.

The furnace has been designed and is being constructed. An assembly drawing is shown in Figure 2 and a flow schematic in Figure 3. Details are presented in Appendix A.

The platinum resistance thermometer and the ignition test cell are being designed. The resistance recording facility has been ordered and partially delivered; final delivery is expected by August 15, 1973.

2.2.2. Task 2. Measurement of Convective Film Coefficients Under Simulated Pyrolysate Evolution.

Decomposition gases emerging from the heated surface effectively protect this surface from impinging gas flames or from cooling air during radiative heating. The interaction between heated surface and environmental gases is described in terms of a convective film coefficient. The objective of this task is to simulate the fabric geometry with inert stainless steel wire mesh cloths and the action of emerging pyrolysates through injection of preconditioned air, and to determine the thermal response of the fabric from the simulated response of the wire cloth by incorporating the cloth directly into a thermocouple circuit which senses true cloth temperature.

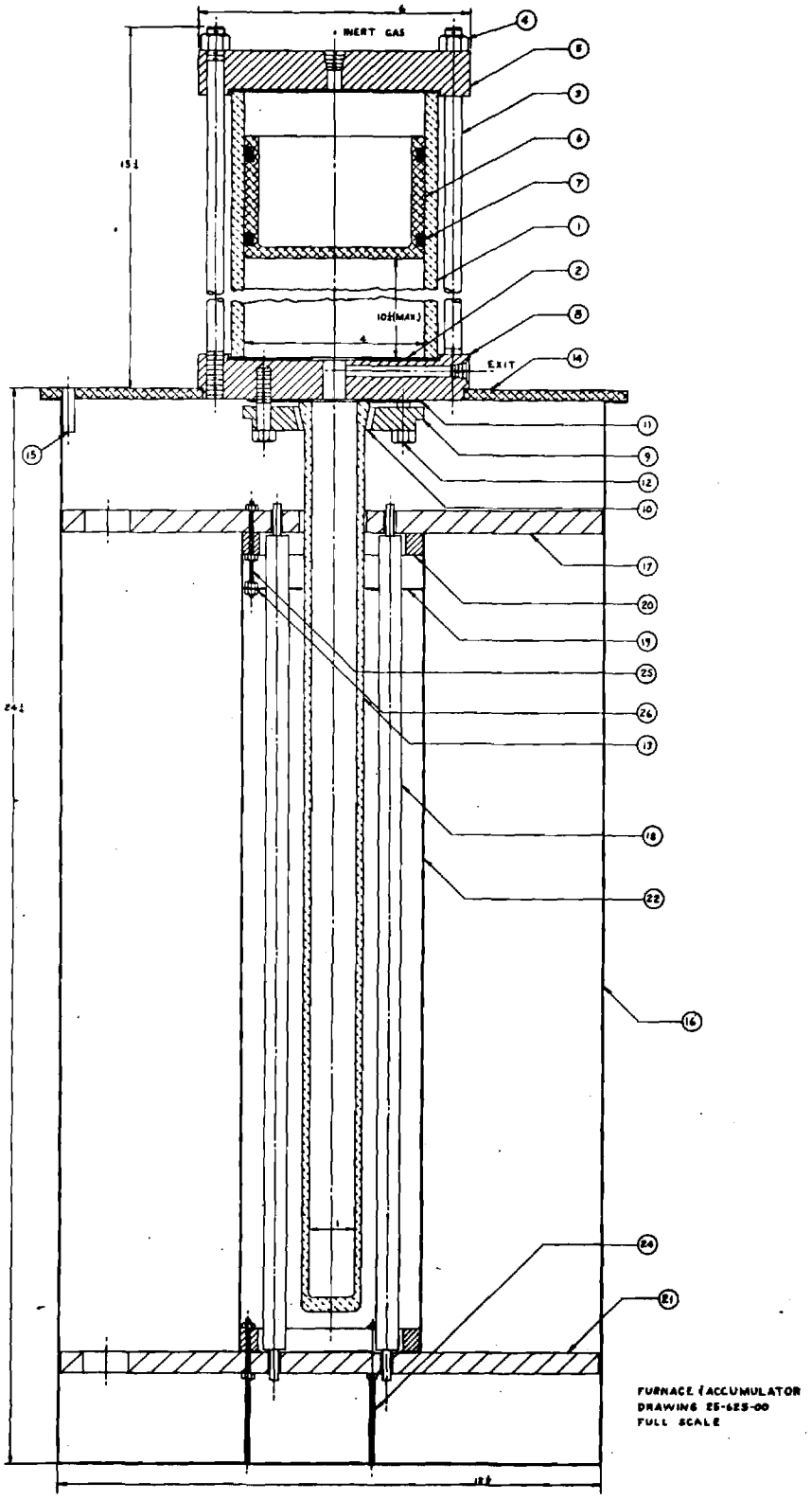

Figure 2. Pyrolysate Generating Furnace

Description of Figure 2

Item	Description
1.	Accumulator Barrel
2.	Accumulator Gasket
3.	Accumulator Tie Rod
4.	Locknut
5.	Accumulator End Cap
6.	Accumulator Piston
7.	"O" Ring
8.	Accumulator Manifold
9.	Flange
10.	Insert
11.	Gasket
12.	Bolt
13.	Furnace Test Tube
14.	Furnace Mounting Plate
15.	Pilot Pin
16.	Furnace Housing
17.	Heating Element Support
18.	Heating Element
19.	Furnace Reflector
20.	Furnace Reflector Support Ring
21.	Heating Element Support
22.	Tubular Reflector
23.	Furnace Reflector (not marked)
24.	Threaded Rod
25.	Threaded Rod
26.	Hex Nut

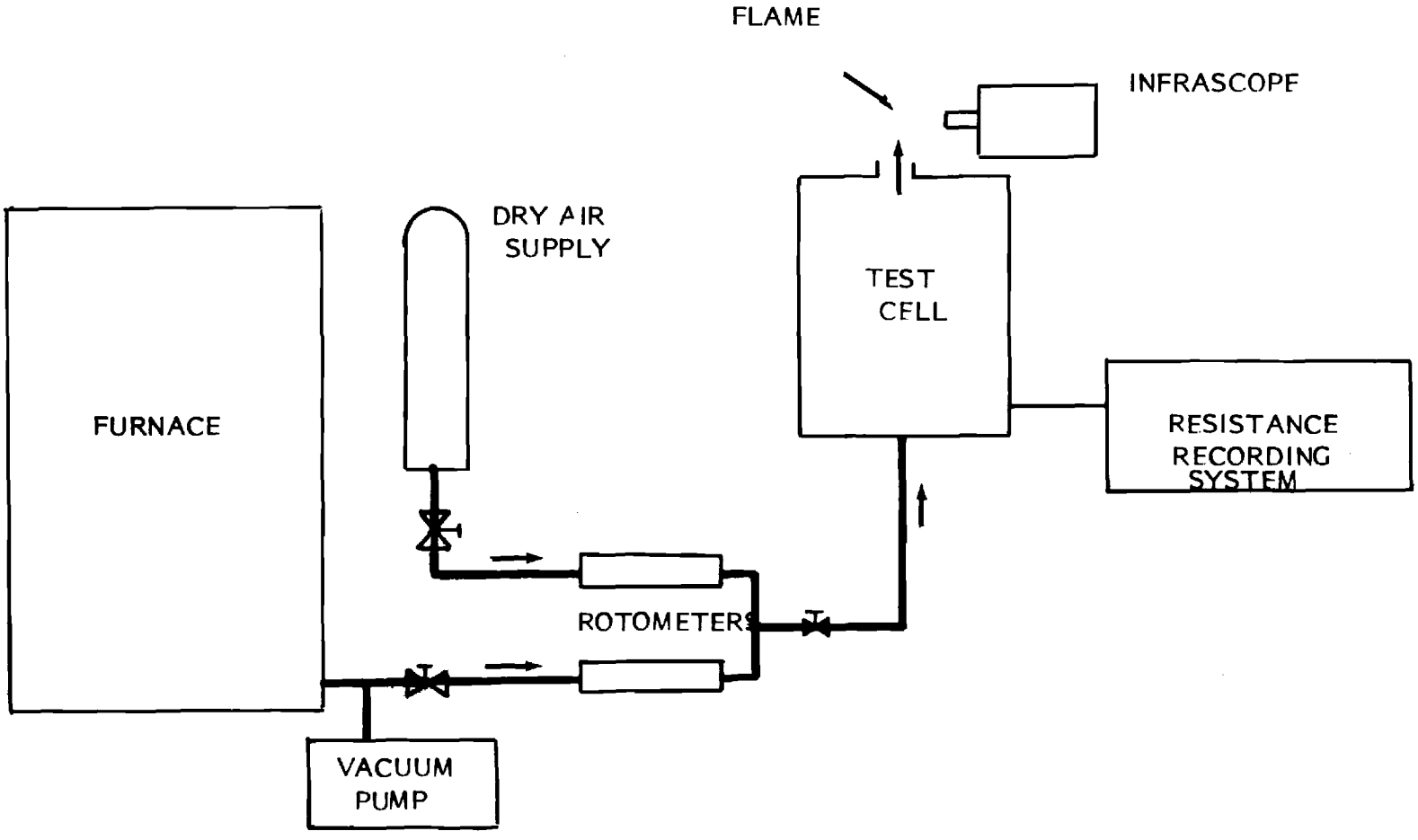

Fig. 3 - FLOW CHART: IGNITION TEMPERATURE MEASUREMENTS OF PYROLYSATE AIR MIXTURE.

An air injection test cell for measuring the convective film coefficient was designed constructed and is being assembled. The cross-sectional view of the stainless steel screen support assembly is shown in Figure 4. Based on an Arrhenius-type decomposition law, the maximum outflow gas velocity was computed to be approximately 3.8 cm/s for pure cotton. From this injection velocity was determined the needed gas flow rate and the necessary instrumentation was selected. Details are presented in Appendix B.

2.2.3. Task 3. Charactenization of Actual Ignition Sources.

The ignition probability P (E/I) defined by Eqs. 1.1 and 1.2 and depicted for cotton fabrics in Figure 1 depends on the exposure time τ_e and on exposure conditions, namely the heating intensity W_o and the environmental humidity level rh, which are all controlled variables in the laboratory experiment. In order to determine the fabric ignition probability for actual exposure conditions and actual human respenses, one must establish, firstly, the probability with which a certain exposure condition is actually encountered, that is the fraction of time during which a specified garment is exposed to a given heating intensity and, secondly the probability or relative frequency with which a given exposure duration is encountered.

The purpose of Task 3 is to determine the probability of encountering heating intensities of a given level. The probability will be based on time fractions of exposure and is intended to be specified separately for different age groups, activities and locations such as private residences, commercial kitchens and factories.

A portable scanning device is being designed which accommodates total heat flux and temperature sensors and which will serve to map flux and temperature distributions in the immediate vicinity of ignition sources. Signal and position will be recorded simultaneously on an x-y plotter. The time of exposure as function of position will be derived from the time studies.

2.2.4. Task 4. Time Ignition Measurements on Fabric Assemblies Under Various Geometric Configurations.

Commencement of work on this task is scheduled for the latter part of September 1973.

2.2.5. Task 5. Measurement of Ignition Time Under Flame Heating on Ten Secondary GIRCFF Fabrics.

This task is a continuation of previously initiated research. The descriptions of the Convective Ignition Time Apparatus CITA, the operating procedures and previously obtained results are presented in Reference (2).

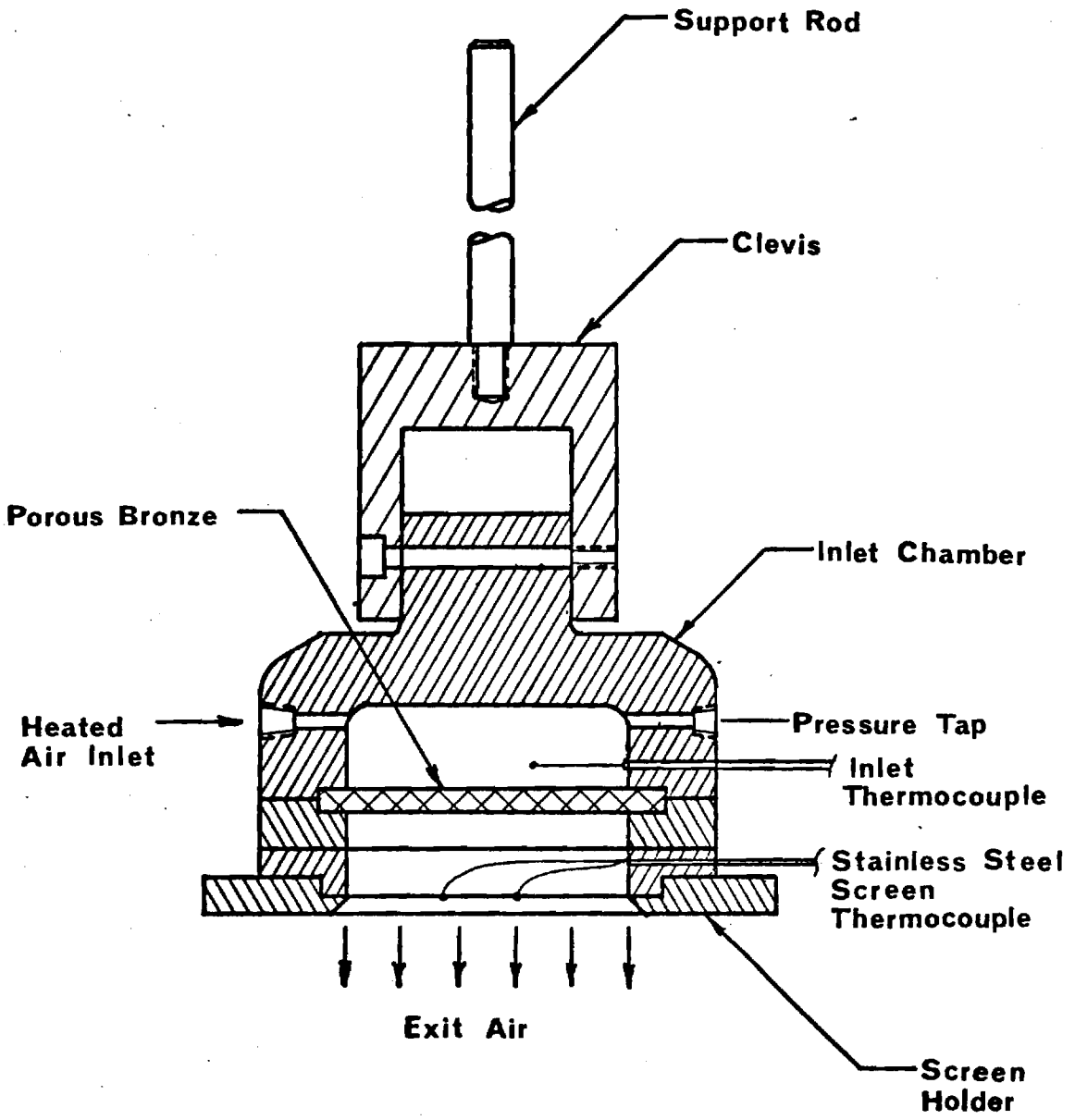

Figure 4. Pyrolysate Injection Simulator

The purpose is to measure fabric destruction time, i.e. ignition or melting time, under gas flame heating and two conditions: (i) the stationary ignition test, where the fabric is suddenly exposed to a time-invarient convective heat source, and (ii) the dynamic ignition test, where the fabric is moved into the convective heat source at a predetermined velocity. In the first case one measures the time between the initial exposure to the heat source, and ignition or melting. In the second case one measures the time from initial contact between fabric and flame at the flame boundary, to ignition or melting, for different rates of fabric motion through the flame.

The schedule calls for completion of the dynamic ignition tests on the ten Primary GIRCFF Fabrics and determination of fabric destruction times on the ten Secondary GIRCFF Fabrics, under both the stationary and dynamic operating modes.

The total of 193 fabric destruction time tests were run in the dynamic ignition test mode on the ten Primary GIRCFF Fabrics by supporting the fabric in the 63.5 mm aperture holder and moving the fabric in the horizontal plane, 1.9 cm above the top of the burner, with velocities between 2 and 25 cm/s. The fabric destruction times obtained ranged from 0.07 seconds to more than 31 seconds.

Fabric destruction time measurements on the ten Secondary GIRCFF Fabrics have been started and the total of 39 tests was carried out. The fabrics were exposed to five different convective heating intensities at the stoichiometric equivalence ratio, of $\phi = 0.86$, and with fabric holder aperture of 63.5 mm. Fabric destruction times were measured successfully for six of the ten Secondary GIRCFF Fabrics. These times range from 1.9 to 11.3 seconds.

The convective fabric destruction time data from the dynamic tests are presented in Figures 5 and 6 for melting and igniting fabrics, respectively.

The normalized destruction time (Fourier number)

$$(N_{Fo})_{i,m} = \left\{ (k/\delta) \;/\; c(\rho\delta) \right\}_{i,m} \tau_{i,m} \qquad (2.1)$$

is plotted versus the sample velocity. The data for zero-velocity are taken from the static tests. The melting times in Figure 5 approach infinity for vanishing sample velocity and the melting time from stationary tests for increasing sample velocity, as would be expected from the consideration of the accumulated heating due to time dependend heat flux impingement during flame traversing. The ignition time data in Figure 6 reveal that ignition may occur after flame traversing and that there is a maximum traversing velocity between 9 and 12 cm/s. for the given burner-aperture combination beyond which ignition does not occur. The maximum traversing velocities are listed in Table 1. The tendency toward large ignition temperatures with vanishing sample velocity could not be observed because of the limitation in the control of low traversing velocities.

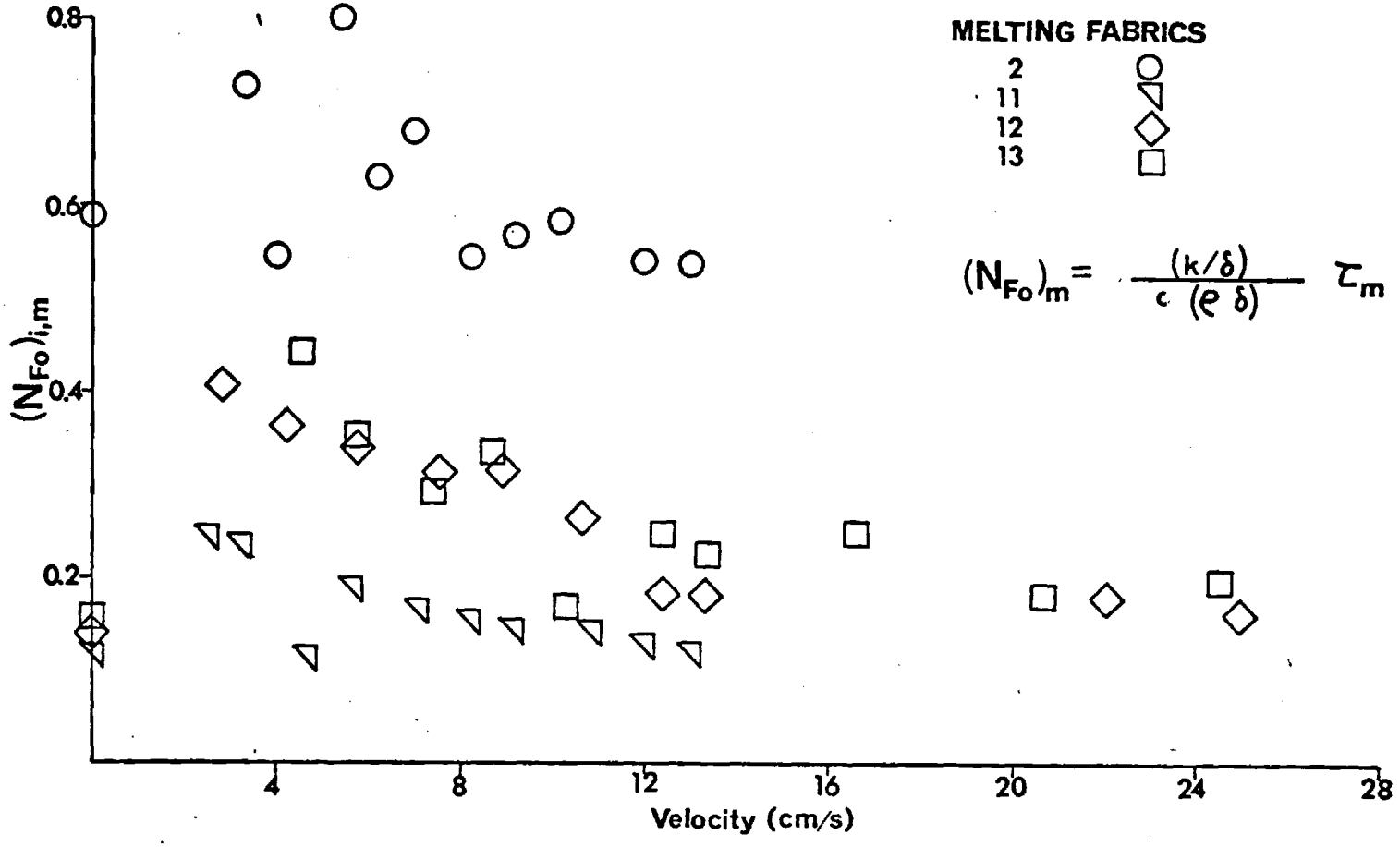

Figure 5. Nondimensional Melting Time versus Sample Velocity; Gas Flame Ignition

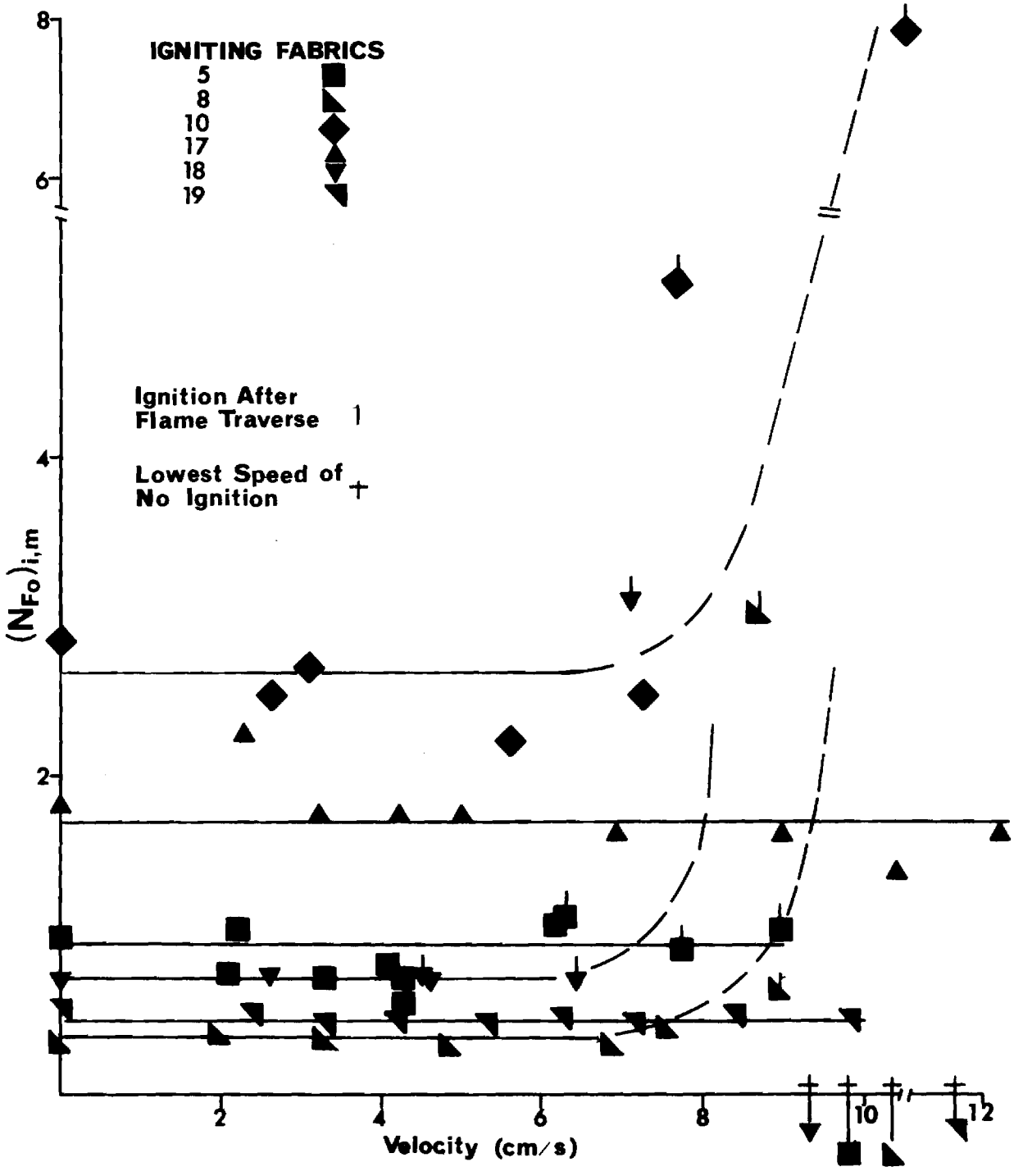

Figure 6. Nondimensional Ignition Time versus Sample Velocity; Flame Ignition

TABLE 1. Maximum Traversing Velocity For Flame Ignition

Vertical Burner, Diameter of 37 mm
Horizontal Fabric Specimen, Diameter of 63.5 mm
Fabric Motion Horizontal, Perpendicular to Flame Axis

GIRCFF Fabric Number	Maximum Velocity cm/s
5	9.88
8	10.6
10	20.6
17	15.9
18	9.42
19	11.67

The convective ignition time data for six of the ten Secondary GIRCFF Fabrics are presented in Figure 7. The nondimensional destruction time $(N_{Fo})_{i,m}$ as defined by Eq. 2.1 is plotted versus the time average, nondimensional heating intensity

$$q_c^* = \left[2 \bar{h}_c / (k/\delta) \right] (\Theta_f - \bar{\Theta}) \qquad (2.2)$$

where Θ stands for normalized temperature

$$\Theta = (T-T_\infty) / (T_{i,m} - T_\infty) , \qquad (2.3)$$

subscript f represents flame temperature and the superscripted bar designates time - averaged fabric temperature as computed from the inert heating analysis presented in Reference [2] .

2.2.6. Task 6. Ignition Time Statistics

Ignition frequencies are measured under controlled exposure times, radiative heating intensities and environmental relative humidity levels for the purpose of evaluting the mean ignition time $\langle \tau_I \rangle$ and the standard deviation σ in Eq. 1.2, by probit analysis. This task is also a continuation of previously performed experiments [2]. The first evaluation of the results from 606 ignition tests is presented in Table 2 below.

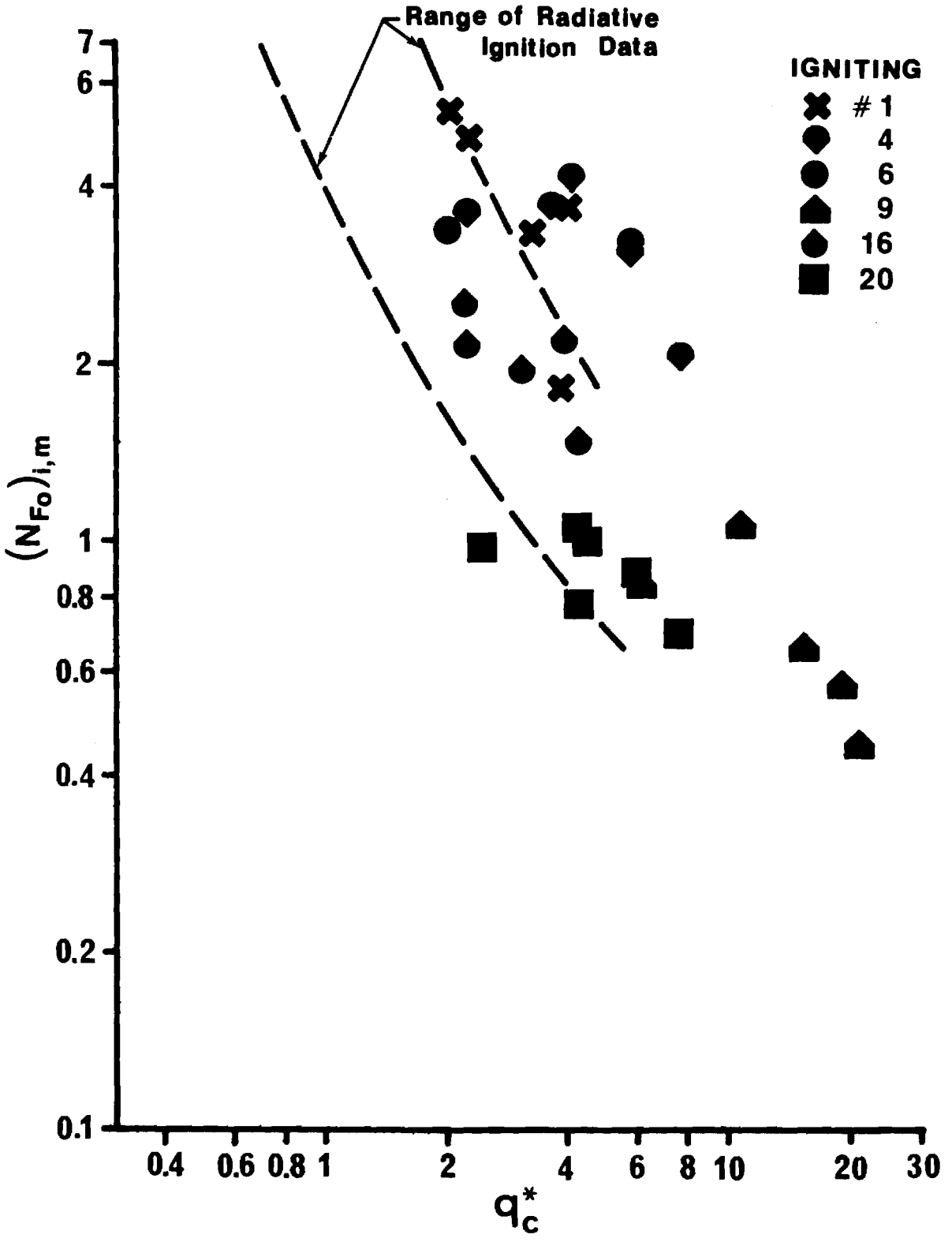

Figure 7. Normalized Destruction Time versus Normalized Convective Heating Intensity

TABLE 2. Ignition Time Statistics of Nylon Tricot

GIRCEFF Fabric No.	Irradiation W_o	Relative Humidity	Number of Tests	Median Ignition Time	Standard Deviation of Ignition Time	
					Mean	Time
				$<\tau_i>$	$\sigma_{<\tau_i>}$	σ
	W/cm^2	%		s	s	s
12	6.50	30	86	12.61	.324	2.246
12	9.52	30	42	6.15	.151	.697
12	13.80	30	57	3.10	.028	.132
12	6.50	90	66	11.63	.191	1.113
12	9.52	90	59	5.87	.062	.348
12	13.80	90	67	3.02	.197	1.235

2.2.7. Task 7. Modeling Analysis

The objective of the analysis is to predict ignition time for thermally decomposing composites, based on an ignition criterion to be imposed on the gaseous reaction in the boundary layer at the heated surface, and on fundamental material properties and process parameters. The prediction of ignition time is based on an integral analysis, describing temperature, degree of decomposition and pyrolysate velocity within the decomposing composite, and temperature and concentration in the reaction boundary layer.

The problem has been formulated for free convection along radiatively heated surfaces and for forced convection from gas flames which impinge normally to the heated surface. The formulation is based on local conservation equations which will be integrated over space to render ordinary differential equations in time which contain suitably space-averaged dependent variables.

Two conservation equations and three constitutive equations govern the fields of temperature, decomposition degree and pyrolysate flow within each decomposing solid. They are the equations of mass and energy conservation, the thermal and caloric equations of state for the pyrolysate and a decomposition rate law. The pressure is taken to be constant and the equations of motion are not necessary.

The gas phase is being considered as a binary mixture and is governed by two equations of mass conservation, the equations of motion and of energy conservation, and by the caloric and thermal equatious of state.

These equations have been developed for one dimensional transient heat transfer in the solid composites and two-dimensional flow in the mixing boundary layer. Further details are presented in Appendix D.

This completes the overview of the progress made during the reporting period.

3. SUMMARY OF ACCOMPLISHMENTS

Below are listed briefly the accomplishments achieved during the six months reporting period. Previously obtained results are found Reference [2].

3.1 Experimental Efforts

The development of new test facilities for new experiments, namely Task 1 through 3 as discussed in Chapter 2, is partly in the design and construction stages, partly in the final assemby stage. Scheduled experimentation with existing and slightly modified instrumentation has progressed as planned, the total of 836 ignition tests has been performed under radiative and convective heating (tasks 5 and 6). The start of Task 4 has been delayed until September as a result of an effort to schedule an M. S. program form Task 4.

3.2. Analytical Effort

The governing equations have been developed to describe the response to heating of themally decomposing composites. The problems were formulated for free convection cooling of radiatively heated surfaces and for forced convection from gas flames. The governing equations are being transformed into integral form with time as the only independent variable.

4. CHANGES IN RESEARCH PLAN, PERSONNEL AND MANAGEMENT

There are no essential changes in the research plan; the initially proposed tasks are being performed or planned to be performed without conceptual changes. Task 6 on ignition time statistics had not been proposed initially and has been earned on primarily to supplement efforts of previous programs, during the time between the termination and renewal of the previous grant.

The previous termination and official renewal date of this Grant GI-31882A#1 is November 1, 1972. The expiration date of the grant is June 30, 1974. Since notification of the grant renewal was received on January 24, 1973, Tasks 1, 2, 3, and 7 were started late, at the beginning of the Spring Quarter, on April 2, 1973. Completion of the program is expected by March 31, 1974. These schedule changes did not interfere with achieving the overall objectives within the current grant period.

Dr. Clavin Lee, who studied under Professor Sibulkin at Brown University in Providence, Rhode Island, joined the research team as Research Associate on July 1, 1973 and works full-time on Tasks 1 and 7. There are no other personnel changes on this program.

There have been no management changes incurred on this program.

5. FUTURE PLANS

Research plans follow in general the originally proposed schedule and are briefly summarized below.

Task 1: Ignition Temperature Measurements on Pyrolysate - Air Mixtures should commence early in September after completion of the test cell construction and final delivery of the resistance recording facility.

Task 2: Measurement of Convective Film Coefficient Under Simulated Pyrolysate Evolution should begin in August and should be completed by the end of September.

Task 3: Characterization of Actual Ignition Sources. Standard household kitchen gas and electric ranges are expected to be surveyed by the end of September. Additional ignition sources will be served by the end of December.

Task 4: Ignition Time Measurement on Fabric Assemblies Under Various Geometric Configurations is expected to commence late in September and to be completed in February.

Task 5: Measurement of Ignition Time Under Flame Heating on Ten Secondary GIRCFF Fabrics will be completed by the end of September.

Task 6: Measurement of Ignition Time Statistics will be completed by the end of August.

Task 7: Modeling Analysis for Composite Systems Ignited by Radiant and Convective Heating Sources will continue through February 1974.

The annual report will be prepared during the month of March 1974. The submission of a new proposal for the expansion of ignition studies is anticipated for November 1973.

6. UTILIZATION EFFORTS

Personnel. There are currently two Principal Investigators, one Research Associate, one Ph. D. Student and four M.S. Students contributing to the research. In addition, there are two students employed on an hourly salary basis during the current Summer Quarter.

Principal Investigator Dr. P. Durbetaki is in charge of Task 5 and supervises jointly with Dr. W. Wulff the execution of Task 2. Principal Investigator Dr. W. Wulff supervises Task 1,3,6, and 7. Task 4 will commence in September and will be organized as an M.S. thesis project in cooperation with a suitable thesis candidate.

Research Associate Dr. Calvin Lee, Ph. D. Student Edward R. Champion and Dr. Wulff are working on the Modeling Analysis, Task 7. Task 7 is anticipated to produce a Ph. D. thesis.

Tasks 1,2 and 3 are M.S. thesis projects and carried out respectively, by Mr. Paul T. Williams, Mr. Gregory L. Wedel and Mr. Oscar A. A. Naveda. Mr. Robert L. Acree is currently working on Tasks 5 and 6 and is expected to select and formulate his M.S. thesis program by the end of September.

Part-time secretary Mrs. Nan B. Hudson contributes approximately one fifth of full time toward this research.

Funding. Research activities to be preformed under this grant are projected at this time to be funded until March 31, 1974. The proposed objectives of this grant are expected to be completed at that date.

7. PUBLICATIONS AND PRESENTATIONS

The following publications, presentations and summary reports have resulted from Grant GK-27189 and its follow-up, Grant GI-31882:

1. W. Wulff, N. Zuber, et al., "Ignition of Fabrics Under Radiative Heating". Combustion Science and Technology, Vol. 6, pp.321-334. (1973)

2. W. Wulff, A. Alkidas, R. W. Hess and N. Zuber, "Fabric Ignition", to be published in Textile Research Journal (1973).

3. W. Wulff and P. Durbetaki, "Study of Hazards from Burning Apparel and the Relation of Hazards to Test Methods", Proceedings of the Flammability Characteristics of Materials, Polymer Conference Series, University of Utah, Salt Lake City, Utah, June 11-15, 1973.

4. W. Wulff and P. Durbetaki, "Fabric Ignition and the Burn Injury Hazard" to be presented and published in the proceedings of the 1973 International Seminar: Heat Transfer from Flames, Trogir, Yugoslavia, August 27-31, 1973

5. W. Wulff, N. Zuber, et al, "Study of Hazards from Burning Apparel and the Relation of Hazards to Test Methods", Final Report, School of Mechanical Engineering, Georgia Institute of Technology, Atlanta, Georgia 30332, NSF Grant No. GK-27189, submitted to the Office of Flammable Fabrics, NBS, Washington, D. C. 20234 (1971).

6. P. Durbetaki, W. Wulff, et al., "Study of Hazards from Burning Apparel and the Relation of Hazards to Test Methods", Second Final Report, School of Mechanical Engineering, Georgia Institute of Technology, Atlanta Georgia, 30332, NSF (RANN Program) Grant No. GI-31882, submitted to the Government-Industry Research Committee on Fabric Flammability Office of Flammable Fabrics, NBS, Washington, D. C. 20234 (1972).

8. BIBLIOGRAPHY

1. W. Wulff, N. Zuber, et al, "Study of Hazards from Burning Apparel and the Relation of Hazards to Test Methods", Final Report, School of Mechanical Engineering, Georgia Institute of Technology, Atlanta, Georgia 30332, NSF Grant No. GK-27189, submitted to the Office of Flammable Fabrics, NBS, Washington, D. C. 20234 (1971).

2. P. Durbetaki, W. Wulff, et al., "Study of Hazards from Burning Apparel and the Relation of Hazards to Test Methods", Second Final Report, School of Mechanical Engineering, Georgia Institute of Technology, Atlanta, Georgia, 30332, NSF (RANN Program) Grant No. GI-31882, submitted to the Government-Industry Research Committee on Fabric Flammability Office of Flammable Fabrics, NBS, Washington, D. C. 20234 (1972).

3. W. Wulff, N. Zuber, et al., "Ignition of Fabrics Under Radiative Heating". Combustion Science and Technology, Vol. 6, pp. 321-334. (1973).

4. W. Wulff, A. Alkidas, R. W. Hess and N. Zuber, "Fabric Ignition", to be published in Textile Research Journal (1973).

5. W. Wulff and P. Durbetaki, "Study of Hazards from Burning Apparel and the Relation of Hazards to Test Methods", Proceedings of the Flammability Characteristics of Materials, Polymer Conference Series, University of Utah, Salt Lake City, Utah, June 11-15, 1973.

6. W. Wulff and P. Durbetaki, "Fabric Ignition and the Burn Injury Hazard" to be presented and published in the proceedings of the 1973 International Seminar: Heat Transfer from Flames, Trogir, Yugoslavia, August 27-31, 1973.

Appendix A

Ignition Temperature of Pyrolysate - Air Mixtures

The objectives of this program phase, the planned approach and principle experimental techniques have been presented in Chapter 2, Section 2.2.1. Pyrolysates are mixed with air and heated until flaming ignition occurs while the mixture temperature is being monitored by resistance thermometry. The apparatus currently designed for this purpose consist of these five parts:

(i) The furnace with accumulator, to decompose thermally degradable materials and to store the decomposition gases,

(ii) the dry air supply with metering and monitoring instruments, to supply oxygen,

(iii) the reaction cell, in which the combushible mixture is heated and its temperature is monitored

(iv) the infrared detector, to sense the occurrence of a flame, and

(v) the resistance recording facility to monitor the mixture temperature.

The functions of these components are described below. The reader is referred tc Figures 2 and 3 in Chapter 2, Section 2.2.1.

A. 1. Experimental Procedure

The fabric sample will be placed in the fused quartz test tube inside the furnace, which will then, along with the rotometers, be repeatedly evacuated and flushed with nitrogen gas. After final evacuation will be sealed off, the fabric sample will be heated to decompose and pyrolysates will collect in the accumulator, located just above the test tube. After the completion of fabric decomposition the pyrolysate will be pushed out of the accumulator at a controlled rate, measured by a rotometer, into the reaction chamber where it will be mixed with dry air, entering at a measured mass flow-rate. At all times will the pyrolysate and pyrolysate-air mixture be kept at a temperature above 200°F to prevent condensation of vapor. As the gas mixture passes through the reaction cell it will be heated at a controlled rate and its temperature rise measured by a resistance thermometer positioned in the gas mixture stream. When the ignition temperature of the pyrolysate-air mixture has been reached, it is expected that ignition will be initated

at the sensor, and a rapid rise in temperature will be recognized at the recording system, while the infrascope responds to the luminous gas flame.

A. 2. Furnace Details

The heat source in the furnace will be 12 tungsten heaters manufactured by General Electric Co. and positioned equally spaced around the test tube. The test tube will be made of "Vitreosil" fuzed quartz and will be 20 1/2 inches long with a 1 inch I. D. The accumulator, located just above the test tube, has a maximum capacity of approximately 2.1 liters and is sealed by a nitrogen gas pressurized piston which controlls the pressure in the accumulator.

A. 3. Resistance Recording System

The system for the measurement and recording of the electrical resistance of the temperature sensor will consist of five components:

(i) DCV/DCA/OHM meter which provides eight ranges of ohms from 1 ohm full scale to 10 mega ohms full scale,

(ii) 5 Digit display unit,

(iii) B C D Module which provides nonisolated B C D output for operation with printers and other devices,

(iv) Digital to Analog Converter accepts the 4 line B C D module, and sends out a signal to the recorder,

(v) Strip Chart Recorder is a 7100BM Hewlett-Packard plug-in recorder with a two channel recording capability.

Appendix B

The Convective Film Coefficient Assembly

The convective film coefficient assembly has been designed to be used with the Convective Ignition Time Apparatus (CITA) to evaluate film coefficients on various mesh size inert metal screens in the presence of pre-heat gas injection through the screen. The shutter system, the gas burner, and the related instrumentation are the major components of CITA to be used. The operating principles of these components remain the same and they have been described in detail in Reference [2], Appendix B. 3. Film coefficient measurements will be carried out with CITA performing in the static mode. Design details of the convective film coefficient assembly, the instrumentation to be used for the tests and the operating procedure are described in the following sections.

B. 1. Screen Support Assembly

The stainless steel screen support assembly is shown in Figure 4. It consists of three primary sections: (i) an aluminum clevis and its support rod, (ii) a transite inlet chamber and porous bronze assembly, and (iii) an inert wire cloth screen and screen holder assembly.

(i) The clevis and support rod have been designed to allow vertical to horizontal positioning of the wire cloth for testing at various angles between the cloth and the flame axis.

(ii) Uniform temperature and velocity profiles are produced by the inlet chamber assembly. Transite has been used to construct the inlet chamber and porous bronze holder. Its low thermal conductivity will help to insulate the heated gases and minimize the heat lossses. In addition a guard heater will be used outside the inlet chamber to further minimize the heat losses. A porous bronze filter is used to produce a uniform velocity profile across the wire cloth. Provision has been made for thermocouple probes to check the temperature profiles for uniformity both upstream and downstream of the bronze filter and for continuous monitoring during testing.

(iii) Since the wire cloth mesh will be varied to determine the effect of the fabric weave on the convective film coefficient,

three screen holder assemblies have been constructed. The holder tops are made of transite for insulation and the holder bases are made of stainless steel for protection from the burner flame and for structural support. During testing, the stainless steel wire cloth will form one leg of the thermocouple with constantan wire forming the other leg and the wires will be routed out through holes provided in the screen holder and using ceramic insulators.

B. 2. Instrumentation

Schematics of the instrumentation associated with the convective film coefficient apparatus are shown on Figures B.1 and B.2. Instrumentation and operation of the burner and shutter systems remain the same as those for the CITA. The mass flow rate through the heater and the film coefficient assembly is determined by means of flow rate, pressure, and temperature measurements. Both temperature and pressure are then measured at the inlet chamber to determine the outflow velocity.

During the film coefficient determination a voltage source and a microswitch, which is activatived by one of the moving shutters, are used to detect the instant of shutter separation and wire cloth exposure to the burner flame. This signal triggers a dual beam type 555 Tektronix Oscilloscope which records the wire cloth temperature on polaroid film.

The signal from the microswitch is also used to produce a spike in one of the traces of a two-channel Hewlett-Packard Type 7100B strip chart recorder at the instant of exposure. The other trace records the output of the thermocouple probe upstream of the porous bronze filter. This record will be used to determine the temperature of the incoming gas.

B.3. Operating Procedure

Stainless steel screens varying from 80 to 400 mesh will be cut to 75mm diameter. A stainless steel and a constantan wire will be attatched such that the screen will form one leg of the thermocouple. The wire leads will then be routed to the oscilloscope input.

The screen support assembly will then be mounted to the convective film coefficient assembly and positioned as required, with respect to its height above the burner axis.

The shutters of CITA are closed and the air tanks pressurized. The burner is stabilized at the desired heating intensity through air and fuel rate selection. It is then inserted into the apparatus, below the water cooled shutters. The screen is then exposed to the gas flame through activation of the solenoid valves which in tern pressurize the air cylinders and retract the shutters.

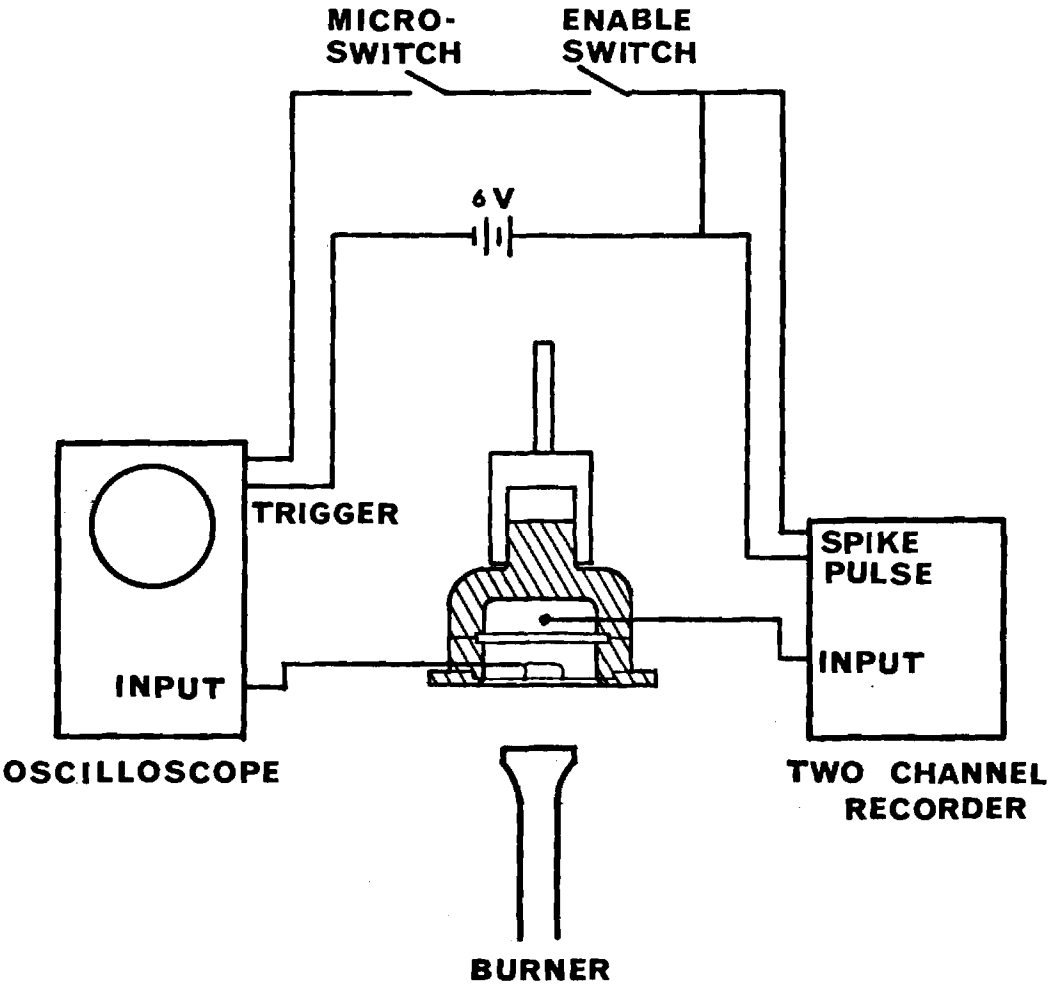

Figure B1. Schematic of Instrumentation for Temperature Measurement in Convective Film Coefficient Test Assembly.

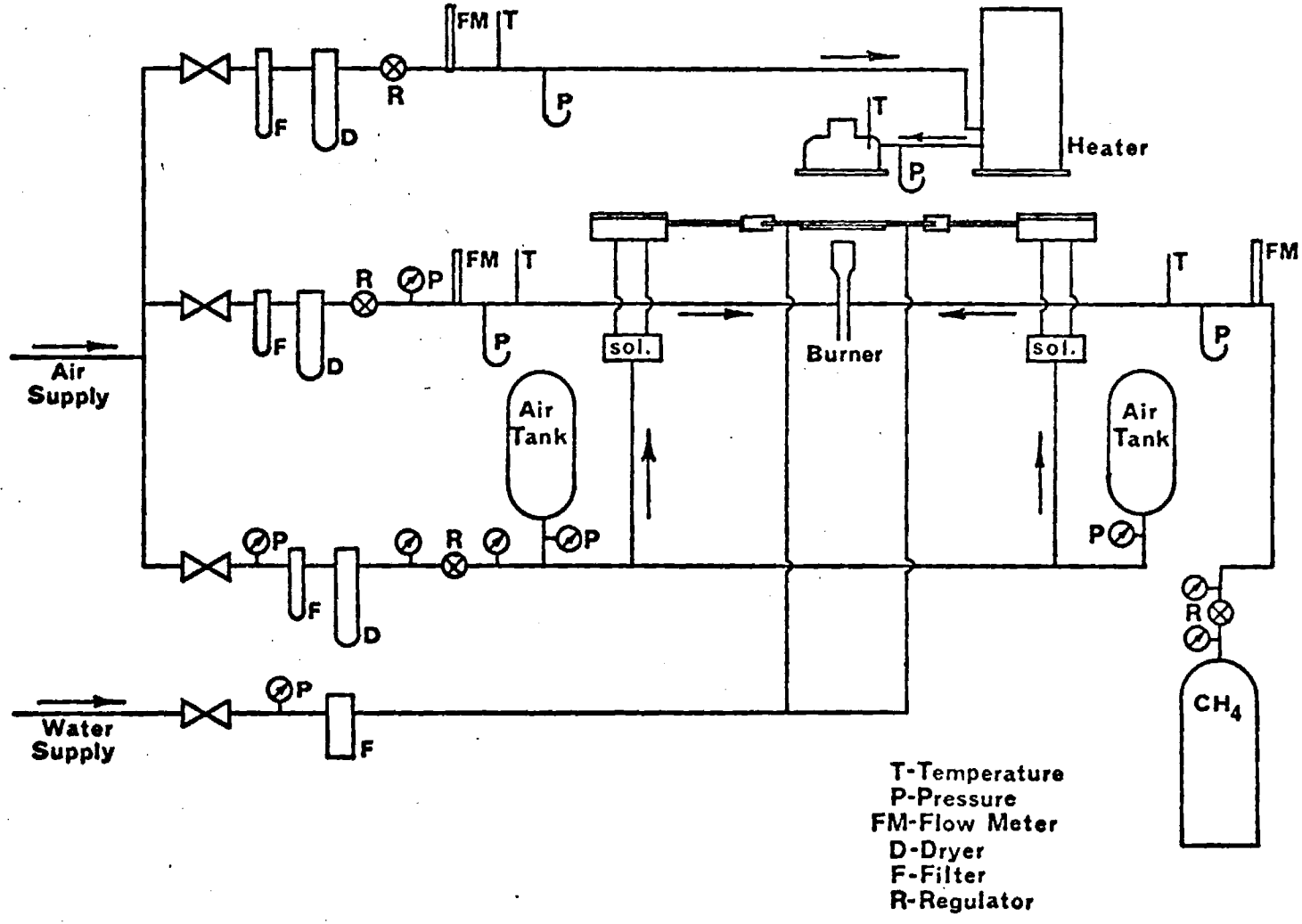

Figure B2. Flow Diagram for Convective Film Coefficient Measurement in Simulated Gasification with CITA

Measurements will be made of the air flow rate, pressure, and temperature, at the flow meter, and pressure and temperature behind the porous bronze plate. The temperature-time profile of the wire cloth will be recorded on polaroid film.

Appendix C

The Convective Ignition Time Apparatus

The Convective Ignition Time Apparatus (CITA) has been operated before for ignition time measurements of the ten Primary GIRCFF Fabrics. These are identified in Table 3 below. A detailed description of the operating principles, design details, and procedures for the static and dynamic modes of operation are given in Reference [2], Appendix B. 3. The tests reported in this report have been performed using the same equipment and following the same procedures.

Table 3 Fabric Identifications and Specific Mass

GIRCFF No.	Classification	Fiber Composition	Color	Finish	Specific Mass mg/cm^2
1	Durable Press Slack	65/35% Pe./C.	White	DP treated	23.49
2*	Textured Woven Blouse	100% Polyester	Yellow	-	7.51
3	Double Knit	100% Polyester	White	-	20.91
4	Denim	100% Cotton	Navy bl.	-	29.63
5*	T-Shirt, Jersey	100% Cotton	White	-	13.71
6	Untreated Slack	65/35% Pe./C.	White	-	23.57
7	Jersey Tube Knit	100% Acrylic	Gold	-	15.13
8*	T-Shirt, Jersey	65/35% Pe./C.	White	-	16.19
9	Terry Cloth	100% Cotton	White	-	26.48
10*	Batiste	100% Cotton	Purple	-	6.65
11*	Tricot	80/20% Acet./ Nyl.	White	-	11.31
12*	Tricot	100% Nylon	White	-	8.91
13*	Tricot	100% Acetate	White	-	9.40
14	Taffeta	100% Nylon	White	-	5.66
15	Durable Press Slack	65/35% Pe./Ray	Brown	DP treated	22.82
16	Shirting	50/50% Pe./C.	White	-	13.14
17*	Batiste	65/35% Pe./C.	White	-	8.55
18*	Flannel	100% Cotton	White	-	12.88
19*	Flannel	100% Cotton	White	Fire retard	14.89
20	Flannel	100% Wool	Navy bl.	-	19.93

*Ten Primary GIRCFF Fabrics.

Appendix D

Modeling Analysis

The fundamental equations describing the thermal response of thermally degrading, porous solids in contact either with other solids or with reacting gases, are briefly listed in vectorial form.

D. 1. Porous Media

Conservation of energy requires that

$$\overline{\rho_s c_s}\frac{\partial T}{\partial \tau} + \rho_f c_{p,f}\, \underset{\sim}{v}\cdot\nabla T = k_{eff}\nabla^2 T - \nabla\cdot \underset{\sim}{q}_{rad}$$

$$- \nabla\cdot(\rho_f \underset{\sim}{v})\left\{\Delta h_f^\circ + \int_{T_o}^{T}\left[c_{p,f}(T') - c_{p,s}(T')\right]dT'\right\} \qquad (D.1)$$

The symbols are defined in the nomenclature. The velocity field $\underset{\sim}{v}$ of the decomposition gases is taken to be onedimensional within the porous solid and the gas pressure is constant. Conservation of mass in the gas phase requires

$$\Psi\frac{\partial \rho_f}{\partial \tau} + \nabla\cdot(\rho_f \underset{\sim}{v}) = \dot{r} \qquad (D.2)$$

and the rate of decomposition is represented by N discrete reactions

$$\dot{r} = \sum_{i=1}^{N}(\Delta_i \rho_s)\,\dot{\lambda}_i \qquad (D.3)$$

in which the degrees of decomposition λ_i satisfy

$$\dot{\lambda}_i = (1-\lambda_i)^{n_i} (k_o)_i \; e^{-\frac{E_i}{RT}} \qquad (D.4)$$

Equations D.1 through 4 are supplemented by the equations of state for the decomposition products (ideal gas) and the boundary conditions expressing continuity of heat flux and gas flow at the solid interfaces.

D. 2. External Gas Phase

The reaching boundary layers, in contact with the thermally degrading porous solid, are modeled as binary mixtures of air and pyrolysates, undergoing changes in composition and temperature until the experinentally established ignition criterion, namely a critical combination of concentration and temperature (flammability limit), is reached.

Conservation of mixture mass requires that

$$\frac{\partial \rho}{\partial \tau} + \nabla \cdot (\rho \underset{\sim}{V}) = 0 \qquad (D.5)$$

while the concentration ω of pyrolysates must satisfy

$$\frac{D\omega}{D\tau} = \frac{1}{\rho} \nabla \cdot [\rho \mathscr{D} \nabla \omega] \qquad (D.6)$$

The equations of motion are, for free convection

$$\rho \frac{D\underset{\sim}{V}}{D\tau} = \mu \nabla^2 \underset{\sim}{V} - \rho \underset{\sim}{g} [\beta (T - T_\infty) + \zeta (x - x_\infty)] \qquad (D.7)$$

and for forced convection

$$\rho \frac{D\underset{\sim}{V}}{D\tau} = \mu \nabla^2 \underset{\sim}{V} - \nabla p \qquad (D.8)$$

Engergy conservation requires that

$$\rho c_p \frac{DT}{D\tau} = k\nabla^2 T + \nabla T \cdot \left\{ \rho \mathcal{D} \sum_{i=1}^{2} c_{p,i} \nabla \omega_i - \rho \underset{\sim}{v} \sum_{i=1}^{2} c_{p,i} \omega_i \right\} \qquad (D.9)$$

These equations are to be suplemented by suitable boundary conditions which describe continuity of heat and mass fluxes at the solid interface and a suitably chosen flow field such as that of a turbulent jet (Fig. D. 1) or of a quiescent atmosphere, far away from the heated surface. Momentum and mass transport properties, namely viscosity and mass diffusivity, appear after the transformation into integral form, in wall shear and mass injection terms which are formulated from known turbulent boundary layer descriptions.

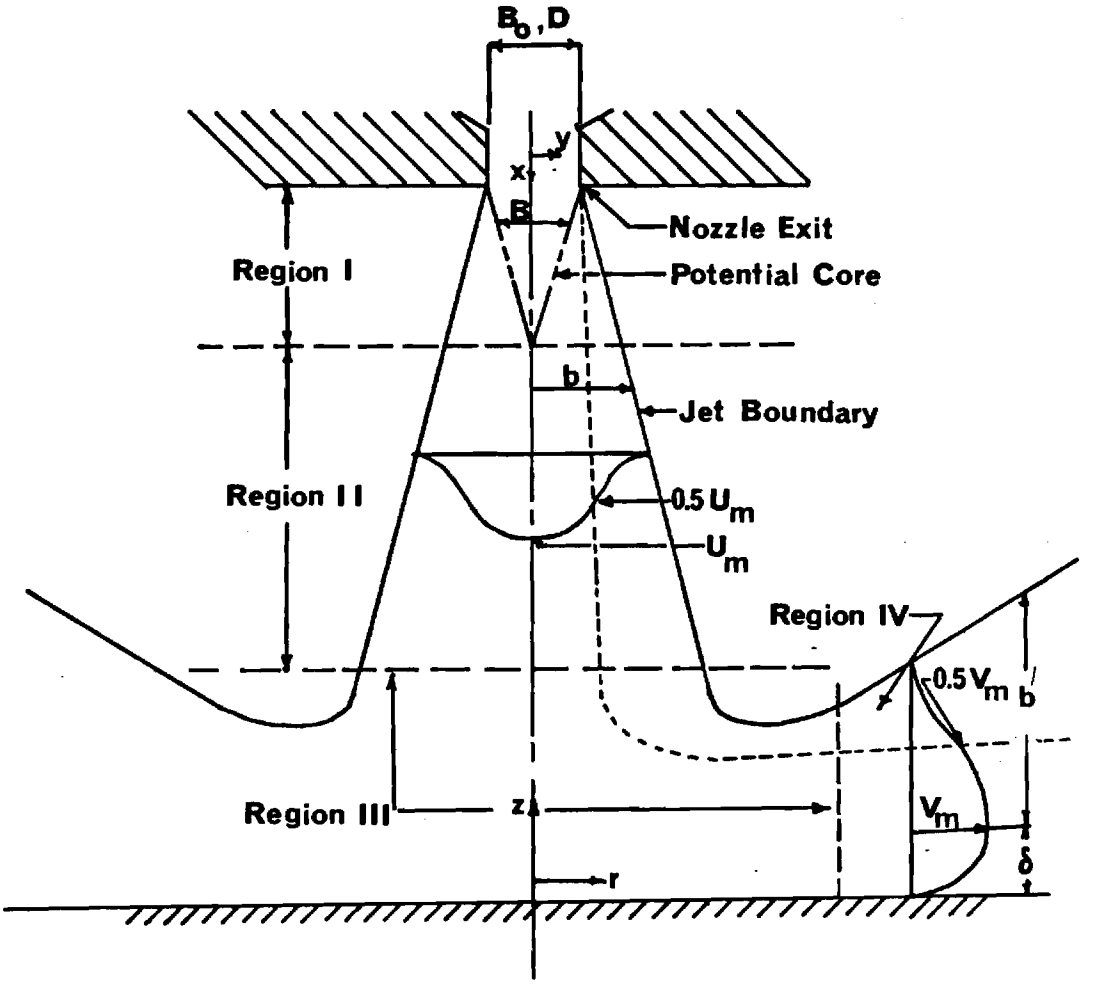

Figure D1. Characteristic Regions in Impinging Jet Flow

GEORGIA INSTITUTE OF TECHNOLOGY
School of Mechanical Engineering
Atlanta, Georgia

PREDICTION OF FIRE HAZARD IN BUILDINGS

Semiannual Progress Report
No. 2

prepared by

K. Annamalai P. Durbetaki G. L. Matson

For The
National Science Foundation
RANN Program

NSF Grant No. GI-31882

March 31, 1975

PREDICTION OF FIRE HAZARD IN BUILDINGS

Semiannual Progress Report No. 2

prepared by

K. Annamalai P. Durbetaki G. L. Matson

School of Mechanical Engineering
Georgia Institute of Technology
Atlanta, Georgia 30332

March 31, 1975

Research Sponsored
By The
National Science Foundation
Under the RANN Program
(Research Applied to National Needs)

NSF Grant No. GI-31882A#3

P. Durbetaki, Principal Investigator

Stothe P. Kezios, Director
School of Mechanical Engineering

FOREWORD

The research described herein is being funded and supported by the National Science Foundation under the RANN Program (Research Applied to National Needs). The work originated in November of 1970 from the need for fabric flammability standards as formulated by the Government-Industry Research Committee on Fabric Flammability (GIRCFF) in an effort to provide the technical background for satisfying the Flammable Fabrics Act of 1953 as amended in 1967.

The project is being performed in the Fire Hazard and Combustion Research Laboratory of the School of Mechanical Engineering at the Georgia Institute of Technology under the direction of the Principal Investigator Dr. Pandeli Durbetaki. Dr. Wolfgang Wulff, who has been a Co-Principal Investigator since November 1970 continued in this capacity and participated in the current program during the period April-June 1974. Participating in the research were M.S. candidates Robert L. Acree, Gregory L. Wedel and Paul T. Williams, and they all completed their research by December 1974. Presently participating in the research are Assistant Research Engineer K. Annamalai, who will be awarded his Ph.D. in June 1975, and M.S. candidates Gary L. Matson and William P. Ryszytiwskyj.

The research is being supported in part by the School of Mechanical Engineering under the matching fund provision of the grant. The interest in, and the support of, this research by the National Science Foundation is greatly appreciated.

ABSTRACT

The fire hazard of a system is quantified by the probability with which use of a system leads to fire loss. This fire loss probability is a function of the subprobabilities with which events occur that lead to a specified loss from fire. The first of the major events which leads to a loss from fire is ignition. The probability of ignition after exposure is a function of the material's ignition time. Experimental and analytical research has been performed to predict thermally thin and thick material ignition time as functions of material properties and heating intensity. Ignition probabilities have been derived from experimental ignition statistics.

The objectives of the current program period are (i) to develop ignition criteria which are applicable to thermally thin and thick materials, (ii) to expand previous experiments on ignition time measurements to thermally thick materials, and (iii) to determine the ignition probability of thermally thin materials under convective heating and of thermally thick materials under radiative heating. The program is subdivided into eight tasks and the accomplishments are:

Task 1: Measurement of Ignition Statistics on Thermally Thin Media, Subject to Convective Heating. The total 653 ignition tests have been performed and the ignition probability under given laboratory conditions has been established for three fabrics at two levels of heating intensity.

Task 2: Measurement of Ignition Temperature on Pyrolysate-Air Mixtures. Ignition tests have been conducted on propane-air mixtures and on pyrolysate-air mixtures with condensibles removed for three cotton fabrics.

Task 3: Measurement of Ignition Statistics on Thermally Thick Media, Subject to Radiative Heating. A large ignition test apparatus has been designed and is currently under construction. With this apparatus it will be possible to expose

samples in sizes up to 40 cm by 40 cm by 5 cm to radiative heating for measurement of ignition times and ignition statistics.

Task 4: Measurement of Convective Film Coefficients Under Simulated Pyrolysate Evolutions. The air injection test cell has been used with 150 mesh and 200 mesh stainless steel wire cloths under injection and suction conditions to determine convective film coefficients during flame-fabric interactions. Modeling analysis was performed to establish scaling parameters and correlate the experimental results.

Task 5: Ignition Time Measurements on Fabric Assemblies Under Various Geometric Configurations. Similar and dissimilar fabric pairs were exposed to radiative heating to measure ignition times. The analysis carried out predicted ignition times for the similar fabric pair at five heating intensities. Edge ignition tests were carried out under gas flame heating for six fabrics at four angles between zero and ninety degrees from the horizontal.

Task 6: Modeling Experiments on Extinguishment. This task has been replaced by Task 7.

Task 7: Modeling Analysis of Ignition for Thermally Thin Media. Using two ignition criteria, the analysis developed for normally impinging flames on fabrics, was employed to predict ignition times. The results have been compared with ignition times from experiments.

Task 8: Modeling Analysis of Ignition for Thermally Thick Media. The governing equations have been formulated to describe the response to radiative heating of thermally thick decomposing solids. The model accounts for free convection and using ignition criteria ignition times will be predicted for the solid.

TABLE OF CONTENTS

Page

LIST OF FIGURES

LIST OF TABLES

NOMENCLATURE

a	coefficient of potential flow velocity u_f/d_f
a_j	polynomial coefficients, equation (F.34)
c	concentration, specific heat
c_p	specific heat at constant pressure
C_s	heat capacity per unit area, equation (2.1)
C_j	coefficients, equation (F.31)
d	hot jet diameter
D	burner diameter, mass diffusivity
D_I	first Damköhler number
E	activation energy
E_b	black body radiation
$f(\eta)$	nondimensional stream function
$F(T^*)$	equation (F.33)
g	acceleration due to gravity
G	inter-fabric air gap
h	convective heat transfer coefficient, enthalpy
$\bar{h}$	mean convective film coefficient
H	convective heat transfer ratio, equation (F.16)
I_v	velocity integral, equation (F.26)
k	thermal conductivity, frequency factor
K	permeability
L	height above burner
$\dot{m}$	mass rate

M	molecular weight
n	order of reaction
N_{Fo}	Fourier number
N_{Gr}	Grashof number
N_{Nu}	Nusselt number
N_{Pr}	Prandtl number
N_{Re}	Reynolds number
p	pressure
p_g	fraction of pyrolysate escaping at $z = 0$
P	porosity
$P(I/E)$	ignition probability given exposure
q	heat flux
$\dot{q}$	heat liberated or absorbed per unit volume
Q	heat of reaction per unit mass
r	radial distance, coordinate
R	screen or fabric radius, gas constant
T	temperature
u	velocity component in x-direction
v	velocity component in z-direction
V	velocity
$\dot{w}$	chemical reaction rate per unit volume
W_o	radiant heat flux
x	height, lateral coordinate
y	normal coordinate
Y	mass fraction
z	axial coordinate; general variable, equation (1.1)

$\tilde{\alpha}$	absorptance
α^*	effective absorptance; equation (2.11)
β	void fraction; coefficient of volume expansion
δ	fabric or screen thickness
ε	decomposable fraction of original mass
$\tilde{\varepsilon}$	emittance
η	similarity variable, equation (F.10)
θ	nondimensional temperature
κ	extinction coefficient for the solid
λ	fraction of decomposable mass which evolves from the fabric
μ	viscosity
ν	kinematic viscosity
π_i	nondimensional groups
ρ	density
$\tilde{\sigma}$	reflectance
σ	standard deviation; refractive index of the solid
τ	time
$<\tau>$	median time
τ^*, $\bar{\tau}$	nondimensional time
$\tilde{\tau}$	transmittance
τ_1	equation (F.28)
ϕ	stoichiometric equivalence ratio
χ	integral limit, equation (1.1)
ψ	stream function

Subscripts

b	burner, back fabric
c	convective, char

d	desorption
e	exposure, potential flow region
f	flame, pyrolysate, front fabric
g	gasification
i	counting index, ignition
j	counting index
m	melting
n	counting index
o	initial
0	oxygen
p	predicted, pyrolysate
r	radiative
s	screen, solid
T	thermal
w	wall
z	z-direction
δ	side exposed to atmosphere
μ	mean
0	injection or perfusion
1	side interacting with flame
2	side exposed to atmosphere
∞	atmosphere

Superscripts

*	nondimensional
-	mean

1. INTRODUCTION

The reduction of loss of life, property and natural resources from fire is essential and requires both education of people toward greater awareness of fire hazard, and reduction of the fire hazard itself. The latter is commonly achieved through the establishment of standards and codes. All codes and standards must be based on test methods and test results which must rationally relate to the potential fire hazard. Such a relationship requires a quantitative measure of the fire hazard itself.

As a quantitative measure of a system's fire hazard, the probability with which use of the system leads to a prescribed loss was first proposed by Myron Tribus [1]. This general concept has been employed for the planning and execution of fabric flammability research [2-5] and currently it is being extended to include research with building material at the School of Mechanical Engineering of Georgia Institute of Technology.

The fire loss probability is composed of all the subprobabilities which are associated with the events and processes connecting the time of hazard assessment with the occurrence of the fire loss. The events and processes generally fall into two categories, the selection processes and the physico-chemical processes.

All the possible choices of use and attendant circumstances to which a system might be subjected fall into the category of selection processes. The subprobabilities associated with these events are equal to the relative frequencies with which such choices are made, subject to the constraints of the system. The relative frequencies are obtained from observation and statistical correlation.

The physico-chemical processes, such as thermal decomposition, ignition, flame propagation, flashover, and extinguishment are predominantly deterministic transient processes. The associated subprobabilites are functions of characteristic times, specifically they depend on the ratio of the time the process is allowed to proceed, over the mean expected value of the time which the process requires for its completion.

The first important event of the physico-chemical process is ignition

after given exposure to a heat source. The associated probability P(I/E) of ignition after given laboratory exposure conditions is

$$P(I/E) = (1/\sqrt{2\pi}) \int_{-\infty}^{\chi} \exp(-z^2/2)dz \qquad (1.1)$$

where the upper limit of the integration encompasses the ratio of the characteristic times τ_e of exposure and $\langle\tau_i\rangle$ of ignition

$$\chi = [\tau_e/\langle\tau_i\rangle - 1]/\sigma \qquad (1.2)$$

and σ represents the standard deviation of ignition time. The standard deviation accounts for the stochastic variation of the material properties.

2. OVERVIEW OF PROGRESS

2.1. Previous Accomplishments

Accomplishments and results of research performed at the School of Mechanical Engineering of Georgia Institute of Technology during the period from November 1970 through March 1974 are detailed in previously published reports [3, 4, 6] and briefly summarized here.

Thermophysical fabric properties which characterize the ignition process have been measured, namely thermal conductance, specific heat, specific mass, ignition or melting temperature, optical properties, reaction kinetic parameters and reaction enthalpy, on cotton, nylon, polyester, acetate and wool fabrics and blends.

Ignition or melting times have been measured on the same fabrics under radiative and convective (gas flame) heating. The median destruction time (ignition or melting) $<\tau_{i,m}>$ as well as the standard deviations σ have been evaluated through probit analysis of destruction time statistics for two igniting cotton fabrics and a melting nylon fabric, as functions of radiative heating intensity and fabric moisture content. Fabric destruction probabilities have been evaluated for all three fabrics as a function of exposure time and heating intensities. Fabric destruction times have been measured on fabrics while these were either held stationary over the flame or moved through the flame at selected speeds. The static fabric destruction measurements under convective heating have been conducted both with normal impingement of the flame on the center of the fabric and with the fabric in a vertial orientation exposing the edge of the fabric to the flame.

Ignition time measurement tests have been performed on fabric assemblies to determine the effect of fabric interaction during radiative heating. The fabric assemblies consisted of two identical cotton fabric samples placed at various interfabric spacings.

Measurements with simulated fabric-flame interaction experiments have

been conducted to evaluate convective film coefficients which may be used in the analysis on prediction of fabric ignition time. Inert stainless steel screens have been used to simulate the fabric and at the same time serve as one leg of a thermocouple to sense its transient mean temperature. The volatile evolution has been simulated by injecting preheated air through the screen.

A lower ignition temperature and concentration apparatus (LITACA) has been constructed with the objective to determine the lowest ignition temperature T_{ig} of cellulose pyrolysis products, premixed with air, as a function of pyrolysate concentration. A pilot test has been carried out using propane-air mixture to test the feasibility of ignition detection with this equipment.

Actual ignition sources such as kitchen gas and electric ranges, and electric hot plates have been characterized using a portable ignition source scanning apparatus (ISSA) and establishing the heat flux and temperature spacial distributions for the purpose of deriving the probability with which laboratory exposure conditions are encountered in real life. Maximum heat flux values and maximum temperatures have been measured in the flames of household matches, a cigarette lighter and a wax candle.

An analytical ignition model has been developed on the basis of energy conservation which accounts for thermal energy storage in the fabric, moisture desorption and endothermic pyrolysis within the condensed phase, and exothermic reaction in the gaseous phase, that is, in the fabric boundary layer. The analysis for both radiative ignition and convective ignition, resulted in an initial value problem with three coupled, nonlinear, first-order, ordinary differential equations. Scaling laws were derived from the differential equations and the numerical solutions were used to elucidate the significance of the above processes on the prediction of ignition time (partial modeling).

An ignition analysis has been developed on the basis of integral techniques. The analysis incorporates a newly developed ignition criterion. This criterion involved the measured ignition temperature of the pyrolysate-air mixture as a function of pyrolysate concentration. The analysis yields ignition time as a function of material properties, heating conditions and geometry, and it yields scaling parameters and the errors

of partial modeling. Analytical results have been compared with measured ignition time.

2.2. Progress During Reporting Period

An overview of the progress is listed here for eight tasks. Task 4 and Task 5 were initiated during the previous reporting period and some of the results were reported in the Third Annual Report [4]. The summary on these two tasks in the present report represent accomplishment during the current period. Task 2 was initiated during the previous period and is currently being continued with expanded objectives. The Appendix presents additional details for some of the tasks.

2.2.1. Task 1. Measurement of Ignition Statistics on Thermally Thin Media, Subject to Convective Heating

Fabric destruction (ignition or melting) are measured under controlled exposure times, convective heating intensity and fabric moisture content for the purpose of evaluating the mean fabric destruction time $\langle \tau_{i,m} \rangle$ and the standard deviation σ in equation (1.2), by probit analysis. The Convective Ignition Time Apparatus (CITA), used previously to measure fabric destruction times on single fabric samples [3,4], has been modified to carry out ignition statistics. A summary of the modification details is given in Appendix A.

The first evaluation of the results from 289 tests is presented in Table 2.1 and the probability of ignition after given exposure for three fabrics is presented on Figures 2.1 - 2.3.

2.2.2. Task 2. Measurement of Ignition Temperature on Pyrolysate-Air Mixtures

Ignition occurs in the gaseous phase near the heated surface of a thermally degrading material. The ignition process must be described in terms of the reactions taking place in the boundary layer near the

Table 2.1. Fabric Destruction Time Statistics, Under Convective Heating

GIRCFF Fabric No.	Convective Heat Flux	Number of Tests	Ignition Time			Standard Deviation of Ignition	
			Shutters in Single Action		Median	Mean	Time
			Solid τ_i, s	Pyrolysate τ_i	$\langle\tau_i\rangle$	σ_μ	σ
	W/cm^2		s	s	s	s	s
2	3.69	49	0.675	--	0.680	0.017	0.091
4	3.36	108	9.556	4.280	4.152	0.054	0.419
17	3.13	69	1.910	1.405	1.398	0.039	0.240
17	9.44	63	0.960	0.960	0.864	0.013	0.073

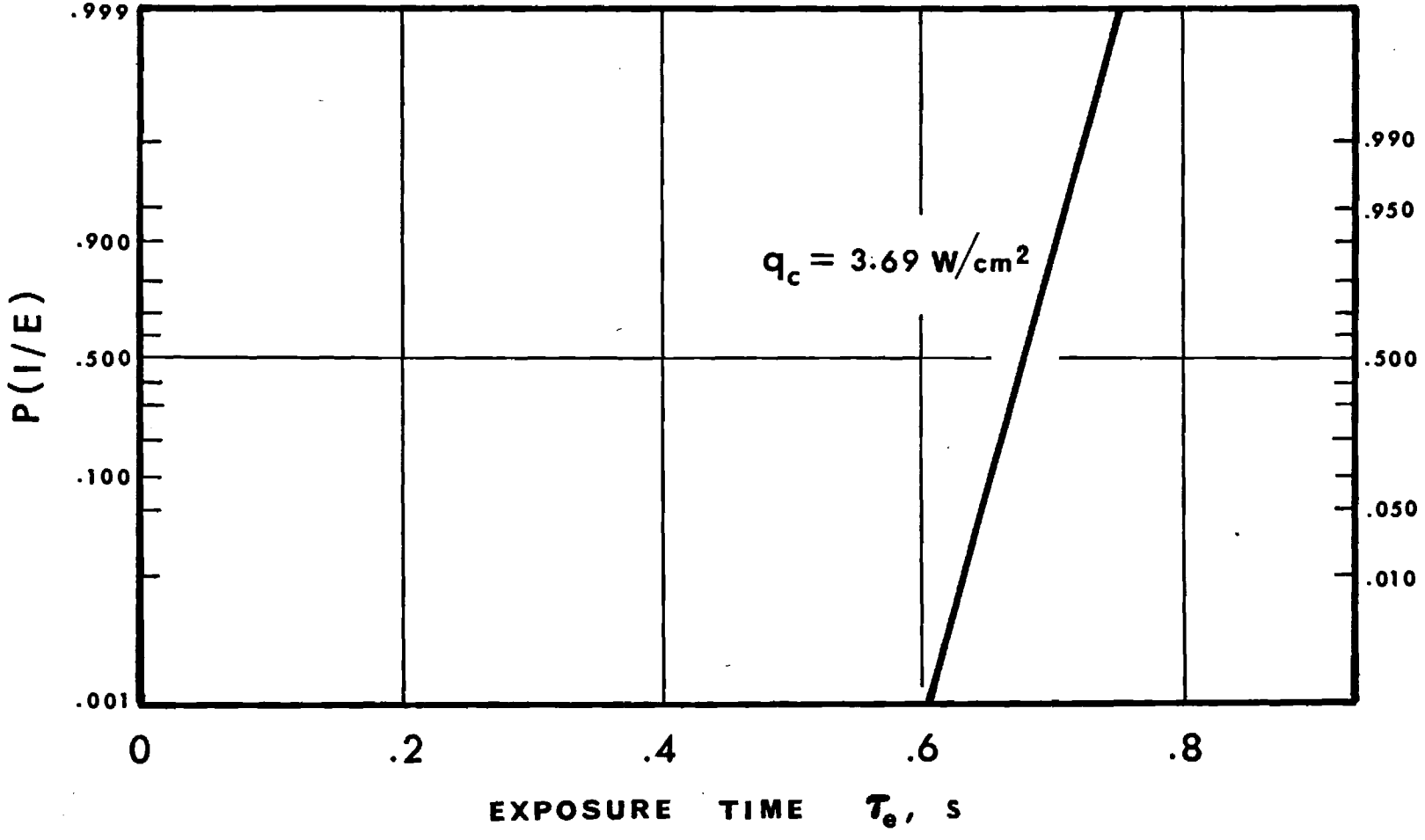

Figure 2.1. Ignition Probability as a Function of Exposure Time at One Heating Intensity, GIRCFF Fabric No. 2, Polyester

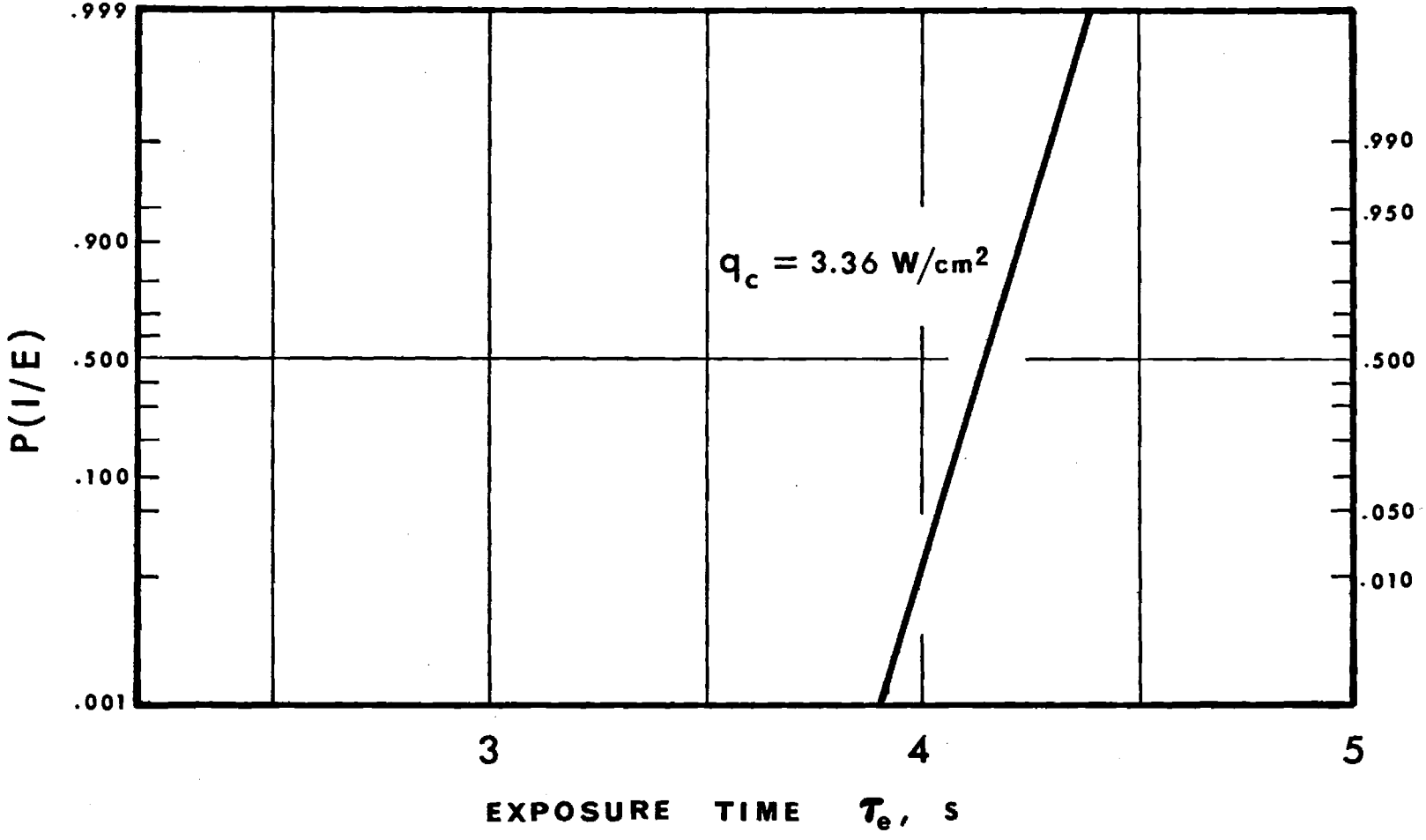

Figure 2.2. Ignition Probability as a Function of Exposure Time at One Heating Intensity, GIRCFF Fabric No. 4, Cotton

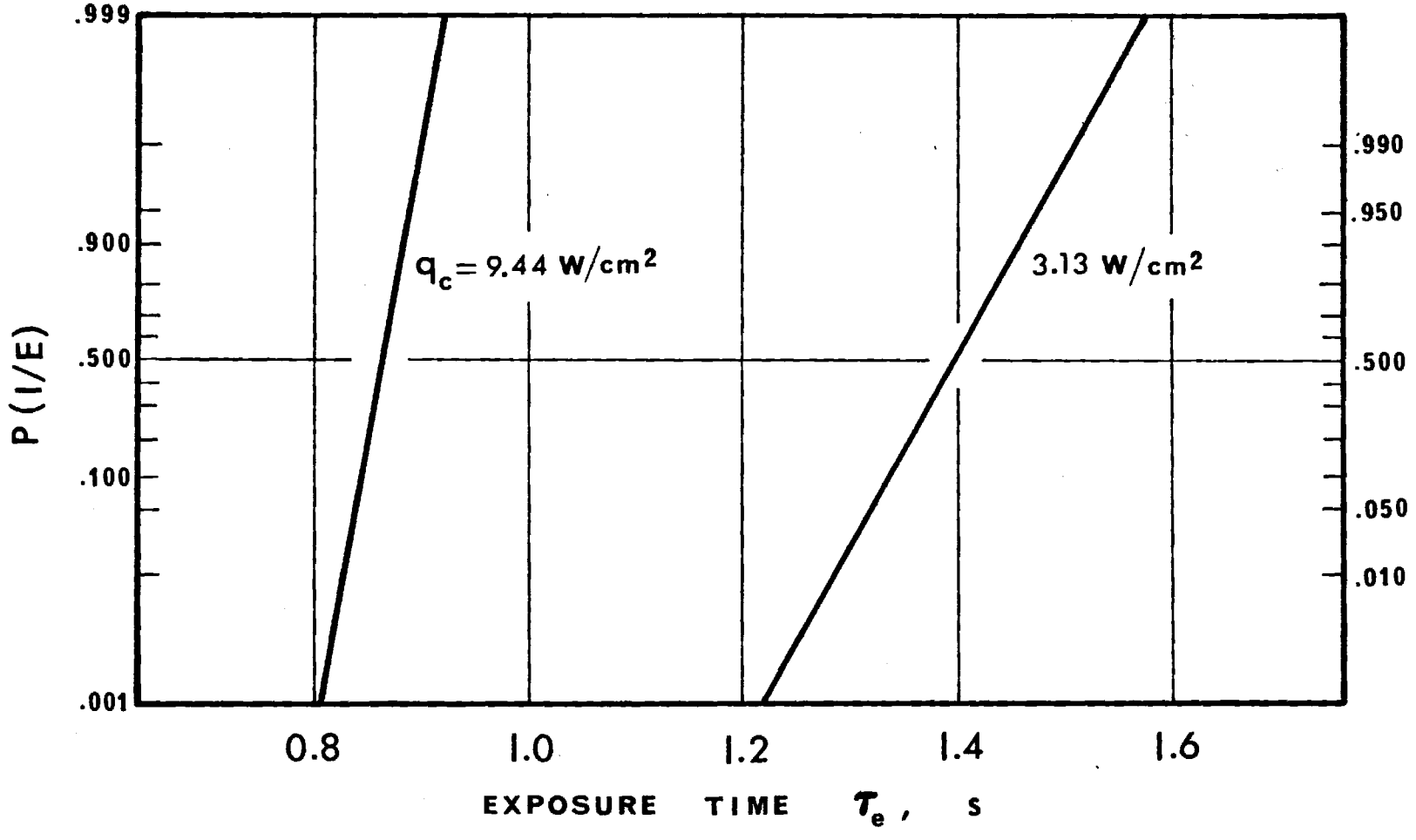

Figure 2.3. Ignition Probability as a Function of Exposure Time and Convective Heating Intensity, GIRCFF Fabric No. 17, 65/35% Polyester/Cotton

heated surface, either in terms of fundamental reaction kinetics or in terms of critical local pyrolysate concentrations and mixture temperatures. The latter approach is taken here.

The Lower Ignition Temperature and Concentration Apparatus (LITACA) was designed, constructed and assembled to meet the following conditions:

(i) thermally decompose pyrolyzing materials,

(ii) store the pyrolysates,

(iii) mix pyrolysates with dry air at controlled mass fractions,

(iv) measure the minimum mixture temperature at which self-ignition occurs, and

(v) afford pyrolysate sampling for molecular weight determinations.

The major components of LITACA are:

(i) the pyrolysate generating furnace,

(ii) the volatile reservoir,

(iii) the pyrolysate and air metering system,

(iv) the reaction cell, and

(v) the temperature recording and ignition detecting instrumentation.

Detailed descriptions of LITACA and the associated calibrating and operating procedures have been presented in Appendix A.1 of Reference[4]. Modifications in the apparatus and operating procedures are discussed in Appendix B of the present report.

The equipment was first used to conduct ignition temperature tests on propane-air mixtures. The results are presented on Figure 2.4. These tests establish the possibility of ignition detection with this equipment. However, the flammability limits do not agree with values found in the literature [7]. At the same time, the lowest temperature for ignition of 660 C is considerably higher than the spontaneous ignition temperature reported for propane [8]. Current investigations with propane are being conducted to check the earlier measurements and investigate the effect of design modifications in the ignition tube, on the ignition temperatures.

Ignition tests were carried out with three 100% cotton fabrics: GIRCFF Fabric No. 5, GIRCFF Fabric No. 4, and Fabric A. The Fabric A was specially prepared at the School of Textile Engineering of Georgia Institute of Technology such that no chemical additives were used during its fabrication. In the initial tests on the cotton fabrics self-ignition of the pyrolysate-air mixtures could not be achieved. A cold trap was

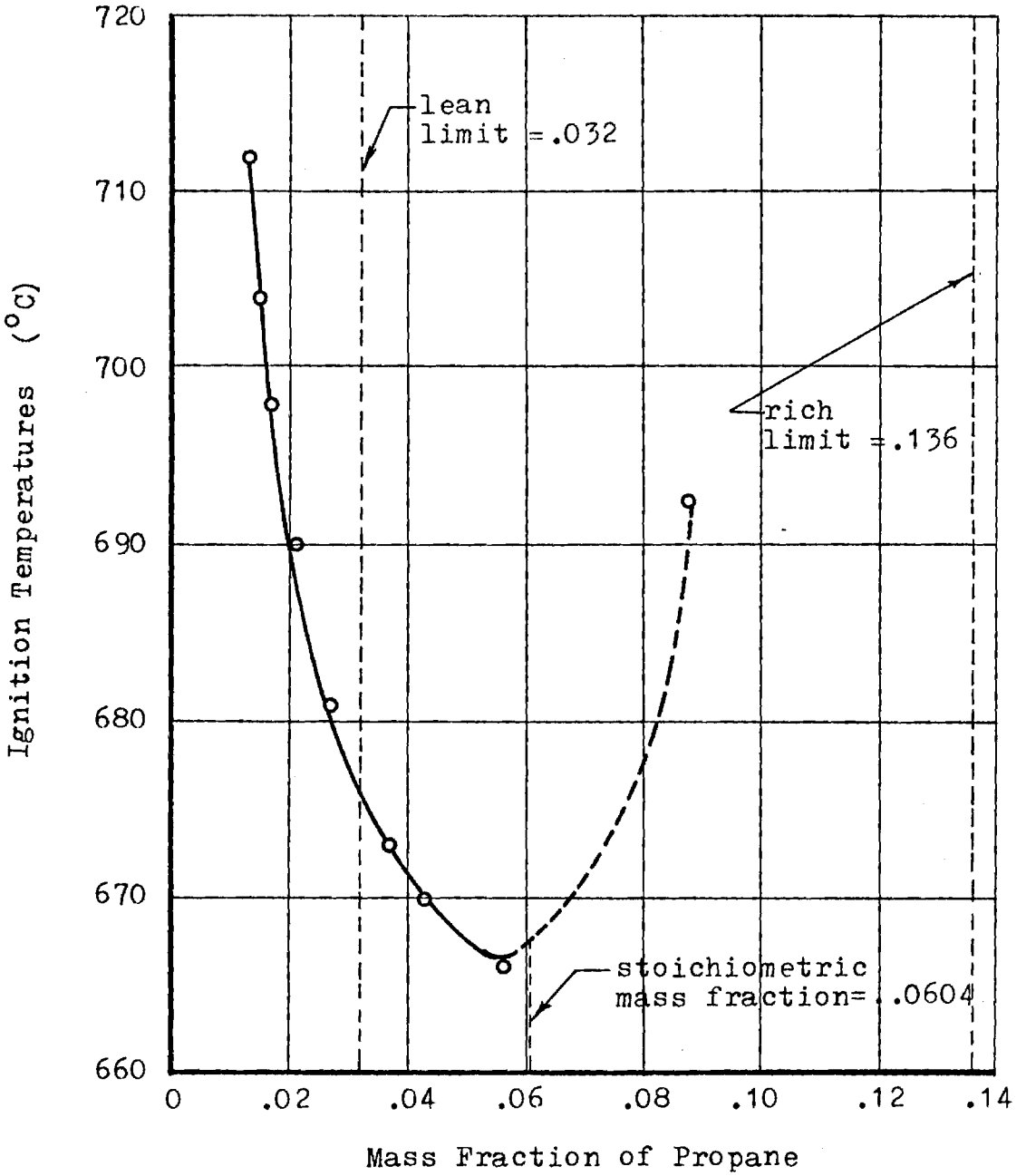

Figure 2.4. Ignition Temperatures of Propane-Air Mixtures; Lean and Rich Limits Were Taken from Reference [7]

installed between the accumulator manifold and the inlet to the pyrolysate flow meter. The ignition temperature tests conducted then were on gas mixtures which have had the condensibles removed by this cold trap. Density measurements on the pyrolysate gases from the three fabrics were taken with and without condensibles in the pyrolysate gases.

The results of the density measurement were used to estimate apparent molecular weights for the pyrolysates. These values are given in Table 2.2 below and the results of the ignition tests are presented on Figures 2.5 - 2.7 [9].

Table 2.2. Apparent Molecular Weights of Pyrolysates

Fabric	Molecular Weight	
	M_w*	M_d**
Fabric A	37.4	15.0
GIRCFF No. 5	36.2	37.7
GIRCFF No. 4	48.8	39.4

*Condensibles present
**Condensibles removed

2.2.3. Task 3. Measurement of Ignition Statistics on Thermally Thick Media, Subject to Radiative Heating

The probability of ignition after given exposure P(I/E) is the first important, highly system-related, quantity required for the assessment of a system's fire hazard. The probability is derived from the system's ignition time for given exposure conditions and the relative frequency with which the given exposure conditions occur.

The objective of this task is first to measure the ignition time and second the ignition frequency for selected ignition time intervals, on thermally thick media, under controlled radiative heating intensity and

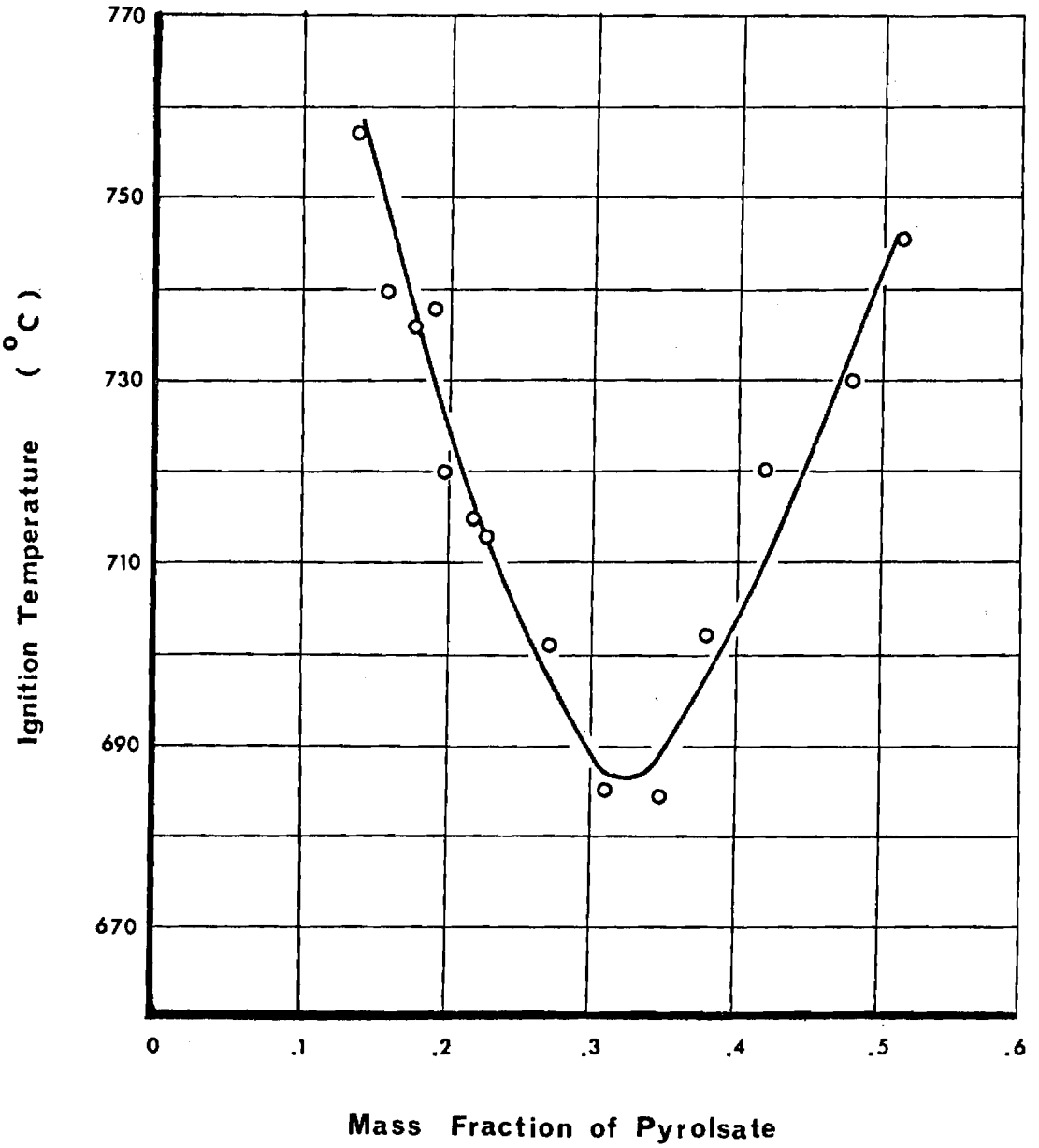

Figure 2.5. Pyrolysate-Air Mixture Ignition Temperatures, GIRCFF Fabric No. 5

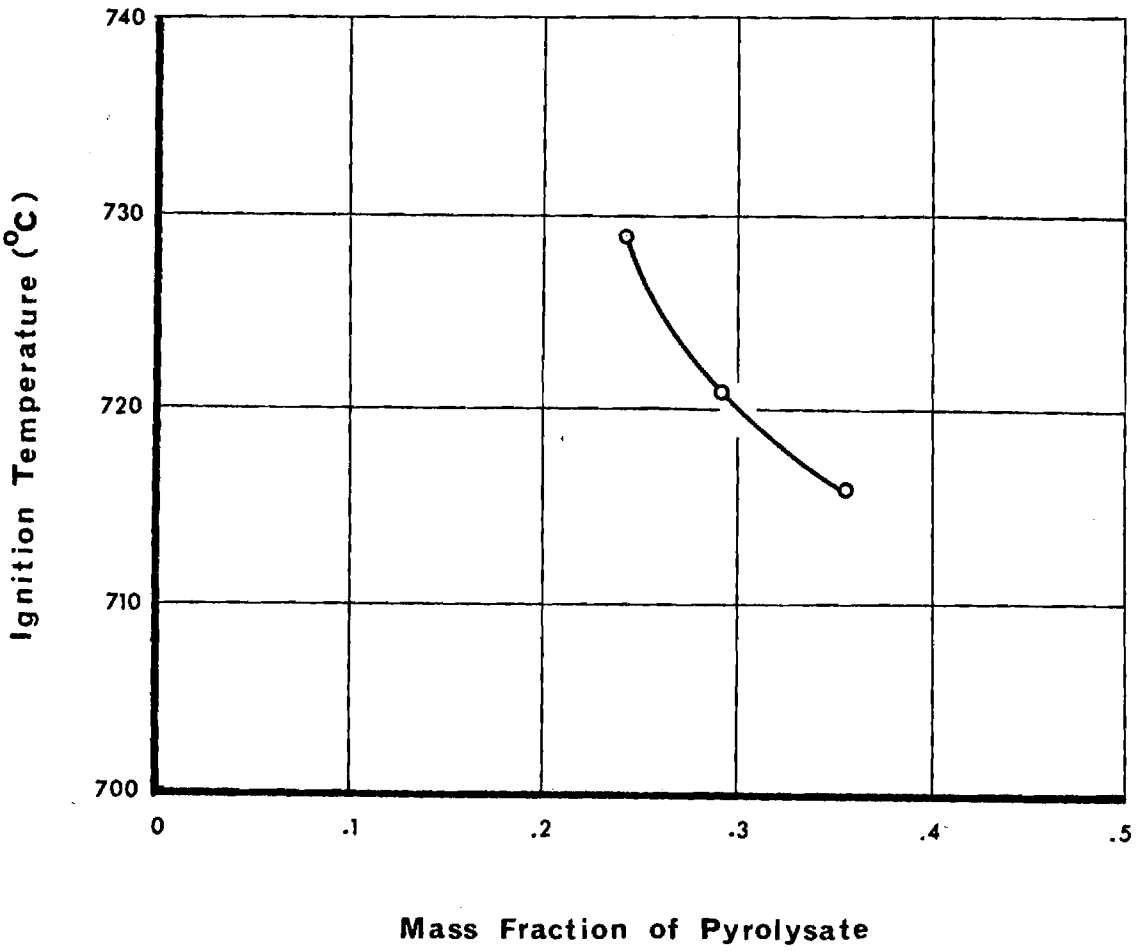

Figure 2.6. Pyrolysate-Air Mixture Ignition Temperatures, GIRCFF Fabric No. 4

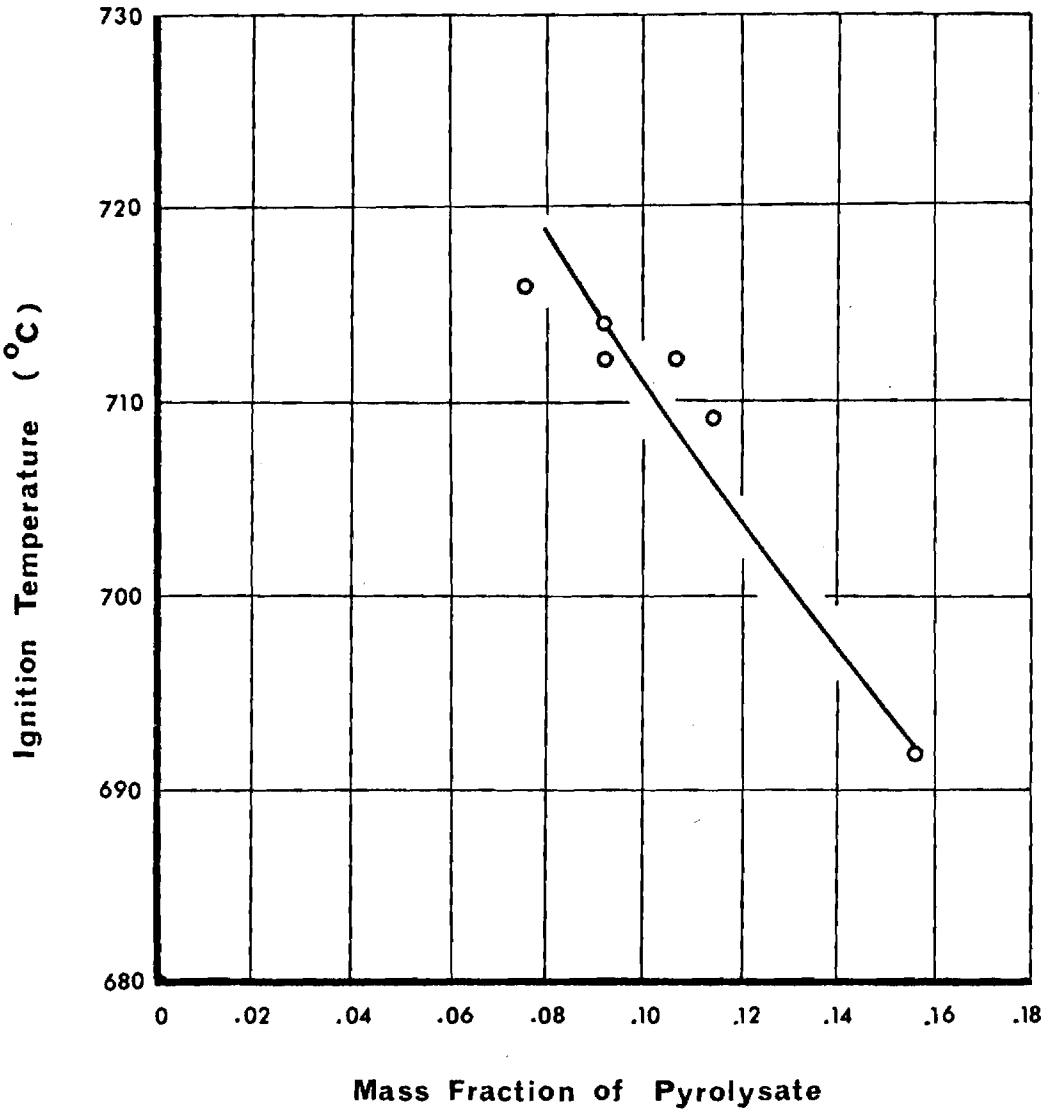

Figure 2.7. Pyrolysate-Air Mixture Ignition Temperatures, Fabric A

controlled sample conditions. The results will provide the ignition probability in the form as shown in Chapter 1 equations (1.1) and (1.2). The ignition times will be presented in nondimensional form, based on the modeling rules developed for thermally thick media.

The Large Ignition Test Apparatus (LITA) has been designed to meet the following conditions:

a. uniform, time-invariant radiative heating on samples in sizes up to 40 cm by 40 cm by 5 cm at power fluxes between 0.25 and 20W/cm^2,
b. sample exposure transients below one per cent of ignition time at both start and the end of the preselected exposure interval,
c. manual time exposure control, and
d. remote infrared detection of flames.

The major sub-assemblies of LITA are (i) the six radiant heater stack, (ii) the two vertical shutter systems, (iii) the sample holder and disposal system, (iv) the supporting structure, (v) the instrumentation for remote control, shutter timing and flame detection, and (vi) the exhaust system. All major components of the apparatus have been designed and constructed. Schematic views of the apparatus assembly are shown in Figures 2.8 and 2.9. Details are presented in Appendix C.

The apparatus is currently being assembled. The assembly is expected to be completed by the end of April 1975 together with the major wiring, water cooling, air cooling and exhaust system. Preliminary testing is expected to start in the first week of May 1975.

2.2.4. Task 4. Measurement of Convective Film Coefficients Under Simulated Pyrolysate Evolution

The release of water vapor and pyrolysate gases by the cellulosic fabric during the preignition period establishes a blanket at the interface which interferes with the heat transfer between the pyrolyzing solid and its environment. This is particularly true with an igniting gas flame in the case of convective heating. The insulating effect from the evolving vapor and pyrolysate gases is similar to that of injection cooling. However, the response of the emerging gaseous mass from the pyrolyzing solid differs significantly from forced coolant injection.

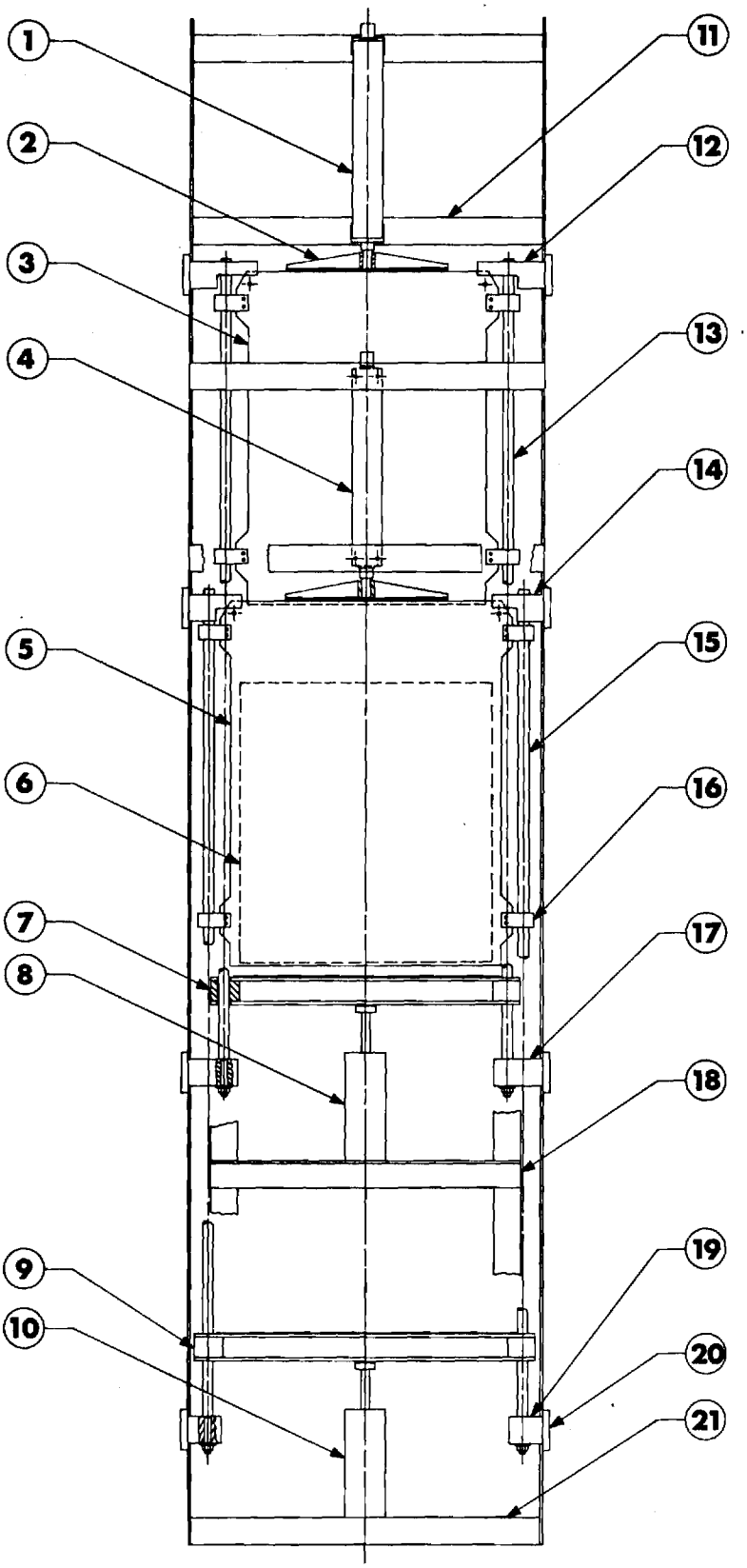

Figure 2.8. Large Ignition Test Apparatus (LITA) for Ignition Time Measurements Subject to Radiative Heating; Front View

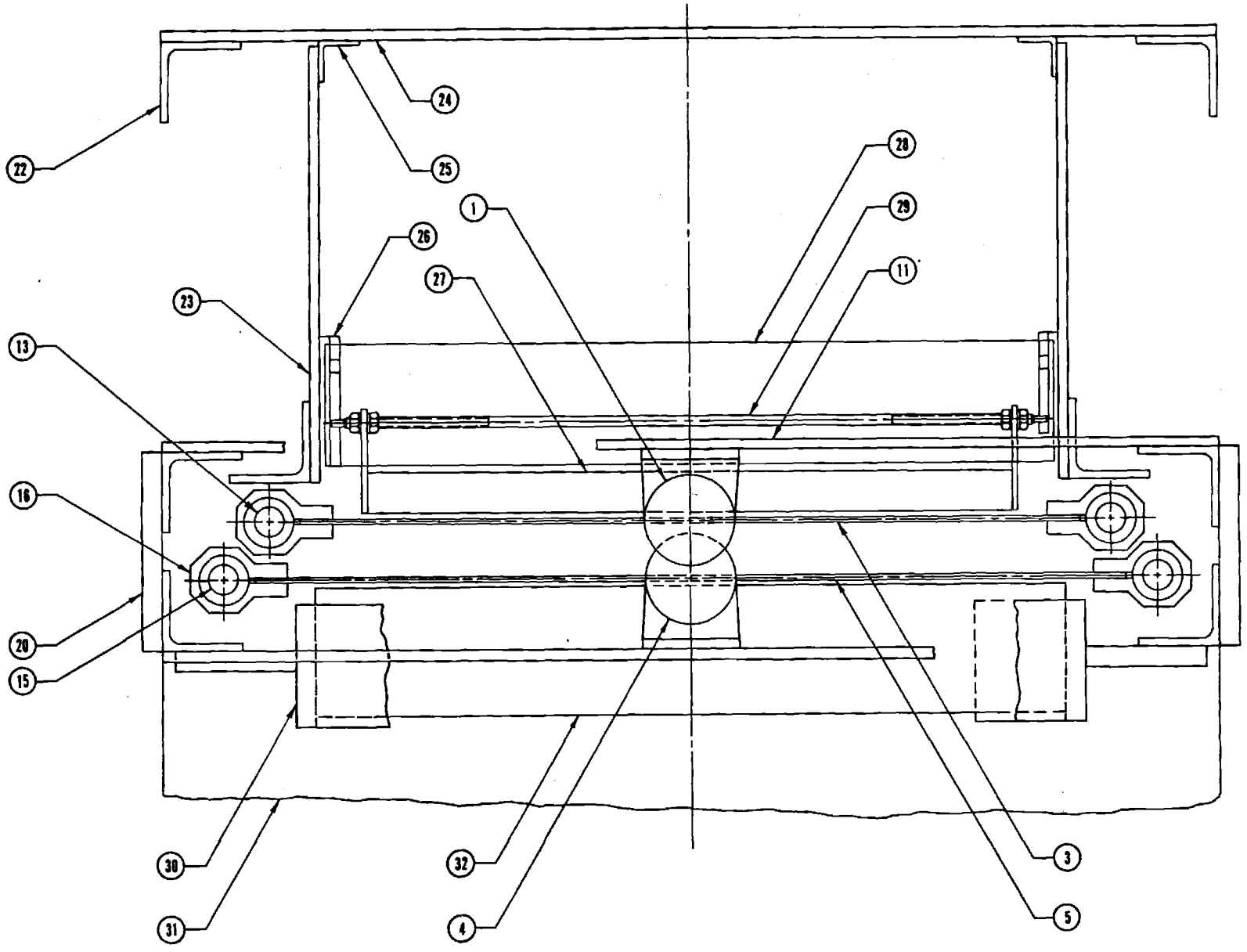

Figure 2.9. Large Ignition Test Apparatus (LITA) for Ignition Time Measurements Subject to Radiative Heating; Top View

Key to Figures 2.8 and 2.9

Part No.	Description
1	Top Air Cylinder
2	Top Accelerator Assembly
3	Top Shutter
4	Bottom Air Cylinder
5	Bottom Shutter
6	Heater Assembly Profile
7	Top Impact Bar
8	Top Shock Absorber
9	Bottom Impact Bar
10	Bottom Shock Absorber
11	Air Cylinder Support
12	Top Shutter Support
13	Top Shutter Guide Rod
14	Bottom Shutter Support
15	Bottom Shutter Guide Rod
16	Bearing Assembly
17	Top Shutter Guide Rod Support
18	Top Shock Absorber Support
19	Bottom Shutter Guide Rod Support
20	Side Plate
21	Bottom Shock Absorber Support
22	Supporting Structure Column
23	Disposal Assembly Support Plate
24	Rear Support Plate
25	Brace Column
26	Disposal Assembly
27	Test Specimen
28	Receptacle
29	Test Specimen Support Rod
30	Heater Support Assembly
31	Heater Support Platform
32	Heater

The objective of this task is to stimulate the fabric geometry with inert stainless steel wire mesh cloths and to simulate the action of emerging pyrolysate through injection of preconditioned air, and to infer the thermal response of the fabric from the response of the wire cloth by incorporating it directly into a thermocouple circuit which senses true wire cloth temperature.

2.2.4.1. Measurements. Measurements with the simulated fabric-flame interaction experiments were conducted to evaluate convective film coefficients which may be used in the analysis on prediction of fabric ignition time [10]. Fabric ignition time has been measured earlier [3-5] by exposing selected fabrics to carefully controlled, premixed methane flames in the Convective Ignition Time Apparatus (CITA). The measurements presented here were performed in the same test facility with the thermally decomposing fabrics replaced by inert stainless steel screens of different mesh sizes. These screens not only simulate the fabric but also serve as one leg of a thermocouple to sense its transient mean temperature. The volatile evolution is simulated by injecting preheated air through the screen, at controlled rate and temperature. The screen is exposed to normally impinging flames of known characteristics.

The heat transfer from the gas flame to the screen is inferred from the screen's temperature rise $dT_s/d\tau$, following its sudden exposure to the flame. An energy balance on the screen yields the following expression for the convective film coefficient

$$\bar{h}_{c,1} = \frac{(\rho\delta)_s c_s (dT_s/d\tau)}{(T_f - T_s)} = \frac{C_s (dT_s/d\tau)}{(T_f - T_s)} \qquad (2.1)$$

where C_s is the heat capacity per unit area of the screen and T_f the flame temperature. The slope of the heating curve $T_s(\tau)$ is evaluated from the initial constant slope of an emf-time oscillogram of the screen-thermocouple.

The action of air injection or suction through the wire screen simulates the evolution of pyrolysates during fabric decomposition and the perfusion through the fabric due to its porosity, respectively.

The Convective Film Coefficient Apparatus (CFCA) was designed to be used with the Convective Ignition Time Apparatus (CITA) (see Appendix A) to determine the film coefficients describing the cloth-flame interaction. Detailed descriptions of the CFCA and the associated operating procedures have been presented in Appendix A.2 of Reference [4]. Modifications in the apparatus and the operating procedures are discussed in Appendix D of the present report.

Table 2.3 gives a representative set of results of the stainless steel screen tests for the evaluation of convective film coefficients with injection or perfusion through the screen.

2.2.4.2. Analysis and Scaling Parameters. The modeling analysis is carried out to describe the fabric-flame interaction, to establish the governing dimensionless groups which correlate the heat transfer data and to provide the relation between test conditions and actual heating conditions.

The model to be used in the analysis consists of a burner whose top is located at a distance L ($z = -L$) from a porous cloth of thickness and the face exposed to the burner fixed at $z = 0$. The burner and the cloth axes are coincident. The hot gases impinging normally to the porous cloth have reacted totally before they arrive at the interface. The back side of the cloth is exposed to the surrounding atmosphere. Due to the porosity of the fabric the flames may perfuse through the matrix of the solid. The pyrolyzing solid generates gas which evolves on both sides of the fabric. The governing equations and the characteristic scaling parameters which evolve from the analysis are presented in Appendix E. It is found that the heat interaction between the flame and the screen in the presence of injection can be correlated by

$$(N_{Nu})_1 = f\{L/D,\ R/D,\ N_{Re}, N_{Pr}, (N_{Re})_0, T_s^*\} \qquad (2.2)$$

2.2.4.3. Data Reduction and Scaling Parameters. The Nusselt number in equation (2.2) is a mean value averaged over the screen radius. The associated mean convective film coefficient was evaluated from the stainless steel screen experiments using equation (2.1). The specific

Table 2.3. Convective Film Coefficients for Screen-Flame Interaction With Injection or Perfusion Through the Screen; 200 Mesh Screen

Exp.	T_s(°C)	T_f(°C)	h(W/cm^2 °C)	N_{Nu}	$(N_{Re})_0$	N_{Re}	N_{Pr}	L/D	V_0(cm/s)
1	38.2	1290	.0029852	9.68	-19.32	227.6	.683	.515	-2.950
2	40.3	1290	.0029682	9.63	-19.17	228.1	.683	.515	-2.947
3	38.2	1352	.0060385	18.94	-19.80	517.1	.681	.515	-3.088
4	38.6	1352	.0058241	18.26	-19.80	518.0	.681	.515	-3.092
5	38.3	1352	.0055423	17.38	-19.80	516.8	.681	.515	-3.089
6	40.1	1347	.0046522	14.63	-19.40	380.3	.681	.515	-3.038
7	38.6	1347	.0043764	13.76	-19.89	382.3	.681	.515	-3.101
8	38.9	1347	.0043943	13.82	-19.87	385.3	.681	.515	-3.101
9	38.2	1347	.0046955	14.76	-19.87	382.4	.681	.515	-3.094
10	38.9	1290	.0027881	9.04	-19.82	228.1	.683	.515	-3.032
11	38.7	1290	.0026114	8.47	-20.27	227.3	.683	.515	-3.099
12	38.1	1290	.0030990	10.05	-9.65	226.5	.683	.515	-1.489
13	38.7	1290	.0032607	10.58	-9.67	227.2	.683	.515	-1.478
14	37.9	1347	.0050836	15.99	-9.47	381.2	.681	.515	-1.488

heat of the screen c_s was evaluated at the initial screen temperature.

The burner Reynolds number N_{Re} was evaluated from the mass flow rate measurements of the combustible mixture to the burner. The burner diameter was used as the characteristic dimension.

The flow rates of the injected air or the perfusion gases through the screen were used to calculate the injection Reynolds number $(N_{Re})_0$. The screen radius was taken as the characteristic dimension. To coincide with the sign of the z-coordinate, negative injection velocity V_0 designates mass efflux from the screen surface exposed to the flame. The associated injection Reynolds number is also negative. A positive V_0 specifies suction through the screen surface exposed to the flame and it is associated with a positive Reynolds number.

The thermodynamic and transport properties of the gases were evaluated at the flame temperature T_f. For the two screens of 200 mesh and 150 mesh used in the tests, the reduced data was correlated through a least-square-fit criterion at each L/D spacing. The scaling parameters for a representative group of tests are given in Table 2.3.

The 200 mesh stainless steel screen has 0.053 mm wire diameter, a specific mass $(\rho\delta)_s = 0.0255$ g/cm^2 and an open area fraction of 33.6%. The resultant correlation equations for this screen are

$$(N_{Nu})_1 = 0.198(N_{Re})_0 + 0.516(N_{Re})^{0.59} \quad \text{for L/D} = 0.515 \qquad (2.3a)$$

$$(N_{Nu})_1 = 0.198(N_{Re})_0 + 14.83(N_{Re})^{0} \quad \text{for L/D} = 1.20 \qquad (2.3b)$$

$$(N_{Nu})_1 = 0.198(N_{Re})_0 + 14.09(N_{Re})^{0} \quad \text{for L/D} = 2.06 \qquad (2.3c)$$

$$(N_{Nu})_1 = 0.198(N_{Re})_0 + 15.07(N_{Re})^{0} \quad \text{for L/D} = 2.83 \qquad (2.3d)$$

The 150 mesh stainless steel screen has 0.066 mm wire diameter, a specific mass $(\rho\delta)_s = 0.0330$ g/cm^2 and an open area fraction of 37.4%. A resultant correlation for this screen is

$$(N_{Nu})_1 = 0.198(N_{Re})_0 + 0.655(N_{Re})^{0.59} \quad \text{for L/D} = 0.515 \qquad (2.4)$$

The predicted Nusselt number $(N_{Nu})_{1,p}$ values from the correlation equations (2.3) and (2.4) are compared with Nusselt number values from measurements $(N_{Nu})_1$, in Figure 2.10. The standard deviation from the 45^o line is 0.835.

2.2.4.4. Application to Prediction of Ignition Time. The discussion in the present section is concerned with the use of the results from the simulation experiments in the analysis for the prediction of fabric ignition times.

A lumped-parameter model has been formulated for the gas flame ignition of fabrics which accounts for (i) convective heating, (ii) thermal energy storage, (iii) radiative heat loss, (iv) desorption of moisture, and (v) pyrolysis [3,4]. The film coefficient $2\bar{h}_c$ in the set of governing equations for this model represents a value averaged over the front and back faces of the fabric. This coefficient can be evaluated from

$$2\bar{h}_c = \frac{\bar{h}_{c,1}(T_f - T) - \bar{h}_{c,2}(T - T_\infty)}{(T_f - T)} \tag{2.5}$$

if the values of $\bar{h}_{c,1}$ and $\bar{h}_{c,2}$ are known.

The film coefficient $\bar{h}_{c,2}$ can be estimated from equation (E.6) where

$$(N_{Nu})_2 = f\{(N_{Gr})_2, V_\delta\} \tag{2.6}$$

The film coefficient $\bar{h}_{c,1}$ can be estimated from a correlation given in equations (2.3) and (2.4).

Following the procedure outlined above film coefficients were evaluated for the thirteen igniting GIRCFF fabrics. To exhibit the common correlation of fabric ignition time as a function of heating intensity a normalized ignition time or Fourier number

$$(N_{Fo})_i = (k/\delta)\,\tau_i/\rho c\delta \tag{2.7}$$

and a normalized convective heat flux are defined [3,4]

$$q_c^* = [2\bar{h}_c/(k/\delta)](\theta_f - \bar{\theta}) \tag{2.8}$$

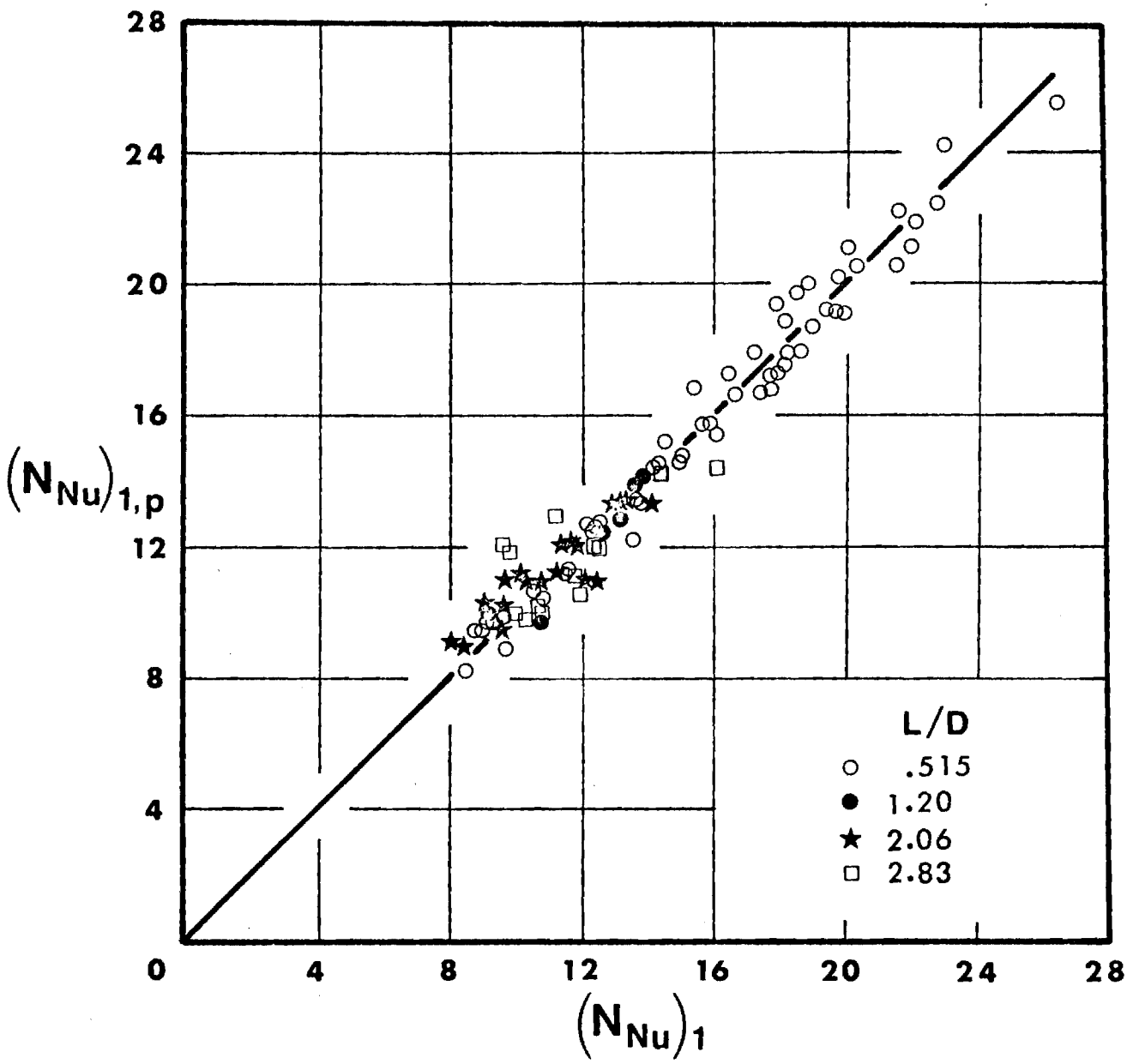

Figure 2.10. Correlation of Experimental Results

With the convective film coefficients determined through the procedure discussed above, measured ignition times for the thirteen fabrics are summarized in Figure 2.11 and compared with the inert heating model. Earlier correlations [5] did not account for the variation of fabric porosity and gas evolution in estimating convective film coefficients for these fabrics. When the present results are compared with these earlier results it is found that the standard deviation of the points from the line of inert heating has been reduced from 0.935 to 0.717 representing a 23% reduction. With some fabrics the reduction in the standard deviation has been found to be as much as 72%.

2.2.5. Task 5. Ignition Time Measurements on Fabric Assemblies Under Various Geometric Configurations

The objective of this task is to determine the effect of fabric interaction during radiative heating, and of fabric geometry and fabric orientation with respect to the flame axis during convective heating, on the ignition time.

2.2.5.1. Fabric Interaction. The Radiative Ignition Time Apparatus (RITA) for fabric ignition time measurements was used for the ignition tests of fabric assemblies. The description of RITA has been presented first in Reference [6]. Supplementary modifications are described in Reference [3]. Additional modifications required for measurements on fabric assemblies together with test procedures have been presented in Section 2.4.3 and Appendix A.3 of Reference [4]. No modifications were effected during the reporting period.

The total of 143 tests were conducted on the RITA to determine the interaction of two parallel fabric layers [16]. Tests were designed to examine the effects of variable heating intensity and variable inter-fabric spacing on the fabric assembly destruction time. The five heating intensities were 6.5, 7.6, 9.25, 13.8, and 16.2 W/cm^2. Fabric spacing was set at 0, 0.16, and 0.32 cm.

The combination of GIRCFF Fabric No. 5 at front (exposed to the radiant heating source) with the same fabric at back (exposed to the

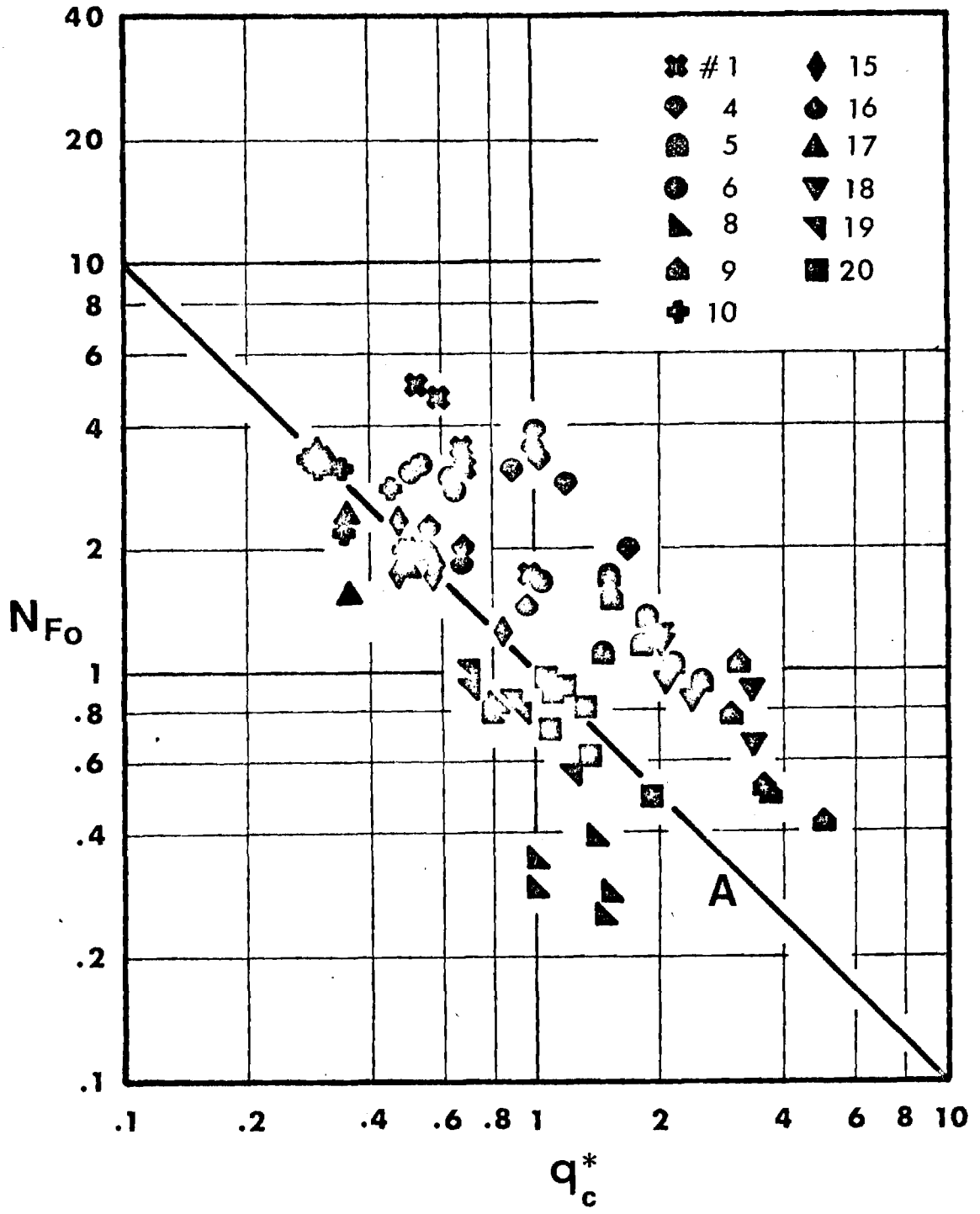

Figure 2.11. Normalized Ignition Times vs Normalized Convective Heat Flux for Thirteen Igniting Fabrics; Curve A is the Inert Heating Model

surroundings) was used for the majority of the tests. Tests were also conducted on the combination of GIRCFF Fabric No. 2 at front with No. 5 at back. Front fabric destruction times for the two combinations are given on Figures 2.12 and 2.13 and are compared with earlier single fabric ignition times [3].

The experimental data in Figure 2.14 are compared with predicted ignition times for the front fabric [16]. The normalized destruction time is defined by

$$(N_{Fo})_{i,m} = [(k/\delta)\tau_{i,m}]/(\rho\delta)c \tag{2.9}$$

and the normalized heat flux by

$$q_r^* = \alpha^* W_o/(k/\delta)(T_{i,m} - T_\infty) \tag{2.10}$$

where

$$\alpha_f^* = \tilde{\alpha}_f[1 + (\tilde{\tau}_f\tilde{\rho}_b)/(1 - \tilde{\rho}_f\tilde{\rho}_b)] \tag{2.11}$$

and

$$\alpha_b^* = \tilde{\alpha}_b\tilde{\tau}_f/(1 - \tilde{\rho}_f\tilde{\rho}_b) \tag{2.12}$$

for the front and back fabrics respectively.

In Figure 2.14 an inert heating model, in the absence of convective and radiative losses, is represented by curve A. A two-fabric assembly with the front fabric subjected to radiative heating and incorporating for both fabrics energy storage, radiative and convective cooling, moisture desorption, endothermic pyrolysis, and exothermic reaction has been used as a model for the analysis represented by curves B and C. Both solutions were carried out for a pair of GIRCFF Fabric No. 5 in the assembly. Curve B utilized kinetic parameters of pyrolysis of McCarter [3], and curve C modiefied kinetic parameters [16].

2.2.5.2. Effect of Geometry. The emphasis in the work presented here is on fabric ignition time for gas flame exposure at the fabric edge.

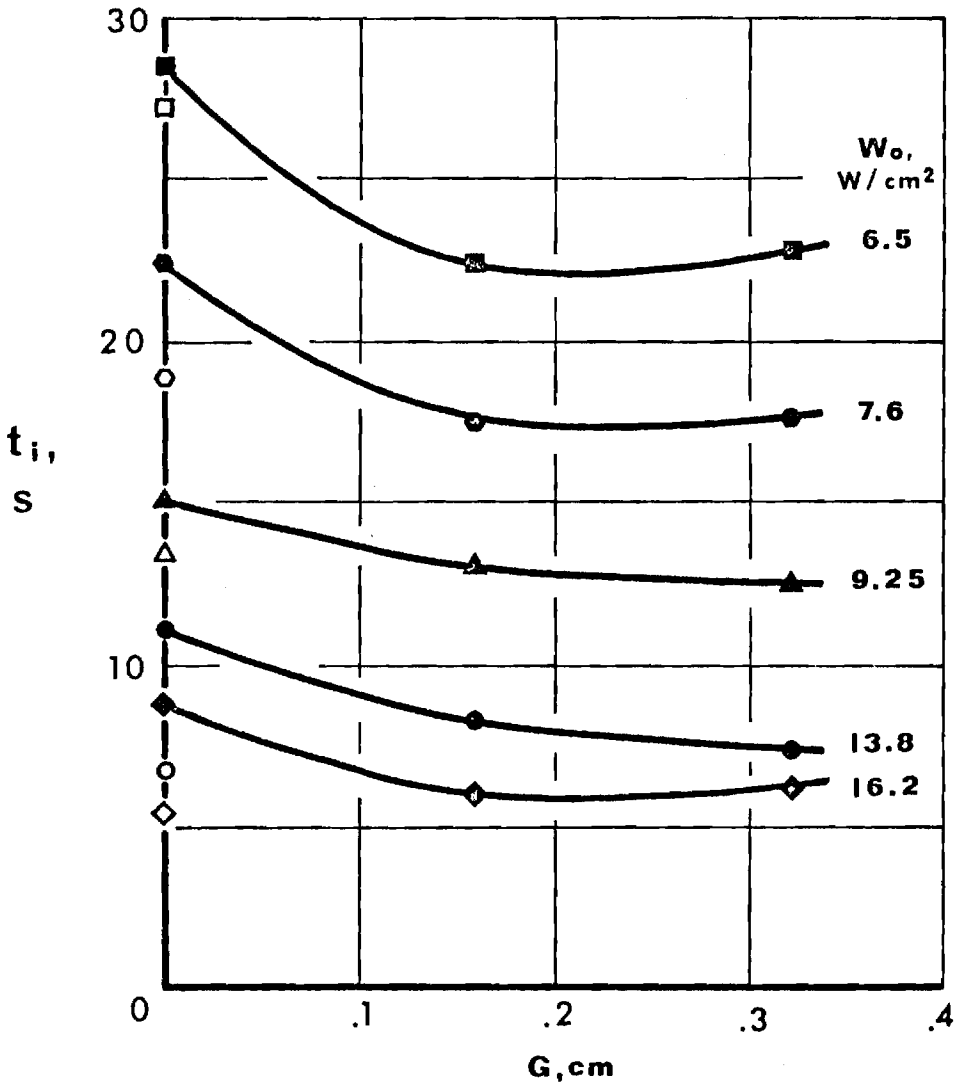

Figure 2.12. Ignition Time of Front Fabric as a Function of Spacing; GIRCFF Fabric No. 5 Front With No. 5 Back; Open Points Designate Single Fabric Ignition Times [3]

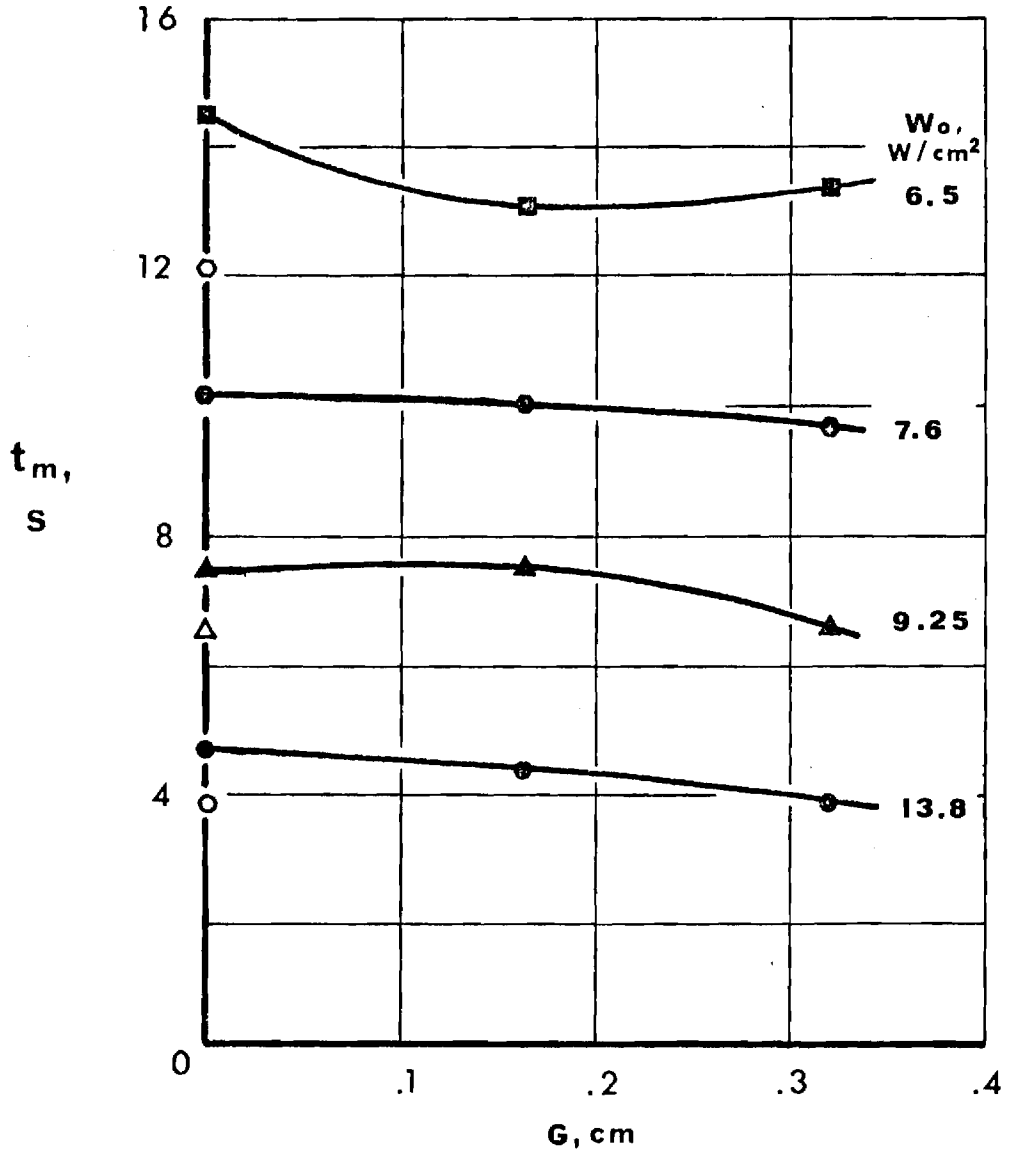

Figure 2.13. Melting Time of Front Fabric as a Function of Spacing; GIRCFF Fabric No. 2 Front With No. 5 Back; Open Points Designate Single Fabric Destruction Times [3]

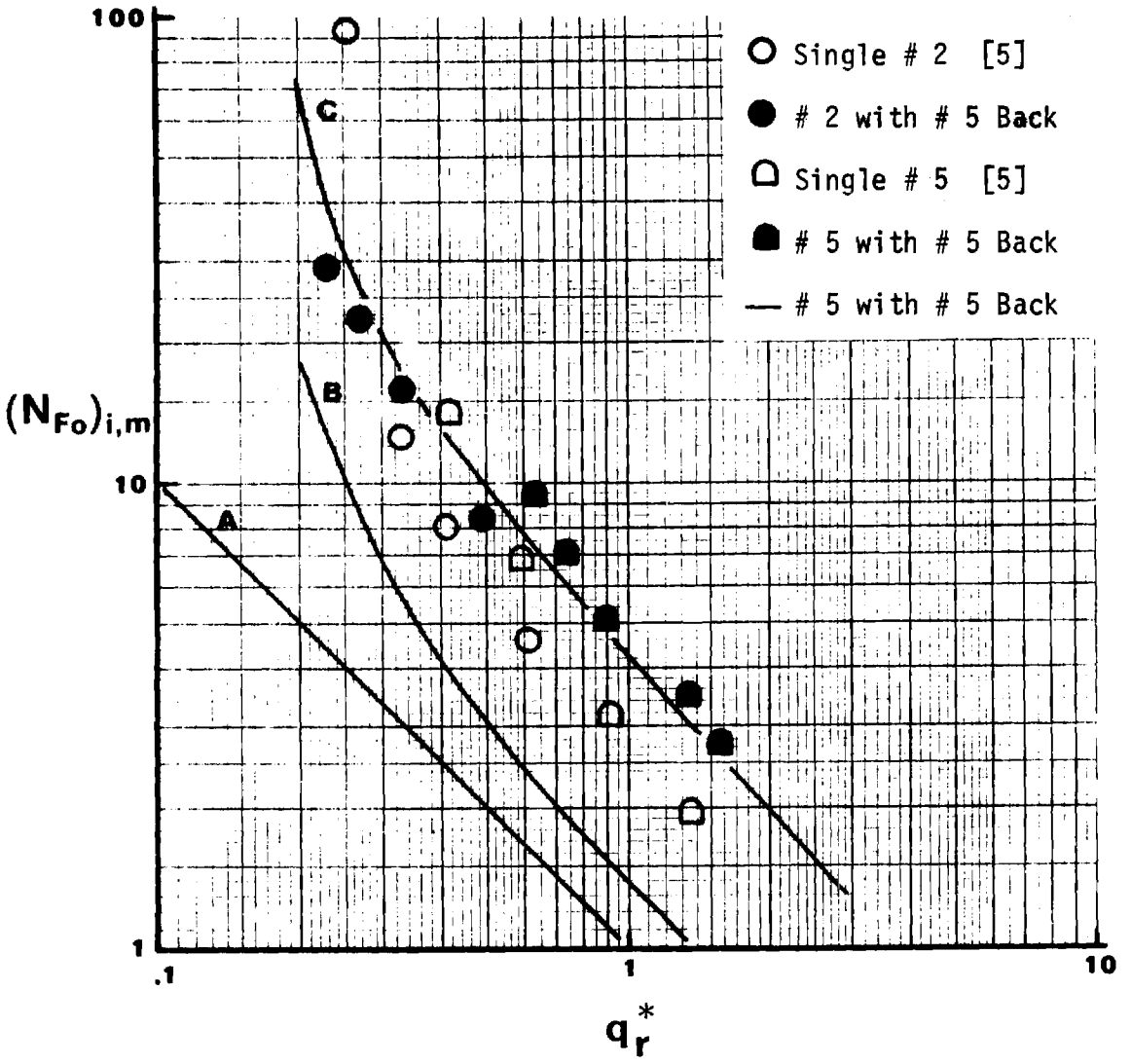

Figure 2.14. Normalized Destruction Times of the Front Fabric Compared With Single Fabric Destruction Times and Analysis; Curve A Inert Heating Model; Curve B With McCarter's Pyrolysis Data; Curver C Modified Pyrolysis Kinetics; Fabric Spacing 0.32 cm

To study these effects, fabric ignition time measurements were conducted with the Convective Ignition Time Apparatus (CITA) (see Appendix A). Modifications required for the fabric edge ignition tests together with the test procedures have been presented in Section 2.4.4 and Appendix A.3 of Reference [4].

Ignition tests were performed with 7.5x7.5 cm fabric samples. The fabric edge was positioned at a line coincident with the burner axis at 7.6 cm above the exit of the burner. The angle of impingement was varied at 0, 30, 60 and 90 degrees. The burner stoichiometric equivalence ratio was held at $\phi = 0.86$ and the burner mixture flow rates at 1260 and 2175 g/h.

Using the normalized ignition time and convective heat flux definitions given by equations (2.7) and (2.8), respectively, the edge ignition time measurements on six of the GIRCFF fabrics are presented on Figure 2.15. Curve A represents the inert heating model and the open symbols are ignition time measurements on fabric with flame impingement to the center of the fabric [3-5].

2.2.6. Task 6. Modeling Experiments on Extinguishment

Commencement of work of this task was scheduled for the early part of April 1975.

2.2.7. Task 7. Modeling Analysis of Ignition for Thermally Thin Media

Ignition times have been measured on single fabrics by exposing them to a time invariant convective source (gas flame) in the Convective Ignition Time Apparatus [3-5]. The purpose of the present investigation is to correlate these fabric ignition time measurements with predicted fabric ignition times from analysis.

The analysis for the ignition of fabric subject to normally impinging flames is presented in Appendix F. The ignition criterion proposed by Wulff [4], which considers ignition to occur in the boundary layer of the pyrolyzing solid, when the pyrolysate-air mixture locally reaches its

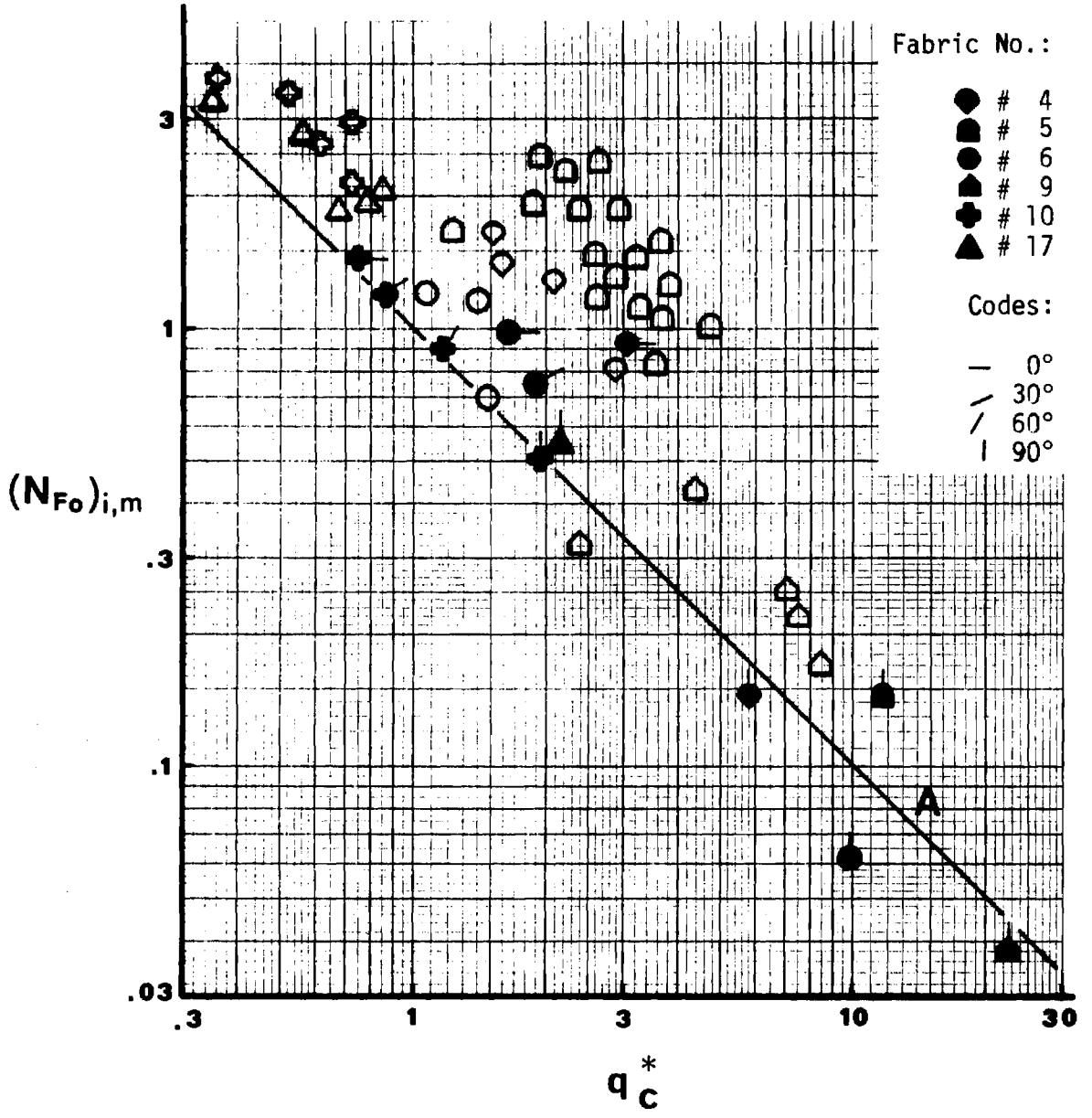

Figure 2.15. Normalized Fabric Edge Ignition Times vs Normalized Convective Heat Flux; Curve A Inert Heating Model; Open Symbols Normal Impingement at Fabric Center [3-5]

concentration-dependent minimum ignition temperature, has been incorporated in the present analysis. A second ignition criterion has also been developed which is called the inflexion method. This criterion considers ignition to occur when the pyrolysate mass fraction of the solid wall varies steeply with temperature.

Using the two criteria for ignition, ignition times have been predicted for five fabrics. The chemical kinetics data for the pyrolysis of these fabrics has been taken from Reference [3]. Concentration dependent ignition temperature data for fabric No. 5 have been obtained from Reference [9] and the coefficients C_0, C_1 and C_2 were evaluated using a least square fit. Comparing the temperature gradient at the fabric surface with the value obtained from numerical integration for frozen stagnation flow of a gaseous mixture over a surface [18], the velocity integral is estimated to be $I_v \simeq 2.02$ for Pr = Sc = 0.74. The free convective heat loss has been estimated using an empirical relation [19].

Predicted fabric ignition times, for GIRCFF Fabric No. 5, using the present analysis and Wulff's Ignition Criterion are presented on Figure 2.16. The heat loss effect on predicted ignition times appears to be significant at low flame temperatures.

The predicted fabric ignition times on five GIRCFF Fabrics using the Inflexion Method are compared with measured ignition times on Figure 2.17. Again, the agreement is quite reasonable at the high heating rates.

2.2.8. Task 8. Modeling Analysis of Ignition for Thermally Thick Media

The objective of the analysis is to predict the ignition time for thermally thick decomposing solids based on an ignition criterion to be imposed on the gaseous reaction in the boundary layer at the heated surface, and on fundamental material properties and process parameters.

The problem has been formulated for free convection along the radiatively heated surface. The governing conservation and constitutive equations for the decomposing solid and the gas phase adjacent to the surface exposed to radiant heating have been presented in detail in Appendix G.

Prediction of ignition time for the decomposing solid will be calculated using three ignition criteria and the results will be correlated.

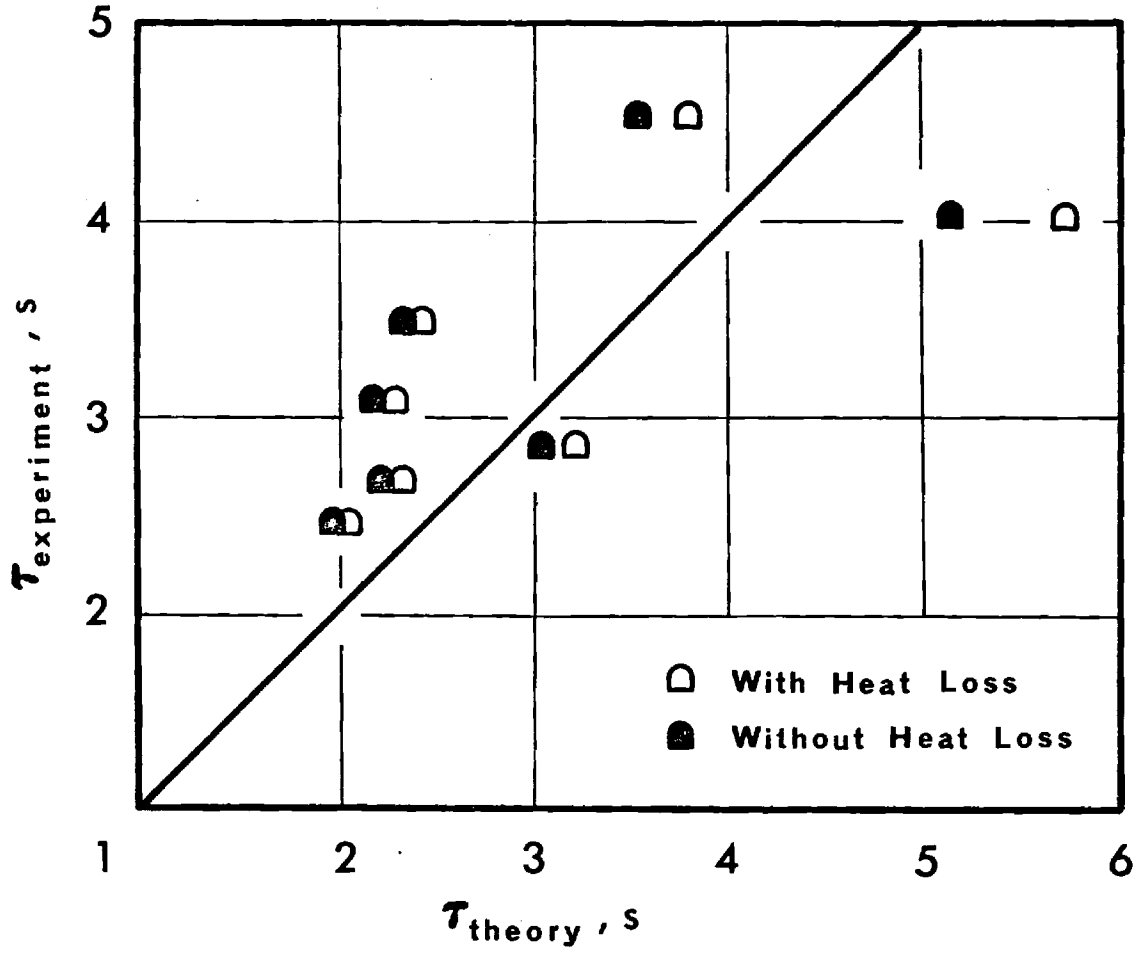

Figure 2.16. Effect of Convective Heat Loss from the Fabric on Predicted Ignition Times; GIRCFF Fabric No. 5

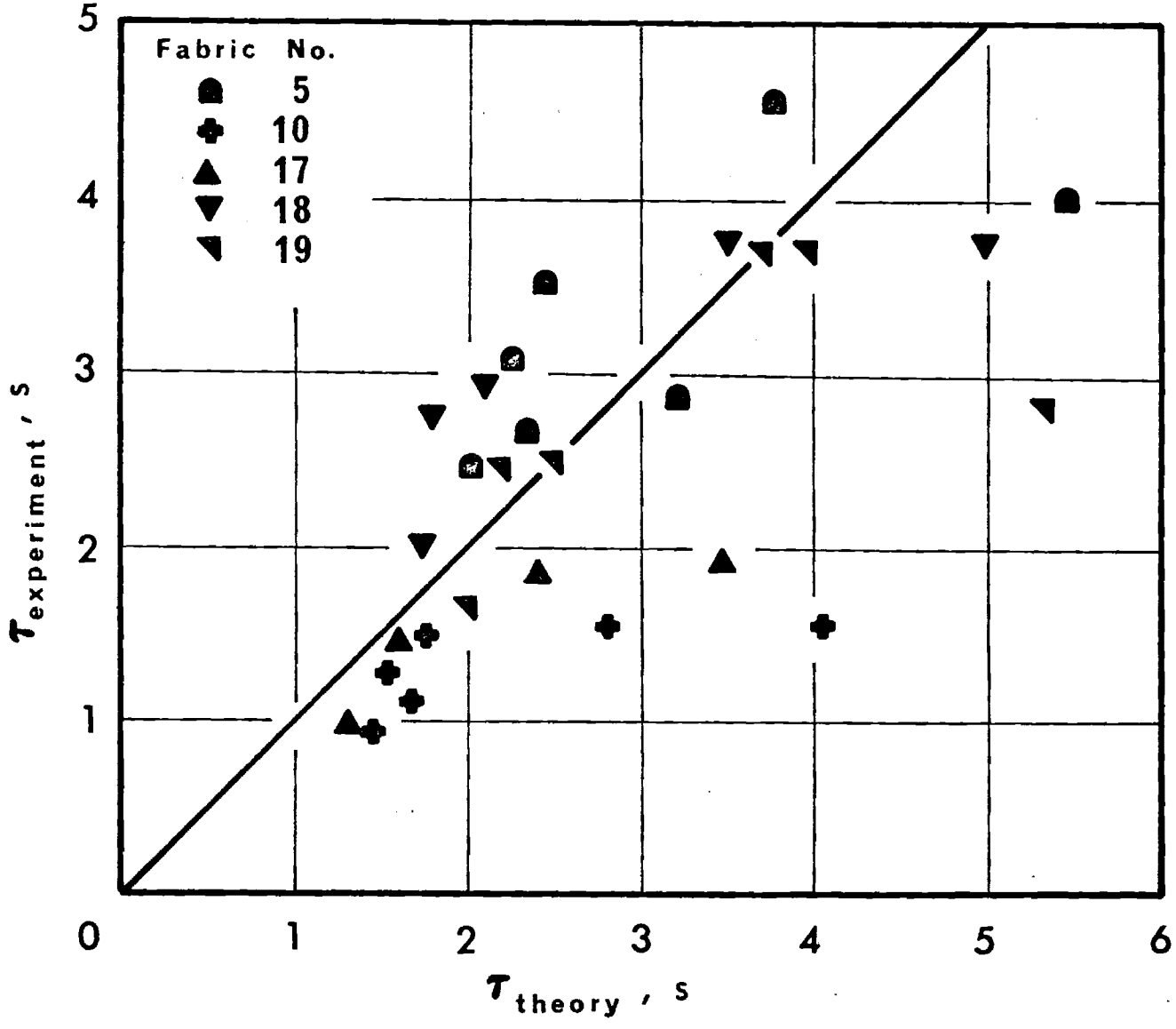

Figure 2.17. Predicted Fabric Ignition Times Using the Inflexion Method

3. SUMMARY OF ACCOMPLISHMENTS

Below are listed briefly the accomplishments achieved during the present reporting period. Previously obtained results are found in References [3, 4, 6].

3.1. Expermiental Efforts

The development of the new test facility for new experiments, namely Task 3, as discussed in Chapter 2, has passed through the design stages and is presently in the assembly stages. Three tasks, namely Task 2, 4 and 5 were initiated during the previous contract period. Tasks 4 and 5 were completed during the present reporting period. The first phase of Task 2 has been completed and is currently being continued under extended objectives.

Scheduled experimentation with existing and slightly modified instrumentation has progressed as planned. This is Task 1, where the total of 653 ignition tests have been performed under convective heating.

3.2. Analytical Effort

The modeling analysis of ignition for thermally thin media subject to convective heating has been completed using two ignition criteria: Wulff's Ignition Criterion and the Inflexion Method. Task 7 was not in the proposed program but has been carried out to augment present analyses for predicting ignition times of fabrics under gas flame heating.

The governing equations have been developed to describe the response to radiative heating of thermally thick decomposing solids. The problem has been formulated for free convection cooling the radiatively heated surface. Prediction of ignition time for the solid will be calculated using three ignition criteria and the results compared.

4. CHANGES IN RESEARCH PLAN, PERSONNEL AND MANAGEMENT

With the exception of Tasks 6 and 7 all other tasks are being performed or planned to be performed, without conceptual changes, as they were initially proposed. Task 6 was originally proposed as part of a two-year program. In view of the one-year funding of the proposal submitted December, 1973, and the present interest to continue with the ignition studies beyond the present grant period, Task 6 was replaced by Task 7. Task 7 was not in the original proposal program.

Grant GI-31882A#2 officially started on April 1, 1974 with Dr. W. Wulff as Project Director and Dr. P. Durbetaki as Co-Principal Investigator. This grant was amended and the present grant GI-31882A#3 designates Dr. P. Durbetaki as the Principal Investigator effective June 1, 1974. The official expiration date of this grant is September 30, 1975. Completion of the program is expected by that time.

Mr. K. Annamalai, who started in this program as a Graduate Research Assistant June, 1974, has been employed as an Assistant Research Engineer beginning with April 1, 1975. He has completed all the requirements for the Ph.D. degree and is working half-time on Tasks 7 and 8.

5. FUTURE PLANS

The research plans for the tasks completed and continuing during the present contract period are summarized below.

Task 1: Measurement of Ignition Statistics on Thermally Thin Media, Subject to Convective Heating will be completed by the middle of May.

Task 2: Measurement of Ignition Temperature on Pyrolysate-Air Mixtures should begin testing with the modified reaction cell during April and complete tests by the end of August 1975.

Task 3: Measurement of Ignition Statistics on Thermally Thick Media Subject to Radiative Heating. The equipment assembly should be completed by the end of April 1975. The ignition tests are expected to commence in May and completed in August 1975.

Task 4: Measurement of Convective Film Coefficients Under Simulated Pyrolysate Evolution was completed October 1974.

Task 5: Ignition Time Measurements on Fabric Assemblies Under Various Geometric Configurations was completed December 1974.

Task 6: Modeling Experiments on Extinguishment. In view of the objectives of the new proposal to continue the ignition studies, this task has been replaced by Task 7.

Task 7: Modeling Analysis of Ignition for Thermally Thin Media was not in the proposed program but was introduced to replace Task 6. The present task has been completed during January 1975.

Task 8: Modeling Analysis of Ignition for Thermally Thick Media will continue through June 1975.

The annual report will be prepared during the month of September 1975. A new proposal for the expansion of ignition studies has been prepared and will be submitted April 1975.

6. UTILIZATION EFFORTS

6.1. Personnel

There are currently one Principal Investigator, one Assistant Research Engineer and two M.S. students contributing to the research. In addition, there is one undergraduate student employed on an hourly salary basis.

Principal Investigator Dr. P. Durbetaki is in charge of the program and supervises the execution of all the tasks. Assistant Research Engineer K. Annamalai completed the modeling analysis, Task 7 and is currently working on the modeling analysis of thermally thick media Task 8.

Tasks 4 and 5 were M.S. thesis projects and were carried out to completion by Gregory L. Wedel and Robert L. Acree respectively. The first phase of Task 2 was an M.S. thesis project and was completed by Paul T. Williams. The continuation of this task is presently being formulated as an M.S. thesis project by William P. Ryszytiwskyj.

Task 3 is an M.S. thesis project and is being carried out by Gary L. Matson. The experimental measurements in Task 1 are being carried out by Wayne C. Davis, undergraduate research assistant.

6.2. Funding

Research activities to be performed under this grant are projected at this time to be funded until September 30, 1975. The proposed objectives of this grant are expected to be completed at that date.

7. PUBLICATIONS AND PRESENTATIONS

The research results from Grant GK-27189 and Grant GI-31882 (A#1-A#3) have been disseminated through a number of different channels and are summarized in the sections that follow.

7.1. Referred Papers

1. Wulff, W., Zuber, N., Alkidas, A., and Hess, R. W., "Ignition of Fabrics Under Radiative Heating", Combustion Science and Technology, 6, 1973, pp. 321-334.

2. Wulff, W., Alkidas, A., Hess, R. W., and Zuber, N., "Fabric Ignition", Textile Research Journal, 43, 1973, pp. 577-588.

3. Wulff, W., and Durbetaki, P., "Fabric Ignition and the Burn Injury Hazard", Heat Transfer in Flames, N. H. Afgan and J. M. Beer, editors, Scripta Book Co., Washington, D. C., 1974, pp. 451-461.

4. Acree, R. L., Durbetaki, P., and Wulff, W., "Ignition of Fabric Assemblies Subject to Radiative Heating", to be presented at the Joint Central and Western States Sections, The Combustion Institute, San Antonio, Texas, April 21-22, 1975.

5. Annamalai, K., and Durbetaki, P., "Ignition of Single Fabrics Subject to Normally Inpinging Flames", to be presented at the Joint Central and Western States Section, The Combustion Institute, San Antonio, Texas, April 21-22, 1975.

6. Durbetaki, P., Wedel, G. L., and Wulff, W., "Flame-Fabric Interaction During Preignition Processes", to be presented at the 15th National Heat Transfer Conference, San Francisco, California, August 10-13, 1975.

Two of the above papers were presented on invitation at these meetings: Paper No. 2 at the Symposium on Textile Finishing Chemistry, 164th National Meeting, ACS, New York, N.Y., August 30 - September 1, 1972; Paper No. 3 at the 1973 International Seminar on Heat Transfer from Flames, Trogir, Yugoslavia, August 27-31, 1973.

7.2. Reports

The research results have been summarized in six Quarterly Progress Reports and one Semiannual Progress Report. They are presented in detail in the three Annual Final Reports:

1. Wulff, W., Zuber, N., et al., "Study of Hazards from Burning Apparel and the Relation of Hazards to Test Methods", (First Annual) Final Report, NSF Grant No. GK-27189, School of Mechanical Engineering, Georgia Institute of Technology, Atlanta, Georgia, 1971, NTIS Accession No. COM-73-10954.

2. Durbetaki, P., Wulff, W., et al., "Study of Hazards from Burning Apparel and the Relation of Hazards to Test Methods", Second Annual Report, NSF (RANN) Grant No. GI-31882, School of Mechanical Engineering, Georgia Institute of Technology, Atlanta, Georgia, 1972, NTIS Accession No. COM-73-10956.

3. Durbetaki, P., Wulff, W., et al., "Fabric Ignition", Third Annual Report, NSF (RANN) Grant No. GI-31882, School of Mechanical Engineering, Georgia Institute of Technology, Atlanta, Georgia, 1974.

7.3. Seminars and Conferences

1. "Seminar on Fabric Flammability", School of Mechanical Engineering, Georgia Institute of Technology, May 19, 1972. Invitations were extended to appropriate executives from Textile Manufacturing and Distributing Industries, from Insurance Industry and from Government in Georgia, and to the Georgia Tech community.

2. Contractors meeting of the National Science Foundation (RANN) Fire Research Program, Applied Physics Laboratory, The John Hopkins University, Silver Springs, Maryland, June 22-23, 1972.

3. Materials Technology, Today and Tomorrow, Georgia Tech Seminar for Whirlpool Corp., Atlanta, Georgia, March 21, 1973.

4. Wulff, W., and Durbetaki, P., "Study of Hazards from Burning Apparel and the Relation of Hazards to Test Methods", Proceedings of the Flammability Characteristics of Materials, Polymer Conference Series, University of Utah, Salt Lake City, Utah, June 11-15, 1973 (Invited Lecture).

5. Wulff, W., and Durbetaki, P., "Study of Hazards from Burning Apparel and the Relation of Hazards to Test Methods", Conference on Firesafety for Buildings: Research - Practice - Needs, Airlie House, Warrenton, Virginia, July 18-20, 1973.

6. Wulff, W., Durbetaki, P., et al., "Ignition Probability and Fire Hazard", Engineering Science and Mechanics Seminar, Georgia Institute of Technology, Atlanta, Georgia, September 27, 1973.

7. Durbetaki, P., and Wulff, W., "The Georgia Tech Fabric Flammability Research", Third Flame-Free Design Conference, Atlanta, Georgia, March 13-15, 1974 (Invited Lecture).

8. Wulff, W., and Durbetaki, P., "Fabric Ignition", NSF/RANN Conference on Fire Research, Georgia Institute of Technology, Atlanta, Georgia, May 28-29, 1974.

9. Durbetaki, P., "Ignition of Thermally Thin Media Subject to Convective Heating", to be presented at the Eleventh Annual Southeastern Seminar on Thermal Sciences, Knoxville, Tennessee, April 28-29, 1975.

10. Naveda, O. A., Durbetaki, P., and Wulff, W., "Probability of Fabric Ignition Under Given Exposure Conditions", to be presented at the International Symposium on Fire Safety of Combustible Materials, Edinburgh, England, October 15-17, 1975.

7.4. Theses and Special Problems

7.4.1. Completed Theses and Special Problems

1. "The Study of Preignition Behavior of Selected Fabrics and Consequent Burn Injury Probability", C. S. Kirkpatrick, M.S. Thesis, June, 1972.

2. "Optical Properties of Fabrics", P. T. Williams, Undergraduate Special Problem, August, 1972.

3. "Reaction Kinetics of Fabrics", W. E. Giddens, M.S. Thesis, March 1973.

4. "Determination of Fabric Ignition Times Through Use of a Convective Heat Source, E. R. Champion, Jr., M.S. Thesis, June 1973.

5. "Study of Actual Ignition Sources of Clothing", O. A. Naveda, M.S. Thesis, June 1974.

6. "Determination of Film Coefficients with Simulated Pyrolysate Injection", G. L. Wedel, M.S. Thesis, October, 1974.

7. "Ignition Temperature Measurement on Pyrolysate-Air Mixtures", P. T. Williams, M.S. Thesis, October, 1974.

8. "Ignition Time Measurement on Fabric Assemblies Under Various Geometric Configurations", R. Acree, M.S. Thesis, December 1974.

7.4.2. Theses in Progress

1. "Measurement of Ignition Statistics on Thermally Thick Media, Subject to Radiative Heating", G. Matson, M.S. Thesis.

2. "Measurement of Ignition Temperature on Pyrolysate-Air Mixtures", W. P. Ryszytiwskyj, M.S. Thesis.

APPENDIX A
CONVECTIVE IGNITION TIME APPARATUS (CITA)

The Convective Ignition Time Apparatus (CITA) has been operated before for ignition time measurements of the twenty GIRCFF fabrics. These are identified in Table A1 below. The two-shutter system, the gas burner, and the related instrumentation are the major components of CITA. A detailed description of the operating principles, design details, and procedures for the static and dynamic modes of operation are given in References [3,4]. The tests conducted in the static modes have the two-shutter system operating in single action. That is, at the appropriate time the two-shutter system is actuated to open, expose the fabric to the convective heat source and remain open through the fabric destruction period.

To conduct the measurements of ignition statistics a shutter control timing system was designed and built. The control timing system consists of the left and right shutter solenoids, a high interval timer, a low interval timer, an electronic counter, and a microswitch. Both timers are General Time solid state timers, Series 2111-IPF-010 and 2111-IPF-001, and provide timed intervals of 0.5-10 seconds and 0.1-1 second respectively. They can be used in series or independently. The Electronic Counter is a Hewlett-Packard Model 5233L and is used to measure the actual elapsed time from shutter separation to closing. The control timing system then provides the means of controlling the exposure of the fabric to the convective heat source by timing and measuring the period when the shutters remain open. For the ignition statistics tests the two-shutter system operates in double action.

Table A1. Fabric Identifications and Specific Mass

GIRCFF No.	Classification	Fiber Composition	Color	Finish	Specific Mass mg/cm^2
1	Durable Press Slack	65/35% Pe./C.	White	DP treated	23.49
2*	Textured Woven Blouse	100% Polyester	Yellow	-	7.51
3	Double Knit	100% Polyester	White	-	20.91
4	Denim	100% Cotton	Navy bl.	-	29.63
5*	T-Shirt, Jersey	100% Cotton	White	-	13.71
6	Untreated Slack	65/35% Pe./C.	White	-	23.57
7	Jersey Tube Knit	100% Acrylic	Gold	-	15.13
8*	T-Shirt, Jersey	65/35% Pe./C.	White	-	16.19
9	Terry Cloth	100% Cotton	White	-	26.48
10*	Batiste	100% Cotton	Purple	-	6.65
11*	Tricot	80/20% Acet./ Nyl.	White	-	11.31
12*	Tricot	100% Nylon	White	-	8.91
13*	Tricot	100% Acetate	White	-	9.40
14	Taffeta	100% Nylon	White	-	5.66
15	Durable Press Slack	65/35% Pe./Ray	Brown	DP treated	22.82
16	Shirting	50/50% Pe./C.	White	-	13.14
17*	Batiste	65/35% Pe./C.	White	-	8.55
18*	Flannel	100% Cotton	White	-	12.88
19*	Flannel	100% Cotton	White	Fire retard	14.89
20	Flannel	100% Wool	Navy bl.	-	19.93

*Ten Primary GIRCFF Fabrics.

APPENDIX B
LOWER IGNITION TEMPERATURE AND CONCENTRATION APPARATUS (LITACA)

An integral part of the evaluation of the newly proposed ignition criterion is the measurement of the lowest ignition temperature of isothermal pyrolysate-air mixtures, as a function of pyrolysate concentration. The Lower Ignition Temperature and Concentration Apparatus has been designed and constructed to accomplish this task. Detailed descriptions of LITACA and the operating procedures have been presented in Appendix A.1 of Reference [4]. This Appendix describes the modifications in the apparatus carried out during the reporting period [9]. The major components of LITACA remain the same and they are shown in a schematic form on Figure B.1.

B.1. Pyrolysate Generating Furnace

The original design of the Pyrolysate Generating Furnace had twelve General Electric tungsten filament lamps installed. During the first test of the furnace the quartz casings of the lamps failed and they were replaced by two cylindrical half-shell, 1720 watt, 230 volt, Model RH 256 heaters from Thermal Corporation, Huntsville, Alabama. The heaters are wired in parallel. The assembly drawing of the modified Pyrolysate Generating Furnace is presented in Figure B.2 together with the volatile reservoir. A chromel-alumel thermocouple has been positioned near the center of the furnace core, outside the quartz furnace tube, to monitor the furnace temperature.

B.2. Reaction Cell

A guard heater has been built by embedding a 10 ohm coil of nichrome wire inside an insulating cap with Sauereisen Insa-Lute adhesive cement.

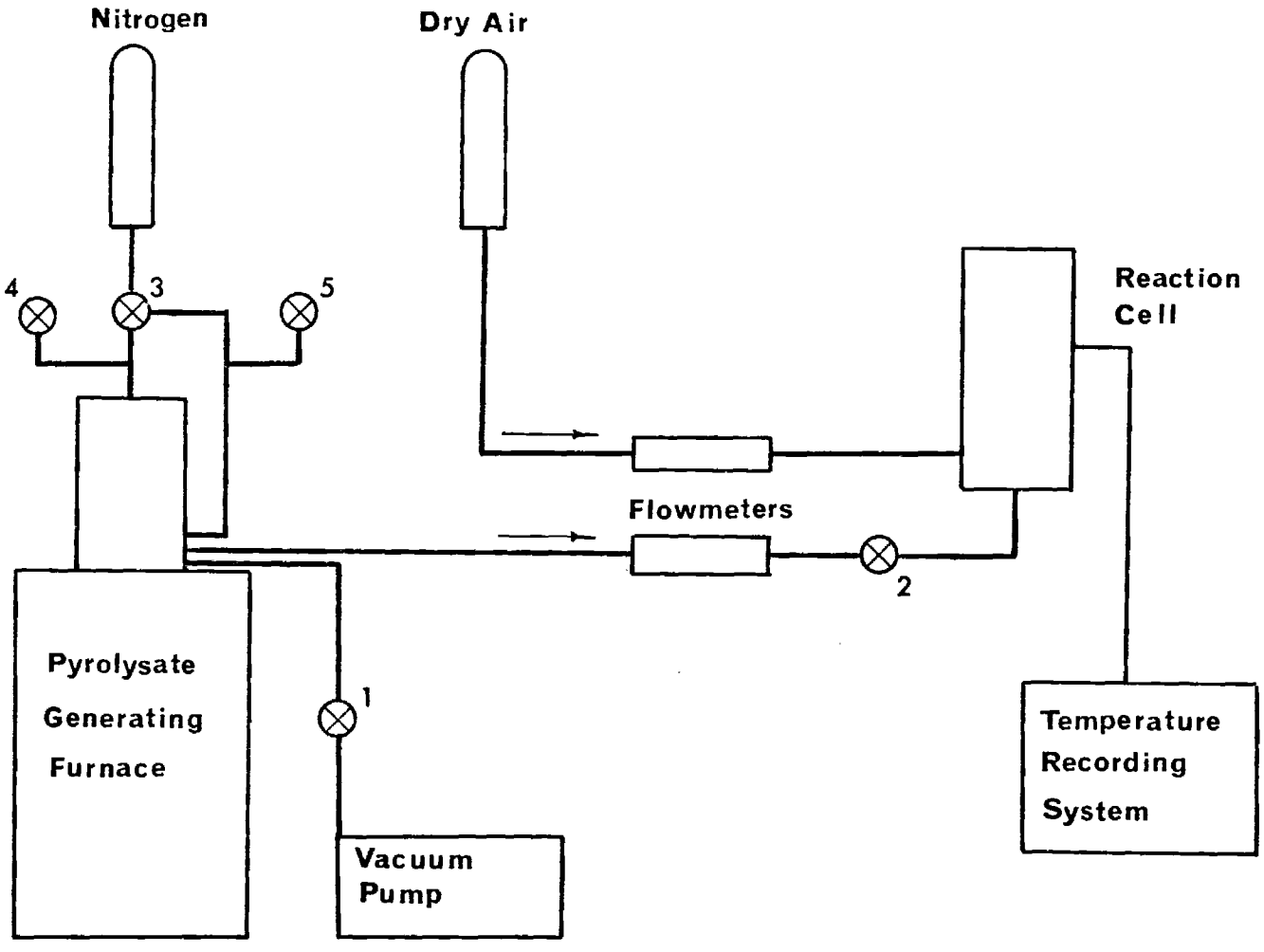

Figure B.1. Schematic Diagram of the Lower Ignition Temperature and Concentration Apparatus (LITACA)

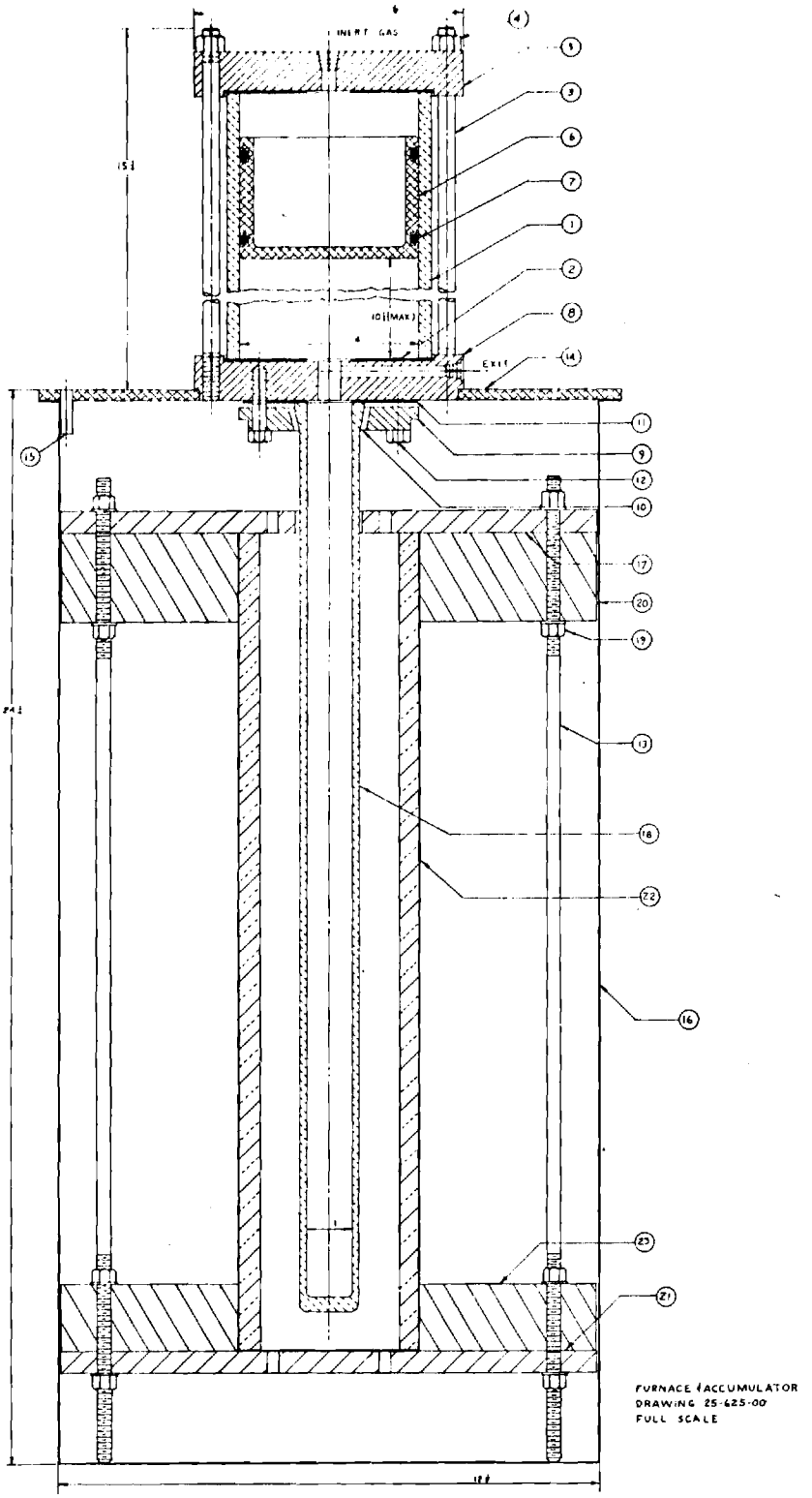

Figure B.2. Cross Section of Pyrolysate Generating Furnace and Accumulator of LITACA

Key to Figure B.2

Part No.	Description	Material	Req'd
1	Accumulator Barrel	Pyrex Glass	1
2	Gasket	Teflon	1
3	Threaded Rod	Cold Worked Steel	6
4	3/8-24 UNF Hex Nut	SAE Grade 5	6
5	Accumulator End Cap	304 Stainless Steel	1
6	Accumulator Piston	6061-T6 Aluminum	1
7	"O" Ring	Neoprene	2
8	Accumulator Manifold	304 Stainless Steel	1
9	Flange	Cast Iron	1
10	Insert	Neoprene	1
11	Gasket	Teflon	1
12	5/16-18UNC Hx Hd Bolt	SAE Grade 5	4
13	5/16-18UNC Threaded Rod	SAE Grade 5	4
14	Furnace Mounting Plate	6061-T6 Aluminum	1
15	ESNA "Rollpin"	Steel	3
16	Furnace Housing	3003-H14 Aluminum	1
17	Furnace Heater Support	Transite	1
18	Furnace Test Tube	Fused Quartz	1
19	5/16-18UNC Hx Hd Nut	SAE Grade 5	16
20	Upper Support Ring	Asbestos	1
21	Furnace Heater Support	Transite	1
22	Heating Element Casing	Ceramic	1
23	Lower Support Ring	Asbestos	1

The insulating cap has been placed on the top of the Reaction Cell, as shown in Figure B.3, to surpress heat losses from the top.

A new quartz tube bundle has been prepared consisting of seventeen 30 mm and two 144 mm long tubes bound together by stainless steel wire rings. Approximately 570 mm of 0.13 mm diameter nickel wire was passed through the tubes and attached to the tungsten terminal pins via a five strand nickel wire lead. A chromel-alumel thermocouple with ceramic insulation was positioned in the center of the tube bundle, with its leads exiting the Reaction Cell through a hole in the center of the insulating cap.

A temperature transverse through the center of the ignition tube, with the Reaction Cell heaters in equilibrium is shown in Figure B.4. It indicates that an isothermal region exists in the ignition tube and it includes the entire length of the 30 mm tube bundle.

B.3. Auxiliary Systems and Components

In view of the inability to achieve self-ignition of the pyrolysate-air mixtures as generated by the furnace, a cold trap type condenser was installed between the accumulator manifold and the inlet to the pyrolysate flow meter. The cold trap consisted of a hollow glass sphere approximately 7.6 cm in diameter. The sphere was immersed in an ice water bath.

All pyrolystate gas lines and the pyrolysate accumulator cylinder have been wrapped with chromel-alumel thermocouple wire. These wires have been connected to variable autotransformers to act as guard heaters and prevent pyrolysate condensation before the gases reach the cold trap.

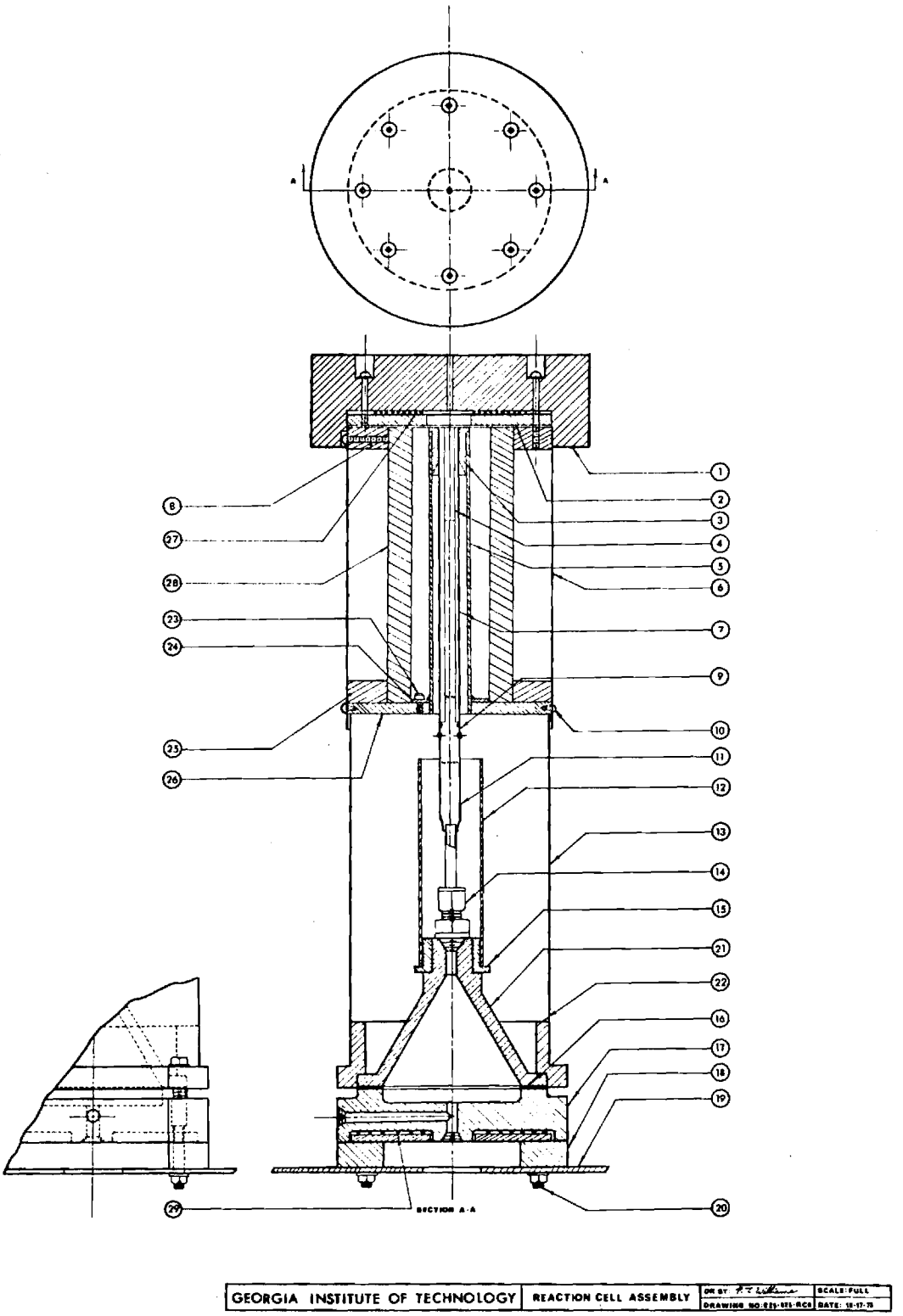

Figure B.3. LITACA Reaction Cell Cross Sectional View

Key to Figure B.3

Part No.	Description	Material	Req'd
1	Insulation Cap	Asbestos	1
2	Reaction Cell Lid	Transite	1
3	Bushing	Transite	1
4	Tube Bundle	Quartz	1
5	Ignition Tube Shield	Stainless Steel	1
6	Upper Cell Housing	6061-T6 Aluminum	1
7	Ignition Tube	Fused Quartz	1
8	Bushing	Transite	1
9	Graded Seal	Quartz-Pyrex Glass	1
10	6-32UNC Rd Hd Mach Scr	SAE Grade 5	4
11	Seal	Pyrex Glass-Kovar	1
12	Lower Guard Htr Support	Stainless Steel	1
13	Lower Cell Housing	6061-T6 Aluminum	1
14	1/8NPT-1/4 Male Conn.	316 Stainless Steel	1
15	Bushing	Transite	1
16	Gasket	Teflon	1
17	Mixing Chamber	Chrome Plated Brass	1
18	Spacer	Transite	2
19	Support Shelf	Aluminum	1
20	1/4-20UNC Nut & Bolt	SAE Grade 5	4
21	Flame Arresting Chamber	Chrome Plated Brass	1
22	Bushing	Transite	1
23	6-32UNC Hx Hd Mach Scr	SAE Grade 5	3
24	Flange	Stainless Steel	1
25	Bushing	Transite	1
26	Upper Cell Floor	Transite	1
27	Upper Guard Heater	Nichrome Wire	1
28	Ignition Heater	Chrome-Al-Fe Wire	1
29	Lower Guard Heater	Nichrome Wire	1

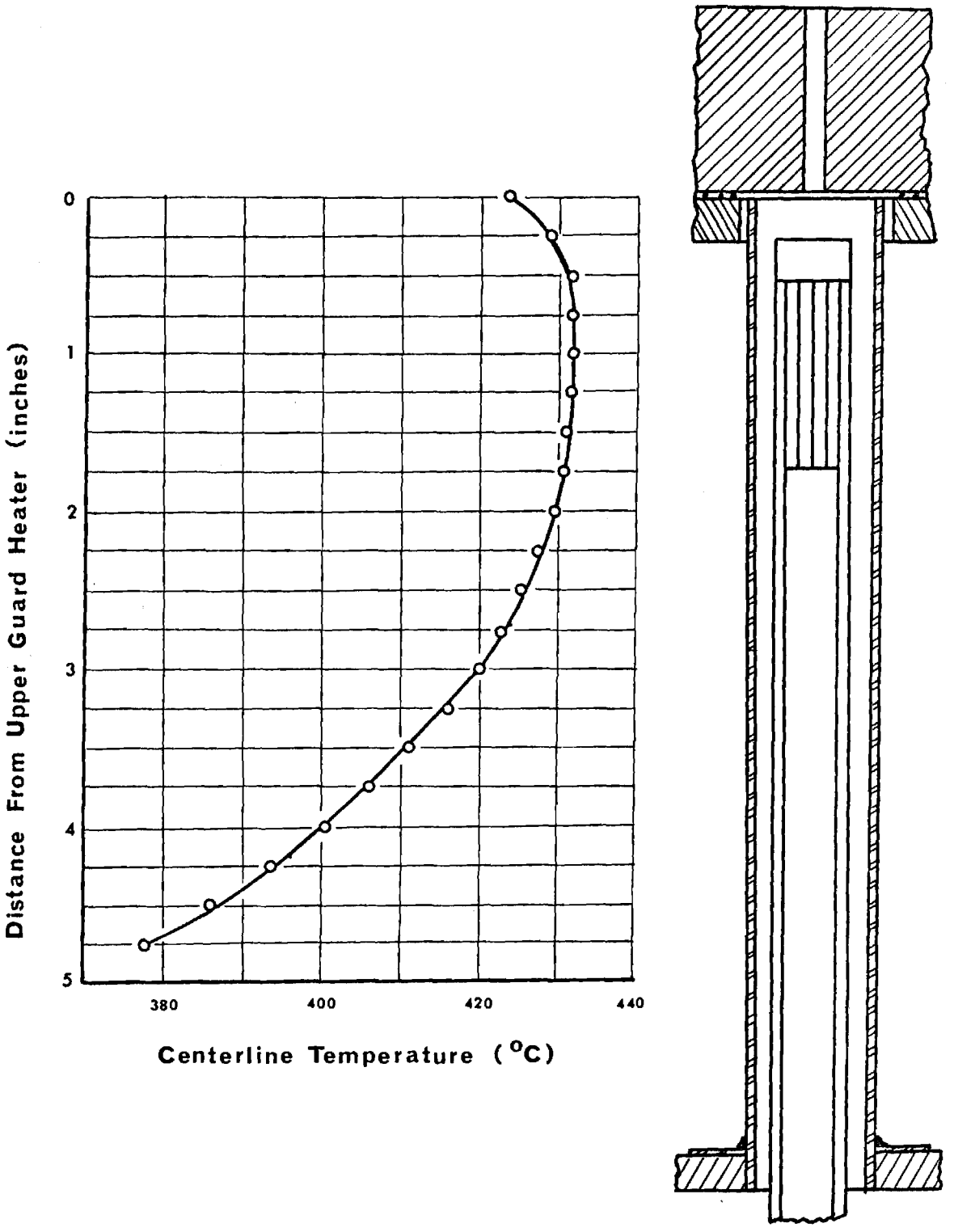

Figure B.4. Temperature Profile Along Axis of Ignition Tube

APPENDIX C
LARGE IGNITION TEST APPARATUS (LITA)

The Large Ignition Test Apparatus (LITA) has been designed to conduct ignition time measurements and ignition statistics on thermally thick media exposed to radiative heating. The apparatus consists of six sub-assemblies:

(i) The radiant heater stack,

(ii) The two vertical shutter systems,

(iii) The sample holder and disposal system,

(iv) The supporting structure,

(v) The instrumentation for remote control, shutter timing and flame detection, and

(vi) The exhaust system.

Details of these sub-assemblies are discussed in the section below. The reader is referred to Figures 2.8 and 2.9 in Section 2.2.3.

C.1. Radiant Heater Stack

The heater assembly consists of six radiant heaters stacked vertically. These six heaters comprise a total heating area of 50 cm by 40 cm. The heaters are Model 5208-16 RI radiant heaters. Each contains six 1600T3/1CL tungsten filament high temperature quartz lamps. The heaters will be operated using 220 volts AC power and providing a maximum of 240 amps. A variac power control will be used to control the input to the heaters which in turn provide a net heat flux at the heater window surface up to 20 watts/cm^2. The heaters are air and water cooled.

C.2. Shutter Systems

The vertical two shutter assembly consists of two systems, each

composed of the following: a shutter, a pneumatic cylinder, a shock absorber, two case hardened guide rods, shutter rod supports and four linear ball bushings.

Both shutters are manufactured from 3.2 mm copper sheet and the lower shutter will be water cooled to prevent pre-exposure heating of the ignition test sample. Attached to each shutter are four Thompson Series A linear ball bushings. These bushings travel on two 19 mm diameter case hardened rods. Prior to the initiation of an ignition test, the shutters are supported each by a pair of spring catch mechanisms. These mechanisms will release when the pneumatic cylinder exerts on the shutter a force in excess of 22 newtons. The pneumatic cylinders are Parker Hannifin Model 2PR16x6 spring return air cylinders. The air cylinders have a 5.1 cm bore and 15 cm stroke. Laboratory air will be used to operate the air cylinders, activated by Modernair three-way solenoid popet valves. The shutters will be stopped each by an Activation "Shok Block" adjustable hydraulic shock absorber, Model ASB1-3PS99. The shock absorber has a storke of 7.6 cm.

C.3. Sample Holder and Disposal

The sample holder assembly will position the samples 4.6 cm from the heater assembly. The sample support will be spring loaded and upon actuation of four remotely controlled Dormeyer Super-C Folded Frame Solenoids the sample will drop vertically into a receptacle for extinguishment.

C.4. Supporting Structure

The supporting structure of LITA consists primarily of eight vertical steel angles. Each of these angles is 2.88 m long. Braces and platform supports are bolted to these angles. The entire structure is bolted to a 1.8 m by 1.8 m steel angle base.

C.5. Instrumentation

The instrumentation consists primarily of the heater power control and monitoring group, shutter activation and exposure time measuring instruments, and heat flux and ignition detection instrumentation. A six stack variac will be used to adjust the level of power supplied to the heaters and monitored on the control panel. Incorporated on the control panel are pre-exposure sequencing switches and light indicators as well as shutter activation switches. A Fisher Model 6-664-30 micro-timer, also mounted on the control panel will be activated through micro-switches by the travelling shutters to measure sample exposure times. Asymptotic heat flux meters will be used to calibrate the heating lamps and infrared detectors to sense ignition of the samples under single shutter mode of operation. The output of the infrared detectors will be fed to oscilloscopes to record changes in the signal on polaroid film.

C.6. Exhaust System

The smoke exhaust system consisting of a large hood and a fan will be used to drive the pyrolysis gases, particulates and combustion gases from test region through a high temperature stack to the outside. The hood is mounted to the top of the four vertical columns of the structure and connected to the 3/4 horsepower fan through a flexible duct. A slide valve in the hood will provide adjustment to the forced convection past the test region.

C.7. Experimental Procedure

Test samples will be conditioned in the enviromental chamber at desired humidity and temperature for a minimum period of twenty-four hours prior to testing. The procedures to be followed during a test will be similar to those used on fabric ignition measurements and fabric ignition statistics with the Radiative Ignition Time Apparatus (RITA) and reported in References [3,4,6].

APPENDIX D
CONVECTIVE FILM COEFFICIENT APPARATUS (CFCA)

The Convective Film Coefficient Apparatus (CFCA) was designed to simulate the flame-fabric interaction and at the same time serve as one leg of a thermocouple to sense its transient mean temperature when exposed to normally impinging flames of known characteristics in the Convective Ignition Time Apparatus. The volatile evolution is simulated by injecting preheated air through the screen. The CFCA consists of three primary components:

(i) an aluminum clevis and its support rod,

(ii) a transite inlet chamber and pprous bronze assembly, and

(iii)an inert wire cloth and screen holder assembly.

Detailed descriptions of the CFCA and the operating procedures have been presented in Appendix A.2 of Reference [4]. This Appendix describes the modification in the apparatus and the procedures carried out during the reporting period [10]. The major components of CFCA remain the same and they are shown in cross-sectional view in Figure D.1.

In addition to injecting preheated air through the screen to simulate volatile evolution, an aspirator was incorporated into the test apparatus to provide suction through the screen and simulate perfusion. This modification is shown schematically on Figure D.2.

For the experiments with the stainless steel screens the burner characteristic parameters were selected to duplicate those used during fabric ignition tests. These were with a stoichiometric equivalence ratio ϕ = 0.86, representing an oxygen-rich flame, and burner mass flow rates $\dot{m}_b$ = 1265, 2185 and 2950 g/h. The screens were placed at 1.9, 7.9 and 10.5 cm above the top of the burner at each burner mixture flow rate to provide the range of flame temperatures needed for the tests.

A 200 mesh and a 150 mesh stainless steel screen were used for the results reported here. The air injection and perfusion rates were varied from 0-300 g/h and 0-400 g/h respectively. The temperature of the injected air was varied from 20-300^{o}C.

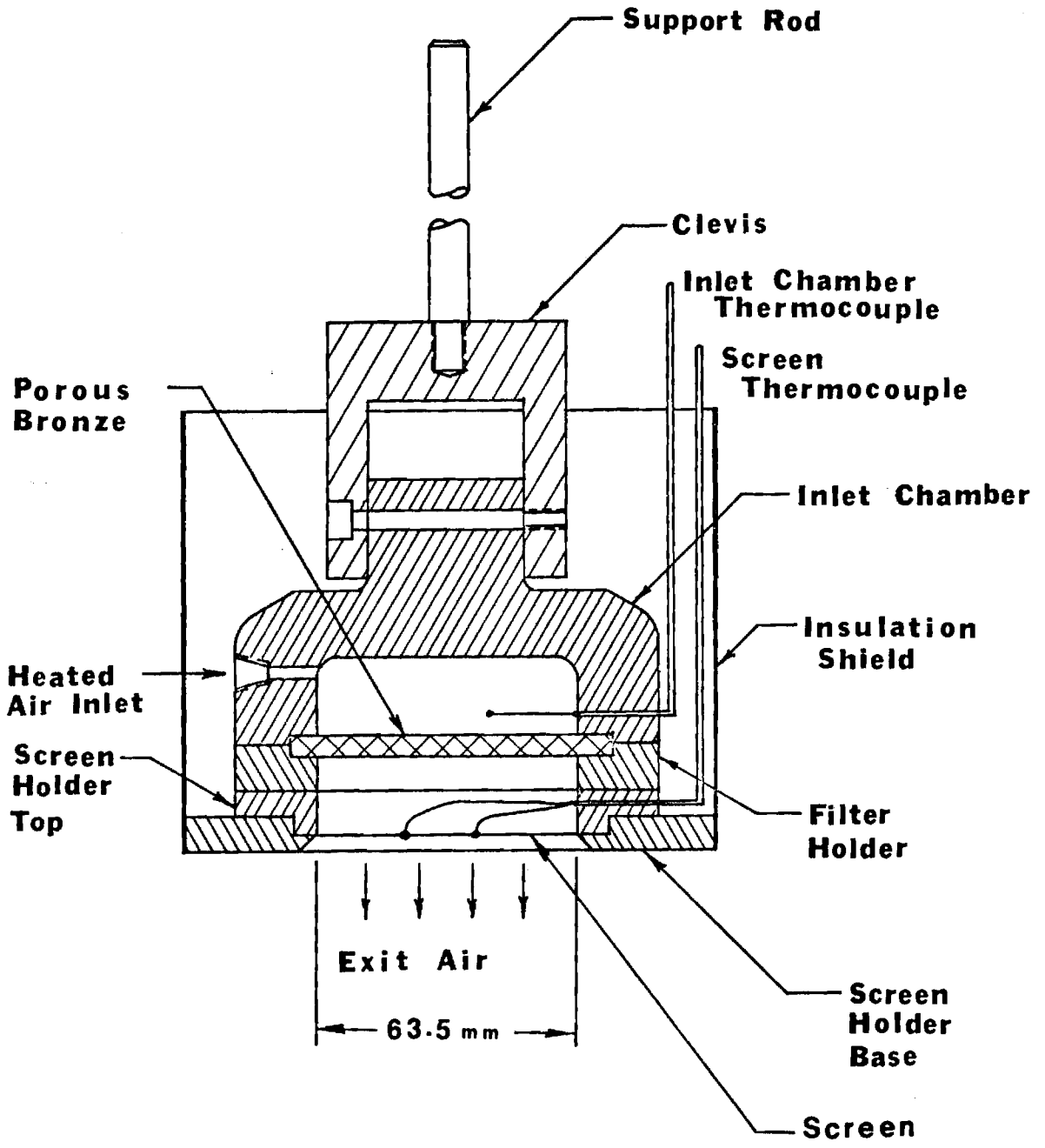

Figure D.1. Cross-sectional View of the Convective Film Coefficient Apparatus (CFCA)

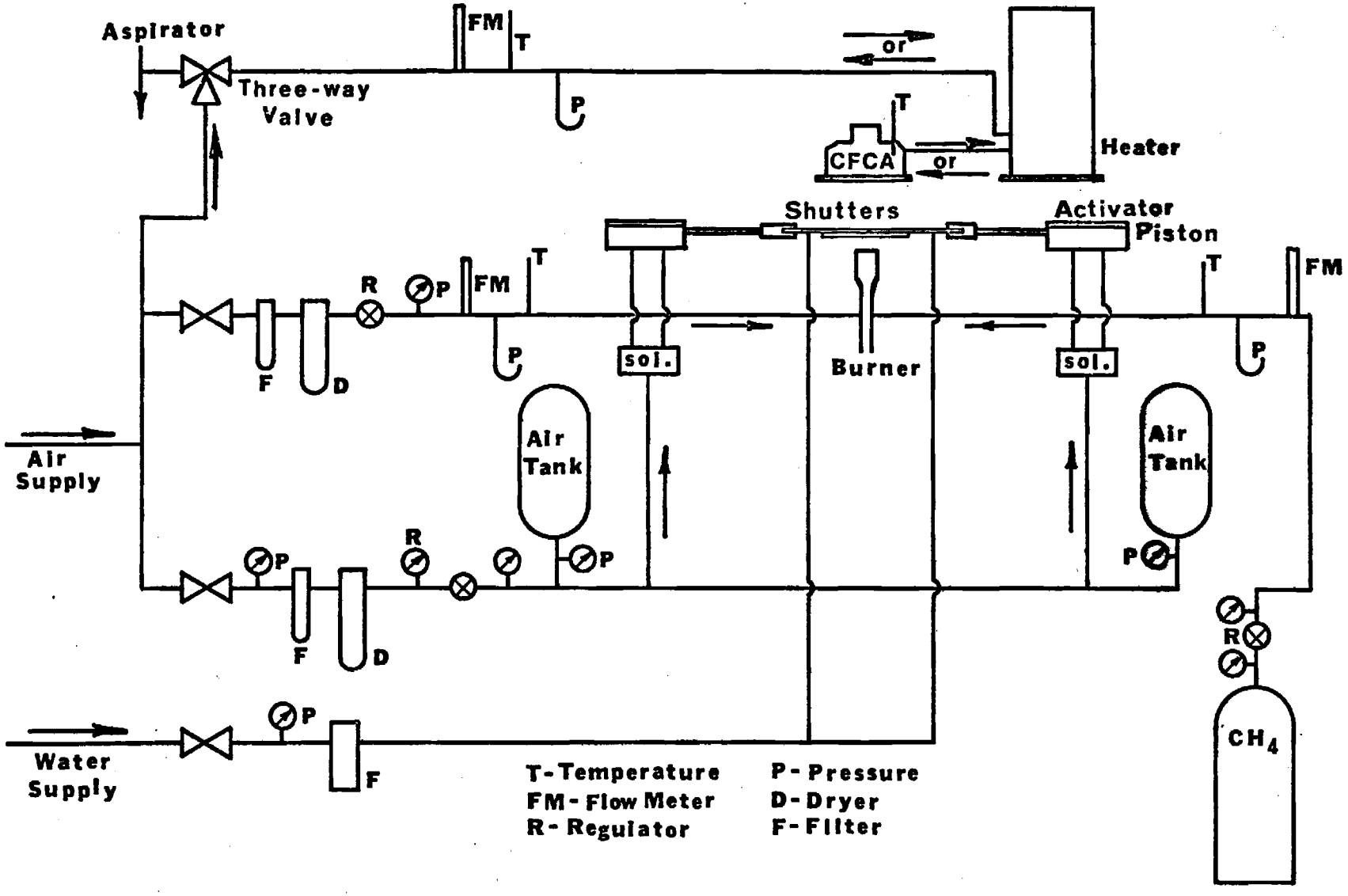

Figure D.2. Schematic View of the Combined Convective Film Coefficient Apparatus and Convective Ignition Time Apparatus.

APPENDIX E
MODELING ANALYSIS FOR FLAME-FABRIC INTERACTION

For the flame-fabric interaction model discussed in Section 2.2.4.2 the momentum and mass conservation for steady, incompressible, axisymmetric flow is [10]

$$\rho(\vec{V}\cdot\nabla)\vec{V} = -\nabla p + \mu\nabla^2\vec{V} + \rho\vec{g} \qquad (E.1)$$

Neglecting the terms of mechanical energy and the viscous dissipation the energy equation is given as

$$\rho c_p\ (\vec{V}\cdot\nabla T) = k\nabla^2 T \qquad (E.2)$$

where the Fourier Law has been used for equation (E.2).

For the pyrolyzing solid using an nth order Arrhenius decomposition law we have

$$\partial(\rho V_z)/\partial(z/\delta) = (\rho\delta)_o \epsilon_g \dot{\lambda}_g \qquad (E.3)$$

where

$$d\lambda_g/d\tau = k_g(1 - \lambda_g)^{n_g} \exp(-E_g/RT_s) \qquad (E.4)$$

and $(\rho\delta)_o$ is the original mass per unit area of the fabric.

The momentum conservation for the flow through a porous solid assuming one dimensional, steady, laminar flow is known as the Darcy law [10,11]

$$\rho V_z = -\rho K(\partial p/\partial z + \rho g)/\mu \qquad (E.5)$$

where K is the average permeability of the porous solid. The gravitational term in equation (E.5) contributes less than 2% of the total driving potential and can be neglected.

Convective heat losses from the fabric surface exposed to the

atmosphere are coupled to mass efflux through this surface due to fabric pyrolysis and gas flame perfusion. This can be expressed in terms of the local Nusselt number $(N_{Nu})_x$, the Grashof number $(N_{Gr})_x$ and a parameter ξ [10, 12-15]

$$(N_{Nu})_x/(N_{Gr})_x^{1/4} = f_2(\xi) \tag{E.6}$$

where

$$\xi = (V_0 x/4\nu)[4\nu^2/g\beta x^3(T_s - T_\infty)]^{1/4}$$

and x is the radial distance from the center of the fabric.

The boundary conditions for the governing equations are

$$\left.\begin{aligned} &\text{at } z = 0: \quad \rho V_z = \rho K(p_1 - p_\delta)/\mu\delta - (\rho\delta)_o \varepsilon_g \dot{\lambda}/2, \\ &\qquad V_r = 0, \; -k\frac{\partial T}{\partial z}\Big|_{z=0} = \bar{h}_{c,1}(T_f - T_s) \end{aligned}\right\} \tag{E.7a}$$

$$\text{at } z = \delta: \quad -k\frac{\partial T}{\partial z}\Big|_{z=\delta} = \bar{h}_{c,2}(T_s - T_\infty) \tag{E.7b}$$

$$\text{at} \begin{Bmatrix} z=-L \\ 0 \le r \le D/2 \end{Bmatrix}: \quad V_r = 0, \; V_z = V_b, \; T = T_f \tag{E.7c}$$

$$\text{as } z \to \infty: \quad T \to T_\infty \tag{E.7d}$$

The mean convective film coefficients are evaluated by integrating from the fabric axis to the fabric radius R and the subscripts 1 and 2 refer to the surfaces interacting with the burner flame and the surrounding atmosphere respectively. D represents the burner diameter.

The governing equations and the associated boundary conditions are normalized using the parameters

$$\left.\begin{aligned} &r^* = r/R, \; z^* = z/R, \; V_r^* = V_r/V_b, \; V_z^* = V_z/V_b \\ &T^* = (T - T_\infty)/(T_f - T_\infty), \; p^* = (p - p_\infty)/\rho_f V_b^2 \end{aligned}\right\} \tag{E.8}$$

$$\rho^* = \rho/\rho_f,\ \dot{\lambda}_g^* = \dot{\lambda}_g/k_g \exp(-E/RT_i) \tag{E.8}$$

and they yield the following nondimensional groups

$$\left.\begin{aligned}
&\pi_1 = \rho_f V_b R/\mu,\ \pi_2 = V_b^2/gR,\ \pi_3 = c_p\mu/k \\
&\pi_4 = \rho K(p_1 - p_\delta)/\ \mu\delta\rho_f V_b \\
&\pi_5 = \{(\rho\delta)_o \varepsilon_g k_g \exp(-E/RT_i)\}/2\rho_f V_b \\
&\pi_6 = \bar{h}_{c,1}R/k,\ \pi_7 = \bar{h}_{c,2}R/k,\ \pi_8 = L/R \\
&\pi_9 = D/R,\ T_s^* = (T_s - T_\infty)/(T_f - T_\infty)
\end{aligned}\right\} \tag{E.9}$$

These scaling parameters are rearranged to evolve into the following groups to characterize

geometry: $\pi_8/\pi_9 = L/D,\ 1/\pi_9 = R/D$ (E.10a)

flame dynamics: $V_b D/\nu = \pi_1\pi_9 = N_{Re}$ (E.10b)

permeability and
injection dynamics: $V_0 R/\nu = \pi_1\pi_4 - \pi_1\pi_5\dot{\lambda}_g^* = (N_{Re})_0$ (E.10c)

heat transfer to the screen: $\bar{h}_{c,1}R/k = \pi_6 = (N_{Nu})_1$ (E.10d)

momentum and energy diffusion: $c_p\mu/k = \pi_3 = N_{Pr}$ (E.10e)

screen temperature: $(T_s - T_\infty)/(T_f - T_\infty) = T_s^*$ (E.10f)

The heat interaction between the flame and the screen in the presence of injection, consequently can be correlated by

$$(N_{Nu})_1 = f\{L/D, R/D, N_{Re}, N_{Pr}, (N_{Re})_0, T_s^*\} \tag{E.11}$$

APPENDIX F
IGNITION OF THERMALLY THIN MEDIA SUBJECT TO NORMALLY IMPINGING FLAMES

The model to be used in the analysis consists of a jet of hot gases impinging normally to a fabric positioned in a horizontal configuration at z = 0 as shown in Figure F.1, the jet and fabric axes coincident. The pyrolyzing solid generates gas which evolves from the fabric surface. The back side of the cloth is exposed to the surrounding atmosphere.

F.1. Solid Phase

The solid is initially (at $\tau < 0$) in stationary thermodynamic equilibrium at temperature T_∞. At time $\tau = 0$ it is exposed to the established hot jet at temperature T_f. Subsequently ($\tau > 0$) the temperature T_s of the solid phase rises and gasification takes place. For the solid phase the model accounts for (i) energy storage, (ii) convective heat loss from the back, and (iii) pyrolysate generation. It assumes (i) absence of moisture desorption, (ii) negligible radiative heat loss, (iii) negligible heat of pyrolysis, and (iv) negligible fraction of the fabric gasified prior to ignition. The conservation equations are:

Energy Conservation

$$k\frac{\partial T}{\partial z}\bigg)_{z=0-} = (\rho_s\delta_s)_o c_{p,s}\frac{\partial T_s}{\partial \tau} + h(T_s - T_\infty) \qquad (F.1)$$

Pyrolysate Conservation

$$\left\{\dot{m}''_p Y_p - \frac{\partial Y_p}{\partial z}\rho D\right\}_{z=0-} = \dot{m}''_p = p_g k_g (1 - \lambda_g)^{n_g} \epsilon_g (\rho_s\delta_s)_o e^{-E_g/RT} \qquad (F.2)$$

where $\dot{m}''_p$ = flux of pyrolysate at z = 0

p_g = fraction of pyrolysate escaping at z = 0

Y_p = mass fraction of the pyrolysate

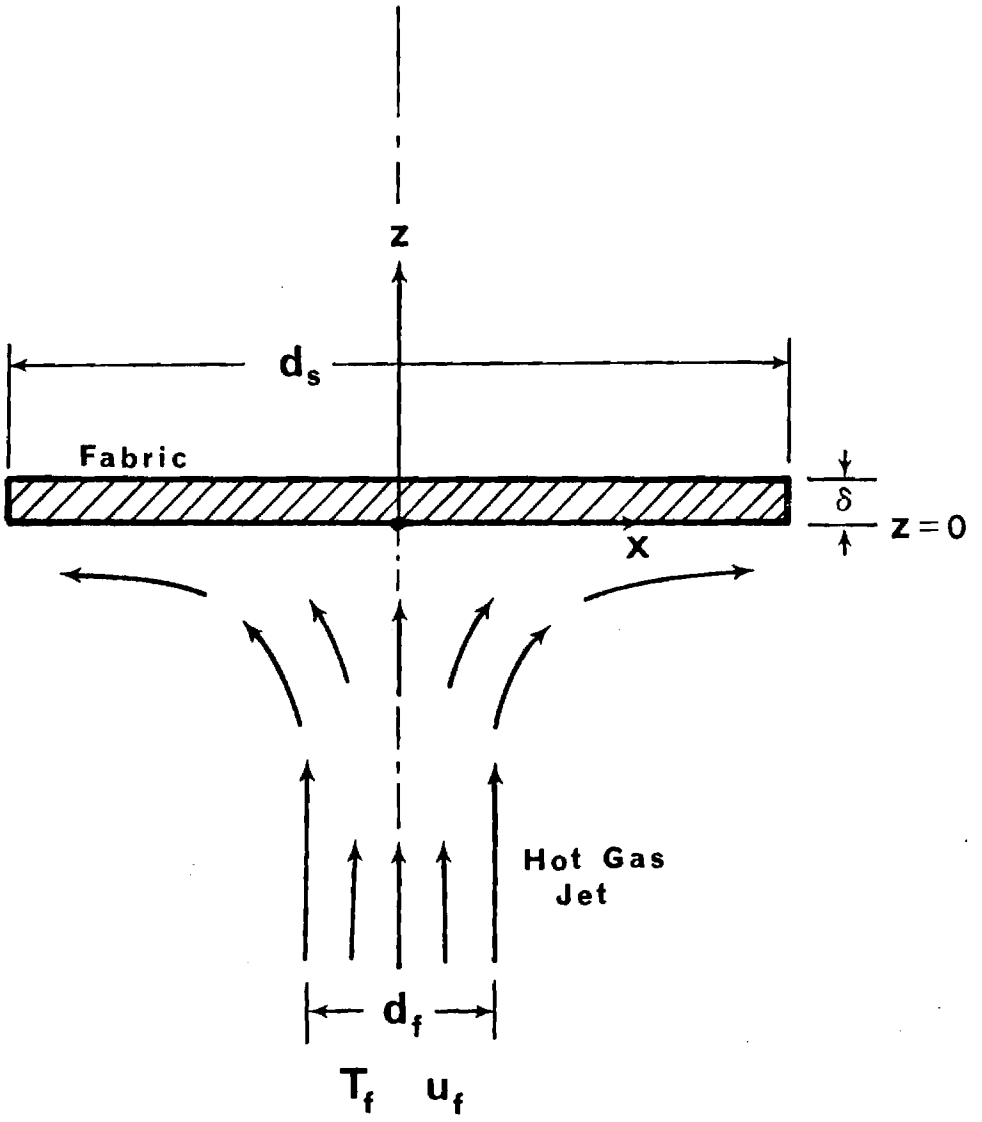

Figure F.1. Pyrolyzing Solid with Normally Impinging Hot Gas Jet

Constitutive equations for thermal and species diffusion were used to obtain equations (F.1) and (F.2). These equations are to be solved subject to the initial conditions

$$\text{at } \tau = 0: \quad T_s = T_\infty \quad \lambda_g = 0 \tag{F.3}$$

F.2. Gas Phase

For the gas phase the model takes into account (i) axisymmetric flow, and (ii) variable properties. It assumes (i) quasi-steady state of a well established jet, (ii) negligible reaction in the gas phase prior to ignition, (iii) negligible injection velocity of pyrolysate, and (iv) Lewis number is unity. The quasi-steady assumption is justifiable when the heat capacity of the solid is very large compared to the heat capacity of the gaseous medium [17]. The conservation equations for the gas phase are:

Mass conservation

$$\frac{\partial}{\partial x}(\rho u x) + \frac{\partial}{\partial z}(\rho v x) = 0 \tag{F.4}$$

Species Conservation

$$\rho u \frac{\partial Y_i}{\partial x} + \rho v \frac{\partial Y_i}{\partial z} = \frac{\partial}{\partial z}\left(\rho D \frac{\partial Y_i}{\partial z}\right) \tag{F.5}$$

Energy Conservation

$$\rho u \frac{\partial T}{\partial x} + \rho v \frac{\partial T}{\partial z} = \frac{\partial}{\partial z}\left(\frac{k}{c_p}\frac{\partial T}{\partial z}\right) \tag{F.6}$$

Momentum Conservation

$$\rho u \frac{\partial u}{\partial x} + \rho v \frac{\partial u}{\partial z} = \frac{\partial}{\partial z}\left(\mu \frac{\partial u}{\partial z}\right) + \rho_\infty u_e \frac{du_e}{dx} \tag{F.7}$$

Equations (F.5) - (F.7) have incorporated constitutive equations for diffusion of species, energy and momentum. These equations are to be

solved subject to the boundary conditions

$$\left.\begin{array}{lll} \text{at } z = 0: & u = 0 & v \simeq 0 \\ & Y_p = Y_{p,w}(\tau) & T = T_w(\tau) \end{array}\right\} \quad (F.8)$$

$$\text{as } z \to -\infty: \quad u = u_f \quad Y_p = 0 \quad T = T_f \quad (F.9)$$

F.3. Transformations

The following quantities are introduced to carry out transformations on the set of equations presented above:

Similarity Variable

$$\eta = (2a/\rho\mu)^{1/2}\int \rho dz \quad (F.10)$$

where

$u_e = ax$, potential velocity

Stream function

$$\psi = \left[\int_0^x 2\rho\mu u_e x^2 dx\right]^{1/2} f(\eta) \quad (F.11a)$$

$$\rho ux = \partial\psi/\partial z \qquad \rho vx = -\partial\psi/\partial x \quad (F.11b)$$

Nondimensional Temperature

$$\theta = T/T_f \quad (F.12)$$

Nondimensional Time

$$\tau^* = \tau c_p \rho^2 D(2a/\rho\mu)^{1/2}/(\rho_s\delta_s)_o c_{p,s} \quad (F.13)$$

Nondimensional Activation Energy

$$E_g^* = E_g/RT_f \tag{F.14}$$

First Damköhler Number at the Surface (z = 0)

$$D_{I,w} = p_g k_g \varepsilon_g (\rho_s \delta_s)_o / \rho^2 D(2a/\rho\mu)^{1/2} \tag{F.15}$$

Convective Heat Transfer Ratio

$$H = h/\rho^2 D c_p (2a/\rho\mu)^{1/2} \tag{F.16}$$

Introducing equations (F.10) - (F.16) into equations (F.1) - (F.9), the following equations are obtained.

Solid Phase

Energy

$$(d\theta/dn)_{0-} = d\theta_w/d\tau^* + H(\theta_w - 1) + H(1 - \theta_\infty) \tag{F.17}$$

Pyrolysate

$$(dY_p/dn)_{0-} = -D_{I,w}(1 - Y_{p,w})\exp(-E_g^*/\theta_w) \tag{F.18}$$

Initial Conditions

$$\text{at } \tau^* = 0: \qquad \theta_w = \theta_\infty \qquad \lambda_g = 0 \tag{F.19}$$

Gas Phase

Pyrolysate

$$Y_p'' = N_{Sc} f Y_p' = 0 \tag{F.20}$$

Energy

$$\theta'' = N_{Pr} f\theta' = 0 \tag{F.21}$$

Momentum

$$f''' = ff'' - (1/2)[(f')^2 - (\rho/\rho_\infty)] = 0 \tag{F.22}$$

Boundary Conditions

$$\text{at } \eta = 0: \quad f' = 0 \qquad f \simeq 0 \qquad Y_p = Y_{p,w} \qquad \theta = \theta_w \tag{F.23}$$

$$\text{as } \eta \to -\infty: \quad f' = 1 \qquad Y_p = 0 \qquad \theta = 1 \tag{F.24}$$

F.4. Solution

The profiles of the pyrolysate and nondimensional temperature are obtained from equations (F.20), (F.21), (F.23) and (F.24)

$$Y_p/Y_{p,w} = (1 - \theta)/(1 - \theta_w) = 1 - \left\{ \int_0^\eta \exp\left[- \int_0^t N_{Pr} f ds \right] dt \right\} \Big/ I_v \tag{F.25}$$

where

$$I_v = \int_0^\infty \exp\left[- \int_0^t N_{Pr} f ds \right] dt \tag{F.26}$$

is the velocity integral.

Substituting equations (F.17), (F.18) and (F.19) into (F.26) to eliminate $Y_{p,w}$ and θ_w, one obtains

$$(1 - \theta)/Y_p = \tau_1^* \left\{ 1 + \exp[E_g^*/(1 - \tau_1^*)] / D_{I,w}^* \right\} \tag{F.27}$$

where

$$\tau_1^* = [(1 - \theta_\infty)/(1 + H)][\exp - \tau(1 + H)/I_v] + (1 - \theta_\infty)H/(1 + H) \tag{F.28}$$

and

$$D^*_{I,w} = D_{I,w} I_v \qquad (F.29)$$

F.5. Prediction of Ignition Time

Two ignition criteria are considered for the prediction of ignition times on fabrics: (i) Wulff's Ignition Criterion which associates the occurrence of ignition in the boundary layer of the hot gaseous mixture of pyrolysate and air, at a location where the local temperature attains a minimum ignition temperature corresponding to the local mass fraction of the pyrolysate [4]. This method requires the quantitative kinetics of pyrolysis and the concentration dependent self-ignition temperature of the pyrolysate. (ii) The Inflexion Method which associates the occurrence of ignition in the boundary layer of the hot gaseous mixture of pyrolysate and air, at a time when the mass fraction of the pyrolysate near the surface varies very steeply with the surface temperature.

F.5.1. Wulff's Ignition Criterion Method

Figure F.2 shows the profiles of the the temperature $(1 - \theta)$ as a function of the pyrolysate mass fraction in the boundary layer, with τ as a parameter. On the same figure the plot of a predetermined concentration dependent ignition temperature $(1 - \theta_i)$ profile of the pyrolysate is superimposed. At a particular time $\tau^*_1 = \tau^*_{1,i}$

$$\theta = \theta_i \qquad (\partial\theta/\partial Y_p)_{\tau^*_1} = (\partial\theta_i/\partial Y_p)_{\tau^*_{1,i}} \qquad (F.30)$$

The pyrolysate ignition temperature τ_i is known as a function of the pyrolysate mass fraction, thus

$$\theta_i = (1/T^*) \left\{ 1/2 Y_p (1 - Y_p) + \sum_{j=1}^{n} C_j Y_p{}^j \right\} \qquad (F.31)$$

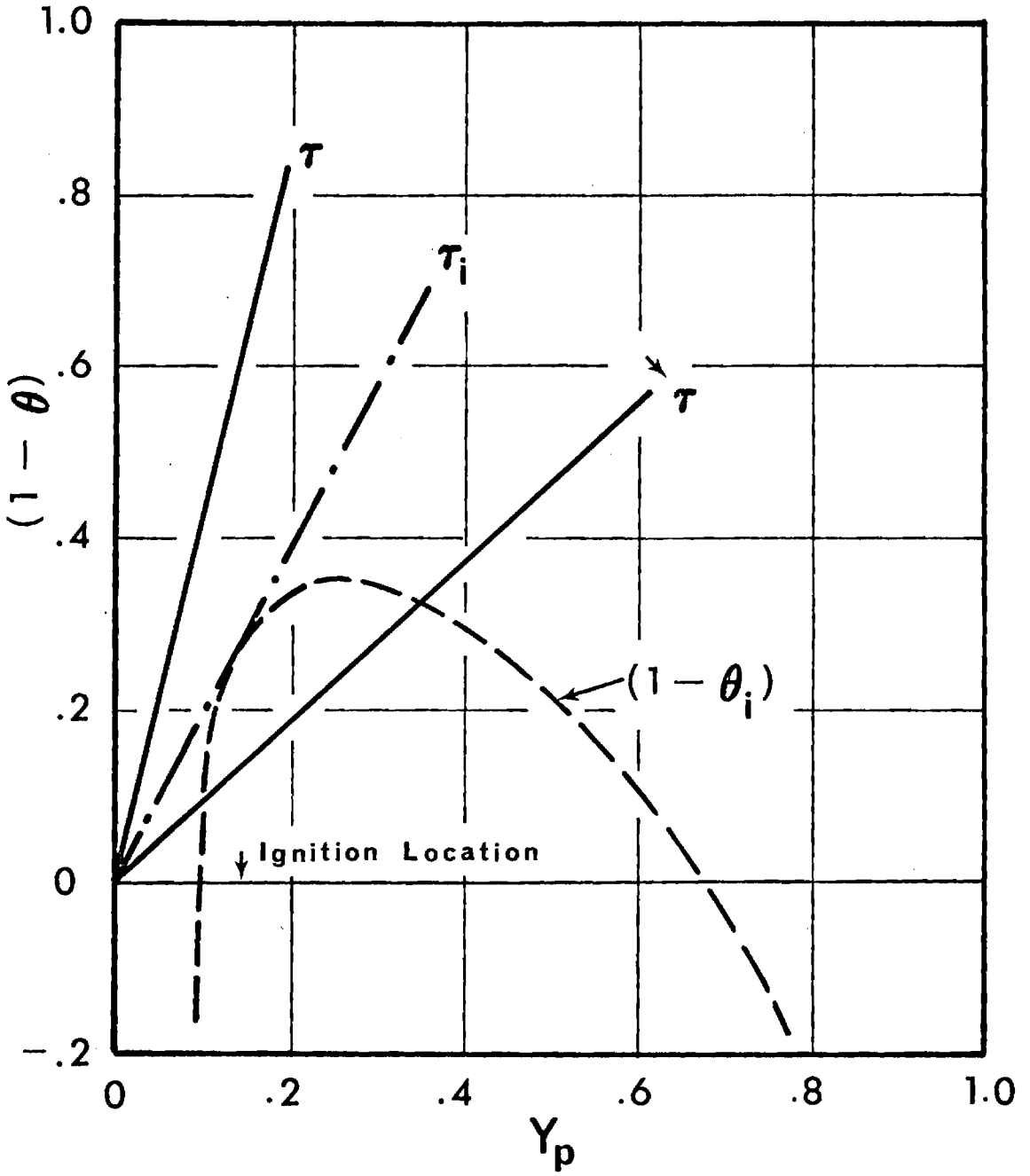

Figure F.2. Temperature Dependent History of the Pyrolysate in the Boundary Layer and Attainment of Wulff's Ignition Criterion For a Fabric Subjected to a Normally Impinging Flame

where

$$T^* = T_f/T_\infty$$

Using equations (F.27), (F.30) and (F.31) the ignition time parameter $\tau^*_{1,i}$ is determined. Thus

$$\tau^*_{1,i} = 1 - E^*_g/\ln\{[F(T^*)/\tau^*_{1,i} - 1]D^*_{I,w}\} \quad (F.32)$$

where

$$F(T^*) = (1 - \theta_i)/Y_{p,i} \quad (F.33)$$

and

$$\sum_{j=0}^{n+3} a_j Y_{p,i}{}^j = 0 \quad (F.34)$$

In equation (F.34) the coefficients a_j are given as follows:

$$a_0 = -1 \quad (F.35a)$$

$$a_1 = 3/2 + T^* - C_0 \quad (F.35b)$$

$$a_2 = 2C_0 - 2T^* \quad (F.35c)$$

$$a_3 = C_2 - C_0 + T^* \quad (F.35d)$$

$$a_m = (m - 4)C_{m-3} + (m - 2)C_{m-1} - 2(m - 3)C_{m-2}, \qquad m \geq 4 \quad (F.36)$$

and C_{n+1}, C_{n+2}, ... are equal to zero according to the polynomial fit given by equation (F.31).

An explicit solution from equation (F.32) can be obtained after simplification. For the quantity inside the square bracket $\tau^*_{1,i}$ can be approximated by $(1-\theta_\infty)$. Then for the condition of negligible heat loss from the side of the fabric exposed to the surrounding atmosphere

$$\tau^*_i \simeq I_v \ln\left[(1 - \theta_\infty)/\{1 - E^*_g/\ln[F(T^*)/(1 - \theta_\infty) - 1]\, D^*_{I,w}\}\right] \quad (F.37)$$

F.5.2 Inflexion Method

When $D^*_{I,w}$ is very large compared to $[F(T^*)/(1 - \theta_\infty) - 1]$ then from equation (F.32)

$$\tau^*_{I,i} = 1 - E^*_g/\ln D^*_{I,w} \qquad (F.38)$$

Equation (F.38) gives the time at which there is a steep rise in the mass fraction of the pyrolysate at the fabric surface (z = 0) with respect to the temperature. Under negligible heat loss from the back of the fabric ($z = \delta$)

$$\tau^*_i \simeq I_v \ln [(1 - \theta_\infty)/(1 - E^*_g/\ln D^*_{I,w})] \qquad (F.39)$$

APPENDIX G
IGNITION OF THERMALLY THICK MEDIA SUBJECT TO RADIATIVE HEATING

A solid of thickness δ is exposed to a uniform time-invariant radiant heating source. The solid is located vertically in a freely convecting atmosphere. The material undergoes thermal degradation throughout the volume of the solid. The generated pyrolysate enters into the boundary layer where it undergoes oxidation. The face of the solid exposed to the radiant heat source is located at $z = 0$ and is cooled by free convection. The face of the solid at $z = -\delta$ is exposed to the ambient air at T_∞.

G.1. Solid Phase

The solid is initially (at $\tau < 0$) in thermodynamic equilibrium with its surroundings at $T = T_\infty$. At time $\tau = 0$ the solid face at $z = 0$ is exposed to a uniform time-invariant radiant heat source. For the solid phase the model accounts for (i) energy storage, (ii) pyrolysate generation, (iii) convective heat loss, (iv) void creation due to pyrolysate generation, and (v) flow of pyrolysate through the porous solid. It assumes (i) one-dimensional heat flow in the z-direction, (ii) all the pyrolysate species can be represented by a single component, (iii) local storage of pyrolysate negligible, and (iv) negligible radiant heat loss. The conservation equations are

Energy Conservation

$$(\rho c_p)_s(\partial T_s/\partial \tau) + (\rho c_p)_p v_p(\partial T_s/\partial z) = \partial(k_s \partial T_s/\partial z)/\partial z + \dot{q}_s - \partial \dot{q}_{r,z}/\partial z \qquad (G.1)$$

Mass Conservation

$$\partial(\rho_p v_p)/\partial z = \dot{w}_{p,s} \tag{G.2}$$

where $\dot{q}_s$, $\dot{w}_{p,s}$ and $\partial\dot{q}_{r,z}/\partial z$ are defined by the following constitutive equations[4,20,21]

$$\dot{q}_s = \dot{w}_{p,s}[Q_g^o + \overline{(\nu_p c_{p,p} + \nu_c c_{p,c} - c_{p,s})}(T - T^o)] \tag{G.3}$$

$$\dot{w}_{p,s} = k_g \rho_{s,o}[(1 - \beta) - (\rho_c/\rho_{s,o})] \exp(-E_g/RT) \tag{G.4}$$

$$\partial\dot{q}_{r,z}/\partial z = 4\kappa\sigma^2 E_b(T_s) - 2\kappa(1 - \beta)W_o E_z(\kappa z) - 2\kappa\sigma^2 \int_0^{-\delta} E_b(t)E_1[|\kappa z - t|]dt \tag{G.5}$$

Boundary Conditions

$$\left.\begin{aligned} \text{at } z = 0: \quad (\rho v)_p &= (\rho v)_f \\ k(\partial T/\partial z)_s &= k(\partial T/\partial z) \end{aligned}\right\} \tag{G.6}$$

$$\left.\begin{aligned} \text{at } z = -\delta: \quad \rho v &= 0 \\ k(\partial T/\partial z)_s &= k(\partial T/\partial z) \end{aligned}\right\} \tag{G.7}$$

Initial Conditions

$$\text{at } \tau = 0: \quad T_s = T_\infty \quad \beta = 0 \quad \text{for } -\delta \leq z \leq 0 \tag{G.8}$$

G.2. Gas Phase

At $\tau < 0$ the solid is surrounded by static ambient air at T_∞. For the gas phase the model takes into account (i) gravitational effects, (ii) viscous dissipation, and (iii) oxidation of pyrolysate in the gas

phase. It assumes (i) quasi-steady state, and (ii) no radiative absorption or emission. The conservation equations are:

Mass Conservation

$$\partial(\rho u)/\partial x + \partial(\rho v)/\partial z = 0 \qquad \text{(G.9)}$$

Pyrolysate Conservation

$$\rho u(\partial Y_f/\partial x) + \rho v(\partial Y_f/\partial z) = \partial[\rho D(\partial Y_f/\partial z)]\ /\partial z + \dot{w}_f \qquad \text{(G.10)}$$

where

$$\dot{w}_f = k_f \rho^n Y_f^{n_f} Y_0^{n_0} \exp(-E_f/RT)$$

Momentum Conservation

$$\rho u(\partial u/\partial x) + \rho v(\partial u/\partial z) = g(\rho_\infty - \rho) + \partial(\mu \partial u/\partial z)/\partial z \qquad \text{(G.11)}$$

$$p = \text{constant}$$

Energy Conservation

$$\rho u(\partial h/\partial x) + \rho v(\partial h/\partial z) = \partial(k\partial T/\partial z)\partial z + \mu(\partial u/\partial z)^2 + \dot{q}_f \qquad \text{(G.13)}$$

where

$$\dot{q}_f = \dot{w}_f Q_0^o$$

Boundary Conditions

$$\left.\begin{array}{l} \text{at } z = 0: \quad u = 0 \qquad (\rho v)_f = (\rho v)_p \\ \qquad\qquad\qquad\quad k(\partial T/\partial z) = k(\partial T/\partial z)_s \end{array}\right\} \qquad \text{(G.14)}$$

$$\text{as } z \to \infty: \qquad u = 0 \qquad T = T_\infty \qquad Y_f = 0 \qquad \text{(G.15)}$$

$$\text{at } x = 0: \qquad u = 0 \qquad T = T_\infty \qquad Y_f = 0 \qquad \text{(G.16)}$$

G.3. Solution

The general solution will be carried out by using the local similarity approach for the gas phase conservation equations. For the solid phase conservation equations the general solution will be presented by first neglecting the convective heat flux and assuming the pyrolysis to be a surface reaction. The two solutions will be matched at the interface to obtain the complete solution.

The prediction of ignition time for the solid will be calculated using three ignition criteria: (i) Inert heating of the solid to a specified temperature [3], (ii) Wulff's Ignition Criterion [4, see also Appendix F], and (iii) Inflexion Method [see Appendix F].

REFERENCES

1. Tribus, M., "Decision Analysis Approach to Satisfying the Requirements of the Flammable Fabrics Act," paper presented at the Textile and Needle Trades Division, American Society of Quality Control, Greensboro, North Carolina, February 12, 1970.

2. Evans, R. B., Wulff, W., and Zuber, N., "The Study of Hazards from Burning Apparel and the Relation of Hazards to Test Method," Research Proposal submitted by the School of Mechanical Engineering, Georgia Institute of Technology, to the Government-Industry Research Committee on Fabric Flammability, Office of Flammable Fabrics, NBS, Washington, D.C., July 1970.

3. Durbetaki, P., Wulff, W., et al., "Study of Hazards from Burning Apparel and the Relation of Hazards to Test Methods," Second Annual Report, NSF Grant GI-31882, School of Mechanical Engineering, Georgia Institute of Technology, Atlanta, Georgia, December 1972, NTIS Accession No. COM-73-10956.

4. Durbetaki, P., Wulff, W., et al., "Fabric Ignition," Third Annual Report, NSF Grant GI-31882, School of Mechanical Engineering, Georgia Institute of Technology, Atlanta, Georgia, March 1974.

5. Wulff, W., and Durbetaki, P., "Fabric Ignition and the Burn Injury Hazard," Heat Transfer in Flames, N.H. Afgan and J.M. Beer, editors, Scripta Book Company, Washington, D.C., 1974, pp. 451-461.

6. Wulff, W., Zuber, N., et al., "Study of Hazards from Burning Apparel and the Relation of Hazards to Test Methods," (First Annual) Final Report, NSF Grant No. GK-27189, School of Mechanical Engineering, Georgia Institute of Technology, Atlanta, Georgia, December 1971, NTIS Accession No. COM-73-10954.

7. Jones, G.W., and Scott, F. E., "Estimation of Propane and Butane Flames by Dichloro-difluoromethane," Bureau of Mines Report of Investigations 3908, 1946, p. 8.

8. Barnett, H. C., and Hibbard, R. R., "Basic Considerations in the Combustion of Hydrocarbon Fuels with Air," NACA Report No. 1300, Government Printing Office, Washington, D.C., 1959, p. 257.

9. Williams, P. T., "Ignition Temperatures of Pyrolysate-Air Mixtures," MS thesis, School of Mechanical Engineering, Georgia Institute of Technology, Atlanta, Georgia, October 1974.

10. Wedel, G. L., "Determination of Convective Film Coefficients Under Simulated Pyrolysate Evolution," MS thesis, School of Mechanical Engineering, Georgia Institute of Technology, Atlanta, Georgia, October 1974.

11. Slattery, J. C., Momentum, Energy and Mass Transfer in Continua, McGraw-Hill, New York, 1972.

12. Fishenden, M., and Saunders, O. A., An Introduction to Heat Transfer, Oxford University Press, London, 1950, pp. 89-101.

13. Rohsenow, W. M., and Hartnett, J. P., Handbook of Heat Transfer, McGraw-Hill, New York, 1973.

14. Sparrow, E. M., and Cess, R. D., "Free Convection with Blowing or Suction," Journal of Heat Transfer, Trans. ASME, Series C, 83, 1961, pp. 387-389.

15. Eichhorn, R., "The Effect of Mass Transfer on Free Convection," Journal of Heat Transfer, Trans. ASME, Series C, 82, 1960, pp. 260-263.

16. Acree, R. L., "Ignition Time Measurements on Fabric Assemblies Under Various Geometric Configurations," MS thesis, School of Mechanical Engineering, Georgia Institute of Technology, Atlanta, Georgia, December 1974.

17. Kashiwagai, T., Macdonald, B. W., Isoda, H. and Summerfield, M., "Ignition of a Solid Polymeric Fuel in a Hot Oxidizing Gas Stream," Thirteenth Symposium (International) on Combustion, The Combustion Institute, Pittsburgh, 1971, pp. 1073-1086.

18. Alkidas, A., and Durbetaki, P., "Ignition Characteristics of a Stagnation Point Combustible Mixture," Combustion Science and Technology, 3, 1971, pp. 187-194.

19. Kreith, F., Principles of Heat Transfer, 3rd edition, Intext Educational Publishers, New York, 1973.

20. Kanury, A. Murty, "Thermal Decomposition Kinetics of Wood Pyrolysis," Combustion and Flame, 18, 1972, pp. 75-83.

21. Viskanta, R., "Radiation Transfer and Interaction of Convection with Radiation Heat Transfer," Advances in Heat Transfer, 4, J. P. Hartnet and T. F. Irvine, Jr., editors, Academic Press, New York, 1966, pp. 175-251.

File: E-25-625

GEORGIA INSTITUTE OF TECHNOLOGY
School of Mechanical Engineering
Atlanta, Georgia

FABRIC IGNITION

Third Annual Report

By

R. L. Acree
E. R. Champion
P. Durbetaki
C. Lee
O. A. A. Naveda
G. L. Wedel
P. T. Williams
W. Wulff

For The

National Science Foundation,

RANN Program

NSF Grant No. GI-31882

March 31, 1974

FABRIC IGNITION

Third Annual Report

By

R. L. Acree
E. R. Champion
P. Durbetaki
C. Lee
O. A. A. Naveda
G. L. Wedel
P. T. Williams
W. Wulff

School of Mechanical Engineering
Georgia Institute of Technology

March 31, 1974

Research Sponsored
By The
National Science Foundation
Under the RANN Program
(Research Applied to National Needs)
NSF Grant No. GI-31882A#1

P. Durbetaki, Principal Investigator

W. Wulff, Principal Investigator

FOREWORD

The research presented in this Third Annual Report was funded and supported by the National Science Foundation under the RANN Program (Research Applied to National Needs). The opportunity to participate in the national research effort toward the reduction of loss from unwanted fires is greatly appreciated.

The project was carried out in the Fire Hazard and Combustion Research Laboratory of the School of Mechanical Engineering under the Principal Investigators Dr. Pandeli Durbetaki and Dr. Wolfgang Wulff.

Dr. Calvin Lee, Research Engineer, assisted in the measurement of fabric synergism effects on ignition time and in the debugging of a computer code for the ignition modeling analysis.

Graduate Research Assistants involved with this research are Mr. Robert L. Acree who measured the effects of fabric synergism and geometry effects on ignition time, Mr. Edward R. Champion who worked on the ignition analysis for forced convection by impinging gas jets, Mr. Oscar A. A. Naveda who carried out all the ignition time frequency measurements and the characterization of actual ignition sources, Mr. Gregory L. Wedel who is measuring forced convection heat transfer coefficients under simulated pyrolysate evolution from fabrics, and Mr. Paul T. Williams who is carrying out the measurement of ignition temperature on pyrolysate-air mixtures.

The participation of graduate research assistants has been supported in part by the School of Mechanical Engineering under the matching fund provision of this grant. The NSF grant which made this research possible is greatly appreciated.

ABSTRACT

This third Annual Report presents the research which was carried out during the time from January 1, 1973 through March 31, 1974, under the National Science Foundation Grant No. GI-31882 as part of the RANN Program (Research Applied to National Needs), and which was performed in the Fire Hazard and Combustion Research Laboratory of the School of Mechanical Engineering at Georgia Institute of Technology. This research constitutes a second continuation program of research previously carried out in the same laboratory, originated on November 1, 1971, jointly by the National Science Foundation as the funding agency and by the Government-Industry Research Committee on Fabric Flammability as the monitoring agency [1.3,4,8 and 9]*.

Fabric ignition plays a dominant role in the occurrence of accidental garment fires, followed by burn injury. It was shown earlier [1.5] that the hazard from fabric-related burn injuries can be measured by the probability that the fabric in question contributes to a burn injury of specified severity. This probability is computed from the probabilities associated with all the possible events which could lead, from the instant of fabric, or end-use product, certification to a burn injury.

Of these possible events, one large class consists of selections and choices by the legislators (selection of standards) and the consumer (material and garment style preferences, frequency of a particular use and activity, etc.). The events are arranged in their logical sequence (decision tree), and the probability of selection events are computed from relative frequency of occurrence.

The other class of events consists of transient thermo-physical processes the probabilities of which are computed from ratios of characteristic times [1.4], namely from the time a certain thermo-physical event is allowed to proceed, divided by the time this process requires, in the mean, for its completion. Such thermo-physical processes are ignition after exposure, flame spread after ignition, extinguishment after ignition, tissue

*Numbers in brackets refer to the Bibliography.

decomposition after flame spread, etc.

The objective of the research presented here and earlier [1.8,9] is to obtain the probability P(I/E) of ignition after exposure which depends on the ratio of exposure time τ_e over mean ignition time $\langle\tau_i\rangle$. The combined experimental and analytical program consists of (i) two tasks to determine constitutive relations for the description of ignition processes, namely the measurement of ignition temperature on air-pyrolysate mixtures and the measurement of forced convection film coefficients on surfaces with pyrolysate evolution, (ii) two tasks to measure fabric ignition time itself, namely on single fabrics, exposed to gas flame heating and on fabric assemblies under various geometric configurations, (iii) the task to determine experimentally the functional relationship $P(I/E) = f(\tau_e/\langle\tau_i\rangle)$, and (iv) the analysis to predict ignition time τ_i as a function of material properties and exposure conditions for pyrolyzing composites, subject to one-dimensional transient heating.

Results

Ignition temperature measurements on pyrolysate-air mixtures are incomplete at this time, primarily because of the chemical instability of the temperature sensor. Preliminary measurements have been performed successfully on propane-air mixtures. The measurements on cellulose are being completed as part of an M.S. Thesis research program.

Forced convection heat transfer coefficients have been measured under conditions simulating the evolution of pyrolysate gases from a fabric screen. This was accomplished by air injection through a stainless steel wire mesh which served as part of a thermocouple circuit to measure its own temperature. Results are presented in nondimensional form and indicate a reduction of convection heat transfer by 20 percent due to air injection.

Fabric ignition times were measured with single fabrics exposed to a well defined gas flame. Experimental results are compared with analytical predictions obtained from lumped-parameter analysis.

Interaction between fabrics during radiative heating is found to be primarily thermal. Depending on fabric spacing, ignition time of two fabrics may be both longer or shorter than that of a single fabric found under the same heating conditions.

Single fabrics exposed edgewise to a gas flame were found to ignite in approximately one fourth of the time required for ignition with normally impinging flames.

Ignition frequency measurements, carried out under radiative heating and with carefully controlled exposure times were evaluated to yield the probability of ignition after laboratory exposure, $P(I/E_\ell)$ in terms of the ratio $\tau_e/\langle\tau_i\rangle$ of exposure time τ_e, divided by the mean ignition time $\langle\tau_i\rangle$ and the normalized standard deviation σ

$$P(I/E_\ell) = 1/\sqrt{2\pi} \int_{-\infty}^{x} \exp(-z^2/2)\, dz \quad ,$$

with $x = (\tau_e/\langle\tau_i\rangle - 1)/\sigma$. Mean ignition times $\langle\tau_i\rangle$ and standard deviations σ were evaluated by probit analysis.

Actual ignition sources normally encountered in households, namely kitchen gas and electric ranges, matches, candles and cigarette lighters were characterized for the purpose of deriving the probability with which laboratory exposure conditions are encountered in actual life. Spacial heat flux and temperature distributions about the ignition source are presented. Maximum heat flux values were measured in diffusion gas flames and found to be approximately 6 W/cm^2.

An ignition analysis was developed on the basis of integral techniques. The analysis incorporates a newly developed ignition criterion. The ignition criterion involves the measured ignition temperature of the pyrolysate-air mixture as a function of pyrolysate concentration. Ignition of the pyrolyzing system is postulated to occur when the binary mixture reaches for the first time, the minimum, concentration-dependent temperature. This criterion takes directly into account the state of thermal decomposition in the condensed phase as well as the effects of the fluid

flow field external to the condensed phase. The criterion takes implicitly into account the heating rate, as well as the heating rate and heating mode-dependent fabric ignition temperature.

The analysis yields ignition time as a function of material properties, heating conditions and geometry, and it yields scaling parameters (scaling laws) and the errors of partial modeling. Analytical results are compared with measured ignition time.

TABLE OF CONTENTS

LIST OF FIGURES

LIST OF FIGURES (Appendices)

LIST OF TABLES

NOMENCLATURE

A	frequency factor
a_{ij}	coefficients, equation (3.4.37)
$\underset{\sim}{B}$	five-dimensional vector, equation (3.4.25)
b_{ij}	coefficients, equation (3.4.38)
$\underset{\approx}{C}$	(5X5) coefficient matrix, equation (3.4.25)
C''	heat capacity per unit area
c	specific heat of solid
c_p	specific heat at constant pressure
D	burner diameter
$\mathscr{D}$	mass diffusivity
d	fabric spacing
E	activation energy
g	acceleration due to gravity
i	enthalpy
Δi_f	reaction enthalpy
H	= h(L)
h	boundary layer thickness
$\overline{h}_c$	average convective film coefficient
k	thermal conductivity
k/δ	thermal conductance
L	height
$\dot{m}$	mass flow rate
$\overline{m}$	exponent, equation (3.4.36)

N	Number of plane-parallel slabs
N_{Fo}	Fourier number, equation (2.3.1)
N_{Nu}	Nusselt number, equation (2.2.2)
N_{Pr}	Prandtl number
N_{Re}	Reynolds number, equation (2.2.3)
N_{Sc}	Schmidt number
n	Order of Reaction
$\overline{n}$	exponent, equation (3.4.36)
$P(E/\hat{U})$	exposure probability for given garment use
$P(I/E)$	ignition probability for given exposure
$P(I/\hat{U})$	ignition probability for given garment use
p	pressure
q	heat flux
q'', $\overline{q}''$	heat flux, averaged heat flux per unit area
q^*	nondimensional heating intensity, equations (2.3.2) and (3.4.42)
R	electrical resistance, screen radius; universal gas constant
r	radial coordinate
s	shear stress
T	absolute temperature
t	relative temperature
U	$= u_m(L)$
u	velocity component along x-coordinate
v	velocity component along y-coordinate
W_o	radiative power flux

w_f	pyrolysate concentration
$w_{f\ell}$	lower limit of ignitable pyrolysate concentration
w_{fu}	upper limit of ignitable pyrolysate concentration
Y_1 through Y_5	System state variables, Eqs. (3.4.20) - (3.4.24)
$\underset{\sim}{Y}$	five-dimensional vector of $(Y_1,\ldots,Y_5)$
x	standard normal variable, equation (2.5.2); traversing position
x,y,z	coordinates
z	general variable
α	radiative absorptivity; temperature coefficient
δ	fabric thickness; slab thickness; coefficient
ζ	normalized Y coordinate, Eq. (3.4.26), Fig. 3.2
η	normalized Y coordinate, Eq. (3.4.26), Fig. 3.2
θ	normalized temperature, equation (2.3.3)
$\overline{\theta}$	time mean of θ
Λ	ignition criterion, equation (3.5.4)
λ	fraction of decomposed mass
μ	dynamic voscosity
ν	kinematic viscosity
ξ	normalized X coordinate, Eq. (3.4.28)
π_0 through π_{14}	scaling groups
$\pi_2^*,\pi_3^*,\pi_5^*,\pi_6^*,\pi_8^*$	scaling groups
ρ	density
$\rho\delta$	specific mass, mass per unit area
$\tilde{\rho}$	radiative reflectance

σ	standard deviation
τ, $<\tau>$	time, median time
$\bar{\tau}$, τ^*	normalized time
$\tilde{\tau}$	radiative transmittance
ϕ	stoichiometric equivalence ratio
ϕ_i	property profile in solid functions, Eq. (3.4.37)
ψ_i	property profile in boundary layer functions, Eq. (3.4.38)

Subscripts

a	oxidizing atmosphere
c	convection
d	desorption
e	exposure
f	flame; pyrolysate
g	gas (pyrolysate)
i	ignition; injection; initial
ig	ignition
j	counter index
ℓ	laboratory
m	melting; maximum
mix	mixture
o	at the interphase; reference
ref	reference
s	solid
∞	environment

1. INTRODUCTION AND PROGRAM OBJECTIVES

1.1 Garment Fire Hazard and Fabric Ignition

The relatively high loss of life, health and property in the United States [1.1]* continues to be of serious concern to the Federal Government, to textile, plastics, building and transportation industries, the armed forces, as well as to the consumer. Of the 12,000 persons dying annually from fire, approximately 3,000 to 5,000 die from injuries inflicted by garment-related fires [1.2].

The Flammable Fabrics Act of 1953, as amended in December of 1967 charged the Secretary of Commerce with the responsibility to establish reasonable fabric safety criteria so as to protect the public from excessive hazards of fabric-related burn injuries. The research reported here is in support of the Flammable Fabrics Act, of the efforts resulting from the Fire Safety and Research Act passed in 1968 and it supports the mission on fire loss reduction of the Consumer Product and Safety Commission. This research began in November of 1970 [1.3,4], initiated and monitored during the first two years by the Government-Industry Research Committee on Fabric Flammability [1.3]** which was charged with formulating and administering research programs to develop the scientific foundation for the legislation sought under the Flammable Fabrics Act. The National Science Foundation provided the funding, during the first year under NSF Grant No. GR-27184, and during the subsequent two years, until now, under the RANN Program through Grant GI-31882.

The determination of the relationship between fabric behavior in a laboratory test, on the one hand, and the hazard it presents in actual use,

---

* Numbers in brackets refer to the bibliography.

** Its members represented the National Science Foundation, the National Bureau of Standards, the American Textile Manufacturers Association, the Cotton Council of America and the Man-Made Fiber Producers Association.

on the other, is the central problem in the development of rational safety standards for the reduction of fabric-related burn injuries [1.3]. The conceptual framework by which to connect burn injury hazard with laboratory test results was first established by Evans, Wulff and Zuber [1.4].

The relationship is based on the quantitative measure of hazard in terms of accident probability, as proposed first by M. Tribus [1.5]. The accident probability is computed from the probabilities with which events occur that could conceivably lead to an accident. It has been demonstrated later [1.6] that the events, considered to start at the time of certification, i.e. application of the intended fire safety standards, and to end with a specified loss or burn injury, fall into two classes, namely the class of selective events and the class of transient physico-chemical events.

The selective events are processes whose outcome is determined by selections and choices made by people in conjunction with the use of a particular system, i.e. either the material such as a fabric, or the end product such as the finished garment. Probabilities associated with these stochastic events are computed from observed relative frequencies and account for human preferences, activities and responses, even to particular standards. Excluded are human responses to the fire itself, once ignition has occurred.

The transient physico-chemical events are processes which are (1) initiated by the action of an ignition source, (2) dominated by transient, physico-chemical material responses, yet affected by stochastic, human response to fire, and (3) terminate in a prescribed fire damage such as a specific burn injury.

The first, primarily but not completely, deterministic process in the chain of events, which lead to burn injury, is fabric ignition after given exposure. This event, together with the later events of fire extinguishment and of thermal tissue decomposition, are considered most indicative of fabric and garment behavior and are deemed particularly important for the characterization of apparel contribution toward the burn injury hazard.

Transient physico-chemical processes are describable in terms of characteristic times. It was recognized by Zuber and Wulff for the first time [1.4] that the controlling processes are exposure and transient heating, that the characteristic times are the time τ_e of exposure and the time $<\tau_{ig}>$ required, on the average, by the fabric to reach ignition, and finally, that the probability of ignition after exposure, P(I/E), should be a function of the ratio $\tau_e/<\tau_{ig}>$.

$$P(I/E) = f(\tau_e/<\tau_{ig}>) \qquad (1.1.1)$$

Here, τ_e characterizes involuntary and voluntary, stochastic response of the potential victim to fire, but $<\tau_{ig}>$ characterizes the system's response and depends on (1) material properties, (2) process parameters describing the interaction between fuel (fabric) and ignition source, and (3) process parameters describing exposure conditions such as heating intensity, forced drafts, etc. Equivalent statements can be made about subsequent events, namely flame spread after ignition, extinguishment after ignition and tissue destruction after ignition (or melting) has occurred.

Therefore, the ignition time τ_e is the first important quantity which is required for the assessment of a material's fire hazard and which is directly related to the material's properties.

1.2 Problem Formulation

To relate burn injury hazard via accident probability to laboratory test results, one has to [1.7]

(i) enumerate all relevant events which could lead from fabric or garment safety certification to burn injury,
(ii) predict the partial probability for each event,
(iii) compute the overall probability of burn injury for every possible succession of events which result in burn injury, and
(iv) add up the overall probabilities for all possible chains of events.

The research program reported here dealt with the process of ignition and with the prediction of the probability of ignition after given exposure P(I/E), i.e. the first, fabric-characterizing process in the chain of events leading to burn injury.

The enormous number of fabrics, fabric assemblies, and garments, combined with uncountably many kinds of human activities and types of ignition sources suggests the separate determinations of, at first the ignition probability under laboratory conditions, $P(I/E_\ell)$, and then the probability with which laboratory exposure conditions occur for a given set of garment uses, $P(E_\ell/\{\hat{U}\})$. The ignition probability for this set of garment uses is then to be computed as the product

$$P(I/\{\hat{U}\}) = P(I/E_\ell)\cdot P(E_\ell/\{\hat{U}\}) \qquad (1.2.1)$$

The determination of the ignition probability under laboratory exposure conditions is achieved by:

(i) the measurement of ignition frequencies following by sensitivity analysis, to obtain the mean ignition time $\langle\tau_i\rangle$ and the function f in Eq. 1.1.1, all for a set of fabrics, fabric assemblies, geometries and exposure conditions,

(ii) the development of an ignition modeling analysis, designed to predict ignition time $\langle\tau_i\rangle$, from fabric properties and process parameters.

The analysis is to be verified by comparison with experimentally obtained ignition time $\langle\tau_i\rangle$. In support of the ignition modeling analysis, there are required:

(iii) the measurement of thermo-physical material properties relevant to the description of the preignition processes,

(iv) the descriptions of fabric and ignition source interactions (constitutive description), and

(v) the establishment of an ignition criterion.

Once the modeling analysis is verified by experiments it can serve to predict ignition time under a large variety of exposure conditions.

Finally, the determination of the probability with which laboratory exposure conditions occur in actual use $\{\hat{U}\}$, namely $P(E_\ell/\{\hat{U}\})$, is obtained from:

(vi) the characterization of ignition sources, that is the measurement of heat flux distribution $q(\vec{r})$ about possible ignition sources, and

(vii) time studies, i.e. the measurement of time frequencies at which garments are exposed at certain positions $(\vec{r})$.

1.3 Previous Achievements

Fabric flammability research performed during the time from November 1, 1970 through December 31, 1972 resulted in the following accomplishments, with results reported in References [1.8 and 9].

1.3.1 The Thermophysical Properties

The thermophysical properties measured on the set of twenty GIRCFF Fabrics, specified in Table 2.1 are:

(i)	fabric mass per unit area	$(\rho\delta)$
(ii)	specific heat of fabric	c_p
(iii)	thermal conductance	(k/δ)
(iv)	ignition temperature	T_{ig}
(v)	radiative properties	
	reflectance	$\tilde{\rho}$
	transmittance	$\tilde{\tau}$
(vi)	reaction kinetic parameters	
	activation energy	E
	frequency factor	A
	reaction degree	n

(vii) reaction calorimetric parameter
reaction enthalpy Δi_f

1.3.2 Ignition Time Measurements

Ignition Time Measurements were carried out on the set of twenty GIRCFF Fabrics, under radiative heating mode with heating intensities varying between 4 and 24 W/cm^2.

1.3.3 Effect of Heating Mode

The effect of heating mode on ignition time τ_{ig} was assessed by ignition time measurements carried out on the first set of ten Primary GIRCFF Fabrics (see Table 2.1 for identification) with a gas flame ignition source.

1.3.4 Effect of Environmental Moisture

The effect of Environmental Moisture on ignition time was determined by carrying out ignition time measurements under radiative heating, in an environmentally controlled enclosure, at relative humidity levels varying between 10 and 95 percent.

1.3.5 Statistical Confidence of Ignition Time Measurements

The statistical confidence of ignition time measurements was obtained from the measurement of ignition time frequencies, carried out with controlled exposure times and evaluated by probit analysis. The standard deviation of mean ignition time $\langle \tau_{ig} \rangle$ was found to be less than 1 percent.

1.3.6 Modeling Analysis

A modeling analysis was performed for the purpose of predicting ignition time $<\tau_{ig}>$ as a function of material properties and exposure conditions. As ignition criterion was employed the attainment of a measured ignition temperature T_{ig} at the heated fabric surface. Individual contributions to the energy requirement during ignition by the processes of desorption, gasification and convective cooling during radiative heating, were assessed by partial modeling.

The modeling analysis revealed that the number of material property and process parameters required to describe the ignition process could be reduced from 21 to 10, by normalization of the governing equations. The expression for ignition probability in Eq. 1.1.1 was shown to take on this form

$$P(I/E) = f(\tau_e/<\tau_1>\{\pi_1,\ldots,\pi_{10}\}) \qquad (1.3.1)$$

where $\{\pi_1,\ldots,\pi_{10}\}$ represents a set of scaling groups.

1.3.7 Publications and Presentations.

The results obtained during the first two years were summarized in six Quarterly Reports and two Annual Final Reports [1.8,9]. The results were orally presented at seven contractor's meetings and at a formal Seminar at the Georgia Institute of Technology in May of 1972. There were two M.S. Theses completed and one special problem carried out under the first two grants. One invited paper was presented at the Symposium on Textile Finishing Chemistry, Division of Cellulose, Wool and Fiber Chemistry, 164th Meeting, ACS, New York, N.Y., August 30, 1972.

These and the more recent publications and presentations are listed in Chapter 5.

1.4 Program Objectives

The program objectives of the research reported here are a natural extension of previous efforts toward the prediction of burn injury probability and are selected to supplement previous accomplishments. The program consists of an experimental and an analytical effort, and is divided into seven tasks.

1.4.1 Experimental Program

The experimental phase consists of six tasks and is intended to (1) describe the fabric response to radiative and gas flame heating, (2) to provide data for experimental verification of the ignition modeling analysis, (3) to develop a new, universally applicable ignition criterion, and (4) to establish constitutive laws which describe fabric interaction with relevant ignition sources. The six tasks are:

Task 1. Ignition Temperature Measurements of Pyrolysate-Air Mixtures are necessary to develop an ignition criterion which takes into account heating history, degree of decomposition and air flow dynamics near the heated surface.

Task 2. Determination of Convective Film Coefficients are required to describe fabric and gas flame interaction, including the shielding effects of pyrolysate evolution from the decomposing fabric.

Task 3. Ignition Time Measurements on Single Fabrics Under Gas Flame Heating were scheduled to complete the second part of an investigation on the effects of heating modes, started during the last grant period.

Task 4. Ignition Time Measurements on Fabric Assemblies Under Various Geometric Configurations are required to assess the effects of

thermal and possibly of chemical fabric interactions, as well as of fabric orientation and fabric shape.

Task 5. Ignition Time Statistics and Ignition Probability. The measurement of ignition frequencies under controlled exposure time are required to determine the actual form of the function f in Eq. 1.1.1, specifically to determine the mean ignition time $<\tau_{ig}>$ and the standard deviation σ of the ignition time τ_{ig} about its mean $<\tau_{ig}>$.

Task 6. Characterization of Ignition Sources

1.4.2 The Analytical Program

The analytical program consists of four subtasks and has these objectives:

Task 6.

(i) To develop a complete modeling analysis, based on integral techniques, which serves to predict ignition time of composites, as a function of material properties and process parameters.

(ii) To incorporate into the modeling analysis the ignition criterion for which experimental data are obtained under Task 1 above.

(iii) To develop the complete scaling laws by which to predict ignition time.

(iv) To assess the errors arising from partial modeling.

The following chapter is a presentation of accomplishments and results from the experimental program. The presentation is made in the order of the task listing above. Significant developments of new test equipment are detailed in Appendix A. Chapter 3 is devoted to the analytical program and Chapter 5 is a summary of publications and presentations which reflect the activities of the entire three-year grant period.

2. EXPERIMENTAL PROGRAM

The purpose of the experimental program is to provide (1) ignition time data for the verification of the modeling analysis described in Chapter 3, (2) constitutive descriptions required for the modeling analysis, namely the description of thermal flame-fabric interaction and the flammability limit for pyrolysate-air mixtures, and (3) the relation between laboratory and actual conditions of fabric exposure to potential ignition sources.

The experimental program originally was subdivided and is now presented in these six tasks:

(i) Ignition Temperature Measurements on Pyrolysate-Air Mixtures
(ii) Determination of Convective Film Coefficients on Pyrolyzing Surfaces
(iii) Ignition Time Measurements on Single Fabrics Subjected to Gas Flame Heating
(iv) Ignition Time Measurements on Fabric Assemblies Under Various Geometric Configurations
(v) Ignition Time Statistics and Ignition Probability
(vi) Characterization of Actual Ignition Sources.

The fabrics previously selected and employed for this program are identified in Table 2.1.

2.1 Ignition Temperature Measurements on Pyrolysate-Air Mixtures

A new ignition criterion has been proposed earlier [2.1], predicated on the assumption that ignition occurs in the boundary layer, where the combustible volatiles interact with the oxygen of the air and when the thermal reaction accelerates itself. Moreover, it is postulated that this thermal excursion begins when locally a concentration-dependent minimum temperature $T_{ig}(w_f)$ is reached.

Table 2.1 Fabric Identifications and Specific Mass

GIRCFF No.	Classification	Fiber Composition	Color	Finish	Specific Mass mg/cm^2
1	Durable Press Slack	65/35% Pe./C.	White	DP treated	23.49
2*	Textured Woven Blouse	100% Polyester	Yellow	-	7.51
3	Double Knit	100% Polyester	White	-	20.91
4	Denim	100% Cotton	Navy bl.	-	29.63
5*	T-Shirt, Jersey	100% Cotton	White	-	13.71
6	Untreated Slack	65/35% Pe./C.	White	-	23.57
7	Jersey Tube Knit	100% Acrylic	Gold	-	15.13
8*	T-Shirt, Jersey	65/35% Pe./C.	White	-	16.19
9	Terry Cloth	100% Cotton	White	-	26.48
10*	Batiste	100% Cotton	Purple	-	6.65
11*	Tricot	80/20% Acet./ Nyl.	White	-	11.31
12*	Tricot	100% Nylon	White	-	8.91
13*	Tricot	100% Acetate	White	-	9.40
14	Taffeta	100% Nylon	White	-	5.66
15	Durable Press Slack	65/35% Pe./Ray	Brown	DP treated	22.82
16	Shirting	50/50% Pe./C.	White	-	13.14
17*	Batiste	65/35% Pe./C.	White	-	8.55
18*	Flannel	100% Cotton	White	-	12.88
19*	Flannel	100% Cotton	White	Fire retard	14.89
20	Flannel	100% Wool	Navy bl.	-	19.93

*Ten Primary GIRCFF Fabrics.

This criterion involves both temperature and pyrolysate concentration and thereby accounts for the effects of heating rate and external fluid flow dynamics.

2.1.1 Purpose

The objective of this measurement is to determine the lowest ignition temperature T_{ig} of cellulose pyrolysis products, premixed with dry air, as a function of pyrolysate concentration. Measurements are required in the range of ignitable concentrations, to produce

$$T_{ig} = f(w_f) \quad , \quad 0 < w_f < 1 \tag{2.1.1}$$

with smooth continuations of f outside the range of ignitable concentrations, that is, for $(0 < w_f \leq w_{fl})$ and $(w_{fu} \leq w_f < 1)$. Here w_{fl} and w_{fu} represent, respectively, the lower and upper limits of ignitable mixture concentrations. It is expected that the smooth continuation implies $T_{ig} \to \infty$ as $w_f(1 - w_f) \to 0$.

2.1.2 Experimental Procedure

The following procedure is employed for the measurement of pyrolysate-air mixture ignition temperatures as a function of pyrolysate concentration.

The cellulosic material is heated in an inert, evacuated furnace, shown in the schematic flow diagram of Figure A.1.1 and in Figure A.1.2 in Appendix A. The volatiles are accumulated in a reservoir and then metered into the mixing chamber of the reaction cell, where they mix with a regulated and monitored stream of dry air.

The mixture of known pyrolysate concentration passes upward through the heated section of the reaction cell where the local mixture temperature rises slowly in time until a flame occurs at the exit of the reaction cell. The flame is detected by an infrascope. The mixture temperature in the heated section of the reaction cell is sensed by a bare, gold-plated

platinum wire resistance thermometer and continuously monitored. The recorded temperature history permits the determination of ignition temperature.

2.1.3 Lower Ignition Temperature and Concentration Apparatus (LITACA)

A special instrument, called Lower Ignition Temperature and Concentration Apparatus (LITACA) has been designed, constructed and assembled which is described in detail in Appendix A and which is shown in Figure A.1.4. It consists of these major components:

(i) Furnace: Quartz glass tube in cylindrical heater, capable of reaching temperatures above 800°C and holding approximately 100 g of cellulosic material.

(ii) Volatile Reservoir: Quartz glass cylinder with pressurized piston, holding up to 2000 cc of volatiles at pressures up to 3 atm.

(iii) Metering System: Heated variable-area flow meters, valves.

(iv) Reaction Cell: Consisting of the mixing chamber filled with glass beads (flame arrestor), and heated quartz tube test section which contains the Pt resistance thermometer.

(v) Resistance Recording Facility, consisting of
Hewlett-Packard 34750 A 5-digit Display Unit
Hewlett-Packard 34721 A BCD Module
Hewlett-Packard 34703 A DCV/DCA/OHM Meter

Detailed descriptions of LITACA and the associated calibrating and operating procedures are presented in Appendix A.1.

2.1.4 Results

A pilot test was carried out using a propane-air mixture to test the feasibility of ignition detection with this equipment. The test has been successful. The work is currently being continued as part of an M.S. Thesis research program and ignition temperature measurements will be conducted on pyrolysate-air mixtures.

2.2 Determination of Convective Film Coefficients for Flame-Fabric Interaction

2.2.1 Purpose

Decomposition gases emerging from the heated fabric surface effectively protects this surface from impinging gas flames or from cooling air during radiative heating. The interaction between heated surface and environmental gases is described in terms of a convective film coefficient. The objective of this task is to simulate the fabric geometry with inert stainless steel wire mesh cloths and to simulate the action of emerging pyrolysates through injection of preconditioned air, and then infer the thermal response of the fabric from the response of the wire cloth by incorporating it directly into a thermocouple circuit which senses true wire cloth temperature.

2.2.2 Achievements

2.2.2.1 Experiments. To simulate thermal decomposition a pyrolysate injection chamber was design constructed and installed. The instrumentation was calibrated. The total of fifty tests were carried out with varying injection velocity, injected air temperature, and burner gas exit velocity. All tests were performed with the stainless steel screen positioned 19 mm above the burner. The burner heating intensities used for the film coefficient measurement were the same as for the fabric ignition time measurements. The results are presented in Section 2.2.4.

2.2.2.2 Analysis. The flame gases envelop the fabric threads (or screen wires) to a degree depending, in part, on the relative magnitudes of the pyrolysis and the porosity of the fabric. The presence of the injection chamber reduces the gas flow through the wire screen, and hence, the heat transfer between gas and screen. This was expected and observed experimentally: the convective film coefficients determined for the screens mounted in the injection chamber were significantly lower than those in which the screen was freely suspended [2.2].

An analysis was therefore developed to correct for the differences in fluid dynamics between freely suspended screens and screens mounted in the injection chamber. The analysis is part of an M.S. Thesis study and not yet completed at the time of report writing. The fundamental equations are developed and are presently being solved. The data reduction in Section 2.2.3.2 is based on the same analysis.

2.2.3 Measurement of Convective Film Coefficients

The convective film coefficient measurements were carried out on the Convective Ignition Time Apparatus (CITA) after suitable modifications in its specimen support. The design details and operating principles of these components of CITA remained the same and are described in Appendix B.3 of Reference [2.3].

The modifications of CITA and specific operating procedures are discussed in the next section. Results are shown in Section 2.2.4.

2.2.3.1 Injection Apparatus. The major components which were added to CITA are

(i) the injection chamber,
(ii) air pre-heater, and
(iii) the related instrumentation.

The design details of the air injection chamber and ancillary equipment is presented in Appendix A.2. Figure 2.1 shows details of the Screen Holder Assembly.

Preheated air is passed, at a selected flow rate, first through a sintered porous bronze plate and then through the screen. Once the flow is established, the screen is rapidly exposed to the gas flame by means of the high-speed shutter system of CITA.

Figure 2.1. Air Injection Apparatus, 64 mm Diameter Stainless Steel Screen.

The screen and gas temperatures are recorded as functions of time. The screen itself is part of a thermocouple junction and thus yields true screen temperature.

2.2.3.2 Experimental Procedures and Data Evaluation. The injection chamber is mounted to the Convective Ignition Time Apparatus and positioned at the selected position and orientation with respect to the burner. The injection air flow rate and temperature are stabilized and the flame established with the shutter separating the flame from the screen.

Activation of the shutters causes the screen to be exposed to the gas flame and a timing mark recorded on the strip chart or oscilloscope recorder monitoring the screen temperature.

The data was evaluated, based on the energy balance for the freely suspended screen. The forced convection film coefficient $\bar{h}_c$ was computed from

$$\bar{h}_c = (C''/2)\,(dT/d\tau)/(T_f - T) \qquad (2.2.1)$$

where C" represents the screen heat capacity per unit area, T and τ stand for screen temperature and time, respectively and T_f for flame gas temperature. The resulting film coefficient is normalized and presented as the Nusselt number

$$N_{Nu} = \frac{\bar{h}_c R}{k} \qquad (2.2.2)$$

and plotted versus the Reynolds number of the approaching gas stream

$$N_{Re} = \frac{\bar{v} R}{\nu} \qquad (2.2.3)$$

with the injection Reynolds number as parameter:

$$(N_{Re})_i = \frac{v_i R}{\nu} \qquad (2.2.4)$$

The symbols R,k and ν represent respectively, the screen radius, the thermal conductivity and the kinematic viscosity of the approaching gas while $\bar{v}$ denotes the average gas velocity normal to the screen and v_i the area-averaged injection velocity of the injected air. The results are shown in the following section.

2.2.4 Results and Conclusions

Measured convective heat transfer coefficients were normalized in terms of Nusselt and Reynolds numbers as defined by Eqs. 2.2.3 and 4. The normalized heat transfer coefficients are plotted for various normalized injection rates, versus normalized free stream velocities in Figures 2.2 and 2.3.

Figure 2.2 shows the results obtained for gas injection temperatures near room temperature, that is, in the range of 20°C to 40°C as indicated. Figure 2.3 presents the results for elevated injection temperatures which are specified on the diagram.

The top curve in Figure 2.2 shows the results obtained without gas injection, $(N_{Re})_i = 0$, on a freely suspended screen. These film coefficients are higher than the values representing the results from the screen mounted in the injection chamber and shown as the second curve from the top. This difference is due to the variation in fluid dynamics and the subject of the analysis described in Section 2.2.3.

The interpretation of the data obtained so far is currently being continued as part of an M.S. thesis research program, but it is apparent from the presented data that injection of gas, or evolution of pyrolysates can effectively reduce the heat transfer from the flame to the pyrolyzing surface by up to 20 percent in the case of fabrics.

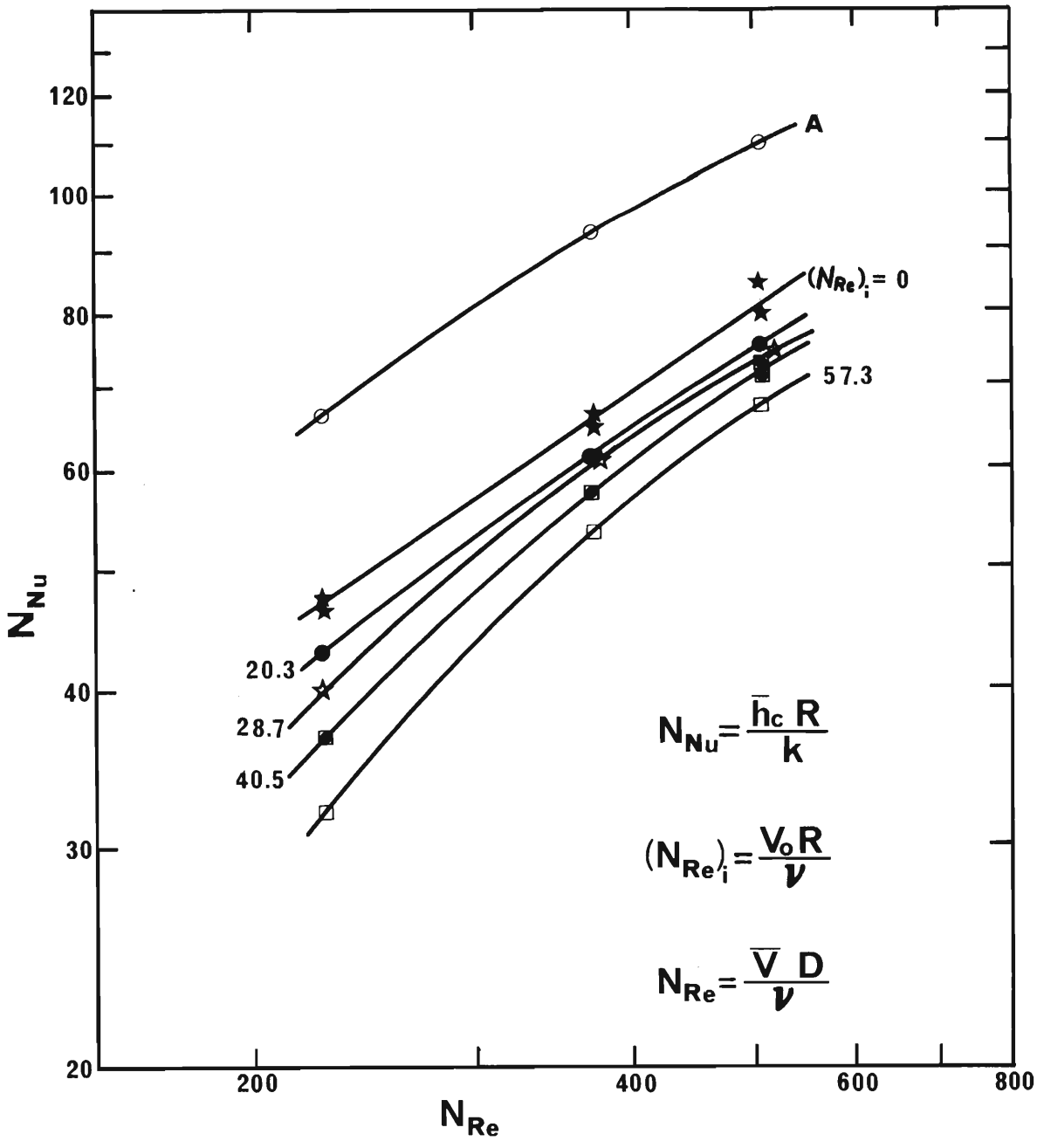

Figure 2.2 Nusselt Number vs. Free-Stream Reynolds Number with Injection Reynolds Number as Parameter, for Low Injection Gas Temperature

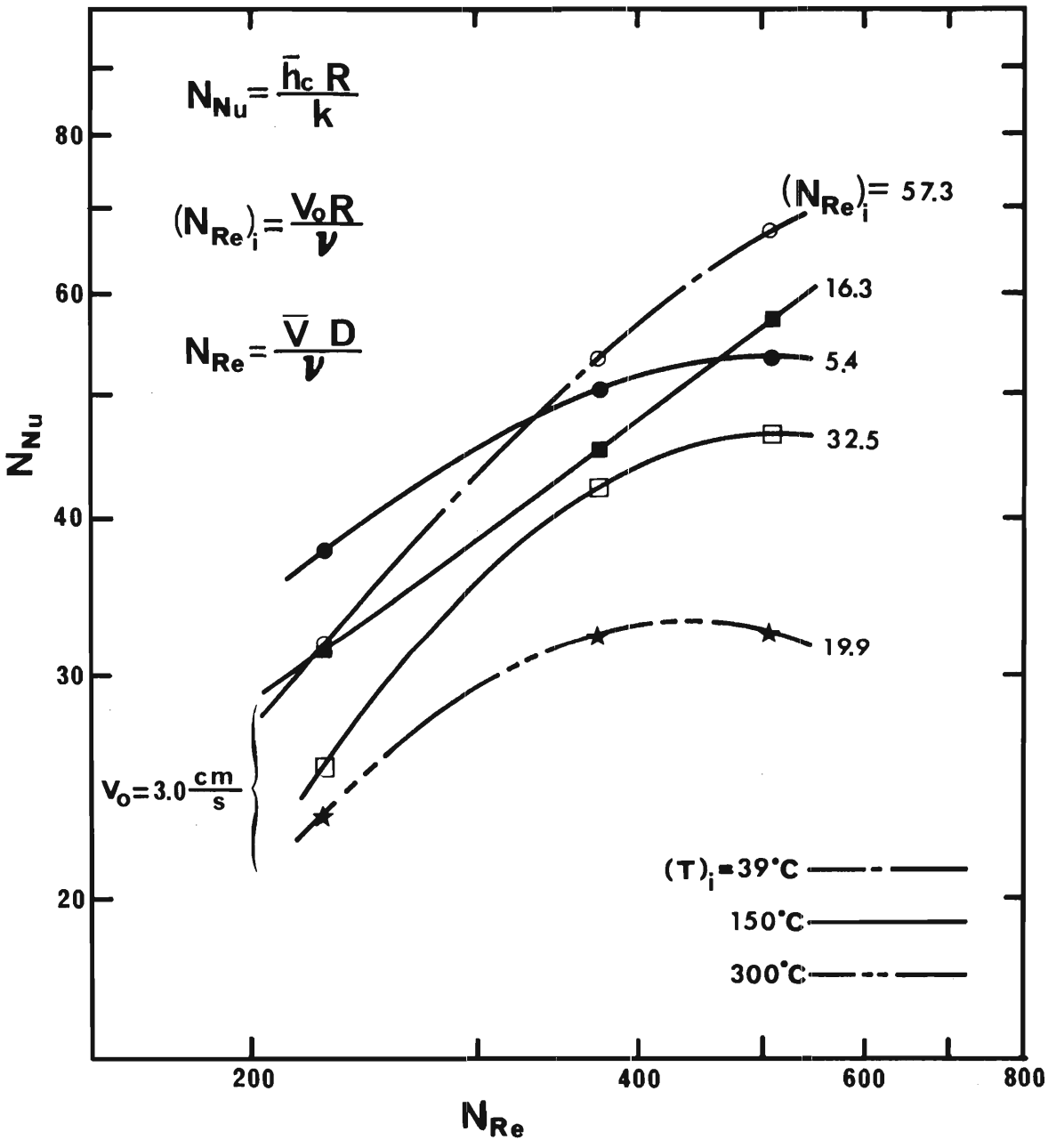

Figure 2.3 Nusselt Number vs. Free-Stream Reynolds Number with Injection Reynolds Number as Parameter, for Elevated Injection Gas Temperature

The analysis carried out to date, on the prediction of ignition times of fabrics under convective heating has made use of convective film coefficients evaluated from inert screen measurements without injection of gases. The results of convective film coefficient measurements with simulated pyrolysate injection will be used to reevaluate the predictions of fabric ignition times.

2.3 Gas Flame Ignition Time Measurements on Single Fabrics

2.3.1 Purpose

The objective is to measure the destruction (ignition or melting) time of single fabrics exposed to a gas flame convective heat source under two conditions: (i) the stationary ignition test, where the fabric is suddenly exposed to a time-invariant convective heat source, and (ii) the dynamic ignition test, where the fabric is moved into the convective heat source at a predetermined velocity. In the first case one measures the time from initial exposure of the fabric to the heat source, to ignition or melting. In the second case one measures the time from initial contact of the fabric with the flame at the flame boundary, to ignition or melting, for different rates of motion of the fabric through the flame.

The Convective Ignition Time Apparatus (CITA) was designed to meet the following conditions [2.3]:

(i) Specimen heating by a gaseous fuel-air flame, provided by a variable fuel rate and variable air rate burner.
(ii) Specimen exposure to the flame, for the static tests, through a shutter providing full exposure of the sample in five-hundredths of a second or less.
(iii) Specimen side of shutter not to exceed 60°C, to avoid preheating of the sample.
(iv) Specimen transport for the dynamic tests at different speeds between 2 and 25 cm/s.

The design features and operating principles of CITA are found in Appendix B.3 of Reference [2.3].

A further objective of this task is to use the fabric ignition time measurements with the gas flame to test the general validity of the analytical model presented in Sections III.C.3.c and III.C.3.d of Reference [2.3].

2.3.2 Achievements

2.3.2.1 Experimental. This task is a continuation of research initiated during the previous grant period. During that period 130 fabric destruction time tests were performed in the stationary ignition test mode on the ten Primary GIRCFF Fabrics.

During the present grant period the total of 193 fabric destruction time tests were run in the dynamic ignition test mode on the ten Primary GIRCFF Fabrics by supporting the fabric in the 63.5 mm aperture holder and moving the fabric in the horizontal plane, 1.9 cm above the top of the burner, with velocities between 2 and 25 cm/s. The fabric destruction times obtained ranged from 0.07 seconds to more than 31 seconds.

Fabric destruction time measurements in the stationary ignition test mode were run on the ten Secondary GIRCFF Fabrics and the total of 71 tests was carried out. The fabrics were exposed to five different convective heating intensities at the stoichiometric equivalence ratio of $\phi = 0.86$, and with fabric holder aperture of 63.5 mm. Fabric destruction times were measured successfully for all of the ten Secondary GIRCFF Fabrics. These times range from 0.33 to 11.3 seconds.

2.3.2.2 Analytical. The analytical model presented in Sections III.C.3.c and III.C.3.d of Reference [2.3] for the gas flame ignition of fabrics was used to predict the time history of the fabric temperature θ, the degrees of desorption λ_d, together with their respective time rates of change, for two of the Primary GIRCFF Fabrics. The solution of the equations was carried out for five different convective heating intensity conditions and using a range of gasification parameters.

2.3.3 Apparatus and Instrumentation

The Convective Ignition Time Apparatus (CITA) was designed, built and used during the previous grant period in the stationary ignition test mode

with the ten Primary GIRCFF Fabrics. The design details of the apparatus and its operating principles in the static and the dynamic test modes are presented in Appendix B.3 of Reference [2.3] together with descriptions of the associated instrumentation used during each test mode. For the present contract period no modifications were made either on the basic apparatus or in the instrumentation used for the stationary and dynamic fabric destruction time measurements.

2.3.4 Experimental Procedures

The fabric samples to be used for fabric destruction time measurements were cut and mounted in the 63.5 mm fabric holders and placed in a desiccated chamber at least twenty-four hours prior to testing. Prior to the conduct of the fabric destruction tests all instrumentation was readied, and the burner was adjusted to the desired air-methane ratio and bulk mixture flow rate. The fabric sample from the desicated chamber was mounted at the desired height in CITA at the last moment to minimize moisture absorption from the atmosphere.

2.3.4.1 Stationary Ignition Tests. Gas flame ignition of the fabric and the occurence of a flame was sensed by an infrared detector focused on the front side of the fabric (the side exposed to the flame), through the gas flame (optically thin in the infrared spectrum). Gas flame melting of the fabric and the onset of a breakthrough in the heated zone was sensed by the infrared detector also, however, this time focused to a small quartz lamp placed no less then 25 cm from the back face of the fabric. A voltage source and a microswitch, which was activated by one of the moving shutters, was used to detect the instant when separation occured in the two shutters and the fabric sample was exposed to the burner flame.

Fabric destruction time was measured from the time the microswitch was activated by the moving shutter to the time where a sharp rise was detected on the infrared detector. The signal of the voltage source interrupted by the microswitch and signal of the infrared detector were recorded on Polaroid film from a dual-beam oscilloscope.

A chromel-alumel thermocouple placed behind the fabric was allowed to record the temperature on a pen-recorder after fabric destruction had occured. In this manner the flame temperature was measured at that point.

2.3.4.2 Dynamic Ignition Tests. The onset of fabric destruction was sensed by a chromel-alumel thermocouple located on the back of the fabric sample. Fabric destruction time was measured from the time the fabric sample crossed the flame boundary to the time when a sharp rise was detected on the thermocouple signal.

2.3.5 Results

2.3.5.1 Experimental. The convective destruction time data from the dynamic tests are presented in Figures 2.4 and 2.5 for melting and igniting fabrics, respectively.

The normalized destruction time (Fourier number)

$$(N_{Fo})_{i,m} = \left\{ (k/\delta) \;/\; c(\rho\delta) \right\} \tau_{i,m} \qquad (2.3.1)$$

is plotted versus the sample velocity. The data for zero-velocity are taken from the static tests. The melting times in Figure 2.4 approach infinity for vanishing sample velocity and the melting time from stationary tests for increasing sample velocity, as would be expected from the consideration of the accumulated heating due to time dependent heat flux impingment during flame traversing. The ignition time data in Figure 2.5 reveal that ignition may occur after flame traversing and that there is a maximum traversing velocity between 9 and 21 cm/s for the given burner-aperature combination beyond which ignition does not occur. The maximum traversing velocities are listed in Table 2.2. The tendency toward large ignition times with vanishing sample velocity could not be observed because of the limitation in the control of low traversing velocities.

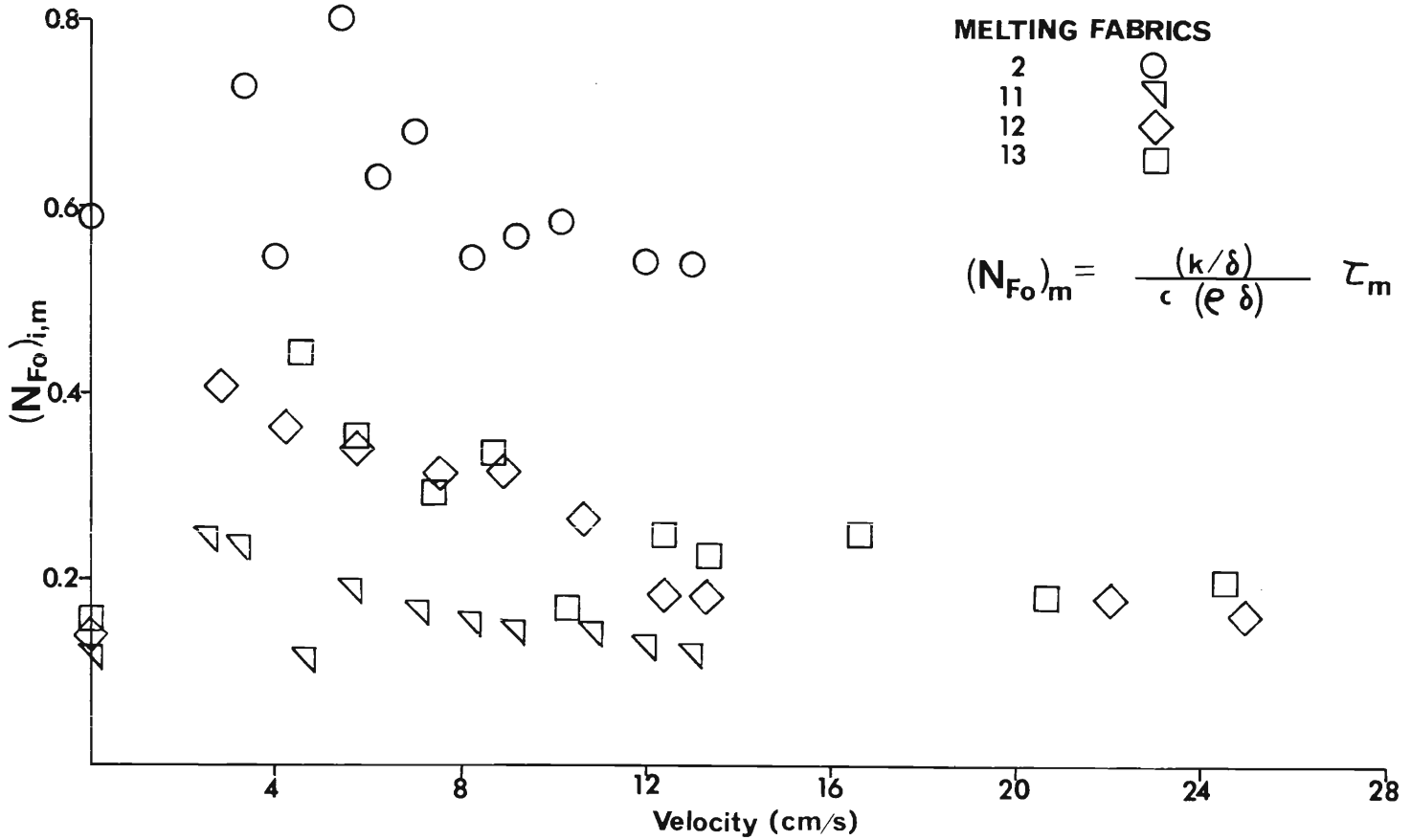

Figure 2.4 Nondimensional Melting Time vs. Sample Velocity, Gas Flame Ignition

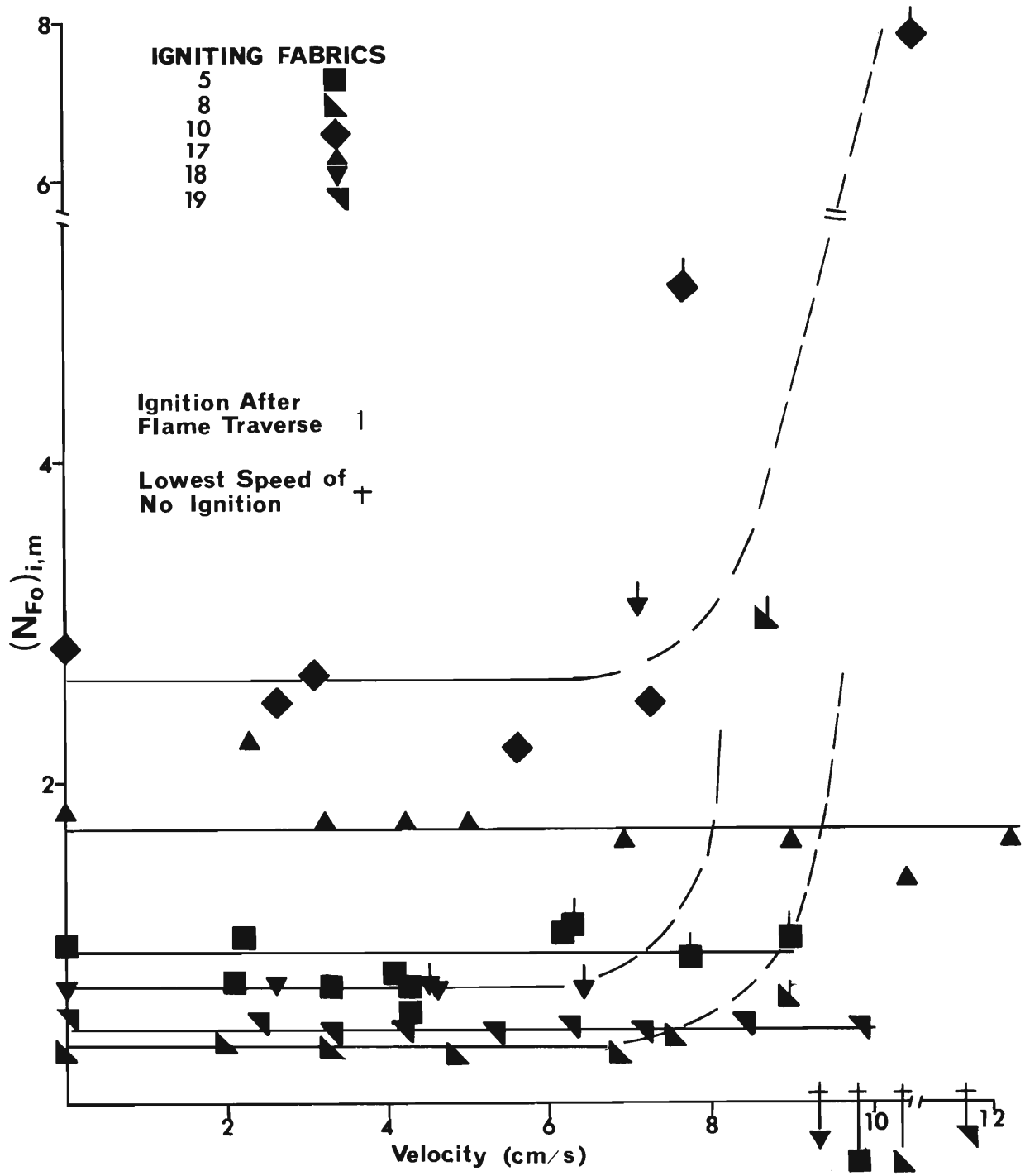

Figure 2.5 Nondimensional Ignition Time versus Sample Velocity; Flame Ignition

Table 2.2 Maximum Traversing Velocity for Flame Ignition

Vertical Burner, Diameter of 37 mm
Horizontal Fabric Specimen, Diameter of 63.5 mm
Fabric Motion Horizontal, Perpendicular to Flame Axis

GIRCFF Fabric Number	Maximum Velocity cm/s
5	9.88
8	10.6
10	20.6
17	15.9
18	9.42
19	11.67

The convective ignition time data for the ten Secondary GIRCFF Fabrics are presented in Figure 2.6. The nondimensional destruction time $(N_{Fo})_{i,m}$ as defined by Eq. 2.3.1 is plotted versus the time average, nondimensional heating intensity

$$q_c^* = \left[2\bar{h}_c \;/\; (k/\delta) \right] (\theta_f - \bar{\theta}) \qquad (2.3.2)$$

where θ stands for normalized temperature

$$\theta = (T - T_\infty) \;/\; (T_{i,m} - T_\infty) \;, \qquad (2.3.3)$$

subscript f represents flame temperature and the superscripted bar designates time-averaged fabric temperature as computed from the inert heating analysis

presented in Reference [2.3]. The convective film coefficient $2\overline{h}_c$ represents the average value over projected front and back faces of the sample. A stainless steel screen, exposed to the gas flame in the same configuration and procedure, was used to infer the convective film coefficients. The details of these measurements and the analysis were reported in Section II.C of Reference [2.3]. The convective film coefficients used in the reduction of the data presented below are summarized in Table A.1 of Appendix A.2.

The experimental data in Figure 2.6 are compared with the inert heating model, which is shown as a solid line curve A. The experimental results of GIRCFF Fabrics number 4 and 9 (both cotton) exhibit the largest difference from the results of the inert heating model. The other igniting fabrics and the melting fabrics exhibit the smallest difference.

The difference between the inert heating model and the experimental results with the convective heating can be attributed to three factors. One of these is pyrolysis. The effect of chemical reactions prior to ignition and the retardation of the ignition process is discussed in the analytical section which follows.

The second factor that is important, when considering the difference between the inert heating model and the experimental data, is the film coefficient. Past measurements of film coefficients were carried out on inert bodies. While these results have been indispensable they are not sufficient for predicting fabric destruction times. One of the tasks of the present contract period has been devoted to consider the desorption and gasification process in the fabric, and the associated outflow of gases from the fabric surface, in the evaluation of the convective film coefficients. The results to date on this effort are reported in Section 2.2 of this report.

The third factor which must be reconciled with in considering the differences between the model and experimental measurements is the fabric ignition temperature. The fabric ignition temperatures used in the modeling analysis and in the reduction of the experimental results presented in this section have been measured in a Setchkin Furnace and reported in Reference

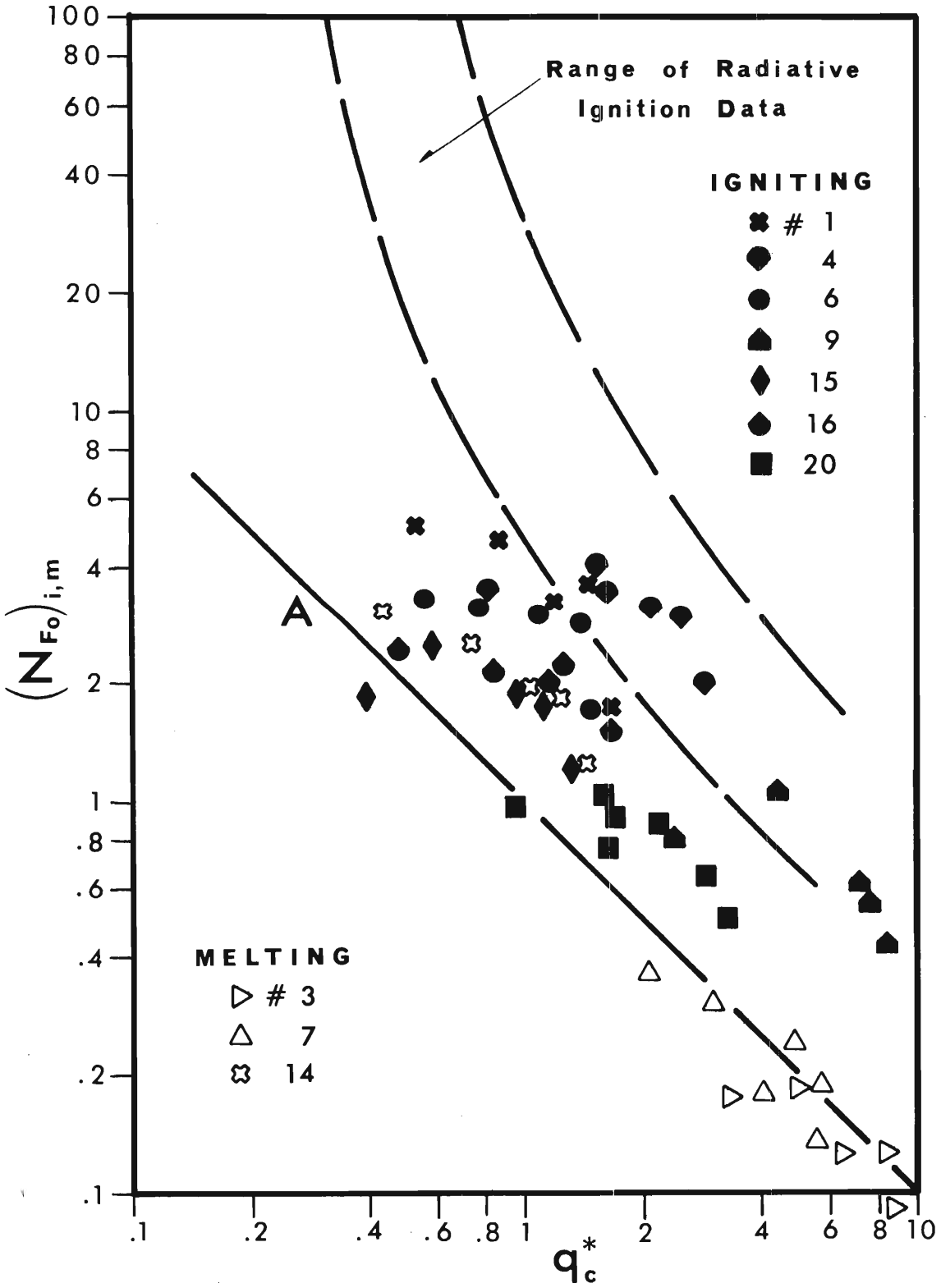

Figure 2.6 Normalized Destruction Time vs Normalized Convective Heat Flux for the Secondary GIRCFF Fabrics

[2.4]. The ignition criterion which has been used assumes attainment of this temperature by the solid-phase as the onset of ignition. A new ignition criterion based on a gas phase ignition temperature has been proposed and the task which has been concerned with the measurement of the pyrolysate-air mixture ignition temperature is reported in Section 2.1 of this report.

2.3.5.2 Analytical. The gas flame ignition model which includes the retarding processes of desorption and gasification was presented in Sections III.C.3.c and III.C.3.d of Reference [2.3]. The derived normalized governing equations are

$$d\theta/d\bar{\tau} = \theta_f - \theta - \pi_2^* \left\{ [1 + \pi_o(\theta - 1)]^4 - [1 - \pi_o]^4 \right\}$$

$$-\pi_3^* (d\lambda_d/d\bar{\tau}) - \pi_6^* (d\lambda_g/d\bar{\tau}) \qquad (2.3.4)$$

$$d\lambda_d/d\bar{\tau} = \pi_5^* (1 - \lambda_d)^{n_d} \exp \left\{ -\pi_4/[1 + \pi_o(\theta - 1)] \right\} \qquad (2.3.5)$$

$$d\lambda_g/d\bar{\tau} = \pi_8^* (1 - \lambda_g)^{n_g} \exp \left\{ -\pi_7/[1 + \pi_o(\theta - 1)] \right\} \qquad (2.3.6)$$

with the following initial conditions

$$\text{at } \bar{\tau} = 0 : \qquad \theta = 0 \qquad \lambda_d = \lambda_g = 0 \qquad (2.3.7)$$

In the above equations the independent variable is the time $\bar{\tau}$, and the dependent variables the temperature θ and the degrees of desorption λ_d and gasification λ_g. The remaining are the eleven scaling parameters on which the ignition time under gas flame ignition depends, i.e.

$$\tau_{i,m} = f(\pi_o, \pi_2^*, \pi_3^*, \pi_4, \pi_5^*, \pi_6^*, \pi_7, \pi_8^*, n_d, n_g; \theta_f) \qquad (2.3.8)$$

These scaling parameters were defined in Tables III-1 and III-2 of Reference [2.3] and they represent the initial condition π_o, the radiative cooling π_2^*, the energy requirement for desorption π_3^*, the desorption activation

energy π_4, the characteristic desorption rate π_5^*, the energy requirement for gasification π_6^*, the gasification activation energy π_7, the characteristic gasification rate π_8^*, the reaction order of desorption n_d, the reaction order of gasification n_g, and the flame temperature θ_f.

The equations (2.3.4) through (2.3.7) were solved numerically using Runge-Kutta Integration to obtain values of the three dependent variables θ, λ_d and λ_g in terms of time along with their respective time rates of change. The solutions were carried out for GIRCFF Fabrics No. 5 and No. 10 at five convective heating intensity conditions. A range of desorption and gasification parameters found in the literature and those reported in Reference [2.3] from measurements carried out during the previous contract period were used to assess the effect of uncertainties in the values of these parameters towards prediction of fabric destruction times.

Sample results for GIRCFF Fabric No. 10 at one heating intensity are presented on Figures 2.7 and 2.8. The four temperature history curves in Figure 2.7 have been calculated with different gasification parameters. These are compared with the inert heating model and the retardation of ignition due to gasification and radiative cooling is apparent. On the same figure the ignition time from experimental measurements has also been displayed for comparison. One set of the gasification parameters underestimates the ignition time while the other three overestimate it.

The degrees of desorption and gasification for the same four cases are shown in Figure 2.8. The desorption and gasification processes progress rather rapidly after the degrees of decomposition achieved 2-4% of their ultimate values.

2.3.6 Conclusions

The ignition time measurements and the ignition model analysis presented here demonstrates that

(i) Fabric destruction time is mainly a function of the heat flux magnitude.

(ii) There exists a minimum heat flux rate below which fabric ignition does not occur.

(iii) Prediction of fabric destruction times by inert heating models is adequate for the melting fabrics but inadequate for the igniting fabrics.

(iv) Desorption does not effect the ignition process of fabrics with a low moisture content.

(v) Radiative cooling and gasification are the two ignition time retarding factors, with gasification playing a more dominant role.

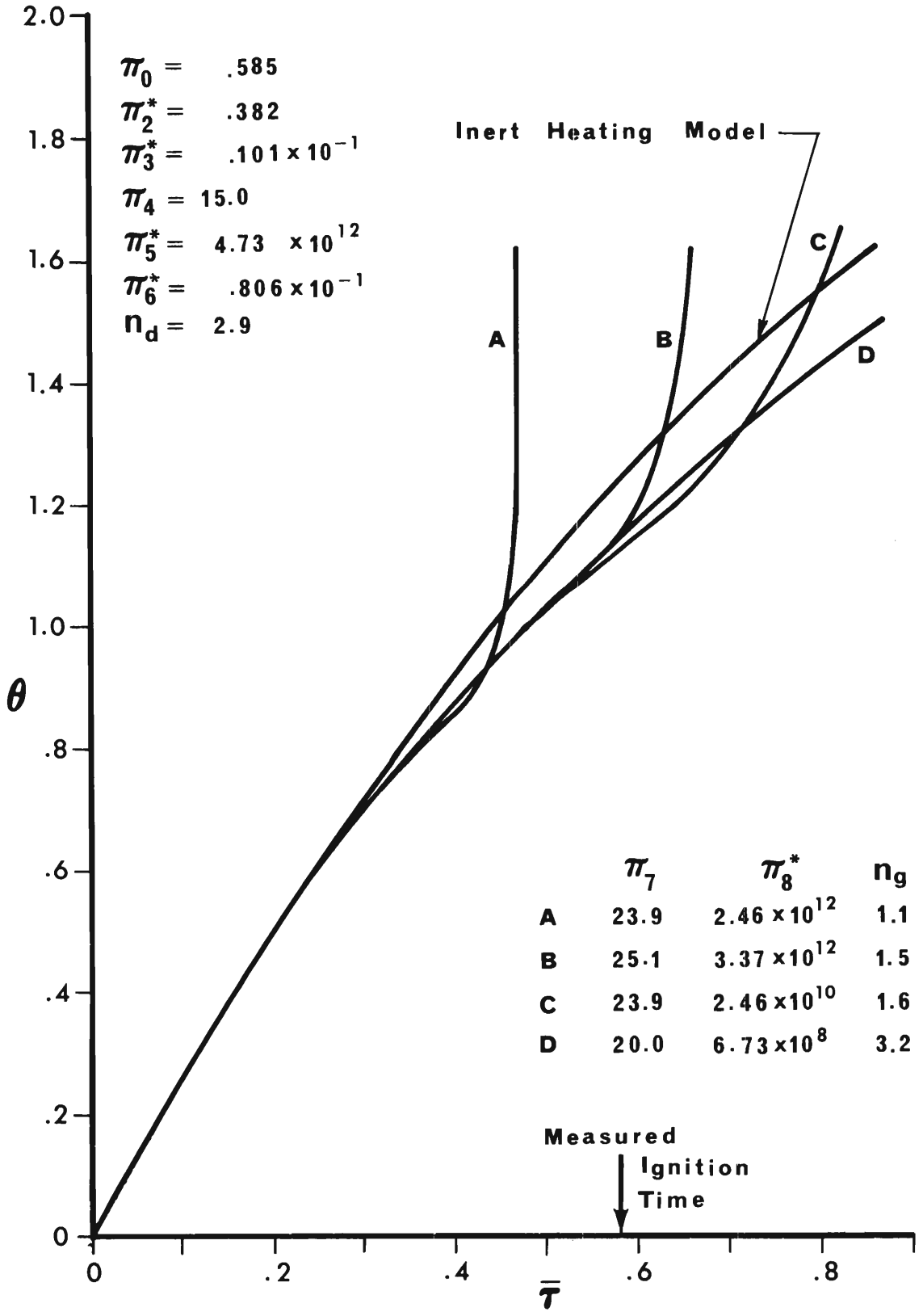

Figure 2.7 Nondimensional Temperature History Curves for GIRCFF Fabric No. 10 at One Heating Intensity and for Different Gasification Parameters

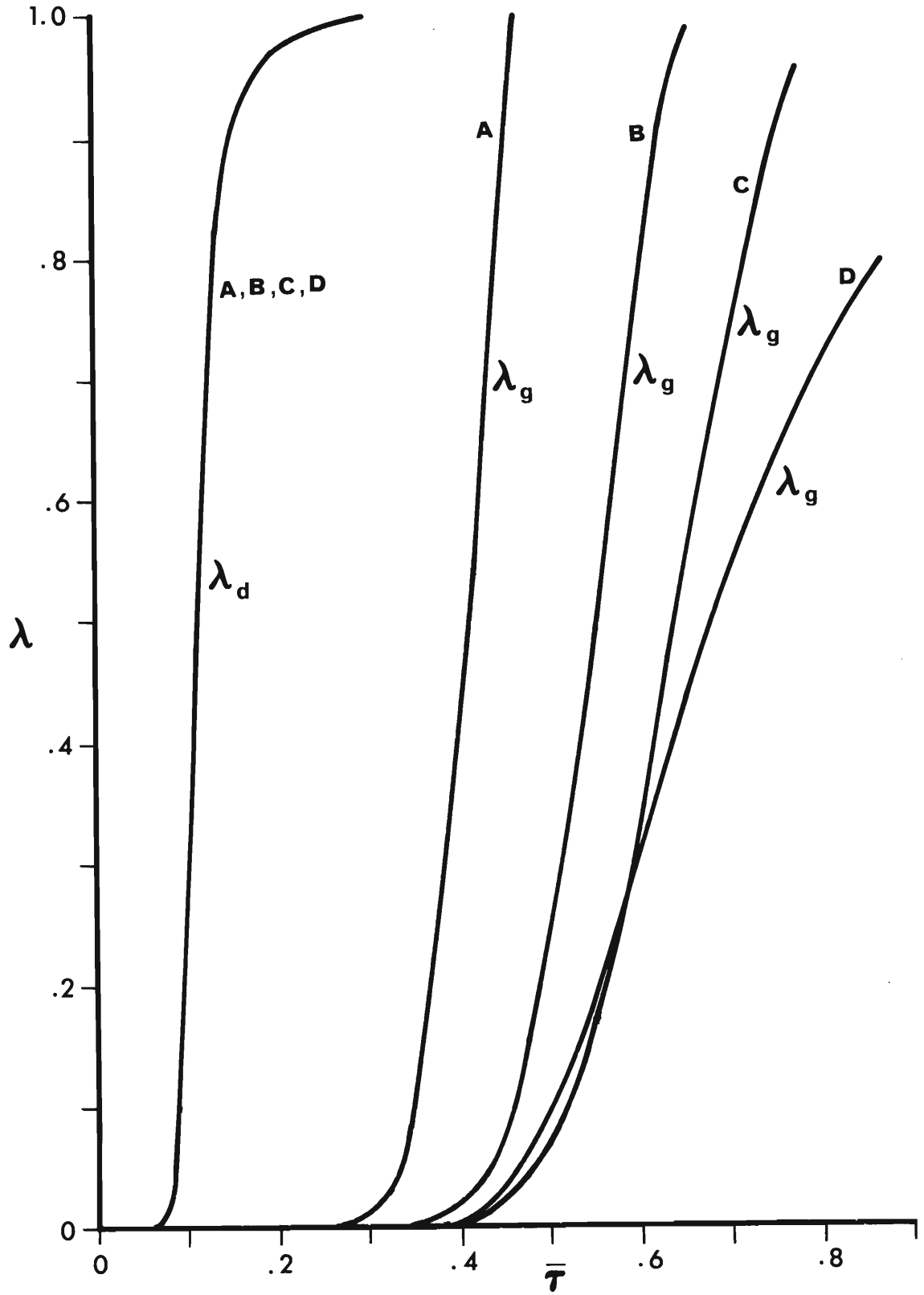

Figure 2.8 Degrees of Desorption and Gasification During the Preignition Period for GIRCFF Fabric No. 10. For definition of A,B,C and D see Figure 2.7.

2.4 Ignition Time Measurements on Fabric Assemblies Under Various Geometric Configurations

2.4.1 Purpose

The objective of this task is to determine the effect of fabric interaction during radiative heating, and of fabric geometry and fabric orientation with respect to the flame axis during convective heating, on the ignition time. Ignition time is defined as the time between the instant of exposure to the first occurrence of a flame anywhere in the system (fabric assembly).

2.4.2 Achievements

The total of 126 ignition tests was performed on fabric assemblies which consisted of two samples of GIRCFF Fabric No. 5 at three fabric spacings and at five heating intensities. The results of ignition time measurements were compared with the ignition times obtained previously [2.3] for a single GIRCFF Fabric No. 5. Results are discussed in the following section.

Seven ignition time measurements were carried out on single fabrics with fabric orientation different from the normal plane to the flame axis, including edge ignition. Results are presented in Section 2.4.4.

Both experimental and analytical work on this task are being continued as part of an M.S. Thesis research program.

2.4.3 Fabric Interaction

The objective of this study is to determine whether fabric interaction during radiative heating can be predicted by heat transfer analysis or whether there is possibly chemical synergism.

Two fabrics were conditioned and mounted, at selected spacings of 0, 1.6 and 3.2 mm, in the Radiative Ignition Time Apparatus (RITA) and radiatively

heated. Front and back faces of the fabric assembly were observed by infrascopes until ignition occurred. The experimental arrangement is shown in Figure 2.9.

2.4.3.1 Apparatus and Instrumentation. The Radiative Ignition Time Apparatus (RITA) for fabric ignition time measurements was used for the ignition tests of fabric assemblies. The description of RITA has been presented first in Reference [2.4]. Supplementary modifications are described in Reference [2.3]. Only additional modifications, required for ignition time measurements on fabric assemblies, are discussed here.

Figure A.3.1 in Appendix A.3 shows the components of a holder to accommodate two fabrics. The fabric holder is identical to that used for single fabrics, except a spacer ring is inserted to separate the two fabrics at the selected distances of 1.6 and 3.2 mm. Details of the holder assembly are shown in Figure A.3.2 of Appendix A.3.

Figure 2.9 shows a schematic of the experimental arrangement which is similar to the one used for single fabric ignition tests, except that there are two additional components, namely, a mirror and a second infrascope to view the front fabric. Two infrascopes were used, one was focused through the mirror on the heated front fabric surface, the other one on the back face of the rear fabric. The mirror did not interfere with the ignition process and reflected the full view of the front fabric into the front fabric infrascope.

2.4.3.2 Data Reduction. Ignition time was measured on the oscillogram (Figure A.3.3) from the instant of exposure to the sharp rise of the trace representing the signal from the front face infrascope, as discussed in Appendix A.3.

2.4.3.3 Results and Conclusion. Results of the ignition time measurements for fabric assemblies are summarized in Table 2.3, together with previously measured ignition times for single fabric under the same test conditions [2.3].

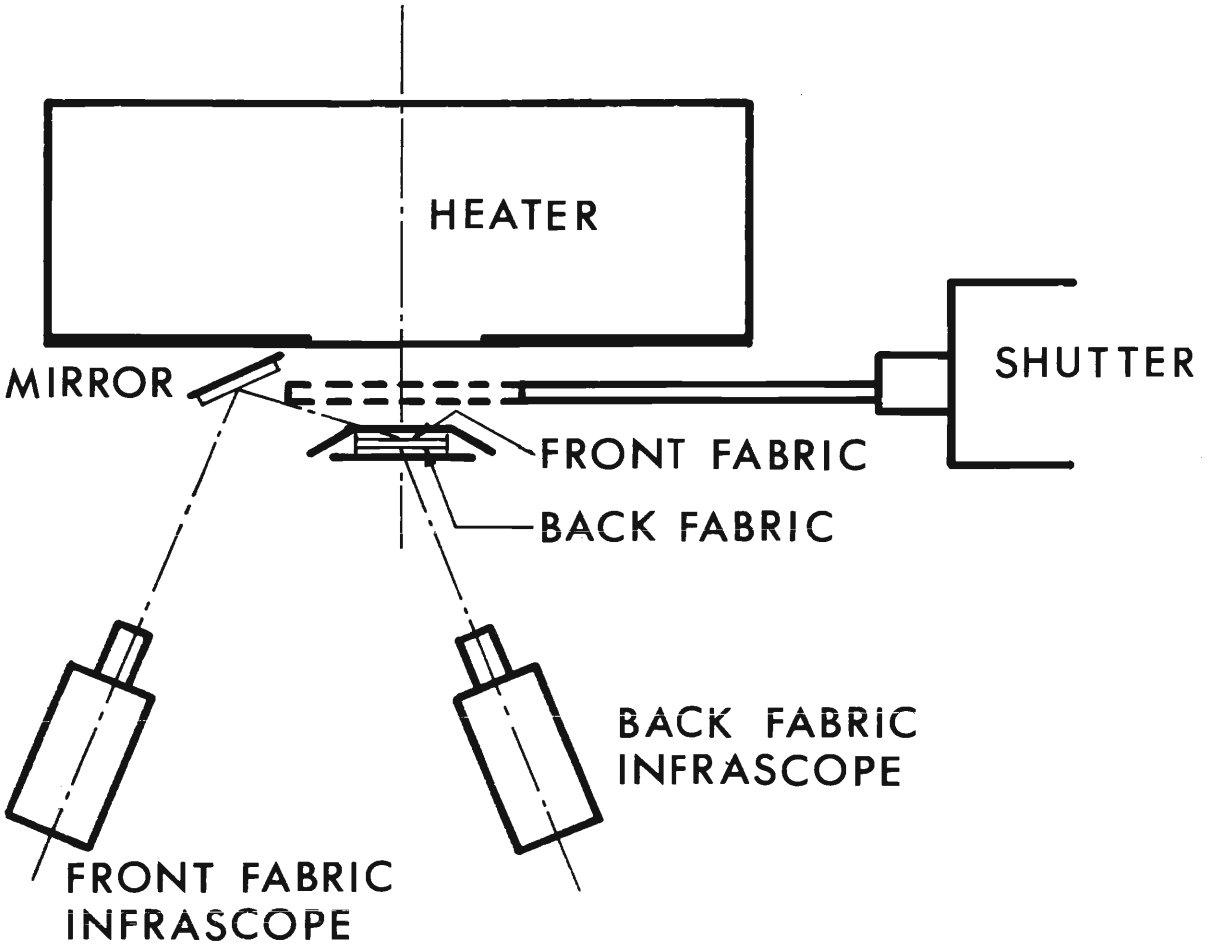

Figure 2.9 Schematic of Experimental Arrangement for Ignition Test on Fabric Assemblies

The data in Table 2.3 have been plotted in Figure 2.10. Figure 2.11 shows the tabulated data to yield the effect of spacing on ignition time.

The experimental results obtained with cotton show that the presence of a second fabric increases ignition time at high heating intensities, but decreases ignition time at low heating intensities. Moreover, ignition time decreases at first with increasing distance between the fabrics and then, at least for low heating rates increases again. This reflects the interplay of two opposing processes, namely the removal of heat by the back fabric acting as a heat sink, and the insulating effect of the back fabric retarding free convection cooling of the front fabric.

An M.S. Thesis research program is currently being conducted to verify analytically the observed trends in fabric ignition time as functions of fabric spacing.

2.4.4 Effect of Geometry

The purpose of this investigation is to determine the effect of fabric orientation, relative to the gas flame axis on ignition time. Ignition time measurements with flame impingement on fabrics, oriented at various angles relative to the flame axis, have been carried out earlier by Factory Mutual [2.5]. The emphasis in the work presented here is on fabric ignition time for gas flame exposure at the fabric edge. To study these effects, fabric ignition time measurements were conducted with the previously constructed Convective Ignition Time Apparatus (CITA), on 69 mm diameter single fabric samples, a segment of which was cut to provide a 43 mm straight edge normal to the burner axis.

2.4.4.1 Apparatus and Instrumentation. Orientation and geometry effects on ignition time were investigated with the use of the Convective Ignition Time Apparatus (CITA) which affords the sudden exposure of stationary and moving fabric samples to a well-defined gas flame. CITA consists of the fabric support and transport mechanism, a shutter system, the gas burner

TABLE 2.3 IGNITION TIME OF FABRIC ASSEMBLIES
GIRCFF FABRIC NO. 5

Initial Temperature 25°C, Relative Humidity 30%, Time in Seconds.

Assembly	Fabric Spacing mm	Irradiation W_o (W/cm^2)				
		6.5	7.6	9.25	13.8	16.2
Two Fabrics	0	24.3	20.0	15.0	9.20	7.10
	1.6	21.6	17.5	12.8	8.06	6.50
	3.2	22.2	17.6	12.3	7.53	6.13
Single Fabric		31.9	-	13.1	7.10	-

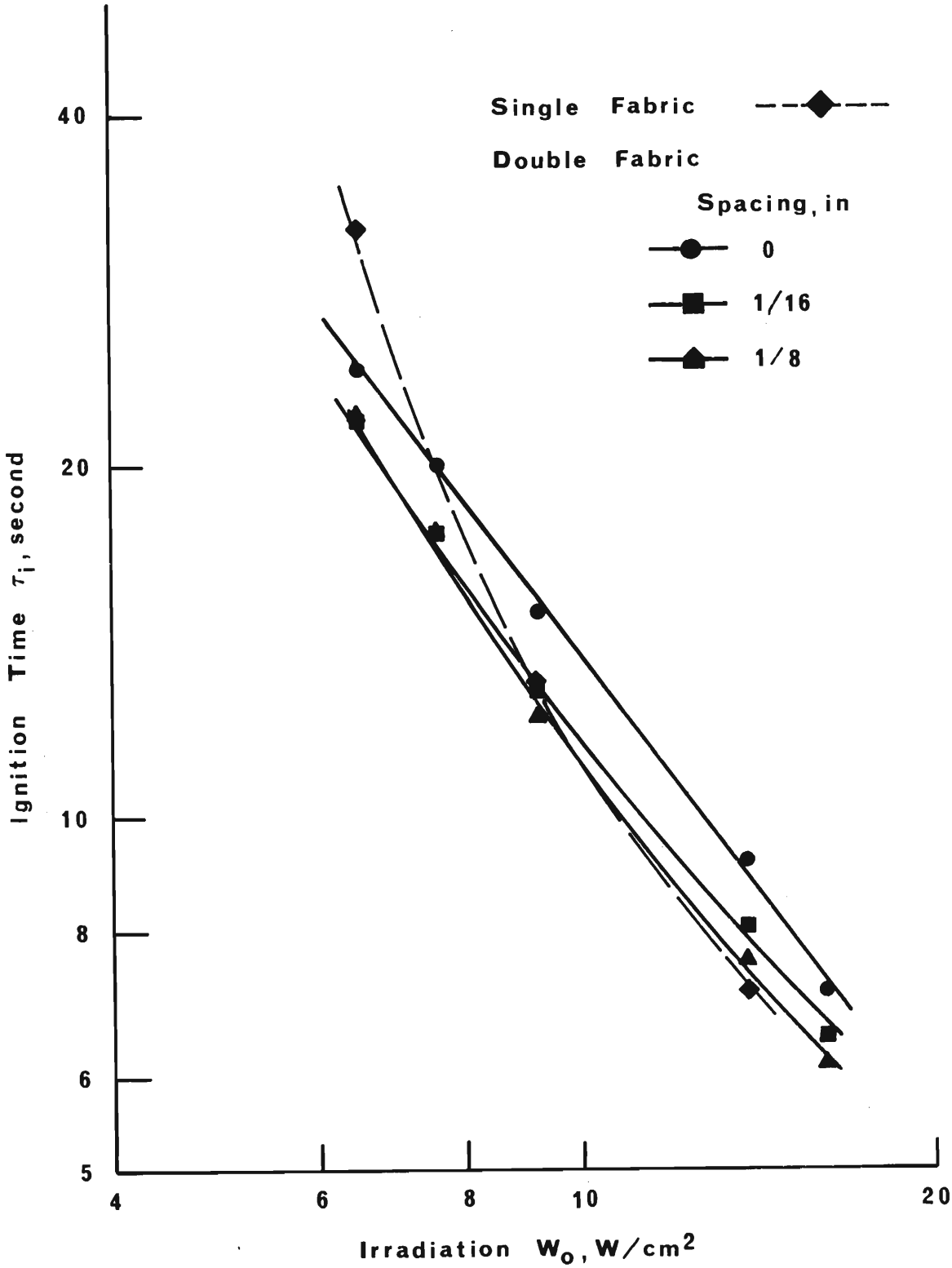

Figure 2.10 Ignition Time of Two-Fabric Composites as Function of Heating Intensity. (Single Fabric Ignition Time for Comparison) GIRCFF Fabric No. 5, Cotton

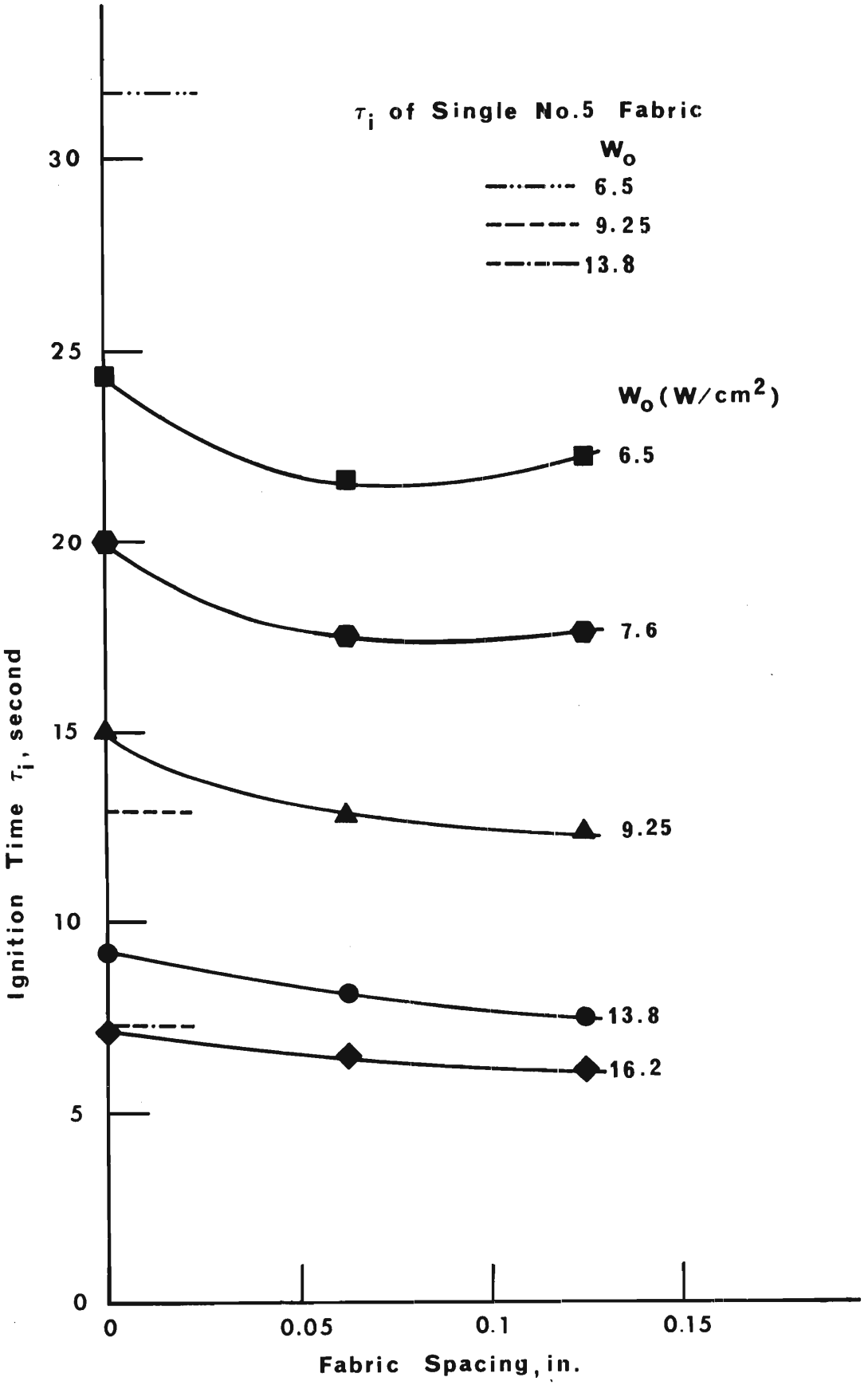

Figure 2.11 Ignition Time of Two-Fabric Composites as Function of Spacing
GIRCFF Fabric No. 5, Cotton

with its fuel and air control and monitoring system, and the flame detection system (see also Section 2.3.1).

The preconditioned fabric and the stabilized gas burner are inserted into CITA. Upon activation of the shutter, the fabric is exposed to the burner flame within 0.05 seconds or less. An infrascope detects the occurrence of the luminous flame from the burning fabric. Further details of CITA are found in Appendix B.3 of Reference [2.3].

A new fabric holder was designed (see Figure A.3.4) to accommodate fabric rotation about a horizontal axis, from 0 to 45° from the vertical. The fabric is held freely between two steel prongs, with its lower edge exposed to the flame. The new fabric holder will be used for all future tests. Infrascope and thermocouples are used to detect the instant of ignition. A view of the experimental arrangement for the fabric ignition time measurements is shown in Figure 2.12.

2.4.4.2 Procedure and Data Reduction. Fabrics to be used for ignition time measurement tests are preconditioned in a desicator for at least twenty-four hours. Through a combination of locating the fabric sample at four different elevations above the top of the burner and varying the combustible mixture rate of the burner at a fixed stoichiometric equivalence ratio, the fabric can be exposed to different convective heat flux intensities. Five different intensities were used for the Primary and Secondary GIRCFF Fabrics tested at the horizontal orientation and reported in Reference [2.3] and in Section 2.3 of the present report. The same convective heat flux intensities are used for the fabric edge ignition time measurements. The procedure of exposing the fabric to the gas flame ignition source is identical to the one used for the horizontal orientation and reported in Section 2.3 and Reference [2.3].

The seven fabric edge ignition time measurements reported in this section were carried out on four different fabrics and at one convective heat flux intensity. Two of the fabric samples were folded in the sample holder to produce a double layer fabric with an edge similar to a hem. This is the

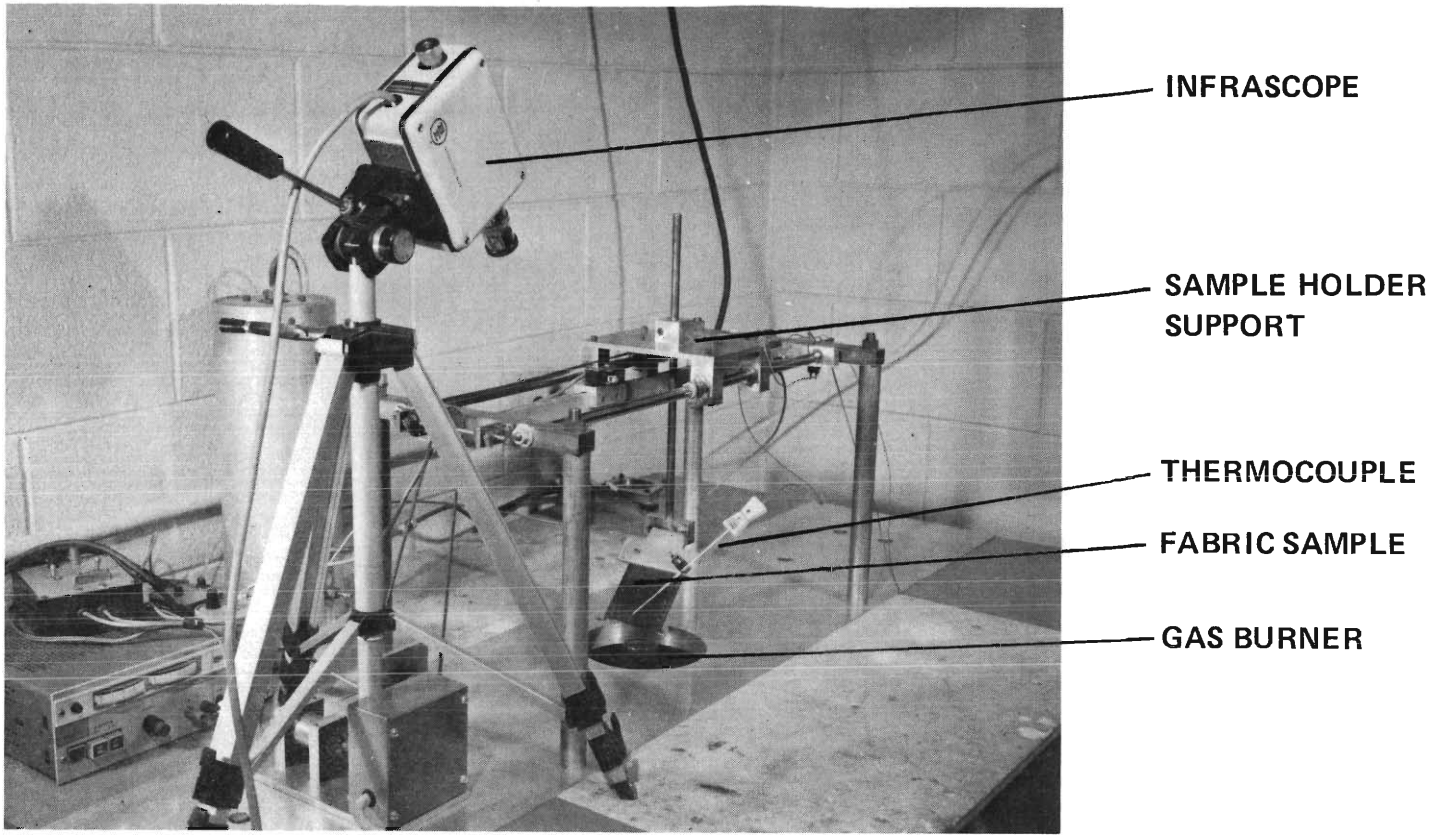

Figure 2.12. Experimental Arrangement of Test Section for Ignition Time Measurement on Single Fabrics at Different Orientations.

edge located nearer to the top of the burner. The other five fabric samples were of single layer exposing a trimmed edge to the burner flame.

The infrascope was focused at the midpoint of the lower edge of the fabric and the fabric ignition time was measured from the point the shutters of CITA separate to expose the fabric to the gas flame, to the time a sharp deflection occurs on the infrascope signal due to the occurrence of a luminous flame on the fabric. The infrascope signal together with the signal from a voltage source interrupted by a microswitch sensing the separating shutters are recorded on Polaroid film from a dual beam oscilloscope. The fabric ignition time was inferred from this record. A chromel-alumel thermocouple located on the back side of the fabric (the side not exposed to the infrascope) and near the lower edge was allowed to record the gas flame temperature after fabric destruction. The temperature readings were corrected for radiation losses from the thermocouple.

2.4.4.3 Results and Conclusions. The results of the fabric edge ignition test measurements are summarized in Table 2.4. All tests were conducted at one convective heat flux intensity characterized by the stoichiometric equivalence ratio ϕ = 0.86, the gas burner combustible mixture flow rate $\dot{m}_{mix}$ = 1272 g/h and the flame temperature T_f = 1502K. The results of the edge ignition time measurement tests are compared with horizontal fabric ignition time measurements carried out under the same convective heat flux intensity. The edge ignition time measurement tests on trimmed edge fabric samples display ignition times which are on the average about four times shorter compared to the corresponding horizontal ignition tests. The folded edge fabrics exhibited slower ignition times than the trimmed edge fabric but still had shorter ignition times than the horizontal fabrics.

These results of the edge ignition tests exhibit the expected trend when compared with the horizontal orientation. The fabric in the vertical orientation is exposed to equal heat flux intensities on both sides.of the fabric as it is interacting directly with the gas flames on both sides. In the horizontal orientations the primary interaction with the gas flame is on the side exposed to the flame and the back interacts mainly with

Table 2.4 Ignition Time Measurement on Fabrics

Under Edge Exposure to Gas Flames

ϕ = 0.86 $\dot{m}_{mix}$ = 1272 g/h T_f = 1502K

Fabric holder aperture = 63.5 mm (horizontal exposure)

Length of fabric edge = 43 mm (edge exposure)

Fabric position above burner (face or edge of fabric) = 7.6 cm

GIRCFF Fabric No.	Fabric Ignition Times, s	
	Edge Exposure	Horizontal Exposure
5	.85	4.530
5	1.05*	4.530
9	2.23	8.800
10	.392	1.550
10	.838*	1.550
16	.490	2.810
16	.780	2.810

*Folded fabric edge

gases that pass through its porous structure.

An M.S. Thesis research program is currently being conducted to expand the measurements to other fabrics and other convective heat flux intensities as well as carry out the needed analysis.

2.4.5 Conclusions

Ignition time measurements on double fabric systems under radiative heating show that the effect of finite spacing between the two fabrics is to reduce ignition time. Physically, the presence of the back fabric has two major effects on the front fabric. The first effect is that the back fabric acts as a heat sink behind the front fabric; this effect would increase the ignition time for the front fabric. The second effect is that the back fabric behaves as an insulator and radiative reflector for the front fabric; this effect would decrease the ignition time for the front fabric. For the three fabric spacings investigated, the second effect dominates the first effect when there is a finite spacing between the two fabrics.

Ignition time measurements on fabrics in a vertical orientation and under convective heating, indicate that they require a shorter period for ignition when compared with fabrics exposed to the same convective heat flux intensities. Exposure of the fabric to equal heat flux on both sides shortens the ignition period.to approximately one fourth of the time observed with normal flame impingement.

2.5 Ignition Time Statistics and Ignition Probability

It is shown in Chapter 1 that the probability of fabric ignition after given exposure, P(I/E), is an important measure in the assessment of garment fire hazards.

2.5.1 Purpose

Previously started [2.3] experiments were to be completed to determine the probability of fabric ignition $P(I/E_\ell)$ under laboratory exposure conditions. As demonstrated earlier [2.3] the probability

$$P(I/E_\ell) = 1/\sqrt{2\pi} \int_{-\infty}^{x} \exp(-z^2/2)\, dz \quad , \tag{2.5.1}$$

where $$x = (\tau_e/\langle\tau_i\rangle - 1)/\sigma \quad , \tag{2.5.2}$$

depends primarily on two measures:

(i) the mean ignition time $\langle\tau_i\rangle$
(ii) the normalized standard deviation σ

and the independent variable τ_e which represents exposure time.

It is the purpose, therefore, of this task to obtain $\langle\tau_i\rangle$ and σ, under controlled environmental conditions, namely initial temperature and environmental humidity.

It must be noted that Eq. 2.5.1 predicts a finite but extremely small ignition probability for the case of vanishing exposure time $\tau_e = 0$. The probability is small enough to be ignored for $\tau_e = 0$ primarily because of the small values found for the deviation σ. The expression in Eq. 2.5.1 represents fabric behavior well for the range of interest, namely for $(|\tau_e - \langle\tau_i\rangle| / \langle\tau_i\rangle) < 1/2$.

2.5.2 Achievements

The experiments were performed with the Radiative Ignition Time Apparatus (RITA) in the Environmental Control Chamber previously developed and constructed [2.3].

The total of 854 new ignition tests was performed on two fabrics, GIRCFF Fabrics No. 10 and 12 (see Table 2.1), at three levels of heating intensities, namely at 6.50, 9.52 and 13.80 W/cm^2 and at two humidity levels, that is at 30 and 90 percent relative humidity. This brings the grand total of dual shutter mode fabric exposures (controlled exposure time) to 1077 tests.

A computer code was developed to perform a probit analysis of the ignition frequency measurements. The objectives of this task have been achieved.

2.5.3 Experimental Apparatus and Methods

Ignition time frequencies were measured by carefully conditioning the fabric at the preselected initial temperature and humidity level. The fabric was inserted into RITA (Radiative Ignition Time Apparatus), then the radiative heater was preheated during a selected and automatically controlled period of time, to reach radiative equilibrium, but without heating the shutter plates. The fabric was then exposed within less than 5 milliseconds to the full radiative power flux and after a selected exposure time shielded, again within less than 5 milliseconds. Exposure times τ_e were selected to vary between $0.9\tau_i$ and $1.1\tau_i$ as measured previously under single-shutter mode [2.4]. Care was exercised to include exposure times at the wings of the frequency distribution, i.e. with both none of the samples and all of the samples ignited. Actual exposure time was measured electronically with the accuracy of $\pm$ 0.01 seconds.

Fabrics were removed from RITA after exposure and found either only charred or ignited and burnt. After dividing all test results into classes of 0.05, 0.1 and 0.2 times the previously found ignition time τ_i, and forming

for each class the fractions of number of ignitions over total number of tests, a sensitivity test was performed, first by the Kaerber Method and then by the Probit Method of Analysis [2.6]. Stimulus levels are exposure time at fixed humidity and heating intensity.

2.5.4 Results, Ignition Probability Measurements

A summary of all ignition time statistics is presented in Tables 2.5 through 2.7. Listed are, in this order, the fabric identification, the heating intensity, the relative environmental humidity, the number of tests evaluated, then the ignition time as measured previously under single shutter mode (without environmental control), and the median ignition time obtained from the sensitivity analysis. Following the ignition times are the estimates for the standard deviations of the median ignition time and the ignition time itself.

The probability of ignition after given laboratory exposure, $P(I/E_{\ell})$ was computed by Eq. 2.5.1 from the listed values of $<\tau_i>$ and σ, and is presented graphically in Figures 2.13, 14, and 15.

The results reveal a generally deterministic response to heating under laboratory exposure conditions.

The results presented here are part of a forthcoming M.S. Thesis by Mr. O. A. A. Naveda.

Table 2.5 Ignition Time Statistics — Cotton Fabric, GIRCFF No. 5

GIRCFF Fabric No.	Irradiation W_o	Relative Humidity	Number of Tests	Ignition Time		Standard Deviation of Ignition	
				Single Shutter τ_i	Median $\langle \tau_i \rangle$	Mean s_μ	Time s
	W/cm^2	%	-	s		s	s
5	6.50	30	77	31.00	31.45	0.37	2.53
5	9.52	30	25	13.35	13.13	0.18	0.49
5	13.80	30	27	7.15	7.35	0.08	0.27
5	6.50	90	17	34.50	35.38	0.34	0.86
5	9.52	90	42	15.00	14.95	0.64	2.97
5	13.80	90	32	7.95	7.93	0.09	0.31

Table 2.6 Ignition Time Statistics Cotton Batiste, GIRCFF Fabric No. 10

GIRCFF Fabric No.	Irradiation W_o	Relative Humidity	Number of Tests	Ignition Time		Standard Deviation of Ignition	
				Single Shutter τ_i	Median $\langle\tau_i\rangle$	Mean s_μ	Time s
	W/cm^2	%	-	s		s	s
10	7.55	30	28	56.00	55.87	3.45	14.38
10	9.52	30	157	22.00	22.56	0.41	3.98
10	13.80	30	44	7.75	7.79	0.19	0.96
10	7.55	90	-	-	-	-	-
10	9.52	90	27	26.50	26.42	0.46	1.83
10	13.80	90	26	8.50	8.42	0.11	0.40

Table 2.7 Ignition Time Statistics — Nylon Tricot, GIRCFF Fabric No. 12

GIRCFF Fabric No.	Irradiation W_o	Relative Humidity	Number of Tests	Ignition Time		Standard Deviation of Ignition	
				Single Shutter τ_i	Median $\langle\tau_i\rangle$	Mean s_μ	Time s
	W/cm^2	%	-	s		s	s
12	6.50	30	86	12.40	12.61	0.32	2.24
12	9.52	30	41	6.35	6.15	0.14	0.70
12	13.80	30	57	3.10	3.10	0.03	0.13
12	6.50	90	66	11.70	11.63	0.19	1.11
12	9.52	90	59	5.90	5.87	0.06	0.35
12	13.80	90	76	3.10	3.07	0.09	0.63

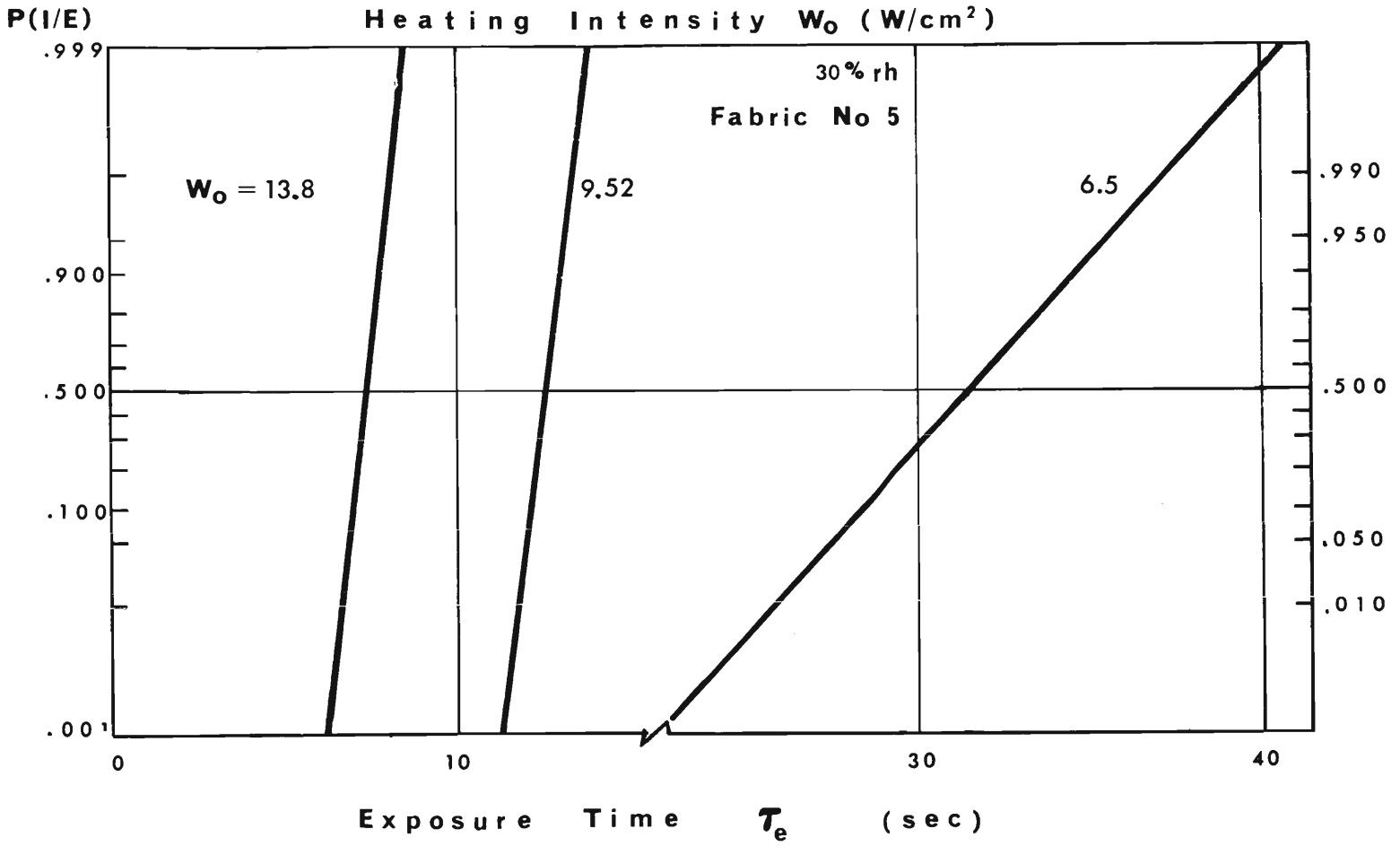

Figure 2.13 Ignition Probability as Function of Exposure Time and Heating Intensity, at 30% r.h. Cotton, GIRCFF Fabric No. 5

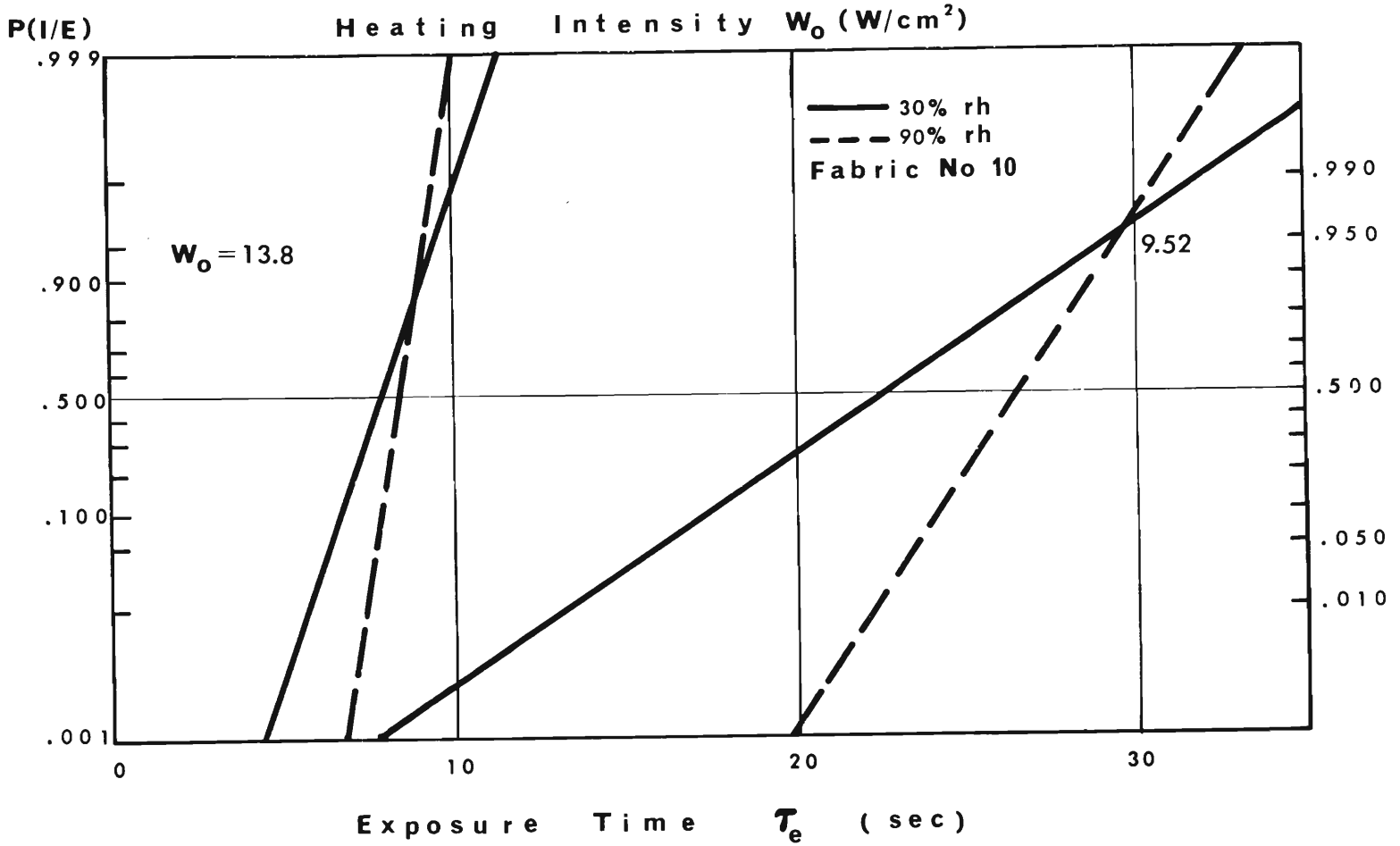

Figure 2.14 Ignition Probability as Function of Exposure Time and Heating Intensity at 30% r.h. and 90% r.h. Cotton Batiste, GIRCFF Fabric No. 10

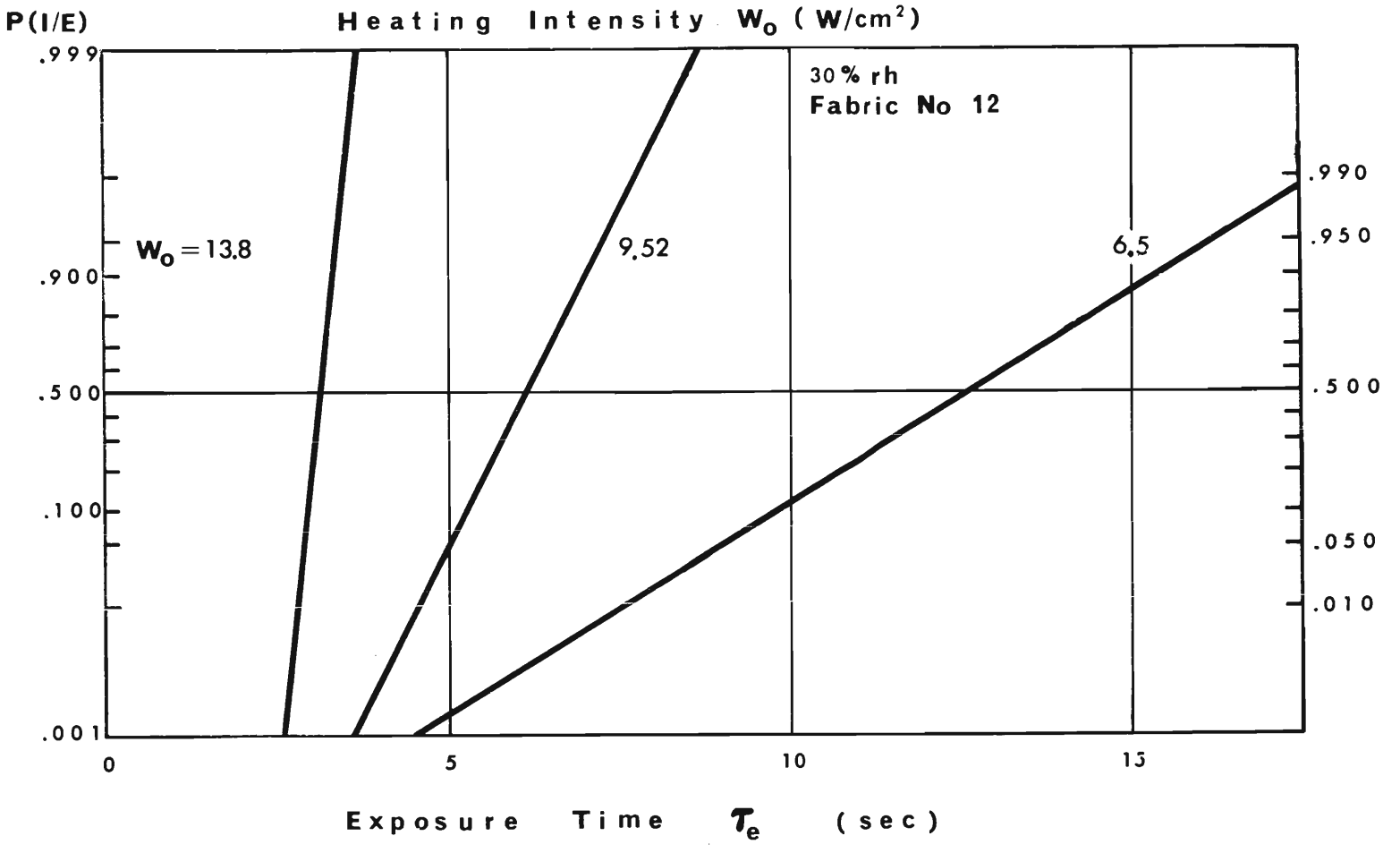

Figure 2.15 Ignition Probability as Function of Exposure Time and Heating Intensity at 30% r.h. Nylon Tricot, GIRCFF Fabric No. 12

2.6 Characterization of Actual Ignition Sources

It is demonstrated in Chapter 1 that the quantitative prediction of garment fire hazards, namely the prediction of burn injury probability, is predicated upon the ability to assess, among other probabilities, the probability of fabric ignition after exposure to an ignition source. There are innumerable permutations to be investigated, arising from all possible combinations of fabrics, fabric assemblies, garment styles, human activities and types of ignition sources. A reasonable approach to this formidable task is to study separately, at first the ignition of fabrics and possible variations of fabric combinations and geometries, then the characteristics of ignition sources and finally the stochastic behavior of people. The results from these three subtasks are to be combined, by probability theory, to yield the probability of ignition after exposure, under actual exposure conditions.

The first subtask is the objective of Section 2.5, and results in the specification of ignition probability after given exposure for a very restricted set of fabrics and exposure conditions. Generalization of the results is afforded through modeling analysis, but the results are always expressed in terms of heating intensity W_o and exposure time τ_e.

The second subtask is to find the spacial distribution of heating intensity $W_o(\vec{r})$ for all relevant ignition sources. The objective of the third subtask remains to determine, through time studies, the fractional time or probability of residing at any given distance from the center of a given ignition source, for any given exposure time. The second subtask is the objective of the study discussed in this section.

2.6.1 Purpose

The purpose of this study is to develop a generally applicable technique for the characterization of ignition sources and to apply this technique to the following types of ignition sources, selected because they are responsible for a relatively high number of ignitions:

(i) kitchen gas ranges,
(ii) electric ranges,
(iii) contained gasoline fire,
(iv) match and cigarette lighter, candles.

Characterization of ignition sources means, for the purpose of this study, to establish the heat flux and temperature distributions as functions of distance from a recognizable source center.

2.6.2 Accomplishments

A portable Ignition Source Scanning Apparatus was constructed to measure heat flux and temperature as functions of space on 90 cm long and 20 cm wide heat sources such as kitchen ranges, broilers, charcoal fires, etc.

The total of 119 temperature and heat flux surveys were obtained on four household ignition sources: two gas ranges and two eletric ranges, with and without utensils covering the burners. Results are presented.

The literature was searched on ignition sources and their relative frequency of involvement in accidental fires. An M.S. Thesis is being prepared in connection with this task.

2.6.3 Apparatus and Experimental Methods

The Ignition Source Scanning Apparatus (ISSA) is shown in Figure 2.16. ISSA consists of these five major components, used for field testing:

(i) the frame with its guide rails,
(ii) the sensor carriage with flux or temperature sensor,
(iii) the sensor carriage drive with speed control,
(iv) the position sensor with power supply,
(v) the recording equipment, i.e. amplifier and x-y plotter.

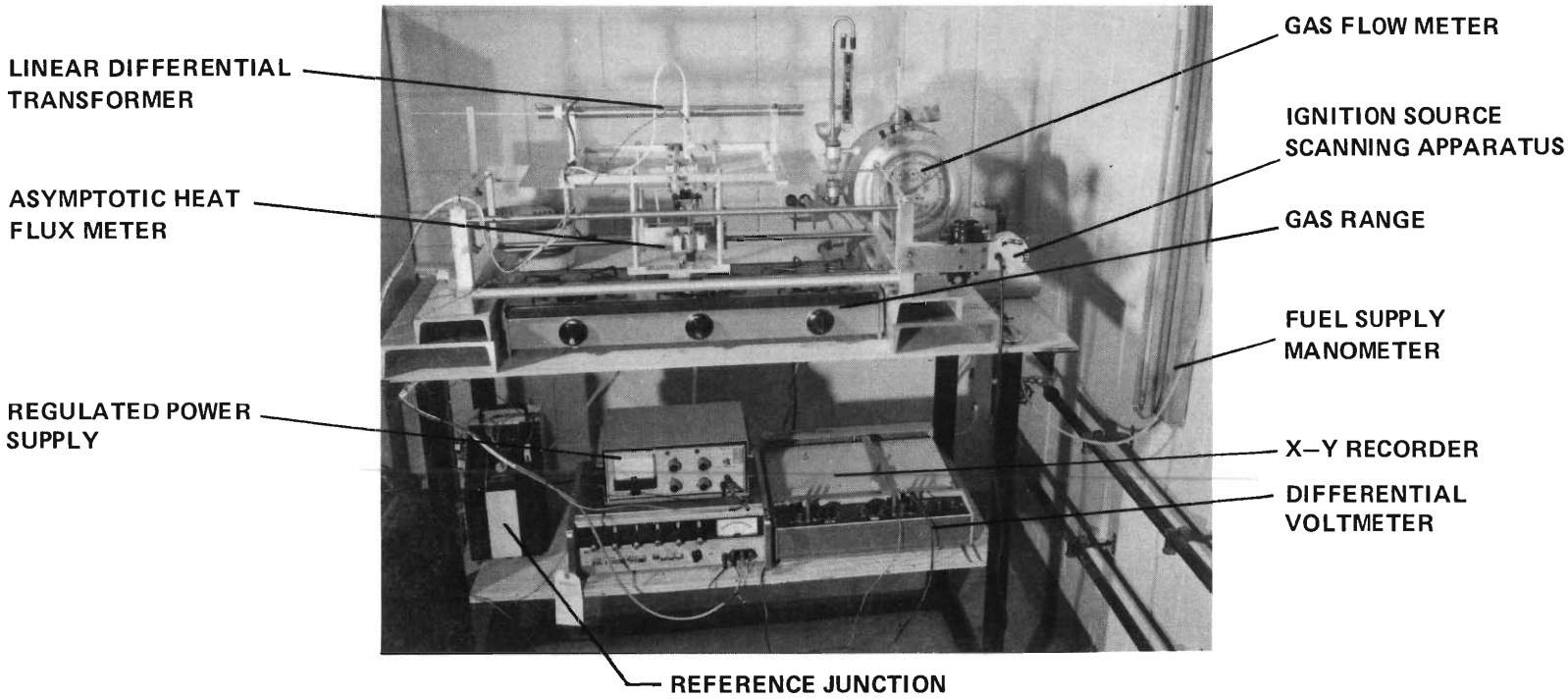

Figure 2.16. Ignition Source Scanning Apparatus (ISSA).

For laboratory testing, the above equipment is supplemented by fuel flow metering equipment, also shown in Figure 2.16 and consisting of a gas flow meter and a manometer.

2.6.3.1 Heat Flux Measurements. The ignition source (burner) is allowed to reach thermal steady state. The water-cooled asymptotic heat flux calorimeter is positioned at the desired height above the burner, at the desired vertical plane through the burner, and at the desired orientation about its horizontal axis.

The sensor carriage is then repeatedly swept through the flame across the burner. The signal is recorded as the ordinate on the x-y recorder.

Coupled with the sensor carriage is the core of a linear differential transformer which serves to sense the heat flux calorimeter position. The transformer signal is proportional to the traversing position (x) and recorded as the abscissa on the x-y recorder.

Three forward and reverse passages are executed at each condition and the resulting six traces of heat flux versus position, $q''(x)$ are averaged to yield $\overline{q}''(x)$.

2.6.3.2 Temperature Measurements. The heat flux sensor is replaced by a chromel-alumel thermocouple, and the same procedure is employed as for the heat flux measurements.

Details of the apparatus, operating and data reduction techniques are deferred to Appendix A.4. Moreover, this task is treated in the forthcoming M.S. Thesis by Oscar A. A. Naveda.

2.6.4 Results and Discussion

The heat flux data $q''(x)$ and temperature data $T(x)$ obtained in parallel vertical planes were evaluated to yield the polar diagrams in Figures 2.17

through 2.22.

Figures 2.17 and 2.18 characterize one 70 mm burner of a three flame gas range, Model Kenmore, Series 119.15031, sold by Sears, Roebuck & Company. Figure 2.17 shows lines of constant total heat flux and Figure 2.18 presents constant temperature lines, in polar coordinates. The burner center is chosen at the vertical axis through the burner and at the top of the flame part.

Figures 2.19 and 2.20 present similarly constant heat flux and temperature distributions for the 85 mm-diameter front burner of a four flame Kenmore Series 71731 30 inch Gas Range.

Electrical hot plates were characterized through total vertical radiative heat flux distribution measurements. Figure 2.21 shows the flux distribution for a 0.8 kW single hot plate whose surface temperature at the open coils was measured to be 920°C. Figure 2.22 shows the total radiative heat flux for a 2.6 kW hot plate, with the diameter of 142 mm, one of four burners of a Westinghouse electrical kitchen range. Its closed coil heating element reached the average temperature of 800°C.

Maximum heat flux values and maximum temperatures measured in the flames of household matches, a dispoz-a-lite type cigarette lighter and a wax candle are summarized in Table 2.8 below. Flux and temperature gradients within these small flames are too large to allow meaningful distribution measurements around such flames. However, fabric ignition probability vanishes rapidly outside such small flames.

The results show that the maximum temperature and the maximum heat flux found in gas flame burners is nearly independent of burner size. Large burners have larger zones of high temperatures and heat fluxes than small burners.

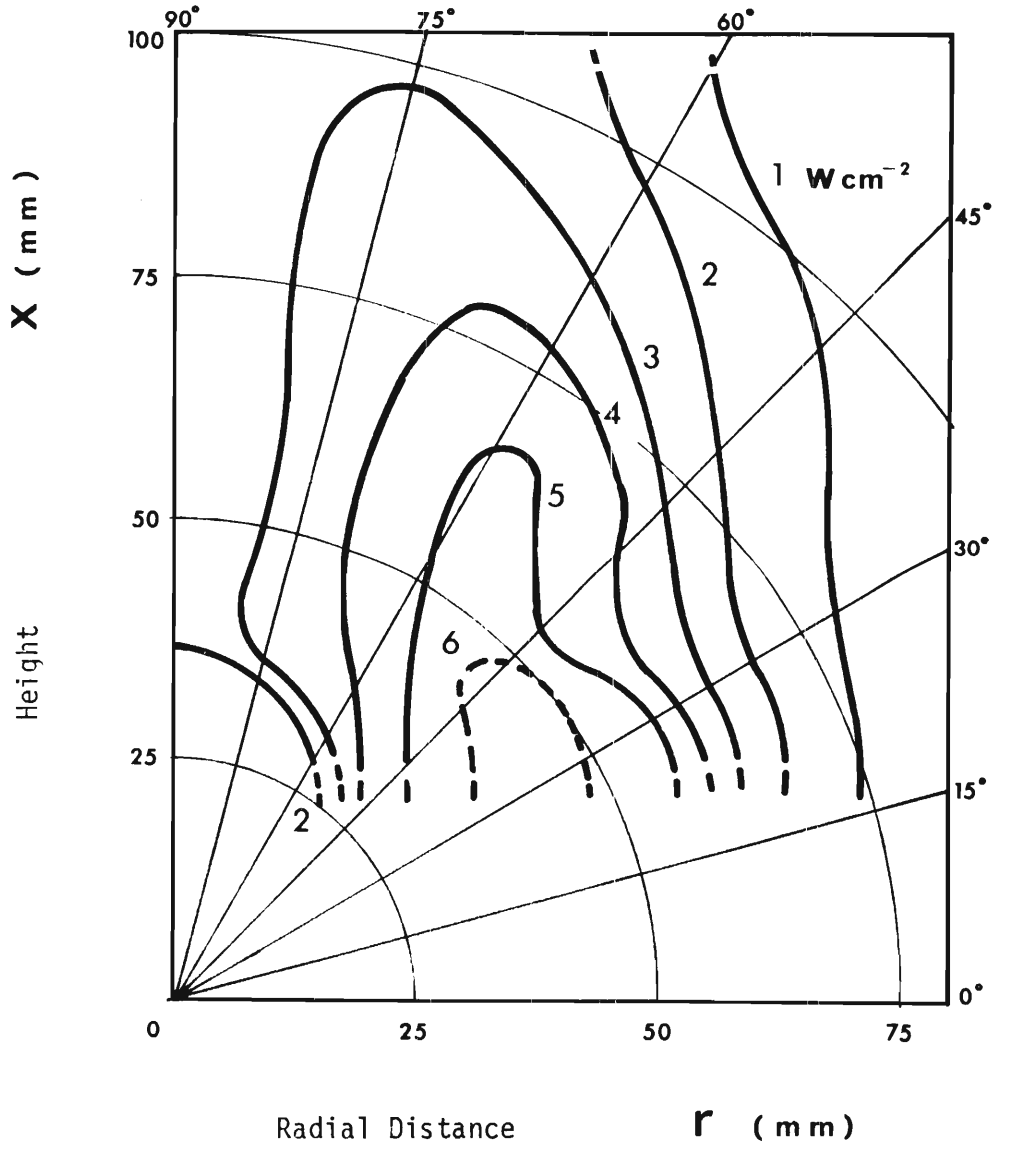

Figure 2.17 Total Heat Flux Distribution, Kenmore Kitchen Gas Range Model 119.15031, Full Open Burner

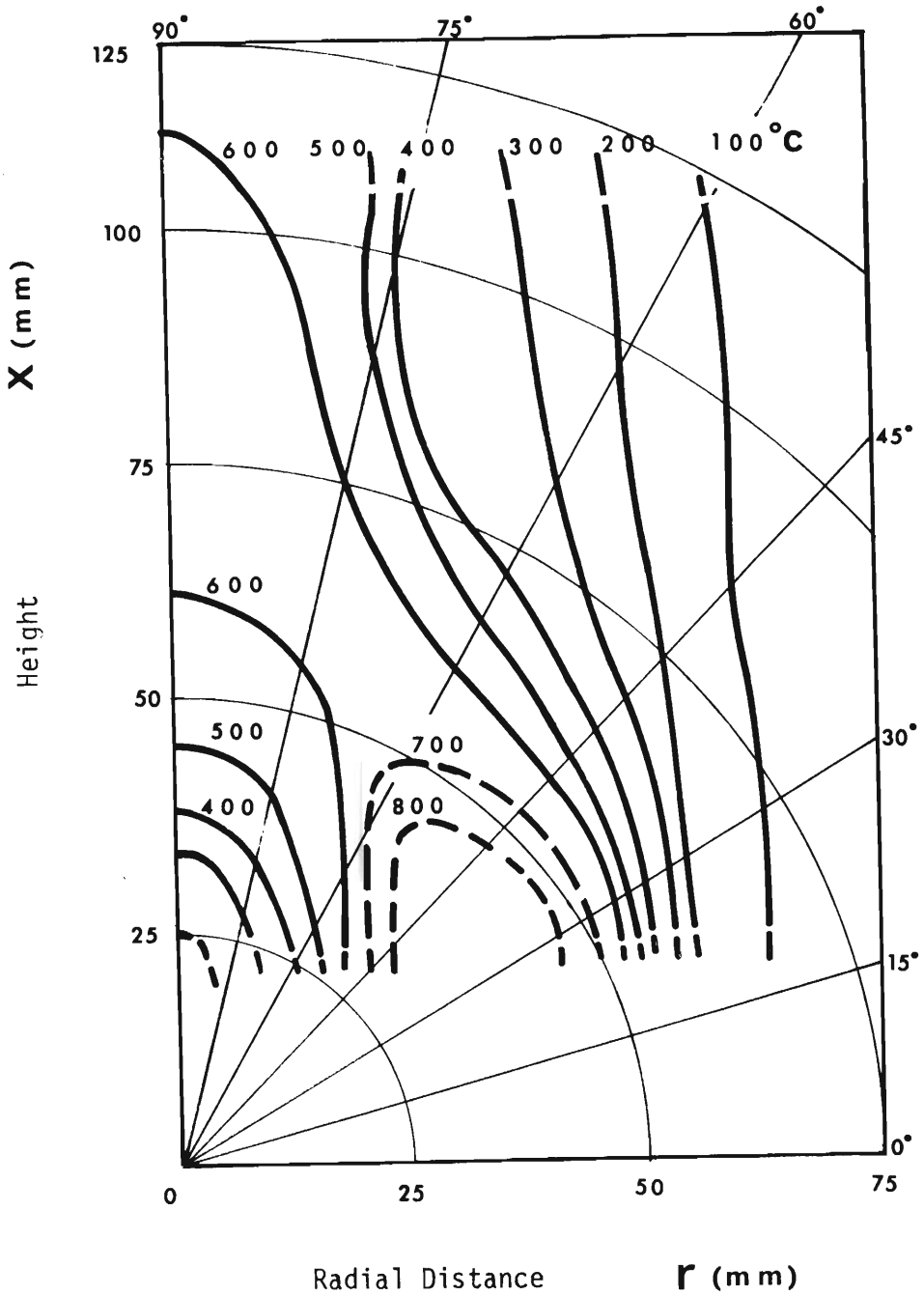

Figure 2.18 Temperature Distribution, Kenmore Kitchen Gas Range Model 119,15031, Full Open Burner

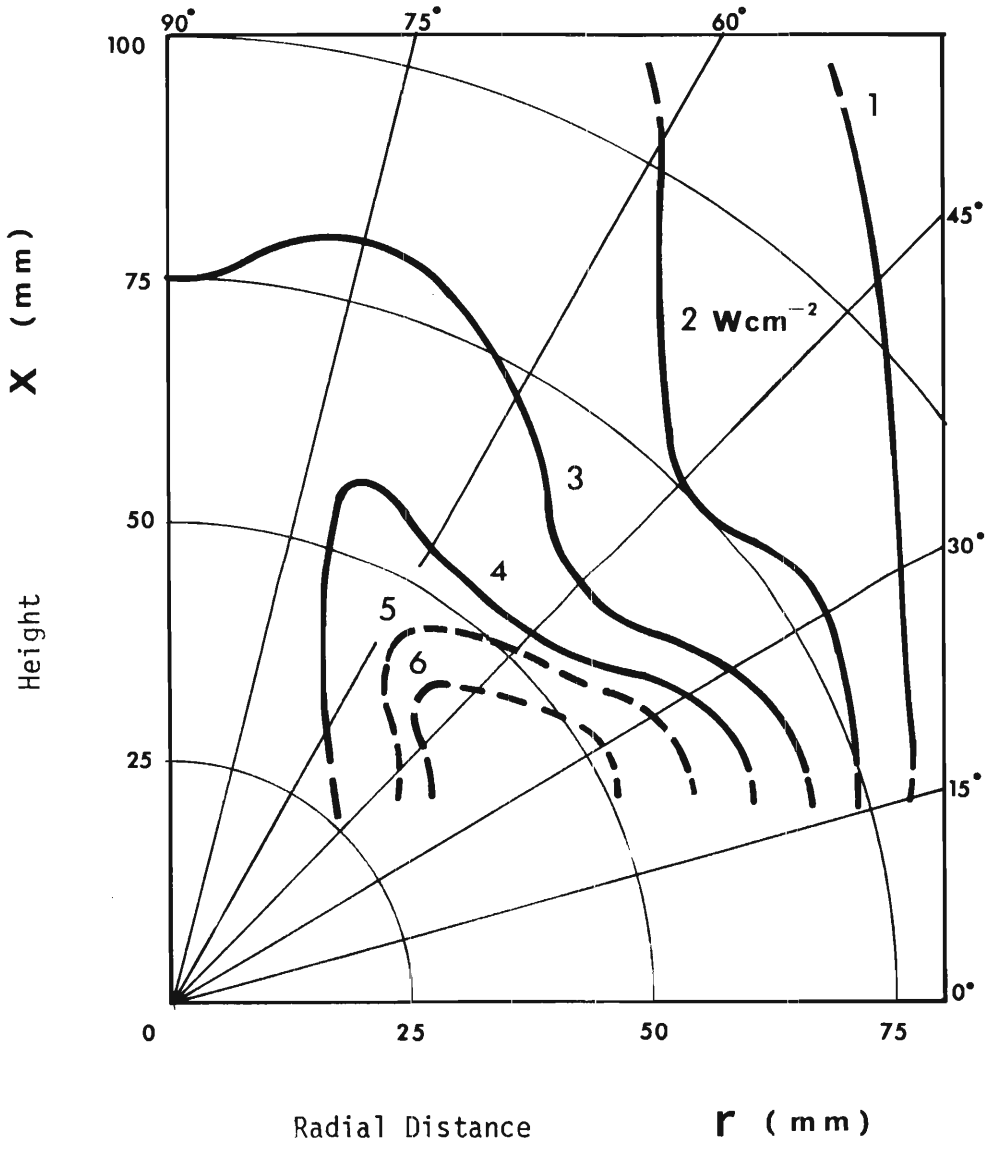

Figure 2.19 Total Vertical Heat Flux Distribution
Kitchen Gas Range, Model Kenmore, 71731 Series

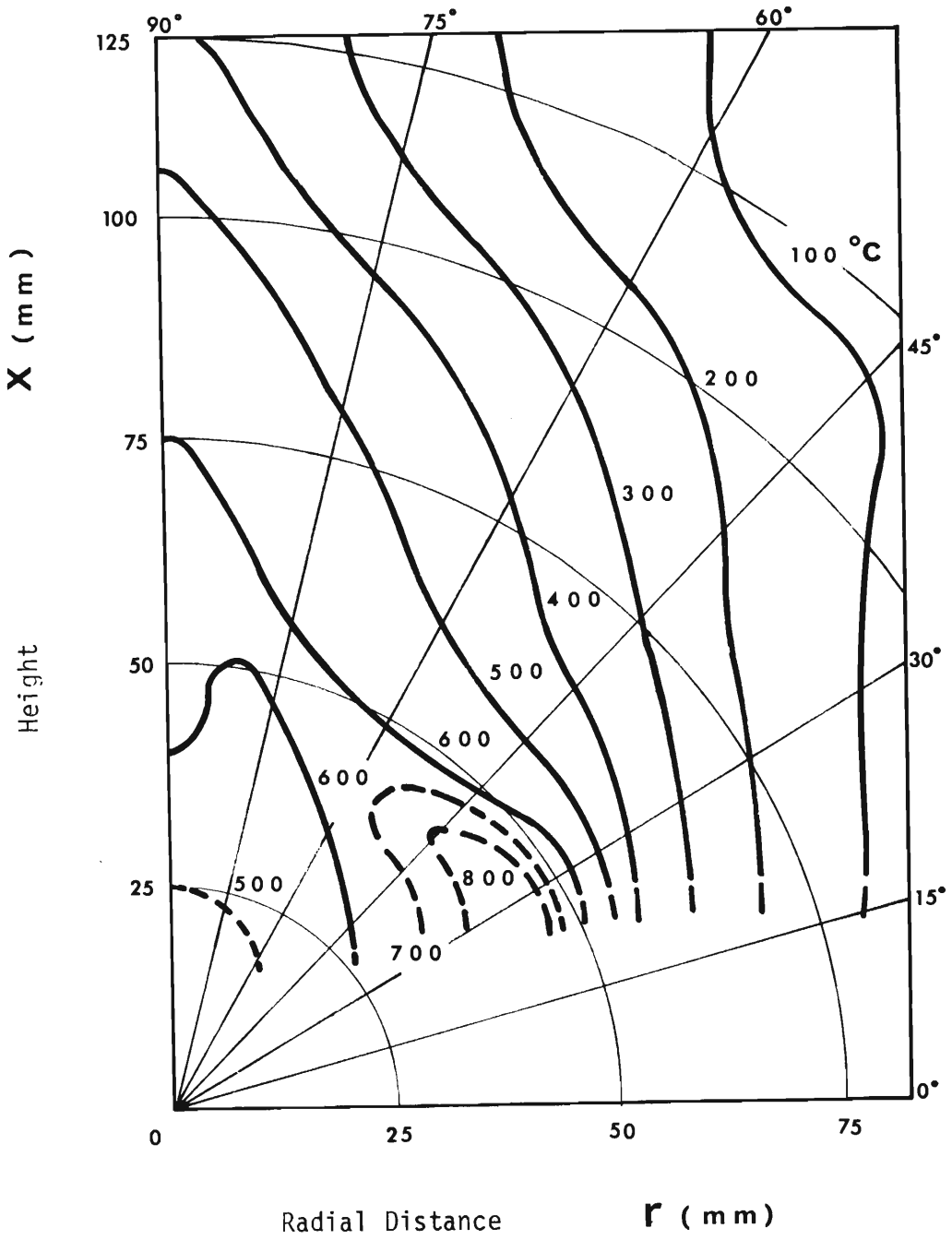

Figure 2.20 Temperature Distribution,
Kitchen Gas Range, Model Kenmore, 7131 Series

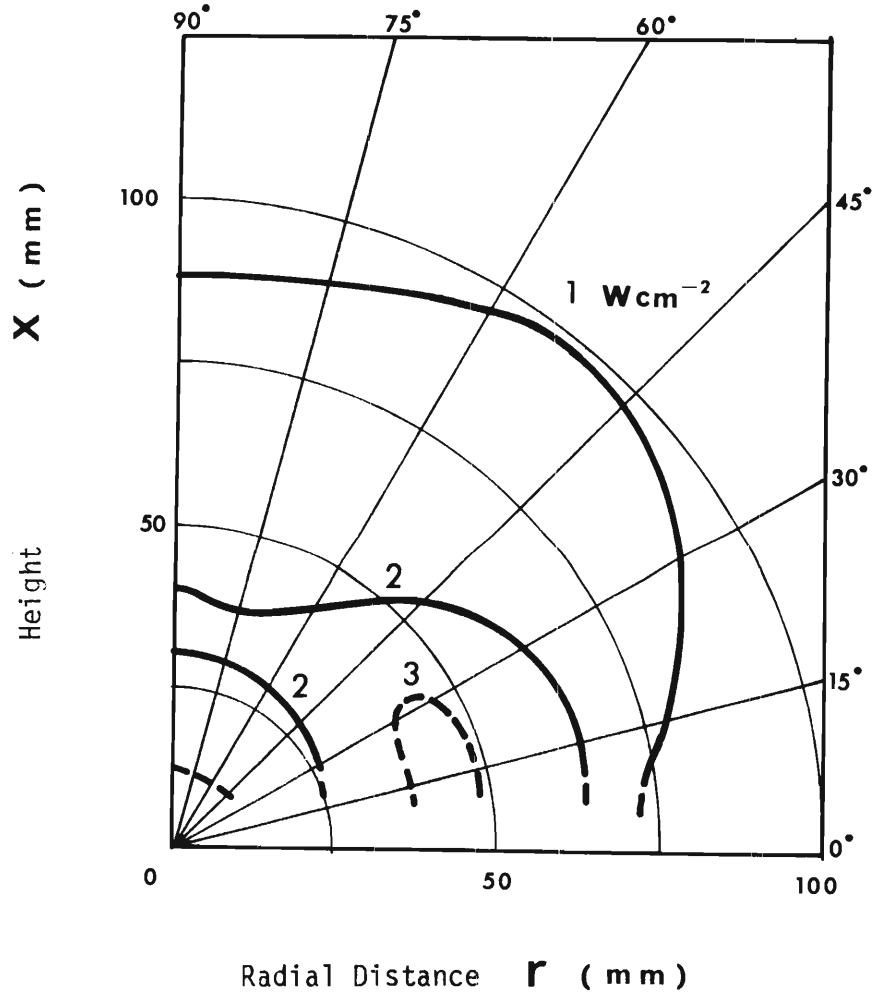

Figure 2.21 Total Vertical Heat Flux Distribution of 0.8 kW Electrical Hot Plate

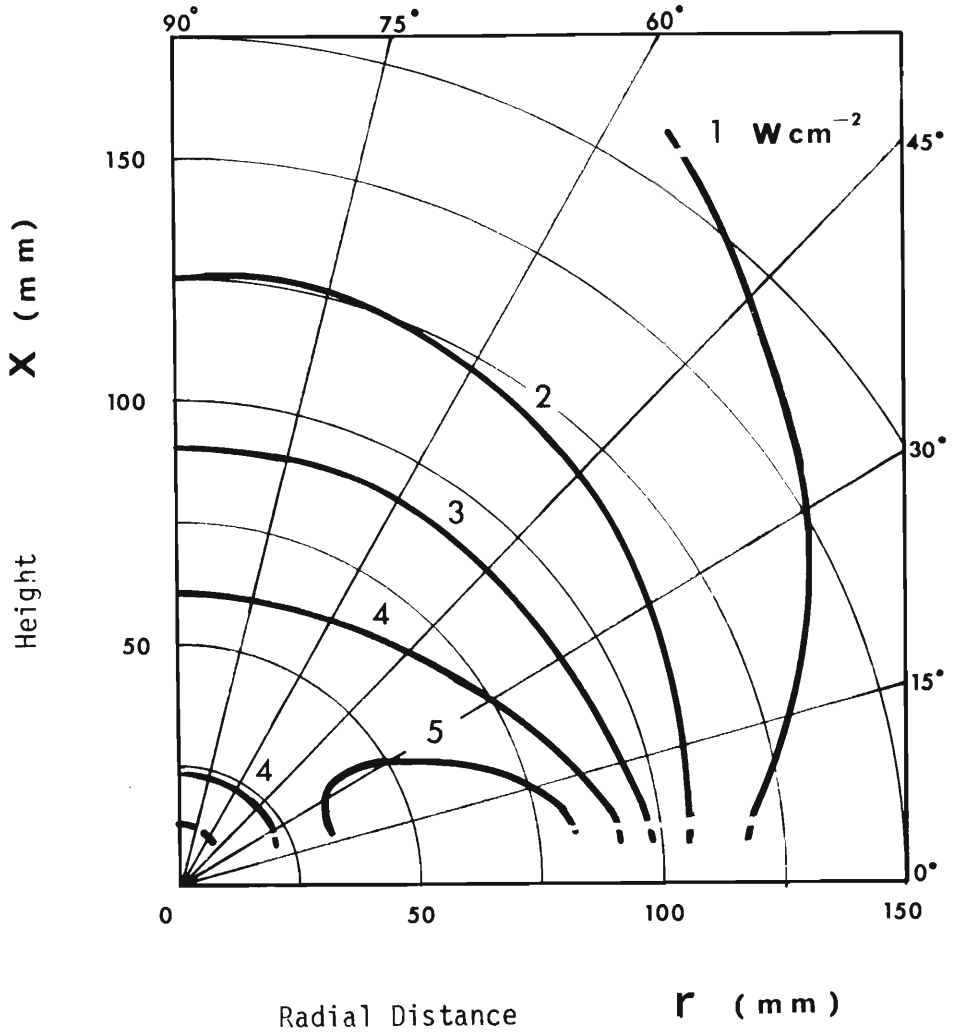

Figure 2.22 Total Vertical Heat Flux Distribution of 2.6 kW Electrical Hot Plate

Table 2.8

Maximum Temperature and Maximum Total Vertical Heat Flux:

Matches, Candles and Cigarette Lighter

Heat Flux Sensor at Temperature t = 40°C

Ignition Source	Average Flame Height cm	Sensor Distance from Base of Flame cm	Heat Flux$_2$ W/cm^2	Flame Temperature °C
Matches	2.5	1.6	3.4	290
		2.2	5.4	540
		2.5	5.4	580
Butane Cigarette Lighter	5.0	2.5	5.8	-
		5.0	5.8	500
Candle	2.5	2.5	4.6	300
		5.0	7.8	650

3. MODELING ANALYSIS

3.1 Purpose and Scope

The objective of the modeling analysis is (1) to describe one-dimensional, transient heat transfer through thermally decomposing composites, (2) to integrate a newly proposed ignition criterion [3.1] into the modeling analysis and (3) to predict the mean ignition time for igniting solid materials in terms of material properties and heating conditions. Scaling laws are developed, and errors arising from partial modeling of the pre-ignition process are assessed.

The modeling analysis is formulated for radiative heating and for forced and natural convective heating. Integral methods are employed to transform the governing partial differential equations into a set of ordinary differential equations [3.2]. The resulting nonlinear initial value problem is solved by numerical techniques for the cases of thermally thin materials subjected to radiative heating and to free convection heating.

It is postulated that sustained autoignition of pyrolyzing solids occurs when, at some point in the gaseous boundary layer adjacent to the heated solid surface, any of the possible combinations of air-volatile concentration with minimum mixture temperature is reached for the first time, provided that, simultaneously the time rate of pyrolysate evolution from the heated solid is sufficient to maintain a flame. This ignition criterion is derived from the assumption that spontaneous exothermal reaction results from local thermodynamic equilibrium within the gaseous boundary layer. Pre-ignition history, heating rate and flow conditions external to the pyrolyzing solid are accounted for in the ignition criterion, seemingly for the first time. The measurement of minimum ignition temperature as a function of pyrolysate concentration is described in Section 2.1 of this report.

Scaling laws are derived by normalyzing the governing conservation and constitutive laws. The resulting large number of nondimensional groups necessitates partial modeling. Errors incurred from partial modeling are estimated from the numerical solution.

3.2 Ignition Time and Fire Hazard

The prediction of ignition time is essential for the development of a rational relation between fire hazards and laboratory experiments [3.3]. It has been shown for the first time by N. Zuber and W. Wulff [3.4] that the mean ignition time $<\tau_i>$ characterizes material response, that the exposure time τ_e characterizes human response and reflexes to fire, and that the ratio of these two characteristic times $\tau_e/<\tau_i>$ defines the probability P(I/E) of ignition after given exposure. The ignition probability P(I/E) is an important contribution to the quantitative fire hazard measure [3.5] namely the fire loss probability, from the first transient, physico-chemical process in the chain of events which lead from flammability certification to a potential fire accident. Therefore, a rational flammability standard requires an estimate of ignition probability.

Ignition probability can be measured as discussed in Sections 2.4 and 2.5 but only for a limited number of carefully controlled experiments. Experimentally determined mean ignition times must be interpreted on the basis of, and, more importantly, supplemented by analytical results.

3.3 Ignition Time Prediction

A set of plane parallel slabs, possibly separated by plane-parallel air gaps as shown in Figure 3.1 is considered to be exposed on one external surface (at $y = \delta$) to either radiative or convective heating. The solid portions of the system are taken to respond to the heating in these five, partially overlapping stages:

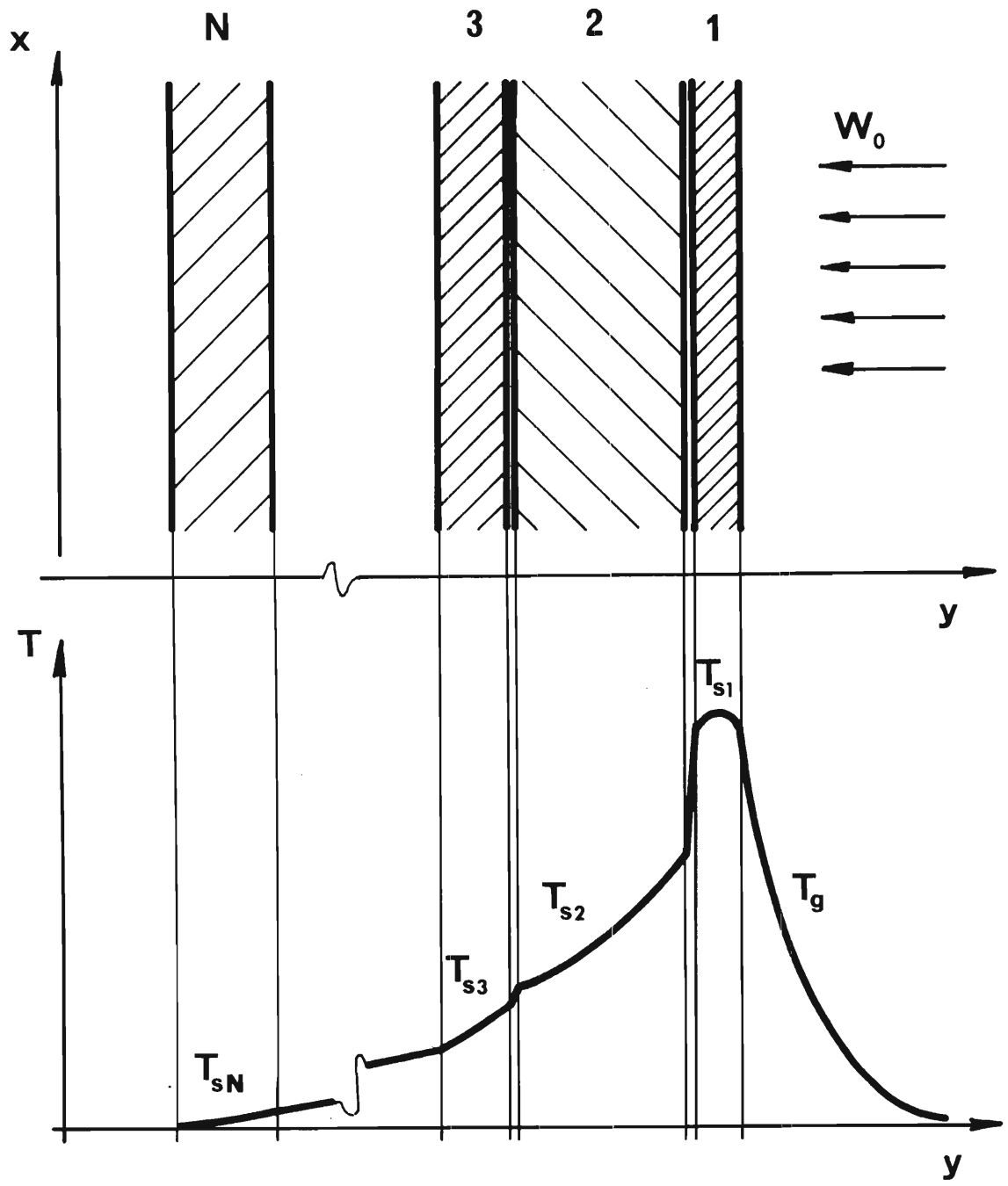

Figure 3.1 Geometry of Analytical Model

(i) inert heating
(ii) desorption of moisture
(iii) pyrolytic gasification, accompanied by pyrolysate convection through, and evolution from the porous solid portions
(iv) thermal excursion in the gaseous phase next to the heated solid surface
(v) combustion and char formation

The onset of the thermal excursion is associated with the appearance of a flame and called ignition. Ignition occurs in the gaseous phase as soon as somewhere in the boundary layer a minimum temperature is reached which depends only on the instantaneous local pyrolysate concentration in the air-pyrolysate mixture.

Previously developed ignition models were formulated on the basis of distributed parameter and lumped parameter descriptions [3.6]. Common to all these ignition models is the assumption that ignition occurs when the heated solid surface reaches a fixed, material-dependent surface temperature. Although very useful insight can be derived from certain closed-form solutions to the lumped-parameter descriptions, the implied ignition criterion appears to yield only limited agreement with ignition time measurements.

Section 3.4 below is a description of the analysis developed for systems which are subjected to a combination of radiative heating and natural convection. The combination of radiative and forced convective heating is discussed in Section 3.5. The presentation of the relevant concepts is as general as possible while detailed descriptions are restricted to a two-zone system, consisting of a single pyrolyzing porous solid and a gaseous boundary layer.

3.4 Radiative Heating and Natural Convection

Radiative heat sources which cause accidental ignitions are electrical space heaters, electrical ranges, broilers and rotisseries, chimney fires and

industrial furnaces. The Radiative Ignition Time Apparatus (RITA), employed for ignition time measurements, (see Sections 2.2 and 2.4 and Reference [3.6]) belongs in the same class of ignition sources. Radiative heating is a dominant mechanism in building fire spread and is responsible for flashover in room fires.

Radiative heating in the atmosphere induces always cooling by free convection at the heated surface. Convective cooling during radiative heating affects strongly the pre-ignition processes, except during extremely intensive radiative heating (above 20 W/cm^2), and consequently must be included in the ignition modeling analysis. The analysis of radiative heating combined with convective cooling is readily specialized to describe convective heating in a quiescent air atmosphere at elevated temperatures.

3.4.1 Problem Formulation

Consider a system of N_1 solid, porous, and $N_2 - 2 = N_1 - 1$ gaseous, plane parallel, large thin slabs ($0 \leq x \leq L >> \delta_j$) with vertical interfaces and surrounded by semi-infinite, gaseous expanses which represent the environment of the system, as depicted in Figure 3.1. In the case of a single solid ($N_1 = 1$), such solid may be semi-infinite ($y \to -\infty$) and replace one external semi-infinite, gaseous expanse.

Initially ($\tau < 0$) the system is in stationary thermodynamic equilibrium at temperature T_i, with all gas phases at rest. At time $\tau = 0$ the heating process is started, either through the imposition of a constant, uniform radiant heat flux W_o, incident at one external solid surface, or through the sudden change of environmental temperature from T_i to $T_o > T_i$, or both.

Subsequently ($\tau > 0$), solid phase temperatures T_{sj}, $j = 1,2,\ldots,N_1$, and gas phase temperatures T_{gj}, $j = 1,2,\ldots,N_2$ rise, desorption and gasification within the porous solids induce "internal" convection normal to and out of the solid-gas interfaces, while buoyancy induces "external" convection, upward and parallel to the interfaces.

Finally, at time $\tau = \tau_{ig}$, the ignition criterion is reached in the gaseous boundary layer at the heated solid surface.

(1) There exists, for every pyrolysate concentration $w_{fl} \leq w_f \leq w_{fu}$ in air, between the lower and upper concentration limits w_{fl} and w_{fu}, respectively ($0 < w_{fl} < w_{fu} < 1$), a minimum temperature $T_{ig}(w_f)$ at which under local thermodynamic equilibrium spontaneous ignition occurs.

(2) A concentration profile $w_f(x,y;\tau)$ establishes itself during pyrolysate evolution from the heated surface (y measures normal and x measures parallel to the heated surface) which, after substitution into the experimentally determined function $T_{ig}(w_f)$, defines for sufficiently large values of time τ a <u>necessary</u> minimum temperature distribution $T_{ig}(x,y;\tau)$.

(3) The actual mixture temperature $(T_g)_{N_2}(x,y;\tau)$ in the boundary layer near the heated solid approaches $T_{ig}(x,y;\tau)$ from below, starting from $(T_g)_{N_2} = T_i$, until at the instant τ_{ig} at some point $(\bar{x},\bar{y})$, $(T_g)_{N_2}(\bar{x},\bar{y};\tau_{ig}) = T_{ig}(\bar{x},\bar{y};\tau_{ig})$ for the first time.

3.4.2 Governing Equations

One-dimensional conductive heat transfer, accompanied by thermal decomposition and pyrolysate convection is described by the equations of mass, energy and momentum balance and constitutive laws for conduction and pyrolysis, and for solid and gas phase material descriptions. Generally this means that there are three balance and five constitutive equations required for each one of the solid regions. In the case of vanishing stress exerted by the porous matrix on the pyrolysate there is no momentum balance needed, and the number of equations is reduced by one.

Each one of the gaseous regions requires three dimensional $(x,y;\tau)$ descriptions of mixture state (pressure p and temperature T), of mixture motion (u,v) and of pyrolysate concentration w_f. This is accomplished with the aid of mixture mass and species conservation equations, of one mixture momentum (x-direction) and one mixture energy balance equations, one

equation each for every one of the N_2 gaseous regions. The balance equations must be supplemented by constitutive descriptions for wall shear stress, heat and mass transport, thermal and caloric mixture behavior and, finally for the ignition criterion.

The necessary equations are listed below for the simple case of $N_1 = N_2 = 1$ as shown in Figure 3.2. This is sufficient to describe all the principles and techniques which are to be applied to the analysis of more complex composite systems. Only significant terms are retained, and the pressure is taken to be uniform throughout (typical of fabric porosity and natural convection).

3.4.2.1 Conservation Equations are obtained by integrating the local conservation equations (partial differential equations) in the y direction across the appropriate regions. With the nomenclature presented in Figure 3.2 one obtains for

energy conservation in the Region (1), i.e. $(0 \leq y \leq \delta)$

$$(\rho c)_1 \frac{\partial}{\partial \tau} \int_0^{\delta} T_1 \, dy + (c_p)_f \int_0^{\delta} (\rho v)_f \frac{\partial T_1}{\partial y} \, dy =$$

$$-(q_y)_{y=\delta} + \alpha W_o - (\Delta\rho)_1 \int_0^{\delta} \dot{\lambda}[\Delta i_f^{\,o} + \overline{\Delta c_p}(T - T_\infty)] \, dy \qquad (3.4.1)$$

pyrolysate mass conservation in Region (1)

$$(\rho v)_f = (\Delta\rho)_1 \int_0^{\delta} \dot{\lambda} \, dy \qquad (3.4.2)$$

conservation of energy for the mixture (2), i.e. $(y>\delta)$

$$\frac{\partial}{\partial \tau} \int_{\delta}^{\tilde{h}} (\rho \Delta i)_2 \, dy + \frac{\partial}{\partial x} \int_{\delta}^{\tilde{h}} (\rho u \Delta i)_2 \, dy - (\rho v \Delta i)_f \Big|_{y=\delta} =$$

$$(q_y)_\delta + \mu_2 \int_{\delta}^{\tilde{h}} \left(\frac{\partial u_2}{\partial y} \right)^2 dy - \left\{ \rho_2 (c_{p,f} - c_{p,a})(T_2 - T_\infty) \mathfrak{D} \frac{\partial w_f}{\partial y} \right\}_{y=\delta} \qquad (3.4.3)$$

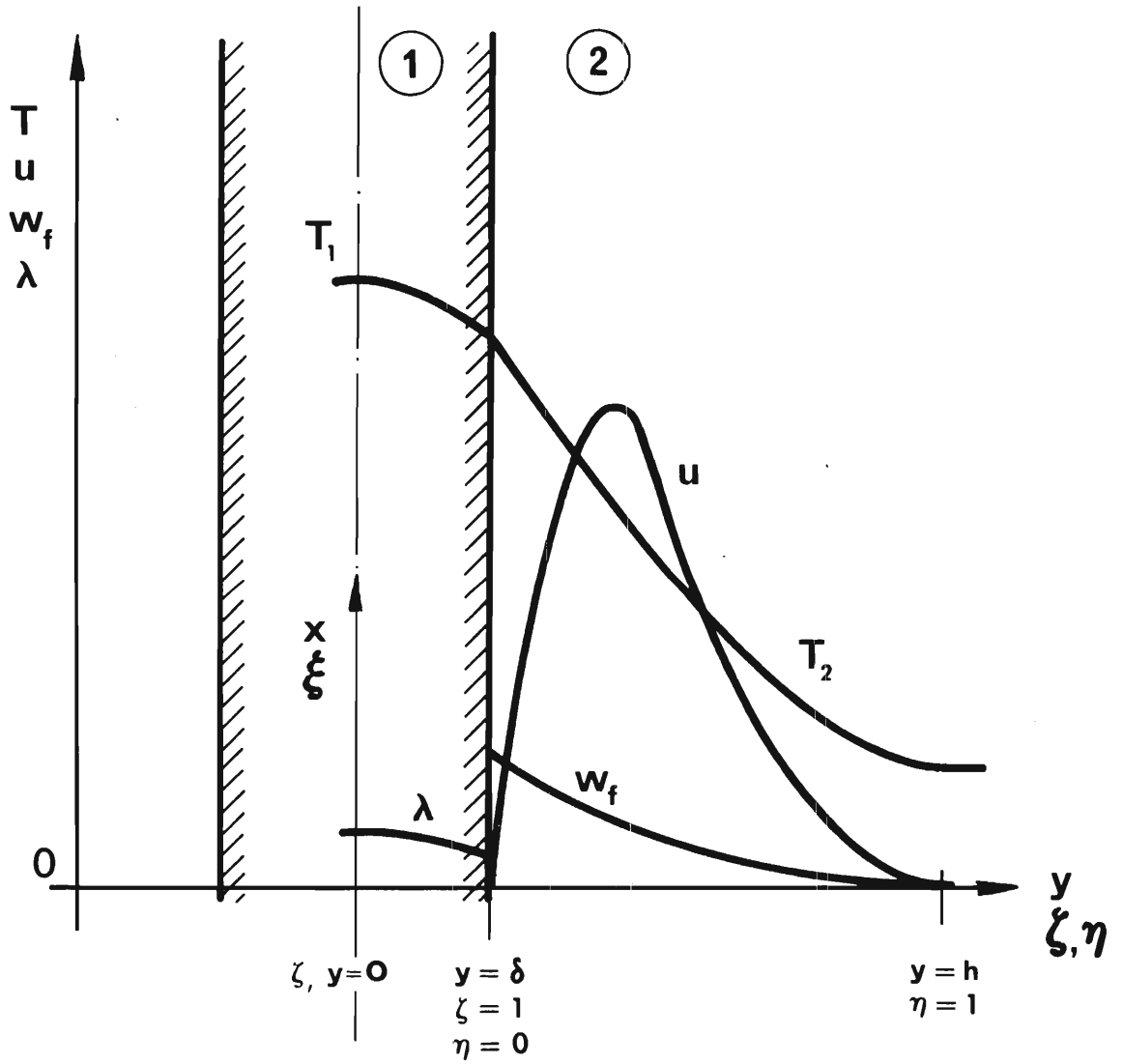

Figure 3.2 Two-Region System and Nomenclature

balance of mixture momentum and mixture mass conservation in Region (2)

$$\frac{\partial}{\partial \tau}\int_{\delta}^{\tilde{h}} (\rho u)_2 \, dy + \frac{\partial}{\partial x}\int_{\delta}^{\tilde{h}} (\rho u^2)_2 \, dy = g\int_{\delta}^{\tilde{h}} (\rho_\infty - \rho_2)\, dy - s_o \tag{3.4.4}$$

and, finally for the

conservation of pyrolysate in Region (2)

$$\frac{\partial}{\partial \tau}\int_{\delta}^{\tilde{h}} \rho_2 w_f dy + \frac{\partial}{\partial x}\int_{\delta}^{\tilde{h}} (\rho u)_2 w_f dy =$$

$$(\Delta\rho)_1 \int_0^{\delta} \dot{\lambda}\, dy - \left\{ \rho_2 \mathfrak{D} \frac{\partial w_f}{\partial y} \right\}_{y=\delta} \tag{3.4.5}$$

Here, the subscripts 1,2,f and a designate, respectively, solid region (1), gaseous region (2), pyrolysate species and air. Symbols ρ,T,u,v represent density, temperature, vertical and horizontal velocity components, $\Delta\rho$ the decomposable solid density portion, c the solid specific heat, c_p the specific heat at constant pressure for the gaseous phase and Δi_f^o the reaction enthalpy of gasification at $T = T_\infty$ ($\Delta i_f^o < 0$ implies exothermic reaction). Moreover

$$\overline{\Delta c_p} = \overline{c_{p,f} - c_1} \tag{3.4.6}$$

is the difference in specific heats of solid and pyrolysate, averaged over the temperature range (T_i, T_{ig}). The symbol

$$(\Delta i)_2 = \overline{c_{p,2}}\,(T_2 - T_\infty) \tag{3.4.7}$$

designates excess enthalpy of the mixture above that of the mixture at the environmental temperature T_∞, $\mathfrak{D}$, $w_f = \rho_f/\rho_2$ stand for diffusion coefficient and mass fraction, respectively, while λ represents the degree

of decomposition. The solid matrix has the time invariant thickness 2δ, and the boundary layer thickness

$$h(x,\tau) = \tilde{h}(x,\tau) - \delta , \tag{3.4.8}$$

common to both the momentum, energy and concentration layers, because

$$N_{Pr} = N_{Sc} = 1 \tag{3.4.9}$$

has been found to be approximately correct for the gas properties involved.

It should be mentioned that uniform and constant pressure is assumed, that the molecular weights of air and pyrolysates have been taken to be the same and that $\rho_f << \rho_1$. Also implied in Eqs. 3.4.3,4 & 5 is the fact that $u = 0$ for $y \geq \tilde{h}$.

3.4.2.2 Constitutive Laws are required to describe firstly

wall shear, which is approximated by [3.7,3.8]

$$S_o(x) = \rho_2 u_m^2 \left[\frac{0.332}{\sqrt{N_{Re,x}}} \right] , \quad N_{Re} \leq 5.5X10^5 \tag{3.4.10}$$

$$= 0.0225\ \rho_2 u_m^2 \left(\frac{\nu_2}{u_m h}\right)^{-1/4} , \quad N_{Re} > 5.5X10^5 \tag{3.4.11}$$

and heat transfer, approximated by [3.9,3.8]

$$(q_y)_\delta (x) = 0.508\ k_2 T_\infty \sqrt[4]{\frac{g(T_{2,\delta} - T_\infty)}{4\ \nu^2 x}}$$

$$\text{for } N_{Re} > 5.5X10^5 \tag{3.4.12}$$

$$= 0.0225\ \rho_2 c_{p,2} u_m (T_{2,\delta} - T_\infty)\left(\frac{\nu_2}{u_m h}\right)^{1/4} N_{Pr}^{-2/3}$$

$$\text{for } N_{Re} > 5.5X10^5 \tag{3.4.13}$$

where u_m, ν and k represent, respectively, the maximum upward velocity $(u_2)_{max}$, kinematic viscosity and thermal conductivity, while N_{Re} and N_{Pr} are the Reynolds and Prandtl numbers.

Equations 3.4,10-13 are correct only in the limit of vanishing pyrolysate evolution $(v_2)\delta/u_m \to 0$. The approximation, however, is adequate except for cases of low heating intensities $\alpha W_o/[(\rho c\delta)_1(T_{ig} - T_i)]<<1$. Pyrolysate injection into the gaseous boundary layer can be accounted for [3.10].

Secondly, one needs to describe the rate of <u>desorption</u> (d) and of gasification (g). Arrhenius-type reaction rates are adequate

$$\dot{\lambda}_{d,g} = (1 - \lambda_{d,g})^{n_{d,g}} A_{d,g} e^{-(E_{d,g}/RT_1)} \qquad (3.4.14)$$

Thirdly, experimentally determined (see Section 2.1) ignition temperature T_{ig} is expressed in terms of pyrolysate mass fraction w_f in the air-pyrolysate mixture

$$T_{ig} = f(w_f) \quad , \quad 0 < w_f < 1 \qquad (3.4.15)$$

Finally, thermal and caloric equations must be specified for the solid porous matrix and the gaseous constituents. Perfect gas and constant transport properties are employed after judicial selection of properly averaged data.

3.4.2.3 <u>Initial and Boundary Conditions are</u>

$$\left.\begin{aligned} T &= T_i \\ u &= v = \lambda = 0 \end{aligned}\right\} \quad \text{in Regions (1) and (2) for } \tau < 0 \qquad (3.4.16)$$

$$v_1 = \frac{\partial T_1}{\partial y} = 0 \quad \text{at } y = 0, \quad \tau \geq 0 \qquad (3.4.17)$$

$$\left.\begin{aligned} (\rho v)_1 &= (\rho v_2) \\ T_1 &= T_2 \end{aligned}\right\} \quad \text{at } y = \delta,\ \tau \geq 0 \qquad (3.4.18)$$

$$T_2 = T_\infty \quad \text{at } y = \tilde{h},\ \tau \geq 0 \qquad (3.4.19)$$

3.4.3 Solution

The five balance equations, Eqs. 3.4.1 through 5, define five system state variables which are considered to be the components $Y_1, Y_2, \ldots, Y_5$ of the five-dimensional vector $\underset{\sim}{Y}$. Chosen as the five components are:

the nondimensional, interfacial excess temperature

$$Y_1 = T_\delta / T_\infty - 1 \qquad (3.4.20)$$

the decomposition rate (desorption effects are ignored)

$$Y_2 = \lambda_g \qquad (3.4.21)$$

the Reynolds number

$$Y_3 = UH/\nu_2 \qquad (3.4.22)$$

the nondimensional maximal boundary layer thickness

$$Y_4 = H/L \qquad (3.4.23)$$

and the pyrolysate mass fraction at the interface

$$Y_5 = w_{f,\delta} \qquad (3.4.24)$$

where $U = u_m(L)$ and $H = h(L)$, with L representing the height of the heated surface.

After substituting the constitutive equations, Eqs. 3.4.10 through 14 into Eqs. 3.4.1 through 5, after expanding Eq. 3.4.14 about the interfacial values $(\lambda_d)_\delta$ and T_δ of decomposition degree and temperature, respectively, and after integrating Eqs. 3.4.1 through 5, first in the y-direction as indicated and then over x from x=0 to x=L, one obtains finally this system of five ordinary differential equations, linear in the derivatives with respect to nondimensional time τ^*

$$\underset{\sim}{C}\dot{\underset{\sim}{Y}} = \underset{\sim}{B} \qquad (3.4.25)$$

The superscripted dot designates $d/d\tau^*$. The (5X5) coefficient matrix $\underset{\sim}{C}$ and the five-dimensional vector $\underset{\sim}{B}$ are functions of $\underset{\sim}{Y}$ and τ^*.

To evaluate the elements of $\underset{\sim}{C}$ and $\underset{\sim}{B}$ in Eq. 3.4.25 we introduce first the normalized x and y coordinates

$$\zeta = y/\delta, \qquad 0 \leq \zeta \leq 1 \qquad (3.4.26)$$

$$\eta = (y - \delta)/(\tilde{h} - \delta)$$
$$= (y - \delta)/(h(x), \qquad 0 \leq \eta \leq 1 \qquad (3.4.27)$$

$$\xi = x/L, \qquad 0 \leq \xi \leq 1 \qquad (3.4.28)$$

and we approximate the spatial property variations, first in the ζ and η direction

for the solid, Region (1), by

$$T_1/T_\infty = \phi_1 + 1 \qquad (3.4.29)$$

$$\lambda/Y_2 = \phi_2 + 1 \qquad (3.4.30)$$

and for the fluid, Region (2) by

$$T_2/T_\infty = \psi_2 + 1 \qquad (3.4.31)$$

$$u_2/u_m = \psi_2 \tag{3.4.32}$$

$$w_f/Y_5 = \psi_3, \tag{3.4.33}$$

and finally in the ξ-direction, for the fluid

$$u_m/U = \xi^{\bar{m}} \tag{3.4.34}$$

$$h/H = \xi^{\bar{n}} \tag{3.4.35}$$

where

$$\left.\begin{aligned} \bar{m} &= 1/2 \\ \bar{n} &= 1/2 \text{ for } N_{Re,L} < 5.5X10^5 \\ \bar{n} &= 7/10 \text{ for } N_{Re,L} \geq 5.5X10^5 \end{aligned}\right\} \tag{3.4.36}$$

The five functions ϕ_i and ψ_i are conveniently expressed by power polynomials with $\underset{\sim}{Y}$-dependent coefficients $a_{ij}(\underset{\sim}{Y})$ and $b_{ij}(\underset{\sim}{Y})$

$$\phi_i = \sum_{j=0}^{N_i} a_{ij} \zeta^j \quad , i = 1,2 \tag{3.4.37}$$

$$\psi_i = \sum_{j=0}^{M_i} b_{ij} \eta^j \quad , i = 1,2,3 \tag{3.4.38}$$

The coefficients are chosen such that Eqs. 3.4.37 and 38 satisfy Eqs. 3.4.17 through 19 and Eqs. 3.4.20 through 24.

A parabolic temperature distribution in the solid requires that

$$a_{10} = Y_1 + q^*/2, \quad a_{11} = 0, \quad a_{12} = -q^*/2 \tag{3.4.39}$$

$$\dot{a}_{20} = \dot{Y}_2/Y_2\left[\frac{q^*}{2(1 + Y_1)^2} - \frac{1 + Y_2(n_g - 1)}{1 - Y_2}\, a_{20}\right] \tag{3.4.40}$$

$$\dot{a}_{2j} = \dot{Y}_2/Y_2 \left[\frac{a_{1j}}{(1 + Y_1)^2} - \frac{1 + Y_2(n_g - 1)}{1 - Y_2} a_{2j} \right]$$

$$j = 1,\ldots,N_2 \qquad (3.4.41)$$

where $q^*(Y_1,Y_3,Y_4) = \dfrac{(q_y)_\delta}{\alpha W_o}$ (3.4.42)

represents the nondimensional heat flux at the fluid solid interface.

A parabolic mixture temperature profile implies

$$b_{10} = Y_1 , \quad b_{11} = -2Y_1 , \quad b_{12} = Y_1 \qquad (3.4.43)$$

The velocity profile was chosen to be represented, by

$$b_{20} = 0 , \quad b_{22} = -2b_{21} , \quad b_{23} = -b_{21}$$

$$\text{and} \quad b_{21} = \frac{1 + \bar{m} + \bar{n}}{\pi_6} \frac{Y_4^2}{Y_3} \qquad (3.4.44)$$

where π_6 is defined in Table 3.1.

Integrations along the ξ-coordinate are trivial, integrations over ζ and η lead to new polynomials, arctangent and natural logarithms with removable singularities for the limits as Y_1, Y_3, Y_4 and Y_5 tend to zero. After the substitution of the profile integrals with Eqs. 3.4.25, this system can be solved (some singularities at $\tau^* = 0$ require special attention) to yield the explicit form

$$\underset{\sim}{\dot{Y}} = \underset{\approx}{C}^{-1} \underset{\sim}{B} \qquad (3.4.45)$$

The initial conditions, Eqs. 3.4.16, require

$$\underset{\sim}{Y}(0) = (\pi_1, 0,0,0,0) \qquad (3.4.46)$$

Table 3.1 Nondimensional Groups for Ignition by Radiation and Free Convection

Definition	Interpretation
$\pi_1 = T_i/T_\infty - 1 = Y_1(0)$	Initial Temperature
$\pi_2 = (\Delta\rho_1)/\rho_1$	Decomposable Mass Fraction
$\pi_3 = \bar{c}_{p,f}/\bar{c}_1$	Specific Heat Ratio in Solid
$\pi_4 = \pi_2 \Delta i_f^o/(\bar{c}_1 T_\infty)$	Ratio of Volumetric Decomposition Enthalpy Density to Volumetric Heat Capacity in Solid
$\pi_5 = gL\tau_{ref}/\nu_2$ *)	Ratio of Buoyancy to Viscous Forces
$\pi_6 = \nu_2 \tau_{ref}/L^2$	Viscous Dissipation
$\pi_7 = \bar{c}_{p,f}/\bar{c}_{p,2}$	Specific Heat Ratio in Fluid
$\pi_8 = \delta(\Delta\rho)_1/(L\rho_\infty)$	Specific Mass Ratio
$\pi_9 = \nu_2^3 \tau_{ref}/(L^4 \bar{c}_{p,2} T_\infty)$	Ratio of Viscous Dissipation to Thermal Energy Storage
$\pi_{10} = N_{sc}$	Schmidt Number
$\pi_{11} = E/(RT_i)$	Activation Energy
$\pi_{12} = A\tau_{ref} e^{-\pi_{11}}$	Decomposition Rate

Definition	Interpretation
$\pi_{13} = n_g$	Reaction Degree
$\pi_{14} = N_{Pr}$	Prandtl Number

---

*) $\tau_{ref} = \delta T_\infty (\rho\overline{c})_1/(\alpha W_o)$ Reference Time

$\tau^* = \tau/\tau_{ref}$ Time

Equations 3.4.45 and 46 are solved numerically, starting from $\tau^* = 0$ and advancing on until the ignition criterion is reached at $\tau^* = \tau^*_{ig}$. This is discussed is Section 3.4.3. The normalization of Eqs. 3.4.1 through 5 leads from twenty dimensional material properties and process parameters to fourteen nondimensional groups π_j , $j = 1,\ldots,14$. Complete modeling analysis yields, therefore, under the assumptions made, the prediction of ignition time τ^*_{ig} in terms of fourteen groups.

$$\tau^*_{ig} = \tau^*_{ig}\,(\pi_1,\pi_2,\ldots,\pi_{14}) \tag{3.4.47}$$

3.5 Ignition Criterion

The experimentally determined flammability limit as defined through Eq. 3.4.15 must be related to the state $\underset{\sim}{Y}$ of the system in order that one can obtain τ^*_{ig} , that is the instant at which the system reaches $\underset{\sim}{Y}_{ig}$ for the first time.

There are two possibilities by which the system can reach ignition conditions, depending on the type of external heating imposed on the system: During convective heating the gas mixture temperature is for all $\tau^* > 0$ large enough, at least at the outer edge of the boundary layer (or else ignition is impossible) and the pyrolysate concentration Y_5 at the solid surface must reach a minimum value. On the other hand, during radiative heating the pyrolysate concentration at the surface increases from zero to one, requiring at first infinitely large, then decreasing and finally again increasingly large solid surface temperatures. This follows from the concave shape of the curve representing $T_{ig}(w_f)$. Therefore, ignition by radiative heating occurs when the surface temperature Y_1 reaches a minimum value.

Substitution of Eq. 4.3.33 into the normalized form of Eq. 4.3.15 yields

$$T_{ig}/T_\infty - 1 = \psi_{ig}(Y_5,\eta) \tag{3.5.1}$$

Ignition occurs at the surface, $\eta = 0$, if for the instantaneous value of $Y_5(\tau^*)$

$$\frac{\partial \psi_{ig}}{\partial \eta}(Y_5,0) \quad \geq \quad \frac{\partial \psi_1}{\partial \eta}\{\psi_{ig}(Y_5), 0\} \tag{3.5.2}$$

as soon as

$$Y_1 = Y_{ig} = \psi_{ig}(Y_5,0) \tag{3.5.3}$$

In this case the critical surface temperature Y_{ig} is reached while there is still sufficient oxygen at the interface. If the pyrolysate concentration reaches saturation, $Y_5 = 1$, before the surface temperature reaches sufficiently high values then ignition occurs at the distance $\eta = \eta_{ig}$ from the surface and as soon as

$$\left.\begin{aligned} \Lambda_1(Y_{ig}, Y_5, \eta_{ig}) &= \psi_{ig} - Y_1 = 0 \\ \Lambda_2(Y_{ig}, Y_5, \eta_{ig}) &= \partial/\partial\eta\ \Lambda_1 = 0 \end{aligned}\right\} \tag{3.5.4}$$

Elimination of η_{ig} yields the ignition criterion for <u>radiative heating</u> in terms of the instantaneous pyrolysate concentration at the surface

$$Y_1 = Y_{ig} = Y_{ig}(Y_5) \tag{3.5.5}$$

or, for <u>convective heating</u> in terms of the instantaneous surface temperature

$$(Y_5)_{min} = f(Y_1) \tag{3.5.6}$$

The system of Eqs. 3.5.4 is readily solved by numerical techniques during integration of Eqs. 3.4.45 and 46. A Newton-Raphson iteration scheme serves to terminate integration precisely when Eq. 3.5.5 or Eq. 3.5.6 is satisfied. This yields the required time τ^*_{ig} of ignition.

3.6 Ignition by Forced Convection Heating

Forced convection heating is the dominant heat transfer mode when gas burners and open flames from burning furnitures or liquid pools, enhanced by induced draft, are responsible for ignition. Domestic and commercial gas kitchen ranges fall into this category and are responsible for a large portion of unwanted fires.

3.6.1 Problem Formulation

Let the heated turbulent gas jet shown in Figure 3.3 impinge normally on the composite system described in Section 3.4.1, thereby replacing the radiant heat flux source.

The system is initially (at $\tau < 0$) in stationary thermodynamic equilibrium at temperature T_i. At time $\tau = 0$ the system is exposed to the established jet. Subsequently ($\tau > 0$), the temperatures T_{sj} of the solid phases rise, desorption and gasification induce convection through and out of the heated solid phase, possibly into the flow of the impinging jet, thereby retarding the heat transfer from the jet to the heated solid.

Ignition occurs at $\tau = \tau_{ig}$, when the combustible pyrolysate has advanced toward the hot gas jet, sufficiently far to reach the minimum temperature T_{ig}. Ignition may occur either at the surface or at some distance $\eta > 0$ from the surface as discussed in Section 3.5. Considered in the analysis is the radial boundary layer ($h/r << 1$). The stagnation region is not treated here at this time.

3.6.2 Governing Equations

The treatment is similar to that in Section 3.4.2. Only the important differences in the governing equations, which result from the differences in geometry and flow pattern, are reproduced here.

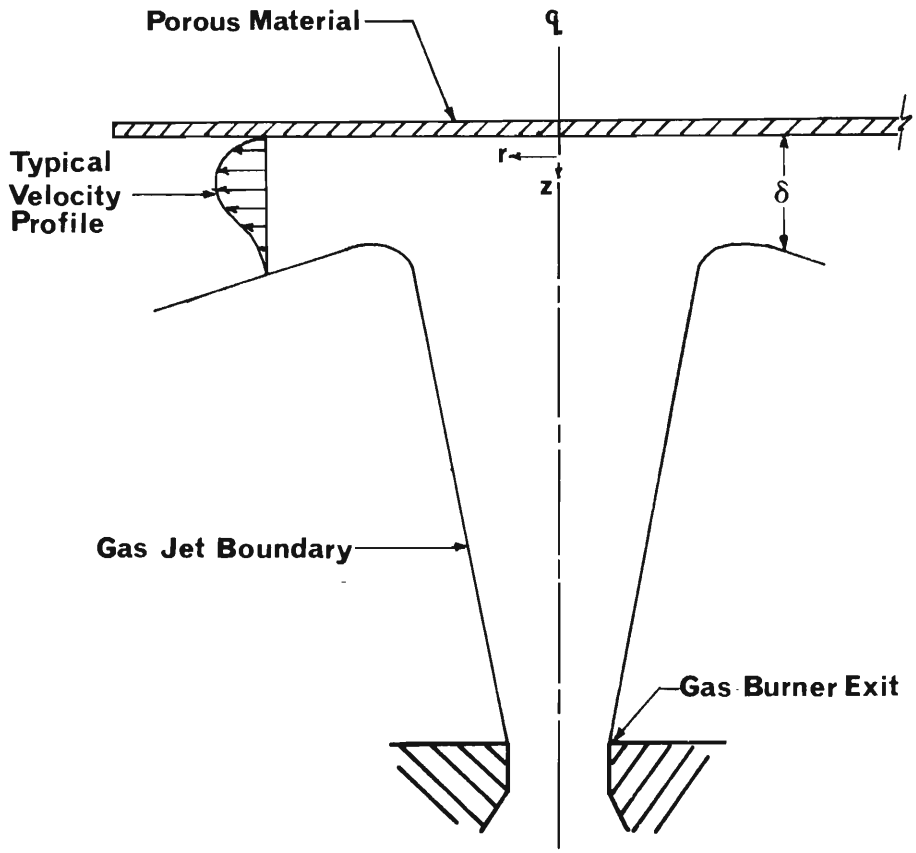

Figure 3.3 Flow Pattern for Ignition by Forced Convection Heating

3.6.2.1 The Balance Equations are derived through integration of local balance equations. For the decomposing porous solid, Region (1), apply Eqs. 3.4.1 and 3.4.2.

The energy equation for the mixture ($z>\delta$) in Region (2), combined with its equation of mass conservation, is

$$\frac{\partial}{\partial \tau}\int_{\delta}^{\tilde{h}} (\rho\Delta i)_2\, dz + \frac{\partial}{r\,\partial r}\int_{\delta}^{\tilde{h}} (r\rho u\Delta i)_2\, dz - (\rho v\Delta i)_f\Big|_{z=\delta} = (q_z)_\delta + \mu_2\int_0^{\tilde{h}} \left(\frac{\partial u_2}{\partial z}\right)^2 dz - \left\{\rho_2(c_{p,f} - c_{p,a})(T_2 - T_\infty)\mathcal{D}\,\frac{\partial w_f}{\partial z}\right\}_{z=\delta} \qquad (3.6.1)$$

Consistent with the flow pattern shown in Figure 3.3, the velocity u at $z = \tilde{h}(r)$ is taken to be zero in Eq. 3.4.54 and in Eqs. 3.4.55 and 56 below.

The balance of momentum and mixture mass conservation in Region (2) reads

$$\frac{\partial}{\partial \tau}\int_{\delta}^{\tilde{h}} (\rho u)_2\, dz + \frac{\partial}{r\,\partial r}\int_0^{\tilde{h}} (r\rho u^2)_2\, dz = -s_o \qquad (3.6.2)$$

since the radial pressure gradient is zero outside of the boundary layer.

The conservation of pyrolysates in Region (2) requires that, prior to ignition

$$\frac{\partial}{\partial \tau}\int_{\delta}^{\tilde{h}} (\rho_2 w_f)\, dz + \frac{\partial}{r\,\partial r}\int_{\delta}^{\tilde{h}} (r\rho u)_2\, w_f\, dz = (\Delta\rho)_1\int_0^{\delta} \dot{\lambda}\, dz - \left\{\rho_2\mathcal{D}\,\frac{\partial w_f}{\partial z}\right\}_{z=\delta} \qquad (3.6.3)$$

3.6.2.2 Constitutive Equations. Heat transfer and wall shear stress are specified by Eqs. 3.4.13 and 3.4.12, respectively. Equations 3.4.14 and 3.4.15 describe chemical reactions and ignition criterion.

3.6.2.3 The Initial and Boundary Conditions are

$$
\left.
\begin{array}{lll}
T = T_i & \text{in Region (1)} & z \leq \delta \\
T = T_f & \text{in Region (2)} & \delta \leq z \leq \tilde{h} \\
\lambda = 0 & & 0 \leq z \leq \delta \\
\tilde{h}(r) = F(r) & & r_o \leq r \leq R
\end{array}
\right\} \quad \tau < 0 \qquad (3.6.4)
$$

$$
\left.
\begin{array}{lll}
2\pi r_o \int_{\delta}^{\tilde{h}} (\rho u)_2 \, dz = \dot{m} & \text{at} & r = r_o \\
v_1 = \dfrac{\partial T_1}{\partial z} = 0 & \text{at} & z = 0 \\
(\rho v)_1 = (\rho v)_2 & \text{at} & z = \delta \\
T_1 = T_2 & \text{at} & z = \delta
\end{array}
\right\} \quad \tau \geq 0 \qquad (3.6.5)
$$

3.6.3 Solution

The solution techniques employed to solve the system of integral balance equations, Eqs. 3.4.1,2; 3.6.1,2 and 3 is the same as described in Section 3.4.3.

3.7 Results and Conclusions

Equations 3.4.45 are integrated by a fourth-order Rung-Kutta algorithm.

The ignition temperature T_{ig} as a function of pyrolysate mass fraction w_f is expressed in two parts. One part represents the singular character at $w_f = 0$ and at $w_f = 1$, and the other part represents the (analytic) complement to be determined by experiment.

$$T_{ig}(w_f) = T_o/[2w_f(1 - w_f)] + \sum_{j=0}^{l_1} c_j w_f^j \qquad (3.7.1)$$

Here T_o represents the conveniently chosen reference temperature $T_o = 298.15°K$, and the l_1 coefficients c_j are determined by experiment. Since the experiments were not concluded at the time of report writing, the following coefficients have been chosen for checking out the integration procedure:

$$c_o = - \quad 298.15 \ °K$$
$$c_1 = \quad 1{,}192.60 \ °K$$
$$c_2 = - \ 1{,}192.60 \ °K$$

These coefficients represent the range of ignition temperatures measured earlier in the Setchkin Furnace [1.8]. The results shown in Figures 3.4,5 and 6 are preliminary, pending final ignition temperature data evaluation.

Figures 3.4 and 5 show the preignition history computed for a cotton fabric, GIRCFF Fabric No. 5 with the following material properties and process parameters:

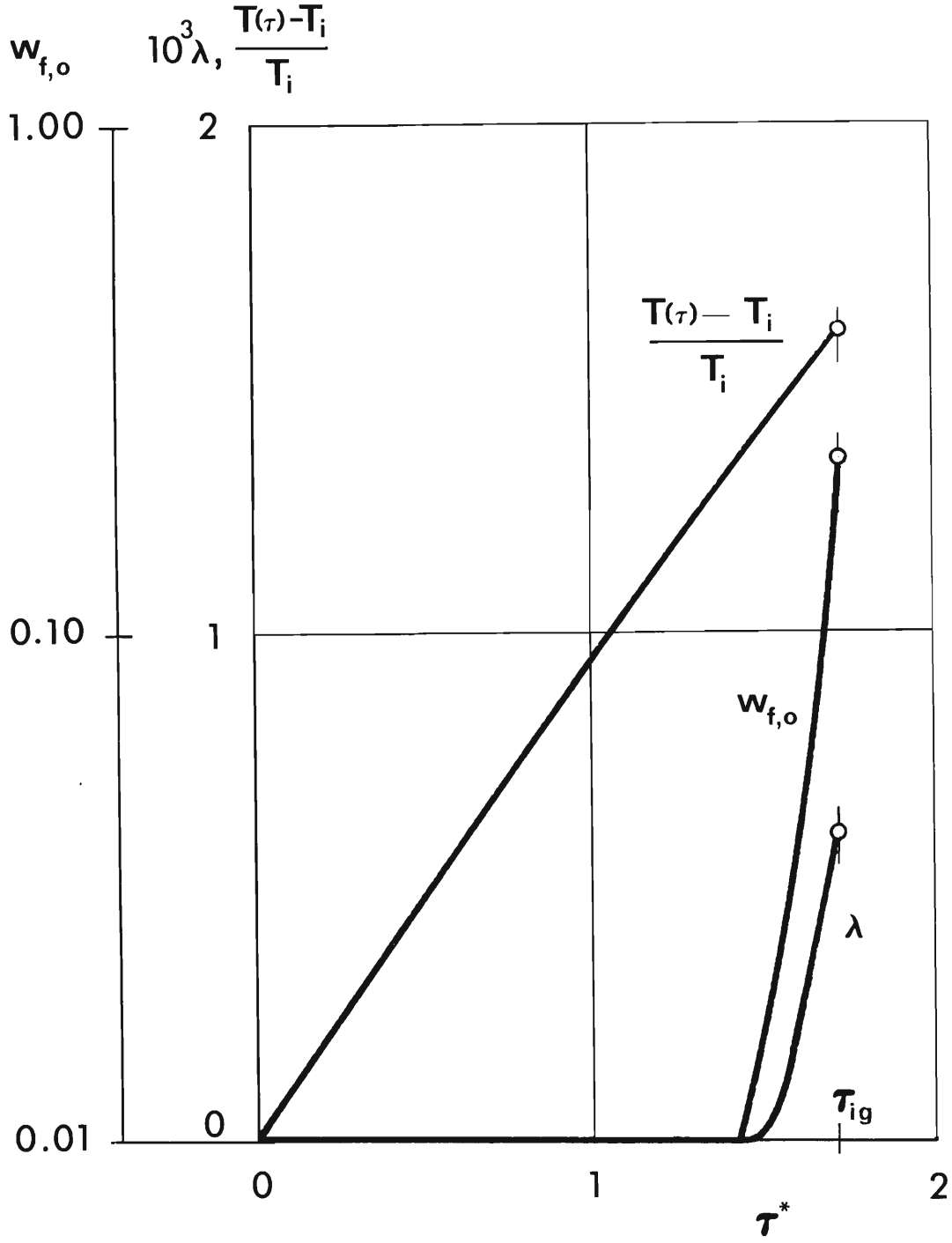

Figure 3.4 Temperature Rise $T/T_i - 1$, Decomposition λ and Surface Pyrolysate Concentration Histories During Preignition Process

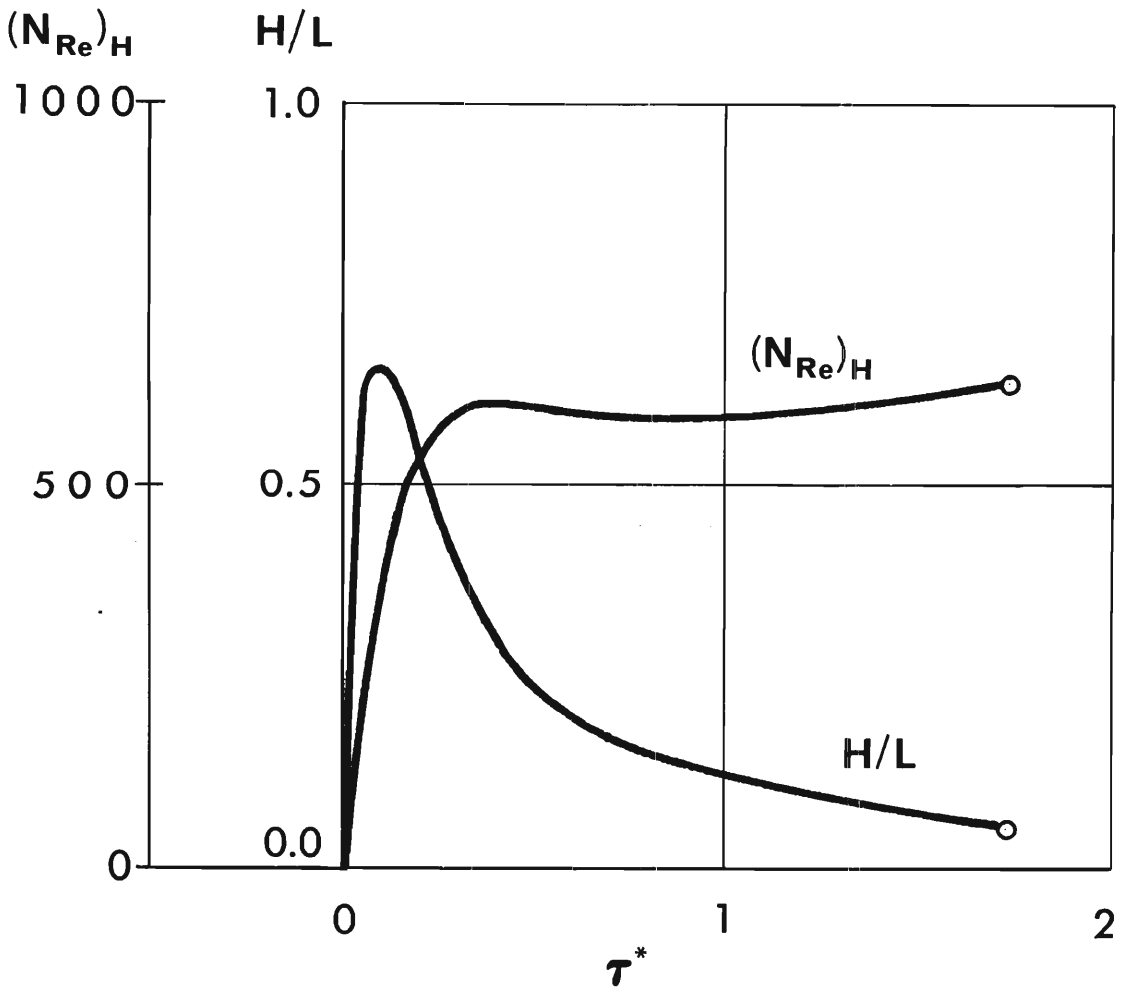

Figure 3.5 Fluid Dynamics During Preignition Process. Reynolds Number and Normalized Boundary Layer Thickness versus Normalized Time

Solid Specific Mass	$.29630 \times 10^{-1}$ g/cm^2
Decomposable Mass Fraction	.90
Radiative Absorptance	.511
Thermal Conductance	$.15000 \times 10^{-1}$ W/(cm^{2}K)
Specific Heat	$.14240 \times 10^{1}$ Ws/(gK)
Reaction Enthalpy (Pyrolysis)	$.90000 \times 10^{2}$ Ws/g
Activation Energy	$.22950 \times 10^{6}$ Ws/mole
Frequency Factor	$.95400 \times 10^{13}$ 1/s
Degree of Reaction	$.26000 \times 10^{1}$
Mixture Density	$.12930 \times 10^{-2}$ g/cm^3
Viscosity	.24630 cm^2/s
Thermal Conductivity	$.33340 \times 10^{-3}$ W/(cmK)
Schmidt Number (PI(10)	1.0
Specific Heat	.80
Pyrolysate Specific Heat	1.0
Irradiance	$.75000 \times 10^{1}$ W/cm^2
Initial Temperature	$.29815 \times 10^{3}$ K
Environmental Temperature	$.29815 \times 10^{3}$ K
Gravity	$.98100 \times 10^{3}$ cm/s^2
Vertical Dimension	$.10000 \times 10^{2}$ cm

The corresponding scaling groups are

$\pi_1 = 0$
$\pi_2 = 0.90$
$\pi_3 = 0.7022$
$\pi_4 = 0.1908$
$\pi_5 = 0.1307 \times 10^{6}$
$\pi_6 = 0.8085 \times 10^{-2}$
$\pi_7 = 1.250$
$\pi_8 = 2.0624$
$\pi_9 = 0.2056 \times 10^{-14}$
$\pi_{10} = 1.0$
$\pi_{11} = 0.9258 \times 10^{2}$
$\pi_{12} = 0.1936 \times 10^{-26}$
$\pi_{13} = 2.6$
$\pi_{14} = 1.0$

Figure 3.4 presents the first three system variables, namely the nondimensional temperature $(T - T_i)/T_i$, the degree of thermal decomposition λ and the pyrolysate concentration $w_{f,o}$ at the interface between the pyrolyzing porous solid and its external boundary layer. All variables are shown as functions of the nondimensional time τ^*.

Figure 3.5 presents the normalized boundary layer thickness H/L and the Reynolds number UH/ν at x = L, also as a function of nondimensional time τ^*. The initial peak in the boundary layer thickness growth represents the initial penetration depth due to thermal diffusion. As the fluid is subsequently accelerated by buoyancy the fluid is swept upwards, and the boundary layer thickness decreases until viscous and buoyancy forces are balanced.

Figure 3.6 shows the normalized dependencies of ignition time τ^*_{ig} and of ignition temperature ψ_{ig} on the relative convective cooling intensity, characterized by $\pi_5 = gL\tau_{ref}/\nu$. This represents in principle the predicted ignition time and ignition temperature as functions of heating intensity.

It can be observed from Figure 3.6 that ignition time τ_{ig} decreases inversely proportional to radiative heating intensity only at high intensities, while convective losses become significant at low heating intensities and retard the heating process. Ignition temperature, that is the temperature of the solid at its heated front face, increases with heating intensity. This agrees with experience. It should be noted that the pyrolysate concentration at the interface reached values between 0.25 at low heating intensities and 0.21 at high heating intensity. All ignitions were predicted to take place at the solid front face.

In conclusion it can be said that integral techniques and the newly proposed ignition criterion are suitable to predict correctly the experimentally observed trends of ignition temperature and ignition time as functions of heating intensity. The ignition time predicted on the basis of the assumed ignition temperature dependence on fuel concentration, however, is lower than the measured ignition time. Final verification of

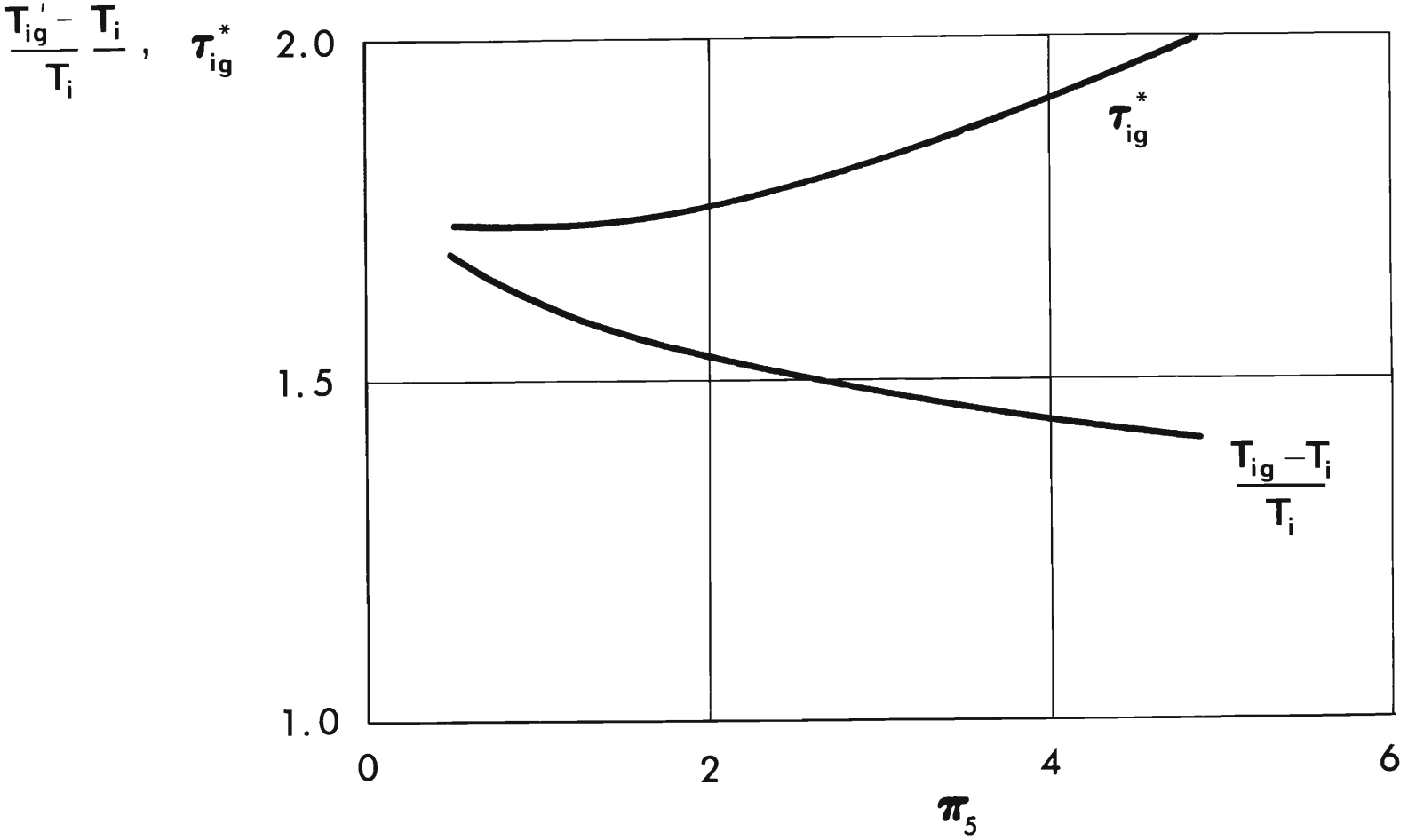

Figure 3.6 Ignition Time and Ignition Temperature Dependences on Heating Intensity. Heating Intensity Decreases from Left to Right.

ignition time predictions will be completed, pending the measurement of ignition temperature as function of fuel concentration.

4. GENERAL CONCLUSIONS

4.1 Concept of Fire Hazard Assessment

(i) The research presented here has lead to the conclusion that fire loss probability is a useful measure of fire hazard.

(ii) The collection and evaluation of statistical data on human activities and responses prior to and during accidental fires, on heating sources for accidental ignition, and on stochastic material behavior serve, along with laboratory experiments and modeling analyses, to predict the fire loss probability.

(iii) Laboratory experiments and modeling analyses are required to predict economically the occurrence probabilities of physico-chemical events which link stochastic events of choice and selection with destruction by fire. Laboratory experiments must be carried out to develop constitutive laws and to verify analytical predictions. The analysis is needed to generalize the results obtained from the necessarily limited number of experiments.

(iv) Occurrence probabilities of transient physico-chemical events depend strongly on the ratio of two characteristic times, namely the time a process is allowed to proceed, divided by the time that the process requires, in the mean, for its completion.

(v) The ignition process is the first significant one of the physico-chemical processes that lead to accidental destruction by fire. The associated probability depends on the ratio of exposure time over mean ignition time. Mean ignition time characterizes the material and therefore contributes significantly to the material fire hazard description. Exposure time characterizes human response to fire.

4.2 Experiments

The experimental work performed during the research phase reported here lead to these conclusions:

4.2.1 Constitutive Laws

(i) Pyrolysate evolution from the heated surface of thermally decomposing solids can effectively reduce the heat transfer between ignition source and heated surface by up to 20 percent.

(ii) The lowest ignition temperature of pyrolysate-air mixtures as a function of pyrolysate concentration constitutes a valid basis for a universal ignition criterion which is applicable to the prediction of pyrolyzing solid ignition.

4.2.2 Experimental Verification of Analytical Ignition Time Prediction

(i) Thermal fabric destruction is governed by the heat transfer process between heating source and fabric, no ignition takes place if heat supply is balanced by heat losses prior to the attainment of an ignition state, defined by temperature and fuel concentration in the reacting boundary layer.

(ii) The instant of melting can be predicted by an inert heating model.

(iii) Moisture desorption and radiative cooling affect pre-ignition processes less than convective cooling during radiative heating and less then convective blanketing by evolving pyrolysates.

(iv) Thermal interaction between fabrics of a composite reduces or increases ignition time depending on the spacing between the fabrics, because of two mutually opposing processes. A neighboring fabric behind the heated fabric retards convective cooling thereby reducing the ignition time. The rear

fabric also absorbs heat from the front fabric for its own heating process, and thereby increases the ignition time for the front fabric.

(v) Fabric Gas Flame heating along trimmed but unfolded fabric edges leads to ignition in about one quarter of the time required with normal flame impingement.

(vi) Fabric response is relatively deterministic only at high heating intensities (standard deviation at irradiation of 13.80 W/cm^2 is $\sigma = 0.1$) but rather stochastic at low heating intensities (irradiation of 6.5 W/cm^2 leads to $\sigma = 0.3$, on the average).

(vii) The characterization of gas flame ignition sources revealed that maximum flame temperatures are essentially independent of burner size, but depend on fuel type.

4.3 Modeling Analysis

(i) Integral techniques are suitable to describe complex pre-ignition processes.

(ii) Complete modeling of a single, pyrolyzing material under radiative heating is describable in terms of five system variables and fourteen scaling groups, the system variables being surface temperature, surface fuel concentration, degree of thermal decomposition, Reynolds number and boundary layer thickness.

(iii) The newly proposed ignition criterion leads to the correct prediction of ignition time and ignition temperature trends with heating intensity.

(iv) Experimental data on flammability limits and additional evaluations of the analysis are required to verify the validity of the ignition criterion, for ignition under both radiative and convective heating.

5. PUBLICATIONS AND PRESENTATIONS

The research results of the first three years have been disseminated through a number of different channels and presented to audiences covering a broad spectrum of background and interest in fire and fire research. These activities are summarized in the sections that follow.

5.1 Refereed Papers

Three papers were prepared and submitted for peer review. All three were accepted and published [1.6,7,10]. Two of the papers were presented on invitation at these meetings: Reference [1.10] at the Symposium on Textile Finishing Chemistry, Division of Cellulose, Wool, and Fiber Chemistry, 164th National Meeting, ACS, New York, N.Y., August 30 - September 1, 1972; Reference [1.7] at the 1973 International Seminar on Heat Transfer from Flames, Trogir, Yugoslavia, August 27 - 31, 1973.

5.2 Reports and Presentations

The research results of the first two years have been summarized in six Quarterly Progress and one Semiannual Reports and presented in detail in two Annual Final Reports [1.8,9]. Both Annual Reports are available for public purchase through the Clearinghouse of the U.S. Department of Commerce.

All of the above reports were presented orally to the Government-Industry Research Committee on Fabric Flammability and their invited guests at the following locations and dates:

(i) Georgia Institute of Technology, Atlanta, Georgia, April 26, 1971.

(ii) Factory Mutual Research Corporation, Norwood, Massachusetts, July 29, 1971 and Massachusetts Institute of Technology, Boston, Massachusetts, July 30, 1971.

(iii) Gillette Company Research Institute, Rockville, Maryland, November 5, 1971.

(iv) National Bureau of Standards, Gaithersburg, Maryland, February 16 - 17, 1972.

(v) Chestnut Run Laboratory, Dupont de Nemours and Co., Inc., Wilmington, Delaware, July 19, 1972.

(vi) Factory Mutual Research Corporation, Norwood, Massachusetts, October 4 - 5, 1972.

(vii) National Bureau of Standards, Gaithersburg, Maryland, April 2 - 3, 1973.

5.3 Seminars, Conferences, and Courses

The research results have also been presented through participation in seminars and conferences. These are summarized as follows:

(i) "Seminar on Fabric Flammability", School of Mechanical Engineering, Georgia Institute of Technology, May 19, 1972. Invitations were extended to appropriate executives from Textile Manufacturing and Distributing Industries, from Insurance Industry and from Government in Georgia, and to the Georgia Tech community.

(ii) Contractors meeting of the National Science Foundation (RANN) Fire Research Program, Applied Physics Laboratory, The John Hopkins University, Silver Spring, Maryland, June 22 - 23, 1973.

(iii) Materials Technology, Today and Tomorrow, Georgia Tech Seminar for Whirlpool Corp., Atlanta, Georgia, March 21, 1973.

(iv) Flammability Characteristics of Materials, Polymer Conference Series, University of Utah, Salt Lake City, Utah, June 11 - 15, 1973 (Invited Lecture).

(v) Conference on Firesafety for Buildings: Research - Practice - Needs, Airlie House, Airlie, Virginia, July 18 - 20, 1973.

(vi) "Ignition Probability and Fire Hazard", Engineering Science and Mechanics Seminar, Georgia Institute of Technology, Atlanta, Georgia, September 27, 1973.

(vii) "The Georgia Tech Fabric Flammability Research", Third Flame-Free Design Conference, the Marriott Hotel, Atlanta, Georgia, March 13 through 15, 1974.

A course entitled "Fire Safety" was instituted and taught for credit during the Spring Quarter 1973, in cooperation with faculty from the Schools of Aerospace Engineering, Architecture and the Georgia Fire Institute. Three outside speakers participated in the lectures. The course was attended by thirty-five (35) students from different academic programs.

5.4 Theses and Special Problems

Student participation during the first three years has encompassed both the undergraduate and the graduate level. The following theses and special problems have been completed:

"The Study of Preignition Behavior of Selected Fabrics and Consequent Burn Injury Probability", C. S. Kirkpatric, M.S. Thesis, June 1972.

"Optical Properties of Fabrics", P. T. Williams, Undergraduate Special Problem, August 1972.

"Reaction Kinetics of Fabrics", W. E. Giddens, M.S. Thesis, March 1973.

"Determination of Fabric Ignition Time Through Use of a Convective Heat Source", E. R. Champion, Jr., M.S. Thesis, June 1973.

The following master theses are in progress:

"Ignition Time Measurement on Fabric Assemblies under Various Geometric Configurations", R. Acree, M.S. Thesis.

"Study of Actual Ignition Sources on Clothing", O. A. Naveda, M.S. Thesis.

"Determination of Film Coefficients with Simulated Pyrolysate Injection", G. Wedel, M.S. Thesis.

"Ignition Temperature Measurement on Pyrolysate-Air Mixtures", P. T. Williams, M.S. Thesis.

APPENDICES

Appendix A.1

Lower Ignition Temperature and Concentration Apparatus (LITACA)

An integral part of the evaluation of the newly proposed ignition criterion is the measurement of the lowest ignition temperature of isothermal pyrolysate-air mixtures, as a function of pyrolysate mass fraction. This Appendix describes the apparatus designed and constructed to accomplish this task.

A.1.1 Purpose and Design Criteria

An apparatus has been designed, constructed and assembled to

(i) thermally decompose pyrolyzing materials,
(ii) store the pyrolysates,
(iii) mix pyrolysates with pure air of controlled mass fractions, and
(iv) measure in an isothermal environment the minimum mixture temperature at which ignition occurs.

The major criteria which this apparatus has to meet are (1) the integrity of the pyrolysate composition should be insured by preventing it from contacting non-inert materials and by preventing water vapor condensation in the apparatus, and (2) the temperature measured should be the true minimum ignition temperature to within $\pm$ 1°C. The apparatus also has to have the provision to let a sample of pyrolysate be drawn off for density measurements.

A.1.2 Major Components and Operating Principles

Figure A.1.1 is a flow diagram for LITACA and its seven components are:

(i) Pyrolysate generating furnace with accumulator, to decompose up to 100 g of thermally degradable materials and to store the decomposition gases,

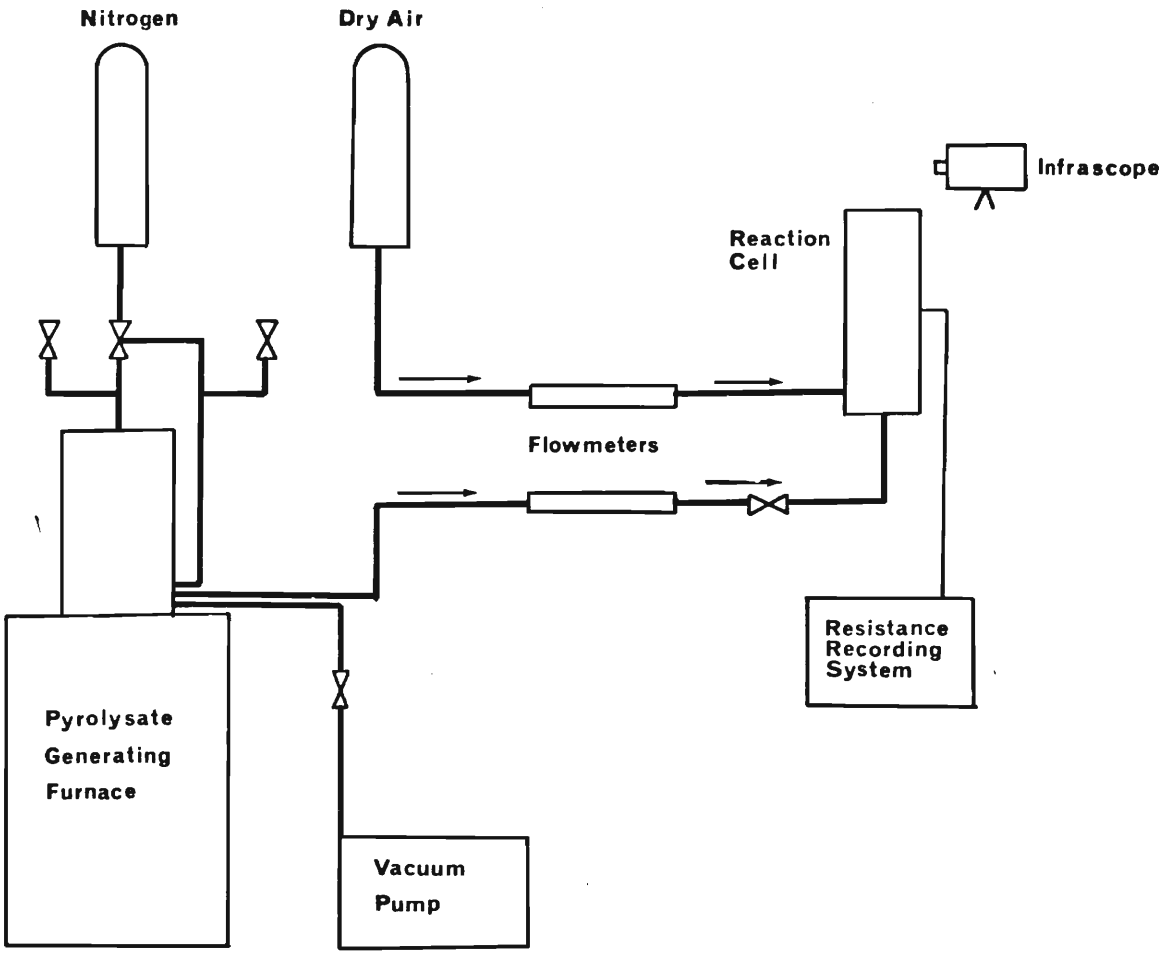

Figure A.1.1 Flow Diagram for Lower Ignition Temperature and Concentration Apparatus (LITACA)

(ii) Supply of dry air, to be mixed at a controlled rate with the pyrolysate gases,

(iii) Supply of nitrogen gas, to pressurize the top side of the accumulator piston which causes ejection of pyrolysate from the generating furnace at a controlled rate and to flush the system of air during the preparatory stages of the experimental procedure,

(iv) Flow Metering System, to measure the volumetric flowrates of the dry air and of the pyrolysate in order to determine and vary the mass-fraction of the pyrolysate-air mixture,

(v) Reach on Cell, in which the dry air and pyrolysate are mixed and in which this mixture is heated and its temperature is monitored,

(vi) Infrared Detector, to sense the occurrence of a flame, and the

(vii) Resistance Recording Facility, to monitor the pyrolysate temperature.

The operating procedure consists of these major steps.

(i) The cellulosic material is placed into the quartz tube of the furnace.

(ii) The system is evacuated and repeatedly flushed with pure nitrogen, and finally evacuated.

(iii) The sample is heated and decomposed.

(iv) Dry air flow is established and the desired rate of temperature rise is selected.

(v) Pyrolysate is introduced at the desired rate.

(vi) Ignition takes place.

The components of LITACA are described in the following section. Experimental procedures are presented in Section A.1.6.

A.1.3 Pyrolysate Generating Furnace

Figure A.1.2 is an assembly drawing of the pyrolysate generating furnace. The heat sources for the furnace consists of two cylindrical half-shell, 1720 watt - 230 volt, Model RH 256 heaters from Thermal Corporation, Huntsville, AL.

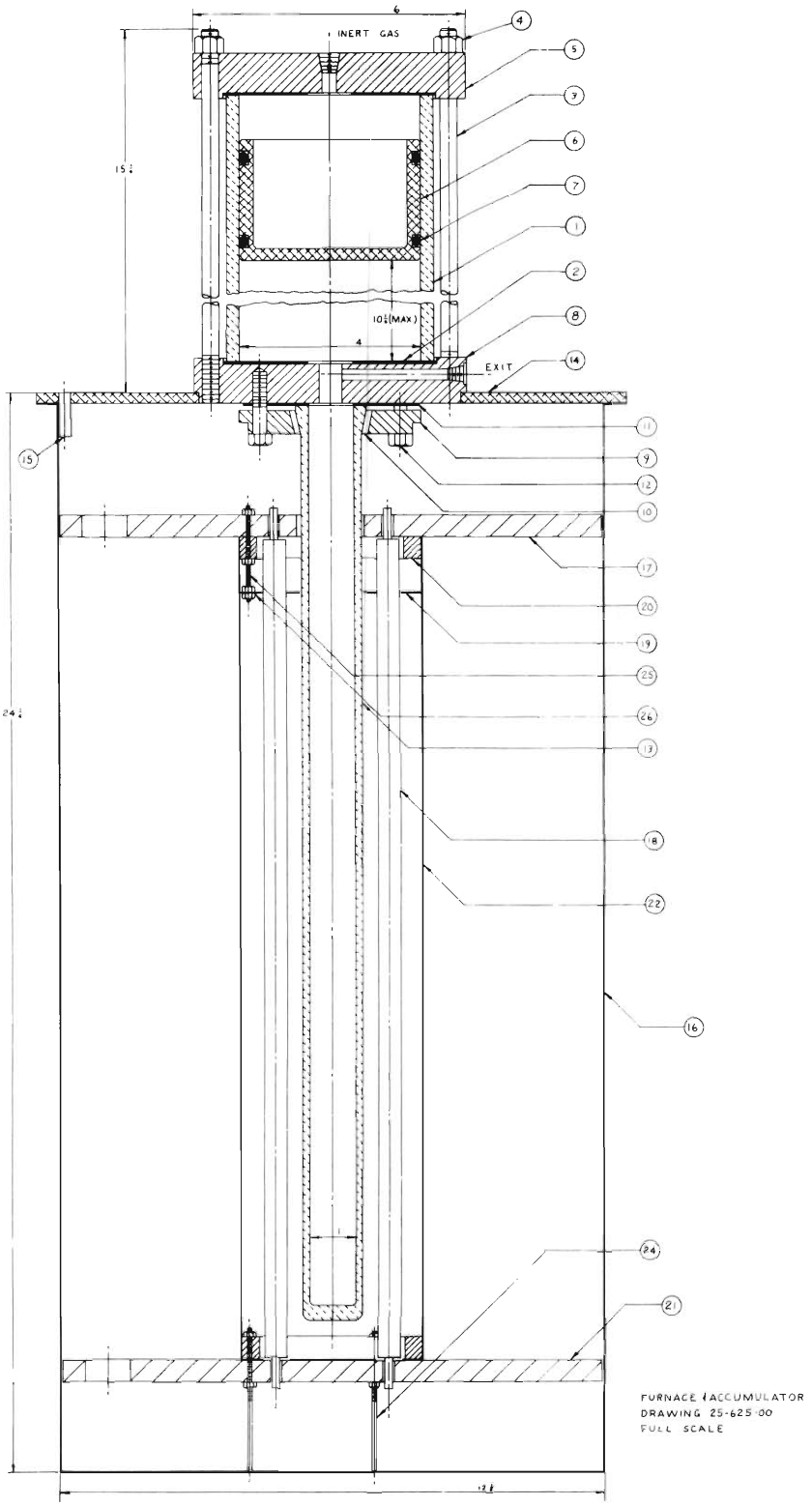

Figure A.1.2 Cross Section of Furnace and Accumulator for LITACA

Description of Figure A.1.2

Item	Description
1.	Accumulator Barrel
2.	Accumulator Gasket
3.	Accumulator Tie Rod
4.	Locknut
5.	Accumulator End Cap
6.	Accumulator Piston
7.	"O" Ring
8.	Accumulator Manifold
9.	Flange
10.	Insert
11.	Gasket
12.	Bolt
13.	Furnace Test Tube
14.	Furnace Mounting Plate
15.	Pilot Pin
16.	Furnace Housing
17.	Heating Element Support
18.	*Heating Element
19.	Furnace Reflector
20.	Furnace Reflector Support Ring
21.	Heating Element Support
22.	Tubular Reflector
23.	Furnace Reflector (not marked)
24.	Threaded Rod
25.	Threaded Rod
26.	Hex Nut

*The 12 tungsten heating element tubes were replaced by two half-shell resistance wire heaters.

The heaters are wired in parallel. The heating elements have the upper operating temperature limit of 2,200°F and are chrome-aluminum-iron resistance wires, helically wound and placed in ceramic backings. These backings are then embedded in a ceramic core. The test tube which holds the sample is made of "Vitreosil" fused quartz. It is 20 1/2 inches long and has a 1 inch I.D. The stainless steel manifold allows access to the furnace from five points in the system, namely the vacuum pump, the glass balloon, the nitrogen supply, the pyrolysate flow meter and the pressure gauge. The accumulator barrel, made of pyrex glass, is positioned on top of the manifold and has a maximum capacity of approximately two liters. It is sealed by a nitrogen gas pressurized piston which controls the pressure in the accumulator. The inner core of the furnace are shown in Figure A.15. The power input to the furnace is controlled by two 20 amp - 115 volt variable-autotransformers, wired in series.

A.1.4 Reaction Cell

Figure A.1.3 is an assembly drawing of the reaction cell in which the pyrolysate is mixed with dry air and then heated to ignition temperature while its temperature is being monitored by the gold-plated, bare-wire platinum resistance thermometer at the exit from the reaction cell. Both the mixing chamber and the flame arresting chamber are made of chrome plated brass with a nickel undercoating. The mixing chamber has a guard heater positioned underneath it in order to prevent condensation in the mixing chamber. The flame arresting chamber is filled with 3 mm diameter glass beads which prevent the upstream propagation of the flame. The ignition heater, positioned in the upper half of the reaction cell, consists of two 515 watt, 115 volt cylindrical half-section heaters, Model RH 221 from Thermal Corporation, Huntsville, AL., wired in parallel. The 2,200°F capacity heating elements are also chrome-aluminum-iron wires, helically wound and placed in ceramic backings, which are then embedded in a ceramic core. The power supply to the heater is controlled by a 15 amp - 115 volt variable-autotransformer.

The key component of the reaction cell is the platinum - resistance thermometer. The temperature vs. electrical resistance curve has been well

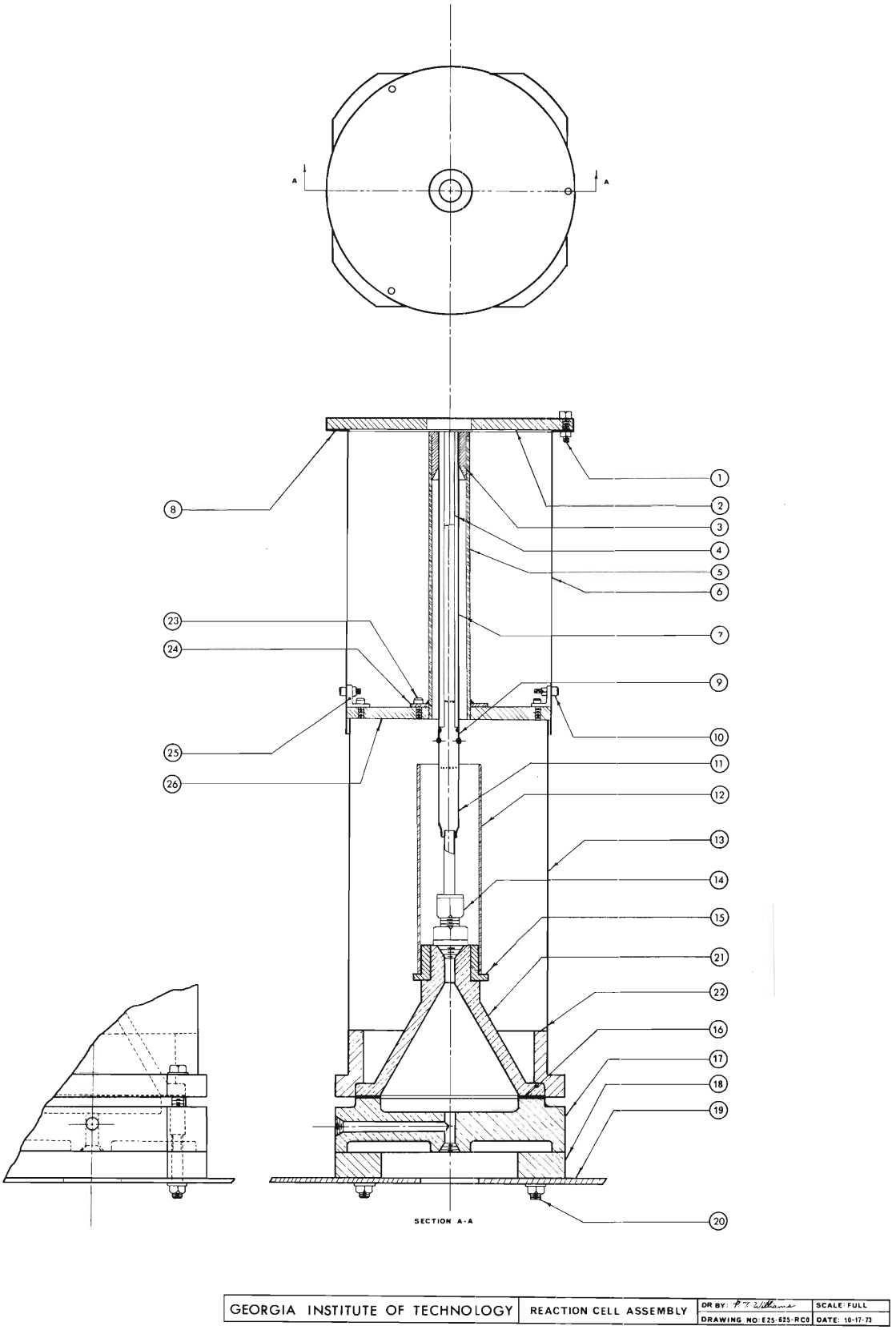

Figure A.1.3. Cross Section of Reaction Cell for LITACA.

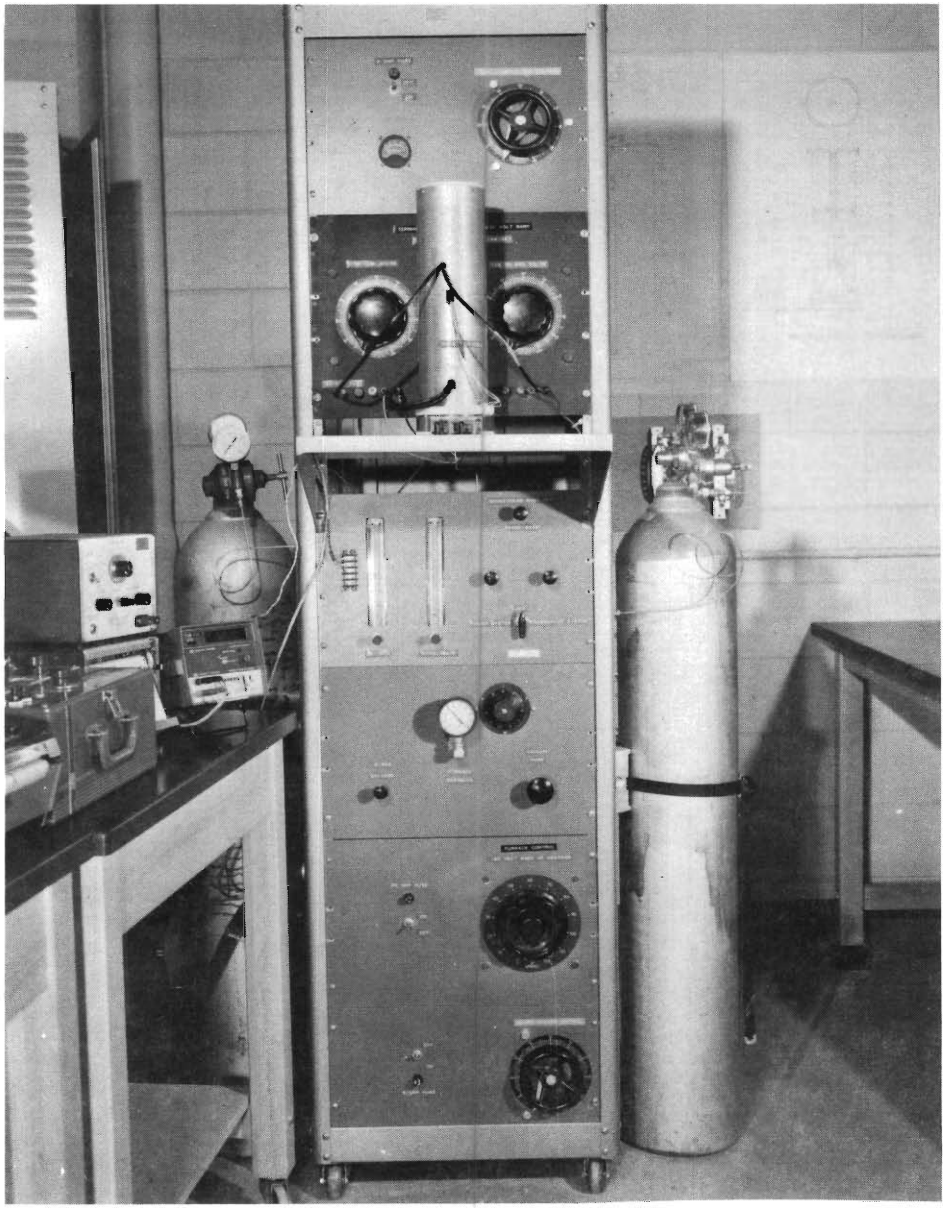

Figure A.1.4. Lower Ignition Temperature and Concentration Apparatus (LITACA).

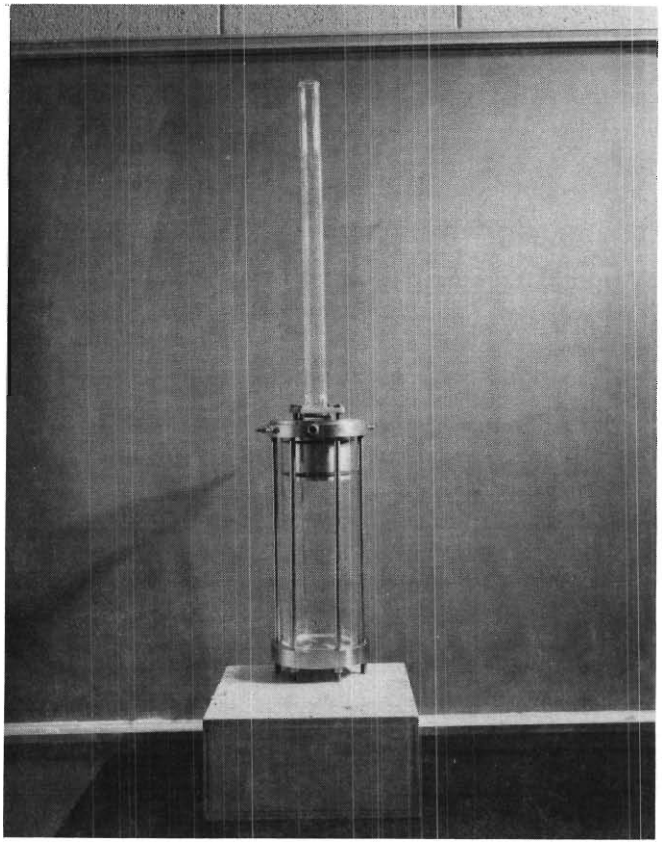

Figure A.1.5. Furnace Core and Accumulator, Overall Height is 90 cm.

established for Platinum by the National Bureau of Standards for a wide range of temperatures. The thermometer is made up of three basic parts: (i) ignition tube, (ii) quartz tube bundle and (iii) the gold-plated platinum wire.

(i) The ignition tube consists of four sections fused together: (1) a 10 mm I.D. quartz tube, 145 mm long, (2) a quartz to glass graded seal, 15 mm long, (3) a pyrex glass tube with 6 mm I.D., 75 mm long and (4) a glass-Kovar graded seal, 1/4 inch O.D. and 35 mm long.

(ii) The quartz tube bundle has five 1 mm O.D. - 7 mm I.D. quartz tubes, 65 mm long, bound together with two 165 mm long quartz tubes by two quartz rings at each end of the bundle. The two long tubes support the bundle and act as conduits for the platinum wire to its two exit points in the glass section of the ignition tube.

(iii) The gold-plated platinum wire (.005 inch DIA) is passed through the tubes in the tube bundle and exits near the middle of the thermometer. The tube bundle is positioned such that approximately 70% of the resistance of the wire lies in the top 65 mm's of the thermometer. While platinum is very inert, it was necessary to gold-plate (an equally inert metal) in order to forestall any catalytic effect the platinum might have on the gas mixture at high temperatures.

The Hewlett-Packard DCV/DCA/OHM meter passes a constant current of 10 milliamperes through the thermometer and measures its resistance up to five significant figures. The tube bundle is in the path of the flow stream, and as the gas mixture passes through the bundle, the gas will come into contact with the bare wire.

A.1.5 Resistance Recording Facility

The resistance recording facility consists of

(i) one Hewlett-Packard Model 34703A DCV/DCA/OHM Meter

(ii) one Hewlett-Packard Model 34750A Five-Digit Display
(iii) one Hewlett-Packard Model 34721A BCD Module
(iv) one Hewlett-Packard Model 581A Digital to Analog Converter
(v) one Hewlett-Packard Model 680 Strip Chart Recorder

The Digital to Analog Converter allows to display any set of three adjacent digits to be recorded with automatic range stepping.

A.1.6 Experimental Procedure

Experiments are currently in progress and the procedure outlined below is tentative.

A fabric sample of 60 - 100 grams is prepared for decomposition by cutting the fabric pieces into 7-inch squares or less and packing it into the quartz test tube of the furnace core. The test tube and sample are then positioned inside the furnace, and a vacuum is drawn on the system. The system is then repeatedly flushed with pure nitrogen, and finally evacuated. The furnace is then energized and thermal decomposition of the fabric begins.

As the pressure builds up in the test tube and accumulator, a sample of the gas can be drawn off into a previously evacuated glass balloon for density measurements.

As the decomposition proceeds and the pressure builds up in the accumulator, the piston rises in the accumulator barrel. The top side of the piston is vented, which allows the complete upward displacement of the piston.

Before the decomposition is complete, the guard heaters are turned on and allowed to come to equilibrium. Dry air is passed through the reaction cell at a selected flowrate, and the ignition heater is energized such that the Pt-resistance thermometer shows the desired steady increase in temperature.

Finally this pyrolysate is introduced into the mixing chamber at a preselected and measured flowrate. For an increasing heat flux into the gas mixture

during its passage through the ignition tube, the gas will reach its maximum temperature at the thermometer. The gold-plated wire represents, because of its higher absorptance in relation to the quartz and the gas, the highest temperature in the reaction cell. Thus, when the resistance wire in the tube bundle shows a sudden excursion from its steady rise, ignition of the mixture should take place on the wire.

After ignition occurs, the flame will propagate down the ignition tube and be stopped in the flame arresting chamber. An infrascope is positioned such that it can see the top of the ignition tube and sense the occurrence of a luminescent flame. In this way an adjustment can be made for any time lag present in the temperature monitoring system. The mass fractions of the dry air and pyrolysate in the mixture are determined from the measured flow-rates, the measured temperatures and the gas pressures in the flow meters (these are 1 atm). This evaluation requires the results of pyrolysate density measurements.

The pyrolysate density is measured by allowing pyrolysate to expand into an evacuated glass sphere which is heated to, and maintained at a known and sufficiently high temperature to prevent condensation. The vapor is weighed on an analytical balance.

A.1.7 Resistance Thermometer Calibration

The gold-plate platinum resistance thermometer is shown in Figure A.1.6 for calibration in the top part of the reaction tube. The reaction tube is submersed, with its top part in the dewar flask shown in Figure A.1.7. The flask is filled with distilled water which is maintained at selected constant temperatures by circulating silicone oil. The circulating oil is heated in the Haake NBS Series Constant Temperature Circulator. The resistance of the object thermometer was calibration at four temperatures between 22 and 95°C against the known resistance of a 100 Ω pure platinum resistance thermometer. The object thermometer was found to have the resistance of R_o = 7.1296 Ω at 0°C, the first temperature coefficient α = 0.003687C^{-1} and the second

coefficient $\delta = -3.623$. Thus its resistance is given by

$$R/R_o = 1 - \alpha[t/C + \delta\ t/100C(1 - t/100C)]$$

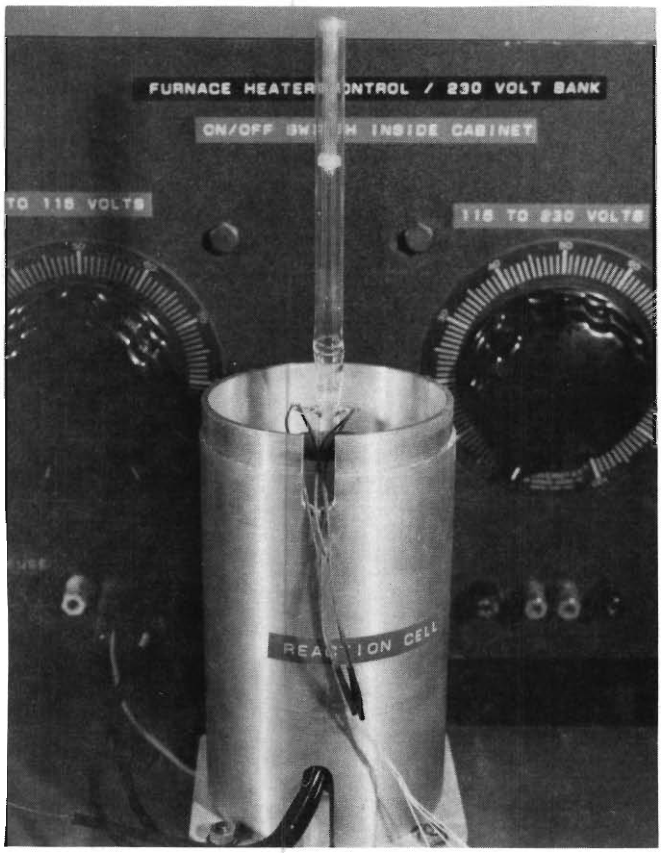

Figure A.1.6. Reaction Cell.

a. A/D CONVERTER
b. RECORDER
c. DC VOLT/AMPERE/OHM METER WITH DIGITAL READOUT
d. CONSTANT TEMPERATURE DEWAR
e. REFERENCE Pt THERMOMETER
f. STIRRER SHAFT
g. HAAKE NBS SERIES CONSTANT TEMPERATURE CIRCULATOR

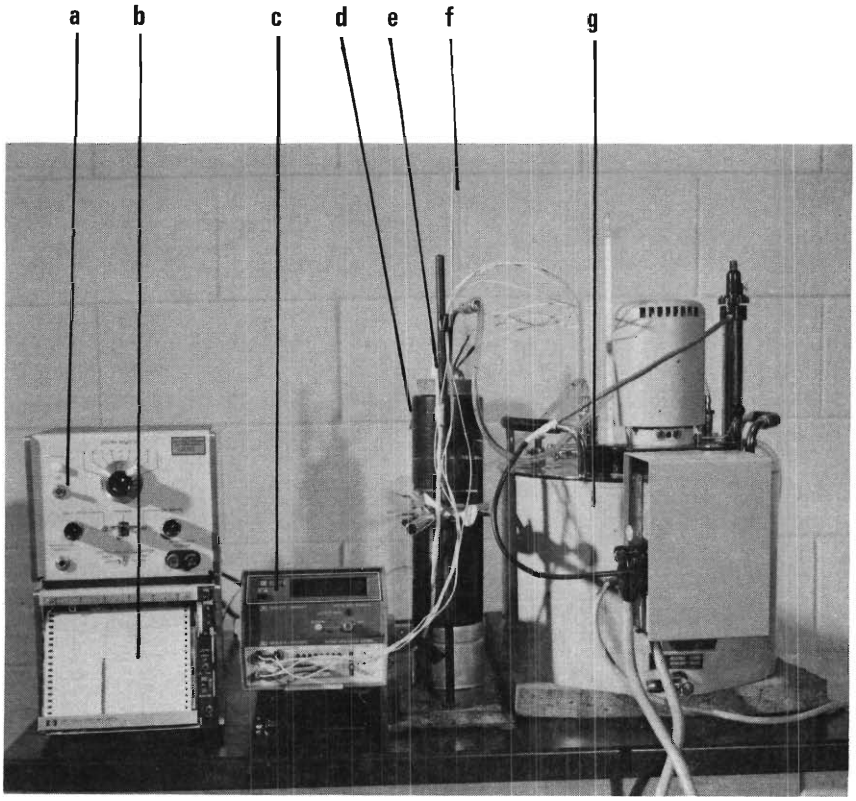

Figure A.1.7. Resistance Thermometer Calibration and Recording Facility.

Appendix A.2

Convective Film Coefficient Measurements

The Injection Apparatus has been designed to be used with the Convective Ignition Time Apparatus (CITA) for the purpose of evaluating film coefficients on various mesh size inert metal screens in the presence of gas injection through the screen. The operating principles of CITA remained the same and have been described in detail in Reference [2.3], Appendix B.3. Film coefficient measurements were carried out with CITA performing in the static mode. Design details of the convective film coefficient assembly, the instrumentation used for the tests, and the operating procedure are described in the following sections.

A.2.1 Screen Support Assembly

The stainless steel screen support assembly is shown in Figure A.2.1. It consists of three primary sections: (i) an aluminum clevis and its support rod, (ii) a transite inlet chamber and porous bronze assembly, and (iii) an inert wire cloth screen and screen holder assembly.

(i) The clevis and support rod have been designed to allow vertical to horizontal positioning of the wire cloth for testing at various angles between the cloth and the flame axis.

(ii) Inlet Chamber. Uniform temperature and velocity profiles are produced by the inlet chamber assembly. Transite has been used to construct the inlet chamber and porous bronze holder. Its low thermal conductivity help to insulate the heated gases and minimize the heat losses. A guard heater is used outside the inlet chamber to suppress the heat losses. A porous bronze filter is used to produce a uniform velocity profile across the wire cloth. Provision has been made for thermocouple probes to check the temperature profiles for uniformity both upstream and downstream of the bronze filter and for continuous monitoring during testing.

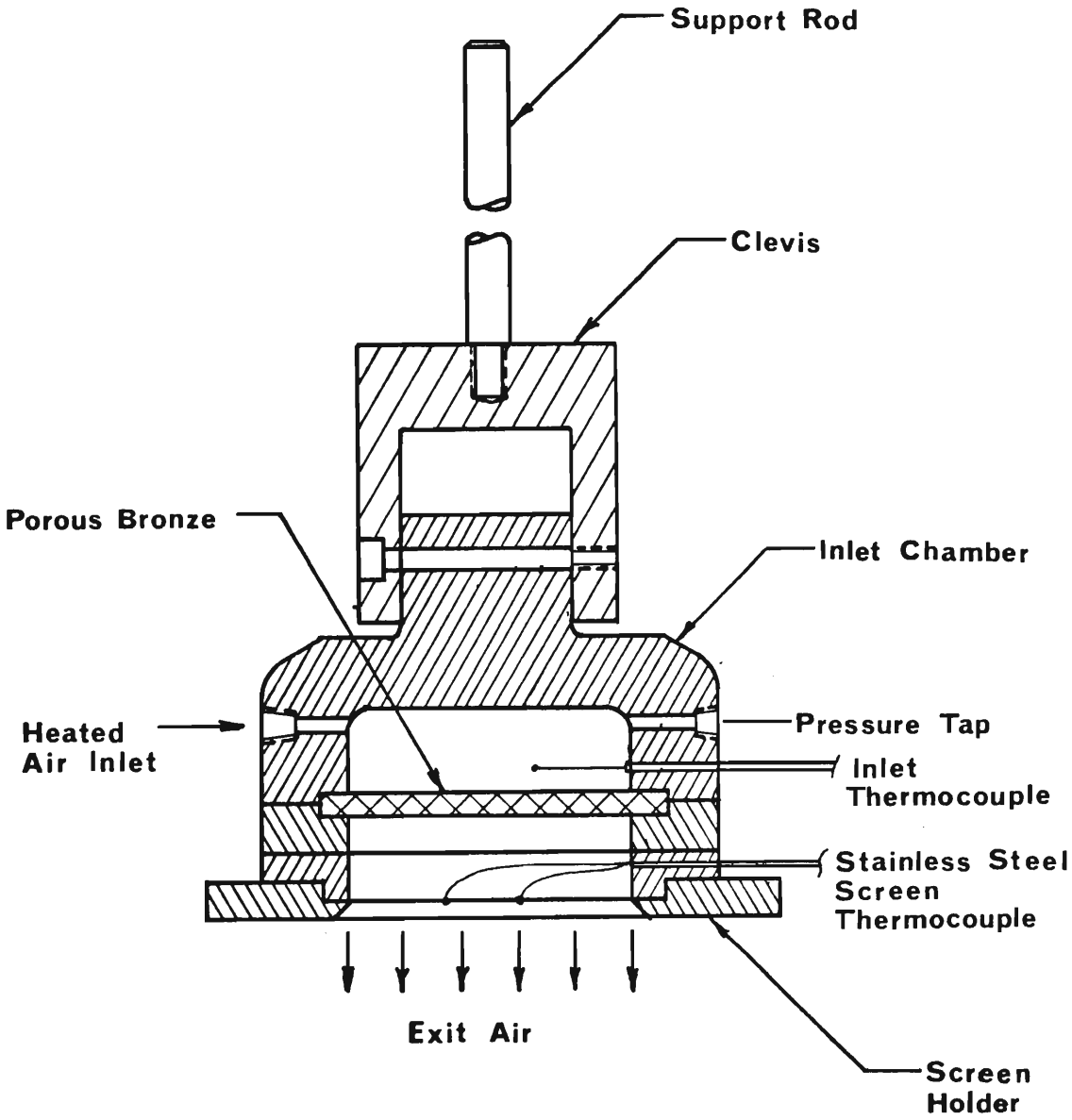

Figure A.2.1 Pyrolysate Injection Simulator

(iii) Screen Holder Assembly. Since the wire cloth mesh size was varied to determine the effect of the fabric weave on the convective film coefficient, three screen holder assemblies have been constructed. The holder tops are made of transite for insultation purposes and the holder bases are made of stainless steel for protection from the burner flame and for structural support. During testing, the stainless steel wire cloth forms one leg of the thermocouple, with constantan wire forming the other leg and the wires are routed out through holes provided in the screen holder and using ceramic insulators. An inconel insulation shield was mounted to the assembly periphery, and special ground wiring was added to eliminate the interference caused by the AC guard heater on the thermocouple response.

A.2.2 Instrumentation

Schematics of the instrumentation associated with the convective film coefficient apparatus are shown on Figures A.2.2 and A.2.3. Instrumentation and operation of the burner and shutter systems remain the same as those for the CITA [2.3]. The mass flow rate through the heater and the film coefficient assembly is determined by means of flow rate, pressure, and temperature measurements. The temperature is measured at the inlet chamber to determine the outflow velocity.

During the film coefficient determination a voltage source and a microswitch, which is activatived by one of the moving shutters, are used to detect the instant of shutter separation and wire cloth exposure to the burner flame. This signal triggers a dual beam type 555 Tektronix Oscilloscope which records the wire cloth temperature on polaroid film.

The signal from the microswitch is also used to produce a spike in one of the traces of a two-channel Hewlett-Packard Type 7100B strip chart recorder at the instant of exposure. The other trace records the output of the thermocouple probe upstream of the porous bronze filter. This record is used

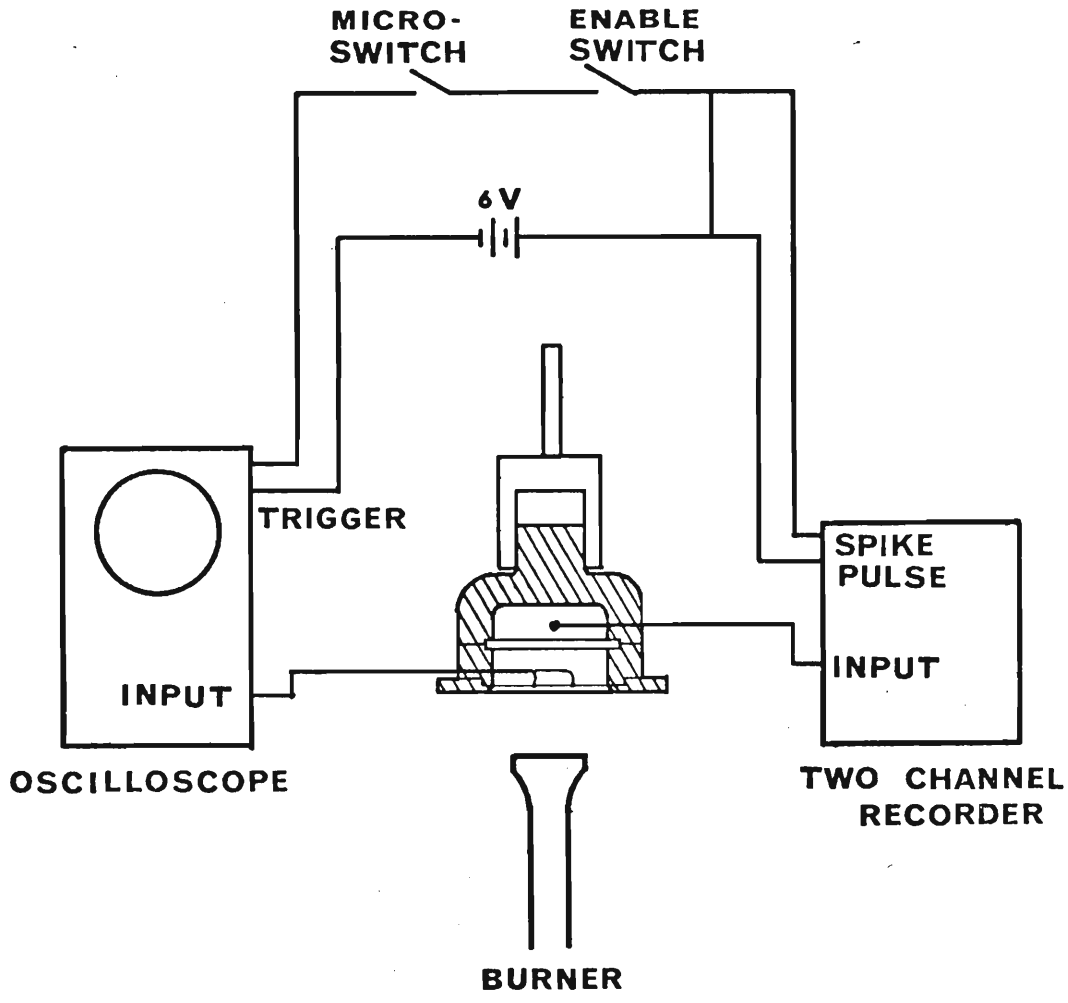

Figure A.2.2 Schematic of Instrumentation for Temperature Recording in Convective Film Coefficient Test Apparatus

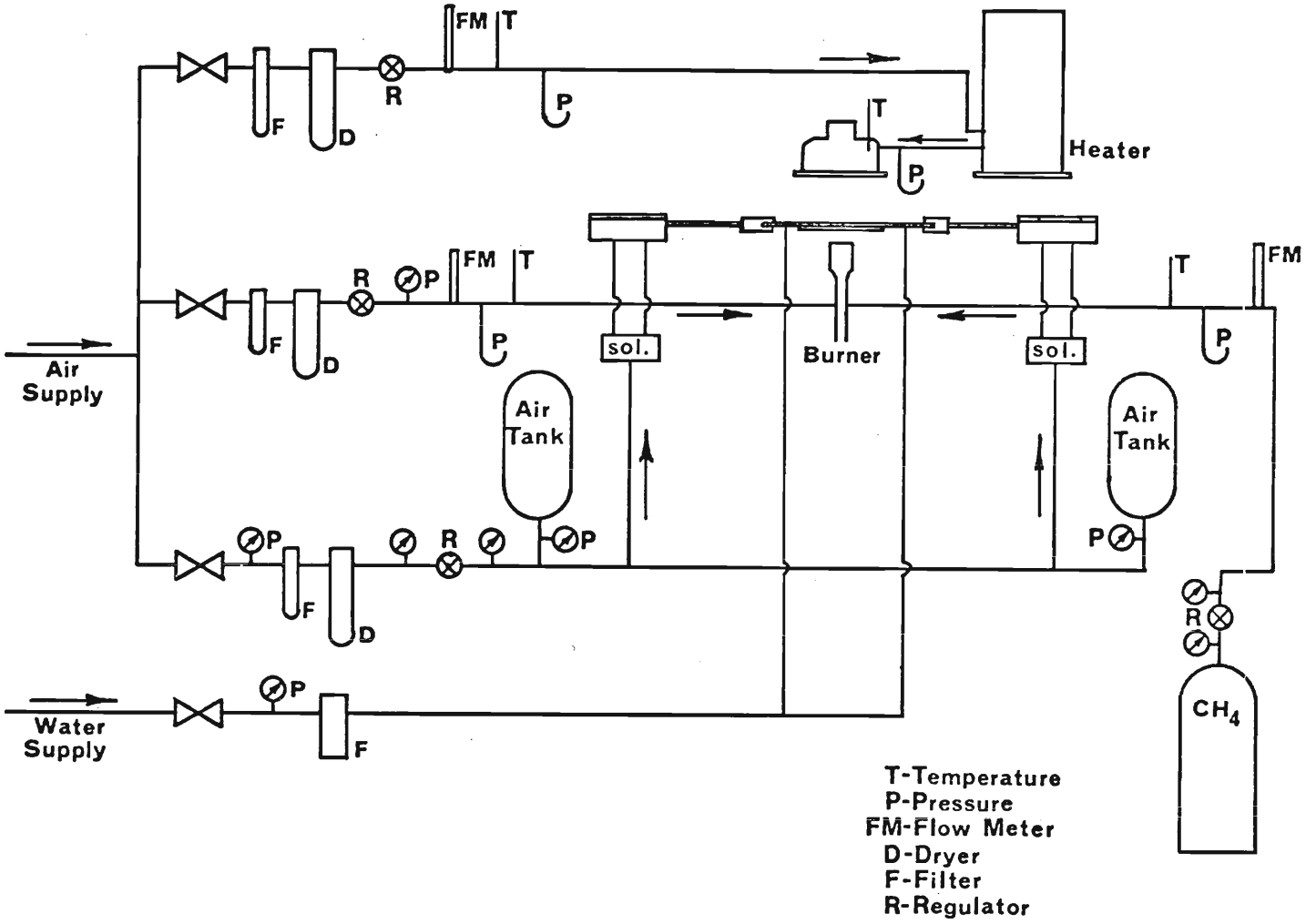

Figure A.2.3 Flow Diagram for Convective Film Coefficient Measurement with Simulated Gasification

to determine the temperature of the incoming gas.

A.2.3 Operating Procedure

Stainless steel screens varying from 80 to 400 mesh were cut in circles of 75 mm diameter. A stainless steel and a constantan wire were welded to the screen forming one leg of the thermocouple.

The screen support assembly is to be mounted to the Injection Apparatus and positioned as required, with respect to its height above the burner and to its orientation relative to the flame axis. The injection air flow rate and temperature were stabilized to give the desired outflow velocity.

The shutters of CITA are closed and the air tanks pressurized. The burner is stabilized at the desired heating intensity through air and fuel rate selections. It is then inserted into the apparatus, below the water cooled shutters. The screen is exposed to the gas flame through activation of the solenoid valves which in turn pressurize the air cylinders and retract the shutters.

Monitored were the air flow rate, the pressure, and the temperature, at the flow meter, and the pressure and temperature behind the porous bronze plate. The temperature-time profile of the wire cloth was recorded on polaroid film, as shown in Figure A.2.4.

A.2.4 Data Reduction Procedure

A sample data sheet is shown in Figure A.2.4. The data was evaluated based on the energy balance for the freely suspended screen in which

$$\overline{h}_c = C''(dT/d\tau)/(T_f - T)$$

GEORGIA INSTITUTE OF TECHNOLOGY
SCHOOL OF MECHANICAL ENGINEERING
FABRIC FLAMMABILITY PROJECT
CONVECTIVE HEAT TRANSFER COEFFICIENT

DATE 12/8/73 TEST NO. 27

DATA BY GLW HOLDER NO. 1

SCREEN TEMP. 6.760 mV MESH 200

SCREEN HEIGHT ABOVE BURNER 3/4 inches.

SCREEN INCLINATION ANGLE 0 degrees.

ROOM TEMPERATURE 72°F

BAROMETRIC PRESSURE 29.176" Hg

INJECTION AIR PRESSURE 13.5 inches, water.

INJECTION AIR I-C THERMOCOUPLE 1.120 mV, 22 °C.

INJECTION AIR FLOW RATE 10.6 cm, 8.17 SCFH.

	P,REG DEL,PSI	P("Hg)	T(mV)	T(°F)	R(cm)	R(CFH)
METHANE	6	13.5	1.1528	72.5	9.45	3.50
AIR	20	13.8	1.1216	71.5	6.85	51.2

A/F: 19.74

PREHEATER AC VOLTAGE 40 V.

GUARD HEATER AC VOLTAGE 15 V.

INLET CHAMBER C-A T.C. 6.560 mv, 160.5 °C.

COLF JUNCTION 0 °C.

-OSCILLOSCOPE-

TIME BASE 50 msec/cm

UPPER BEAM 2.0 V/cm

LOWER BEAM 1.0 mV/cm

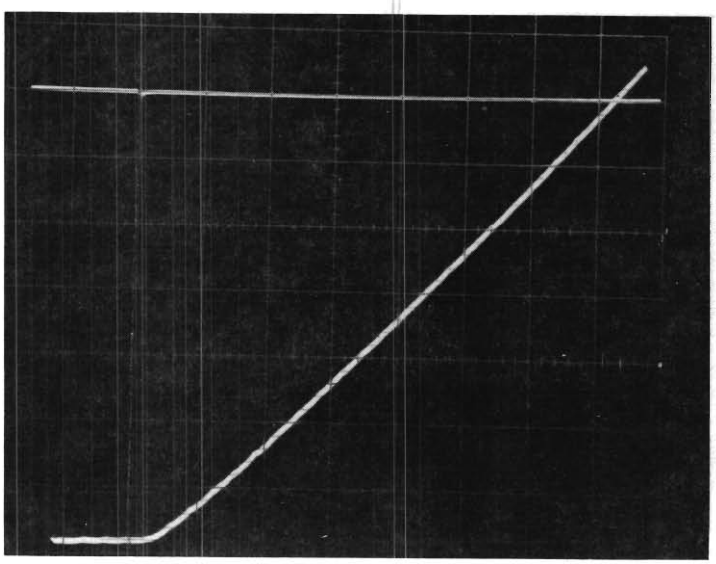

Figure A.2.4

Figure A.2.4.

The mass per unit area ($\rho\delta$) was determined by weighing the 75 mm stainless steel screens on a Christian Beckers Analytical balance. For the 200 mesh, .0021" diameter wire screen, it was found to be

$$\rho\delta = .025541 \text{ g/cm}^2$$

The specific heat of the screen as a function of temperature was found in the literature for stainless steel SS316. A third order polynomial was used to fit the data using the least-square fit.

The time rate of temperature ($dT/d\tau$) was evaluated from the slope of $T(\tau)$ curves after conversion of EMF (τ) traces as shown in Figure A.2.4. The slopes were evaluated at the initial instant $\tau = 0$ when screen and injection gas were in thermal equilibrium. Gas flame temperatures T_f were measured earlier [2.3] and used here.

The film coefficients were normalized to obtain the Nusselt number

$$N_{Nu} = \frac{\bar{h}_c R}{k}$$

and then plotted versus normalized approach velocity of the gas flame jet. The average velocity $\bar{v}$ was computed from the mass flow rate through the burner and the gas temperature above the burner. The normalized approach velocity is the Reynolds number, defined as

$$N_{Re} = \frac{\bar{v} D}{\nu}$$

where R and D are, respectively the screen radius and the burner diameter, and the kinematic viscosity ν is evaluated at the flame temperature T_f.

The Nusselt numbers are given (Figures 2.2 and 2.3) for various injection rates which are normalized to yield the injection Reynolds number

$$(N_{Re})_i = \frac{v_i R}{\nu}$$

where v_i is the area-averaged injection velocity.

A.2.5 Calibration of Screen-Thermocouple

The constantan-stainless steel screen thermocouples were calibrated in the temperature range from 25°C to 540°C. Three test screens of different mesh size were placed in a radiatively shielded enclosure within a Thermolyne Type 1400 furnace. The furnace temperature was monitored by an iron-constantan thermocouple which was placed in the enclosure with the test screens.

It was found that the EMF signals obtained as functions of temperature were nearly the same for each test screen. A single polynomial least-square polynomial of fourth order was derived to relate screen temperature to the EMF signal.

A.2.6 Convective Film Coefficients Without Injection

Convective film coefficients without pyrolysate simulation were measured during the previous contract period. These coefficients were inferred from stainless steel screen measurements, whereby the screen was exposed to the convective heat source in the same geometrical configuration as the fabric. The details of these measurements and the analysis were reported in Section II.C of Reference [2.3]. The convective film coefficients used in the reduction of the data discussed in Section 2.3.5.1 of the present report are summarized in Table A.1.

Table A.1 Summary of SS Screen Convective Film Coefficients Without Injection

ϕ = 0.86 Fabric Holder Aperture = 63.5 mm

L cm	$\dot{m}_{mix}$ g/h	t_f °C	$2\overline{h}_{c_2}$ W/cm^{2}K
10.5	1265	995	0.004362
	2158	-	-
	2951	1257	0.009559
7.6	1265	1205	0.005965
	2158	1319	0.007602
	2951	1320	0.008140
4.4	1265	1256	0.004677
	2158	1351	0.007114
	2951	1359	0.008528
1.9	1265	1290	0.006319
	2158	1347	0.007732
	2951	1352	0.010130

where L = height of stainless steel screen above top of burner

$\dot{m}_{mix}$ = combustible methane-air mixture rate to the burner

t_f = flame temperature at the designated mixture flow rate and position above top of burner

Appendix A.3

Apparatus for Ignition Time Measurement on Fabric Assemblies Under Various Geometric Configurations

A.3.1 Fabric Interaction

Figure A.3.1 shows the fabric holder elements used to support two fabrics parallel to, and at selected distances from, each other during radiative heating in the Radiative Ignition Time Apparatus (RITA). Details of the holder are shown in the cross-sectional views of Figure A.3.2. RITA has been described in detail in References [1.8 and 2.3]. The arrangement of the samples relative to the heater and the infrascopes used for viewing the heated front surface of the front fabric and the rear side of the back fabric are shown in Figure 2.9 of Chapter 2.

The two circular fabric samples are inserted into the holder and conditioned in the environmental chamber at the selected humidity level and initial temperature. The sample holder is inserted into RITA, and the sample assembly is suddenly, within less than 10 milliseconds, exposed to a uniform, time-invariant radiant heat flux until ignition has occurred.

Ignition is defined as the occurrence of a flame anywhere in the system, that is at the front or the back fabric.

Figure A.3.3 shows a typical oscillogram with two infrascope traces, one representing the radiosity originated from the front fabric and seen through the mirror by a Temptron Model IT-7310 infrascope, the other representing radiant energy transmitted through and emitted from the back fabric and sensed by a Mark 1 Model 3-1C00-15 infrascope. The destruction, either by ignition or melting, is recognized by the onset of a sudden radiosity change, resulting from flame emission or sudden change in transmitted or reflected radiant energy.

The ignition of fabrics is also visually observed (through darkened glasses) and the ignition time is measured with a stop watch. Visual

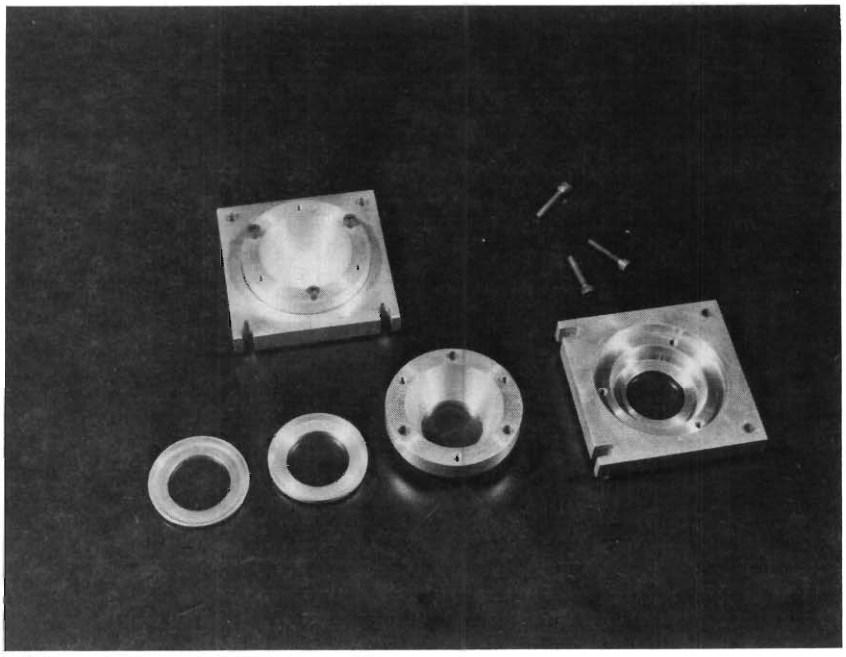

Figure A.3.1. Fabric Holder for Fabric Assemblies. Exposed Area Measures 1 Inch in Diameter.

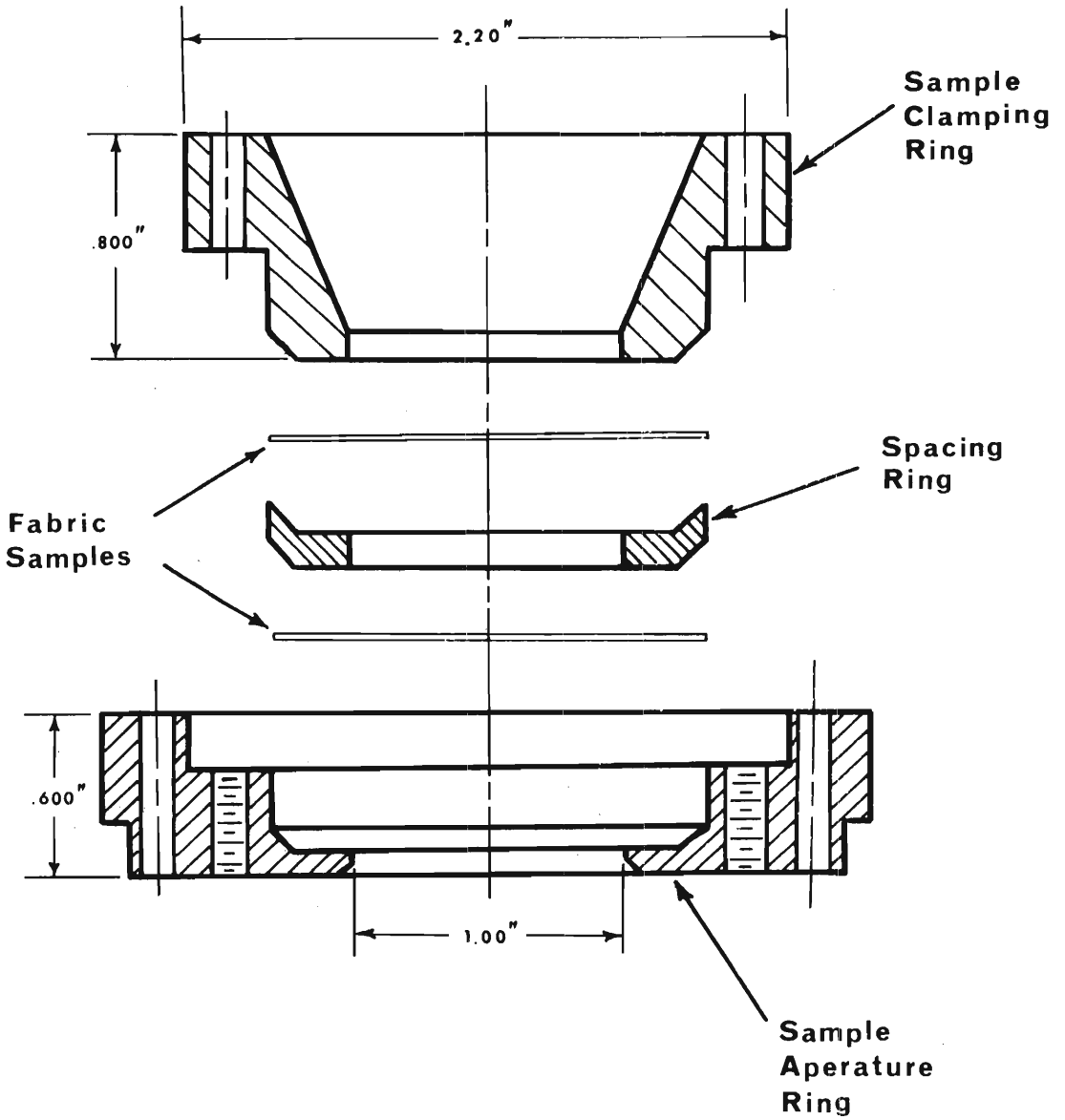

Figure A.3.2 Cross-Section of Fabric Holder

FABRIC ASSEMBLY IGNITION TIME TEST

Test No. 82

Date MARCH 1, 1974

Experimentors R.A & C.L.

Remarks

GIRCFF FABRIC NO.:

Front #5 Back =5

IRRADIATION:

Idle Voltage 75 V

Incident Heat Flux (W_o) 6.5 W/cm^2

Relative Humidity 30 %

Spacing Between Fabrics 1/16 in

INFRASCOPE TRACE

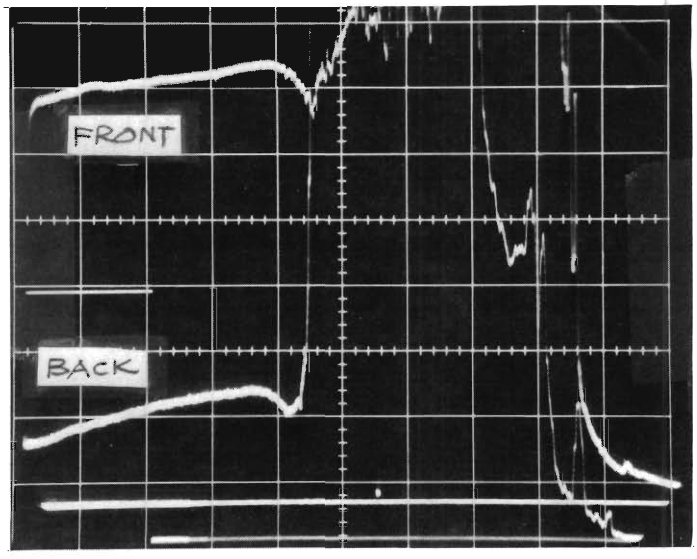

U.B. Sensitivity 5 mV/cm (B)

L.B. Sensitivity 50 mV/cm (T)

Sweep Rate 5 s/cm

INFRASCOPE READING:

Temperature Scale Setting A(B) - BLUE (T)

Emissivity 1.0 BOTH

Ignition Time 4.5 cm

Ignition Time 22.5 s

SAMPLE FABRIC

Time (s)	Observation
22.7	FLAME OBSERVED VISUALLY (Front)

Front Back

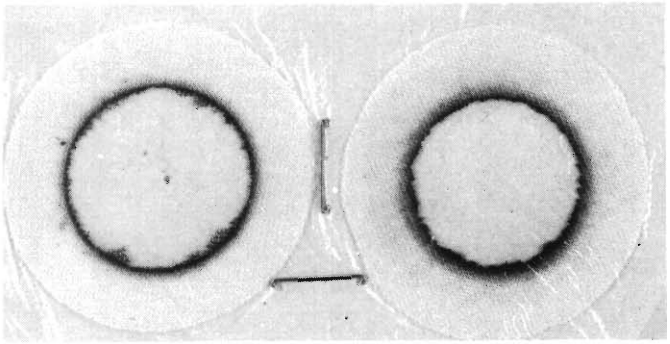

Figure A.3.3.

observation and oscillogram interpretation are in agreement.

A.3.2 Effects of Geometry

The Convective Ignition Time Apparatus (CITA) is used to study the effects of geometry and orientation on the ignition time. The procedures, equipment and instrumentation used are identical to the horizontal orientation tests and a complete description is found in Appendix B.3 of Reference [2.3]. The only change introduced for the edge ignition tests is a new fabric holder shown in the schematic drawing Figure A.3.4. A 7.5 X 7.5 cm fabric sample is mounted between the two 3.2 mm diameter rods. The rods are adjustable to provide sufficient tension on the fabric without causing distortion in the fabric structure. The holder plate can swivel on the clevis to produce fabric orientations 0 to 90° from the vertical axis.

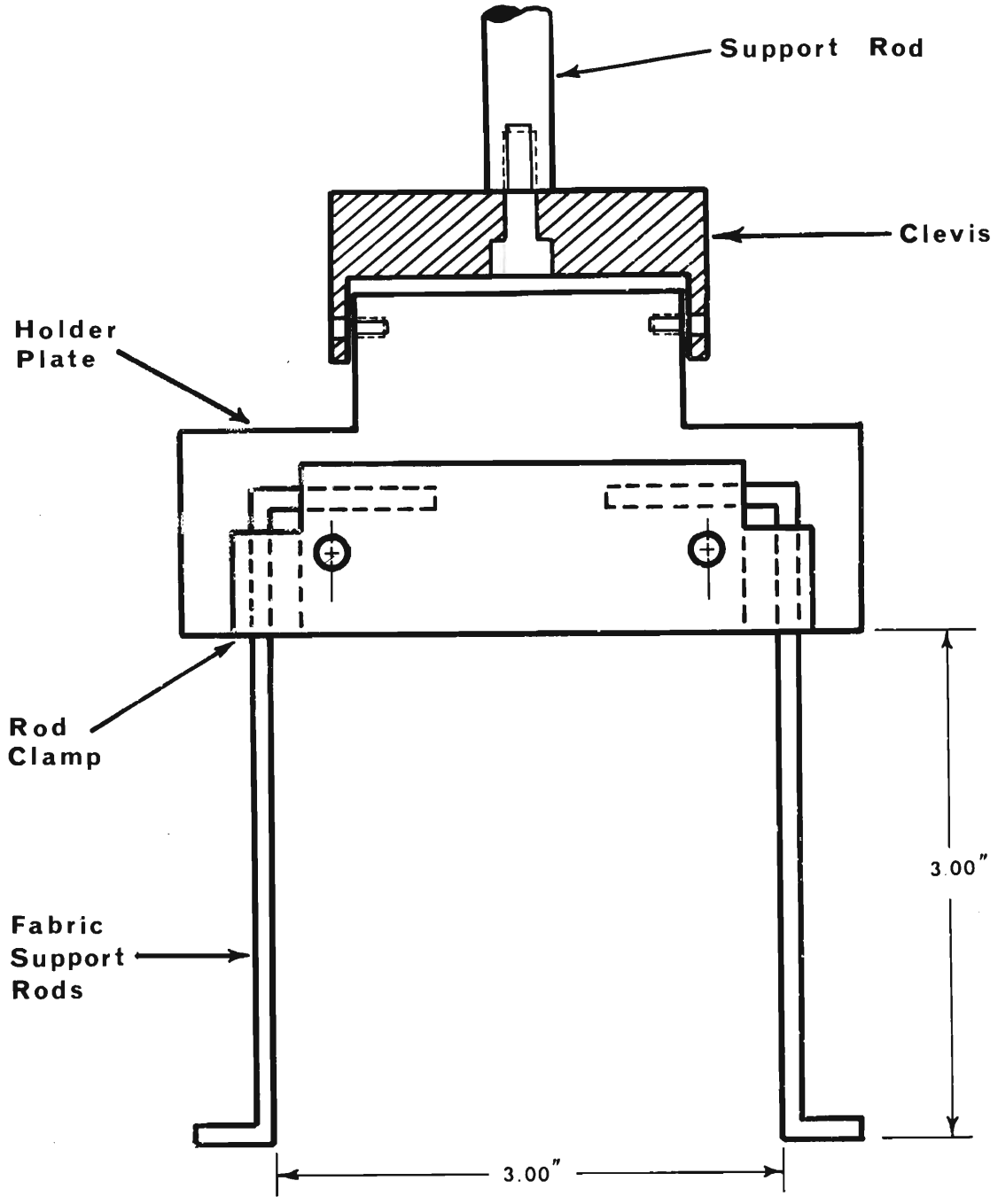

Figure A.3.4 Fabric Holder for Ignition Time Measurement of Single Fabrics at Various Orientations

Appendix A.4

Characterization of Ignition Sources

A.4.1 Ignition Source Scanning Apparatus (ISSA) and Operating Principles

An Ignition Source Scanning Apparatus, called ISSA, was specially designed, constructed and calibrated to characterize ignition sources with

length	90 cm
width	25 cm
height	25 cm
maximum power flux	60 W/cm^2
maximum temperature	1500°C

so that power flux and temperature can be measured as functions of position, in three dimensions. Heat flux measurements can be performed also at any angle relative to the vertical, from zero to ninety degrees.

ISSA is shown in the photograph of Figure 2.16 and consists of five major components, namely

(i) the frame with its guide rails
(ii) the sensor carriage, with heat flux or temperature sensor
(iii) the carriage drive with speed control
(iv) the position sensor with its power source
(v) the recording equipment

ISSA produces directly diagrams of heat flux q" as functions of lengthwise position x for selected heights and lateral positions, or of temperature T(x) for selected heights and lateral positions. The apparatus guides the sensor across the ignition source at a speed sufficienlty low to average out turbulent fluctuations, and produces two electrical signals, one for position and the other for heat flux or temperature. These signals are recorded on the x-y plotter.

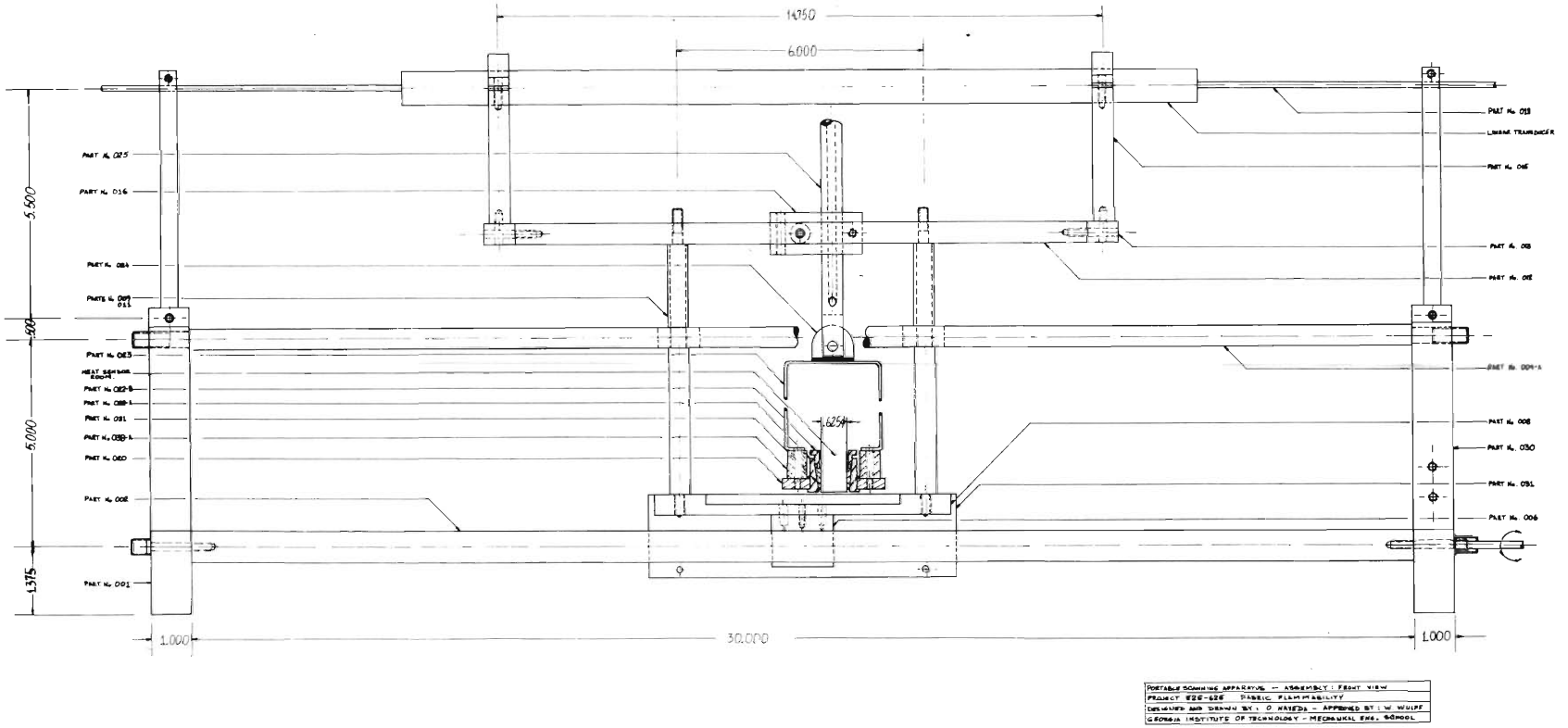

Figure A.4.1 Ignition Source Scanning Apparatus, Elevated View

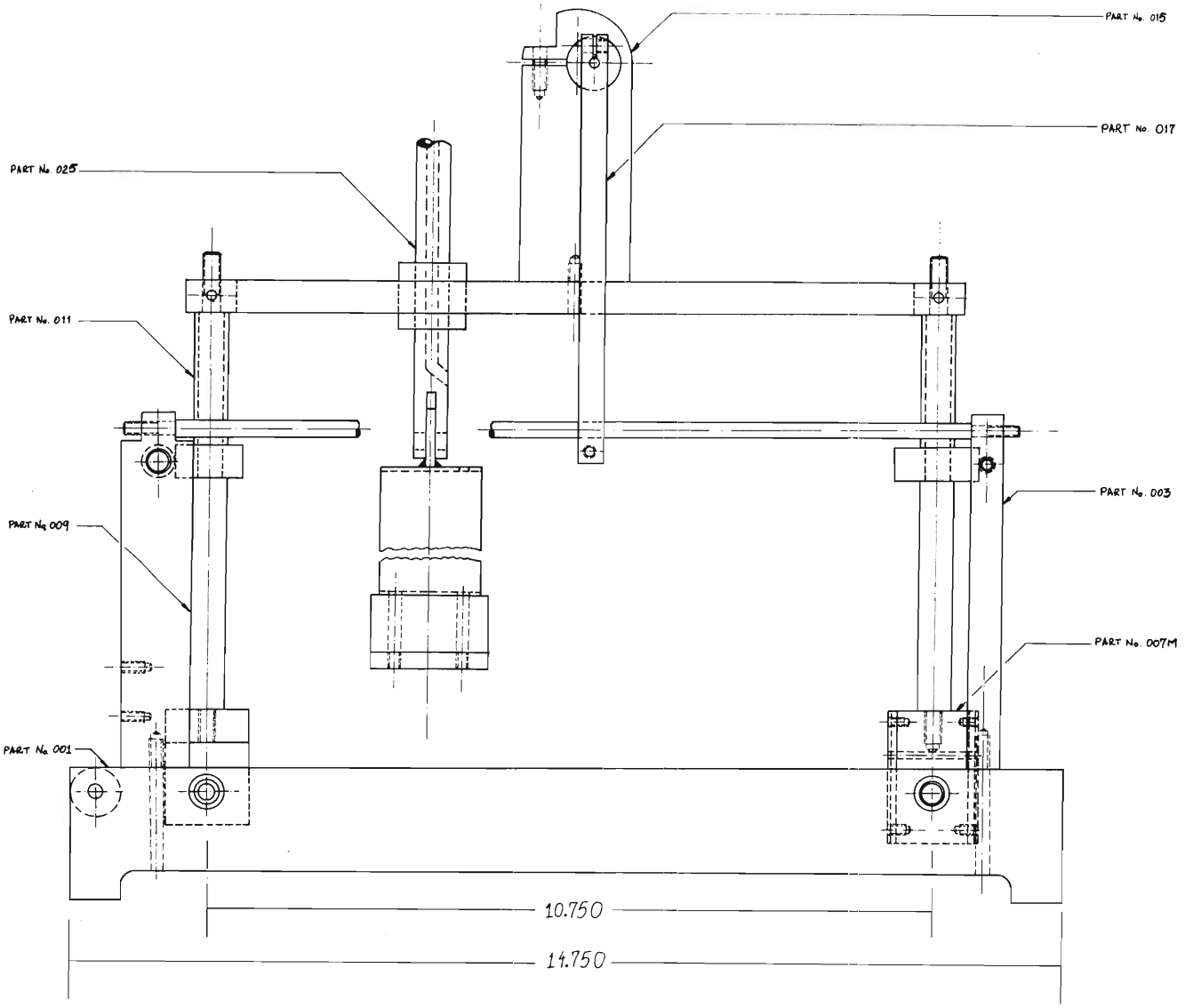

Figure A.4.2 Ignition Source Scanning Apparatus, Side View

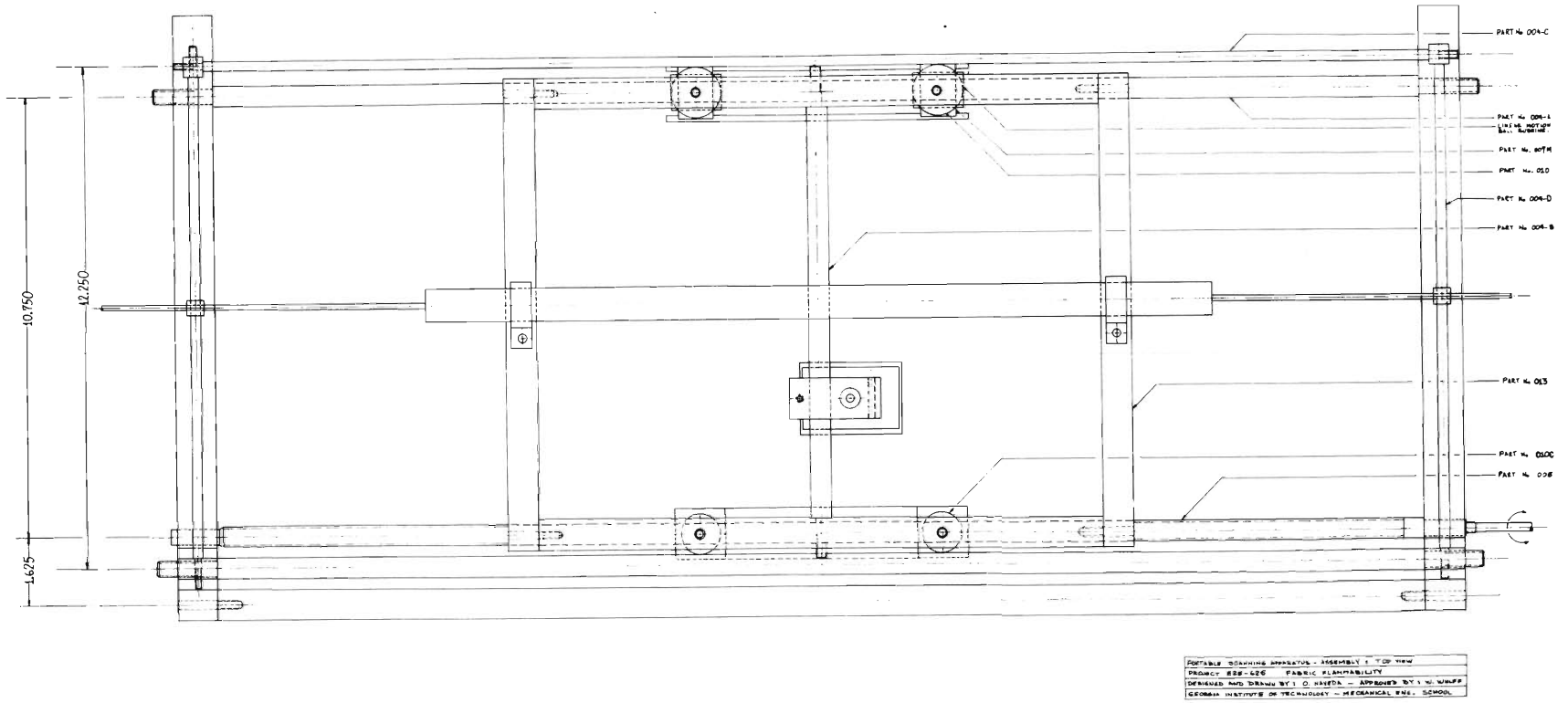

Figure A.4.3 Ignition Source Scanning Apparatus, Top View

A.4.2 Instrumentation

The Frame is shown in three assembly drawings, Figures A.4.1,2 and 3. The carriage is guided by linear ball bearings and traversed through a rotating threaded spindle.

The Sensor Carriage accommodates a water cooled High-Cal Asymptotic Heat Flux Calorimeter, Model No. C-1301-A-60 or a Chromel-Alumel thermocouple with exposed junction. The carriage allows for lateral and vertical positioning of the sensor, as well as for its rotation about a horizontal axis, anywhere between 0 and 90 degrees from the horizontal plane to the sensor plane.

The Carriage Drive consists of a 1/100 HP Bodine motor, Model 102, with built in worm gear reduction and a voltage regulator by Talboys Engineering Corporation. The motor drives a 1/2 inch threaded spindle with 13 threads per inch.

The Position Sensor is a Schaevitz Model 5000 HR-DC linear differential transducer with a linear displacement response range of six inches. The transducer requires 24 V exitation and is energized by a Heath Kit Regulated Power Supply, Model IP-27.

The Recording Equipment consists of

(i) Hewlett-Packard Model 7005 B x-y Recorder
(ii) Hewlett-Packard Model 3420 B Differential Volt/Ratio Meter
(iii) Leeds and Northrup Millivolt Potentiometer, Catalog No. 8686

Gas pressures were measured by U-tube manometers, the fuel gas flow rate by a Precision Wet Test Meter, manufactured by Precision Scientific Corporation. Surface temperatures of electric hot plate heating elements were measured with a Pyro Micro-Optical Pyrometer, Model No. 95. Temperatures were measured on the heating coil surface at eight different, uniformly distributed points and then averaged.

A.4.3 Experimental Procedure

Any ignition source surveyed was first allowed to come to thermal equilibrium at the selected operating conditions, either uncovered or covered by cooking utensils.

The volume above the ignition source was then traversed in the lengthwise direction of ISSA with the sensor arrested at a selected height above the source and in a vertical plane at a selected distance from the source axis. A typical heat flux diagram obtained is shown in Figure A.4.4 The diagram resulted from three left-to-right and three right-to-left traverses, carried out to obtain long-time averages for the local heat flux. The traversing speed was selected to average out turbulent fluctuations.

The heat flux sensor was cooled to remain at 55°C so that water vapor cound not condense onto the sensor. The manufacturers certified calibration was used to convert the emf-signal to heat flux.

A.4.4 Data Reduction

Five diagrams as that shown in Figure A.4.4 were each visually averaged to obtain the heat flux distribution in a vertical center plane. The results were transformed from rectangular Cartesian coordinates to polar coordinates, to yield Figures 2.17 through 2.22.

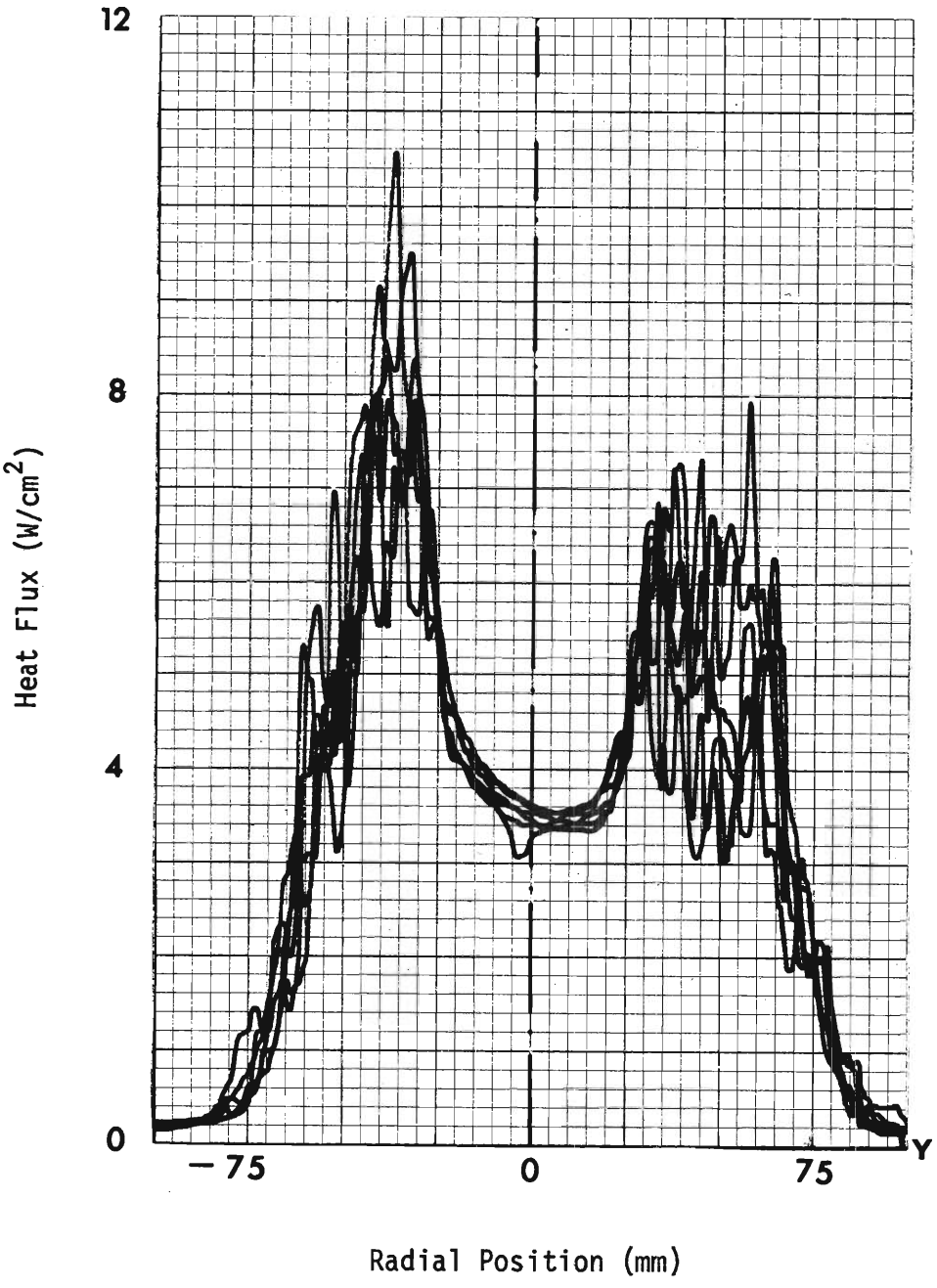

Figure A.4.4 Heat Flux Distribution. At X = 25mm above Burner Top, in the Vertical Center Plane. Kenmore Gas Hot Plate, Model No. 119.1503

BIBLIOGRAPHY*

1.1 "America Burning", The Report of the National Commission on Fire Prevention and Control, May 1973, GPO Bookstore Stock Number 5200-00004.

1.2 "Flammable Fabrics", Fourth Annual Report by U.S. Department of Health, Education and Welfare, 1972, for sale by Superintendent of Documents, U.S. Government Printing Office, Washington, D.C. 20402.

1.3 Government-Industry Research Committee on Fabric Flammability, "Study of Hazards from Burning Apparel and the Relation of Hazards to Test Methods". A work statement prepared by the Research Committee, Dr. E. Passaglia, Chairman, National Bureau of Standards, June 1970.

1.4 Evans, R. B., Wulff, W. and Zuber, N., "The Study of Hazards from Burning Apparel and the Relation of Hazards to Test Methods", Research Proposal submitted by the School of Mechanical Engineering, Georgia Institute of Technology, to the Government-Industry Research Committee on Fabric Flammability, July 1970.

1.5 Tribus, M., "Decision Analysis: Approach to Satisfying the Requirements of the Flammable Fabrics Act", Paper presented at the Textile and Needles Trades Division, American Society of Quality Control, Greensboro, North Carolina, February 12, 1970.

1.6 Wulff, W., Zuber, N., Alkidas, A. and Hess, R. W., "Ignition of Fabrics Under Radiative Heating", Combustion Science and Technology, 1973, Vol. 6, pp. 321-334.

1.7 Wulff, W. and Durbetaki, P., "Fabric Ignition and Burn Injury Hazard", Proceedings, 1973 International Seminar on Heat Transfer from Flames, Trogir, Yugoslavia.

1.8 Wulff, W., Zuber, N., et. al. "Study of Hazards from Burning Apparel and the Relation to Test Methods", First Final Report, NSF Grant No. GK-27189, December 1971, National Technical Information Access No. COM-73-10954.

---

*The first digit refers to the chapter in which the reference is cited for the first time.

1.9 Durbetaki, P. and Wulff, W., "The Study of Hazards from Burning Apparel and the Relation of Hazards to Test Methods", a Research Proposal submitted to the National Science Foundation by the School of Mechanical Engineering at Georgia Institute of Technology, September 1972.

1.10 Wulff, W., Alkidas, A., Hess, R. W. and Zuber, N., "Fabric Ignition", Textile Research Journal, Vol. 43, No. 10, October 1973, pp. 577-588.

2.1 Same as 1.9.

2.2 Durbetaki, P., Wulff, W., et. al. "Fabric Ignition", Seminannual Progress Report No. 1, NSF Grant No. GI-31882, July 31, 1973.

2.3 Wulff, W., Durbetaki, P. et al. "Study of Hazards from Burning Apparel and the Relation of Hazards to Test Methods", Second Final Report, NSF Grant No. GI-31882, December 1972, National Technical Information Service Access No. COM-73-10956.

2.4 Same as 1.8.

2.5 Heskestad, G., "Ease of Ignition of Fabrics Exposed to Flaming Heat Sources", Final Report, FMRC Service No. 199967, 1973.

2.6 Natrella, M. G., "Experimental Statistics, Handbook 91, United States Department of Commerce, National Bureau of Standards (Portion of AMC Handbook).

3.1 Same as 1.9.

3.2 Goodman, T.R., "Application of Integral Methods to Transient Nonlinear Heat Transfer", Advances in Heat Transfer, Irvine, T.F. Jr. and Hartnett, J.P., editors, Vol. 1, 1973, Academic Press, pp. 52-122.

3.3 Same as 1.7.

3.4 Same as 1.4.

3.5 Same as 1.5.

3.6 Same as 2.3.

3.7 Schlichting, H., Boundary-Layer Theory, Sixth Edition, McGraw-Hill, 1968, p. 128.

3.8 Eckert, E.R.G. and Jackson, T.W., "Analysis of Turbulent Free Convection Boundary Layer on a Flat Plate". NACA Report 1015, 1951.

3.9 Schlichting, H., Boundary-Layer Theory, Sixth Edition, McGraw-Hill, 1968, p. 301.

3.10 Ibid, p. 647.

E-25-625

GEORGIA INSTITUTE OF TECHNOLOGY
School of Mechanical Engineering
Atlanta, Georgia

STUDY OF HAZARDS FROM BURNING APPAREL AND THE RELATION OF HAZARDS TO TEST METHODS

Second Final Report

By

A. Alkidas
E. R. Champion
P. Durbetaki
W. E. Giddens
R. W. Hess
B. Kumar
O. A. A. Naveda
P. T. Williams
W. Wulff

For The

GOVERNMENT-INDUSTRY RESEARCH COMMITTEE
ON FABRIC FLAMMABILITY
Office of Flammable Fabrics
National Bureau of Standards
Washington, D. C. 20234

NSF Grant No. GI-31882

December 31, 1972

STUDY OF HAZARDS FROM BURNING APPAREL

AND

THE RELATION OF HAZARDS TO TEST METHODS

Second Final Report
December 31, 1972

By

A. Alkidas
E. R. Champion
W. E. Giddens
R. W. Hess
B. Kumar
O. A. A. Naveda
P. Durbetaki
P. T. Williams
W. Wulff

School of Mechanical Engineering
Georgia Institute of Technology
Atlanta, Georgia 30332

For The

GOVERNMENT-INDUSTRY RESEARCH COMMITTEE
ON FABRIC FLAMMABILITY

Office of Flammable Fabrics
National Bureau of Standards
Washington, D. C. 20234

N.S.F. Grant No. GI-31882

W. Wulff, Principal Investigator

N. Zuber, Principal Investigator

Stothe P. Kezios, Director
School of Mechanical Engineering

GEORGIA INSTITUTE OF TECHNOLOGY

School of Mechanical Engineering

FOREWORD

The research presented here was funded and supported by the National Science Foundation under the RANN program (Research Applied to National Needs), and monitored by the Government-Industry Research Committee on Fabric Flammability. The opportunity to participate in this nationally coordinated research effort is greatly appreciated.

The project was carried out in the Fire Hazard and Combustion Research Laboratory of the School of Mechanical Engineering under the Principal Investigators Dr. Wolfgang Wulff and Dr. Novak Zuber. Dr. Pandeli Durbetaki directed the experimental investigation of fabric ignition in gas flames and the associated data evaluation.

The research assistants involved were Dr. Alexandros Alkidas, responsible for the measurements of ignition and melting temperatures, of fabric enthalpy and thermal conductivity, further Mr. Richard W. Hess who performed radiative fabric ignition time measurements, Mr. Edward R. Champion who constructed the Convective Ignition Time Apparatus and measured fabric gas ignition time, Mr. Williams E. Giddens who measured reaction kinetics and enthalpies. Mr. Oscar A. A. Naveda carried out the experimental ignition statistics under radiative heating, Mr. Kumar assisted in the evaluation of free convection film coefficients and Mr. Paul T. William, M.E. Senior, measured optical properties on charred fabrics.

The permission to use the DTA/TGA Facility in the School of Chemistry at Georgia Institute of Technology and the assistance by Dr. E. C. Ashby in the use of that facility, as well as the expert advise given by Dr. P. Claudy during the DTA/TGA investigation, are acknowledged with great appreciation.

The participation of the graduate research assistants has been supported in part by the School of Mechanical Engineering under the matching fund provision of the grant. The NSF grant in support of this research is greatly appreciated.

Stothe P. Kezios, Director
School of Mechanical Engineering

December 29, 1972

ABSTRACT

This second Final Report presents the research carried out during the time from January 1, 1972 through December 31, 1972 on that portion of the analytical and experimental program, monitored by the Government-Industry Research Committee on Fabric Flammability (GIRCFF), and sponsored by the National Science Foundation under the RANN Program, which has been performed at the Georgia Institute of Technology. This research is the continuation of the research previously carried out at Georgia Institute of Technology between November 1, 1970 and December 31, 1971, also under NSF funding and GIRCFF administration and reported on in the previous Final Report [I-1]*.

It was shown [I-2] that the hazard from fabric-related burn injuries can be quantitatively assessed in terms of the probability that such injury is suffered. This probability depends upon the probabilities associated with the possible events leading to the injury, such as ignition after exposure combustion after ignition and tissue decomposition during and after burning. It was also shown that the probability of fabric ignition under given exposure depends on the ratio of fabric ignition time to exposure time; hence that the ignition time is an important characteristic required to assess the hazards of fabric-related burn injuries. Therefore, this experimental and analytical program has been carried out to predict the fabric ignition time as a function of exposure parameters and fabric properties.

The objective of the experimental phase is two-fold, firstly, to measure the ignition times of a selected set of cotton, nylon, polyester and acetate fabrics and blends, at well defined exposure and fabric conditions, secondly to measure, on the same fabrics, the thermophysical properties which characterize the ignition process. These properties are the thermal conductance,

*Numbers in brackets refer to the Bibliography.

the specific heat, the mass per unit area, the ignition or melting temperature, further the optical properties, namely infrared reflectance and transmittance, and the reaction kinetic parameters activation energy, pre-exponential factor and reaction enthalpy. In addition, the characterization of exposure conditions requires the measurement of the convective heat transfer film coefficients, for forced convection during gas flame ignition and for free convection losses during radiative heating.

The objective of the analytical phase is to predict fabric ignition time as a function of fabric properties and exposure conditions. The complete modeling analysis previously performed to establish the modeling rules necessary for the prediction of fabric ignition time was extended to include desorption and gasification processes. Partial modeling rules are discussed, and error estimates appropriate for partial modeling are presented. Modeling experiments are specified which are required to predict ignition time.

Results

The following property measurements were performed on the second set of ten fabrics, selected by GIRCFF and called the secondary GIRCFF Fabrics. These and previously treated Primary GIRCFF Fabrics are specified in Table II-1.*

Thermal conductance was measured in a guarded hot plate for single layers of fabrics in the temperature range from $70^{o}C$ to $200^{o}C$ at the contact pressures of 528 and 866 N/m^2. The thermal conductance, i.e. the ratio of thermal conductivity to fabric thickness, was found to vary between 60 and 300 W/m^2C) and to increase almost linearly with increasing temperature and pressure, by a factor of up to two.

*Roman numerals refer to the Chapters of this report.

The specific heat was obtained from enthalpy measurements in a drop calorimeter, carried out in the temperature range between 100°C and 220°C. The enthalpy versus temperature data were graphically smoothed, represented by a power polynomial, and the results were differentiated with respect to temperature. Specific heats were found to vary between 1.2 and 2.5 Ws/(g C) and to agree well with previously published data.

The fabric auto ignition temperature was measured by immersion of the fabric into a modified, preheated Setchkin furnace, flushed by preheated air at the velocity of 0.61 m/s. Pilot ignition temperatures were measured by triggering intermittently a small electric arc near the sample. Melting temperatures are recorded for fabrics which melt prior to ignition. Thermoplastic fabrics were found to melt above 230°C while cellulosic fabrics ignited at temperatures between 280°C and 500°C.

Optical properties were measured on charred fabric samples in an integrating sphere reflectometer under infrared irradiation. By measuring the apparent reflectance of the fabric, once with a reflecting and once with an absorbing background, both the reflectance and the transmittance were obtained. Most fabrics proved to absorb approximately 20% of the incident radiant flux in their original, but 40% in their charred conditions.

Reaction kinetic parameters were measured on the ten Primary GIRCFF Fabrics for the desorption and fusion processes prior to ignition, by thermogravimetric methods. Pyrolysis data were evaluated from the measurements carried out by Dr. McCarter of NBS.

Reaction enthalpies were measured on the same fabrics and for the same processes by means of differential thermal analysis.

The literature was reviewed concerning data on reaction kinetics and calorimetry to cover the exothermic processes following endothermic gasification.

Ignition times were measured under radiative heating on the ten Secondary GIRCFF Fabrics after desiccation and on selected fabrics at two additional levels of environmental relative humidity. Measurements were also performed under convective heating in gas flames on the ten Primary GIRCFF Fabrics, also after fabric desiccation.

A special Radiative Ignition Time Apparatus (RITA) had been previously designed and constructed, capable of exposing a 1 in.-diameter fabric sample area to a uniform, constant radiant heating pulse of 0.25 to 16.0 W/cm^2 with transients of no more than 5 ms. The energy transmitted through the fabric during the ignition process is being monitored by a thermoelectric heat flux meter and the instant of fabric destruction (melt-through or ignition of back face) is being sensed by an infrared detector. Ignition times obtained vary between 1 and 70 s.

RITA was enclosed in a temperature and humidity-controlled environmental chamber and equiped with automated timing and monitoring circuits to operate under dual shutter mode operation. This allowed preconditioning of fabrics and control of exposure time for the study of the effect of moisture and of ignition statistics.

To assess the effects of heating modes a special Convective Ignition Time Apparatus (CITA) was constructed during this reporting period, capable of exposing fabric samples suddenly to a well defined gas flame, and of sensing the onset of ignition as well as of melt-through. The heating intensity was varied from approximately 10 to 200 W/cm^2 by controlling vertical distance of the fabric from the burner opening, air to fuel ratio, and total fuel and air flow rates. Heating intensities were inferred from measured gas flame temperatures and from measured forced convection heat transfer coefficients. Composition profiles for CO_2 and O_2 were established and ignition times are presented in nondimensional form, suitable for direct comparison with radiative ignition time data.

The probability of ignition under laboratory exposure conditions was measured for a cellulosic fabric at three levels of irradiation and two levels of humidity. The variance of mean ignition time and the variance of ignition time about the mean were evaluated and found to be extremely small for high heating intensity and only moderately large for low intensities.

A detailed, distributed-parameter ignition model and a lumped-parameter model had been developed previously. The lumped-parameter modeling analysis has been extended to include desorption, gasification in the condensed phase and exothermal reaction in the gaseous phase. Analytical and experimental ignition times have been compared. Necessary advances for future research have been identified in a separate proposal [1-3].

TABLE OF CONTENTS

LIST OF FIGURES

LIST OF TABLES

NOMENCLATURE*

C'	ratio of heated fabric height over thickness of gas boundary layer
C''	areal heat capacity
c	specific heat
c_p	specific heat at constant pressure
d	sample diameter
E	activation energy
$E_n(Z) = \int_0^1 y^{n-2} \exp(-z/y)\, dy,\ n = 1,2$	exponential integral
$\bar{F}_{s\infty}$	average sample view factor with respect to its environment
h_c	convection heat transfer coefficient
$\bar{h}_c$	average (front and back face average or time average) conv. heat transf. coeff.
Δi	reaction enthalpy
k	thermal conductivity
k/δ	thermal conductance
k_d, k_e, k_q	frequency factors of desorption, oxidation and pyrolysis respectively
L	vertical distance above burner oxidation
$\dot{m}$	mass flow rate
N_{Bi}	Biot number $N_{Bi} = h_c\, \delta / k$

* Symbols used in Appendices are defined in the Appendix in which they occur.

N_{Fo}	Fourier number, Eq. II-B.1
P(I/E)	probability of ignition for given exposure
q	volumetric heat generation rate
q*	nondimensional heat flux, Eqs. II-B.2 and II-C.2
R	universal gas constant
s	estimate for standard deviation σ
T	absolute temperature
t	relative temperature
W_o	radiative power flux
x	coordinate normal to fabric surface
Y =	$(\bar{\pi}_1)^{1/5}$, Eq. III-14
y	integration variable
z	general variable
α	absorpance
β	argument in Eq. III-13, defined in Eq. III-14
δ	fabric thickness
ε	decomposable mass fraction
Θ	nondimensional temperature, Eq. III-18
θ	nondimensional temperature, Table III-2
θ	time mean of θ
κ	extinction coefficient
$\kappa\delta = \kappa^*$	optical thickness
λ	fraction of decomposable mass fraction

μ	ratio $\langle \tau_i \rangle / \tau_i$ of statistical mean ignition time over single-shutter ignition time
$\pi = 3.1415 \ldots$	
π_o through π_{10}	scaling groups, defined in Table III-1
$\pi_2^*, \pi_3^*, \pi_5^*, \pi_6^*, \pi_8^*$	scaling groups, defined in Table III-2
$\pi_{20}, \pi_{21}, \pi_{22}, \pi_{23}$	scaling groups defined, respectively, by Eqs. III-16, 17, 19 and 21
ρ	fabric density
$\rho\delta$	specific mass, mass per unit area
ρ	reflectance
σ	Stefan-Boltzmann constant
σ	standard deviation
τ	time
τ^*	nondimensional time, Table III-1
$\bar{\tau}$	nondimensional time, Table III-2
$\langle \tau^* \rangle$	median of nondimensional time
τ	radiative transmittance
ϕ	heating rate
ϕ	stoichiometric equivalence ratio
χ^*	standard normal variable, Eq. III-3
$\psi = \tau_e / \tau_i$	

Subscripts

b	boundary
c	convection

d	desorption
e	exposure
e	exothermic
f	flame
g	gas (pyrolysate)
i	ignition
l	laboratory
m	melting
mix	mixture
rad	radiative
∞	environment and initial
o	initial

I. INTRODUCTION AND PROGRAM OBJECTIVE

A. Introduction

1. The Hazard From Burning Apparel And Related Test Methods

The Flammable Fabrics Act of 1953 as amended in 1967 demands that the Secretary of Commerce establish reasonable criteria based on standard tests to be imposed on fabrics so as to protect the public from excessive hazards of fabric related burn injuries. In order to establish the technical and scientific foundation for the required legislation, the United States textile industry and the United States Government have initiated a cooperative effort in sponsoring, jointly, research programs designed to lay down this foundation. The task of formulating and administrating these programs has been delegated to the Government-Industry Research Committee on Fabric Flammability.

In initiating the research in support of the Flammable Fabrics Act, the Government-Industry Research Committee made the following statement in Reference [I-1]*:

"The determination of the relationship between fabric behavior in a test method, on the one hand, and the hazard it presents in actual use, on the other, is necessary in order to develop meaningful standards."

The determination of this relation can be considered therefore as the central problem of fabric flammability studies.

The principle connection between burn injury hazard on one side and both stochastic and deterministic processes leading to burn injury on the other side were established in Reference [I-2]. The relationship is based on the quantitative assessment of hazard in terms of accident probability, and the

*Numbers in brackets refer to the Bibliography.

dependence of accident probability on subsidiary probabilities associated with all conceivable events occurring between intended fabric certification and accidental burn injury.

Predominantly stochastic events are dictated statistically by human characteristics such as habits, preferences and, most importantly, response to accident conditions. The more, but not completely, deterministic processes in the chain of events which lead to burn injury are fabric ignition after exposure and tissue decomposition after fabric ignition. These two events are considered most indicative of fabric behavior and deemed to be of particular importance for the characterization of apparel contribution toward the burn injury hazard.

The probability of fabric ignition for given exposure, P(I/E), was related, in principle, in Reference [I-2] to the ratio of the time it takes a fabric to ignite under given exposure conditions, called the ignition time τ_i, over the time the fabric is exposed to a given ignition source, that is the exposure time τ_e

$$P(I/E) = f\,(\tau_e/\tau_i)\,. \qquad (I\text{-}1)$$

While the exposure time τ_e depends on human response and reaction the ignition time τ_i depends on (1) physical fabric properties, (2) process parameters describing the interactions between fabric, heating source and environment and (3) fundamental physico-chemical processes such as heat and mass transfer and chemical reactions. Equivalent statements can be made about the other event, tissue decomposition after fabric ignition (or melting) has occurred [I-2].

Consequently, in order to relate burn injury hazard via accident probability to laboratory test methods one has to establish (1) which thermophysical fabric properties are relevant to the description of ignition and burn processes, (2) which skin and tissue properties are involved in the description of

thermal tissue decomposition, (3) the descriptions of heat source and fabric interaction, (4) the description of fabric and skin interaction, including the possible direct interaction between heat source and tissue, (5) the modeling analysis required to describe the physical processes of ignition and burning and to evolve the scaling laws, (6) the functional relationships given by Eq. (I-1) for fabric ignition and an equivalent relation for tissue decomposition, both under laboratory conditions and, finally, (7) the statistical relation between laboratory and actual exposure conditions. The last relation and the scaling laws provide the connection between laboratory test methods and real-life hazard conditions.

The investigations which are being carried out in the School of Mechanical Engineering at Georgia Tech under the sponsorship of NSF and monitored by the Government-Industry Research Committee on Fabric Flammability (GIRCFF), are designed to provide the modeling rules and experimental data which are required for determining the probability of fabric ignition P(I/E) after given exposure.

2. Previous Objectives and Accomplishments

The purpose of the research program performed during the period from November 1, 1970 through December 31, 1971 [I-2] was to predict the fabric ignition time as a function of relevant fabric properties and exposure conditions. Emphasis was placed on inert heating and the research was restricted to fabric ignition by radiative heating alone. The research program consisted of an experimental and an analytical phase.

The specific objectives of the experimental program were to measure

a. the fabric ignition time under well-controlled exposure conditions, and
b. all the relevant fabric properties which describe the fabric behavior during the heating process until ignition or melting occurs.

Originally, these fabric properties were anticipated to be

the constant-pressure specific heat c_p

the enthalpy of reaction Δi

the thermal conductivity k normal and parallel to the fabric

the fabric thickness δ

the fabric density ρ

the ignition temperature T_i

but it became evident during the program that, after the choice of radiation heating as the first and simplest heating source, optical properties are most relevant. The above list was changed to include the optical properties reflectance $\tilde{\rho}$ and transmittance $\tilde{\tau}$ instead of the reaction enthalpy Δi.

The specific objectives of the analytical program were:

c. a complete modeling analysis for the purpose of determining the relevant modeling rules needed to assess the ignition time; the analysis was to be carried out by examining the governing differential equations and to take into account (1) fabric material properties, (2) physical processes such as heating modes and boundary conditions, and (3) different geometries;

d. the development of the rules for partial modeling on the basis of the governing differential equations;

e. an assessment of the errors involved with partial modeling.

Tasks (a) and (b) above were carried out on ten of the twenty fabrics selected by the Government-Industry Research Committee on Fabric Flammability (GIRCFF). Results are reported in Reference [I-2].

The analysis was performed. A distributed-parameter model was developed to describe radiative heating with in-depth absorption, associated by endothermic gasification and exothermic fabric reaction. Numerical integration of the governing partial differential equations revealed that, under expected environmental conditions of natural convection, the simpler lumped-parameter description adequately represents the ignition process. This leads to the reduction from ten to seven in the number of nondimensional groups which define the problem solution. Closed-form

solutions were presented for inert heating with convective losses included, and heating with zero-order reaction but without convection. The complete problem was solved numerically. Partial modeling errors were listed, the insignificant role of thermal diffusion established and the importance of free convection and endothermic reaction was demonstrated by comparison of experimental with analytical results.

B. Program Objective

The purpose of the research program reported on herein is to assess quantitatively the effects of

(1) heating mode,

(2) fabric humidity and

(3) pre-ignition endothermic gasification of fabric ignition.

In order to establish the fabric ignition probability under laboratory exposure conditions statistical ignition time data were to be collected to determine

(4) the statistical confidence (standard errors) of the mean ignition time and the ignition time itself.

The last objective was to complete

(5) fabric property measurements on the ten Secondary CIRCFF Fabrics.

The effect of heating mode was to be investigated through gas flame ignition studies, associated with comprehensive flame characterization and subsequent comparison of results obtained from gas flame and radiative ignition studies.

Humidity effects were to be studied experimentally by ignition time measurements on preconditioned fabrics in a temperature and humidity-controlled environment, and analytically by including desorption of water into the governing differential equations.

Endothermic gasification effects were to be considered on the basis of

thermogravimetric and differential thermal analysis data.

Ignition time statistics were to be measured by precise control of exposure time and by monitoring the frequency of ignition.

Chapter II is a presentation of the experimental accomplishments. Details of instrumentation and experimental procedures are presented in Appendix B. The analysis and the comparison between experimental and analytical results are discussed in Chapter III. The conclusions are summarized in Chapter IV. A fabric-by-fabric property summary for all GIRCFF Fabrics, selected by the Government-Industry Research Committee on Flammable Fabrics, is presented in Appendix A. Finally, a summary of the literature survey on fabric reaction kinetics and calorimetry is given in Appendix C.

II. EXPERIMENTAL PROGRAM

The objective of the experimental program is to measure the thermophysical fabric properties which characterize the fabric behavior during the ignition process and to measure the fabric ignition time itself under well-defined heating conditions so that the analytically predicted ignition time may be verified or the analysis modified and refined until sufficient agreement is reached between analysis and experiment. The particular fabric properties to be measured are density, ignition temperature, thermal conductivity, specific heat at constant pressure, radiative reflectance and absorptance, and the reaction kinetics parameters: activation energy, frequency factor and order of reaction, as well as the reaction enthalpy, all for preignition reactions that affect significantly the ignition time.

Discussed below are at first the property measurements, each measurement as a separate task, and then the measurements of ignition time. Ignition time measurements were performed in four separate phases: firstly the measurement of ignition time under radiative heating of desiccated fabrics, secondly the assessment of the influence of fabric moisture on ignition time, thirdly the measurement of the effect of heating mode on the ignition processes and finally the evaluation of ignition time statistics.

A. Property Measurements (Tasks 1 through 6)

1. Purpose

Fabric ignition is recognized as a transient heating process. The relevant fabric properties which characterize fabric response to heating are

(i)	Fabric Mass Per Unit of Area	$(\rho\delta)$
(ii)	Specific Heat of Fabric	(c_p)
(iii)	Thermal Conductance	(k/δ)
(iv)	Ignition Temperature	(T_i)
(v)	Radiative Properties	$(\tilde{\rho}, \tilde{\tau})$
(vi)	Properties of Reaction Kinetics and Calorimetry.	$(n, E, k_o, \Delta i)$

This listing order is not intended to imply a universal order of priority in which the properties affect ignition processes. Items (i) and (ii) are composite properties, their composition being stipulated by reasons of analysis. Fabric mass per unit area is the product of thickness δ and density ρ, thermal conductance the quotient of thermal conductivity k over thickness δ. The two radiative properties are reflectance $\tilde{\rho}$ and transmittance $\tilde{\tau}$. The parameter of reaction kinetics are: order of reaction n, activation energy E and frequency factor k_o. The parameter of reaction calorimetry is the reaction enthalpy Δi.

The objective of the property measurement program is to provide the above listed fabric properties, to the extent necessary for describing the ignition process.

Below are presented the achievements and the results of the property measurement program. The measurements were performed on the twenty fabrics listed in Table II-1. These fabrics were selected and numbered by the Government-Industry Research Committee on Fabric Flammability. They are called GIRCFF Fabrics and identified by the numbers in accordance with Table II-1.

Table II-1 Fabric Identifications and Specific Mass

GIRCFF No.	Classification	Fiber Composition	Color	Finish	Specific Mass mg/cm^2
1	Durable Press Slack	65/35% Pe./C.	White	DP treated	23.49
2*	Textured Woven Blouse	100% Polyester	Yellow	-	7.51
3	Double Knit	100% Polyester	White	-	20.91
4	Denim	100% Cotton	Navy bl.	-	29.63
5*	T-Shirt, Jersey	100% Cotton	White	-	13.71
6	Untreated Slack	65/35% Pe./C.	White	-	23.57
7	Jersey Tube Knit	100% Acrylic	Gold	-	15.13
8*	T-Shirt, Jersey	65/35% Pe./C.	White	-	16.19
9	Terry Cloth	100% Cotton	White	-	26.48
10*	Batiste	100% Cotton	Purple	-	6.65
11*	Tricot	80/20% Acet./ Nyl.	White	-	11.31
12*	Tricot	100% Nylon	White	-	8.91
13*	Tricot	100% Acetate	White	-	9.40
14	Taffeta	100% Nylon	White	-	5.66
15	Durable Press Slack	65/35% Pe./Ray	Brown	DP treated	22.82
16	Shirting	50/50% Pe./C.	White	-	13.14
17*	Batiste	65/35% Pe./C.	White	-	8.55
18*	Flannel	100% Cotton	White	-	12.88
19*	Flannel	100% Cotton	White	Fire retard	14.89
20	Flannel	100% Wool	Navy bl.	-	19.93

*Ten Primary GIRCFF Fabrics.

2. Achievements, Property Measurements

Task 1. Fabric Mass Per Unit Area ($\rho\delta$)

The total of ten weighings was performed on 5 inch by 5 inch large, desiccated samples by means of an analytical balance. The results agree well with those obained by NBS and are presented in Table II-1, along with the previously obtained results.

Task 2. Specific Heat of Fabrics (c_p)

The experimental arrangements and procedures described in Reference [I-2], Appendix B. 2 were used to perform the total of 51 enthalpy measurements on the ten Secondary GIRCFF Fabrics, in the temperature range between 120°C and 220°C. The enthalpy data obtained as functions of temperature were visually smoothed as shown in Reference [I-2], pp. 29 through 39, then approximated by power polynomials and differentiated with respect to temperature.

Task 3. Thermal Conductance of Fabrics (k/δ)

The total of forty guarded hot plate measurements were performed as described in Reference [I-2], Appendix B.3.

Task 4. Fabric Ignition and Melting Temperatures ($T_{i,m}$)

The previously developed modification of the Setchkin Furnace was further improved by the design, construction and installation of a purge air preheater. The totals of 32 auto-ignition and 26 pilot ignitions were performed on the ten Secondary GIRCFF Fabrics.

Task 5. Radiative Fabric Properties ($\tilde{\rho}$, $\tilde{\tau}$)

Twenty GIRCFF Fabrics were charred in a thermostatically controlled furnace at the arithmetic mean temperatures between room temperature and the fabrics' destruction temperature.

Reflectances and absorptances were derived from measured apparent reflectances, produced by the fabrics with selected backgrounds, in accordance with the procedures described in Appendix B.5 of Reference [I-2]. Reflectance, transmittance, absorptance and optical thickness, i.e. the product of fabric thickness and extinction coefficient, are reported for all twenty GIRCFF Fabrics.

Task 6. Reaction Kinetics Parameters and Calorimetry (n, E, k_o, Δi)

Simultaneous Differential Thermal Analysis and Thermogravimetric Analysis (DTA/TGA) measurements were performed to derive activation energy E, reaction order n, pre-exponential frequency factor k_o and reaction enthalpy Δi for the endothermic decomposition processes prior to ignition. Eighty-one thermal analysis tests were run on the METTLER Thermoanalyzer 2 of the School of Chemistry at Georgia Tech. Of these, forty DTA/TGA measurements were carried out with aluminum oxide powder as the reference material and twenty-three DTA/TGA measurements with gold powder as the reference material. All tests were performed on the ten Primary GIRCFF Fabrics. A total of sixteen tests was made for calibration purposes and for finding the optimum crucible position for symmetric heating. Two separate computer codes were developed for data reduction. Chemical reaction parameters, namely the reaction enthalpy, the order of reaction, the activation energy, and the pre-exponential factor, were evaluated for twenty DTA/TGA tests with gold powder as the reference material and for nine thermal decomposition tests carried out by Dr. R. J. McCarter of the National Bureau of Standards.

Exothermal oxidization kinetics were also evaluated for the total of 5 non-melting primary GIRCFF Fabrics.

Not all of the DTA/TGA experiments are considered successful. Considered as sufficiently reliable for the purposes of the analysis are the desorption kinetics data and the oxidation kinetics data, obtained from measurements in the dynamic air atmosphere. Calorimetric data of desorption, although in general agreement with data computed from moisture regain and desorption enthalpy, are considered less reliable than the computed data. Computed data were used in support of the analysis. Pyrolysis data which were derived from measurements carried out in inert atmospheres by Dr. McCarter at NBS, exhibit consistently appreciable pyrolytic decomposition only at temperatures too far above the measured ignition temperature to be useful for the modeling analysis of ignition. This observation is attributed to the effect of the inert atmosphere rather than to uncertainties in the data reduction.

3. Experimental Results, Property Measurements

A summary of results is presented here for each of the six tasks in the property measurement program. Appendix A is a data collection, summarized for each fabric.

Task 1. Fabric Mass Per Unit Area ($\rho\delta$)

The specific mass is listed for each of the twenty GIRCFF Fabrics in the last column of Table II-1.

Task 2. The Specific Heat (c_p)

Specific heat was obtained from the differentiation with respect to temperature of measured enthalpy data, after visual smoothing and polynomial collocation. Detailed descriptions on the calorimeter used, on calibration and data reduction procedures are found in Appendix B.2 of Reference [I-2] pp. 29 through 39. The results are listed in Table II-A.1 for all twenty GIRCFF Fabrics.

Task 3. Thermal Conductance (k/δ)

Thermal conductance was measured on single layers of fabrics, cut into squares of 12.7 cm edge length and placed between plane-parallel brass plates, in a guarded hot plate. Tests were performed in the temperature range from $120^{o}C$ to $220^{o}C$ and at two contact pressures of 528 N/m^2 and 866 N/m^2.

Detailed descriptions on the guarded hot plate and measurement techniques are found in Appendix B.3 of Reference [I-2]. A graphical representation of thermal conductance as a function of temperature is given in Figure II-A.1 for the contact pressure of 528 N/m^2. The results of thermal conductance measurements, obtained with the contact pressure of 866 N/m^2, are listed in Table II-A.2, along with measured fabric thicknesses [I-2]. Increasing the contact pressure leads generally to increased conductance, as has been observed before. The exception is the wool (GIRCFF Fabric No. 20) whose conductance did not change appreciably with pressure.

Table II-A.1 Specific Heat of Fabrics in W s /(g C) as Function of Temperature

GIRCFF No.	Temperature, °C 50	75	100	125	150	175	200	250
1	1.19	1.24	1.29	1.34	1.38	1.43	1.47	1.53
2	1.42	1.42	1.42	1.42	1.42	1.42	1.42	-
3	1.03	1.10	1.17	1.25	1.36	1.50	1.67	2.16
4	1.17	1.23	1.29	1.35	1.40	1.46	1.50	1.55
5	1.05	1.19	1.33	1.47	1.62	1.77	1.91	-
6	1.10	1.16	1.21	1.26	1.32	1.39	1.48	-
7	1.27	1.40	1.53	1.71	1.92	2.23	-	-
8	1.23	1.37	1.44	1.54	1.65	1.75	1.86	-
9	1.13	1.21	1.32	1.45	1.53	1.61	1.64	-
10	1.37	1.50	1.64	1.77	1.91	-	-	-
11	1.45	1.45	1.45	1.45	1.45	1.45	1.45	-
12	1.51	1.70	1.90	2.09	2.29	2.42	2.68	-
13	1.24	1.38	1.51	1.65	1.78	1.92	2.05	-
14	1.59	1.66	1.73	1.69	1.86	1.96	2.13	-
15	0.91	1.03	1.15	1.26	1.37	1.47	1.55	1.66
16	1.16	1.21	1.26	1.31	1.37	1.41	1.44	-
17	1.27	1.33	1.40	1.47	1.53	1.60	1.66	-
18	1.44	1.50	1.56	1.63	1.69	1.75	1.82	-
19	1.33	1.42	1.51	1.60	1.69	1.78	1.87	-
20	1.27	1.27	1.27	1.27	1.27	1.27	1.27	-

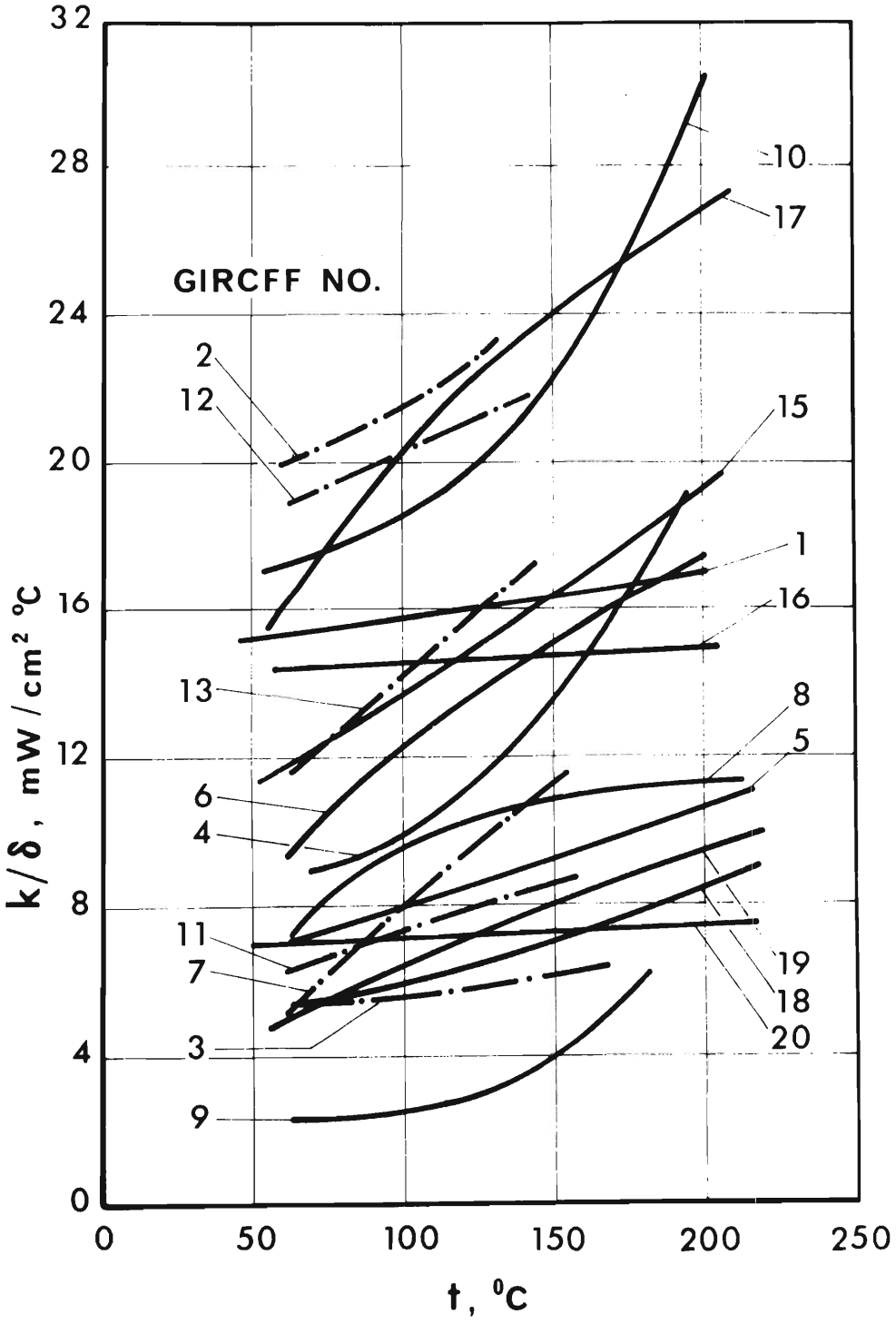

Figure II-A.1. Thermal Conductance as Functions of Temperature.

Table II-A.2 Thermal Conductance Secondary GIRCFF Fabrics. At Contact Pressure of 866 N/M^2

GIRCFF Fabric Number	Mass Per Unit Area mg/cm^2 N.B.S.	Mass Per Unit Area mg/cm^2 G.T.	Original Fabric Thickness cm	Mean Temperature ^oC	Specific Conductance $mW\ cm^{-2}C^{-1}$
1	24.04	23.49	0.0464	88.7	15.71
3	19.82	20.91	0.0953	92.0	5.46
4	29.44	29.63	0.0575	90.2	13.05
6	23.77	23.57	0.0476	88.9	14.53
7	8.98	15.13	0.0791	88.3	7.93
9	25.23	26.48	0.2080	95.3	2.98
14	5.68	5.66	0.0110	88.2	27.80
15	22.51	22.82	0.0421	89.0	15.37
16	13.29	13.14	0.0321	90.7	19.72
20	22.03	19.93	0.0721	91.7	7.00

Task 4. Fabric Ignition Temperature Measurements ($T_{i,m}$)

Auto and pilot ignition temperature ranges as measured in accordance with the procedures described in Appendix B. 4 of Reference [I-2] are listed in Table II-A.3 for fabrics which ignite. The melting temperatures of fabrics which were found to melt prior to ignition are listed in the same table and indicated by M.

The temperatures listed are the lower and upper limits of the furnace purge air at which fabric destruction was not and was observed, respectively, The air flow velocity past the fabric specimen was 0.6m/s. For more detailed descriptions of the apparatus used and the procedures followed see Reference [I-2].

Task 5. Radiative Fabric Properties ($\tilde{\rho}, \tilde{\tau}$)

The directional-hemispherical reflectance and transmittance were measured in an integrating sphere reflectometer for the purpose of describing the fabric-heater interaction. Details of instrumentation and operating procedures are presented in Appendix B. 5, of Reference [I-2].

Measurements were first carried out at incidence of 20^{o} from the normal. Then the effect of incidence was measured at various angles between 0^{o} and 40^{o} and found negligible. The fabrics measured can be considered as Lambertian reflectors and transmittors.

. Reflectance and transmittance was measured both in the infrared spectrum between 0.6μm and 2.5μm and the combined visible (less than I2%) and infrared spectrum as produced by a tungsten filament projector lamp at $3,200^{o}K$ filament temperature.

The reflectance, transmittance and absorptance was evaluated for all twenty GIRCFF Fabrics in their original condition (virgin and after charring

Table II-A.3 Auto and Pilot Ignition and Melting Temperatures

Temperatures in Centigrade

GIRCFF Fabric No.	Self-Ignition, Melting	Pilot-Ignition
1	416-409	337-331
2	262-255 M**	
3	255-246 M	
4	297-287 290-280*	290-280
5	311-301 327-318	311-301
6	416-409	345-337
7	246-236 M	
8	450-439 443-416	316-304
9	308-297	297-290
10	439-429 443-434	351-339
11	237-218 M	
12	255-237 M	
13	237-218 M	
14	246-236 M	
15	426-419	337-331
16	473-466	360-353
17	480-463	384-368
18	311-301	294-278
19	497-480	329-316
20	480-463	329-316

* check on reproducibility

** M represents melting

at the mean temperature between room temperature ($25^{o}C$) and their respective destruction temperatures. Optical properties obtained from charred fabrics are considered representative mean properties for the ignition process.

Table II-A.4 below lists optical properties of original fabrics for two kinds of irradiation as indicated. Table II-A.5 lists optical data for charred fabrics, along with the charr temperatures.

Task 6. Reaction Kinetics and Calorimetry

Differential thermal analysis and thermogravimetric analysis data obtained as described in Appendix B.1 were evaluated to yield

(i) activation energy E,

(ii) frequency factor k_o,

(iii) reaction order n, and

(iv) reaction enthalpy Δi

for each of these three processes:

(α) water desorption of cellulosic fabrics

(β) endothermic pyrolysis or fusion

(γ) exothermic oxidization.

The kinetics parameters (E, k_o, n) were evaluated from thermograms by three different techniques:

Method I consists of finding the best straight line through mass loss rate vs. reciprocal absolute temperature data, suitably normalized in accordance with Eq. B-2, then deriving n and E from the intercept and slope, respectively, of that line and computing finally k_o directly from the Arrhenius law.

Method II consists of evaluating the reaction order n, the activation Energy E and the frequency factor k_o from the known heating rate ϕ, from the decomposition λ_m, the decomposition rate $\dot{\lambda}_m$ and from the temperature T_m at the time of maximum decomposition rate,

Table II-A.4 Optical Properties of Original Fabrics

Subscript 1 refers to Tungsten Filament Source, T=3,160°K
Subscript 2 refers to Infrared Source, $0.6 \leq \lambda \leq 2.5 \mu m$

CIRCFF No.	Reflectance		Transmittance		Absorptance		Optical Thickness	
	$\tilde{\rho}_1$	$\tilde{\rho}_2$	$\tilde{\tau}_1$	$\tilde{\tau}_2$	α_1	α_2	κ^*_1	κ^*_2
1	0.605	0.522	0.211	0.289	0 184	0.189	0.375	0.296
2	0.560	0.501	0.276	0.346	0.164	0.153	0.272	0.208
3	0.560	0.619	0.250	0.238	0.190	0.143	0.335	0.276
4	0.450	0.491	0.105	0.137	0.445	0.372	1.106	0.855
5	0.533	0.521	0.288	0.296	0.179	0.183	0.284	0.282
6	0.581	0.581	0.220	0.284	0.199	0.135	0.388	0.223
7	0.536	0.549	0.262	0.159	0.202	0.292	0.340	0.855
8	0.562	0.560	0.264	0.276	0.174	0.164	0.298	0.272
9	0.681	0.623	0.206	0.231	0.113	0.146	0.274	0.288
10	0.418	0.406	0.361	0.394	0.221	0.200	0.280	0.236
11	0.523	0.508	0.320	0.329	0.157	0.163	0.230	0.232
12	0.447	0.397	0.380	0.433	0.173	0.170	0.214	0.188
13	0.490	0.443	0.344	0.390	0.166	0.167	0.227	0.203
14	0.348	0.348	0.508	0.434	0.144	0.218	0.136	0.234
15	0.515	0.413	0.259	0.331	0.226	0.256	0.375	0.340
16	0.613	0.499	0.219	0.294	0.168	0.207	0.338	0.312
17	0.485	0.464	0.364	0.372	0.151	0.164	0.198	0.208
18	0.599	0.573	0.231	0.251	0.170	0.176	0.326	0.312
19	0.590	0.602	0.229	0.197	0.181	0.201	0.348	0.428
20	0.336	0.365	0.119	0.102	0.545	0.533	1.149	1.226

Table II-A.5 Optical Properties of Charred Fabrics

Fabrics irradiated by Tungsten Filament Source at 3,160°K

FABRIC GIRCFF No.	Reflectance $\tilde{\rho}$	Transmittance $\tilde{\tau}$	Absorptance $\alpha=1-\tilde{\tau}-\tilde{\rho}$	Optical Thickness κ^*	Charr Temper. °C
1	0.366	0.285	0.349	0.490	219
2	0.582	0.243	0.175	0.305	134
3	0.506	0.294	0.200	0.306	134
4	0.401	0.088	0.511	1.305	162
5	0.491	0.284	0.225	0.348	162
6	0.339	0.288	0.373	0.510	219
7	0.113	0.167	0.720	1.115	230
8	0.346	0.308	0.346	0.460	230
9	0.627	0.131	0.242	0.660	162
10	0.219	0.394	0.387	0.413	230
11	0.566	0.256	0.178	0.303	134
12	0.465	0.346	0.189	0.289	134
13	0.492	0.326	0.182	0.291	134
14	0.399	0.408	0.193	0.222	134
15	0.239	0.158	0.603	1.040	247
16	0.322	0.437	0.241	0.256	247
17	0.255	0.320	0.425	0.520	252
18	0.527	0.232	0.241	0.431	162
19	0.248	0.254	0.498	0.688	252
20	0.105	0.286	0.609	0.725	252

*This source produces 11.3% visible and ultraviolet and 88.7% infrared radiation.

by applying Eqs. B. 7, 5 and 6, in that order. These equations are derived by differentiation and integration of the Arrhenius law.

Method III is a successive approximation procedure (Newton Raphson technique), based on the integral of the Arrhenius law, Eq. B.8. The procedure is designed to converge to that optimum value of the implicitely appearing reaction order n in Eq. B. 8 which yields the least-square fit for Eq. B.8 with the highest possible measure of determinateness, namely the greatest square (B) of the correlation coefficient (r) (s. Eq. B. 12).

It should be clear that Methods I and II require analog or digital differentiation of measured data resulting in loss of accuracy. Method III is considered the most reliable one of the three methods.

Apparatus, operating procedures, sample preparation, data evaluation techniques and thermograms are presented in Appendix B. I of this report.

The following tables list the results of the kinetics data evaluation; a separate table is presented for each method employed and for each process evaluated. Tables produced by Methods I and III list the GIRCFF Fabric Number, the heating rate, the temperature range of the reaction, the mass fraction decomposed or removed from the fabric during the process, then the three reaction parameters n, E and k_o, and finally the number B which is equal to unity for perfect fit (all data points fall on straight line of least-square fit), and equal to zero for useless correlations (circular cloud of uniform data point density). Tables produced by Method II show, instead of the temperature range, the temperature T_m, the decomposition λ_m and the rate $\dot{\lambda}_m$ at the time of maximum decomposition rate $\dot{\lambda}_m$.

Tables II-A. 6, 7 and 8 represent water desorption data, measured at Georgia Tech and evaluated by Methods I, II and III, respectively.

Table II-A.6 Kinetics Parameters for Moisture Desorption of GIRCFF Fabrics In Dynamic Air Atmosphere Evaluated by Method I.

GIRCFF Fabric No.	Heating Rate (^{o}C/min.)	Temperature Range (^{o}C)	$\frac{m_{\infty}}{m_{o}}$ (%)	Order of Reaction	Activation Energy (kcal./mole)	Pre-exponential Factor (1/sec.)	B
5	25	28-146	4.28	2.5	24.4	2.73×10^{14}	0.958
5	10	36-120	1.85	2.1	23.4	1.00×10^{13}	0.973
10	25	28-169	3.05	2.4	20.0	1.26×10^{11}	0.982
10	10	25-120	4.04	2.2	20.7	5.55×10^{11}	0.964
18	25	31-140	2.87	2.2	23.9	5.68×10^{13}	0.977
18	10	30-103	2.35	2.4	33.4	6.43×10^{20}	0.954
19	25	28-120	2.52	2.1	23.0	2.52×10^{13}	0.955
19	10	35-90	1.29	2.0	30.8	4.86×10^{18}	0.951
11	25	28-94	2.24	2.2	28.8	6.72×10^{17}	0.976

Table II-A.7 Kinetic Parameters for Moisture Desorption on GIRCFF Fabrics In Dynamic Air Atmosphere Evaluated by Method II.

GIRCFF Fabric No.	Heating Rate (^{o}C/min.)	$\frac{m_{\infty}}{m_{o}}$ (%)	λ_m (1/sec) $\times 10^{-3}$	λ_m	t_m (^{o}C)	Order of Reaction	Activation Energy (kcal./mole)	Pre-exponential Factor (1/sec.)
5	25	4.28	3.50	0.47	58	2.3	22.4	7.87×10^{10}
5	10	1.85	2.84	0.53	71	1.7	24.2	1.35×10^{11}
10	25	3.05	3.50	0.49	67	2.1	22.2	2.48×10^{10}
10	10	4.04	2.00	0.48	56	2.2	18.4	8.55×10^{7}
18	25	2.87	5.00	0.54	68	1.6	30.7	1.54×10^{15}
18	10	2.35	2.50	0.54	52	1.6	18.6	5.87×10^{8}
19	25	2.52	3.67	0.52	60	1.8	16.5	2.64×10^{7}
19	10	1.29	3.17	0.58	56	1.3	19.9	2.14×10^{9}
11	25	2.24	4.34	0.52	50	1.8	20.2	9.65×10^{9}

Tables II-A.9 and 10 list the parameters of exothermic reactions as measured at Georgia Tech. Method II was not employed in the evaluation of this process.

Tables II-A.6 through 10 represent processes in atmospheric air.

Tables II-A.11 and 12 present the data evaluation by Georgia Tech of the measurements obtained by Dr. McCarter at NBS [B.48], from thermal decompositions in nitrogen atmosphere. These measurements produce decomposition rates directly and differentiation of decomposition history with respect to time is not necessary.

It can be seen from the tabulated data that

(i) data reduction by Method III produces the best representation,

(ii) decomposition of cellulosic fabrics in nitrogen (Dr. McCarter data) reach peak decomposition rates at temperatures above the ignition temperature measured in oxidizing atmospheres.

The last observation does not neccessarily constitute an inconsistency but the high values of E and k_o for GIRCFF Fabrics indicate that pyrolysis of thermoplastics takes place above the melting temperature and does not contribute to the destruction processes investigated here.

Table II-A.8 Kinetic Parameters for Moisture Desorption on GIRCFF Fabrics In Dynamic Air Atmosphere Evaluated by Method III.

GIRCFF Fabric No.	Heating Rate (^{o}C/min.)	Temperature Range (^{o}C)	$\frac{m_{\infty}}{m_{o}}$ (%)	Order of Reaction	Activation Energy (kcal./mole)	Pre-exponential Factor (1/sec.)	B
5	25	28-146	4.28	2.6	23.3	4.88×10^{13}	0.994
5	10	36-120	1.85	2.3	25.4	2.12×10^{14}	0.993
10	25	28-169	3.05	2.9	21.4	1.77×10^{12}	0.992
10	10	25-120	4.04	2.2	21.2	1.00×10^{12}	0.985
18	25	31-140	2.87	2.5	25.1	4.74×10^{14}	0.993
18	10	30-103	2.35	2.3	30.4	3.40×10^{18}	0.981
19	25	28-120	2.52	2.3	24.3	2.00×10^{14}	0.991
19	10	35-90	1.29	3.3	48.2	7.70×10^{30}	0.989
11	25	28-94	2.24	2.9	36.1	1.28×10^{23}	0.994

Table II-A.9 Kinetic Parameters for Exothermal Decomposition of GIRCFF Fabrics In Dynamic Air Atmosphere Evaluated by Method I.

GIRCFF Fabric No.	Heating Rate (^{o}C/min.)	Temperature Range (^{o}C)	$\frac{m_{\infty}}{m_{o}}$ (%)	Order of Reaction	Activation Energy (kcal./mole)	Pre-exponential Factor (1/sec.)	B
2	25	337-490	95.4	2.1	67.9	2.30×10^{19}	0.914
2	10	333-477	95.8	1.6	70.6	2.01×10^{20}	0.969
5	25	248-392	90.9	2.8	53.6	1.26×10^{18}	0.796
5	10	240-394	90.0	3.2	50.2	2.09×10^{16}	0.621
8	25	240-411	93.3	4.7	41.0	3.24×10^{12}	0.829
10	25	178-579	91.6	2.5	24.4	5.60×10^{6}	0.985
10	10	191-416	91.4	0.9	30.2	3.95×10^{8}	0.878
11	25	256-426	90.6	3.6	56.8	2.89×10^{18}	0.553
11	10	249-392	86.9	3.9	53.6	2.58×10^{17}	0.554
12	10	235-505	93.0	2.1	29.2	9.50×10^{6}	0.461

Table II-A.9 (Continued)

GIRCFF Fabric No.	Heating Rate (^{o}C/min.)	Temperature Range (^{o}C)	$\frac{m_{\infty}}{m_{o}}$ (%)	Order of Reaction	Activation Energy (kcal./mole)	Pre-exponential Factor (1/sec.)	B
13	25	253-425	94.9	2.6	55.0	9.49×10^{17}	0.855
13	10	246-433	91.4	1.5	47.4	6.07×10^{14}	0.901
17	25	240-415	99.3	6.2	36.7	7.19×10^{10}	0.918
17	10	224-380	94.7	2.6	36.6	3.58×10^{10}	0.987
18	25	238-408	90.4	2.5	55.8	4.87×10^{18}	0.730
18	10	245-349	90.9	2.8	79.8	5.17×10^{27}	0.695
19	25	202-389	88.4	3.9	34.6	1.43×10^{11}	0.872
19	10	166-376	87.7	4.7	32.8	2.82×10^{10}	0.562

Table II-A.10 Kinetic Parameters for Exothermal Decomposition of GIRCFF Fabrics in Dynamic Air Atmosphere Evaluated by Method III.

GIRCFF Fabric No.	Heating Rate (^{o}C/min.)	Temperature Range (^{o}C)	$\frac{m_{\infty}}{m_{o}}$ (%)	Order of Reaction	Activation Energy (kcal./mole)	Pre-exponential Factor (1/sec.)	B
2	25	337-490	95.4	0.8	48.7	9.81×10^{12}	0.980
2	10	333-477	95.8	1.2	54.4	8.35×10^{14}	0.964
5	25	248-392	90.9	1.5	35.8	1.26×10^{11}	0.955
5	10	240-394	90.0	1.6	34.1	9.20×10^{9}	0.976
8	25	240-411	93.3	1.8	30.7	3.12×10^{8}	0.986
10	25	178-579	91.6	3.2	28.6	2.52×10^{8}	0.985
10	10	191-416	91.4	1.0	22.6	3.30×10^{5}	0.966
11	25	256-426	90.6	1.4	31.3	6.97×10^{8}	0.941
11	10	249-392	86.9	1.0	29.3	8.63×10^{7}	0.966
12	10	235-505	93.0	0.1	18.8	9.78×10^{2}	0.983

Table II-A.10 (continued)

GIRCFF Fabric No.	Heating Rate (^{o}C/min.)	Temperature Range (^{o}C)	$\frac{m_{\infty}}{m_{o}}$ (%)	Order of Reaction	Activation Energy (kcal./mole)	Pre-exponential Factor (1/sec.)	B
13	25	253-425	94.9	1.4	32.7	3.08×10^{9}	0.937
13	10	246-433	91.4	2.0	33.7	5.88×10^{9}	0.904
17	25	240-415	99.3	3.0	25.2	2.67×10^{6}	0.986
17	10	224-380	94.7	2.0	25.9	2.86×10^{6}	0.994
18	25	238-408	90.4	1.2	37.3	2.20×10^{11}	0.956
18	10	245-349	90.9	0.5	44.0	5.89×10^{13}	0.944
19	25	202-389	88.4	1.8	22.0	8.60×10^{5}	0.957
19	10	166-376	87.8	0.8	20.4	7.79×10^{4}	0.973

Table II-A.II Kinetic Parameters Evaluated from McCarter's Data on GIRCFF Fabrics Decomposing in Dynamic Nitrogen Atmosphere by Method I

GIRCFF Fabric No.	Heating Rate (^{o}C/min.)	Temperature Range (^{o}C)	$\frac{m_{\infty}}{m_{o}}$ (%)	Order of Reaction	Activation Energy (kcal./mole)	Pre-exponential Factor (1/sec.)	B
2	60	414-529	96.0	1.7	87.0	1.04×10^{24}	0.983
5	60	324-466	91.0	1.4	71.0	3.07×10^{21}	0.995
10	60	319-478	87.5	1.2	56.6	3.38×10^{16}	0.995
11	60	350-457	100.0	2.9	123.0	6.71×10^{38}	0.989
12	60	404-535	100.0	2.1	118.5	1.65×10^{33}	0.987
13	60	360-476	98.0	2.4	128.8	7.56×10^{40}	0.935
17	60	348-443	90.2	2.1	87.4	1.28×10^{27}	0.994
18	60	333-478	90.4	1.6	81.3	7.26×10^{24}	0.992
19	60	319-396	55.8	2.1	144.4	5.33×10^{49}	0.978

Table II-A.12 Kinetic Parameters Evaluated for McCarter's Data on GIRCFF Fabrics Decomposing in Dynamic Nitrogen Atmosphere by Method II.

GIRCFF Fabric No.	Heating Rate (^{o}C/min)	$\frac{m_{\infty}}{m_{o}}$ (%)	$\dot{x}_{m}$ (i/sec) $\times 10^{-2}$	x_{m}	t_{m} (^{o}C)	Order of Reaction	Activation Energy (kcal./mole)	Pre-exponential Factor (1/sec.)
2	60	96.0	2.05	0.59	487	1.2	71.7	3.15×10^{16}
5	60	91.0	1.93	0.61	417	1.1	52.5	9.54×10^{12}
10	60	87.5	1.97	0.61	425	1.1	54.6	2.85×10^{13}
11	60	100.0	2.50	0.44	407	2.7	112.3	1.06×10^{30}
12	60	100.0	2.80	0.60	473	1.2	92.1	8.33×10^{21}
13	60	98.0	2.62	0.59	409	1.2	73.7	1.20×10^{19}
17	60	90.2	2.27	0.54	409	1.6	74.2	1.80×10^{19}
18	60	90.4	1.93	0.60	420	1.2	54.9	4.98×10^{13}
19	60	55.8	4.64	0.47	354	2.3	159.7	7.90×10^{46}

The measurements of reaction enthalpy was derived from the thermal analysis of transient heating as experienced by sample and reference crucibles. This analysis is presented in Appendix B.1, Section e.(ii).

Table II-A.13 presents the measured enthalpies of water desorption which differ from the values computed on the basis of experimental data in "Moisture in Textiles", edited by J. W. S. Hearle and R. H. Peters [II-3]. Particulary the data obtained for the fire retardant GIRCFF Fabric No. 19 and the cotton GIRCFF Fabric No. 18 are higher by a factor of as much as two.

Table II-A.14 presents the heat of fusion for melting fabrics which agree with literature data (Appendix C.)

This completes the description of the results obtained from the property measurement program. This program should not be considered complete in as much as there is still considerable detail left to be investigated, primarily temperature dependence and rate dependence of properties. However enough information has been gathered to advance the analytical understanding of ignition far beyond its present state.

Table II-A.13 Reaction Enthalpies for Endothermal Decomposition of GIRCFF Fabrics in Dynamic Air Atmosphere.

GIRCFF Fabric No.	Heating Rate (°C/min.)	Temperature Range (°C)	$\frac{w_\infty}{m_o}$ (%)	Enthalpy of Reaction (cal./g.)
5	10	36-120	1.85	40.2
10	10	25-120	4.04	14.1
18	25	31-140	2.87	17.7
18	10	30-103	2.35	38.1
19	25	28-120	2.52	66.1
19	10	35-90	1.29	32.2
11	25	28-94	2.24	25.7

Table II-A.14 Heats of Fusion of Thermoplastic GIRCFF Fabrics and Blends Undergoing Melting in Dynamic Air Atmosphere.

GIRCFF Fabric No.	Heating Rate (°C/min.)	Temperature Range (°C)	Melting Temp. (°C)	Heat of Fusion (cal./g.)
2	25	194-307	252	22.2
8	25	199-280	242	10.5
11	25	210-288	245	20.0
12	25	225-357	283	23.4
17	25	225-272	240	6.8

B. Fabric Ignition and Moisture Effects

1. Objective

The purpose is to measure the ignition or destruction time, defined as the time between the instantaneous fabric exposure to a well-known, uniform and time-invariant heat flux and the fabric ignition or destruction, as recognized through the appearance of a flame or the melt-through of the fabric. The strict destinction is made, however, between ignition and destruction.

The destruction time is the key parameter (Eq. III-4) in the definition of destruction probability and must be measured to verify its analytical prediction.

A Radiative Ignition Time Apparatus (RITA) was designed, constructed and operated with design specifications established to meet the above objective as follows [I-2]:

a. Uniform and time-invariant, radiative sample heating at heat fluxes between 0.25 and 15.8 W/cm^2 (800 to 50,000 $Btu/(hr\ ft^2)$), and over circular sample areas of 25 mm diameter (1 inch).
b. Sample exposure transients of less than two milliseconds to achieve sufficiently time-independent exposures of as low as 20 milliseconds. Maximum exposure time of 60 seconds.
c. Remote infrared flame detection consistent in response time with Item (b).
d. Radiative heat pulse control from 5 to 30 seconds with accuracy of ± 0.2 seconds. Monitoring pulse times with an accurarcy of ± 0.01 seconds.
e. Fabric sample conditioning and fabric exposure in a temperature and humidity controlled environment, between the limits of 5 and $32^{o}C$ and between 5 and 95% relative hummidity.

The design features and operating principles of RITA are found in Appendix B. 1 of Reference [I-2]. Supplementary modifications implemented during this contract period are discussed in Appendix B.2. Achievements and results are discussed below.

2. Achievements, Radiative Ignition Time Measurement

a. Apparatus Modification. The ignition time under radiative heating is measured in the Radiative Ignition Time Apparatus in accordance with the procedures described in Reference [I-2], Appendix B1. The Radiative Ignition Time Apparatus has been installed in a thermally and psychrometrically controlled enclosure. Air and water cooling lines, electrical power and signal lines were fed through the enclosure walls. The timing and time monitoring circuit was revised to prevent cross-coupling and interference. The apparatus works satisfactorily in both single and double shutter modes. For additional details see Appendix B.2.

b. Convective Heat Loss Measurements. A chromel-alumel thermocouple of 0.02 in diameter was interwoven with a sample of cotton fabric, GIRCFF Fabric No. 5, to measure fabric heating prior to exposure, as a result of shutter warm-up and to measure the convective film coefficient on the fabric directly. The results obtained served to select the correct preheating time to attain radiative equilibrium on the heater without preheating the fabric.

A 200-mesh stainless steel screen was mounted in place of the fabric and used as one leg of a thermocouple junction. The convective film coefficient was evaluated from heating and cooling curves of the screen, subjected to radiative heating and passive cooling.

c. Ignition Time Measurements. The total of 94 ignition time measurements (single shutter mode) has been carried out at 30 and 90 percent relative humidity on both thermoplastic and cellulosic fabrics, in the power flux range between 0.25 and 15 W/cm^2.

An ignition and melting time summary for 18 of 20 GIRCFF fabrics has been prepared and is presented.

d. The Effect of Moisture on Ignition Time was found to be small and consistent for the cotton fabric No. 5. Here moisture prolonges ignition time between 11 and 13 percent in the range of irradiation from 6 to 13.80 W/cm^2. For cotton Fabric No. 18, however, an apparently doubled ignition time was observed. Results for Fabric No. 5 are averaged from 200 ignition tests while the results for Fabric No. 18 are from a single series of four ignition tests.

3. Results, Radiative Ignition Time

a. Ignition Time Summary. Figure II-B.1 presents the summary of the ignition and melting times, in non-dimensional form, for the Primary and Secondary GIRCFF Fabrics. Presented are the non-dimensional destruction time $(N_{Fo})_{i,m}$ (i for ignition, m for melting) versus the normalized radiant heating intensity q^*_{rad}, namely

$$(N_{Fo})_{i,m} = \frac{(\frac{k}{\delta})\tau_{i,m}}{c(\rho\delta)} \qquad \text{(II-B.1)}$$

versus

$$q^*_{rad} = \frac{(1-\tilde{\rho})\, W_o}{(\frac{k}{\delta})\ (T_{i,m}-T_\infty)} \qquad \text{(II-B.2)}$$

where

(k/δ) thermal conductance (W/cm^2c), or ratio of thermal conductivity k over thickness δ

$\tau_{i,m}$ ignition time (s), or melting time

$(\rho\delta)$ mass per unit of fabric area, (g/cm^2), ρ is fabric density

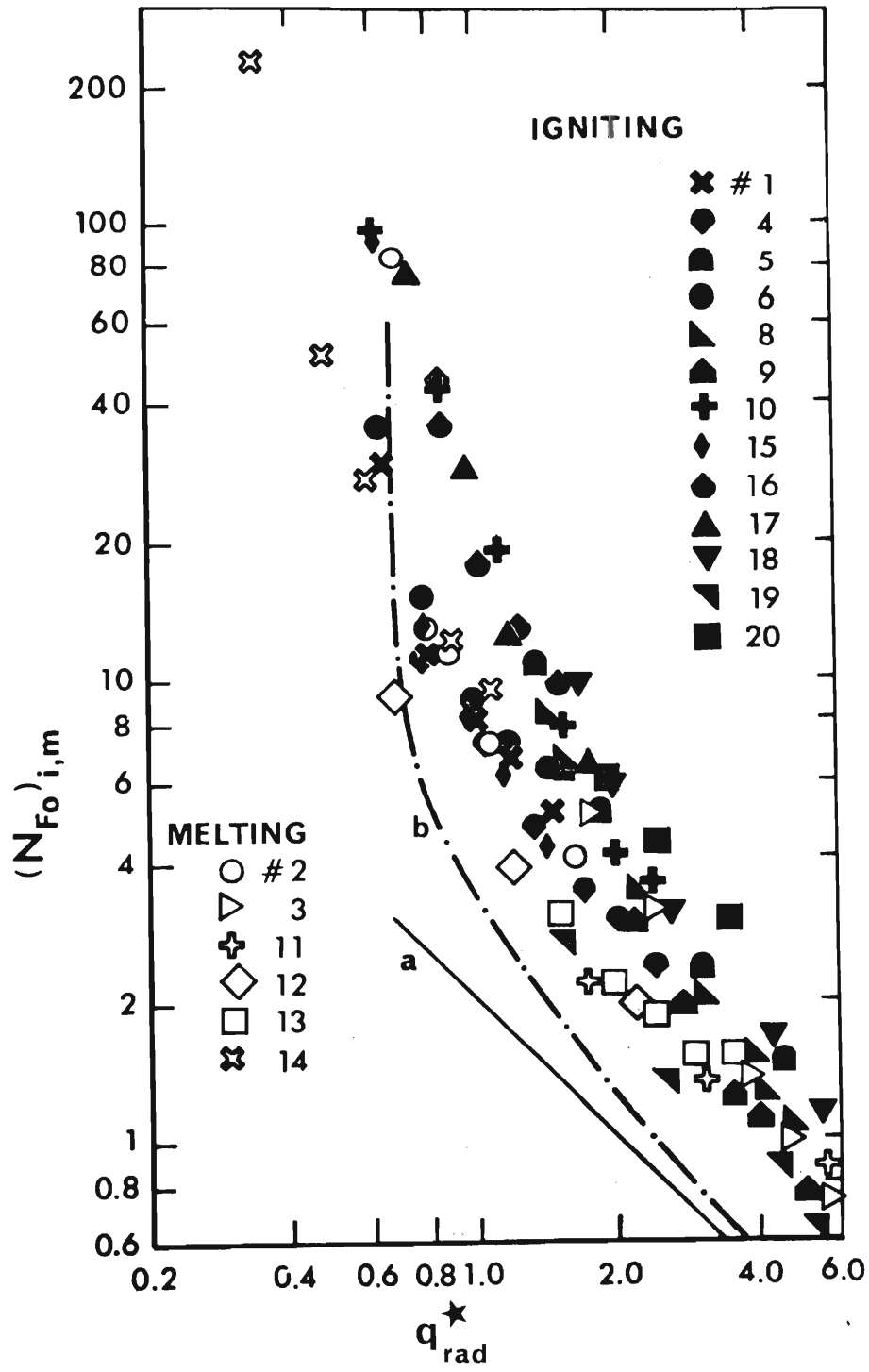

Figure II-B.1. Normalized Ignition or Melting vs Normalized Radiative Heating Intensity Curve a represents inert heating without losses, Curve b represents inert heating with convective loss, both computed for Fabric No. 10.

c specific heat of fabric, (Ws/g K)

$T_{i,m}$ ignition temperature (self ignition) (K), or melting temperatures

T_{∞} initial fabric temperature, equal to environmental temperature, (K)

$\tilde{\rho}$ radiative fabric reflectance, (-)

Open symbols in Figure II-B.1 represent melting, solid symbols igniting fabrics.

Figure II-B.1 reveals, by virtue of the nondimensional presentation that all the fabrics shown undergo essentially thermally similar processes prior to ignition despite of considerable differences in properties. The variation of ignition times at constant heating rate, exhibited in Figure II-B.1 is due to the differences in optical thickness (see Equation III-5) and in endothermic reactions prior to ignition or melting. The choice of parameters is derived as shown in Reference [I-2] in Chapter III of this report.

b. The Effect of Moisture on Ignition Time is shown in Table II-B.1 below. Given are the ignition time at relative hummidity below 10% and the times obtained at 30% and 90% r.h. No significant humidity effect could be detected below 30% r.h.

Humidity effects appear to vary greatly from fabric to fabric. The data reported for GIRCFF Fabric No. 5 were derived from the statistical analysis discussed in Section C below and are far better confirmed than the data for other fabrics. Further investigation of the moisture effect is in progress, particularly for the fabrics whose τ_{90}/τ_{30} ratio was found to be far in excess of the theoretically expected value of approximately 1.30. Data on GIRCFF Fabric No. 18 are preliminary.

4. Conclusions

The following conclusions can be drawn from the experimental experience gained through radiative ignition time measurements so far:

Table II-B.1
Effect of Moisture on Ignition Time

GIRCFF Fabric No.	Irradiation W/cm^2	Ignition Time sec ≤10%	Ignition Time sec 30%	Ignition Time sec 90%	Ratio $\frac{\tau_{90}}{\tau_{30}}$
4	5.80	27.0	27.0		
(cotton)	7.90	17.2	21.0		
	8.80	14.9	14.2		
	13.00	8.8	8.8		
	15.80	6.8	7.0		
5	6.50		31.9	35.5	1.112
(cotton)	9.25		13.1	15.7	1.199
	13.80		7.1	7.8	1.100
6	7.60	40.0	38.0		
(P.E.)	9.60	22.8	21.0		
	13.70	13.6	12.0		
9	6.50		37.2	41.7	1.22
(cotton)	9.50		20.0	25.2	1.260
	13.70		12.2	16.0	1.311
18	7.55		20.9	25.9	1.240
(cotton)	11.00		11.1	19.0	1.712
	13.70		8.2	15.3	1.867
	17.50		5.8	13.0	2.24

(i) Radiative ignition time measurements are repeatable and produce results of higher consistency than other heating modes.

(ii) Ignition and melting of fabrics is preceeded by similar processes with endothermic reaction, radiative and convective cooling.

(iii) No single process appears to affect radiative ignition as strongly as convective cooling. Free convection can prevent ignition at heating rates below specific levels, defined as the product of convective film coefficient times the excess fabric temperature at ignition, over the environmental temperature. Convection will prevent ignition under these circumstances in the absence of exothermic processes. The difficulty in predicting the critical level of net power absorption lies in the problem of predicting the convection film coefficient and the radiative absorptance at ignition temperature.

(iv) Moisture contained in hygroscopic fabrics (condensation and hydroxyl-water combinations) retards ignition significantly. It can be said that at 90% relative humidity the cellulosic fabric can gain enough moisture such that its ignition time is 30% longer than the ignition time of the dry fabric. Moisture effects below 30% r.h. are insignificant.

C. Effect of Heating Mode on Fabric Ignition Time

1. Objectives

The purpose is to provide a well defined convective heat source in the form of a gas flame and to measure fabric ignition time under two conditions: (i) the stationary ignition test, where the fabric is suddenly exposed to a time-invariant convective heat source, and (ii) the dynamic ignition test, where the fabric is moved into the convective heat source at a predetermined velocity. In the first case one measures the time from initial exposure of the fabric to the heat source, to ignition or melting. In the second case one measures the time from initial contact of the fabric with the flame at the flame boundary, to ignition or melting, for different rates of motion of the fabric through the flame.

The Convective Ignition Time Apparatus was designed to meet the following conditions:

(a) Specimen heating by a gaseous fuel-air flame, provided by a variable fuel rate and variable air rate burner.

(b) Specimen exposure to the flame, for the static tests, through a shutter providing full exposure of the sample in five-hundredths of a second or less.

(c) Specimen side of shutter not to exceed 150^{o}F, to avoid preheating of the sample.

(d) Specimen transport for the dynamic tests at different speeds between 2 in/sec and near zero.

The major components of the Convective Ignition Time Apparatus are the shutter system, the gas burner, the sample transport system, and instrumentation for flame characterization, ignition detection and timing.

2. Achievements

a. Flame Characterization

The experimentally controlled independent variables of static fabric exposure are

(i) fabric position within the flame,

(ii) air-fuel mass ratio, and

(iii) total air and fuel mass flow rate.

All three variables affect flame temperature and convective film coefficient at the fabric, i.e. convective heat flux to the fabric, as well as oxygen availability within the flame.

The instrumentation used in the measurement of air and fuel flow rates, flame temperature and temperature distributions, species distribution in the flame, and inert body film coefficients, is discussed in detail in Appendix B.3.

(i) Air-Fuel Ratios

After some preliminary tests the mass flow rates of the fuel and the air were mapped to establish the usable ranges of the Blast Type, Fisher Scientific Co. Burner. Specifically the flow rates were used to evaluate the stoichiometric equivalence ratios and the volumetric flow rate of the reactive mixture prior to combustion. The results are used for the selection of constant stoichiometric equivalance ratios at different mixture flow rates for use in the fabric ignition tests.

(ii) Temperature Distribution

A thermocouple probe was constructed and used along with associated instrumentation (see Appendix B.3) to measure the temperature distributions in the flame. These were recorded for the two stoichiometric equivalence ratios used in the fabric ignition tests, at three different reactive mixture flow rates and at four different elevation planes above the top of the burner.

The flame temperature was recorded during each fabric test by the thermocouple placed in the fabric plane.

(iii) Composition

After some exploratory experiments in gas chromatography this method of gas sampling was abandoned for the present, due to the excessive time required for each sample analysis and the lack of adequate personnel to carry out these measurements. Consequently, the mass spectrometer was used alone to record CO_2 and O_2 concentration distribution in the flame, without fabric specimen. The records of the concentration distributions were obtained for each of the two stoichiometric equivalence ratios, at three different reactive mixture flow rates and at four different elevation planes above the top of the burner.

(iv) Convective Film Coefficient

In order to predict gas flame ignition time it is necessary to describe the fabric-flame interaction. The convective film coefficient must be known when the fabric is exposed to the convective heat source. Consequently seventy-three tests were carried out with a 200-mesh stainless steel screen, whereby the screen was exposed to the convective heat flux source in the same geometrical configuration as the fabric. Construction and other details concerning the stainless steel screen are given in Appendix B.3.

Of the seventy-three tests with the stainless steel screen fifty were carried out with the one-inch aperture fabric holder and twenty-three with the two-and-one-half-inch aperture fabric holder.

b. Ignition Time Under Convecting Heating

A total of 130 ignition time tests were run in the stationary ignition test mode. Each of the ten Primary GIRCFF Fabrics was exposed to a minimum of five

different intensities of convective heat flux at a stoichiometric equivalence ratio, ϕ, of 0.86, and with a fabric holder aperture of 2.5 inches. In additon, three of the fabrics were exposed to the convective heat flux source through a one-inch fabric holder aperture, two of the fabrics were exposed to the convective heat flux source with $\phi = 1.2$, and one fabric was exposed to the convective heat flux source at a 45^{o} angle from the horizontal. Ingnition or destruction times were measured successfully for all ten Primary GIRCFF Fabrics. These times range range from 0.15 to 9.20 seconds.

The Convective Ignition Time Apparatus was tested to determine the interval of time from the instant the two shutters separate to full exposure of the fabric. This interval of time is about 6 milliseconds and 15 milliseconds for the one-inch and two-and-one-half-inch fabric holders, respectively. Both of these are well within the design specifications. However, for the lowest fabric destruction time measured the 15 milliseconds represent 10% of this time.

The construction of the transport system for the dynamic tests has been completed and the assembly of the components on the Convective Ingition Time Apparatus carried out. In view of the effort spent in the determination of the convective film coefficients, ignition time tests in the dynamic mode were post-poned. These tests will be performed in the near future and the results will be reported later.

3. Experimental Results

a. Flame Characterization

(i) Air-Fuel Ratios

The mass flow rates of the fuel and the air measured for the Blast Type, Fisher Scientific Co. Burner were used to evaluate the stochiometric equi-valance ratios. The results are shown on Figures II-C.1, II-C.2 and II-C.3 for three ranges of total volumetric flow rates. The calibration curves of the

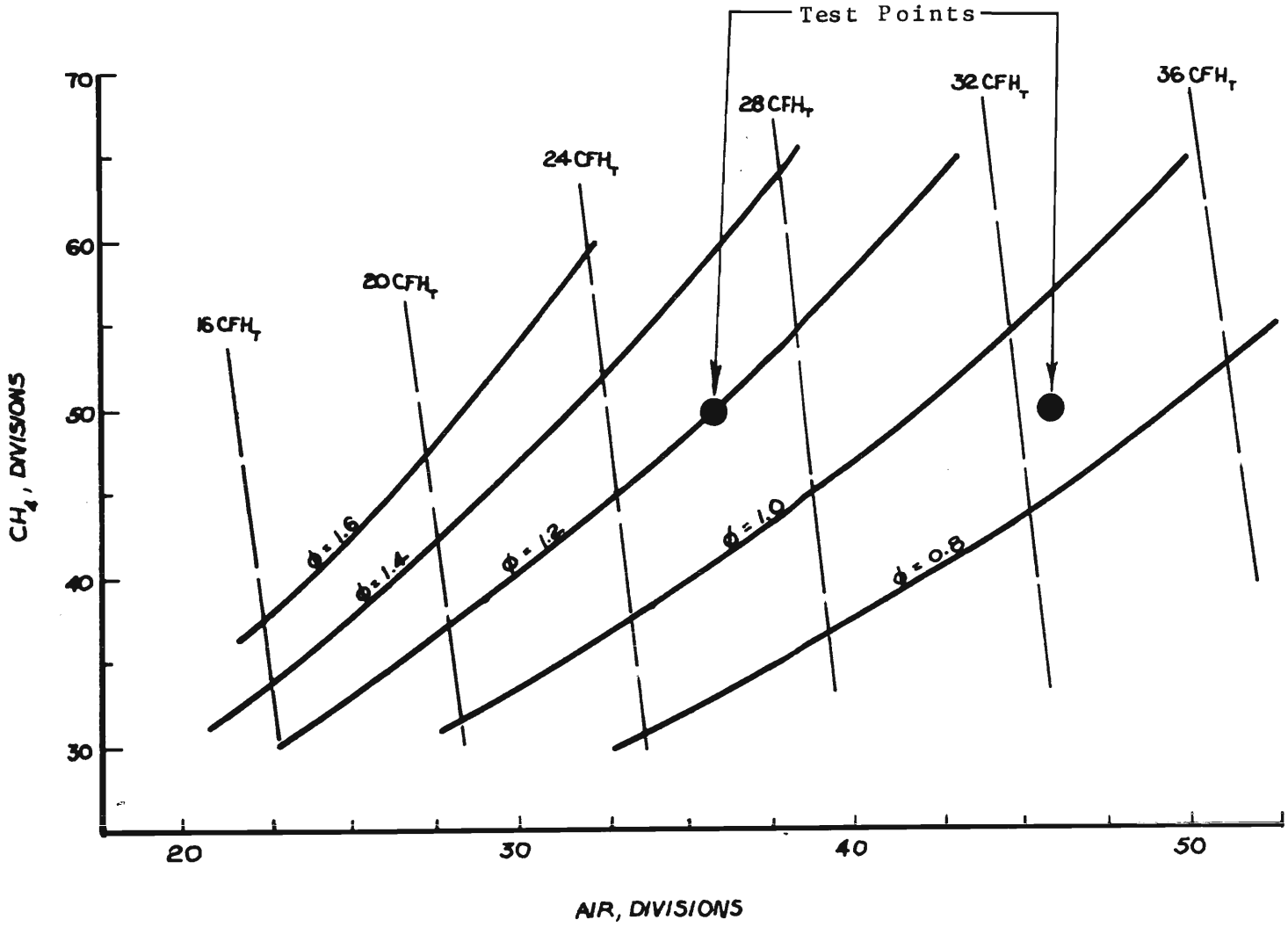

Figure II-C.1. Stoichiometric Equivalence Ratio ϕ and Total Volumetric Flow Rates $\dot{V}$ for the 37 mm Diameter Burner at Low Flow Rates.

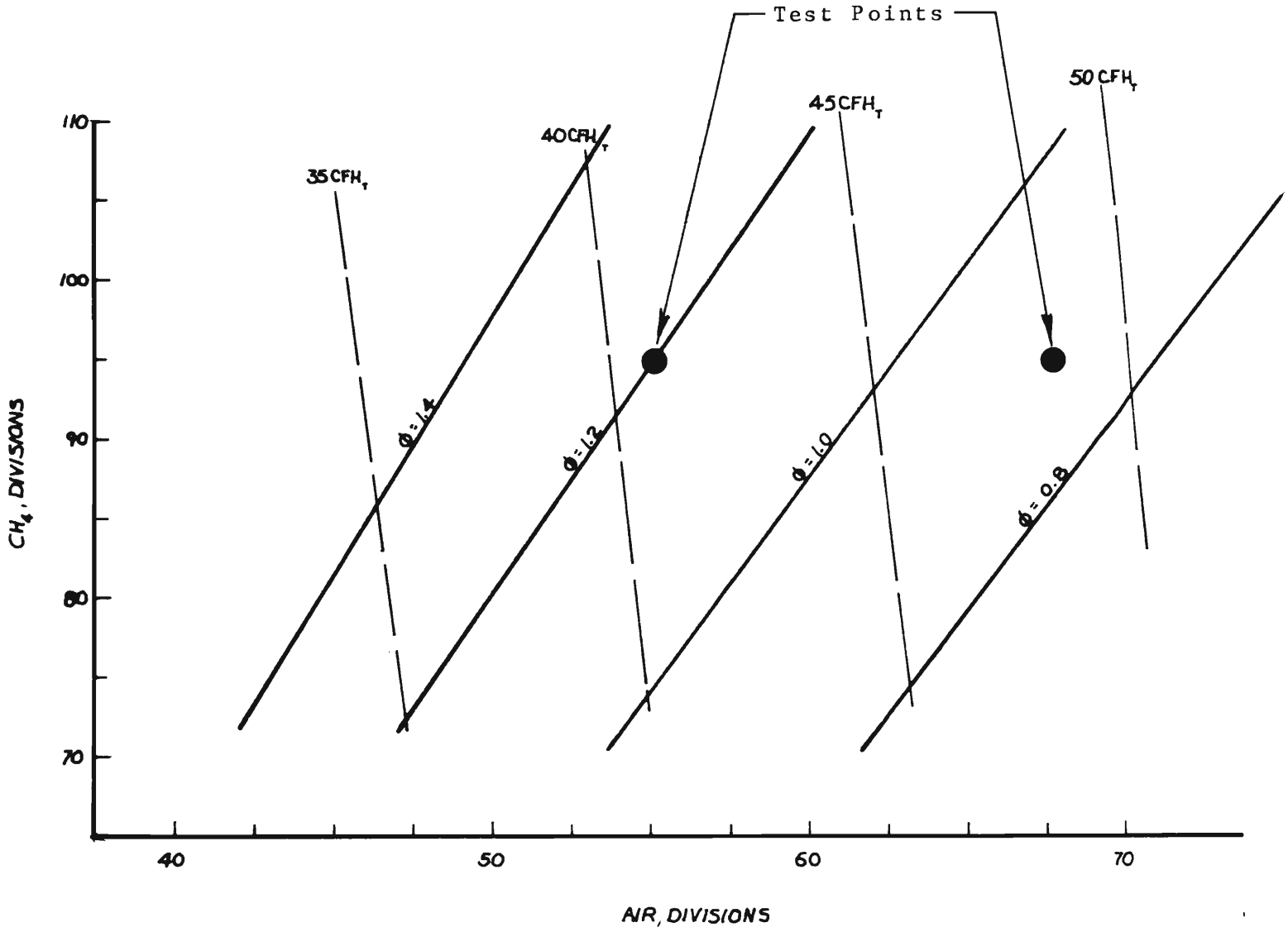

Figure II-C.2. Stoichiometric Equivalence Ratio ϕ and Total Volumetric Flow Rates $\dot{V}$ for the 37 mm Diameter Burner at Intermediate Flow Rates.

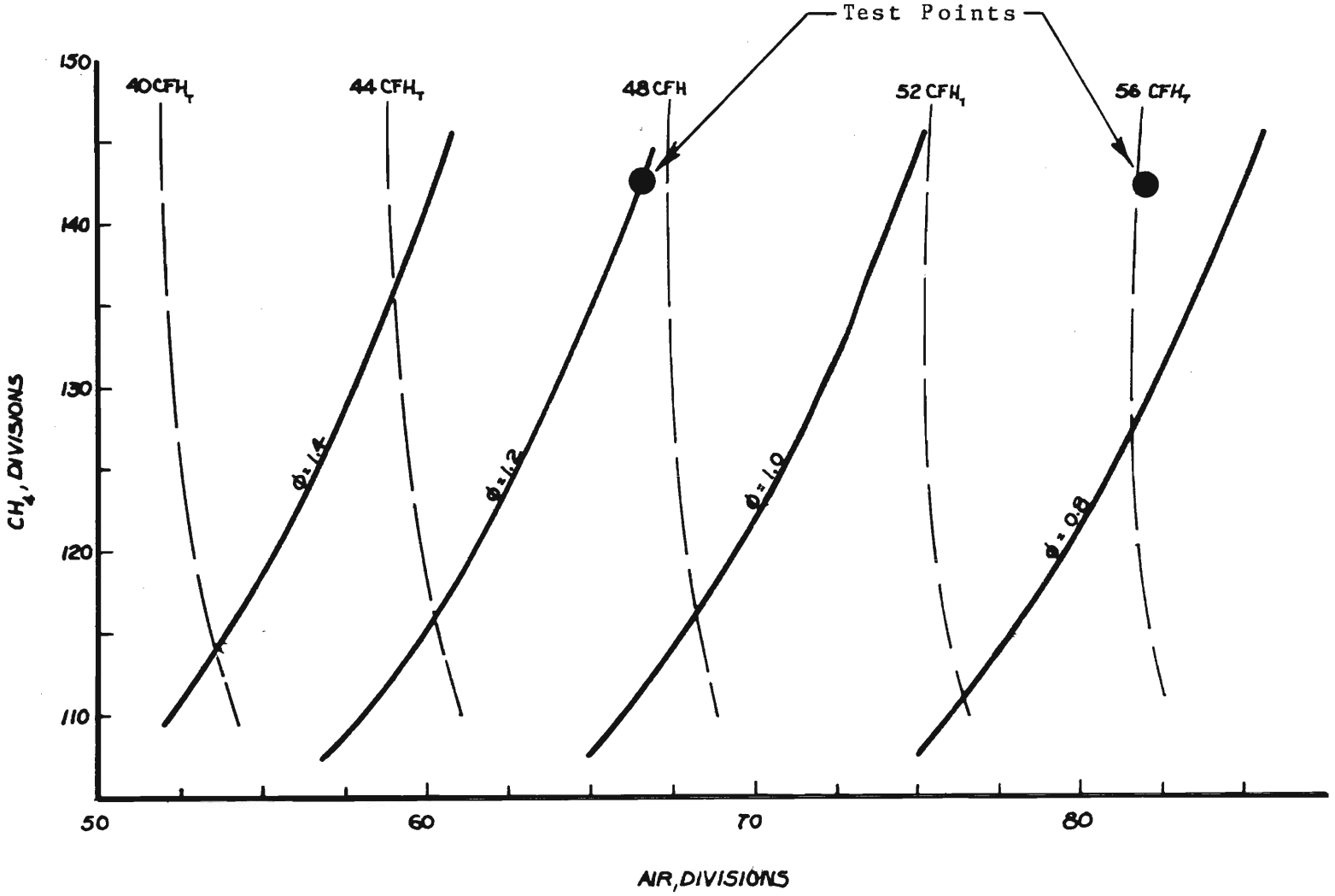

Figure II-C.3. Stoichiometric Equivalence Ratio ϕ and Total Volumetric Flow Rates V for the 37 mm Diameter Burner at High Flow Rates.

air and fuel meters are included in Appendix B.3. On the same three figures constant total volumetric flow rate curves are also shown. The six test conditions selected for the ignition time tests are shown as solid circles on these curves.

(ii) Temperature Distribution

Records of the Chromel Alumel thermocouple output, (EMF) obtained as the temperature probe is moved through the flame are shown on Figure II-C.4 through Figure II-C.8. These correspond to the different reactive mixture flow rates used at the two stochiometric equivalence ratios. The position of the thermocouple bead above the top of the burner is indicated on each curve. In each figure a scale representing one-inch of radial distance in the plane of the thermocouple motion, is shown.

(iii) Composition

The main interest, at present, in characterizing the flame with regards to the stable species, lies in the oxygen concentration in the plane where the fabric is exposed to the convective heat source. The mass spectrometer, with its associated instrumentation is capable of continuous sampling and analysis of one or two species. Qualitative records of radial CO_2 and O_2 concentrations, at several heights, as obtained with the quartz microprobe traversing the flame, are shown on Figures II-C.9 through II-C.17. The vertical position of the tip of the quartz microprobe above the top of the burner is indicated on each figure. Also, a scale representing a one-inch radial distance in the plane of the microprobe motion, is shown on each figure.

(iv) Convective Film Coefficient

The gas flame temperature T_f, the temperature T and its time rate of change, $dT/d\tau$ of the stainless steel screen after sudden exposure to the gas flame are used to infer the convective film coefficient, averaged over projected

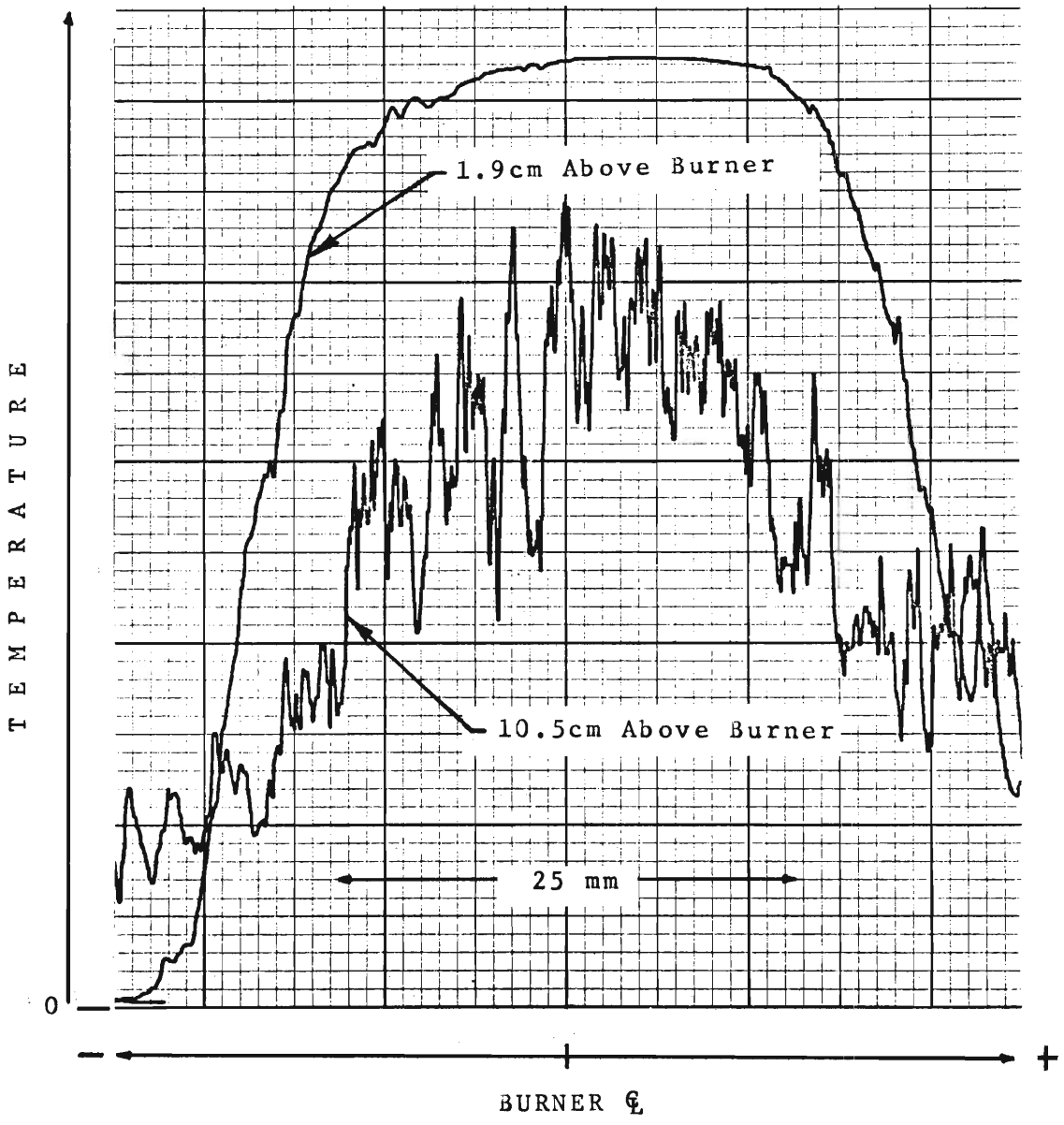

Figure II-C.4. Flame Temperature Profiles Obtained with Stoichiometric Equivalence Ratio $\phi = 0.86$ and for Low Flow Rate, $\dot{m}_{mix} = 1,285$ g/h.

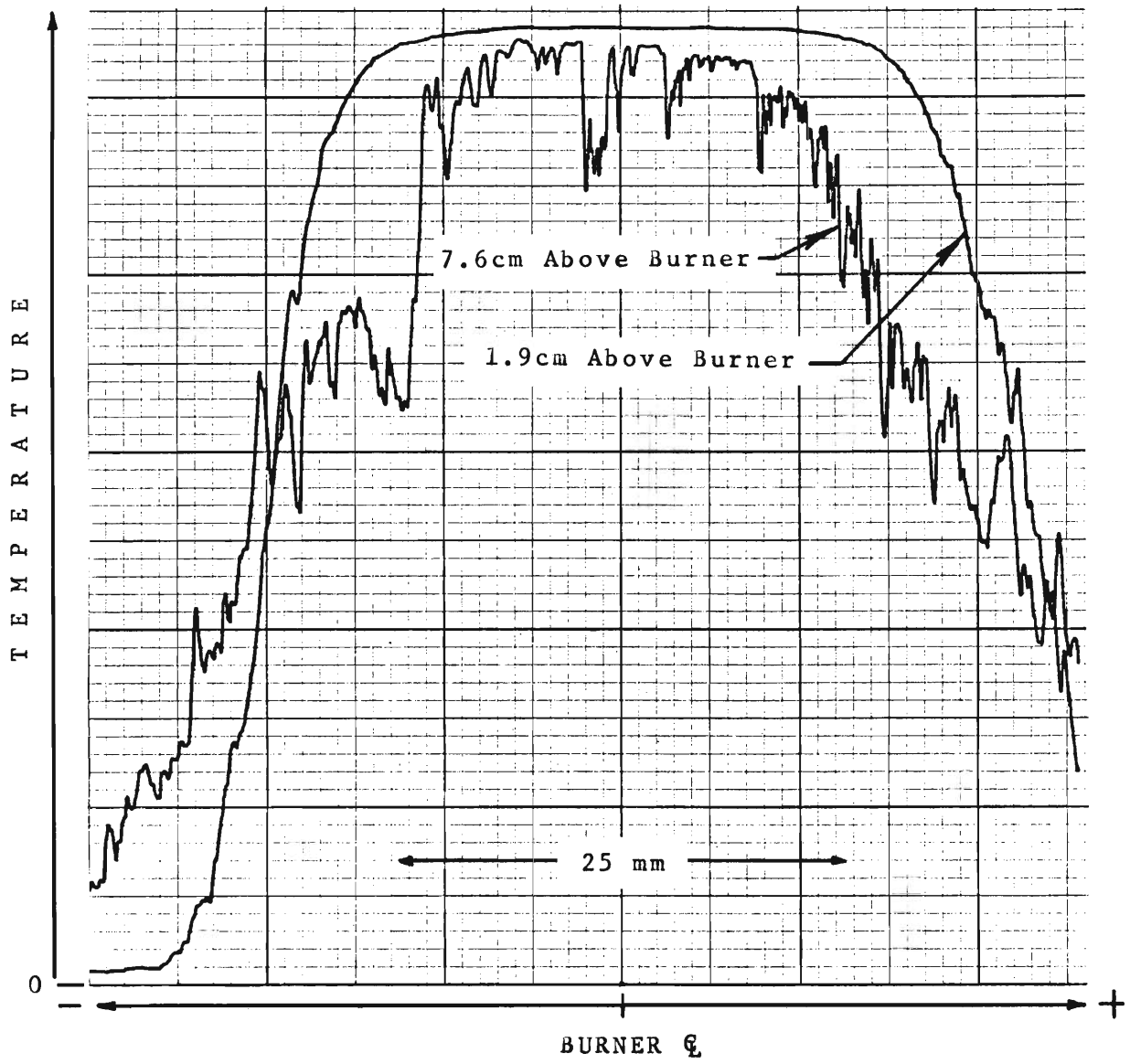

Figure II-C.5. Flame Temperature Profiles Obtained with Stoichiometric Equivalence Ratio $\phi = 0.86$ and for Intermediate Flow Rate, $\dot{m}_{mix} = 2,158$ g/h.

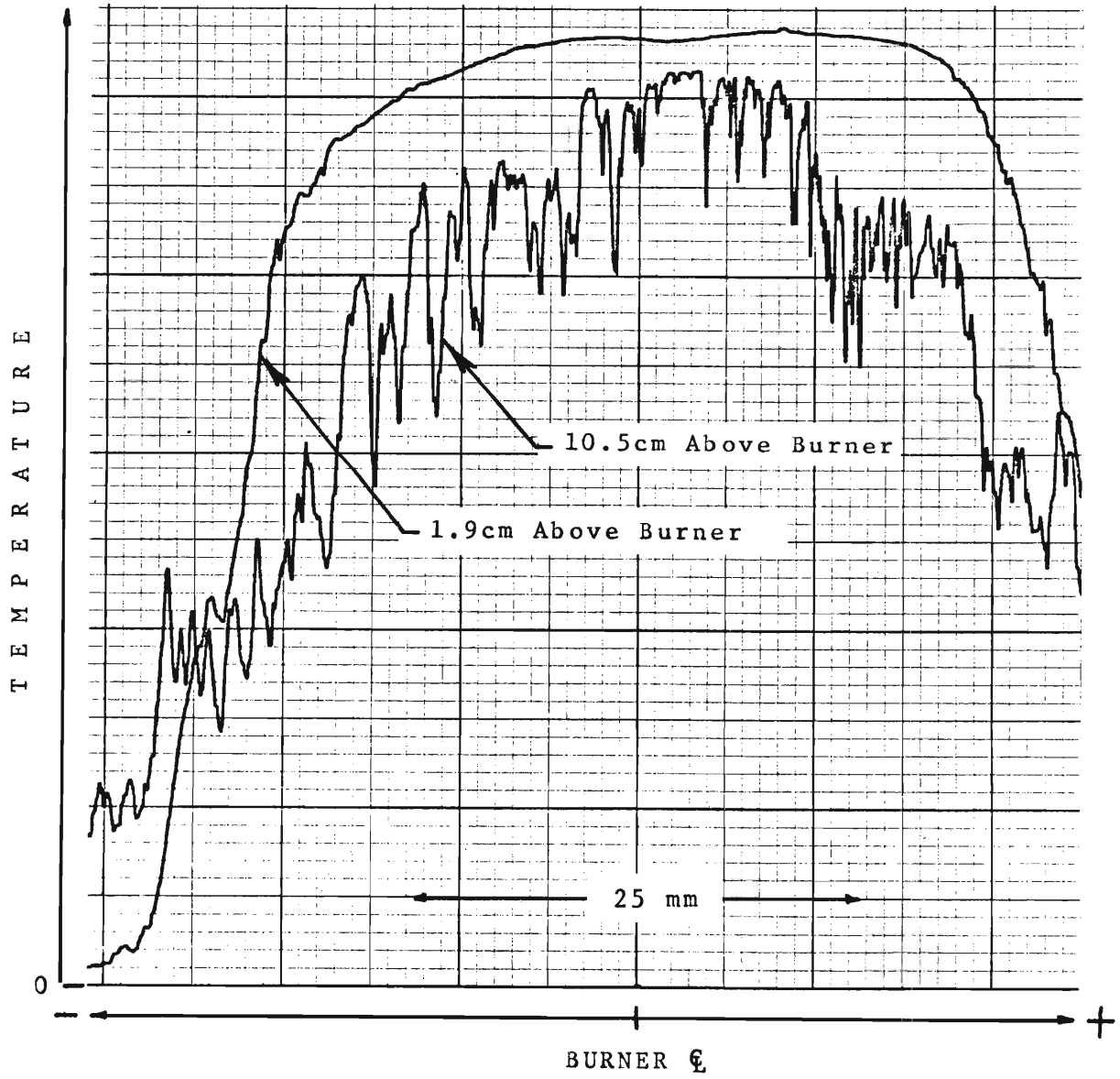

Figure II-C.6. Temperature Profiles Obtained with Stoichiometric Equivalence Ratio $\phi = 0.86$ and for High Flow Rate $\dot{m}_{mix} = 2,951$ g/h.

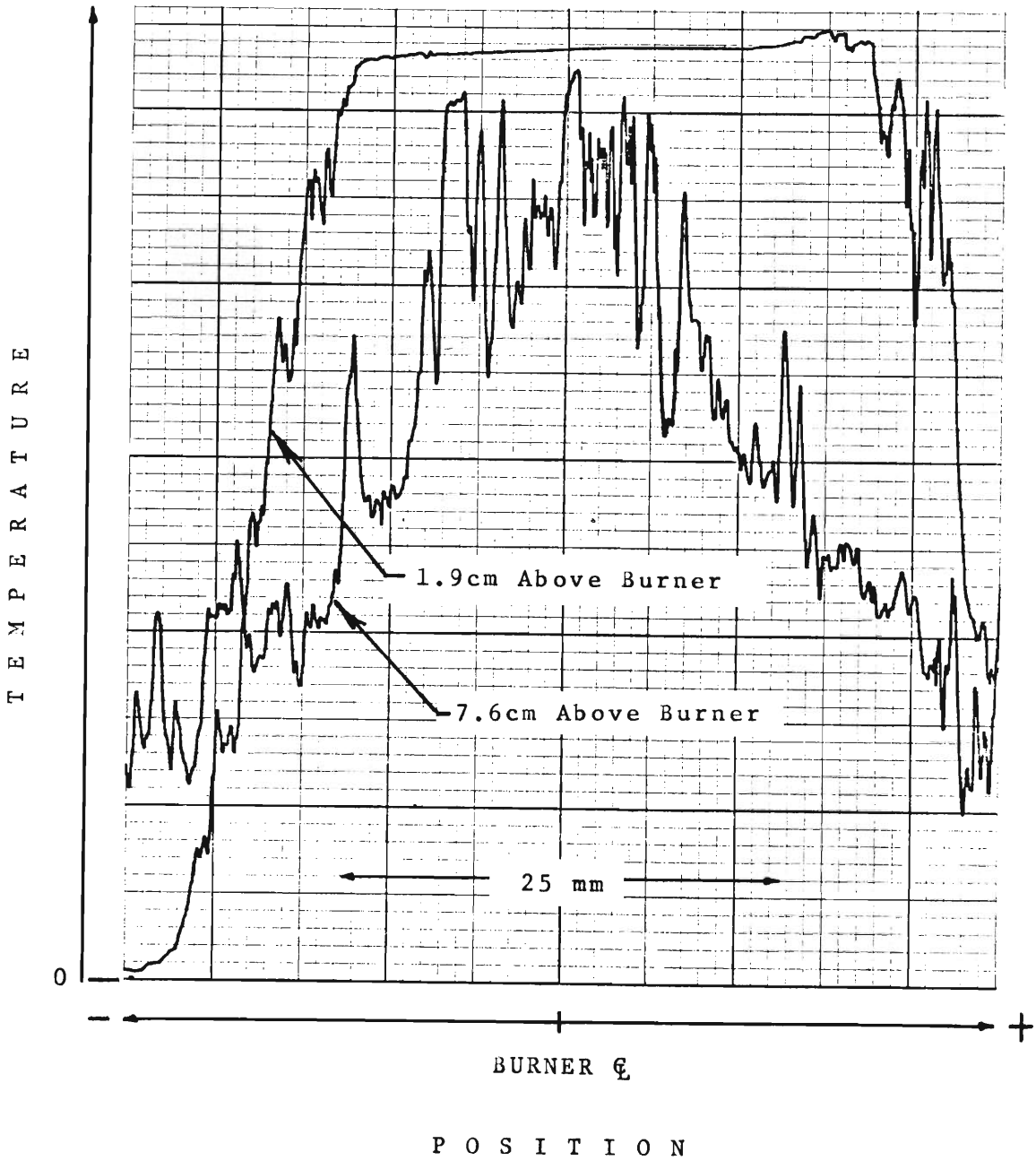

Figure II-C.7. Flame Temperature Profiles Obtained with Stoichiometric Equivalence Ratio $\phi = 1.20$ and for Low Flow Rate, $\dot{m}_{mix} = 928$ g/h.

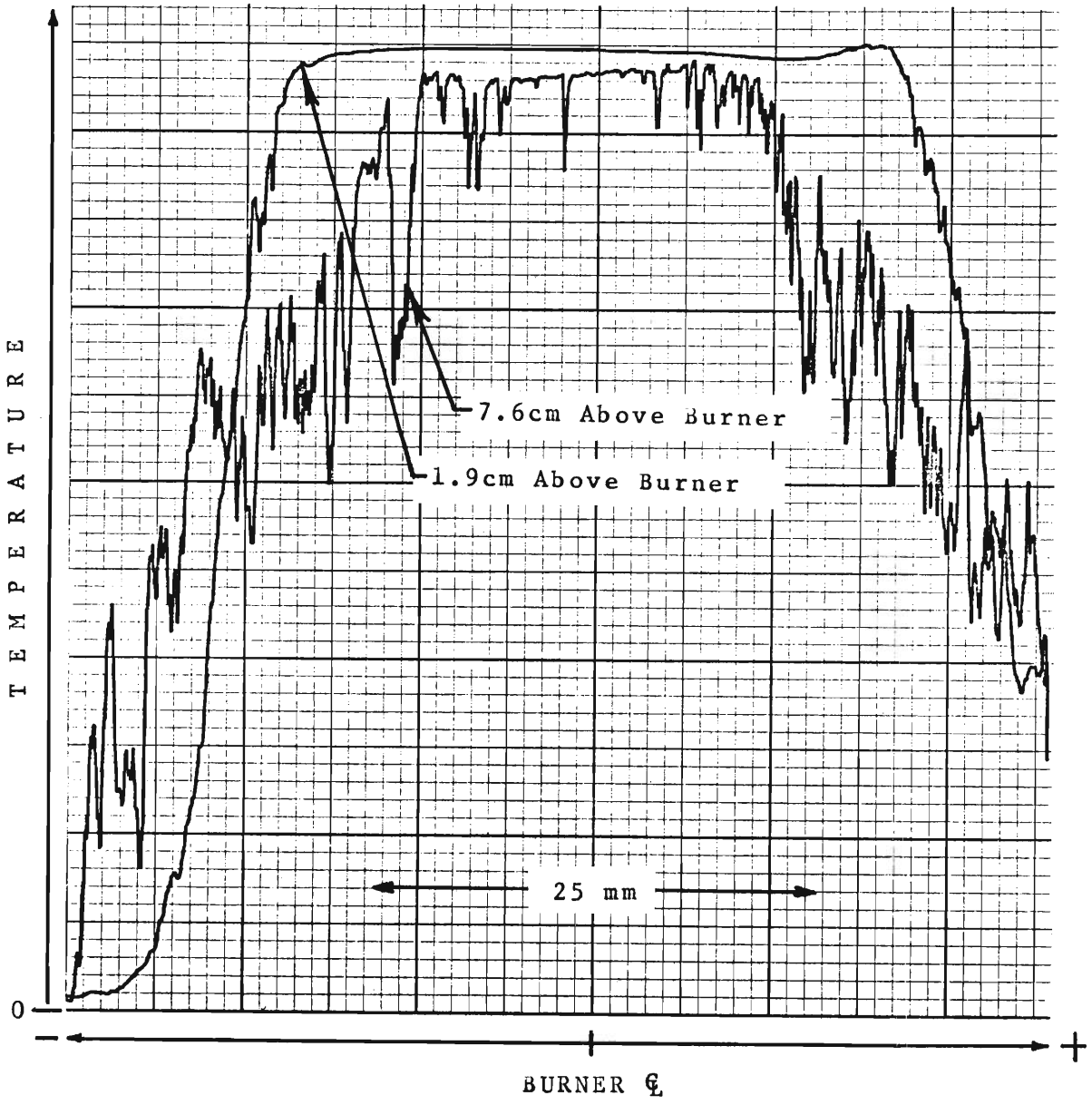

Figure II-C.8. Flame Temperature Profiles Obtained with Stoichiometric Equivalence Ratio $\phi = 1.20$ and for Intermediate Flow Rate, $\dot{m}_{mix} = 1,655$ g/h.

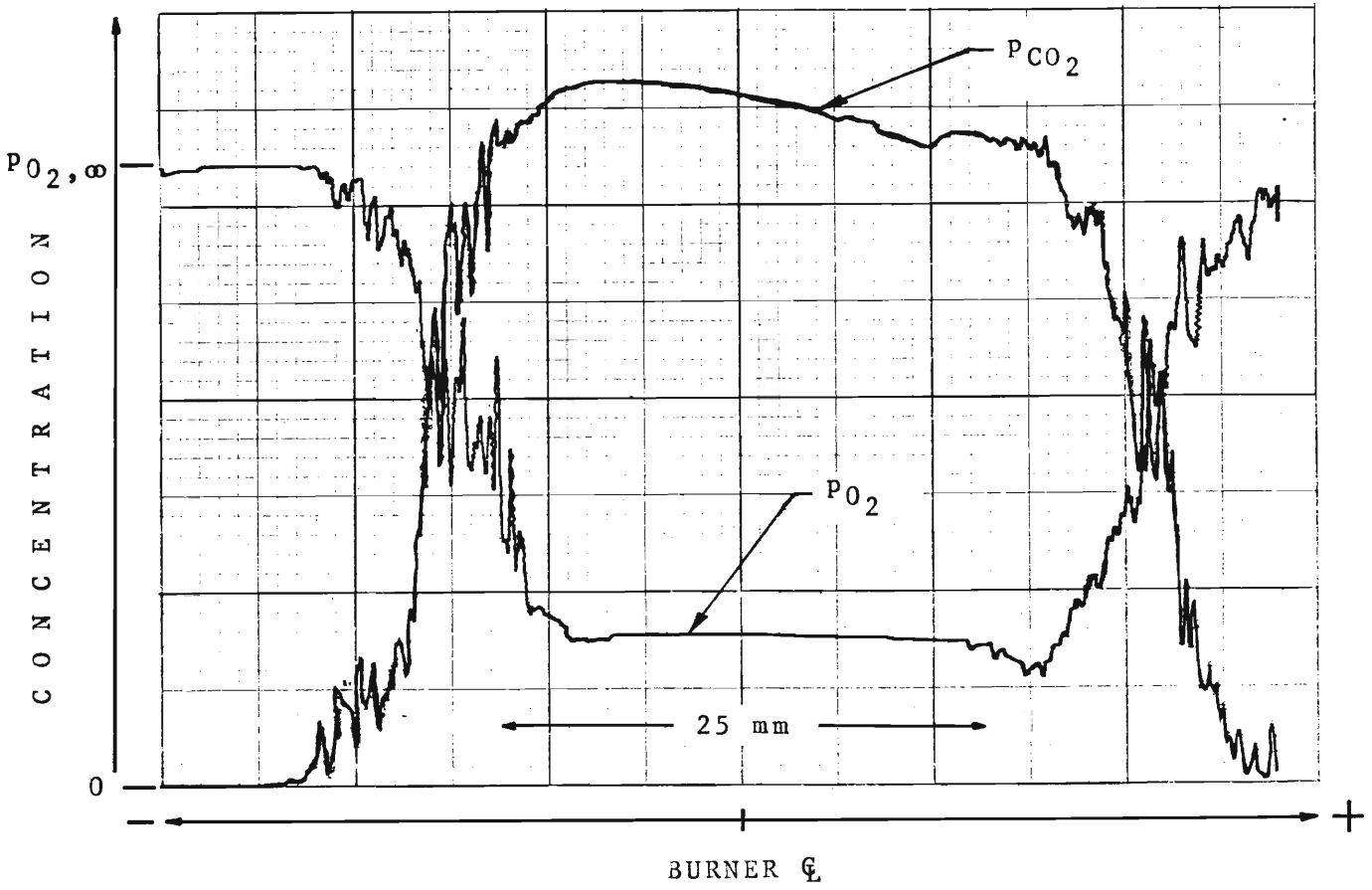

Figure II-C.9. Concentration Profiles of CO_2 and O_2, Obtained with Stoichiometric Equivalence Ratio $\phi = 0.86$ and Mass Flow Rate $\dot{m}_{mix} = 1,265$ g/h at 19 mm Above Burner Opening.

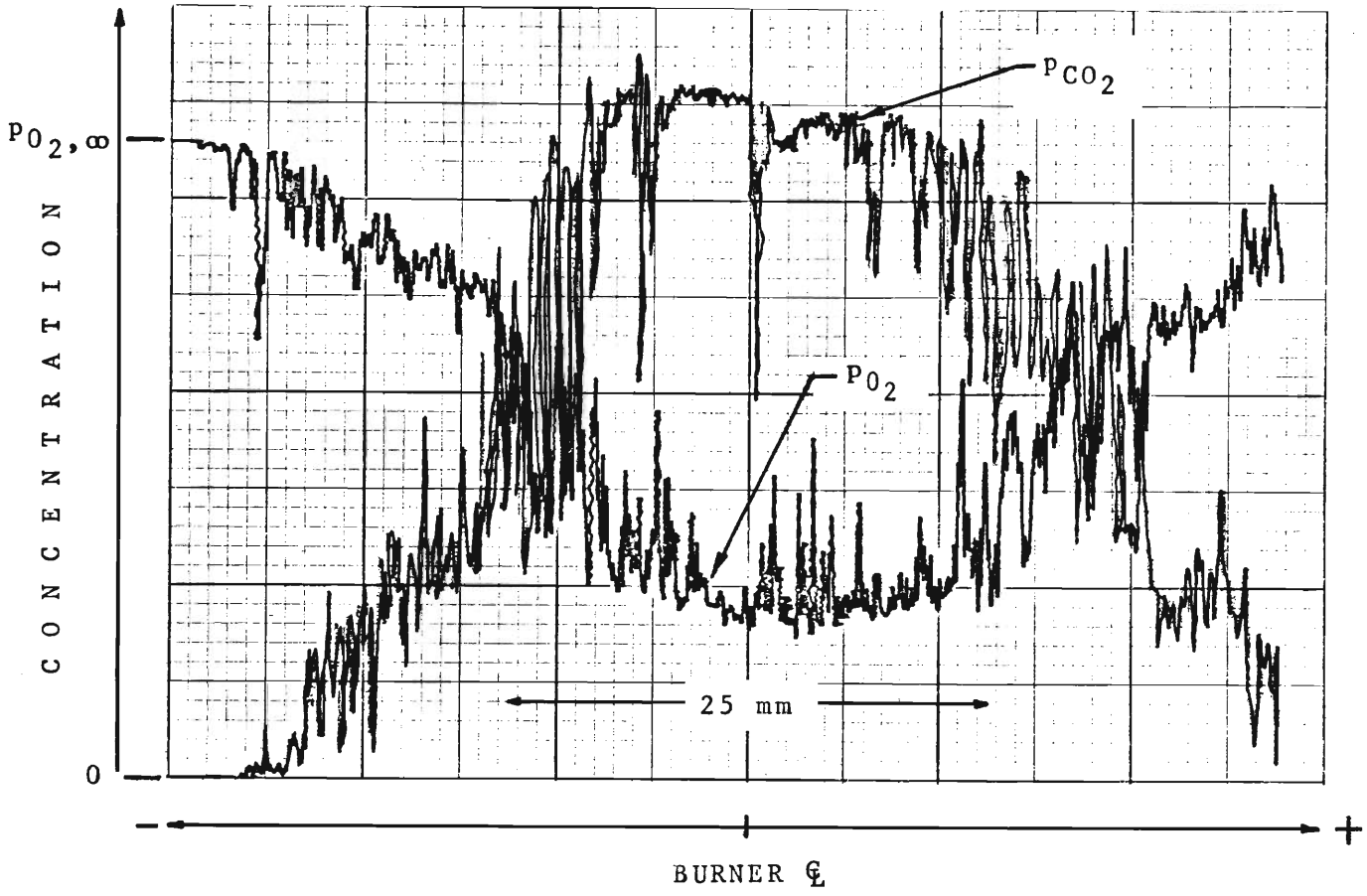

Figure II-C.10. Concentration Profiles of CO_2 and O_2, Obtained with Stoichiometric Equivalence Ratio $\phi = 0.86$ and Mass Flow Rate $\dot{m}_{mix} = 1,265$ g/h at 44 mm Above Burner Opening.

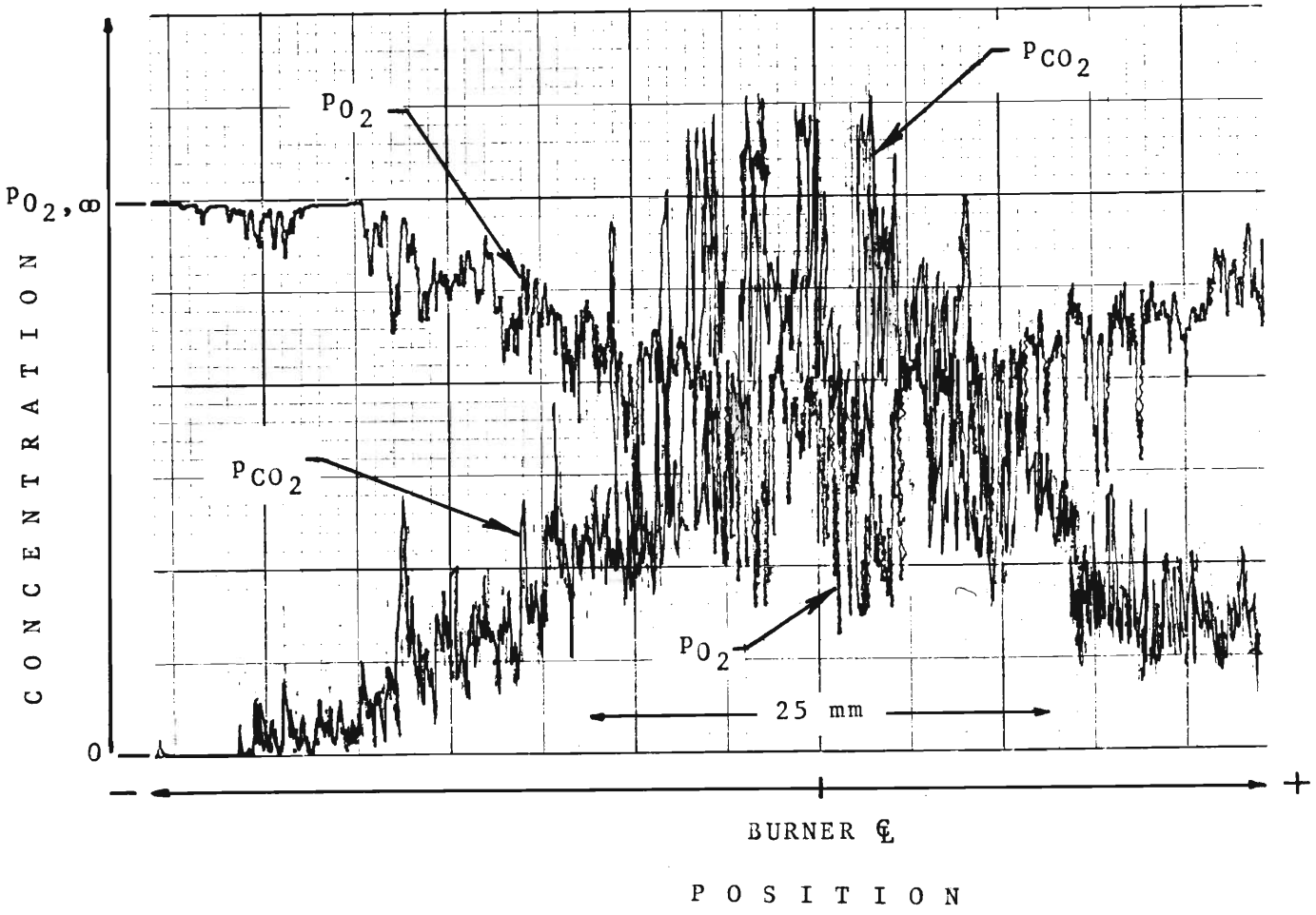

Figure II-C.11. Concentration Profiles of CO_2 and O_2, Obtained with Stoichiometric Equivalence Ratio ϕ = 0.86 and mass Flow Rate $\dot{m}_{mix}$ = 1,265 g/h at 76mm Above Burner Opening

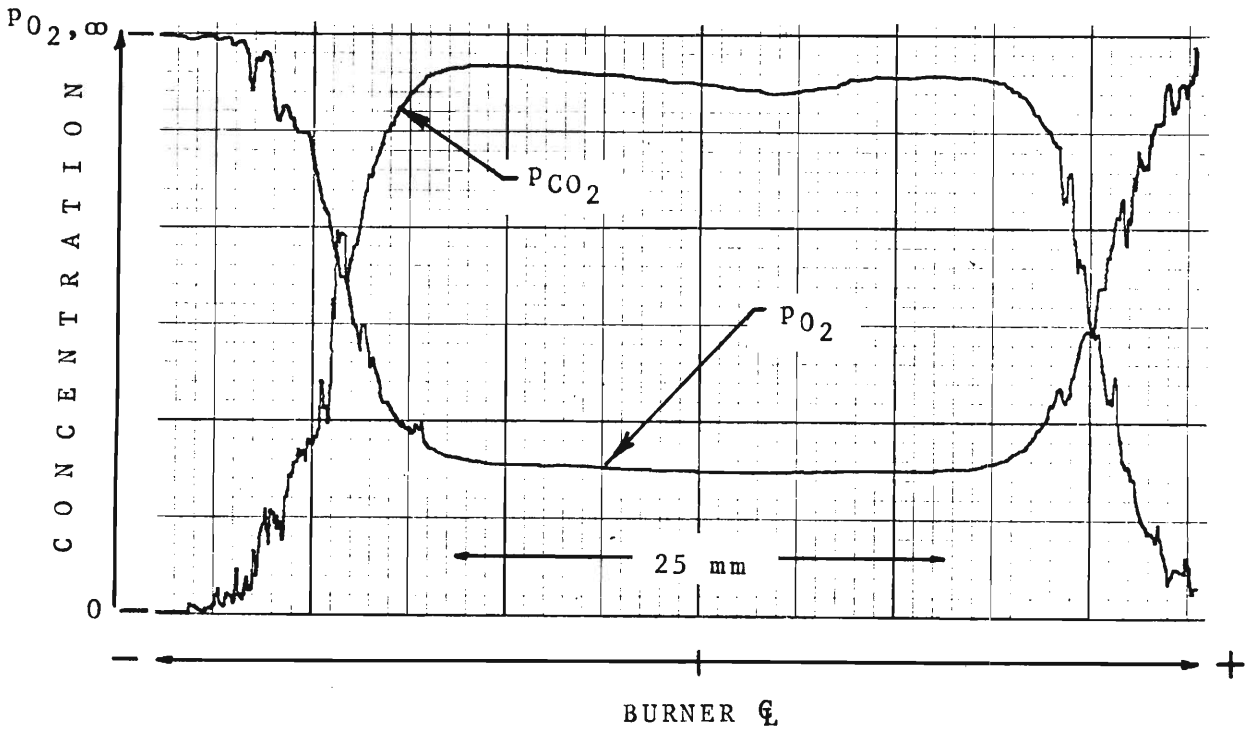

Figure II-C.12. Concentration Profiles of CO_2 and O_2, Obtained with Stoichiometric Equivalence Ratio $\phi = 0.86$ and Mass Flow Rate $\dot{m}_{mix} = 2,158$ g/h at 19 mm Above Burner Opening.

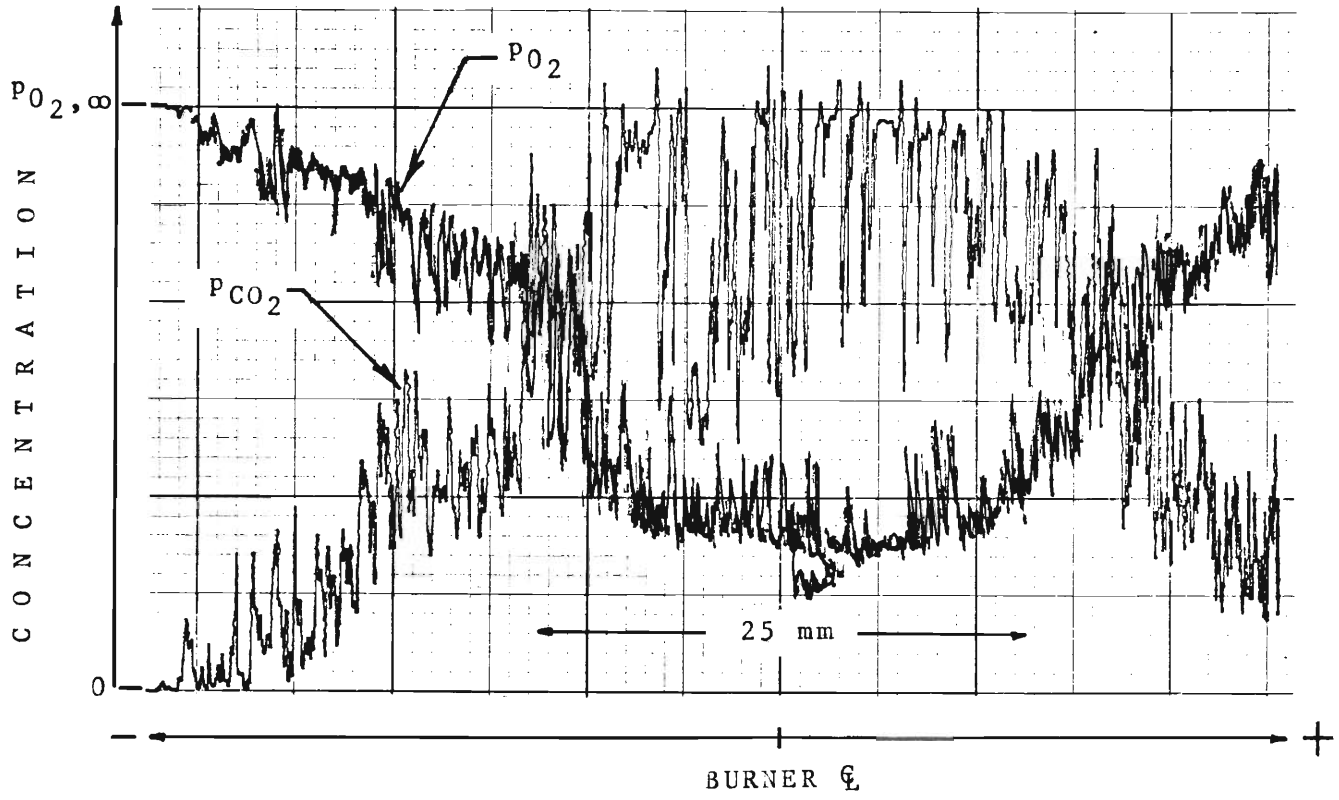

Figure II-C.13. Concentration Profiles of CO_2 and O_2, Obtained with Stoichiometric Equivalence Ratio $\phi = 0.86$ and Mass Flow Rate $\dot{m}_{mix} = 2,158$ g/h at 76 mm Above Burner Opening.

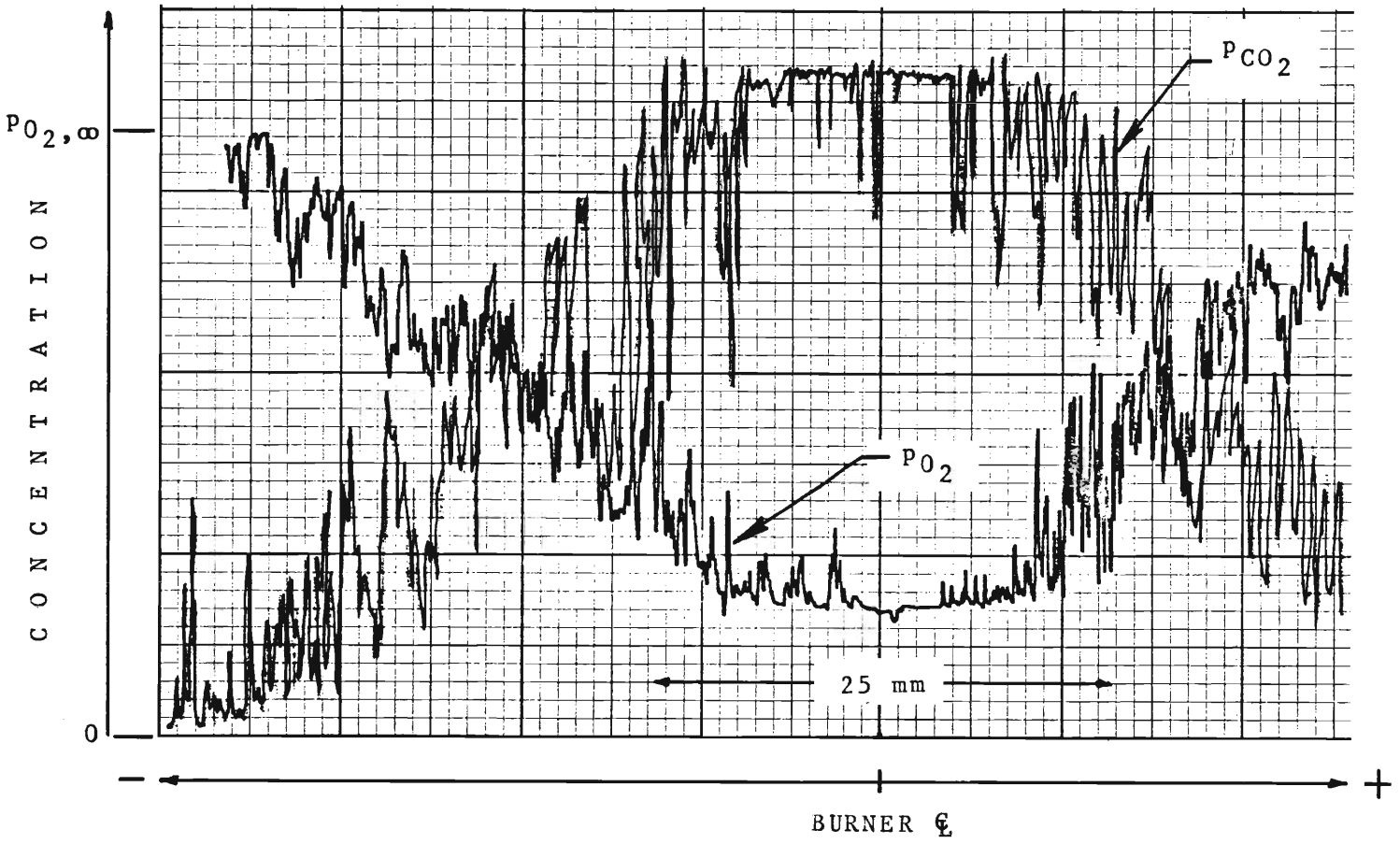

Figure II-C.14. Concentration Profiles of CO_2 and O_2, Obtained with Stoichiometric Equivalence Ratio $\phi = 0.86$ and Mass Flow Rate $\dot{m}_{mix} = 2,951$ g/h at 76 mm Above Burner Opening.

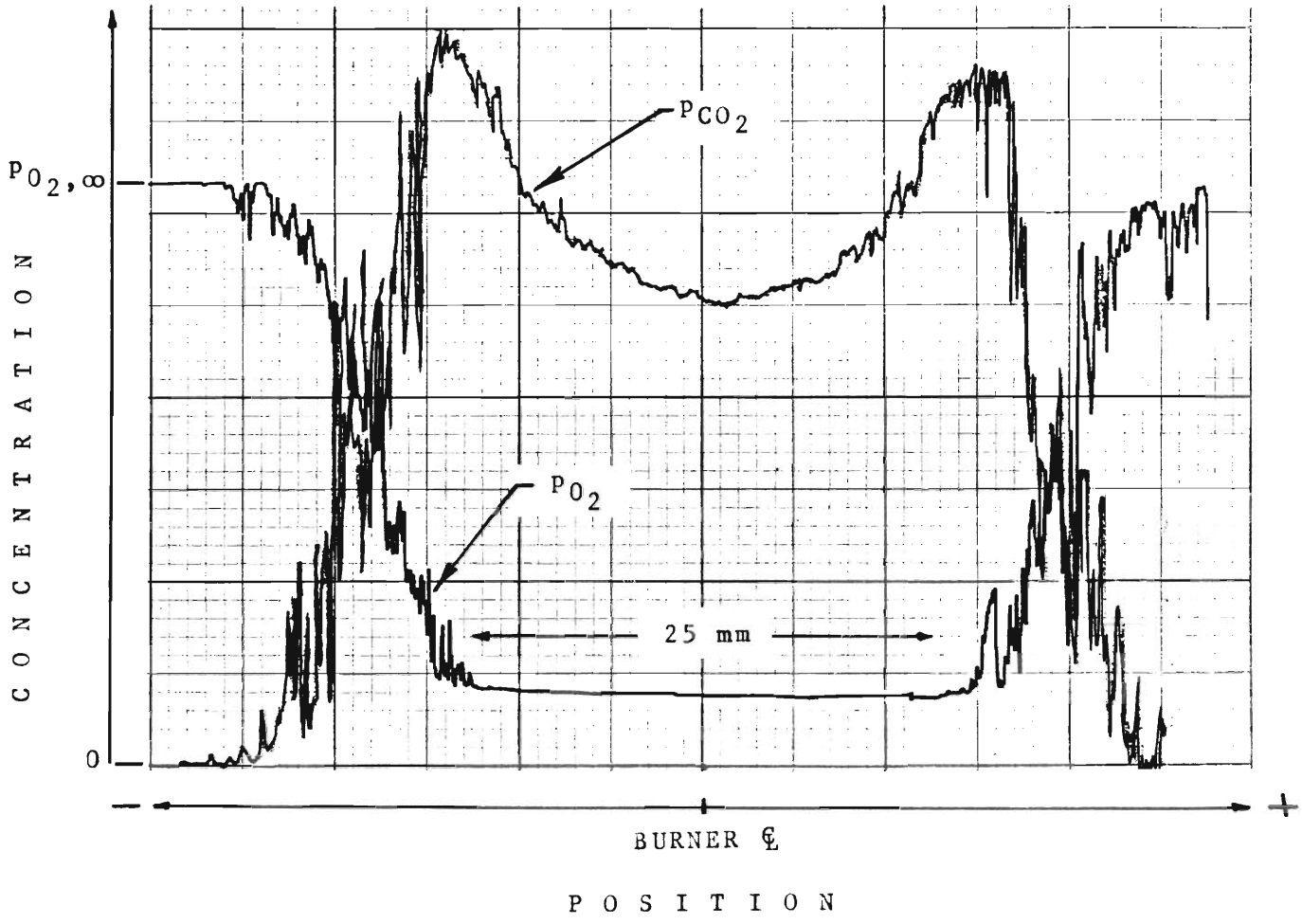

Figure II-C.15. Concentration Profiles of CO_2 and O_2, Obtained with Stoichiometric Equivalence Ratio $\phi = 1.2$ and Mass Flow Rate $\dot{m}_{mix} = 928$ g/h at 19 mm Above Burner Opening.

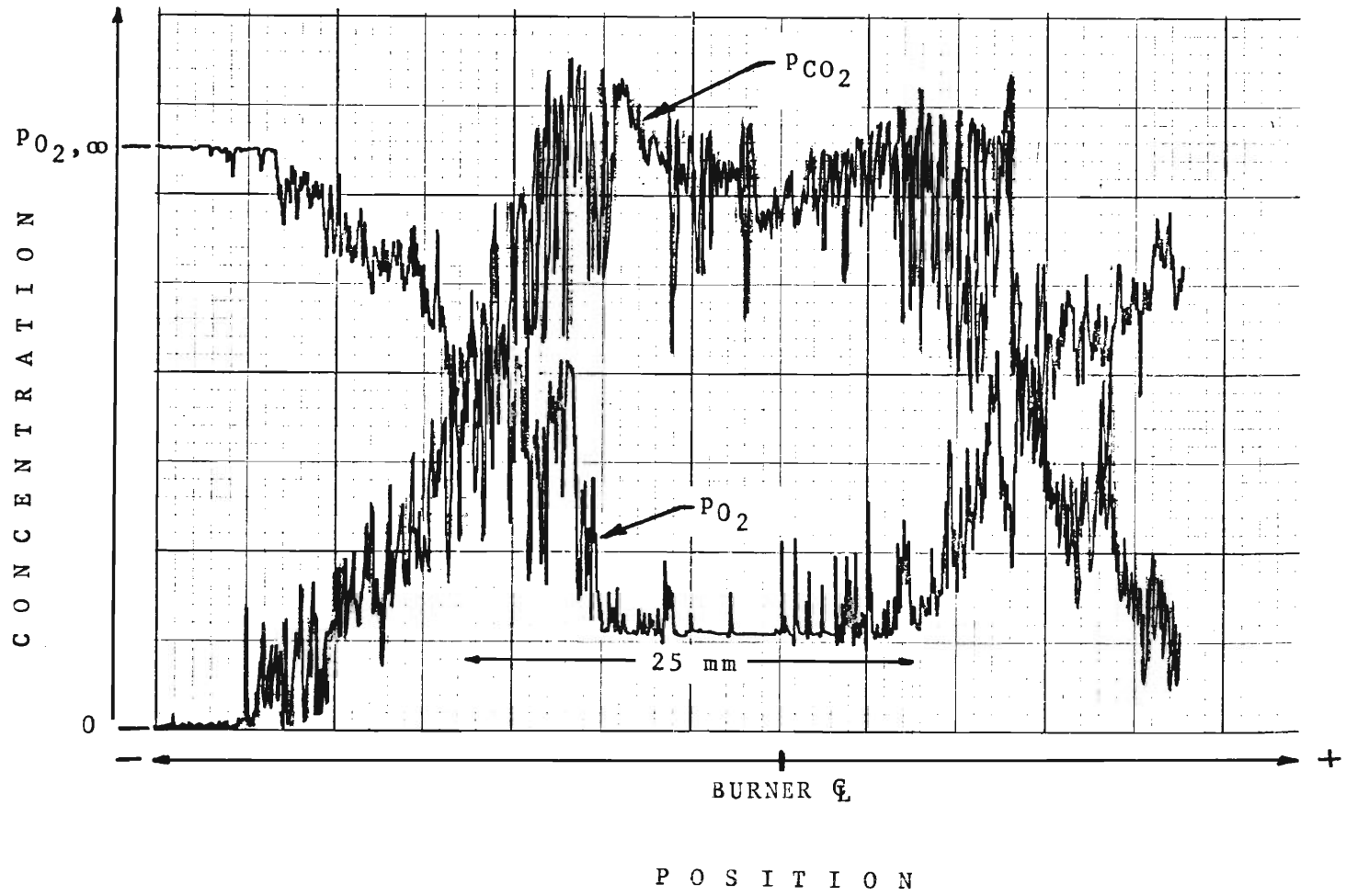

Figure II-C.16. Concentration Profiles of CO_2 and O_2, Obtained with Stoichiometric Equivalence Ratio ϕ = 1.2 and Mass Flow Rate $\dot{m}_{mix}$ = 928 g/h at 44 mm Above Burner Opening.

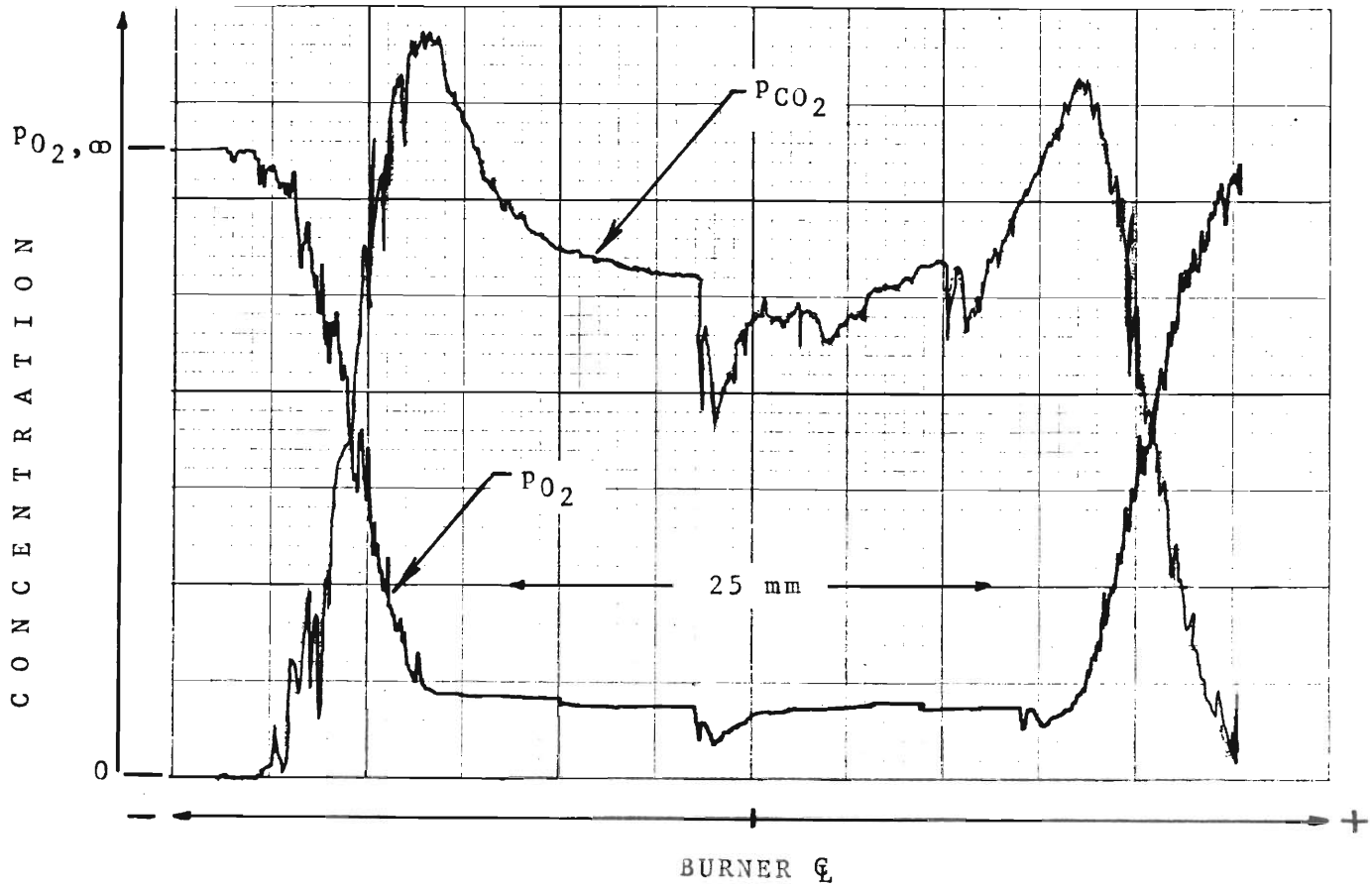

Figure II-C.17. Concentration Profiles of CO_2 and O_2, Obtained with Stoichiometric Equivalence Ratio $\phi = 1.2$ and Mass Flow Rate $\dot{m}_{mix} = 1,655$ g/h at 19 mm Above Burner Opening.

front and back faces of the screen from

$$\bar{h}_c = C'' \, dT/d\tau / [2(T_f - T)] \qquad \text{(II-C.1)}$$

where C" represents the heat capacity per unit area of the screen. The slope of the heating curve $T(\tau)$ is observed to remain constant during the early heating period, that is until the screen temperatures reach the fabric destruction temperatures.

Screen heating curves were recorded at first with a two-channel Hewlett Packard Model 7100 B. Strip Chart Recorder and then on the Tektronix 502A oscilloscope because the response time of the recorder was recognized to be too long.

Tables II-C.1, 2 and 3 present the summary of convective film coefficients obtained. All data presented pertain to the flame diameter at burner opening of 37 mm. Table II-C.1 lists film coefficients obtained for the fabric sample holder diameter d = 25mm and the stoichiometric equivalence ratio $\phi = 0.86$. Tables II-C.2 and 3 represent data for the large holder opening d = 63.5 mm (2.5 in); Table II-C.2 for $\phi = 0.86$ (oxygen surplus) and Table II-C.3 for $\phi = 1.2$. The first two columns represent the vertical distance L above the burner opening, $\dot{m}_{mix}$ in the third column is the mass flow rate of the reactive gas mixture to the burner and t_f in the fourth column is the flame temperature. In Table II-C.2 the convective film coefficients evaluated from the pen recorder record are compared with those evaluated from the oscilloscope traces. As expected the larger descrepencies occur at the high heat flux conditions.

b. Ignition Time Under Convective Heating

The instrumentation used in association with the Convective Ignition Time Apparatus, record the times associated with the occurence of a flame at the front face of igniting fabrics or with the onset of a breakthrough in the heated zone of melting fabrics. Gas flame ignition of the fabric and the occurence of

Table II-C.1. Summary of SS Screen Convective Film Coefficients*

ϕ = 0.86 Fabric Holder Aperture = 25 mm

L		$\dot{m}_{mix}$	t_f	$2\bar{h}_c$
in	cm	g/h	^oC	W/cm^2K
4 1/8	10.5	1285	1006	0.01210
		2158	-	-
		2951	1257	0.02074
3	7.6	1285	1215	0.01372
		2158	1317	0.01822
		2951	1320	0.02152
1 3/4	4.4	1285	1256	0.01276
		2158	1351	0.01563
		2951	1356	0.02097
3/4	1.9	1285	1290	0.01554
		2158	1347	0.02372
		2951	1354	0.02552

*All the convective film coefficient tests for this group were carried out using the pen recorder.

Table II-C.2. Summary of SS Screen Convective Film Coefficients, II

ϕ = 0.86 Fabric Holder Aperture = 63.5 mm

L		$\dot{m}_{mix}$	t_f	$2\bar{h}_c$	$2\bar{h}_c$
in	cm	g/h	^oC	W/cm^2K (Oscilloscope)	W/cm^2K (Pen Recorder)
4 1/8	10.5	1265	995	0.01108	0.01120
		2158	-	-	-
		2951	1257	0.02428	0.01912
3	7.6	1265	1205	0.01515	0.01428
		2158	1319	0.01931	0.01898
		2951	1320	-	-
1 3/4	4.4	1265	1256	-	-
		2158	1351	-	-
		2951	1359	-	-
3/4	1.9	1265	1290	0.01605	0.01373
		2158	1347	0.01964	0.01920
		2951	1352	0.02573	0.02285

Table II-C.3. Summary of SS Screen Convective Film Coefficients, III

ϕ = 1.2 Fabric Holder Aperture = 63.5 mm

L		$\dot{m}_{mix}$	t_f	$2\bar{h}_c$
in	cm	g/h	^oC	W/cm^2K
3/4	1.9	2151	1375	0.01922

The convective film coefficient test was carried out using the oscilloscope.

the flame is sensed by an infrared detector focused on the front side of the fabric (the side exposed to the flame), through the gas flame (optically thin in the infrared spectrum). Gas flame melting of the fabric and the onset of a breakthrough in the heated zone is sensed by the infrared detector also, however, this time focused to a small quartz lamp placed no less than twelve inches from the back face of the fabric.

The convective ignition time data are presented in summary form suitable for comparison with previously presented (Fig. II-B.1) radiative ignition time data. Presented are, in Figure II-C. 18, the normalized destruction times $(N_{Fo})_{i,m}$ defined by Eq. II-B. 1, with $\bar{\tau}$ as in Table III-2, as functions of normalized convective heating intensity, q_c^*, namely the product of Biot number times normalized average excess flame temperature above the fabric temperature:

$$q_c^* = [2\bar{h}_c/(k/\delta)](\theta_f - \bar{\theta}) \qquad \text{(II-C.2)}$$

Here $\theta_f = (T_f - T_\infty)/(T_{i,m} - T_\infty)$ is the nondimensional flame temperature consistent with the definition of θ in Table III-2. The quotient of film coefficient $\bar{h}_c$ over thermal conductance k/δ is the Biot number. The average, normalized fabric temperature is defined by

$$\bar{\theta} = 1/\bar{\tau}_{i,m} \int_0^{\bar{\tau}_{i,m}} \theta \, d\bar{\tau} \qquad \text{(II-C.3)}$$

and evaluated from the solution to Eq. III-35 for inert heating, namely

$$\theta = \theta_f [1 - \exp(-\bar{\tau})], \qquad \text{(II-C.4)}$$

with the nondimensional destruction time $\bar{\tau}_{i,m}$, as in Table III-2, computed from

the condition that $\theta = 1$ at the time of destruction, $\bar{\tau} = \bar{\tau}_{i,m}$. The result for the average normalized convective heat flux is

$$q_c^* = 2\left\{1/\ln\left[\theta_f/(\theta_f-1)\right]\right\} \bar{h}_c/(k/\delta) \qquad \text{(II-C.5)}$$

The ignition time data for the ten Primary GIRCFF Fabrics are presented in Figure II-C.18. The figure shows, for all fabrics, a clear trend of increasing ignition times with decreasing heat flux. Curve A drawn on this figure represents the solution to the inert heating analysis, Eq III-39 and the two broken lines show the range of radiative ignition time data from Figure II-B.1 for comparison.

The convective heat fluxes obtained in this group of experiments overlap in part the range of the radiative heat fluxes obtained with the Radiative Ignition Time Apparatus. At the same time, the convective heat source extended the range toward higher heating intensities.

GIRCFF Fabrics No. 5 and 18 (both cotton) are grouped together and exhibit trends different from those of the other eight fabrics. Their ignition times fall above the upper limit of the radiative ignition time data, in the same range of heat fluxes. For the remaining eight fabrics, on the average, the convective ignition times are shorter than those obtained with the radiative heat source, for the same range of heat fluxes because there is no convective cooling in the gas flame.

Comparing the result of the inert heating model, which is shown as curve A in Figure II-C.18, with the experimental data, it shows that the melting fabrics provide the smallest difference, while the igniting fabrics the largest. Average ratios of measured to computed destruction times for the melting group are 2.3 while for the igniting group they are 6.3.

The large difference between the inert heating model and the experimental results with the convective heat source can be attributed to two factors. One of these is pyrolysis. The effect of chemical reactions prior to ignition has already been discussed in relation to ignition time experiments with the radiative heat

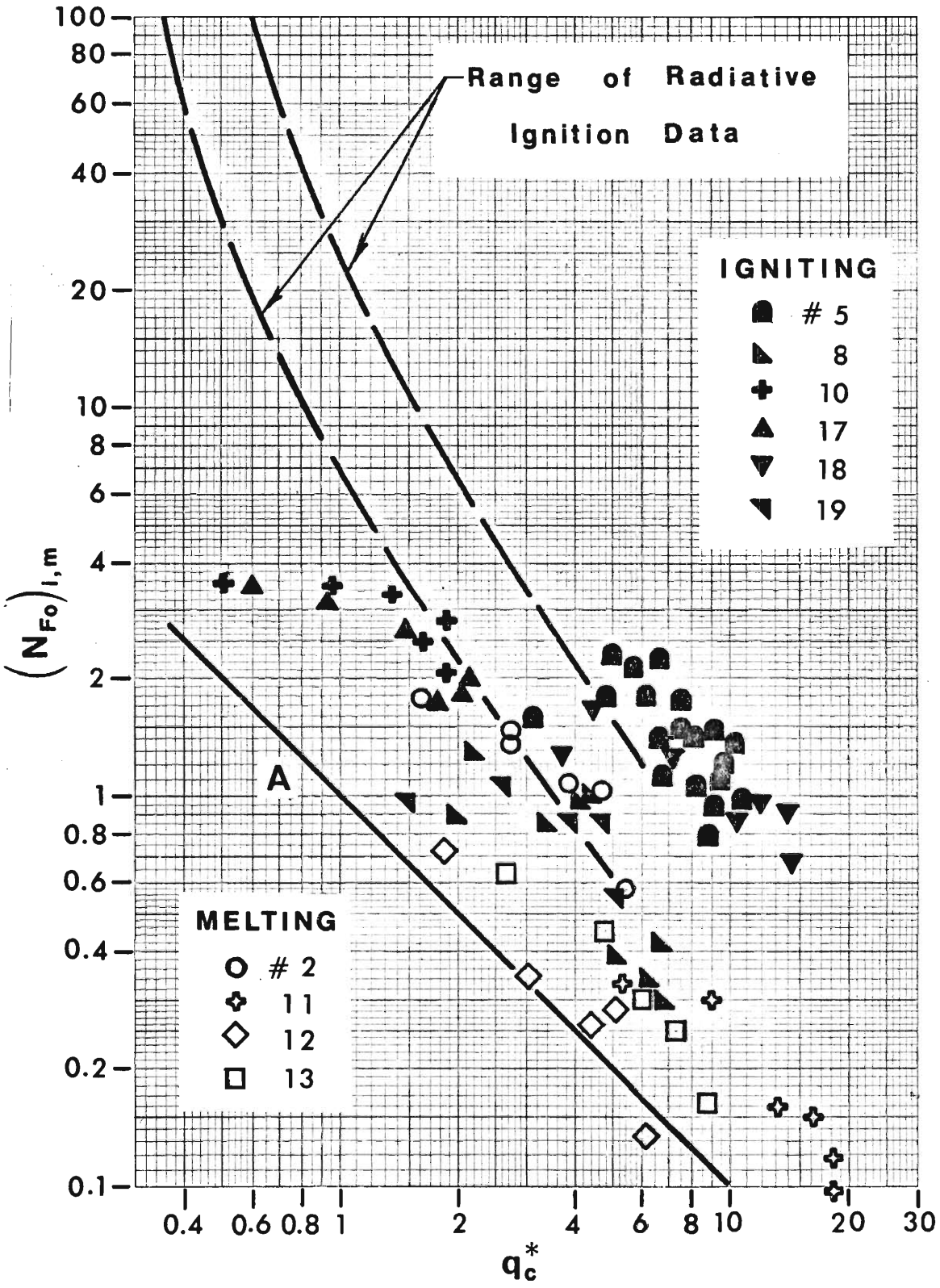

Figure II-C.18. Normalized Destruction Time vs Normalized Convective Heat Flux.

source.

The second factor that is important, when considering the difference between the inert heating model and experimental data, is the film coefficient. The importance of the fabric film coefficient in the analysis can be emphasized by noting that when the fabric is exposed to a heat flux source, desorption and gasification take place, which are associated with an outflow of gases from the fabric surface. The physical effect of the gas outflow from the pyrolyzing fabric is similar to transpiration cooling. A glimpse in the literature on transpiration cooling [II-4] reveals a reduction in the convective film coefficient with increasing normal velocity of the injected fluid. Consequently, while current measurements of film coefficients on inert bodies are indispensable, they are not sufficient for predicting fabric destruction times. This fact then accounts for part of the difference between experiment and inert model fabric destruction times. The remaining difference can then be attributed to the retardation of fabric destruction time due to the chemical reaction during the pre-ignition period.

Oxygen starvation is the third factor that must be considered important in measuring fabric destruction times when the fabric is exposed to a convective heat flux source. For the experimental data reported here the stoichiometric equivalence ratio was kept at 0.86 and thus providing excess oxygen in the reactive mixture. The existance of excess oxygen is clearly shown on the concentration profiles presented in Section 3, a. iii.

Finally the difference between convective and radiative fabric ignition appears to be minor. The essential variable is the magnitude of the net heat flux entering the fabric.

4. Conclusions

Fabric destruction time is mainly a function of the heat flux magnitude and not of the heating mode. Prediction of fabric destruction times by inert heating models is inadequate. On the average cellulosic fabrics ignite about 6.3

times slower then predicted by the inert heating model and plastic polymers about 2.3 times slower. Factors that are important in the measurement and analysis of fabric destruction times with a convective heat flux source are: (i) the chemical reactions prior to ignition, (ii) the convective film coefficient, (iii) oxygen starvation.

D. Measurement of Ignition Time Statistics

1. Purpose

Ignition time frequencies were to be measured to determine

(i) the statistical confidence in previously obtained ignition time data, and

(ii) the probability of fabric ignition under given laboratory exposure conditions.

As discussed later in Chapter III.A the assessment of ignition probability under laboratory conditions is a crucial step toward burn injury probability. It is also shown in CHapter III.A that the laboratory ignition probability P_I (I/E) is defined through three measures

(i) the mean (median) value $<\tau_i^*>$ of ignition time,

(ii) the standard deviation σ of ignition time about the mean ignition time $<\tau_i^*>$, and

(iii) the standard deviation σ_μ of $<\tau_i^*>$.

These three measures were obtained.

2. Achievements

Developments performed in relation to the environmental enclosure, its controls and the automatic timing and monitoring circuits for the operation of RITA have been discussed in Section B.2 of this chapter, details of the latest modifications are presented in Appendix B.2. The total of 223 dual shutter mode ignition tests was performed at three power and two humidity levels and with one fabric. Ignition time variance was much smaller than originally expected, thus requiring more tests at highly resolving time intervals, but for fewer fabrics than expected because the ignition time is nearly deterministic.

3. Results, Ignition Time Statistics

Ignition time frequencies were measured by carefully conditioning the fabric at the preselected initial temperature and humidity level. The fabric was inserted into RITA (Radiative Ignition Time Apparatus, Appendix B.2), then the radiative heater was preheated during a selected and automatically controlled period of time, to reach radiative equilibrium. The fabric was then exposed within less than 5 milliseconds to the full radiative power flux and after a selected exposure time shielded, again within less than 5 milliseconds. Exposure times τ_e were selected to vary between $0.9\tau_i$ and $1.1\tau_i$ as measured previously under single-shutter mode ([I-2] and Section B of this report). Care was exercised to include exposure times at the wings of the frequency distribution, i.e with both none of the samples and all of the samples ignited. Actual exposure time was measured electronically with the accuracy of ± 0.01 seconds.

Fabrics were removed from RITA after exposure and found either only charred or ignited and burnt. After dividing all test results into classes of 0.1 and 0.2 times the previously found ignition time τ_i, and forming for each class the fraction of ignitions over total tests, a sensitivity test was performed, first by the Kaerber Method and then by the Probit Method of Analysis [II-5] Stimulus levels are exposure time at fixed humidity and heating intensity.

The results are shown in Table II-D.I below. Listed are, in this order, the fabric identification, the heating intensity, the relative environmental humidity, the number of tests evaluated, then the ignition time as measured previously under single shutter mode (without environmental control), and the median ignition time obtained from the sensitivity analysis. Following the ignition times are the ratio of ignition time obtained under single shutter mode operation over ignition time from dual shutter mode, and finally the estimates for the standard deviations of the median ignition time and the ignition time itself. It was impossible to compute standard deviations of the median ignition times for two levels, namely 13.80 W/cm^2 at 30% r.h., and 6.50 W/cm^2 at 90% r.h., because of insufficient resolution.

Table II-D.1. Ignition Time Statistics.

GIRCFF Fabric No.	Irradiation W_o	Relative Humidity	Number of Tests	Ignition Time		Relative Mean μ =	Standard Deviation of Ignition Mean	Time
				single shutter τ_i	median $\langle\tau_i\rangle$	$\langle\tau_i\rangle/\tau_i$	s_μ	s
	W/cm^2	%	-	s		-	s	s
5	6.50	30	77	27.2	31.93	1.174	0.38	2.55
5	9.52	30	25	12.8	13.08	1.022	0.14	0.353
5	13.80	30	18	6.9	7.11	1.030	-	0.781
5	6.50	90	17	-	35.49	-	-	0.175
5	9.52	90	43	-	15.75	-	0.57	2.62
5	13.80	90	32	-	7.91	-	0.07	0.246

4. Conclusion

The statistical data evaluation shows for the cotton fabric, CIRCFF No. 5 that

(i) ignition time measured in a single test under single shutter operating mode deviates from the statistical mean, at with 50 percent of all exposures are expected to result in ignition, by less than 20 percent,

(ii) the 95 percent confidence interval for the mean or median ignition time $<\tau_i>$ is two percent of the mean at low humidity levels and four percent at 90% r.h.; the interval shrinks with increasing heating intensity,

(iii) the probability that the fabric ignites within a given fraction of its mean ignition time $<\tau_i>$ increases with heating intensity.

More specifically, at 30% relative humidity it can be expected that 95 percent of all exposures cause ignition if the ignition times fall within ± 15.7, 5.1 and 2.2 percent of the median ignition time at the respective irradiation levels of 6.50, 9.52 and 13.80 W/cm^2.

Finally, the entries in the sixth and last columns of Table II-D.1 are the parameters required to predict ignition time under laboratory exposure in accordance with Eqs. III-2 through 4. The mean or median $<\tau_i>$ is required to evaluate ψ in Eq. III-4 and s is an estimate for the deviation σ.

III. ANALYSIS

A. Objective

Rational flammability standards require some logical, experimentally verified connection between the properties of the material to be certified, the statistically relevant conditions which could lead to material ignition, and the extent and severity of damage. There are currently a large number of so-called flammability tests in use, each one singling out one particular property or one response to a particular set of circumstances. Generally there is no convincing connection between the measured quantity and a measure of burn injury [III-1]. Nevertheless, flammability standards must evolve from, and be administered through, laboratory experiments because well-controlled and instrumented experiments on the human itself are impossible on a routine basis. The purpose of this analysis is to provide the scaling laws necessary to reach the first phase of relating relevant fabric properties to burn injury measures, namely to predict the probability P(I/E) of fabric ignition for given exposure, as formulated in Eq. (I-1), from fabric properties and exposure conditions. The scaling laws are derived from fundamental conservation principles and constitutive laws.

As demonstrated previously [I-2] the transient nature of ignition processes stipulates that ignition probability P(I/E) should depend on the ratio $\Psi = \tau_e/\tau_i$ of exposure over ignition times (Eq. (I-1)). Here, the exposure time τ_e reflects human activities and reflex responses, while the ignition time τ_i characterize the fabric behavior under given exposure conditions. The complexity of the ignition processes, together with the stochastic behavior of people suggest this two step approach toward establishing the ignition probability P(I/E): firstly, to derive the probability P_I (I/E) of ignition under given laboratory exposure conditions and, secondly, to relate experimentally laboratory to

real-life exposure conditions.

The analysis presented here is developed to predict

$$P_I(I/E) = f(\psi) \qquad (III-1)$$

from thermophysical fabric properties and exposure conditions under radiative and gas flame heating. To reach this goal a relation between $P_I(I/E)$ and ignition time τ_i is established first and followed by the analysis to predict τ_i from properties and exposure conditions.

B. Ignition Probability And Ignition Time

Experiments discussed in Chapter II, Section D have shown an essentially normal distribution of ignition frequency as a function of exposure time τ_e. The normal distribution is characterized by the mean value $<\tau_i>$ of ignition time and the standard deviation σ, both dependent on exposure conditions such as heating mode and intensity, and fabric conditions such as moisture content.

The normal or Gaussian distribution yields this ignition probability $P_I(I/E)$ under laboratory exposure conditions:

$$P_I(I/E) = 1/\sqrt{2\pi} \int_{-\infty}^{\chi^*} \exp(-z^2/2)\ dz \qquad (III-2)$$

where the upper integration limit χ^* is given by

$$\chi^* = (\psi-1)/\sigma \qquad (III-3)$$

and

$$\psi = \tau_e/<\tau_i> . \qquad (III-4)$$

The integral in Eq. (III-2) is tabulated in standard handbooks on statistics [III-2*]. Notice that $<\tau_i>$ is equal to that exposure time at which half of all exposures result in ignition, and that 68.3 percent of all ignitions are expected to occur within the exposure time limits of $<\tau_i>(1\pm\sigma)$.

The median ignition time $<\tau_i>$ and the standard deviation σ are obtained from the measurement of ignition frequencies. An analytical estimate τ_i derived from material properties and exposure conditions, can serve to predict the ignition probability $P_I(I/E)$ under laboratory conditions provided that (1) the predicted time τ_i compares favorably with the measured median time $<\tau_i>$ and (2) the standard deviation is known from experiments for any desired set of conditions

The purpose of the following analysis is to predict the ignition time τ_i, or the destruction time $\tau_{i,m}$, from fabric properties and exposure conditions. Previously obtained results [I-2] are reviewed in part, and then extended. A new formulation is proposed to account for fabric desorption and gasification. Nondimensional groups are developed to identify scaling laws. The significance of the parameters and the processes they characterize are demonstrated from the numerical solution to the complete differential equations. Finally, experimental results are compared with the analytical solution.

C. Prediction of Ignition Time

The single fabric will be considered, first under radiative and then under convective heating. The fabric is taken to respond to heating in these partially overlapping stages:

(i) inert heating,

(ii) desorption of water,

---

*Observe the difference in lower integration limits and add 1/2 to all values in the column headed by "Area".

(iii) pyrolytic gasification, accompanied by the evolution of combustible and non-combustible gases, of smoke with entrained particles, or by shrinking and melting

(iv) thermal excursion (ignition, beginning of exponential temperature rise in gas phase or condensed phase), appearance of flame,

(v) combustion and char formation.

The completion of stage (iii) or the onset of stage (iv) is identified with the instant of destruction, $\tau_{i,m}$, namely the ignition time for igniting fabrics and the melting time for fabrics which melt prior to ignition.

The attainment of a surface temperature, the ignition temperature T_i is associated with the thermal excursion. The ignition temperature may be measured as discussed in Section A of Chapter II or inferred from reaction kinetics.

I. Previous Results

One-dimensional heat transfer by simultaneous conduction and diffuse radiation, accompanied by internal chemical reactions, was formulated in Reference [I-2] for the fabric and skin system depicted in Figure III-1. The analysis is based on the equation of energy conservation

$$\rho c(\partial T/\partial \tau) = \partial/\partial x\,(k\,\partial T/\partial x) + 2(1-\tilde{\rho})\,\kappa E_2(\kappa x)\,W_o + q'''\{T(x)\} \qquad \text{(III-5)}$$

where

ρ	fabric density	g/cm^2
c	specific heat of fabric	Ws/(gK)
T	fabric temperature	k
τ	time	s
x	coordinate	cm
k	thermal conductivity	W/(cm K)

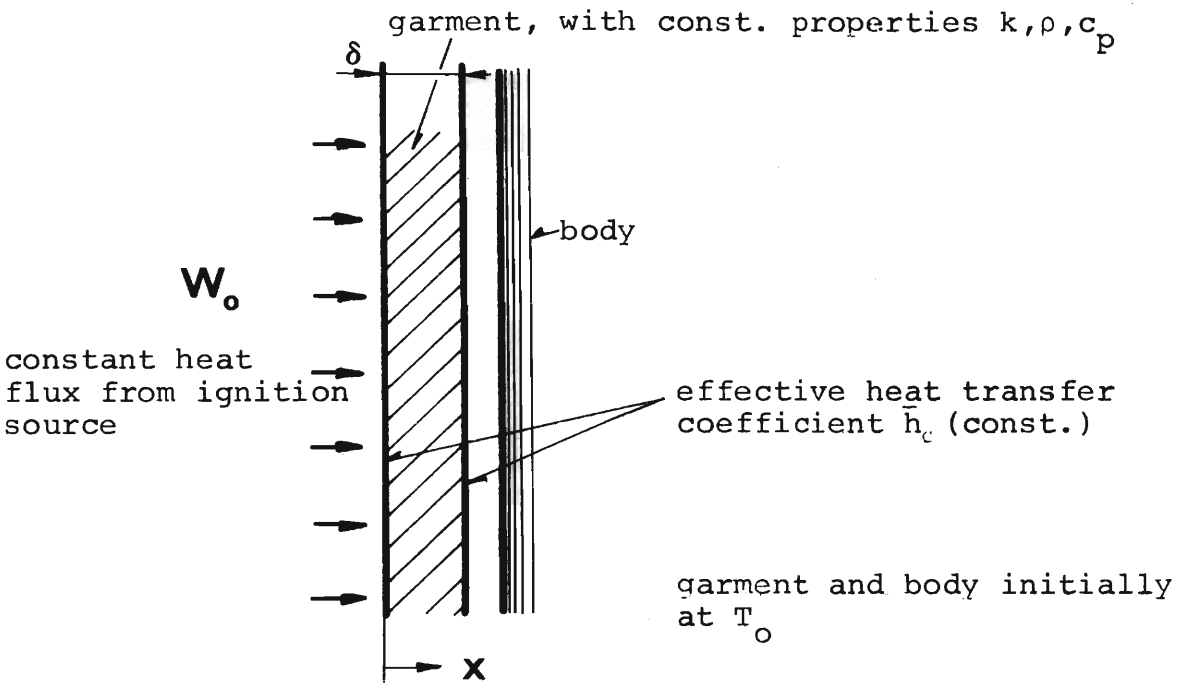

Figure III-1. Geometry of Ignition Model

$\tilde{\rho}$	fabric reflectance	
κ	radiative extinction coefficient	1/cm
W_o	incident radiant flux	W/cm^2

$$E_2(\kappa x) = \int_1^\infty t^{-2} e^{-(\kappa x)t} dt$$

The volumetric heat generation q''' was based on the average heat generation in gaseous and condensed phases. It was formulated in terms of Arrhenius-type reaction rate laws. Convective boundary conditions were imposed to describe fabic cooling at the front and the back faces.

The problem description involved 21 parameters, namely twelve fabric properties, five process parameters, the two dependent variables T and degree of reaction, λ, and the independent variables x and τ. Normalization of the problem resulted in the parameter reduction to the total of fourteen nondimensional groups or modeling parameters. Consequently the nondimensional destruction time was related to ten modeling parameters.

Partial modeling revealed that three modeling parameters are sufficient to predict ignition of inert, opaque fabrics, four parameters for semitransparent inert fabrics and ten additional parameters are necessary to include two thermal reactions, a first and a zero-order reaction.

Equation III-5 was solved numerically to yield ignition time under inert heating of semitransparent fabrics. The solution [I-2] lead to the conclusion that internal thermal diffusion is insignificant under normally expected conditions of natural convection and that lumped-parameter modeling techniques are justified.

Integration of Eq. III-5 yields a first-order ordinary differential equation involving eight nondimensional groups. For radiative heating of an inert slab, subject to convective cooling on both sides the governing equations are

$$\left.\begin{aligned} d\theta/d\tau^* &= 1 - \pi_1\theta \\ \theta(0) &= 0 \\ \theta(\tau^*_{i,m}) &= 1 \end{aligned}\right\} \quad \text{(III-6)}$$

with $\theta = (T-T_\infty)/(T_{i,m}-T_\infty)$ representing the nondimensional temperature and $\tau^* = \alpha W_o \tau/[\rho c\delta (T_{1,m}-T_\infty)]$ the nondimensional time. The destruction temperature $T_{i,m}$ stands for ignition or melting temperature, T_∞ for environmental temperature and α for radiative absorptance. The nondimensional destruction time $\tau^*_{i,m}$ depends on the single parameter

$$\pi_1 = 2\bar{h}_c(T_{i,m}-T_o)/\alpha W_o \quad \text{(III-7)}$$

which represents the fraction of absorbed radiant power which is lost by convection at the time of ignition. In Eq. III-7, $\bar{h}_c$ stands for the average convection film coefficient. The solution to Eq's.III-6 is [II-2]

$$\tau^*_{i,m} = -1/\pi_1 \ \ln(1-\pi_1) \quad \text{(III-8)}$$

and shows (1) that without convective losses or for extremely intense irradiation, that is for $\pi_1 \to 0$

$$\lim_{\pi_1 \to o} \tau^*_{i,m} = 1 \quad \text{(III-9)}$$

and $\tau_{i,m} \to \rho c\delta (T_{i,m}-T_o)/\alpha W_o$, (2) that convection can delay destruction and (3) that ignition is impossible when irradiation is balanced by convective cooling at least at the time the fabric reaches ignition temperature; for ignition to occur without chemical heat evolution π_1 must be less than unity, and $\tau^*_{i,m} \to \infty$ as $\pi_1 \to 1$.

2. Extension To Previous Results

a. Variable Film Coefficients. Ignition time measurements under radiative heating reveal that convective losses are significant. Experience on natural convection, expressed in familiar relationships between the Nusselt, the Grashof and the Prandtl numbers, establishes the temperature dependence of the convective film coefficient, namely $h_c \sim (T-T_\infty)^n$ with $n = 1/4$ for laminar and $n = 1/3$ for turbulent free convection on vertical surfaces. Laminar convection occurred during the radiative ignition time measurements. The corresponding convection parameter π_1 becomes

$$\pi_1 = \bar{\pi}_1 \, \theta^{\frac{1}{4}} \tag{III-10}$$

where

$$\bar{\pi}_1 = [(T_{i,m}-T_\infty)/(T_r-T_\infty)]^{\frac{1}{4}} \pi_r \tag{III-11}$$

and π_r is obtained from Eq. III-7 with h_c evaluated at a reference temperature T_r. Substitution of Eq. III-10 into the first of Eqs. III-6 yields

$$d\theta/d\tau^* = 1 - \bar{\pi}_1 \, \theta^{5/4} \tag{III-12}$$

the solution for which is

$$\begin{aligned} \tau^*_{i,m} &= 4/Y^4 \int_0^Y y^3/(1-y^5)\, dy \\ &= -(4/5)/Y^4 \Bigg[\ln(1-z) + \\ &\sum_{j=1}^{2} \cos 4\beta \cdot \ln(1 + 2z\cos\beta + z^2) + \\ &\sum_{j=1}^{2} \sin 4\beta \cdot \operatorname{arctg}[(z+\cos\beta)/\sin\beta] \Bigg]_{z=0}^{Y} \end{aligned} \tag{III-13}$$

with $\beta = \pi(2j - 1)$

and $Y = (\bar{\pi}_1)^{1/5}$ (III-14)

The solution is graphically represented in Figure III-2 together with that given by Eq. III-8. The comparison shows that $\tau^*_{i,m}$ computed by Eqs. III-13 and 14 is larger than that computed by Eq. III-8.

b. Inert Heating Combined with Isothermal Reactions. Endothermic reactions retard destruction while exothermic reactions deliberate heat and accelerate destruction. Experimentally obtained destruction times always appear to be longer than the times computed from inert heating models. An extremely efficient method may be developed to account for the ignition delays due to water desorption and melting if one assumes these reactions to be isothermal. This assumption is well supported by the occurrence of horizontal plateaus in the temperature - time oscillogram obtained from optical surface temperature measurements during gas flame ignition.

For n isothermal, endothermic reactions each taking place at its temperature T_j, each removing the fraction ε_j of the original fabric mass, and each requiring the change in enthalpy $(\Delta i)_j$, measured in terms of original fabric mass, a separate delay can be computed from the time it takes the radiative energy source to supply the net energy $\varepsilon_j(\Delta i)_j$. Accounting for the heating between reactions on the basis of Eq. III-8 one obtains this result:

$$\tau^*_{i,m} = -1/\pi_1 \ln(1-\pi_1) + \sum_{j=1}^{n} (\pi_{20})_j / [1 - \pi_1 (\pi_{21})_j] \quad \text{(III-15)}$$

where $(\pi_{20})_j = \varepsilon_j(\Delta i)_j / [c(T_{i,m} - T_\infty)]$ (III-16)

and $(\pi_{21})_j = (T_j - T_\infty) / (T_{i,m} - T_\infty)$ (III-17)

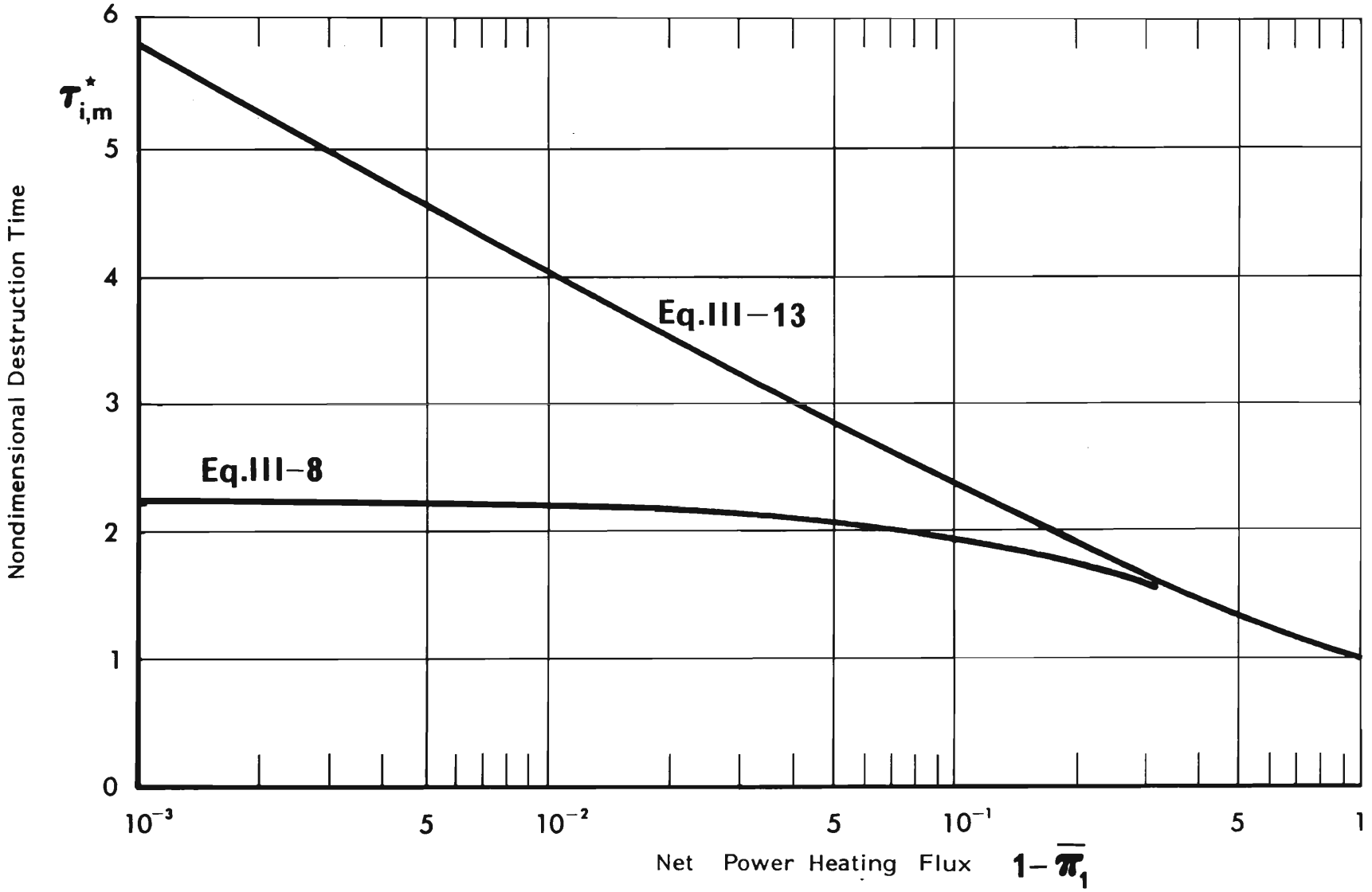

Figure III-2. Effect of Free Convection on Ignition Time.

Equation III-15 shows that reactions at high temperatures require more time than at lower temperatures even when both reactions require the same enthalpy Δi.

c. Two-Stage Heating Without Convective Losses: The final closed-form solution presented here is applicable for intense heating and relative low convective losses. The heating process is assumed to be inert up to a certain temperature T_c and then to proceed in a zero-order Arrhenius reaction. Introduce

$$\Theta = (T - T_{i,m}) / (T_{i,m} - T_\infty) \tag{III-18}$$

$$\pi_{22} = \Delta i \, \rho \delta \, k_o / (\alpha W_o) \tag{III-19}$$

$$\pi_o = 1 - T_\infty / T_{i,m} \tag{III-20}$$

and

$$\pi_{23} = E/(RT_{i,m}) \tag{III-21}$$

where E and k_o represent activation energy and frequency factor, respectively. The reaction enthalpy Δi is taken to be positive for endothermic reactions. The energy balance requires that

$$\left.\begin{aligned} d\Theta/d\tau^* &= 1 \quad \text{for} \quad -1 \leq \Theta \leq \Theta_c \\ &= 1 - \pi_{22} \exp\left[-\pi_{23}/(1+\pi_o\Theta)\right] \quad \text{for} \quad \Theta_c < \Theta \leq 0 \end{aligned}\right\} \tag{III-22}$$

and that

$$\Theta(0) = -1$$

$$\Theta(\tau^*_{i,m}) = 0$$

Provided that $|\pi_o \Theta_c| << 1$ the solution may be found to yield

$$\tau^*_{i,m} = 1 + 1/(\pi_o \pi_{23}) \times$$

$$\ln \left\{ \left\{ 1 - \pi_{22} \exp[-\pi_{23}(1 - \pi_o \theta_c)] \right\} \Big/ \left\{ 1 - \pi_{22} \exp(-\pi_{23}) \right\} \right\} \qquad \text{(III-23)}$$

Evaluation of Eq. (III-23) shows for cotton fabric typical ignition delays by approximately fifty percent of the ignition time computed for inert heating.

3. New Formulation of the Problem

The apparently consistent experience of experimentally obtaining longer ignition times than those computed from inert heating with convective losses for radiative ignition and from inert heating by convection for gas flame ignition lead to the attempt to extend the ignition model so as to include primarily retarding processes, that is processes which require energy in appreciable quantities. A new model was formulated to account for

(i) radiative heating
(ii) internal energy storage
(iii) convective heat loss
(iv) radiative heat loss
(v) desorption of moisture
(vii) exothermal reaction in gaseous phase with feed-back to the fabric.

a. Governing Equations for Radiative Ignition conservation of Energy requires that

$$\begin{aligned} \rho \delta c (dT/d\tau) = {} & \alpha W_o - 2h_c(T - T_\infty) - 2\alpha\sigma \bar{F}_{s\infty}(T^4 - T_\infty^4) \\ & + (\Delta i)_d [d(\rho\delta)/d\tau]_d \\ & + (\Delta i)_g [d(\rho\delta)/d\tau]_g \\ & + h_c(T_b - T) \end{aligned} \qquad \text{(III-24)}$$

The symbols not yet defined are:

$\bar{F}_{s\infty}$ view factor of sample with respect to environment, averaged over front and back faces,

T_b temperature of gaseous phase in boundary layer of fabric.

Subscripts d and g designate, respectively, desorption and gasification. Expressing the mass which participates in a particular reaction through the reacted mass fraction of the completed reaction, designated by λ_d for desorption and λ_g for gasification, one obtains

$$\left.\begin{aligned} (\rho\delta)_d &= \varepsilon_d(\rho\delta)_o(1-\lambda_d) \\ (\rho\delta)_g &= \varepsilon_g(\rho\delta)_o(1-\lambda_g) \end{aligned}\right\} \quad \text{(III-25)}$$

where ε stands for the fraction of the original mass per unit area, $(\rho\delta)_o$, that participates in the reaction. With this definition, Eq. III-24 can be recognized to contain three dependent variables, namely T, λ_d and λ_g. The two additional equations required describe the rate of reaction

$$\left.\begin{aligned} d\lambda_d/d\tau &= k_d(1-\lambda_d)^{n_d}\exp[-E_d/(RT)] \\ d\lambda_g/d\tau &= k_g(1-\lambda_g)^{n_g}\exp[-E_g/(RT)] \end{aligned}\right\} \quad \text{(III-26)}$$

A global energy balance applied to the boundary layers at both fabric faces yields this estimate for the mean gas temperature in the boundary layers

$$T_b - T = (-\Delta i)_e/(c_v + Cc_p)_b \times k_e/(d\lambda_g/d\tau) \times (\rho\delta)_b/[\varepsilon_g(\rho\delta)_o]\exp[-E_e/RT] \quad \text{(III-27)}$$

It may be noted that Eq. III-27 contains the solid-phase temperature T on the right side instead of the gas-phase temperature T_b. The discrepance introduced can be avoided only by the vigorous treatment of the boundary layer which is proposed for a later program, but the error introduced appears tolerable at

this time because thermal excursion is expected when the solid-phase temperature T becomes equal to the measured ignition temperature T_i. The nature of the thermal excursion gives little cause to seek accurate gas properties for the evaluation of Eq. III-27 which is dominated by the power of k_e and the value of E_e.

Finally, the solution to Eqs. III-24 and 26 calls for the initial conditions at $\tau = 0$:

$$\left.\begin{aligned} T(0) &= T_\infty \\ \lambda_d &= \lambda_g = 0 \end{aligned}\right\} \quad \text{(III-28)}$$

Ignition or melting occurs at $\tau = \tau_{i,m}$ when $T = T_{i,m}$.

Normalization of Eqs. III-24, 26 and 27 gives this system of equations in terms of the scaling parameters summarized in Section b below:

$$\begin{aligned} d\Theta/d\tau^* = {} & 1 - \bar{\pi}_1(\Theta+1)^{5/4} - \pi_2[(1+\pi_o\Theta)^4 - (1-\pi_o)^4] \\ & - \pi_3(1-\lambda_d)^{n_d}\exp[-\pi_4/(1+\pi_o\Theta)] \\ & - \pi_6(1-\lambda_g)^{n_g}\exp[-\pi_7/(1+\pi_o\Theta)] \\ & + \pi_9/(1-\lambda_g)^{n_g}\exp[-\pi_{10}/(1+\pi_o\Theta)] \end{aligned} \quad \text{(III-29)}$$

$$d\lambda_d/d\tau^* = \pi_5(1-\lambda_d)^{n_d}\exp[-\pi_4/(1+\pi_o\Theta)] \quad \text{(III-30)}$$

$$d\lambda_g/d\tau^* = \pi_8(1-\lambda_g)^{n_g}\exp[-\pi_7/(1+\pi_o\Theta)] \quad \text{(III-31)}$$

The initial conditions:

$$\left.\begin{aligned} &\text{at } \tau^* = 0 \quad \Theta = -1, \\ &\lambda_d = \lambda_g = 0 \end{aligned}\right\} \quad \text{(III-32)}$$

The parameters Θ, τ^*; π_o and $\bar{\pi}_1$ were defined previously. The physical interpretation of these and the remaining parameters are given next.

b. The Scaling Parameters For Radiative Ignition are the independent variable of temperature Θ and degrees of reaction λ_d and λ_g, and eleven parameters π_o, $\bar{\pi}_1$, $\pi_2, \ldots, \pi_{10}$. The ignition time sought depends on these thirteen parameters

$$\tau^*_{i,m} = f(\pi_o, \bar{\pi}_1, \pi_2, \pi_3, \ldots, \pi_{10}, n_d, n_g) \qquad \text{(III-33)}$$

(i) The effects of inert heating by a radiative source is characterized by $\tau^*_{i,m}$ which reduces to unity in the absence of all other effects (see Eq. III-9).

(ii) The effect of convective losses on ignition time is completely characterized by the single parameter $\bar{\pi}_1$, defined by Eqs. III-11.

(iii) Radiative effects are accounted for by two parameters, namely π_o, representing a measure of initial temperature, and π_2, the ratio of emitted over received power fluxes.

(iv) The descriptions of desorption and gasification each require four parameters, namely the fraction of power converted to the power absorbed characterized by π_3 for desorption, the ratio of reaction to ignition temperatures, designated by π_4 for desorption, the characteristic time, π_5 for desorption, and the order of reaction n. Corresponding parameters for gasification are designated by subscripts 6, 7 and 8 instead of 3, 4 and 5, respectively.

(v) The reaction within the boundary layer and its coupling with the condensed phase are approximately represented in this model by two parameters, the relative power exchange parameter π_9 representing the fraction of the incident power that is supplied by the burning gas and the relative reaction temperature π_{10}.

All parameters are summarized in Table III-1. At the present time convection, desorption and exothermal reaction are deemed significant, with their relative importance reflected in the above order.

TABLE III-1. Definition of Radiative Ignition Parameters

Parameter Symbol	Definition	Interpretation
π_o	$1-T_\infty/T_{i,m}$	initial condition
$\bar{\pi}_1$	$2(h_c)_r(T_{i,m}-T_\infty)/(\alpha W_o)\,[(T_{i,m}-T_\infty)/(T_r-T_\infty)]^{1/4}$	convective cooling
π_2	$2\sigma\bar{F}_{s\infty}T_{i,m}^4/W_o$	radiative cooling
π_3	$\varepsilon_d(\rho\delta)_o(\Delta i)_d k_d/(\alpha W_o)$	power requirement for desorption
π_4	$E_d/(RT_{i,m})$	desorption rate dependence on temperature
π_5	$(\rho\delta)_o c(T_{i,m}-T_\infty)k_d/(\alpha W_o)$	characteristic desorption rate
π_6	$\varepsilon_g(\rho\delta)_o(\Delta i)_g k_g/(\alpha W_o)$	power requirement for gasification

TABLE III-1 (continued) Definition of Radiative Ignition Parameters

Parameter Symbol	Definition	Interpretation
π_7	$E_g/(RT_{i,m})$	gasification rate dependence on temperature
π_8	$\pi_5\, kg/k_d$	characteristic desorption rate
π_9	$(-\Delta i)_e/(c_v + C\, c_p)_b \cdot h_c/(\alpha W_o) \cdot (\rho\delta)_b/[\varepsilon_g(\rho\delta)_o]\, k_e/k_g$	thermal interaction between gas and solid phases
π_{10}	$(E_e - E_g)/(RT_{i,m})$	temperature dependence of thermal feedback from boundary layer
Θ	$(T - T_{i,m})/(T_{i,m} - T\infty)$	fabric temperature
τ^*	$\alpha W_o\, \tau / [\rho\delta c(T_{i,m} - T_o)]$	time
n_d, n_g	Eq. III-26	reaction orders

c. Governing Equations For Gas Flame Ignition. The same model as used for radiative ignition yields, when applied to convective heating, this equation of energy conservation

$$\rho\delta c(dT/d\tau) = 2\bar{h}_c(\bar{T}_f - T) - 2\alpha\sigma\bar{F}_{s\infty}(T^4 - T_\infty^4)$$

$$+ (\Delta i)_d[d(\rho\delta)/d\tau]_d$$

$$+ (\Delta i)_g[d(\rho\delta)/d\tau]_g \qquad \text{(III-34)}$$

where the flame temperature T_f is the effective mean between the gas temperatures in front and back of the fabric. The exothermic pyrolysate reaction, together with its ensuing thermal feedback to the fabric are ommitted because the energy evolution during oxidization is overwhelmed by the energy supply from the gas flame.

Equation III-34 is to be solved simultaneously with Eqs. III-26 and subject to the initial conditions given by Eq. III-28.

Normalization of Eq. III-34 in terms of parameters discussed in the following section yields:

$$d\theta/d\bar{\tau} = \theta_f - \theta - \pi\,[1 + \pi_o(\theta-1)]^4 - [1-\pi_o]^4$$

$$-\pi_3^*(d\lambda_d/d\bar{\tau}) - \pi_6^*(d\lambda_g/d\bar{\tau}) \qquad \text{(III-35)}$$

For gas flame ignition, Eqs. III-26 reduce to

$$d\lambda_d/d\bar{\tau} = \pi_5^*(1-\lambda_d)^{n_d}\exp\left\{-\pi_4/[1+\pi_o(\theta-1)]\right\} \qquad \text{(III-36)}$$

and

$$d\lambda_g/d\bar{\tau} = \pi_8^*(1-\lambda_g)^{n_g}\exp\left\{-\pi_7/[1+\pi_o(\theta-1)]\right\} \qquad \text{(III-37)}$$

The initial conditions are

$$\left.\begin{aligned} \text{at } \bar{\tau} = 0 \quad & \theta = 1 \\ & \lambda_d = \lambda_g = 0 \end{aligned}\right\} \text{(III-32)}$$

The unstarred parameters π_0, π_4 and π_7 are defined in Table III-1; the other parameters are discussed below

d. The Scaling Parameters For Gas Flame Ignition are the independent variable of time $\bar{\tau}$, the dependent variables of temperature θ (Table III-2), and of decomposition degrees λ_d and λ_g (Eq. III-25), moreover the flame characteristic θ_f and the parameters π_o, π_4 and π_7 (Table III-1) and π_2^*, π_3^*, π_5^*, π_6^* and π_8^*, together with the reaction orders n_d and n_g. The parameters not yet listed in Table III-1 are summarized in Table III-2. The ignition time gas flame ignition depends consequently on eleven parameters.

$$\bar{\tau}_{i,m} = f(\pi_o, \pi_2^*, \pi_3^*, \pi_4, \pi_5^*, \pi_6^*, \pi_7, \pi_8^*, n_d\, n_g;\ \theta_f) \qquad \text{(III-38)}$$

(i) Inert heating is characterized by two parameters, by the destruction time as a function of flame temperature

$$\bar{\tau}_{i,m} = \ln[\theta_f/(\theta_f - 1)]. \qquad \text{(III-39)}$$

(ii) Radiative cooling introduces two additional parameters namely π_o and π_2^*.

(iii) Desorption and gasification processes each require four parameters as discussed in Paragraph b for radiative ignition, and also the parameter π_o. Isothermal decomposition approximations as discussed in Section 1.b of this chapter, for radiative heating, assume this form in terms of five parameters for gas flame ignition.

TABLE III-2. Definition of Gas Flame Ignition Parameters

Parameter Symbol	Definition	Interpretation
θ	$(T-T_\infty)/(T_{i,m}-T_\infty)$	temperature (with subscr. f: Flame Temp.)
$\bar{\tau}$	$2\bar{h}_c\tau/(\rho\delta c)$	time
π_o	As in Talbe III-1	
π_2^*	$\alpha\sigma\bar{F}_{s\infty}T_{i,m}^4/[\bar{h}_c(T_{i,m}-T_\infty)]$	radiative cooling
π_3^*	$\varepsilon_d(\Delta i)_d/[c(T_{i,m}-T_\infty)]$	quotient of energy requirements for desorption over sensible heat
π_4	As in Table III-1	
π_5^*	$(\rho\delta)_o c k_d/(2\bar{h}_c)$	characteristic desorption rate
π_6^*	$\varepsilon_g(\Delta i)_g/[c(T_{i,m}-T_\infty)]$	quotient of energy requirement for gasification over sensible heat.

Table III-2 (Continued) Definition of Gas FLame Ignition Parameters

Parameter Symbol	Definition	Interpretation
π_7	As in Table III-1	
π_8^*	$(\rho\delta)c\,k_g/(2\bar{h}_c)$	characteristic gasification rate
n_d, n_g		reaction orders

$$\bar{\tau}_{i,m} = \ln[\theta_f/(\theta_f-1)] + \pi_3/(\theta_f-\theta_d) + \pi_6/(\theta_f-\theta_g) \qquad \text{(III-40)}$$

Equation III-40 shows again, as Eq. III-15, that of two endothermic reactions which require equal reaction enthalpies the reaction advancing at higher temperature ($\theta_g > \theta_d$) requires more time for completion.

4. Numerical Solution and Parameter Study

Equations 29 through 32 were solved by Runge-Kutta Integration to yield the temperature Θ, the degrees of decomposition λ_d and λ_g, together with their respective time rates of change, and to yield the ignition time $\tau^*_{i,m}$ in accordance with Eq. III-33. The input variables are the thirteen parameters π_o, $\pi_1, \ldots, \pi_{10}$; n_d and n_g.

Also computed are the instantaneous power requirements due to convective cooling, radiative cooling, desorption and gasification, and the thermal feedback power from the reacting pyrolysates. Finally, the computation yields also the integrated power requirements, that is the energy requirements for each of the above processes.

Figure III-3 shows the computed temperature and decomposition history for cotton, GIRCFF Fabric No. 5.

Figure III-4 depicts the computed influence of convection on the ignition time, and exhibits the computed effect of moisture on ignition time.

Figure III-5 demonstrates the retarding effects of endothermic gasification.

5. Errors Arising from Partial Modeling

Error estimates given below are derived from the numerical solution to Eq. III-29 by evaluating the contribution of the processes listed below, to the

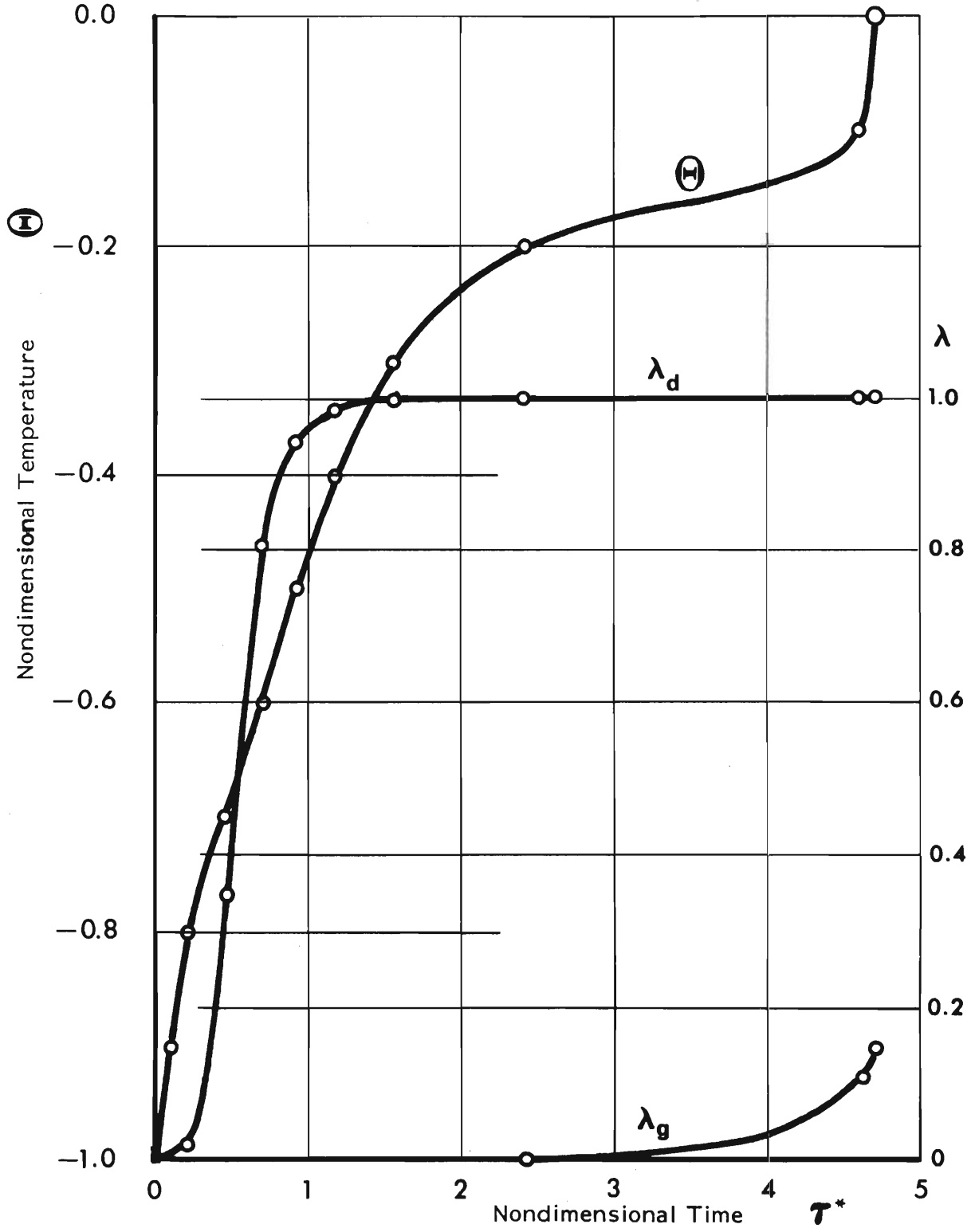

Figure III-3. Computed Temperature Rise θ, Desorption λ_d And Gasification λ_s During Ignition Process.

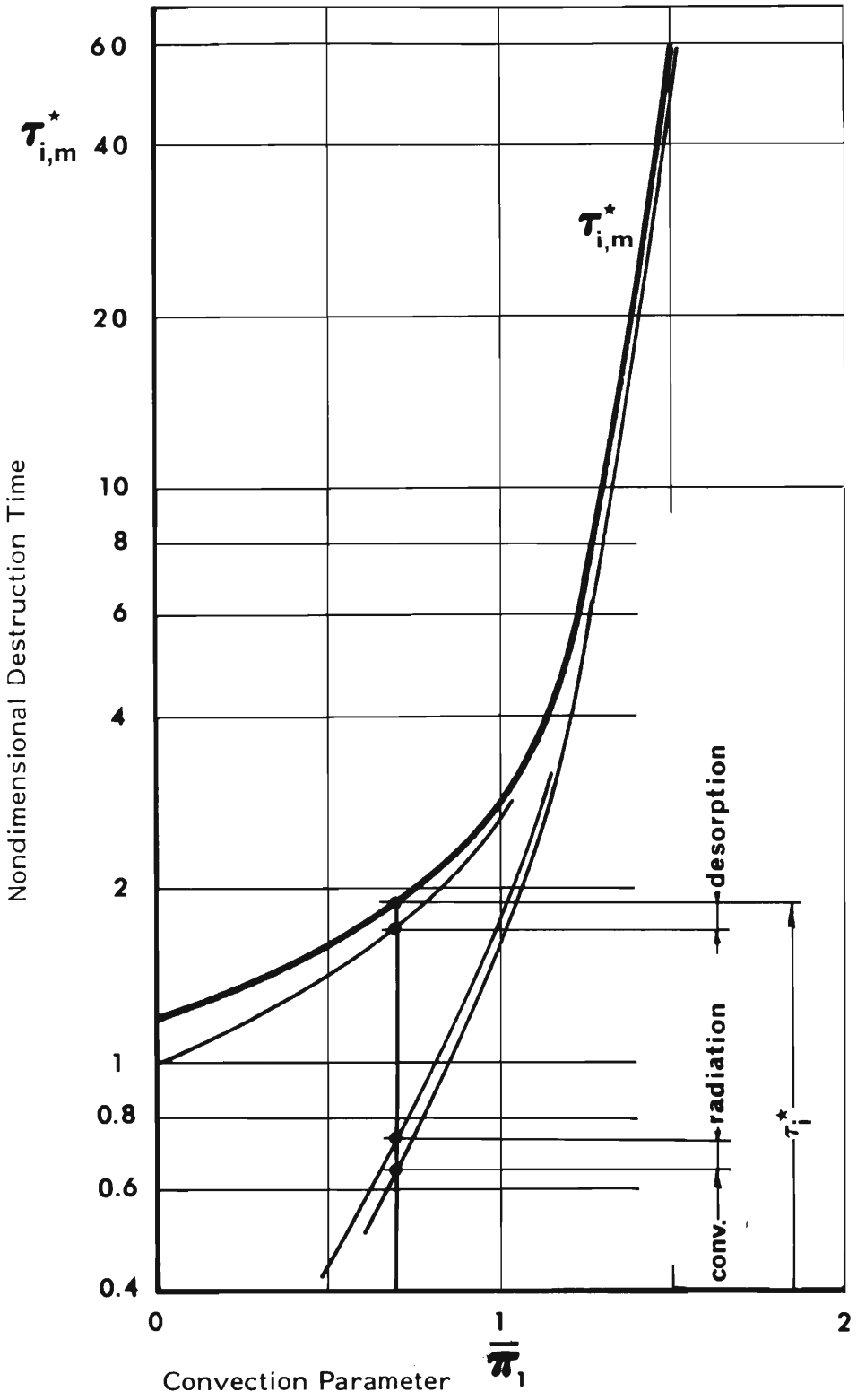

Figure III-4. Convection and Moisture Effects on Destruction Time (Computed).

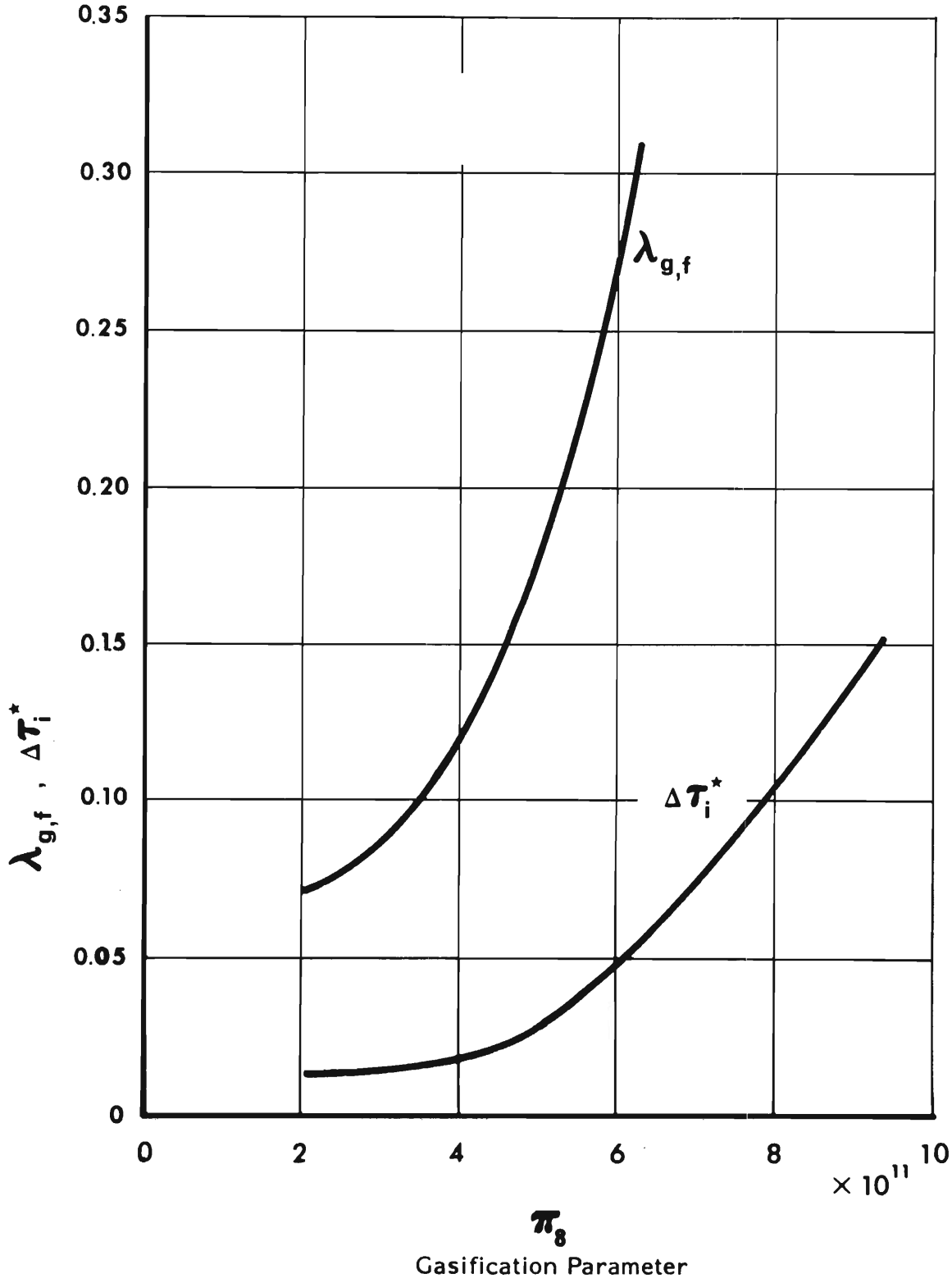

Figure III-5. Endothermic Gasification Effects: Ignition Time Delay $\Delta\tau_i^*$ and Fabric Decomposition λ_g.

destruction time $\tau^*_{i,m}$. These contributions are expressed as multiples of the time necessary to heat the fabric in the absence of convective and radiative losses and of chemical processes. All errors must be understood to vary with heating intensity. The example is listed for the cotton fabric GIRFF No. 5. for which all processes are describable in terms of available fabric properties and process parameters.

The errors listed are understood to arise from partial modeling as a result of omitting the specified process:

Table III-3. Errors Due to Partial Modeling

Sensible heating	100 %
Convective cooling	zero to complete prevention of destruction
Radiative cooling	10 %
Desorption	30 %
Gasification	65 %
Oxidation	10 %

From the above table can be seen that radiative cooling, desorption after low regain and partial pyrolysis may be ignored in that order, if the expected ignition time is to be accurate to within 30% of the time required for inert heating ($\tau^*_{i,m} = 1$). However, even these errors depend strongly on heating rate and on degree of decomposition at the time of ignition. Free convection cannot be ignored in the analysis of radiative fabric ignition unless the irradiation level is above 30 W/cm^2.

Error estimates can also be derived directly from Eqs. III-8 and 13 for convection (see Fig. III-4) from Eq. III-15 for endothermic reactions, and

from Eq. III-23 for neglecting a zero-order reaction. Equation III-40 allows to estimate the error of omitting chemical reactions in the prediction of ignition time for gas flame ignition.

6. Comparison of Analytical With Experimental Results.

The comparison presented here is for the cotton and nylon fabrics, GIRCFF Nos. 5 and 12, for which reaction kinetics and calorimetric data are available at this time.

Presented are in Figure III-6 the nondimensional ignition time τ_i^* plotted versus the radiative net power flux entering the fabric at ignition, namely $1-\bar{\pi}_2$. The parameters τ_i^* and $\bar{\pi}_1$ are evaluated from process parameters and fabric properties according to their respective definitions given in Table III-1. The fabric properties used are as listed in Appendices A.5 and 12; the convective film coefficient employed is $h_c = 1.49 \times 10^{-3}$ W/cm^{2}C at 50^{o}C (reaching 2.76×10^{-3} W/cm^{2}C at ignition according to Eq. III-11), and the viewfactor $\bar{F}_{s\infty}$ was computed to be 0.827.

The solid symbols in Figure III-6 represent experimental data obtained from cotton ignition time measurements under both single and dual shutter mode operations. Open symbols represent measured melt-through times of nylon. The solid lines are computed from Eqs. III-29 through 32.

7. Conclusions

The analytical results obtained from the ignition model presented here demonstrate that

(i) an inert heating model, combined with the ignition criterion involving a solid-phase ignition temperature, cannot adequately describe the ignition process under radiative heating,

(ii) free convection cannot be responsible by itself for the ignition delay observed on cellulosic fabrics,

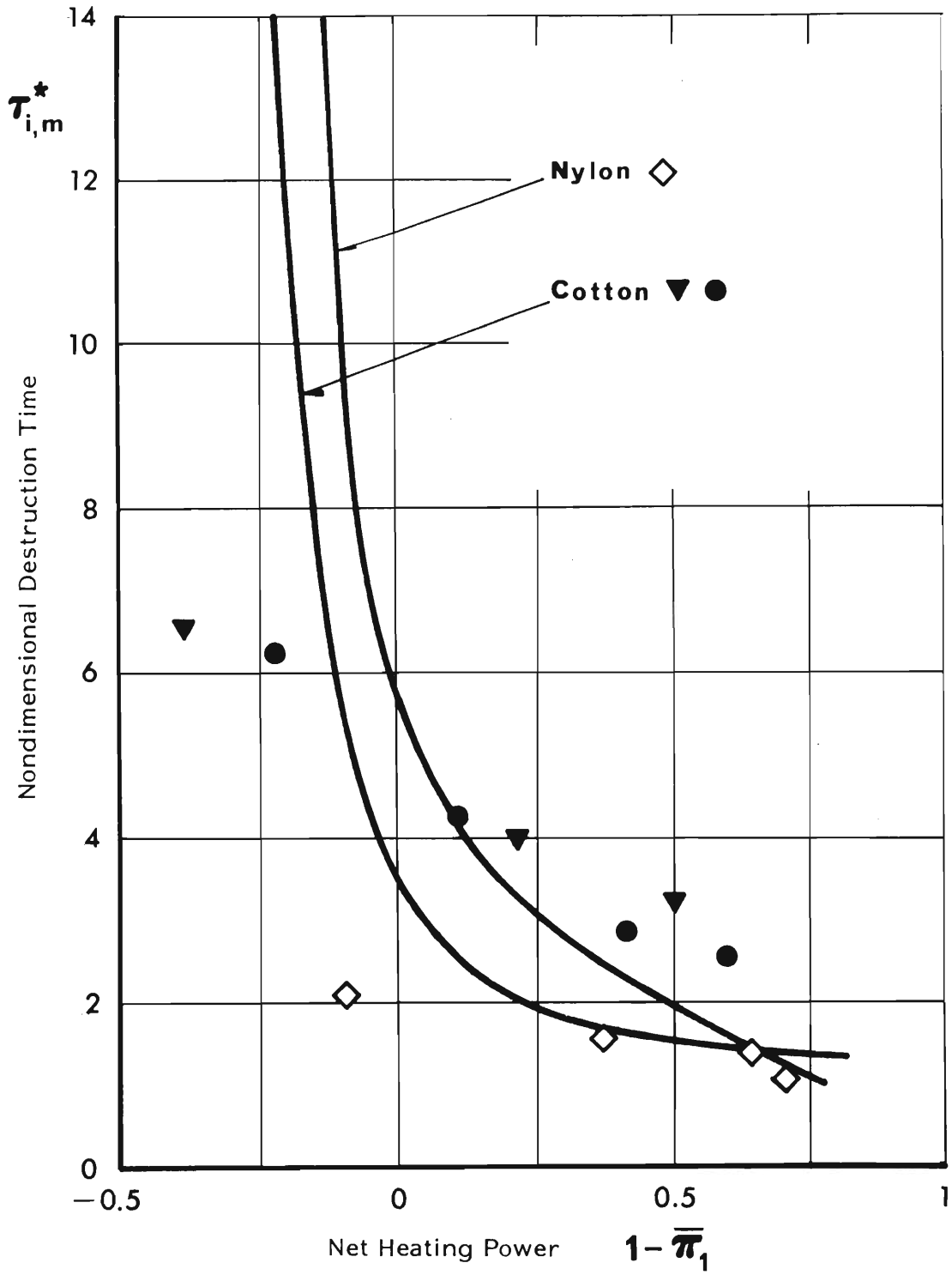

Figure III-6. Comparison of Experimental And Analytical Results of Ignition Time Analysis.

(iii) reaction kinetics of desorption do not affect the ignition time but the enthalpy of desorption,

(iv) reaction kinetics of pyrolysis and of oxidation affect ignition significantly; ignition may occur due to chemical reaction even where otherwise suppressed by convective and radiative losses, but ignition may also be significantly delayed by pyrolysis.

Items (i) and (ii) above imply that experimentally obtained radiative ignition time data cannot be fitted by either a single nor a reasonably varying, free convection film coefficient. A high film coefficient (twice the coefficient measured on the stainless steel screen) may accommodate ignition time data at high levels of irradiation but will lead to stationary fabric temperature prior to ignition at low heating intensity. Exothermic reaction is required in this case to support the external heating source. A low film coefficient (75 percent of the measured film coefficient) would predict correctly the long ignition times at low heating intensity, but would not predict the ignition delay at high heating levels.

The prediction of melt-through is less problematic than the prediction of ignition. It is recognized that ignition involves transient processes in the gaseous phase which apparently cannot be linked uniquely to the solid-phase temperature alone.

IV GENERAL CONCLUSIONS

A. Experiments

1. The fabric ignition process is describable in terms of four groups of parameters, namely
   a. Fabric Properties:
      mass per unit area,
      specific heat,
      optical properties for radiative ignition,
      enthalpies of reactions,
      reaction kinetics
   b. Heating Source Descriptions:
      radiant power emission (radiative source),
      flame temperature distributions,
      species distributions,
   c. Process Parameters Describing The Interaction Between Heat Source and Fabric:
      view factors,
      convective film coefficients,
   d. Ignition Criteria.

It may be noted that a complete description of reaction kinetics renders separate ignition criteria unnecessary. Ignition occurs whenever and wherever an exothermic reaction rate grows exponentially.

Thermal conductance must be included under (a) for heavy, opaque fabrics subject to intensive convective cooling or heating.

2. Radiative ignition of fabrics in air is strongly affected by free convection. Depending on heating intensity, free convection may retard the ignition

process and prevent ignition at low heating intensity.

3. Convective ignition of fabrics (flame ignition) is strongly governed by the fluid dynamics of the flame as exhibited by the influence of the forced convection heat transfer coefficient on ignition time.

4. Radiative cooling of the fabric during both radiative and convective heating is not significant.

5. Gas flame ignition measurements have revealed that, as under radiative heating, the net energy entering the fabric is the dominant quantity related to ignition time. Chemical effects in the gaseous phase have not been observed to influence the ignition time, except the elimination of oxygen in the vicinity of the fabric.

6. Moisture in fabrics does not affect fabric ignition time below equilibrium moisture concentrations corresponding to 24^{o}C and 30 percent relative humidity in the fabrics' pre-exposure environment. Ignition times increase up to approximately 30 percent in cellulosic fabrics preconditioned at 90 percent relative humidity.

7. The probability of fabric ignition is characterized by a small standard deviation of the ignition time about its median value, typically of only five percent of the ignition time.

B. Analysis

1. The comparison of experimental with analytical results revealed that an inert heating model with convective interaction between fabric and its environment cannot describe the fabric ignition process under radiative or convective heating over the entire range of heating conditions. The characteristic behavior of fabrics is affected by chemistry.

2. Under intensive heating the ignition time approaches the quotient of the total energy required to reach ignition criterion, over the mean rate of heating. The required energy consists of sensible heat and reaction enthalpies associated with pre-ignition processes.

3. Under decreasing heating intensities the statement given under (2) above is to be modified to include in the total energy requirement the process-dependent heat losses, and in the mean heating rate the variation of heating intensity.

4. For fabrics with low moisture content and insignificant gasification the destruction time $\tau_{i,m}$ is
under radiative heating

$$\tau_{i,m} = \rho c \delta (T_{i,m} - T_\infty) / \alpha W_o$$

and under gas flame heating

$$\tau_{i,m} = \rho c \delta / (2h_c) \cdot \ln [\theta_f / (\theta_f - 1)]$$

where the symbols are defined in the Nomenclature. These expressions involve fabric properties (ρ, c, δ, α), source descriptions (W_o, T_f) parameters of interaction (h_c) and of ignition criteria ($T_{i,m}$).

5. Any endothermic reaction delays fabric ignition or melting the more the higher the temperature at which the reaction takes place. This applies for radiative as well as convective heating of the fabric.

6. Rigorous ignition analysis involves the description of the aerochemical processes in the gaseous phase.

V APPENDICES

Appendix A. Fabric Properties Summary

Appendix A.1

Thermophysical Property Summary

Durable Press Slack

GIRCFF Fabric No.1

1. Description

   Fiber Composition: 65/35% Polyester/Cotton

   Color: White

2. Mass Per Unit Area: 23.49 mg/cm^2

3. Specific Heat

Temperature	50	125	200	°C
Spec. Heat	1.19	1.34	1.47	Ws/g C

4. Thermal Conductance

(i)	Contact Pressure	528 N/m^2			
	Temperature	63.4	108.6	161.6	°C
	Conductance	15.45	13.31	16.56	W/cm^{2}K
(ii)	Contact Pressure	866 N/m^2			
	Temperature	88.7			°C
	Conductance	15.71			W/cm^{2}K
(iii)	Contact Pressure	1,370 N/m^2			
	Temperature				°C
	Conductance				W/cm^{2}K

5. Temperature, self 413°C, pilot 334°C

6. Infrared Optical Properties

	Original		Charred at 219 °C
Source:	3,160°K	3,160°K	0.6-2.5 μm
Absorptance	0.184	0.189	0.349
Reflectance	0.605	0.522	0.366
Transmittance	0.211	0.289	0.285
Optical Thickness	0.375	0.296	0.490

7. Reaction Parameters

Reaction	Ref.	Temperature Range °C	Heating Rate °C/min	Environment	Activation Energy Kw/mole	Preexponential Factor 1/s	Order of Reaction	Enthalpy Ws/g		
								30% r.h	65% r.h	95% r.h
(i) Desorption	[II-3]							35.6	67.2	134.6
(ii) Pyrolysis	3.48	348 - 443	60	N_2	365.5	1.28×10^{27}	2.1			
(iii) Exothermic Reaction (Combustion)			See GIRCFF No. 17							

Appendix A.2

Thermophysical Property Summary

Textured Woven Blouse
GIRCFF Fabric No.2

1. Description

   Fiber Composition: 100% Polyester

   Color: Yellow

2. Mass Per Unit Area: 7.51 mg/cm^2

3. Specific Heat

Temperature	50	125	200	°C
Spec. Heat	1.42	1.42	1.42	Ws/g C

4. Thermal Conductance

(i)	Contact Pressure		528 N/m^2		
	Temperature	73.0	93.1	124.6	°C
	Conductance	20.3	21.0	22.8	W/cm^{2}K
(ii)	Contact Pressure		866 N/m^2		
	Temperature	83.3	86.3		°C
	Conductance	21.0	22.7		W/cm^{2}K
(iii)	Contact Pressure		1,370 N/m^2		
	Temperature	75.8			°C
	Conductance	22.5			W/cm^{2}K

5. Temperature, self 259 °C, pilot °C

6. Infrared Optical Properties

	Original		Charred at 134 °C
Source:	3,160°K	3,160°K	0.6-2.5 μm
Absorptance	0.164	0.153	0.175
Reflectance	0.560	0.501	0.582
Transmittance	0.276	0.346	0.243
Optical Thickness	0.272	0.208	0.305

7. Reaction Parameters

Reaction	Ref.	Temperature Range °C	Heating Rate °C/min	Environment	Activation Energy Kw/mole	Preexponential Factor 1/s	Order of Reaction	Enthalpy Ws/g		
								30% r.h	65% r.h	95% r.h
(i) Desorption										
(ii) Melting (252°C)	GIT	194 - 307	25	Air				92.9		
Pyrolysis	[B.48]	414 - 529	60	N_2	363.8	1.04×10^{24}	1.7			
(iii) Exothermic Reaction (Combustion)	GIT	337 - 490	25	Air	203.6	9.81×10^{12}	0.8			
	GIT	333 - 477	10	Air	227.5	8.35×10^{14}	1.2			
	[B.2]	260-450	5	Air	146.3	2.70×10^{9}	1.2			

See also Tables C.1 and 2.

Appendix A. 3

Thermophysical Property Summary

Double Knit
GIRCFF Fabric No. 3

1. Description

   Fiber Composition: 100% Polyester

   Color: White

2. Mass Per Unit Area: 20.91 mg/cm^2

3. Specific Heat

Temperature	50	125	200	°C
Spec. Heat	1.03	1.25	1.67	Ws/g C

4. Thermal Conductance

(i)	Contact Pressure	528 N/m^2			
	Temperature	63.2	109.7	161.0	°C
	Conductance	5.40	5.54	6.29	W/cm^{2}K
(ii)	Contact Pressure	866 N/m^2			
	Temperature	92.0			°C
	Conductance	5.46			W/cm^{2}K
(iii)	Contact Pressure	1,370 N/m^2			
	Temperature				°C
	Conductance				W/cm^{2}K

5. Melting Temperature, self 251 °C, pilot °C

6. Infrared Optical Properties

	Original		Charred at 134 °C
Source:	3,160°K	3,160°K	0.6-2.5 μm
Absorptance	0.190	0.143	0.200
Reflectance	0.560	0.619	0.506
Transmittance	0.250	0.238	0.294
Optical Thickness	0.335	0.276	0.306

7. Reaction Parameters

Reaction	Ref.	Temperature Range °C	Heating Rate °C/min	Environment	Activation Energy Kw/mole	Preexponential Factor 1/s	Order of Reaction	Enthalpy Ws/g		
								30% r.h	65% r.h	95% r.h
(i) Desorption								-	-	-
(ii) Melting Pyrolysis			See GIRFF No. 2							
(iii) Exothermic Reaction (Combustion)			See GIRFF No. 2							

See also Tables C.1 and 2.

Appendix A. 4

Thermophysical Property Summary

Denim

GIRCFF Fabric No.4

1. Description

   Fiber Composition: 100% Cotton

   Color: Navy Blue

2. Mass Per Unit Area: 29.63 mg/cm^2

3. Specific Heat

Temperature	50	125	200	°C
Spec. Heat	1.17	1.35	1.50	Ws/g C

4. Thermal Conductance

(i)	Contact Pressure	528 N/m^2			
	Temperature	65.2	107.7	159.1	°C
	Conductance	9.02	10.88	14.62	W/cm^2K
(ii)	Contact Pressure	866 N/m^2			
	Temperature	90.2			°C
	Conductance	13.05			W/cm^2K
(iii)	Contact Pressure	1,370 N/m^2			
	Temperature				°C
	Conductance				W/cm^2K

5. Ignition Temperature, self 288 °C, pilot 285 °C

6. Infrared Optical Properties

	Original		Charred at 162°C
Source:	3,160°K	3,160°K	0.6-2.5 μm
Absorptance	0.445	0.372	0.511
Reflectance	0.450	0.491	0.401
Transmittance	0.105	0.137	0.088
Optical Thickness	1.106	0.855	1.305

7. Reaction Parameters

Reaction	Ref.	Temperature Range °C	Heating Rate °C/min	Environment	Activation Energy Kw/mole	Preexponential Factor 1/s	Order of Reaction	Enthalpy Ws/g		
								30% r.h	65% r.h	95% r.h
(i) Desorption	[II-3]							101.6	191.5	384.7
	GIT	28 - 146	25	Air	97.4	4.88×10^{13}	2.6			
	GIT	36 - 120	10	Air	106.2	2.12×10^{14}	2.3			
(ii) Pyrolysis*										
(iii) Exothermic Reaction * (Combustion)										

* See also GIRCFF No. 5
Tables C.1 and 2.

Appendix A. 5

Thermophysical Property Summary

T-Shirt, Jersey
GIRCFF Fabric No. 5

1. **Description**

   Fiber Composition: 100% Cotton

   Color: White

2. **Mass Per Unit Area:** 13.71 mg/cm^2

3. **Specific Heat**

Temperature	50	125	200	°C
Spec. Heat	1.05	1.47	1.91	Ws/g C

4. **Thermal Conductance**

(i)	Contact Pressure	528 N/m^2			
	Temperature	70.9	130.5	206.0	°C
	Conductance	7.32	8.81	10.82	W/cm^{2}K
(ii)	Contact Pressure	866 N/m^2			
	Temperature	57.4	79.8		°C
	Conductance	7.31	11.28		W/cm^{2}K
(iii)	Contact Pressure	1,370 N/m^2			
	Temperature	76.5			°C
	Conductance	13.02			W/cm^{2}K

5. Ignition Temperature, self 314°C, pilot 306°C

6. **Infrared Optical Properties**

	Original		Charred at 162 °C
Source:	3,160°K	3,160°K	0.6-2.5 μm
Absorptance	0.179	0.183	0.225
Reflectance	0.533	0.521	0.491
Transmittance	0.288	0.296	0.284
Optical Thickness	0.284	0.282	0.384

7. Reaction Parameters

Reaction	Ref.	Temperature Range °C	Heating Rate °C/min	Environment	Activation Energy Kw/mole	Preexponential Factor 1/s	Order of Reaction	Enthalpy Ws/g		
								30% r.h	65% r.h	95% r.h
	[II-3]							101.6	191.5	384.7
(i) Desorption	GIT	28 - 146	25	Air	97.4	4.88×10^{13}	2.6			
	GIT	36 - 120	10	Air	106.2	2.12×10^{14}	2.3			
(ii) Pyrolysis*	[B.48]	324-466	60	N_2	206.9	3.07×10^{21}	1.4			
	[B.48]	324-466	60	N_2	219.5	9.54×10^{12}	1.1			
	[B.8]	265-357	3	H_e	351.2	3.80×10^{25}	1.0			
	[B.8]	251-354	3	He	231.2	8.40×10^{14}	1.0			
(iii) Exothermic Reaction (Combustion)	GIT	248-392	25	Air	149.7	1.26×10^{11}	1.5			
	GIT	240-394	10	Air	142.6	9.20×10^{9}	1.6			
	[B.27]	320-380	5	Air	234.6	2.20×10^{14}	1.6			
	[B.33]	275-450	12	O_2				-1.478×10^{4}		

* See also Tables C.1 and 2.

Appendix A.6

Thermophysical Property Summary

Untreated Slack
GIRCFF Fabric No. 6

1. Description

   Fiber Composition: 65/35% Polyester/Cotton

   Color: White

2. Mass Per Unit Area: 23.57 mg/cm^2

3. Specific Heat

Temperature	50	125	200	°C
Spec. Heat	1.10	1.26	1.48	Ws/g C

4. Thermal Conductance

(i)	Contact Pressure	528 N/m^2			
	Temperature	66.8	12.68	160.6	°C
	Conductance	9.90	107.4	15.60	W/cm^{2}K
(ii)	Contact Pressure	866 N/m^2			
	Temperature	88.9			°C
	Conductance	14.53			W/cm^{2}K
(iii)	Contact Pressure	1,370 N/m^2			
	Temperature				°C
	Conductance				W/cm^{2}K

5. Ignition Temperature, self 412 °C, pilot 341 °C

6. Infrared Optical Properties

	Original		Charred at 219 °C
Source:	3,160°K	3,160°K	0.6-2.5 μm
Absorptance	0.199	0.135	0.373
Reflectance	0.581	0.581	0.339
Transmittance	0.220	0.284	0.288
Optical Thickness	0.388	0.223	0.510

7. Reaction Parameters

Reaction	Ref.	Temperature Range °C	Heating Rate °C/min	Environment	Activation Energy Kw/mole	Preexponential Factor 1/s	Order of Reaction	Enthalpy Ws/g		
								30% r.h	65% r.h	95% r.h
(i) Desorption	[II-3]							35.6	67.2	134.6
(ii) Pyrolysis	[B.48]	348 - 443	60	N_2	365.5	1.28×10^{27}	2.1			
(iii) Exothermic Reaction (Combustion)			See GIRFF No. 17							

Appendix A. 7

Thermophysical Property Summary

Jersey Tube Knit
GIRCFF Fabric No. 7

1. Description

   Fiber Composition: 100% Acrylic

   Color: Gold

2. Mass Per Unit Area: 15.13 mg/cm^2

3. Specific Heat

Temperature	50	125	200	°C
Spec. Heat	1.27	1.71		Ws/g C

4. Thermal Conductance

(i)	Contact Pressure	528 N/m^2			
	Temperature	66.4	106.6	142.7	°C
	Conductance	5.44	8.66	9.92	W/cm^{2}K
(ii)	Contact Pressure	866 N/m^2			
	Temperature	88.3			°C
	Conductance	7.93			W/cm^{2}K
(iii)	Contact Pressure	1,370 N/m^2			
	Temperature				°C
	Conductance				W/cm^{2}K

5. Melting Temperature, self 241°C, pilot °C

6. Infrared Optical Properties

	Original		Charred at 230 °C
Source:	3,160°K	3,160°K	0.6-2.5 μm
Absorptance	0.202	0.292	0.720
Reflectance	0.536	0.549	0.113
Transmittance	0.262	0.159	0.167
Optical Thickness	0.340	0.855	1.115

7. Reaction Parameters

Reaction	Ref.	Temperature Range °C	Heating Rate °C/min	Environment	Activation Energy Kw/mole	Preexponential Factor 1/s	Order of Reaction	Enthalpy Ws/g		
								30% r.h	65% r.h	95% r.h
(i) Desorption										
(ii)										
(iii) Exothermic Reaction (Combustion)										

Appendix A.8

Thermophysical Property Summary

T-Shirt, Jersey
GIRCFF Fabric No.8

1. Description

   Fiber Composition: 65/35% Polyester/Cotton

   Color: White

2. Mass Per Unit Area: 16.19 mg/cm^2

3. Specific Heat

Temperature	50	125	200	°C
Spec. Heat	1.23	1.54	1.86	Ws/g C

4. Thermal Conductance

(i)	Contact Pressure	528 N/m^2			
	Temperature	68.4	129.6	205.9	°C
	Conductance	7.63	10.50	11.13	W/cm^{2}K
(ii)	Contact Pressure	866 N/m^2			
	Temperature	56.0	81.7		°C
	Conductance	7.99	9.13		W/cm^{2}K
(iii)	Contact Pressure	1,370 N/m^2			
	Temperature	75.4			°C
	Conductance	10.74			W/cm^{2}K

5. Ignition Temperature, self 437 °C, pilot 310 °C

6. Infrared Optical Properties

	Original		Charred at 230 °C
Source:	3,160°K	3,160°K	0.6-2.5 μm
Absorptance	0.174	0.164	0.346
Reflectance	0.562	0.560	0.346
Transmittance	0.264	0.276	0.308
Optical Thickness	0.298	0.272	0.460

7. Reaction Parameters

Reaction	Ref.	Temperature Range °C	Heating Rate °C/min	Environment	Activation Energy Kw/mole	Preexponential Factor 1/s	Order of Reaction	Enthalpy Ws/g		
								30% r.h	65% r.h	95% r.h
(i) Desorption	[II-3]							35.6	67.2	134.6
(ii) Melting (242°C)	GIT	199 - 280	25					43.9		
Pyrolysis	[B.48]	348 - 443	60	N_2	365.5	1.28×10^{27}	2.1			
(iii) Exothermic Reaction (Combustion)	GIT	233 - 263	10	Air				133.0		
	GIT	240 - 411	25	Air	128.4	3.12×10^{8}	1.8			

Appendix A.9

Thermophysical Property Summary

Terry Cloth
GIRCFF Fabric No. 9

1. Description

   Fiber Composition: 100% Cotton

   Color: White

2. Mass Per Unit Area: 26.48 mg/cm^2

3. Specific Heat

Temperature	50	125	200	°C
Spec. Heat	1.13	1.45	1.64	Ws/g C

4. Thermal Conductance

(i) Contact Pressure 528 N/m^2

Temperature	69.7	117.4	175.3	°C
Conductance	2.34	2.79	3.62	W/cm^2K

(ii) Contact Pressure 866 N/m^2

Temperature	95.3	°C
Conductance	2.98	W/cm^2K

(iii) Contact Pressure 1,370 N/m^2

Temperature	°C
Conductance	W/cm^2K

5. Ignition Temperature, self 302°C, pilot 294 °C

6. Infrared Optical Properties

	Original		Charred at 162 °C
Source:	3,160°K	3,160°K	0.6-2.5 μm
Absorptance	0.113	0.146	0.242
Reflectance	0.681	0.623	0.627
Transmittance	0.206	0.231	0.131
Optical Thickness	0.274	0.288	0.660

7. Reaction Parameters

Reaction	Ref.	Temperature Range °C	Heating Rate °C/min	Environment	Activation Energy Kw/mole	Preexponential Factor 1/s	Order of Reaction	Enthalpy Ws/g		
								30% r.h	65% r.h	95% r.h
(i) Desorption	[II-3]							101.6	191.1	384.7
	GIT	28 - 146	25	Air	97.4	4.88×10^{13}	2.6			
	GIT	36 - 120	10	Air	106.2	2.12×10^{14}	2.3			
(ii) Pyrolysis*	[B.48]	324 - 466	60	N_2	206.9	3.07×10^{21}	1.4			
(iii) Exothermic Reaction * (Combustion)										

* See also GIRCFF No. 5
Tables C.1 and 2.

Appendix A.10

Thermophysical Property Summary

Batiste
GIRCFF Fabric No.10

1. Description

   Fiber Composition: 100% Cotton

   Color: Purple

2. Mass Per Unit Area: 6.65% mg/cm^2

3. Specific Heat

Temperature	50	125	200	°C
Spec. Heat	1.37	1.77	—	Ws/g C

4. Thermal Conductance

(i)	Contact Pressure	528 N/m^2			
	Temperature	67.8	128.4	195.8	°C
	Conductance	17.48	20.19	29.67	W/cm^{2}K
(ii)	Contact Pressure	866 N/m^2			
	Temperature				°C
	Conductance				W/cm^{2}K
(iii)	Contact Pressure	1,370 N/m^2			
	Temperature	7.65			°C
	Conductance	25.36			W/cm^{2}K

5. Ignition Temperature, self 437 °C, pilot 345 °C

6. Infrared Optical Properties

	Original		Charred at 230 °C
Source:	3,160°K	3,160°K	0.6-2.5 μm
Absorptance	0.221	0.200	0.387
Reflectance	0.418	0.406	0.219
Transmittance	0.361	0.394	0.394
Optical Thickness	0.280	0.236	0.413

7. Reaction Parameters

Reaction	Ref.	Temperature Range °C	Heating Rate °C/min	Environment	Activation Energy Kw/mole	Preexponential Factor 1/s	Order of Reaction	Enthalpy Ws/g		
								30% r.h	65% r.h	95% r.h
(i) Desorption	[II-3]							101.6	191.5	384.7
	GIT	28 - 169	25	Air	89.5	1.77×10^{12}	2.9			
	GIT	25 - 120	10	Air	88.6	1.00×10^{12}	2.2			
(ii) Pyrolysis*	[B.48]	319 - 478	60	N_2	228.3	2.85×10^{13}	1.1			
(iii) Exothermic Reaction (Combustion)	GIT	178 - 579	25	Air	119.6	2.52×10^{8}	3.2			
	GIT	191 - 416	10	Air	94.5	3.30×10^{5}	1.0			

* See also GIRCFF No. 5
Tables C.1 and 2.

Appendix A.11

Thermophysical Property Summary

Tricot

GIRCFF Fabric No. 11

1. Description

   Fiber Composition: 80/20% Acetate/Nylon

   Color: White

2. Mass Per Unit Area: 11.31 mg/cm^2

3. Specific Heat

Temperature	50	125	200	°C
Spec. Heat	1.45	1.45	1.45	Ws/g C

4. Thermal Conductance

(i)	Contact Pressure	528 N/m^2			
	Temperature	75.2	95.2	130.9	°C
	Conductance	6.60	7.08	8.08	W/cm^2K
(ii)	Contact Pressure	866 N/m^2			
	Temperature	86.2			°C
	Conductance	7.46			W/cm^2K
(iii)	Contact Pressure	1,370 N/m^2			
	Temperature	77.7			°C
	Conductance	8.13			W/cm^2K

5. Melting Temperature, self 228°C, pilot °C

6. Infrared Optical Properties

	Original		Charred at 134 °C
Source:	3,160°K	3,160°K	0.6-2.5 μm
Absorptance	0.157	0.163	0.178
Reflectance	0.523	0.508	0.566
Transmittance	0.320	0.329	0.256
Optical Thickness	0.230	0.232	0.303

7. Reaction Parameters

Reaction	Ref.	Temperature Range °C	Heating Rate °C/min	Environment	Activation Energy Kw/mole	Preexponential Factor 1/s	Order of Reaction	Enthalpy Ws/g		
								30% r.h	65% r.h	95% r.h
(i) Desorption	[II-3]							84.0	158.0	327.0
	GIT	28 - 94	25	Air	150.9	1.28×10^{23}	2.9			
(ii) Melting (245°C)	GIT	210 - 288	25	Air				83.6		
	[B.48]	350 - 457	60	N_2	469.6	1.06×10^{30}	2.7			
(iii) Exothermic Reaction (Combustion)	GIT	256 - 426	25	Air	130.9	6.97×10^{8}	1.4			
	GIT	249 - 392	10	Air	122.5	8.63×10^{7}	1.0			

Appendix A.12

Thermophysical Property Summary

Tricot

GIRCFF Fabric No. 12

1. Description

   Fiber Composition: 100% Nylon

   Color: White

2. Mass Per Unit Area: 8.91% mg/cm^2

3. Specific Heat

Temperature	50	125	200	°C
Spec. Heat	1.51	2.09	2.68	Ws/g C

4. Thermal Conductance

(i)	Contact Pressure	528 N/m^2			
	Temperature	76.1	96.3	122.6	°C
	Conductance	19.3	17.00	20.93	W/cm^{2}K
(ii)	Contact Pressure	866 N/m^2			
	Temperature	56.1	92.2		°C
	Conductance	17.35	20.8		W/cm^{2}K
(iii)	Contact Pressure	1,370 N/m^2			
	Temperature	73.5			°C
	Conductance	17.89			W/cm^{2}K

5. Melting Temperature, self 246 °C, pilot °C

6. Infrared Optical Properties

	Original		Charred at 134 °C
Source:	3,160°K	3,160°K	0.6-2.5 μm
Absorptance	0.173	0.170	0.189
Reflectance	0.447	0.397	0.465
Transmittance	0.380	0.433	0.346
Optical Thickness	0.214	0.188	0.289

7. Reaction Parameters

Reaction	Ref.	Temperature Range °C	Heating Rate °C/min	Environment	Activation Energy Kw/mole	Preexponential Factor 1/s	Order of Reaction	Enthalpy Ws/g		
								30% r.h	65% r.h	95% r.h
(i) Desorption	[II-3]							38.9	87.6	155.7
(ii) Melting	GIT	225 - 357	25	Air				97.8		
Pyrolysis	[B.48]	404 - 535	60	N_2	385.1	8.33×10^{21}	1.2			
(iii) Exothermic Reaction (Combustion)	[B.27]	380 - 480	10	Air	209.1	3.30×10^{13}	1.0			
	[B.27]	380 - 480	5	Air	209.1	3.30×10^{13}	1.0			
	GIT	235 - 505	10	Air	78.6	9.78×10^{2}	0.1			

See also Tables C.1 and 2.

Appendix A.13

Thermophysical Property Summary

Tricot

GIRCFF Fabric No.13

1. Description

   Fiber Composition: 100% Acetate

   Color: White

2. Mass Per Unit Area: 9.40 mg/cm^2

3. Specific Heat

Temperature	50	125	200	°C
Spec. Heat	1.24	1.65	2.05	Ws/g C

4. Thermal Conductance

(i)	Contact Pressure	528 N/m^2			
	Temperature	72.1	94.9	125.1	°C
	Conductance	12.21	18.07	15.86	W/cm^{2}K
(ii)	Contact Pressure	866 N/m^2			
	Temperature	91.7			°C
	Conductance	18.82			W/cm^{2}K
(iii)	Contact Pressure	1,370 N/m^2			
	Temperature	76.9			°C
	Conductance	17.56			W/cm^{2}K

5. Melting Temperature, self 227 °C, pilot °C

6. Infrared Optical Properties

	Original		Charred at 134 °C
Source:	3,160°K	3,160°K	0.6-2.5 μm
Absorptance	0.166	0.167	0.182
Reflectance	0.490	0.443	0.492
Transmittance	0.344	0.390	0.326
Optical Thickness	0.227	0.203	0.291

7. Reaction Parameters

Reaction	Ref.	Temperature Range °C	Heating Rate °C/min	Environment	Activation Energy Kw/mole	Preexponential Factor 1/s	Order of Reaction	Enthalpy Ws/g		
								30% r.h	65% r.h	95% r.h
(i) Desorption	[II-3]							95.3	175.6	370.5
(ii) Pyrolysis	[B.48]	360 - 476	60	N_2	308.2	1.20×10^{19}	1.2			
	[B.19]	180 - 465	Static	vac.	192.3	2.60×10^{12}	1.0			
	[B.19]	180 - 465	Static	vac.	188.2	1.30×10^{12}	1.0			
(iii) Exothermic Reaction (Combustion)	GIT	253 - 425	25	Air	136.7	3.08×10^{9}	1.4			
	GIT	246 - 433	10	Air	149.9	5.88×10^{9}	2.0			

Appendix A. 14

Thermophysical Property Summary

Taffeta
GIRCFF Fabric No. 14

1. Description

   Fiber Composition: 100% Nylon

   Color: White

2. Mass Per Unit Area: 5.66 mg/cm^2

3. Specific Heat

Temperature	50	125	200	°C
Spec. Heat	1.59	1.69	2.13	Ws/g C

4. Thermal Conductance

(i)	Contact Pressure	528 N/m^2			
	Temperature	63.2	104.4	156.4	°C
	Conductance	33.91	35.71	41.91	W/cm^{2}K
(ii)	Contact Pressure	866 N/m^2			
	Temperature	88.2			°C
	Conductance	27.80			W/cm^{2}K
(iii)	Contact Pressure	1,370 N/m^2			
	Temperature				°C
	Conductance				W/cm^{2}K

5. Melting Temperature, self 241°C, pilot °C

6. Infrared Optical Properties

	Original		Charred at 134 °C
Source:	3,160°K	3,160°K	0.6-2.5 μm
Absorptance	0.144	0.218	0.193
Reflectance	0.348	0.348	0.399
Transmittance	0.508	0.434	0.408
Optical Thickness	0.136	0.234	0.222

7. Reaction Parameters

Reaction	Ref.	Temperature Range °C	Heating Rate °C/min	Environment	Activation Energy Kw/mole	Preexponential Factor 1/s	Order of Reaction	Enthalpy Ws/g		
								30% r.h	65% r.h	95% r.h
(i) Desorption	[II-3]							38.9	87.6	155.7
(ii) Pyrolysis	[B.48]	404 - 535	60	N_2	495.5	1.65×10^{33}	2.1			
(iii) Exothermic Reaction (Combustion)			See GIRFF No. 12							

See also Tables C.1 and 2.

Appendix A.15

Thermophysical Property Summary

Durable Press Slack
GIRCFF Fabric No.15

1. Description

   Fiber Composition: 65/35% Polyester/Rayon

   Color: Brown

2. Mass Per Unit Area: 22.82 mg/cm^2

3. Specific Heat

Temperature	50	125	200	°C
Spec. Heat	0.91	1.26	1.55	Ws/g C

4. Thermal Conductance

(i)	Contact Pressure	528 N/m^2			
	Temperature	64.1	104.7	159.8	°C
	Conductance	12.01	13.91	16.91	W/cm^2K
(ii)	Contact Pressure	866 N/m^2			
	Temperature	89.0			°C
	Conductance	15.37			W/cm^2K
(iii)	Contact Pressure	1,370 N/m^2			
	Temperature				°C
	Conductance				W/cm^2K

5. Ignition Temperature, self 432 °C, pilot 334 °C

6. Infrared Optical Properties

	Original		Charred at 247 °C
Source:	3,160°K	3,160°K	0.6-2.5 μm
Absorptance	0.226	0.256	0.603
Reflectance	0.515	0.413	0.239
Transmittance	0.259	0.331	0.158
Optical Thickness	0.375	0.340	1.040

7. Reaction Parameters

Reaction	Ref.	Temperature Range °C	Heating Rate °C/min	Environment	Activation Energy Kw/mole	Preexponential Factor 1/s	Order of Reaction	Enthalpy Ws/g		
								30% r.h	65% r.h	95% r.h
(i) Desorption	[II-3]							67.3	118.4	255.5
(ii)										
(iii) Exothermic Reaction (Combustion)										

Appendix A.16

Thermophysical Property Summary

Shirting
GIRCFF Fabric No. 16

1. **Description**

   Fiber Composition: 50/50% Polyester/Cotton

   Color: White

2. **Mass Per Unit Area:** 13.14 mg/cm^2

3. **Specific Heat**

Temperature	50	125	200	°C
Spec. Heat	1.16	1.31	1.44	Ws/g C

4. **Thermal Conductance**

(i)	Contact Pressure	528 N/m^2			
	Temperature	63.9	105.9	135.6	°C
	Conductance	14.49	14.62	19.03	W/cm^2K
(ii)	Contact Pressure	866 N/m^2			
	Temperature	90.7			°C
	Conductance	19.72			W/cm^2K
(iii)	Contact Pressure	1,370 N/m^2			
	Temperature				°C
	Conductance				W/cm^2K

5. Ignition Temperature, self 470°C, pilot 357 °C

6. **Infrared Optical Properties**

	Original		Charred at 247 °C
Source:	3,160°K	3,160°K	0.6-2.5 μm
Absorptance	0.168	0.207	0.241
Reflectance	0.613	0.499	0.322
Transmittance	0.219	0.294	0.437
Optical Thickness	0.338	0.312	0.256

7. Reaction Parameters

Reaction	Ref.	Temperature Range °C	Heating Rate °C/min	Environment	Activation Energy Kw/mole	Preexponential Factor 1/s	Order of Reaction	Enthalpy Ws/g		
								30% r.h	65% r.h	95% r.h
(i) Desorption	[II-3]							50.8	95.7	192.3
(ii)										
(iii) Exothermic Reaction (Combustion)										

Appendix A.17

Thermophysical Property Summary

Batiste

GIRCFF Fabric No. 17

1. Description

   Fiber Composition: 65/35% Polyester/Cotton

   Color: White

2. Mass Per Unit Area: 8.55 mg/cm^2

3. Specific Heat

Temperature	50	125	200	°C
Spec. Heat	1.27	1.47	1.66	Ws/g C

4. Thermal Conductance

(i)	Contact Pressure	528 N/m^2			
	Temperature	72.6	128.0	199.3	°C
	Conductance	17.34	22.48	26.75	W/cm^2K
(ii)	Contact Pressure	866 N/m^2			
	Temperature				°C
	Conductance				W/cm^2K
(iii)	Contact Pressure	1,370 N/m^2			
	Temperature	77.3			°C
	Conductance	30.41			W/cm^2K

5. Ignition Temperature, self 471°C, pilot 376 °C

6. Infrared Optical Properties

	Original		Charred at 252 °C
Source:	3,160°K	3,160°K	0.6-2.5 μm
Absorptance	0.151	0.164	0.425
Reflectance	0.485	0.464	0.255
Transmittance	0.364	0.372	0.320
Optical Thickness	0.198	0.208	0.520

7. Reaction Parameters

Reaction	Ref.	Temperature Range °C	Heating Rate °C/min	Environment	Activation Energy Kw/mole	Preexponential Factor 1/s	Order of Reaction	Enthalpy Ws/g		
								30% r.h	65% r.h	95% r.h
(i) Desorption	[II-3]							35.6	67.2	134.6
(ii) Melting (240°C)	GIT	225 - 272	25	Air				28.4		
		231 - 252	10	Air				20.1		
Pyrolysis	[B.48]	348 - 443	60	N_2	310.3	1.80×10^{19}	1.6			
(iii) Exothermic Reaction (Combustion)	GIT	240 - 415	25	Air	105.4	2.67×10^{6}	3.0			
	GIT	224 - 380	10	Air	108.3	2.86×10^{6}	2.0			

Appendix A. 18

Thermophysical Property Summary

Flannel
GIRCFF Fabric No.18

1. Description

   Fiber Composition: 100% Cotton

   Color: White

2. Mass Per Unit Area: 12.88 mg/cm^2

3. Specific Heat

Temperature	50	125	200	°C
Spec. Heat	1.44	1.63	1.82	Ws/g C

4. Thermal Conductance

(i)	Contact Pressure	528 N/m^2			
	Temperature	73.0	134.4	205.3	°C
	Conductance	5.55	6.72	8.74	W/cm^2K
(ii)	Contact Pressure	866 N/m^2			
	Temperature				°C
	Conductance				W/cm^2K
(iii)	Contact Pressure	1,370 N/m^2			
	Temperature	78.6			°C
	Conductance	7.06			W/cm^2K

5. Ignition Temperature, self 306°C, pilot 286 °C

6. Infrared Optical Properties

	Original		Charred at 162 °C
Source:	3,160°K	3,160°K	0.6-2.5 μm
Absorptance	0.170	0.176	0.241
Reflectance	0.599	0.573	0.527
Transmittance	0.231	0.251	0.232
Optical Thickness	0.326	0.312	0.431

7. Reaction Parameters

Reaction	Ref.	Temperature Range °C	Heating Rate °C/min	Environment	Activation Energy Kw/mole	Preexponential Factor 1/s	Order of Reaction	Enthalpy Ws/g		
								30% r.h	65% r.h	95% r.h
(i) Desorption	[II-3]							101.6	191.5	384.7
	GIT	31 - 140	25	Air	104.9	4.74×10^{14}	2.5			
	GIT	30-103	10	Air	127.1	3.40×10^{18}	2.3			
(ii) Pyrolysis*	[B.48]	338 - 470	60	N_2	229.6	4.98×10^{13}	1.2			
(iii) Exothermic Reaction * (Combustion)	GIT	238 - 408	25	Air	156.00	2.20×10^{11}	1.2			
	GIT	245 - 349	10	Air	184.00	5.89×10^{13}	0.5			

* See also GIRCFF No. 5
Tables C.1 and C.2

Appendix A.19

Thermophysical Property Summary

Flannel
GIRCFF Fabric No.19

1. Description

   Fiber Composition: 100% Cotton, Fire retardant

   Color: White

2. Mass Per Unit Area: 14.89 mg/cm^2

3. Specific Heat

Temperature	50	125	200	°C
Spec. Heat	1.33	1.60	1.87	Ws/g C

4. Thermal Conductance

(i)	Contact Pressure	528 N/m^2			
	Temperature	73.0	134.1	203.5	°C
	Conductance	5.38	7.55	9.46	W/cm^{2}K
(ii)	Contact Pressure	866 N/m^2			
	Temperature				°C
	Conductance				W/cm^{2}K
(iii)	Contact Pressure	1,370 N/m^2			
	Temperature	77.8			°C
	Conductance	8.55			W/cm^{2}K

5. Ignition Temperature, self 488°C, pilot 323 °C

6. Infrared Optical Properties

	Original		Charred at 252 °C
Source:	3,160°K	3,160°K	0.6-2.5 μm
Absorptance	0.181	0.201	0.498
Reflectance	0.590	0.602	0.248
Transmittance	0.229	0.197	0.254
Optical Thickness	0.348	0.428	0.688

7. Reaction Parameters

Reaction	Ref.	Temperature Range °C	Heating Rate °C/min	Environment	Activation Energy Kw/mole	Preexponential Factor 1/s	Order of Reaction	Enthalpy Ws/g		
								30% r.h	65% r.h	95% r.h
(i) Desorption	[II-3]							101.6	191.5	384.7
	GIT	28 - 120	25	Air	101.6	2.00×10^{14}	2.3			
	GIT	35 - 90	10	Air	201.5	7.70×10^{30}	3.3			
(ii) Pyrolysis*	[B.48]	319 - 396	60	N_2	603.0	5.33×10^{49}	2.1			
(iii) Exothermic Reaction * (Combustion)	GIT	202 - 389	25	Air	92.0	8.60×10^{5}	1.8			
	GIT	166 - 376	10	Air	85.3	7.79×10^{4}	0.8			

* See also GIRCFF No. 5
Tables C.1 and C.2.

Appendix A. 20

Thermophysical Property Summary

Flannel
GIRCFF Fabric No. 20

1. **Description**

   Fiber Composition: 100% Wool

   Color: Navy Blue

2. **Mass Per Unit Area:** 19.93 mg/cm^2

3. **Specific Heat**

Temperature	50	125	200	°C
Spec. Heat	1.27	1.27	1.27	Ws/g C

4. **Thermal Conductance**

(i)	Contact Pressure	528 N/m^2			
	Temperature	63.9	107.5	142.5	°C
	Conductance	7.12	7.29	7.55	W/cm^{2}K
(ii)	Contact Pressure	866 N/m^2			
	Temperature	91.7			°C
	Conductance	7.00			W/cm^{2}K
(iii)	Contact Pressure	1,370 N/m^2			
	Temperature				°C
	Conductance				W/cm^{2}K

5. Ignition Temperature, self 471 °C, pilot 322 °C

6. **Infrared Optical Properties**

	Original		Charred at 252 °C
Source:	3,160°K	3,160°K	0.6-2.5 μm
Absorptance	0.545	0.533	0.609
Reflectance	0.336	0.365	0.105
Transmittance	0.119	0.102	0.286
Optical Thickness	1.149	1.226	0.725

7. Reaction Parameters

Reaction	Ref.	Temperature Range °C	Heating Rate °C/min	Environment	Activation Energy Kw/mole	Preexponential Factor 1/s	Order of Reaction	Enthalpy Ws/g		
								30% r.h	65% r.h	95% r.h
(i) Desorption	[II-3]							199.5	365.0	657.1
(ii)										
(iii) Exothermic Reaction (Combustion)										

Appendix B.I

Reaction Kinetics and Calorimetry

a. Objectives. The fabric ignition models presented in Chapter III for the purpose of predicting ignition time in terms of heating conditions and fabric properties involve the enthalpies of reactions and kinetics parameters activation energy, frequency factor and order of reaction, each averaged over representative process stages, namely desorption, pyrolysis or melting, and oxidation. These parameters are derived from simultaneous differential thermal analysis (DTA) and thermogravimetric analysis (TGA).

Differential Thermal Analysis is performed to obtain the enthalpy of reaction. This calorimetric quantity is derived by comparing the temperature response of the material of interest to the response of an inert reference material while both materials are subjected to the same controlled environmental temperature change. The difference between sample material and reference enthalpy changes is due to (1) differences in specific heat, (2) differences in mass or mass changes and (3) chemcal reactions, be they exothermic or endothermic.

The reaction enthalpy is derived from the energy balances written for both the sample and the reference systems, which is evaluated on the basis of appropriate calibration runs with known sample materials and from the recordings of the difference between sample and reference temperatures as functions of time.

Thermogravimetric Analysis yields the three kinetics parameters activation energy, frequency factor and reaction order through evaluation of the continuously recorded change in weight suffered by the object material while it undergoes controlled heating. The three parameters are derived from fitting the weight loss history sectionally to Arrhenius type reaction rate laws.

b. The Apparatus Used for DTA/TGA Measurements.

The apparatus used for DTA/TGA measurements is the METTLER Thermoanalyzer 2 which is owned by the School of Chemistry and which was supplemented appropriately by the School of Mechanical Engineering both at Georgia Institute of Technology. The thermoanalyzer is shown in Figure B.1 and consists of the Control and Recording Facility shown in Figure B.2, the Furnace shwon in Figure B.3 and the electromagnetic substitution balance housed in the cabinet beneath the Furnace (Figure B.1). The sample and reference materials are retained in the METTLER Macro-TGA Platinum Crucibles and supported by the ceramic sample holder shown in Figure B.4.

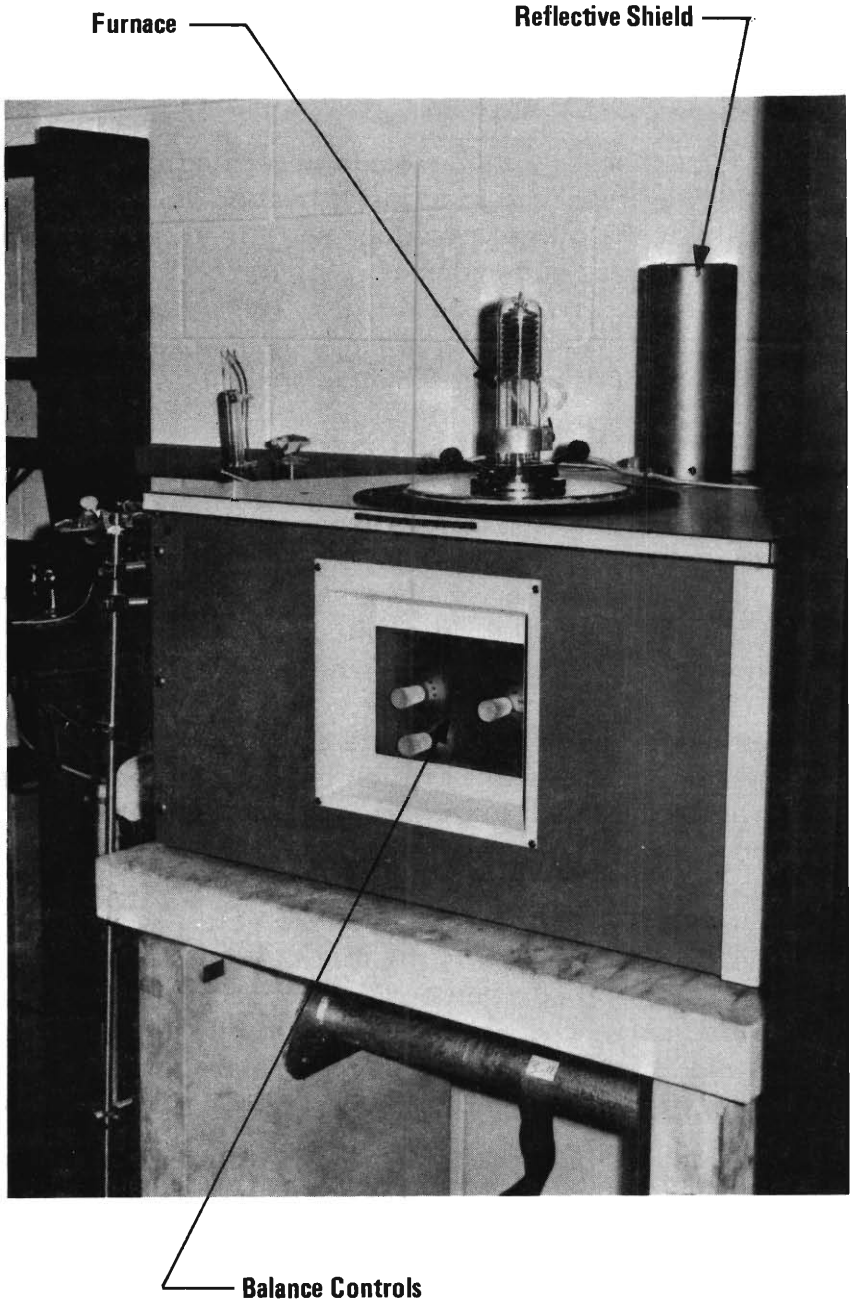

Figure B.1. DTA/TGA Apparatus.

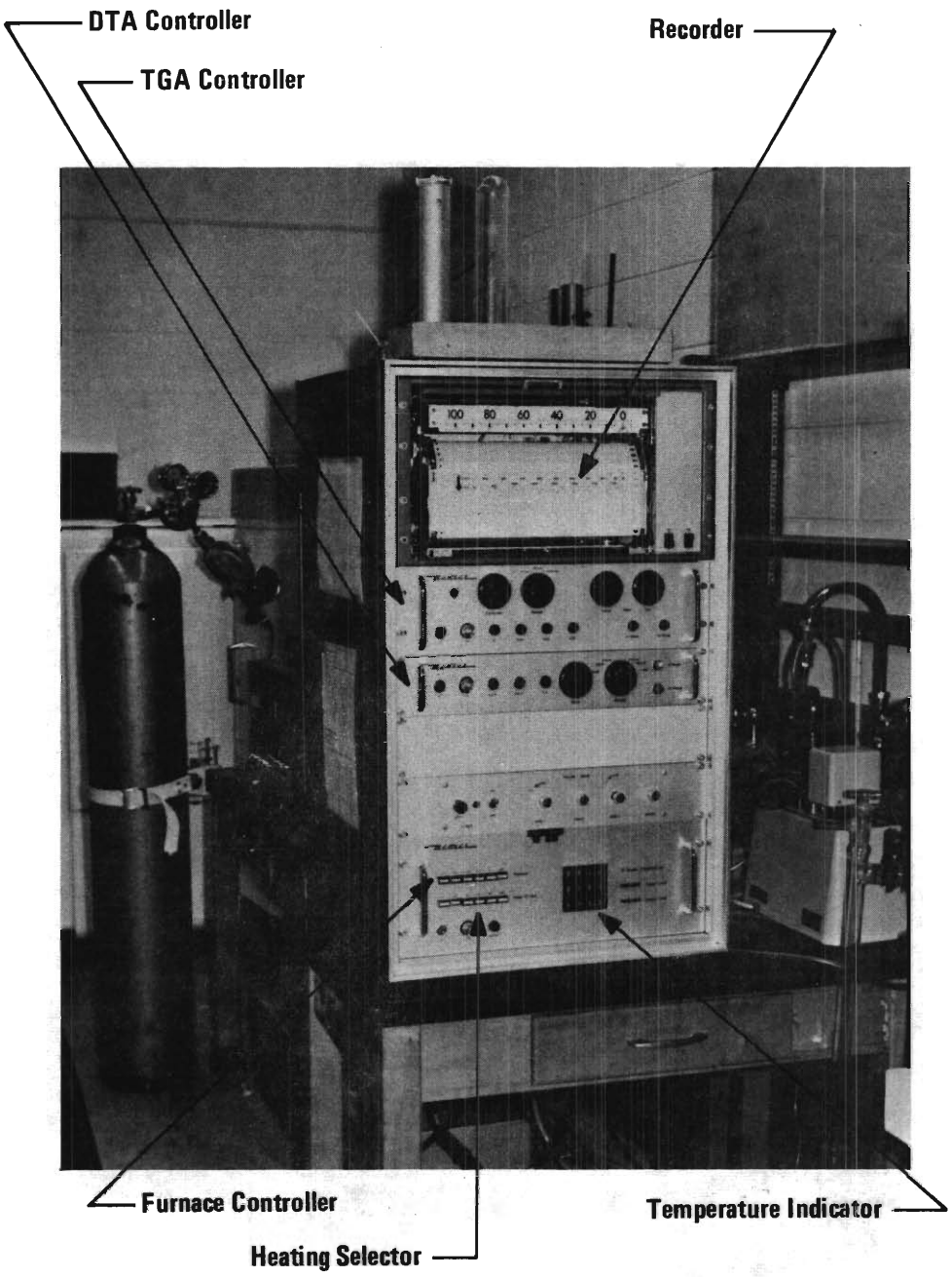

Figure B.2. DTA and TGA Control Elements and Recording Facility.

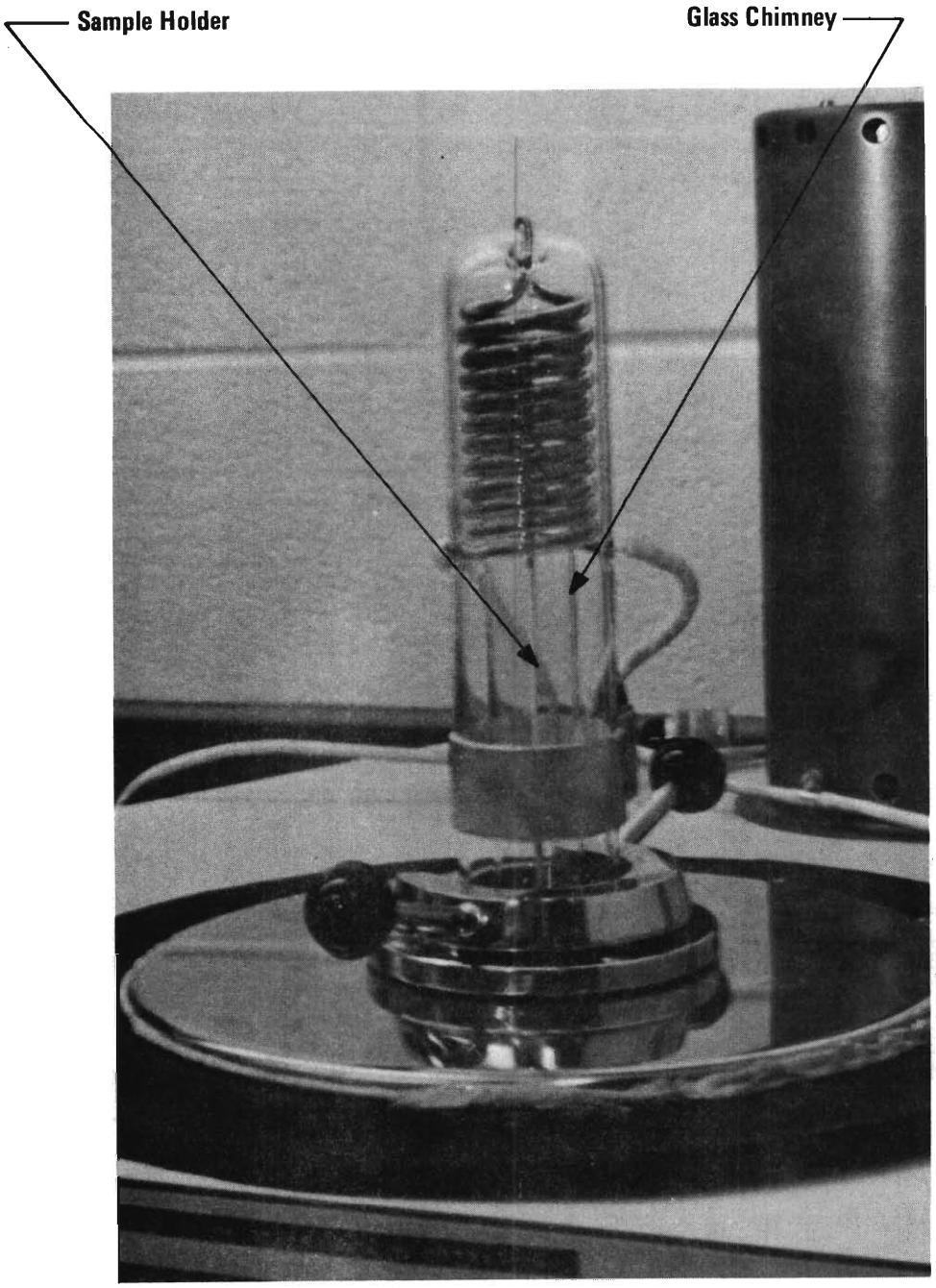

Figure B.3. Close-Up of Furnace.

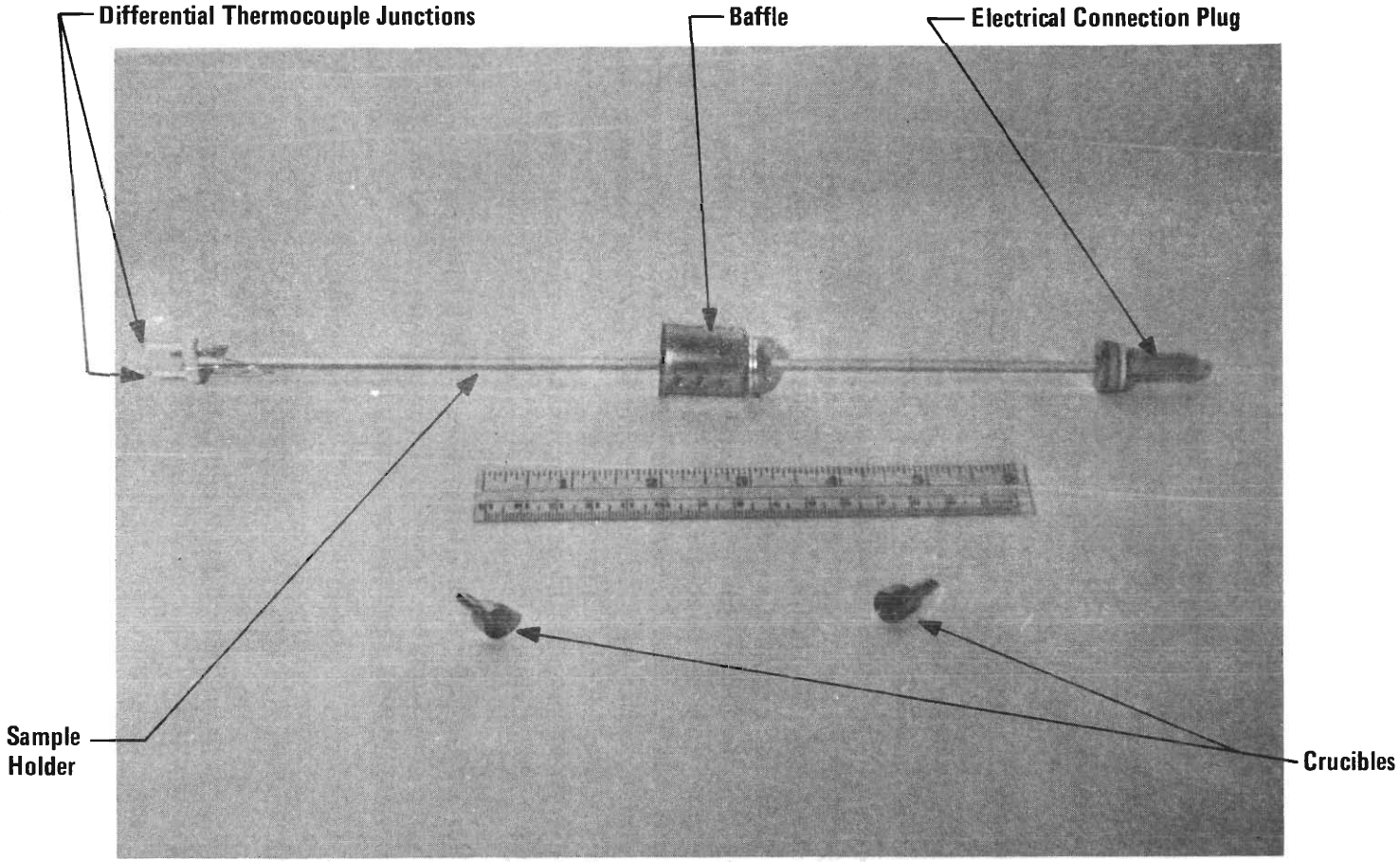

Figure B.4. Close-Up of Sample Holder and Crucibles.

The furnace used is the middle-range Quartz Furnace, heating the crucibles radiatively at the rates between 1 and 25°C/min, in the temperature range between 25 and 1000°C.

Crucible and differential temperatures are sensed by Pt/Pt - 10% Rh thermocouples whose junctions are pressed against the bottom of the crucibles.

The Mettler balance is an electromagnetically compensated balance. Changes in sample weight are detected by a photocell which sends a compensating electrical signal to an electromagnet. The amount of electrical power sent to the balance is read out as a measure of weight loss. The maximum recording sensitivity is 25.4 mm/mg.

c. Procedure for DTA/TGA Measurements.

Samples were prepared by finely cutting a piece of each of the ten Primary GIRCFF Fabrics with scissors to obtain a loose fuzz. It was felt that further subdivision would lead to loss of integrity of the sample as fabric. The mass of sample material as specified for each test was mixed with gold or aluminum oxyde powder and hard packed into the platinum sample crucible. A mass of aluminum oxyde or gold powder equal to the sum of sample and diluent masses, was hard packed into the platinum reference crucible. The two crucibles were then placed on the ceramic support rod and the furnace was placed over the whole assembly of the METTLER Thermoanalyzer 2. A dynamic atmosphere of dry air from a compressed air bottle was provided at a flow rate of twelve cubic centimeters per minute. Simultaneous DTA/TGA measurements were made with each fabric on the METTLER Thermoanalyzer 2 at two heating rates, 25 and 10°C per minute. A six channel recorder operating at twelve inches per minute was used to record furnace temperature, mass loss and differential temperature.

The optimum position of the crucibles with respect to the furnace was established (Figure B.5). The buoyancy correction was determined and KNO_3 was used for the calorimetric calibration substance.

d. Data Evaluation

(i) Reaction Kinetics were evaluated by three different methods, called Method I, II and III, respectively. All methods are based on the Arrhenius reaction rate law

$$\dot{\lambda} = d\lambda/d\tau = (1 - \lambda)^n \, k_o \exp(-E/RT) \qquad (B.1)$$

where λ is the reacted mass fraction of the decomposable mass fraction, T is

the absolute temperature, τ the time, k_o the frequency factor, E the activation energy, R the universal gas constant and n the reaction order. The aim is to determine E, k_o and n from the thermogram $\lambda(\tau)$.

Method I involves the entire thermogram and requires problematic differentiation, Method II involves measured data only at the single point of maximum decomposition rate while Method III is an iterative process optimizing simultaneously the reaction order and the activation energy. The three methods are discussed below.

e. Thermograms of DTA/TGA Test Runs.

Thermograms of DTA/TGA test runs used in the kinetic parameter evaluations are shown in Figures B.9 through B.21 along with the DTA/TGA data sheet for each test. Figures B.5 and B.6 show the optimum furnace position test and the buoyancy calibration tests.

Method I consists of writing Eq. B.1 twice, once for an arbitrary instant and once for the instant maximum decomposition rate $\dot{\lambda}_m$, and of forming the ratios

$$[\ln(\dot{\lambda}/\dot{\lambda}_m)] / \ln[(1-\lambda)/(1-\lambda_m)] =$$

$$n - \left\{ E/[R(1/T - 1/T_m)] \right\} / \ln[(1-\lambda)/(1-\lambda_m)] \qquad (B.2)$$

Plotting of Eq. B.2 on semi-logarithmic paper allows fitting a least-square straight line to the decomposition rate data, with intercept n, and slope proportional to $-E/RT_m$. Numerical differentiation was used to derive $\dot{\lambda}$ from $\lambda(\tau)$ traces. The evaluation was coded in FORTRAN. The singularity of Eq. B.2 encountered when $\lambda \to \lambda_m$ at $T \to T_m$ was removed with the aid of d'Hospital's rule which yields

$$-\ddot{\lambda}_m (1-\lambda_m) / (\dot{\lambda}_m)^2 = n - (E/RT_m)\ \phi\ (1-\lambda_m) / (T_m \dot{\lambda}_m)$$

$$\text{for} \quad T \to T_m \qquad (B.3)$$

where ϕ is the known heating rate.

After having obtained n and E from the least-square fit, the frequency factor k_o was evaluated directly from Eq. B.1, by averaging over all discrete data points.

The quality of least-square fit was evaluated in terms of the square of the correlation coefficient as described under Method III. For results see Chapter II.

For Method II, Eq. B.1 is differentiated with respect to time, the result set

equal to zero, to yield the decomposed fraction λ_m at the instant of maximum decomposition rate $\dot{\lambda}_m$, which is substituted back into Eq. B.1. The fraction λ_m is found first

$$[\ (1-\lambda_m)^{1-n}\ ] / n \ = \ k_o\, RT_m^2 \,/\, (E\phi)\ \exp\ (-E/RT_m) \qquad (B.4)$$

and then the maximum rate

$$\dot{\lambda}_m \ = \ (1-\lambda_m) \ / \ n \ . \ [\ E\phi/RT_m^2)\ ] \qquad (B.5)$$

Integrating Eq. B.1 and ignoring insignificant terms gives, after approximating the exponential integral by asymptotic expansion appropriate for large values of its argument,

$$[\ (1-\lambda_m)^{1-n} -1\ ] / (n-1) \ \approx \ k_o\, RT_m^2 \,/\, (\phi E)\ .\ \exp\ (-E/RT_m) \qquad (B.6)$$

Combining Eqs. B.4 and 6 gives this implicit expression for the reaction order n

$$(1-\lambda_m)^{1-n} \ = \ n \qquad (B.7)$$

Having solved Eq. B.7 by Newton-Raphson iteration for n one obtains E from Eq. B.5 and k_o from Eq. B.6, in that order.

This method not only relays heavily on a particular instant of the reaction but also involves numerical differentiation for the evaluation of E by Eq. B.5. The method is, however, very simple and requires no least-square fit. Results are shown in Chapter II, Section A.

Method III was developed to avoid numerical differentiation of the weight loss trace, $\lambda(\tau)$. The procedure leading to Eq. B.6 was repeated for arbitrary instances $(\lambda, T; \tau)$ to give

$$\ln \left\{ [1-(1-\lambda)^{1-n}\ ] / (1-n)\ .\ (T_o/T)^2 \right\} \ =$$

$$\ln\ [k_o\, RT_o^2 \,/\, (\phi E)\ ] \ - E/(RT) \qquad (B.8)$$

where T_o represents the initial temperature. Plotting the left-hand side of Eq. B.8 on semi-log paper versus 1/T yields again the activation energy E through the slope of the best straight line through the data points (λ, T). But the reaction order n must be known before such a plot can be prepared, and the quality of the least-square, straight line fit depends on the choice of n.

If one selects the square $B = r^2$ of the correlation coefficient r as the measure of determinateness or quality of least-square fit one has B = 1 in the case of a perfect fit and B = 0 for a useless fit, i.e. the attempt to pass a line through a circular cloud of uniformly distributed data points. Moreover one can consider

B as a function of reaction order n and optimize n by maximizing B(n). For this purpose introduce Z_i for the left-hand side of Eq. B.8 as evaluated at discrete points (λ_i, T_i), and $y_i = 1/T_i$. Then define for N data points

$$s_{yz} = 1/N \sum_{i=1}^{N} y_i z_i - \bar{y}\,\bar{z} \qquad (B.9)$$

where superscripted bars indicate arithmetic means, and

$$s_y^2 = 1/N \sum_{i=1}^{N} y_i^2 - (\bar{y})^2$$

along with a corresponding expression for s_z^2. With these definitions one gets the best straight line Z(Y)

$$Z = \bar{z} + b\,(Y - \bar{y}) \qquad (B.10)$$

where $$b = s_{yz}/s_y^2 \qquad (B.11)$$

Clearly, the regression coefficient b depends on the reaction order n, as does

$$B = r^2 = [b\, s_y/s_z]^2 \qquad (B.12)$$

A Newton-Raphson iteration was coded in FORTRAN to converge to the optimum reaction order n, via the maximum determinatenes, B(n), the maximum being identified by $dB/dn = 0$ and $d^2B/dn^2 < 0$. After having found the optimum n we computed E/R from the regression coefficient b and found the frequency factor k_o from the intercept of the line defined by Eq. B.10. Results are presented in Chapter II.

Dr. McCarter's Decomposition Rate Data were evaluated by Methods I and II. Differentiation was obviously not necessary but the total and fractional fabric masses decomposed had to be evaluated by Simpson Integration of the given decomposition rate histories, $\lambda(\tau)$. Results are also presented in Chapter II.

ii. Reaction Calorimetry. Since previously published techniques [B.8] for evaluating the reaction enthalpy from differential thermal analysis (DTA) data do not account for the effects of mass loss, a procedure was developed from the energy conservation principle, applied to the sample and the reference systems. The unknown instrument characteristics were evaluated either from

calibration runs performed with a known substance (KNO_3) or direct weighings and published material properties. Discussed are at first the calibration methods, then the evaluation technique for desorption and finally for melting reactions.

Calibration. The potassium nitrate (KNO_3) thermogram in Figures B.7 and 8 were used to infer the overall coefficient K of heat transfer between the radiating tungsten filament of the furnace (fu) and the crucibles. Conservation of energy, i.e.

$$C\,dT = -dH + K\,(T_{fu} - T)\,d\tau \qquad (B.13)$$

was written with appropriate values of heat capacities, known from weighings (m_i) and specific heats c_i

$$C = \sum_i m_i\, c_i, \qquad (B.14)$$

with known reaction enthalpies (ΔH_{KNO_3}), and known heating histories $T(\tau_{fu})$ and then integrated to yield

$$K = \left\{ -\Delta H_{KNO_3} + C_s\,[(\Delta T_i - \Delta T_f) + \varepsilon\,(T_i - T_f)_r\,] \right\} / A \qquad (B.15)$$

Here, ΔT designates the difference between sample (KNO_3) and reference (Al_2O_3 or gold) temperatures, subscripts i and f designate, respectively, beginning and end of reaction while subscripts s and r represent sample and reference, respectively. The symbols ε and A stand for

$$\varepsilon = C_r / C_s - 1 \qquad (B.16)$$

and

$$A = \int_i^f \Delta T\, d\tau. \qquad (B.17)$$

The specific data used are listed in Table B.1 below and the average value of K was found to be

$$K = 3.27 \times 10^{-2}\ W/^oK \qquad (B.18)$$

Desorption, Pyrolysis, Oxidation processes can also be described by an equation of the form as Eq. B.13, except the heat capacity of the sample system changes with time

$$C_s = C_{so} + m\,(\tau)\,.\,c \qquad (B.19)$$

Table B.1. Parameters Used in Evaluation of Overall Heat Transfer Coefficient, Reaction Calorimetry

m_{c_s}	=	1.025 g.
m_{c_r}	=	1.037
c_c^*	=	0.0328 cal./g. ^oK
c_g^*	=	0.0316 cal./g. ^oK
$c_{KNO_3}^*$	=	0.228 cal./g. ^oK
$\Delta H_{KNO_3}^*$	=	28.1 cal./g.

Test No.: 60
ϕ = 25 ^oC/min.

m_{KNO_3}	=	0.0504 g.
m_{g_s}	=	0.0489 g.
m_{g_r}	=	0.0979 g.
C_s	=	0.0470 cal./ ^oC
ε	=	-0.202
A	=	-345 sec. - ^oC
$\Delta T_o - \Delta T_\infty$	=	0.15 ^oC
$T_{r,\infty} - T_{r,o}$	=	129 ^oC

Test No.: 72
ϕ = 10 ^oC/min.

m_{KNO_3}	=	0.0500 g.
m_{g_s}	=	0.0489 g.

Table B.1. (Continued)

m_{g_r}	=	0.0984 g.
C_s	=	0.0470 cal./ ^{o}C
E	=	-0.202
A	=	227
$\Delta T_o - \Delta T_\infty$	=	-0.14 ^{o}C
$T_{r,\infty} - T_{r,o}$	=	52 ^{o}C

* Reported from NBS Circular 500.

where C_{so} is heat capacity of crucible, diluent and fabric residue. Integration of the difference between sample and reference energy conservation equations yields

$$\Delta H_{fabric} = C_{so} \left[(\Delta T_i - \Delta T_f) + \varepsilon (T_f - T_i)_r \right] - KA - C \left[\phi \int_i^f (m_o - m)\, d\tau + \int_i^f (m_l - m)\, d(\Delta T) \right] \quad (B.20)$$

The area A is obtained from the thermogram by Simpson integration, K from Eq. B.18 and ε is computed from known masses and specific heats. Temperatures, differential temperatures and mass of sample are read off from the thermogram. Equation B.20 was evaluated by computer and the results are given in Chapter II.

Melting is a special case of the previously treated reactions in that there is no appreciable change in sample mass. The result of the same analysis as above reduces to

$$\Delta H_{fabric} = (\Delta H)_{KNO_3} \left[A_{fabric} / A_{KNO_3} \right] \quad (B.21)$$

Equation B.21 was also evaluated by computer. The results are listed in Chapter II.

GEORGIA INSTITUTE OF TECHNOLOGY - MECHANICAL ENGINEERING

FABRIC FLAMMABILITY PROJECT

DTA/TGA DATA SHEET

DATE: 8/1/72 TEST NO.: 59

SAMPLE MATERIAL : GOLD POWDER

SAMPLE AMOUNT : 99.3 MG.

DILUENT MATERIAL : NONE

DILUENT AMOUNT : _____ MG.

REFERENCE MATERIAL : GOLD POWDER

REFERENCE AMOUNT : 99.8 MG.

THERMOCOUPLE : PT / PT - RH 10 %

HEATING RATE : 25 °C / MIN.

TEMPERATURE LIMITS : 25 TO 700 °C

GASEOUS ATMOSPHERE : AIR

FLOW RATE : 12 ML. / MIN.

CHART PAPER FEED RATE : 12 INCH / HR.

DTA SENSITIVITY : 5 μV / INCH

TG I SENSITIVITY : 10 MG. / INCH

TG II SENSITIVITY : 1 MG. / INCH

TEST INITIATION TIME : 11:05

REMARKS : FURNACE POSITION AND ATMOSPHERE BUOYANCY CALIBRATION.

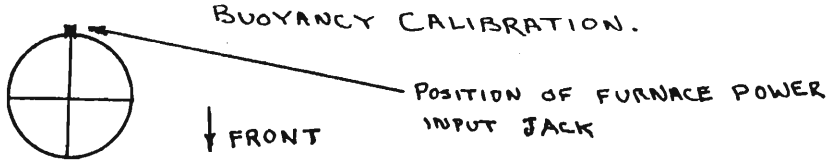

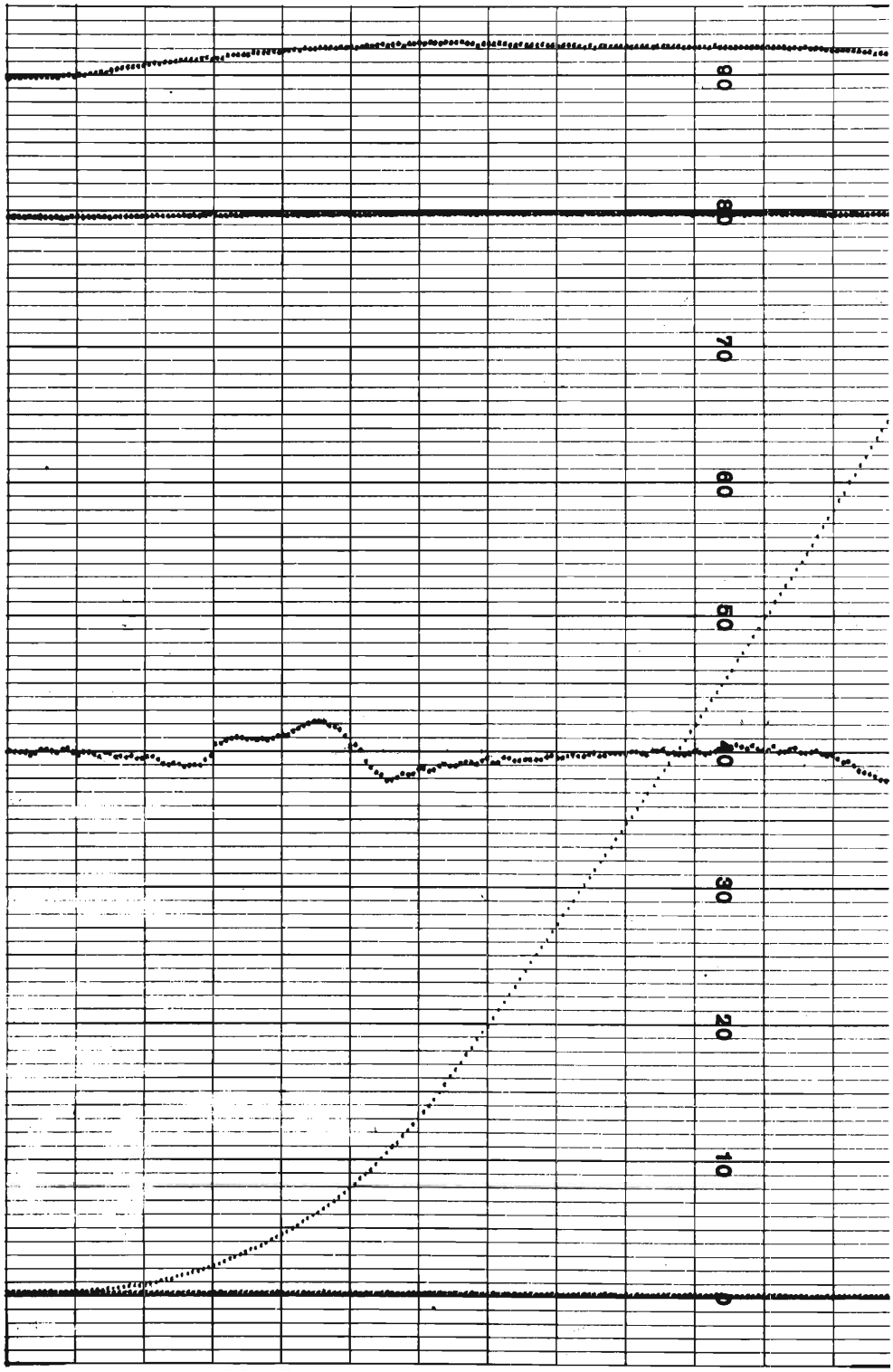

Figure B.5. Selection of Optimum Furnace Position and Calibration of Buoyancy, DTA/TGA Test at Ø=25°C/min. (Linear Reduction=78%)

GEORGIA INSTITUTE OF TECHNOLOGY - MECHANICAL ENGINEERING

FABRIC FLAMMABILITY PROJECT

DTA/TGA DATA SHEET

DATE: 8/10/72 TEST NO.: 84

SAMPLE MATERIAL: Gold Powder

SAMPLE AMOUNT: 100.1 Mg.

DILUENT MATERIAL: None

DILUENT AMOUNT: _____ Mg.

REFERENCE MATERIAL: Gold Powder

REFERENCE AMOUNT: 99.8 Mg.

THERMOCOUPLE: Pt / Pt - Rh 10 %

HEATING RATE: 10 °C / Min.

TEMPERATURE LIMITS: 25 to 720 °C

GASEOUS ATMOSPHERE: Air

FLOW RATE: 12 Ml. / Min.

CHART PAPER FEED RATE: 12 Inch / Hr.

DTA SENSITIVITY: 5 μV / Inch

TG I SENSITIVITY: 10 Mg. / Inch

TG II SENSITIVITY: 1 Mg. / Inch

TEST INITIATION TIME: 10:40

REMARKS: Atmosphere Buoyancy Calibration

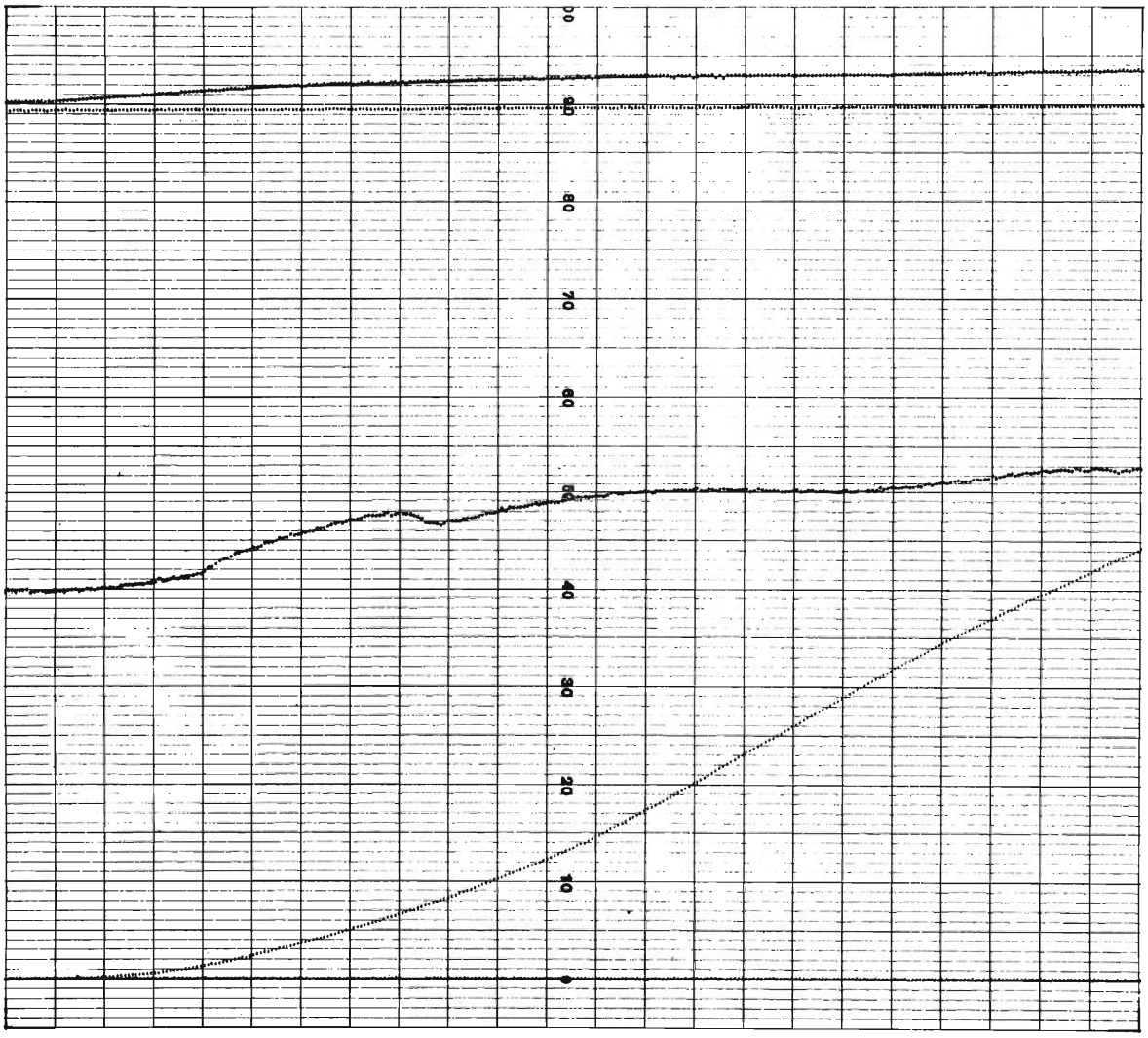

Figure B.6. Buoyancy Calibration DTA/TGA Test at $\emptyset$=10°C/min. (Linear Reduction=52%)

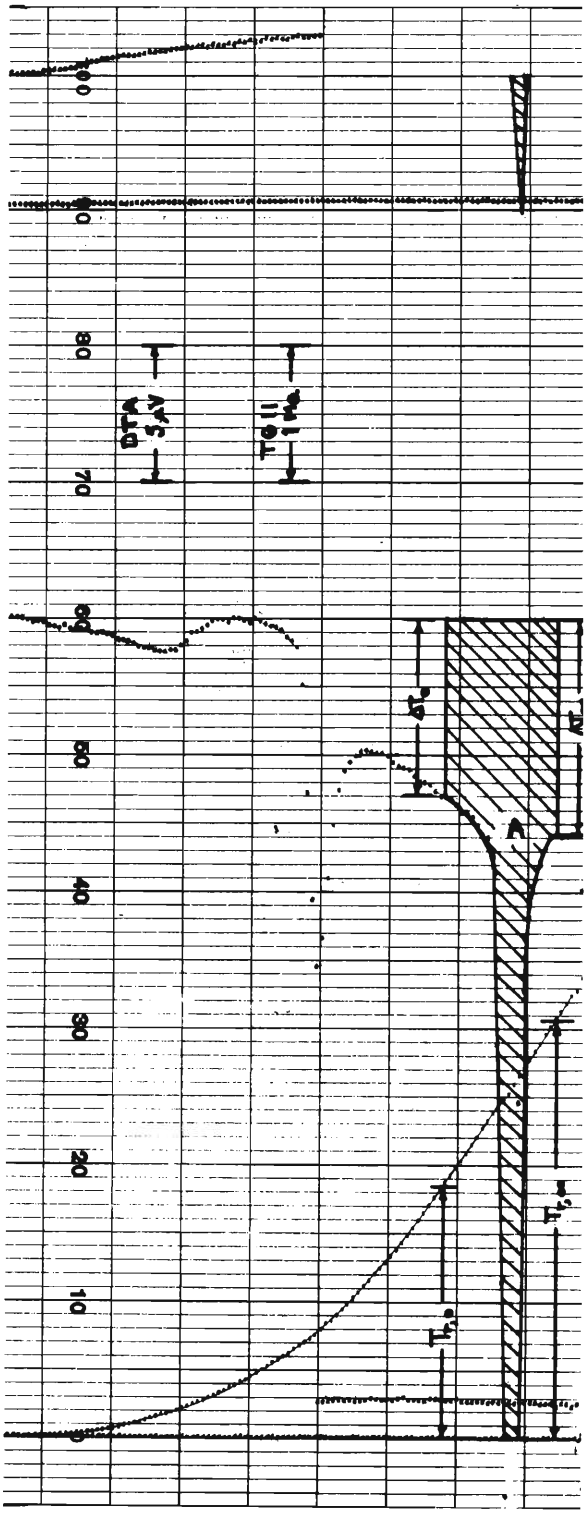

Figure B.7. DTA Thermogram of KNO_3 Reaction Enthalpy Calibration Test at a Heating Rate of 25°C per minute. (Linear Reduction=71%)

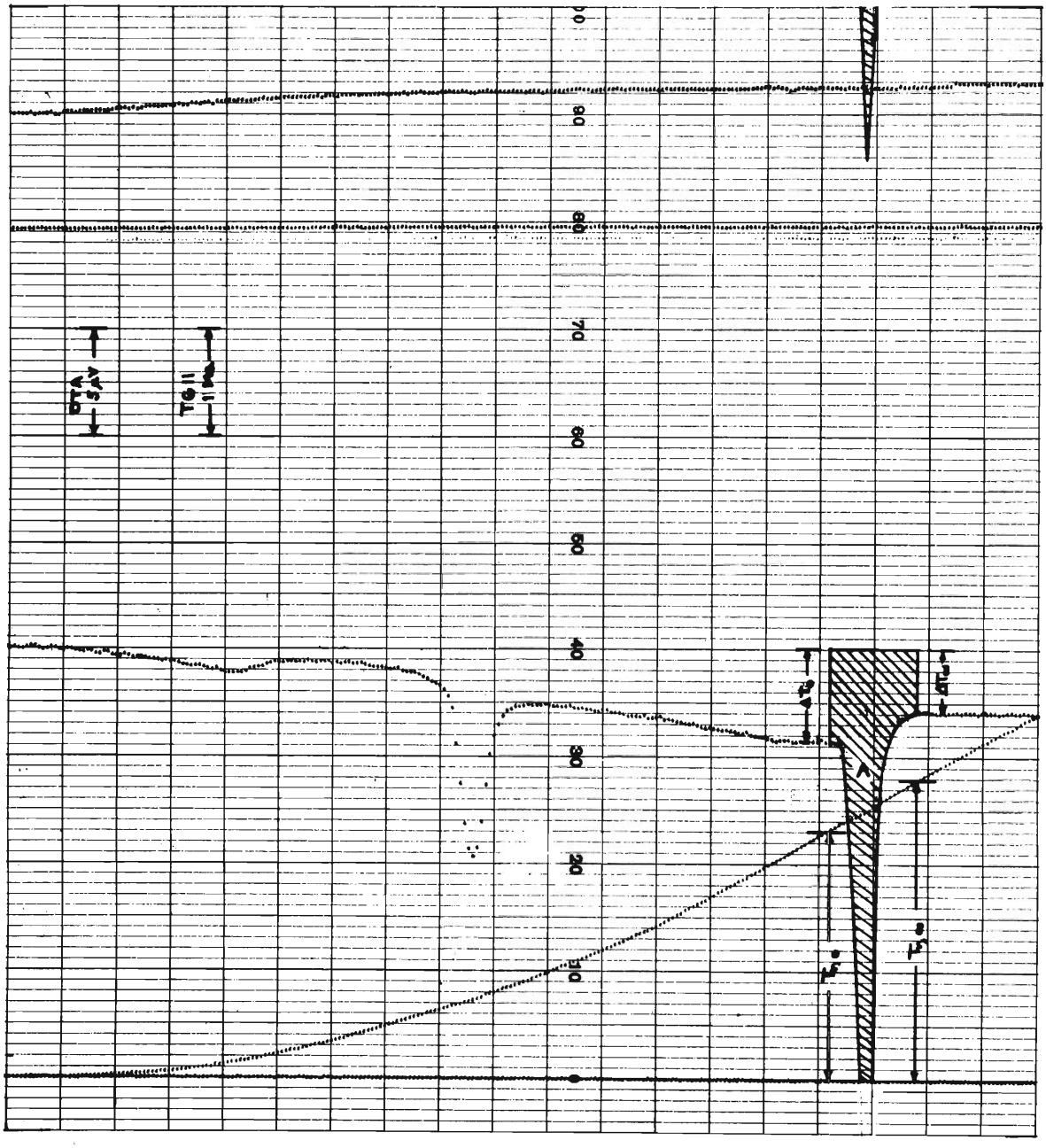

Figure B.8. DTA Thermogram of KNO_3 Reaction Enthalpy Calibration Test at a Heating Rate of 10°C per minute. (Linear Reduction=63%)

GEORGIA INSTITUTE OF TECHNOLOGY - MECHANICAL ENGINEERING

FABRIC FLAMMABILITY PROJECT

DTA/TGA DATA SHEET

DATE: 8/3/72 TEST NO.: 65

SAMPLE MATERIAL : GIRCFF NO. 2

SAMPLE AMOUNT : 20.0 MG.

DILUENT MATERIAL : GOLD POWDER

DILUENT AMOUNT : 79.6 MG.

REFERENCE MATERIAL : GOLD POWDER

REFERENCE AMOUNT : 99.9 MG.

THERMOCOUPLE : PT / PT - RH 10 %

HEATING RATE : 25 °C / MIN.

TEMPERATURE LIMITS : 25 TO 740 °C

GASEOUS ATMOSPHERE : AIR

FLOW RATE : 12 ML. / MIN.

CHART PAPER FEED RATE : 12 INCH / HR.

DTA SENSITIVITY : 5 μV / INCH

TG I SENSITIVITY : 10 MG. / INCH

TG II SENSITIVITY : 1 MG. / INCH

TEST INITIATION TIME : 10:05

REMARKS : _____

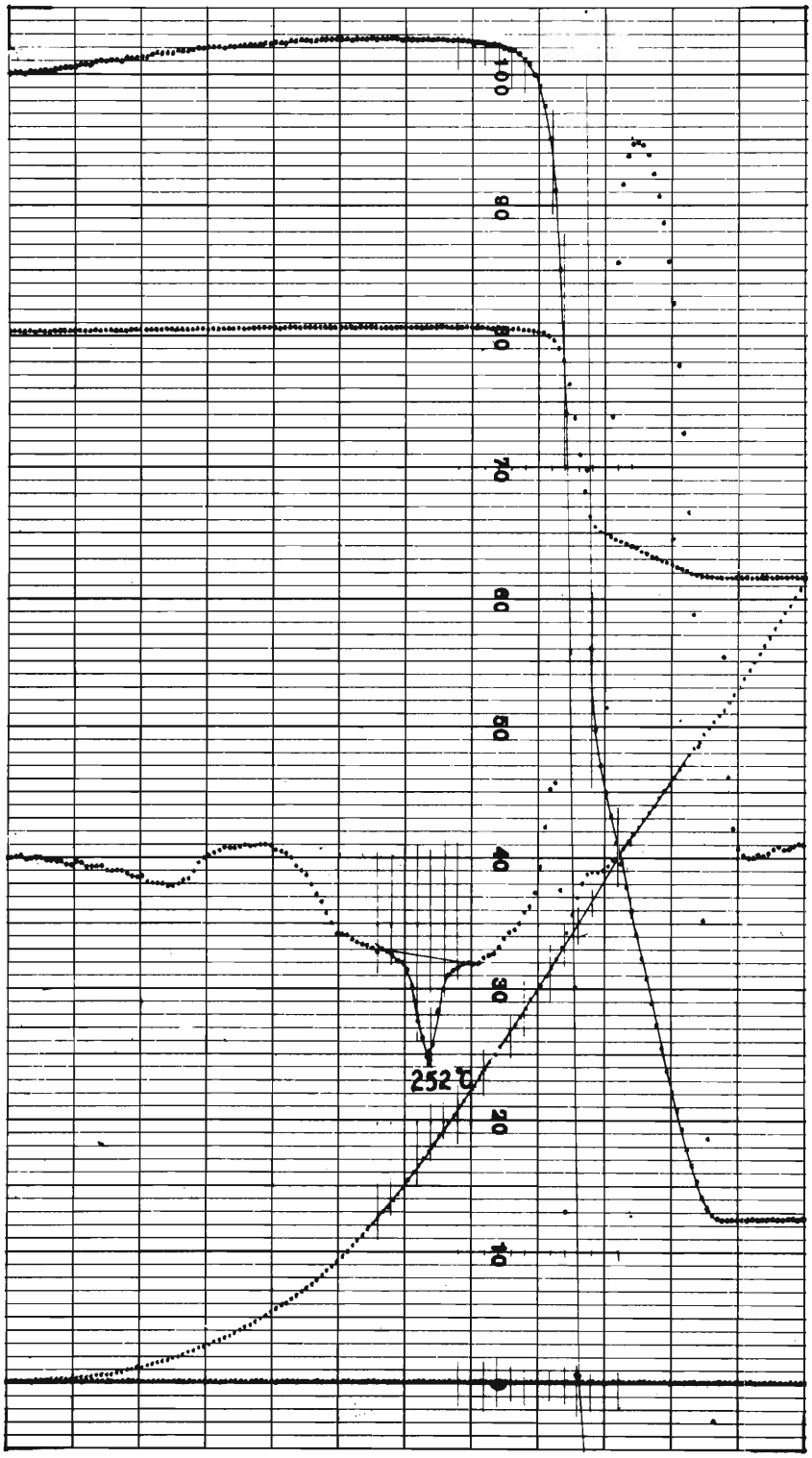

Figure B.9. DTA/TGA Test of GIRCFF Fabric No. 2, Polyester, at $\emptyset$=25°C/min. (Linear Reduction=71%)

GEORGIA INSTITUTE OF TECHNOLOGY - MECHANICAL ENGINEERING

FABRIC FLAMMABILITY PROJECT

DTA/TGA DATA SHEET

DATE: 8/2/72 TEST NO.: 61

SAMPLE MATERIAL : GIRCFF NO. 5

SAMPLE AMOUNT : 20.1 MG.

DILUENT MATERIAL : GOLD POWDER

DILUENT AMOUNT : 79.7 MG.

REFERENCE MATERIAL : GOLD POWDER

REFERENCE AMOUNT : 99.7 MG.

THERMOCOUPLE : PT / PT - RH 10 %

HEATING RATE : 25 °C / MIN.

TEMPERATURE LIMITS : 25 TO 730 °C

GASEOUS ATMOSPHERE : AIR

FLOW RATE : 12 ML. / MIN.

CHART PAPER FEED RATE : 12 INCH / HR.

DTA SENSITIVITY : 5 μV / INCH

TG I SENSITIVITY : 10 MG. / INCH

TG II SENSITIVITY : 1 MG. / INCH

TEST INITIATION TIME : 11:55

REMARKS : _____

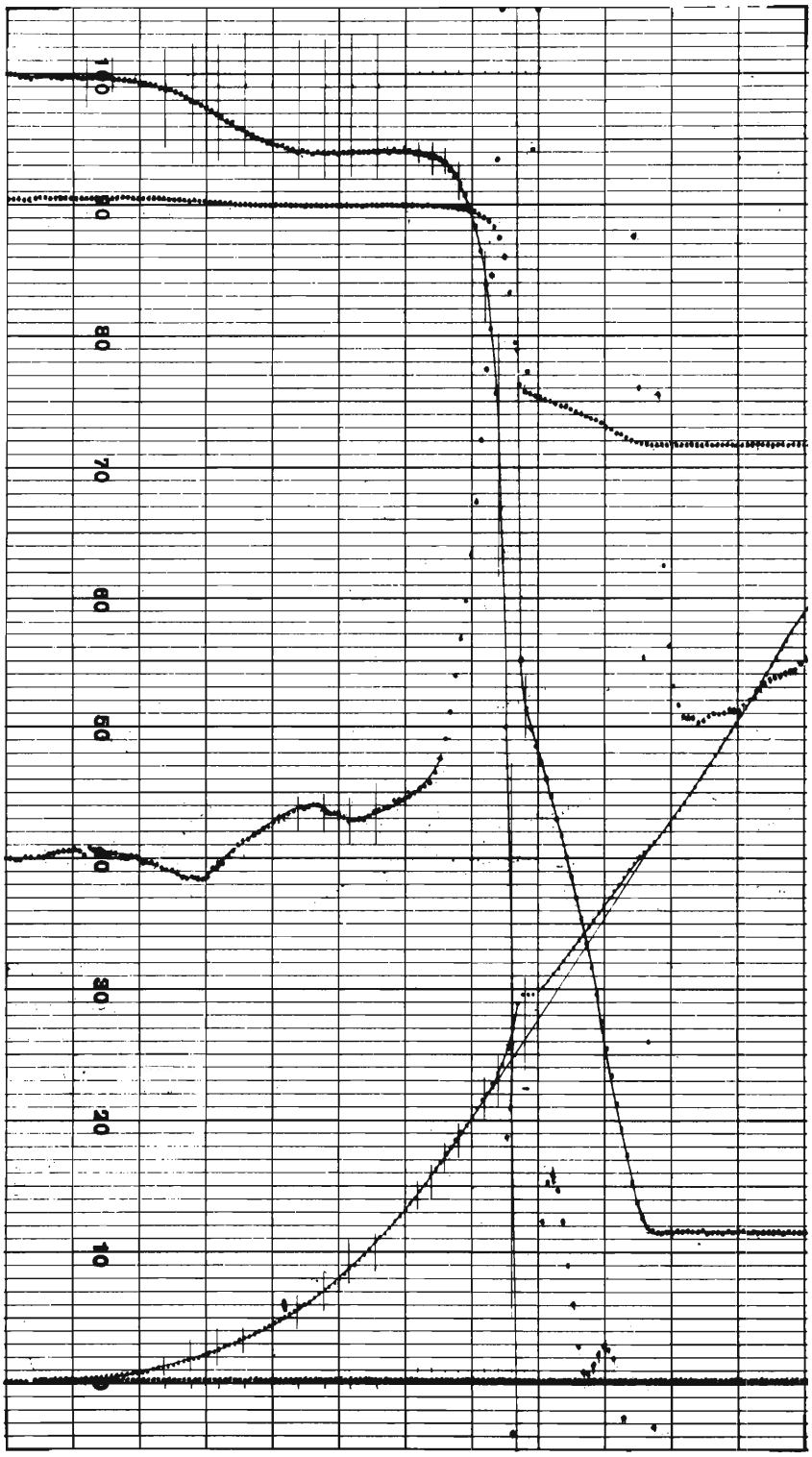

Figure B.10 DTA/TGA Test of GIRCFF Fabric No. 5, Cotton, at Ø=25°C/min. (Linear Reduction=71%)

GEORGIA INSTITUTE OF TECHNOLOGY - MECHANICAL ENGINEERING

FABRIC FLAMMABILITY PROJECT

DTA/TGA DATA SHEET

DATE: 8/4/72 TEST NO.: 73

SAMPLE MATERIAL : GIRCFF NO. 5

SAMPLE AMOUNT : 20.0 MG.

DILUENT MATERIAL : GOLD POWDER

DILUENT AMOUNT : 79.9 MG.

REFERENCE MATERIAL : GOLD POWDER

REFERENCE AMOUNT : 99.6 MG.

THERMOCOUPLE : PT / PT - RH 10 %

HEATING RATE : 10 °C / MIN.

TEMPERATURE LIMITS : 25 TO 510 °C

GASEOUS ATMOSPHERE : AIR

FLOW RATE : 12 ML. / MIN.

CHART PAPER FEED RATE : 12 INCH / HR.

DTA SENSITIVITY : 5 μV / INCH

TG I SENSITIVITY : 10 MG. / INCH

TG II SENSITIVITY : 1 MG. / INCH

TEST INITIATION TIME : 13:45

REMARKS : _____

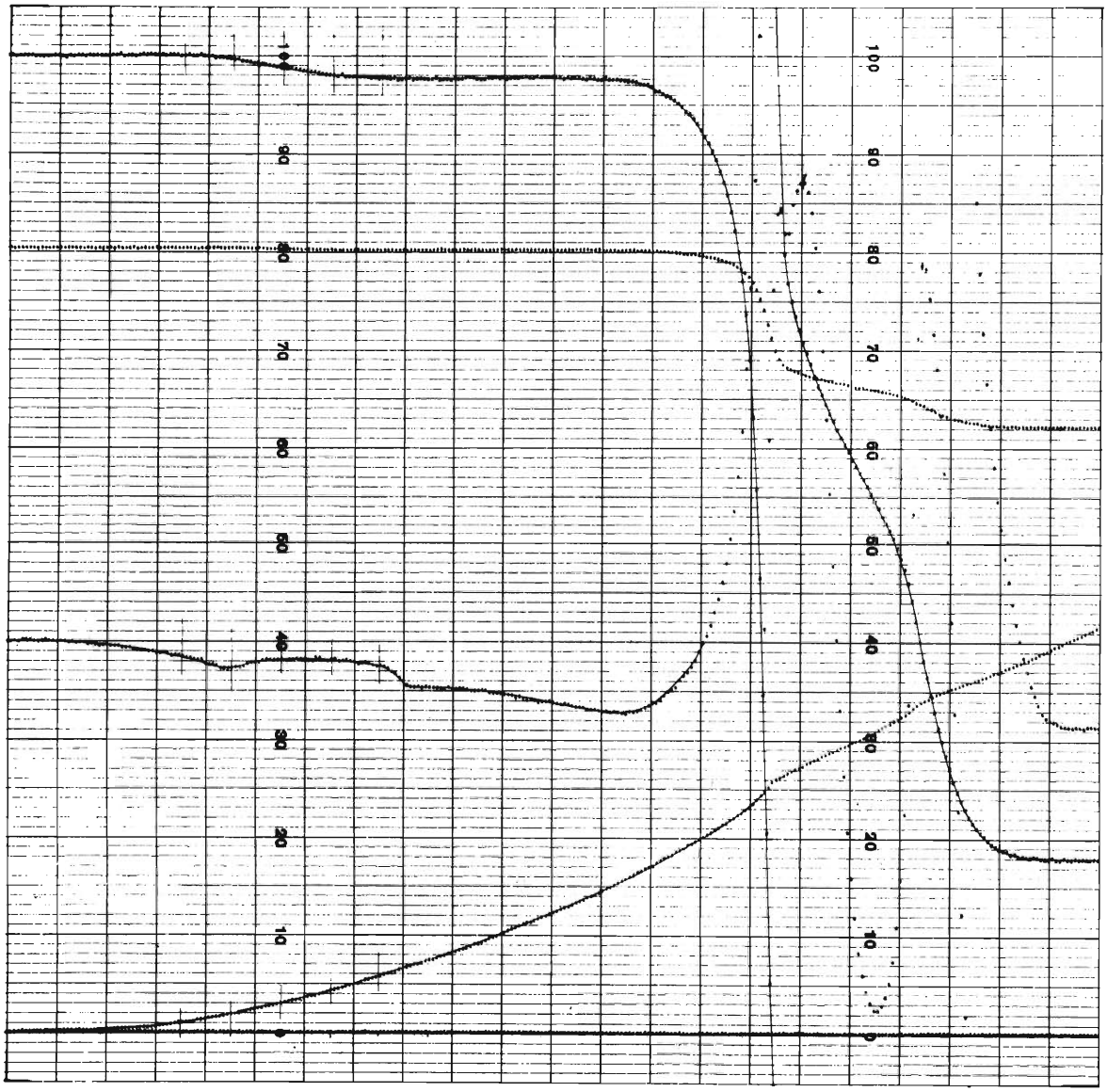

Figure B.11. DTA/TGA Test of GIRCFF Fabric No. 5, Cotton at Ø=10°C/min. (Linear Reduction=54%)

GEORGIA INSTITUTE OF TECHNOLOGY - MECHANICAL ENGINEERING

FABRIC FLAMMABILITY PROJECT

DTA/TGA DATA SHEET

DATE: 8|3|72 TEST NO.: 69

SAMPLE MATERIAL : GIRCFF NO. 8

SAMPLE AMOUNT : 20.1 MG.

DILUENT MATERIAL : GOLD POWDER

DILUENT AMOUNT : 79.9 MG.

REFERENCE MATERIAL : GOLD POWDER

REFERENCE AMOUNT : 99.9 MG.

THERMOCOUPLE : PT / PT-RH 10 %

HEATING RATE : 25 °C / MIN.

TEMPERATURE LIMITS : 25 TO 660 °C

GASEOUS ATMOSPHERE : AIR

FLOW RATE : 12 ML. / MIN.

CHART PAPER FEED RATE : 12 INCH / HR.

DTA SENSITIVITY : 5 μV / INCH

TG I SENSITIVITY : 10 MG. / INCH

TG II SENSITIVITY : 1 MG. / INCH

TEST INITIATION TIME : 15:35

REMARKS : _____

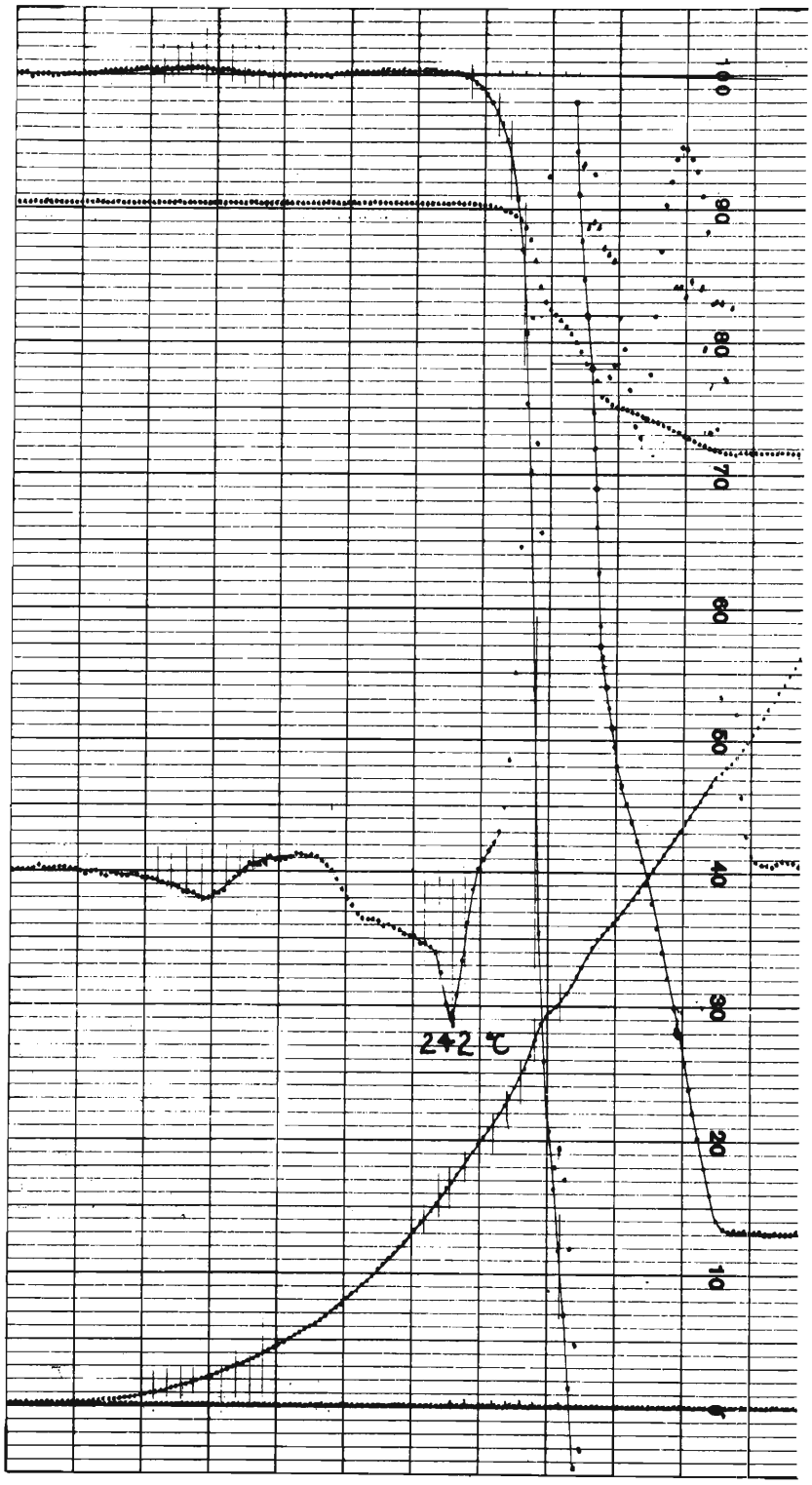

Figure B.12. DTA/TGA Test of GIRCFF Fabric No. 8, Cotton-Polyester Blend, at Ø=25°C/min. (Linear Reduction=71%)

GEORGIA INSTITUTE OF TECHNOLOGY - MECHANICAL ENGINEERING

FABRIC FLAMMABILITY PROJECT

DTA/TGA DATA SHEET

DATE: 8/2/72 TEST NO.: 62

SAMPLE MATERIAL : GIRCFF NO. 10

SAMPLE AMOUNT : 19.7 MG.

DILUENT MATERIAL : GOLD POWDER

DILUENT AMOUNT : 79.7 MG.

REFERENCE MATERIAL : GOLD POWDER

REFERENCE AMOUNT : 99.8 MG.

THERMOCOUPLE : PT / PT - RH 10 %

HEATING RATE : 25 °C / MIN.

TEMPERATURE LIMITS : 25 TO 690 °C

GASEOUS ATMOSPHERE : AIR

FLOW RATE : 12 ML. / MIN.

CHART PAPER FEED RATE : 12 INCH / HR.

DTA SENSITIVITY : 5 μV / INCH

TG I SENSITIVITY : 10 MG. / INCH

TG II SENSITIVITY : 1 MG. / INCH

TEST INITIATION TIME : 14:15

REMARKS : _____

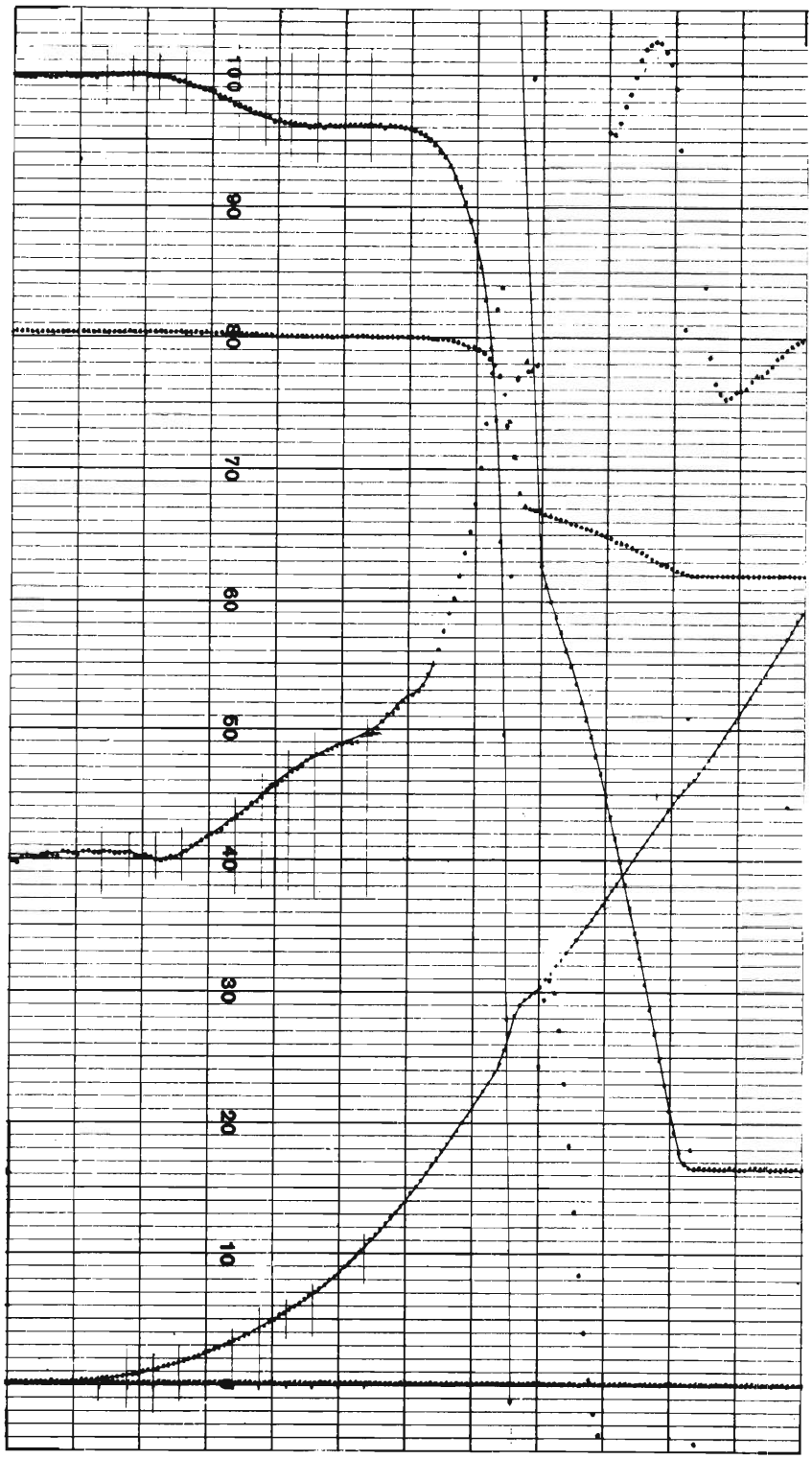

Figure B.13. DTA/TGA Test of GIRCFF Fabric No. 10, Cotton, at $\emptyset$=25°C/min. (Linear Reduction=71%)

GEORGIA INSTITUTE OF TECHNOLOGY - MECHANICAL ENGINEERING

FABRIC FLAMMABILITY PROJECT

DTA/TGA DATA SHEET

DATE: 8/7/72 TEST NO.: 74

SAMPLE MATERIAL : GIRCFF NO. 10

SAMPLE AMOUNT : 19.8 MG.

DILUENT MATERIAL : GOLD POWDER

DILUENT AMOUNT : 79.7 MG.

REFERENCE MATERIAL : GOLD POWDER

REFERENCE AMOUNT : 99.3 MG.

THERMOCOUPLE : PT / PT - RH 10 %

HEATING RATE : 10 °C / MIN.

TEMPERATURE LIMITS : 25 TO 530 °C

GASEOUS ATMOSPHERE : AIR

FLOW RATE : 12 ML. / MIN.

CHART PAPER FEED RATE : 12 INCH / HR.

DTA SENSITIVITY : 5 μV / INCH

TG I SENSITIVITY : 10 MG. / INCH

TG II SENSITIVITY : 1 MG. / INCH

TEST INITIATION TIME : 10:05

REMARKS : _____

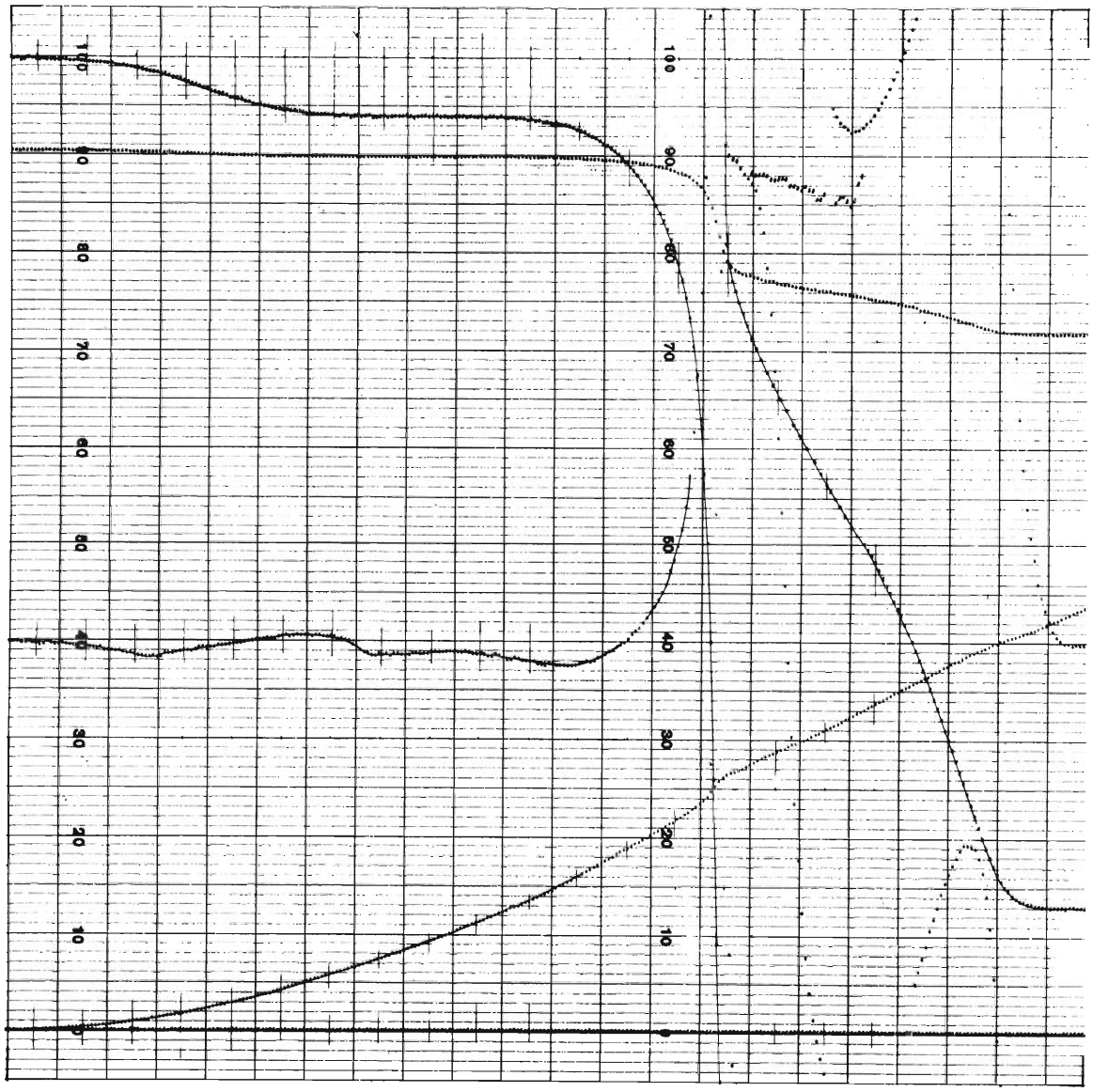

Figure B.14. DTA/TGA Test of GIRCFF Fabric No. 10, Cotton, at $\emptyset$=10°C/min. (Linear Reduction=54%)

GEORGIA INSTITUTE OF TECHNOLOGY - MECHANICAL ENGINEERING

FABRIC FLAMMABILITY PROJECT

DTA/TGA DATA SHEET

DATE: 8/4/72 TEST NO.: 70

SAMPLE MATERIAL : GIRCFF NO. 11

SAMPLE AMOUNT : 20.5 Mg.

DILUENT MATERIAL : GOLD POWDER

DILUENT AMOUNT : 79.7 MG.

REFERENCE MATERIAL : GOLD POWDER

REFERENCE AMOUNT : 99.4 MG.

THERMOCOUPLE : PT / PT - RH 10 %

HEATING RATE : 25 °C / MIN.

TEMPERATURE LIMITS : 25 TO 125 °C

GASEOUS ATMOSPHERE : AIR

FLOW RATE : 12 ML. / MIN.

CHART PAPER FEED RATE : 12 INCH / HR.

DTA SENSITIVITY : 5 μV / INCH

TG I SENSITIVITY : 10 MG. / INCH

TG II SENSITIVITY : 1 MG. / INCH

TEST INITIATION TIME : 8:25

REMARKS : _____

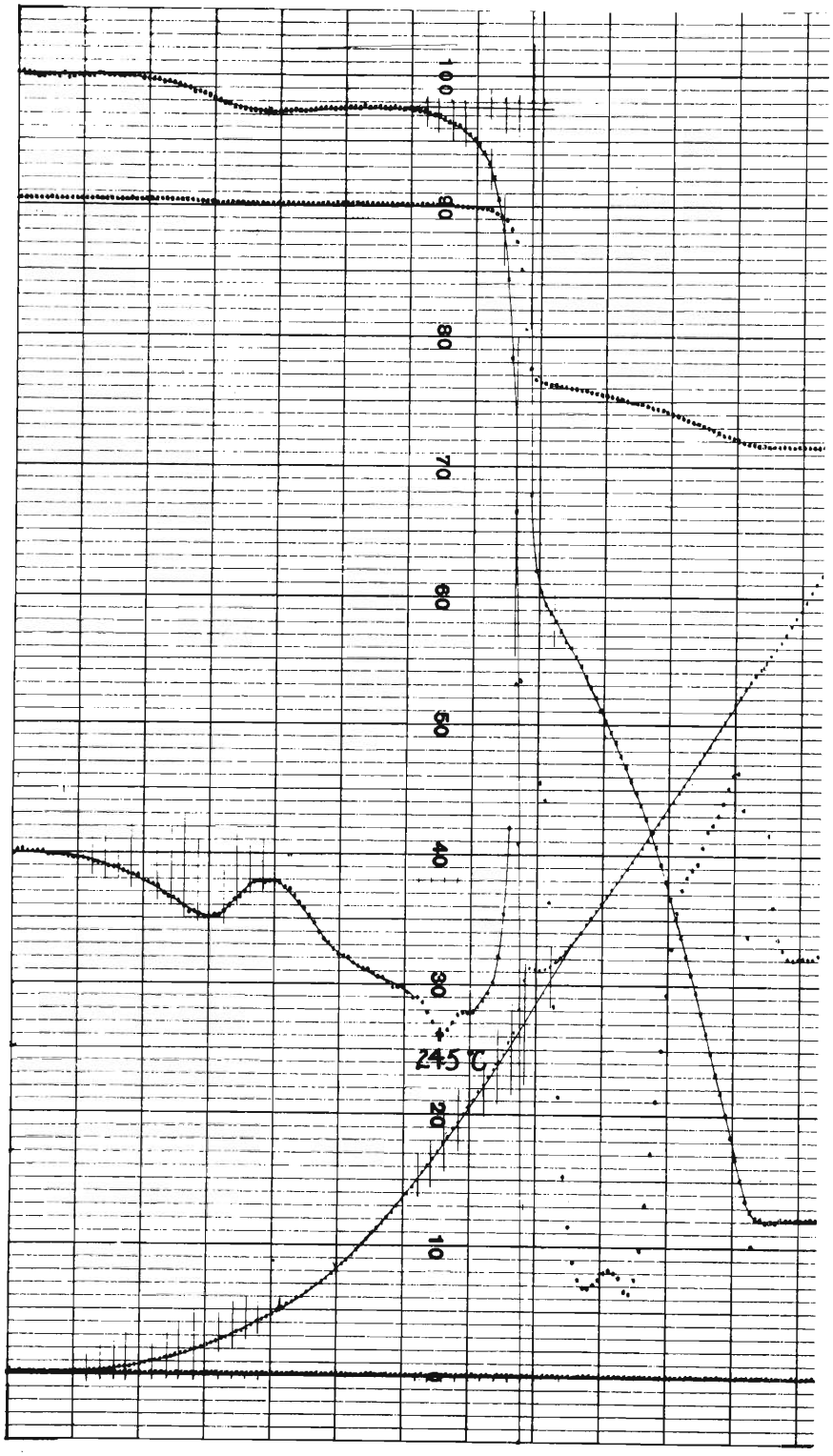

Figure B.15 DTA/TGA Test of GIRCFF Fabric No. 11, Nylon-Acetate Blend, at $\emptyset$=25°C/min. (Linear Reduction=71%)

GEORGIA INSTITUTE OF TECHNOLOGY - MECHANICAL ENGINEERING

FABRIC FLAMMABILITY PROJECT

DTA/TGA DATA SHEET

DATE: 8/3/72 TEST NO.: 66

SAMPLE MATERIAL : GIRCFF NO. 12

SAMPLE AMOUNT : 20.2 MG.

DILUENT MATERIAL : GOLD POWDER

DILUENT AMOUNT : 79.6 MG.

REFERENCE MATERIAL : GOLD POWDER

REFERENCE AMOUNT : 99.7 MG.

THERMOCOUPLE : PT / PT - RH 10 %

HEATING RATE : 25 °C / MIN.

TEMPERATURE LIMITS : 25 TO 740 °C

GASEOUS ATMOSPHERE : AIR

FLOW RATE : 12 ML. / MIN.

CHART PAPER FEED RATE : 12 INCH / HR.

DTA SENSITIVITY : 5 μV / INCH

TG I SENSITIVITY : 10 MG. / INCH

TG II SENSITIVITY : 1 MG. / INCH

TEST INITIATION TIME : 11:45

REMARKS :

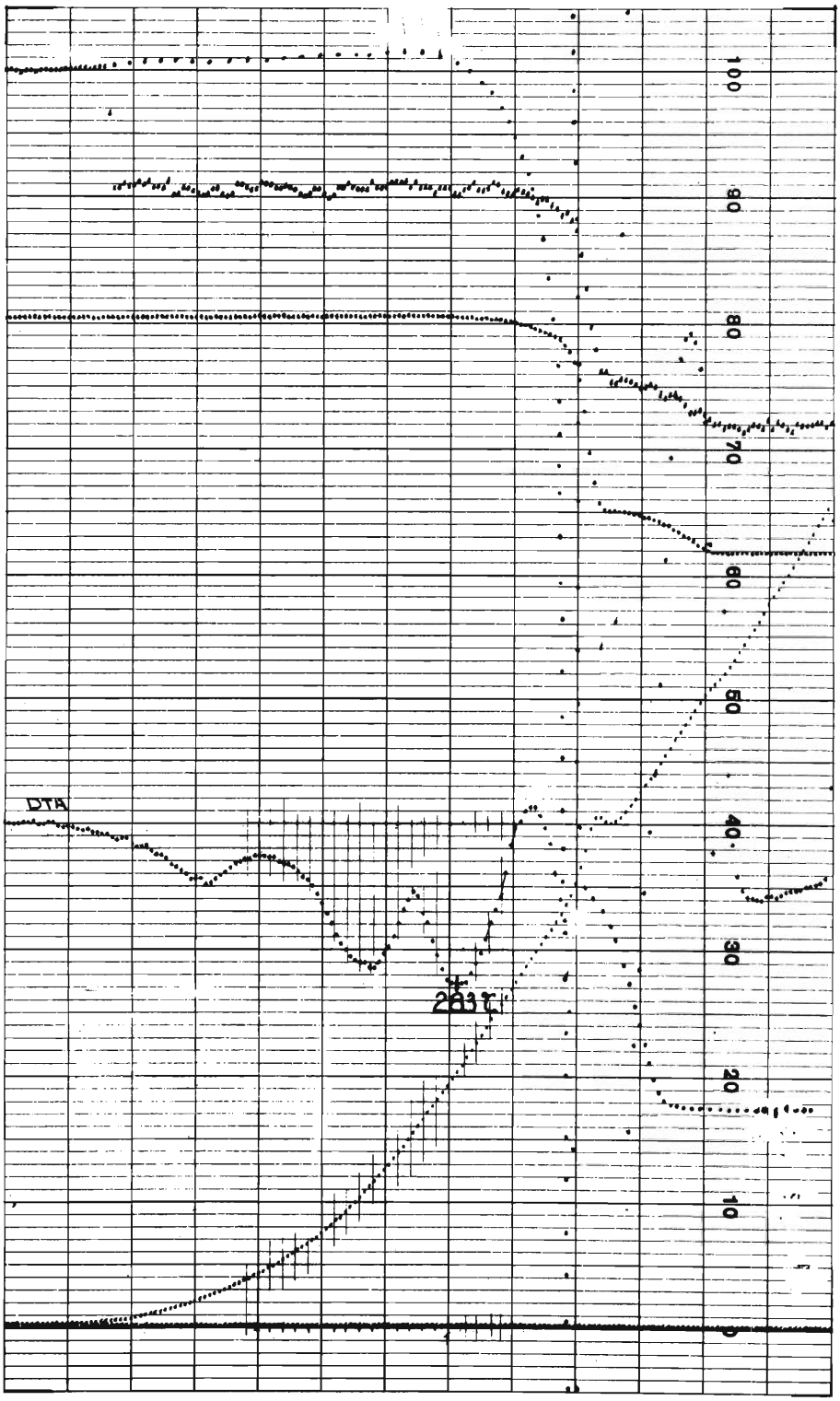

Figure B.16. DTA/TGA Test of GIRCFF Fabric No. 12, Nylon, at Ø=25°C/min. (Linear Reduction=71%)

GEORGIA INSTITUTE OF TECHNOLOGY - MECHANICAL ENGINEERING

FABRIC FLAMMABILITY PROJECT

DTA/TGA DATA SHEET

DATE: 8/4/72 TEST NO.: 71

SAMPLE MATERIAL : GIRCFF NO. 17

SAMPLE AMOUNT : 20.0 MG.

DILUENT MATERIAL : GOLD POWDER

DILUENT AMOUNT : 80.1 MG.

REFERENCE MATERIAL : GOLD POWDER

REFERENCE AMOUNT : 99.8 MG.

THERMOCOUPLE : PT / PT - RH 10 %

HEATING RATE : 25 °C / MIN.

TEMPERATURE LIMITS : 25 TO 645 °C

GASEOUS ATMOSPHERE : AIR

FLOW RATE : 12 ML. / MIN.

CHART PAPER FEED RATE : 12 INCH / HR.

DTA SENSITIVITY : 5 μV / INCH

TG I SENSITIVITY : 10 MG. / INCH

TG II SENSITIVITY : 1 MG. / INCH

TEST INITIATION TIME : 10:10

REMARKS : _____

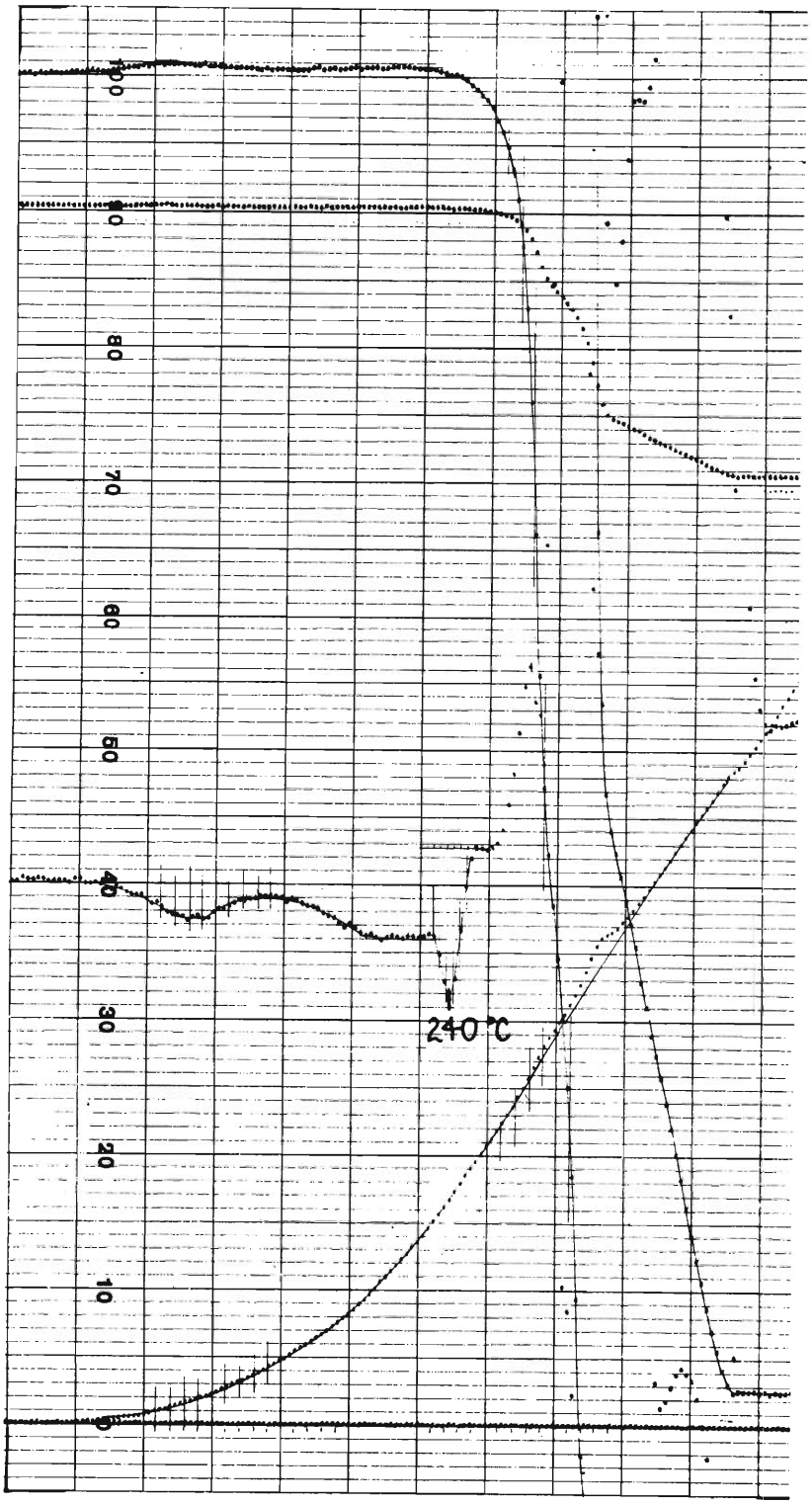

Figure B.17. DTA/TGA Test of GIRCFF Fabric No. 17, Cotton-Polyester Blend, at Ø=25°C/min. (Linear Reduction=71%)

GEORGIA INSTITUTE OF TECHNOLOGY - MECHANICAL ENGINEERING

FABRIC FLAMMABILITY PROJECT

DTA/TGA DATA SHEET

DATE: 8/2/72 TEST NO.: 63

SAMPLE MATERIAL : GIRCFF NO. 18

SAMPLE AMOUNT : 20.2 MG.

DILUENT MATERIAL : GOLD POWDER

DILUENT AMOUNT : 79.9 MG.

REFERENCE MATERIAL : GOLD POWDER

REFERENCE AMOUNT : 99.5 MG.

THERMOCOUPLE : PT / PT - RH 10 %

HEATING RATE : 25 °C / MIN.

TEMPERATURE LIMITS : 25 TO 630 °C

GASEOUS ATMOSPHERE : AIR

FLOW RATE : 12 ML. / MIN.

CHART PAPER FEED RATE : 12 INCH / HR.

DTA SENSITIVITY : 5 μV / INCH

TG I SENSITIVITY : 10 MG. / INCH

TG II SENSITIVITY : 1 MG. / INCH

TEST INITIATION TIME : 15:50

REMARKS : _____

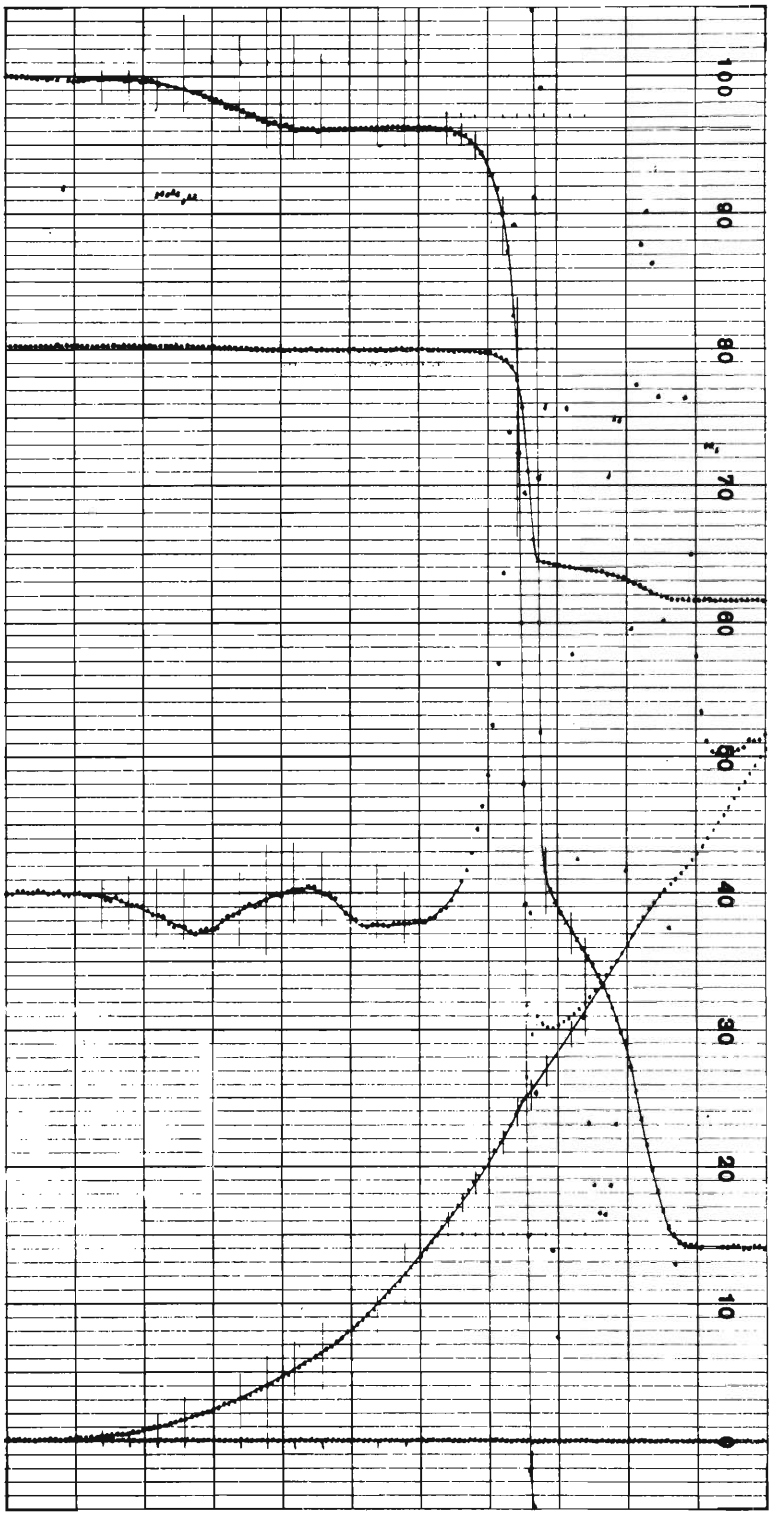

Figure B.18. DTA/TGA Test of GIRCFF Fabric No. 18, Cotton, at $\emptyset$=25°C/min. (Linear Reduction=71%)

GEORGIA INSTITUTE OF TECHNOLOGY - MECHANICAL ENGINEERING

FABRIC FLAMMABILITY PROJECT

DTA/TGA DATA SHEET

DATE: 8/7/72 TEST NO.: 75

SAMPLE MATERIAL : GIRCFF NO. 18

SAMPLE AMOUNT : 20.2 MG.

DILUENT MATERIAL : GOLD POWDER

DILUENT AMOUNT : 79.8 MG.

REFERENCE MATERIAL : GOLD POWDER

REFERENCE AMOUNT : 99.6 MG.

THERMOCOUPLE : PT / PT - RH 10 %

HEATING RATE : 10 °C / MIN.

TEMPERATURE LIMITS : 25 TO 520 °C

GASEOUS ATMOSPHERE : AIR

FLOW RATE : 12 ML. / MIN.

CHART PAPER FEED RATE : 12 INCH / HR.

DTA SENSITIVITY : 5 μV / INCH

TG I SENSITIVITY : 10 MG. / INCH

TG II SENSITIVITY : 1 MG. / INCH

TEST INITIATION TIME : 11:50

REMARKS : _____

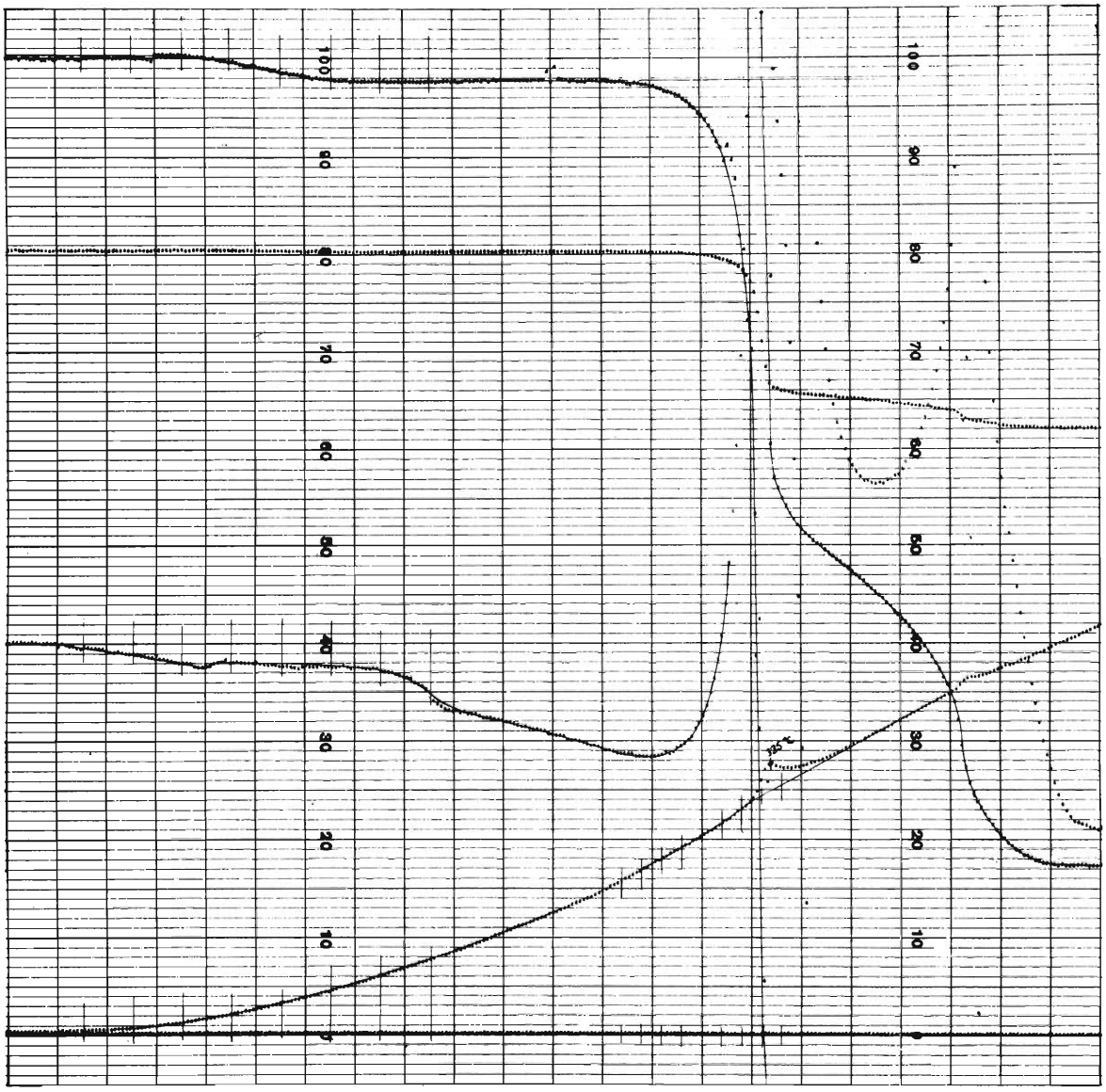

Figure B.19. DTA/TGA Test of GIRCFF Fabric No. 18, Cotton at $\emptyset$=10°C/min. (Linear Reduction=54%)

GEORGIA INSTITUTE OF TECHNOLOGY - MECHANICAL ENGINEERING

FABRIC FLAMMABILITY PROJECT

DTA/TGA DATA SHEET

DATE: 8/3/72 TEST NO.: 64

SAMPLE MATERIAL : GIRCFF NO. 19

SAMPLE AMOUNT : 19.8 MG.

DILUENT MATERIAL : GOLD POWDER

DILUENT AMOUNT : 79.1 MG.

REFERENCE MATERIAL : GOLD POWDER

REFERENCE AMOUNT : 99.9 MG.

THERMOCOUPLE : PT / PT - RH 10 %

HEATING RATE : 25 °C / MIN.

TEMPERATURE LIMITS : 25 TO 860 °C

GASEOUS ATMOSPHERE : AIR

FLOW RATE : 12 ML. / MIN.

CHART PAPER FEED RATE : 12 INCH / HR.

DTA SENSITIVITY : 5 μV / INCH

TG I SENSITIVITY : 10 MG. / INCH

TG II SENSITIVITY : 1 MG. / INCH

TEST INITIATION TIME : 8:30

REMARKS : _____

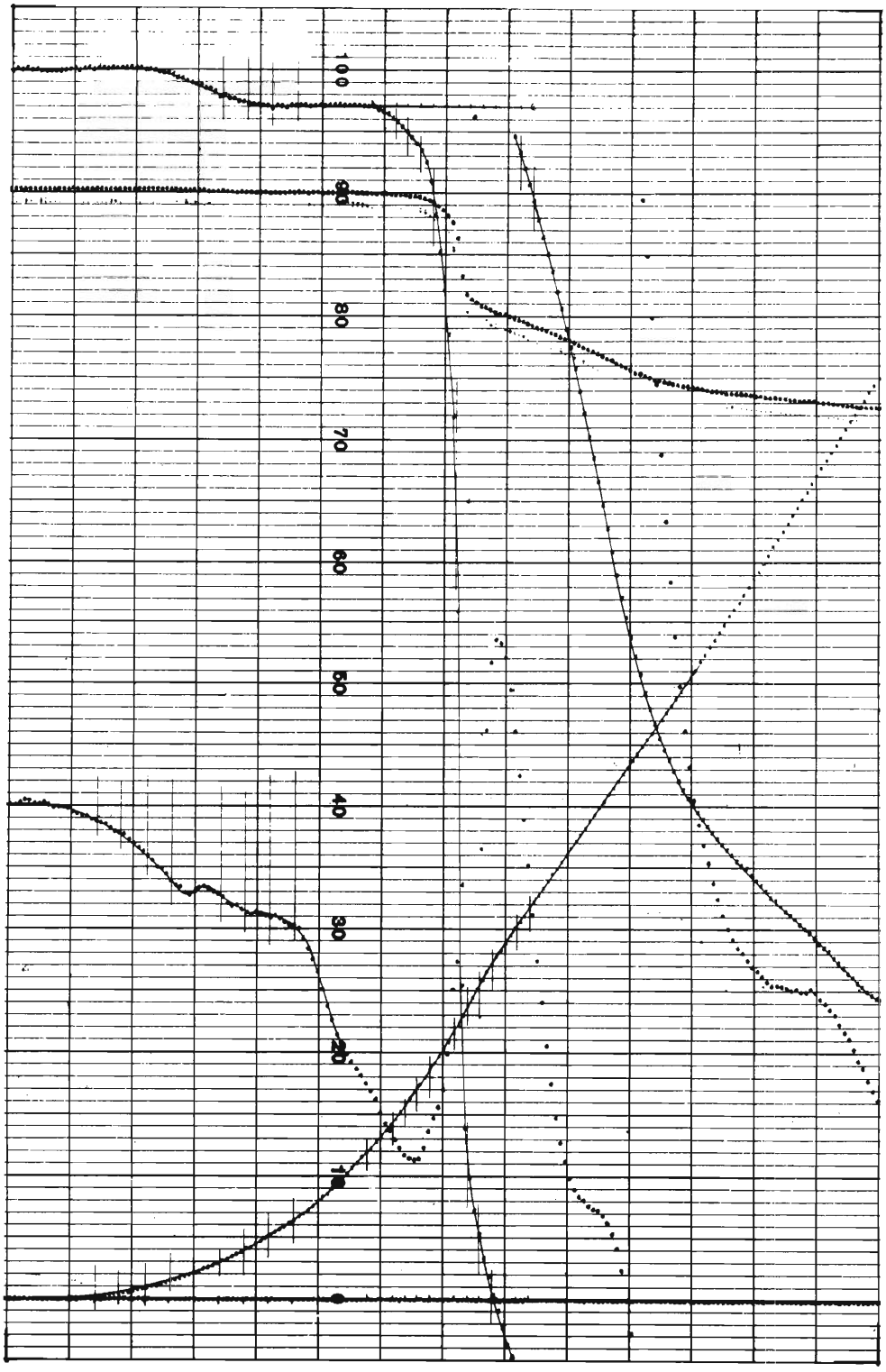

Figure B.20. DTA/TGA Test of GIRCFF Fabric No. 19, Treated Cotton, at Ø=25°C/min. (Linear Reduction=71%)

GEORGIA INSTITUTE OF TECHNOLOGY - MECHANICAL ENGINEERING

FABRIC FLAMMABILITY PROJECT

DTA/TGA DATA SHEET

DATE: 8/7/72 TEST NO.: 76

SAMPLE MATERIAL : GIRCFF NO. 19

SAMPLE AMOUNT : 20.2 MG.

DILUENT MATERIAL : GOLD POWDER

DILUENT AMOUNT : 80.0 MG.

REFERENCE MATERIAL : GOLD POWDER

REFERENCE AMOUNT : 99.4 MG.

THERMOCOUPLE : PT / PT - RH 10 %

HEATING RATE : 10 °C / MIN.

TEMPERATURE LIMITS : 25 TO 835 °C

GASEOUS ATMOSPHERE : AIR

FLOW RATE : 12 ML. / MIN.

CHART PAPER FEED RATE : 12 INCH / HR.

DTA SENSITIVITY : 5 μV / INCH

TG I SENSITIVITY : 10 MG. / INCH

TG II SENSITIVITY : 1 MG. / INCH

TEST INITIATION TIME : 13:45

REMARKS : _____

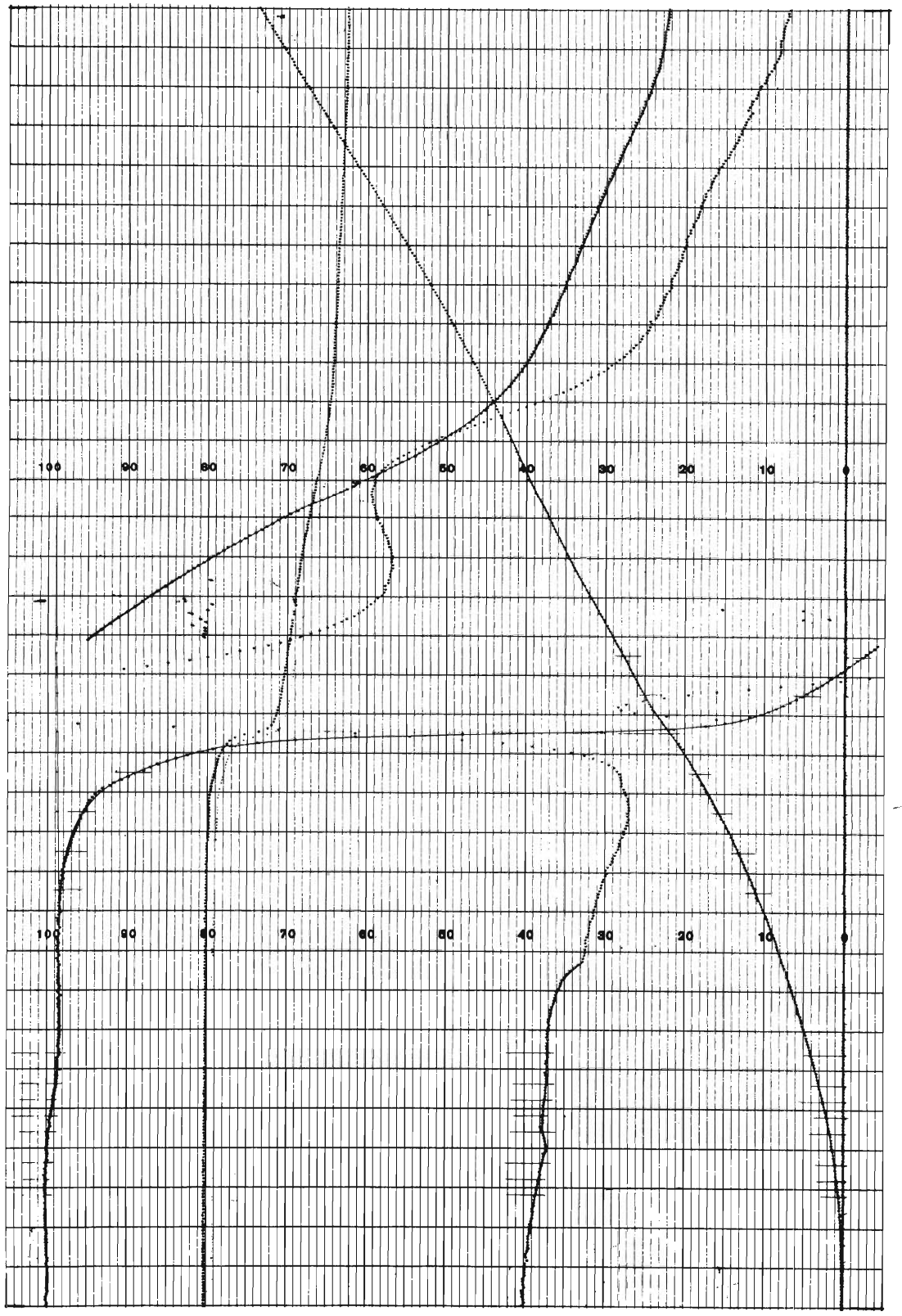

Figure B.21. DTA/TGA Test of GIRCFF Fabric No. 19, Treated Cotton, at Ø=10°C/min. (Linear Reduction=50%)

Appendix B.2

Completion of Radiative Ignition Time Apparatus

The Radiative Ignition Time Apparatus (RITA) had been operated previously under single shutter mode operation as discussed in Appendix B.1 of Reference [I-2]. After conditioning of the radiative heater to reach radiative equilibrium, a single shutter exposed the fabric sample to the radiative heat flux and triggered simultaneously two oscilloscopes. The fabric specimen was exposed to the heater until destruction occurred as recognized from the steep rise on the oscilloscope traces recording the signals from an infrared detector and a heat flux sensor, both focused on the back face of the fabric.

Under dual shutter mode the exposure time is controlled to ± 0.2 seconds, and the fabric is observed after exposure either to be only charred or to be destroyed. Under this method of fabric exposure it is possible to measure definitely ignition time, without the difficult observation of ignition during heating, and to measure ignition frequencies for the purpose of assessing ignition probability. The major improvement implemented in the design of RITA are the modifications which allow dual-shutter mode operation and the humidity and temperature controlled environment which provide for fabric moisture conditioning and for ignition time measurements under well defined conditions. These two features are discussed below; additional details are presented in Reference [I-2].

a. Environmental Humidity and Temperature Control

The thermostatically and psychrometrically controlled enclosure shown in Figure B.22 was purchased from Environair Systems, Inc., East Longmeadow, Massachusetts. The interior dimensions of the enclosure are

length	8'4"	or	2.54 m
width	5'4"	or	1.62 m
height	6'10"	or	2.08 m

The temperature is automatically controlled and recorded in the temperature range between 40°F and 95°F or 4.5°C and 35°C. The relative humidity is automatically maintained and recorded between 25 and 95 percent. The temperature as observed with an independent mercury-in-glass thermometer

was stable within ± 0.2°C during operation; humidity fluctuated, according to the recorder, within ± 2% r.h. during normal operation. Steady humidity recording (Honeywell) was verified by measurements with a wet-bulb psychrometer.

RITA was installed into the enclosure as shown in Figure B.23. Cooling air and water lines were fed through the chamber walls from external filters and pressure regulators to the radiative fabric heater. Power lines were fed through the enclosure wall from the external voltage regulator and timing relays to the radiative heater.

Separate, multi-purpose low voltage lines were also fed through the enclosure wall to pass the signals from microswitches, heat flux sensors and the infrared detector to external recording units.

The fabric specimen were mounted in fabric holders and stored for at least 12 hours in the enclosure prior to exposure. They were installed immediately before exposure without having been removed from the chamber. The mounting of the fabric and the loading of the shutters of RITA required two quick door openings between any two exposures. Normally nobody was inside the enclosure during fabric exposure.

b. Dual Shutter Mode Operation was developed to control precisely the exposure time in addition to power flux and fabric conditions. This was achieved by constructing the timing circuit which allows repeatable and fully automatic sequencing of

radiator preheating
termination of exposure
radiator shut-down,

} with transients of 5 μs

accompanied by automatic trigger actions which start and stop the electronic time counter. The timing circuit is housed in the instrument rack shown in Figure B.23 and consists of two electric timers to select preheating and exposure periods, of a mercury power relay to activate and deactivate the heater, and of a separate dc circuit to trigger either the oscilloscopes (single shutter mode operation) or the counter.

The counter is triggered by the first shutter plate which activates, after fabric exposure, the first microswitch. This starts the counter. The second shutter plate activates, after terminating fabric exposure, the second microswitch which stops the counter and interrupts the power to the mercury power relay causing it to shut off the heater power.

The time interval of exposure is measured to an accuracy of ± 0.01 seconds

and recorded together with the condition of the fabric after exposure: either charred or destroyed.

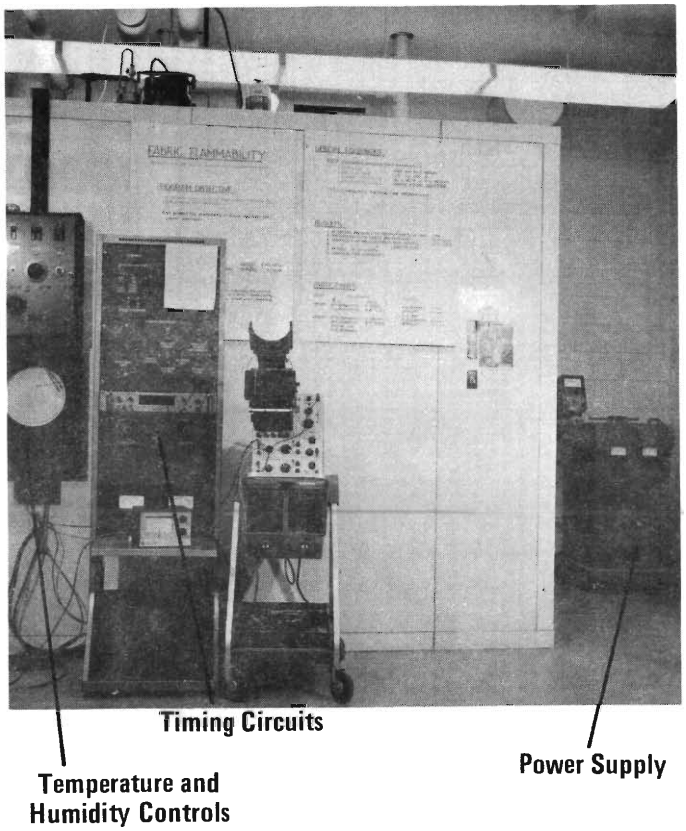

Figure B.22. Environmental Chamber and Ancillary Equipment.

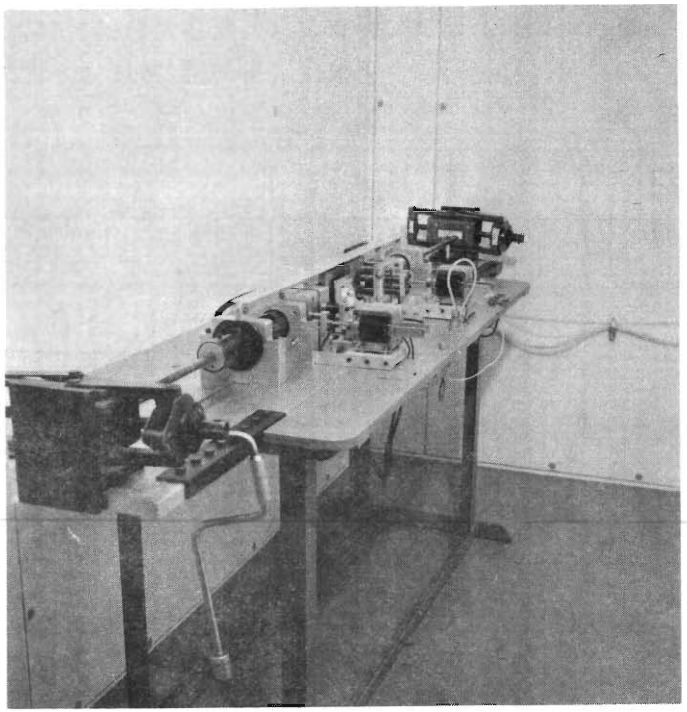

Figure B.23. Radiative Ignition Time Apparatus Inside of Environmental Chamber.

Appendix B.3

The Convective Ignition Time Apparatus

The Convective Ignition Time Apparatus (CITA) was designed to meet the specifications listed in Chapter II - C.1. The CITA is shown schematically in Figures B.24, B.25 and B.26, and the assembly is shown in Figures B.27, B.28, and B.33. The apparatus consists of four major components which are discussed in Part b. of this Appendix. The four major components are:

i) the shutter system
ii) the superstructure and sample transport system
iii) the gas burner
iv) the instrumentation for flame characterization, ignition detection and timing.

a. Operating Principle of CITA

The CITA functions in two different modes: (i) the "static" test mode and (ii) the "dynamic" test mode. Prior to any test, the fabric samples are cut to size and placed in the fabric holders. The entire assembly is then desiccated for a minimum of twenty hours. Tests are carried out within one or two minutes after removal from the desiccator.

(i) Static Ignition Test

For static testing, the shutters of the CITA are closed and the air tanks are pressurized. The burner outisde of CITA is ignited and stabilized at the desired heating intensity through fuel and air flow rate selections. The fabric holder assembly is removed from the desiccator and placed in the fabric holder support which has been adjusted for position both horizontally and vertically. The burner is placed beneath the water-cooled shutter plates. The solenoids are activated allowing compressed air to enter the air-cylinders thus causing the shutters to retract and expose the fabric sample to the flame.

The electric switch which activates the two solenoids is also used to trigger a dual-beam oscilloscope. A microswitch, connected to a D.C. voltage source is activated by one of the moving shutters. This microswitch causes a "spike" on the upper beam of the oscilloscope trace which denotes the beginning of shutter separation and exposure of the fabric sample to the flame. When ignition occurs, the infrared flame emission activates the infrared detector, focussed on the heated front face of the fabric, and causes one channel of the oscilloscope

to deflect from its base position. A chromel-alumel thermocouple, placed adjacent and behind the fabric, monitors the temperature and senses fabric destruction. When fabric destruction occurs this thermocouple is allowed to record the flame temperature on a two-channel pen recorder. This completes the static ignition test. The burner is removed from beneath the shutters, the shutters are closed and the test cycle is repeated with a new fabric sample.

(ii) Dynamic Ignition Test

In the dynamic test, the shutters of CITA are left open. The burner is adjusted so that its top is in the same plane as the top of the base plate. The fabric holder assembly is locked in the preselected vertical position. The burner is ignited and stabilized at the desired heating intensity. The traversing mechanism is then started and the complete assembly moves into and out of the flame or it is stopped at some point in the flame.

The electric switch which triggers the motion of the traversing mechanism also triggers a dual-beam oscilloscope. One of the channels registers the voltage across a helipot, which is coupled to a D.C. voltage source and relates to the position of the traversing mechanism. A chromel-alumel thermocouple placed adjacent and behind the fabric, monitors the temperature and senses fabric destruction. The output of this thermocouple is recorded on the second channel of the oscilloscope. After fabric destruction the thermocouple is also used to record the flame temperature on a two-channel pen recorder. This completes the dynamic ignition test. The traversing assembly is returned to its original position and the test cycle can be repeated with a new fabric sample.

b. Design Details

All components of the shutter system and the sample transport system were designed and mounted onto a one-inch thick base plate. This plate, made of aluminum tooling plate, forms a table for the apparatus. The assembly drawings of the Convective Ignition Time Apparatus (CITA) are shown on Figures B.24 and B.25. A schematic diagram of CITA with the sample transport system is shown on Figure B.26. A six-inch diameter opening in the base plate exposes the fabric sample to the burner flame either through use of the shutter system for the static tests or through employment of the sample transport system in the dynamic tests. Overall views of CITA with its superstructure and fabric holder transport system are shown on Figures B.27 and B.28.

(i) Shutter System

Each of the two shutter plates is an eight inch by eight inch by one-eighth inch copper plate. One plate has a 1/4 inch by 1/8 inch by 7 3/8 inch

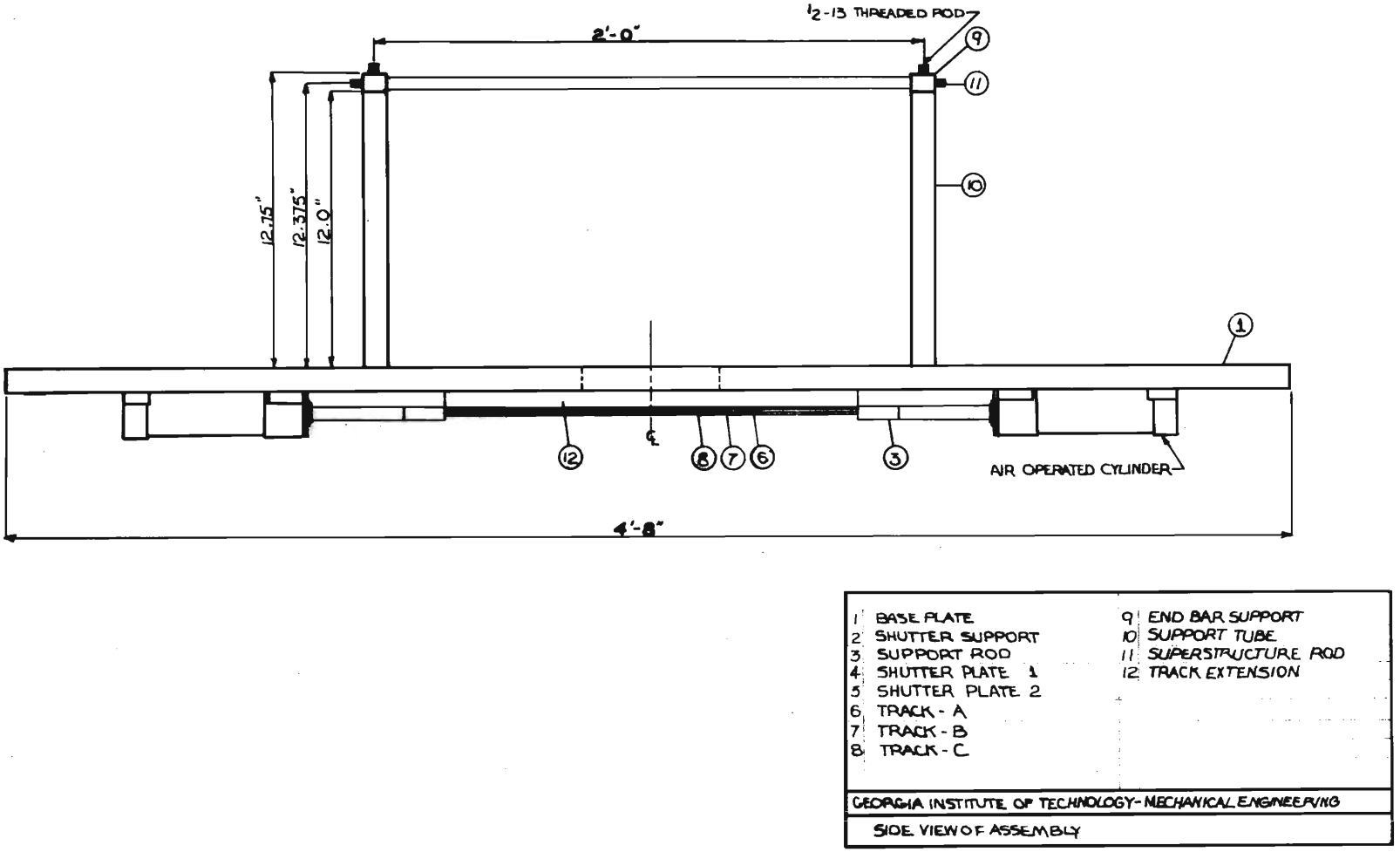

Figure B.24. Side View of Convective Ignition Time Apparatus.

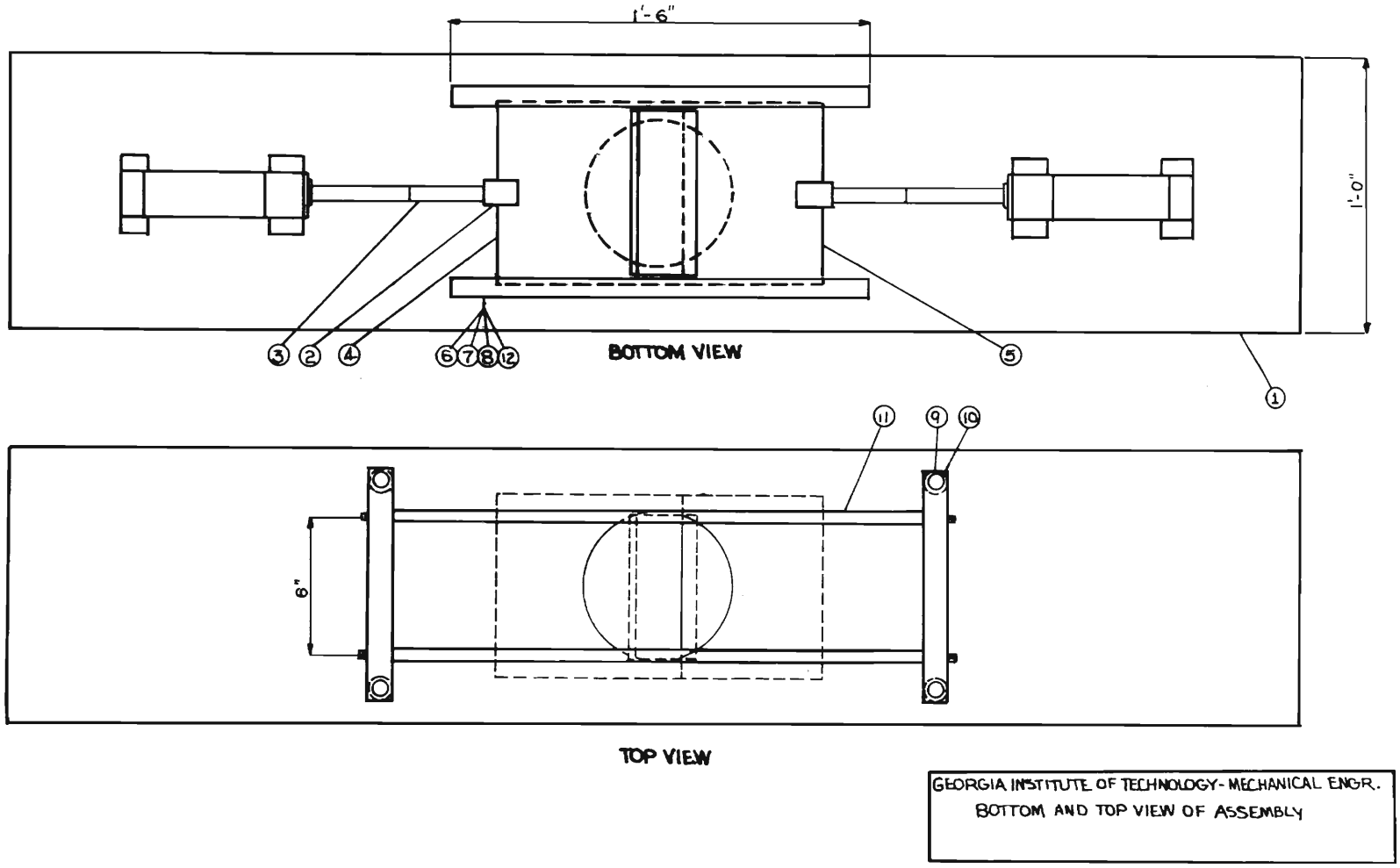

Figure B.25. Top and Bottom Views of Convective Ignition Time Apparatus.

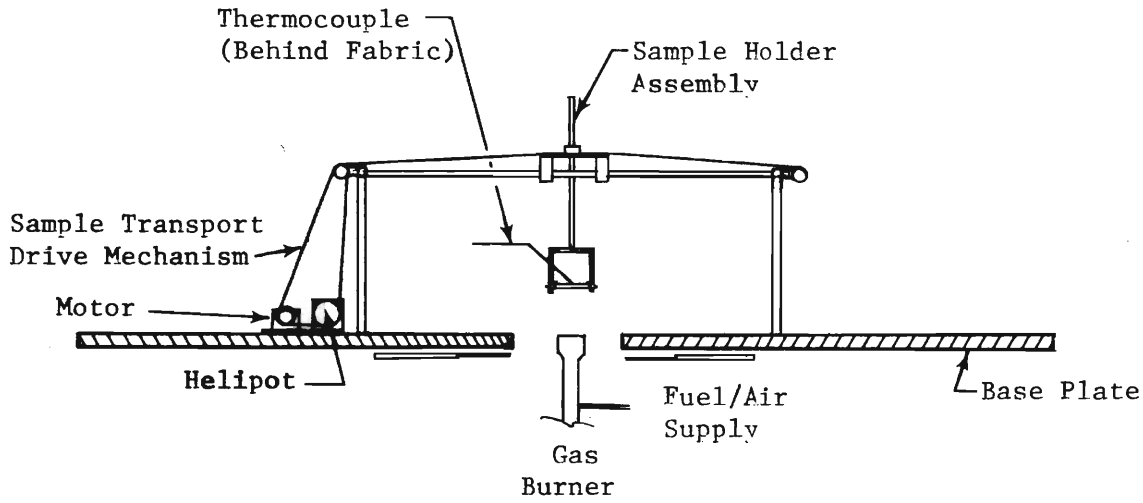

Figure B.26. Schematic of Convective Ignition Time Apparatus with Sample Transport System.

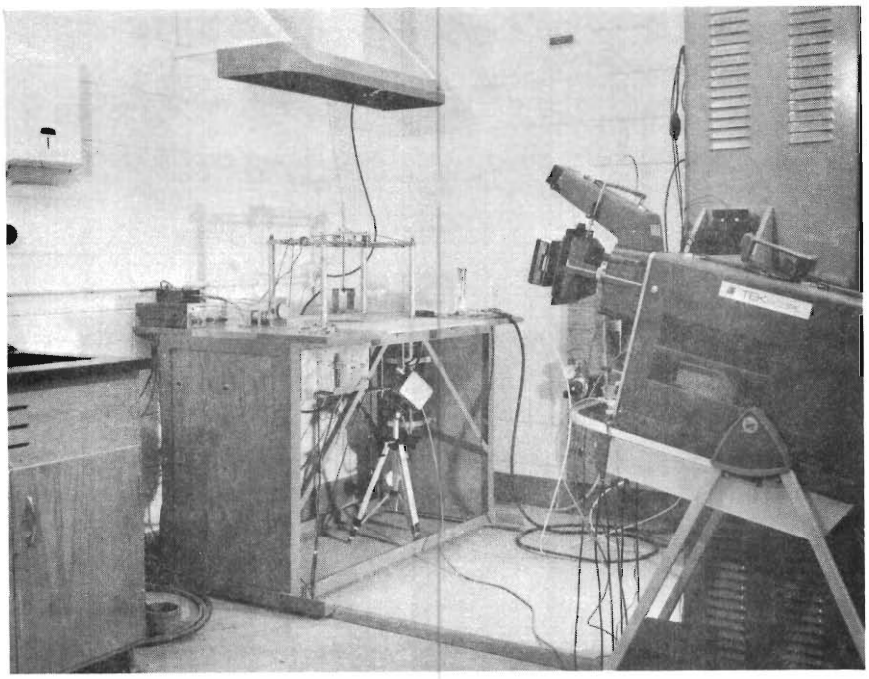

Figure B.27. Overall View of Convective Ignition Time Apparatus with Exhaust Hood

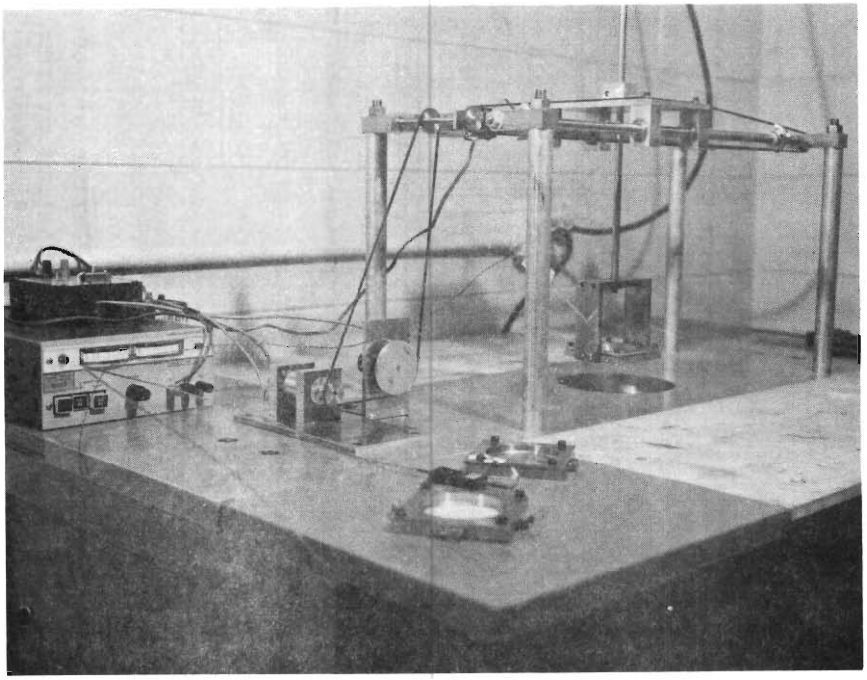

Figure B.28. CITA Superstructure with Fabric Holder Transport System, Power Drive and Power Supply

stop for the other shutter plate which, in turn, is constructed such that it has a 2 1/2 inch by 1/8 inch by 7 3/8 inch portion that overlaps the stop of the first plate to shield the center portion of the flame. The overlap of the two plates allows acceleration of the plate before exposure to make possible a short time for the transient interval of the total exposure of the sample to the flame (See Figures B.24 and B.25).

In the original design each shutter was positioned below and adjacent to the base plate and thus, was some distance above the action axis of the air cylinders. A spacer (14) was placed between the base plate and the shutter track. This modification necessitated modification of the shutter support (2) and the shutter support rod (3). With these modifications all moving components of the shutter system were aligned along a common center line.

High temperatures of the gaseous flame required the shutter plates to be cooled. To provide cooling, a one-eighth inch diameter copper tube coil was soldered to the heated bottom side of each plate. Flexible plastic hoses connect the cooling coils to the water source and the drain.

(ii) Superstructure and Sample Transport System

The superstructure consists of four 1/2 inch diameter by fourteen inch long threaded rods threaded into the base plate, four one inch o. d. by twelve inch long brass end supports (11), and two 5/8 inch diameter by twenty-six inch long Thompson Case Hardened and Ground Shafts (See Figures B.24 and B.25).

The sample transport system consists of the sample holder (Figure B.26), the supporting vertical adjusting rod, the supporting cradle and the transport drive mechanism.

Sets of two different size aperture fabric sample holders were designed and machined from stainless steel. Each fabric holder is composed of an upper body, a lower body, and four hex socket head cap screws. Design details of the fabric holders are shown in Figures B.29 and B.30. Both sizes of fabric holders have the same overall outside dimensions but, as stated before, vary in aperture size. The smaller size has a 25 mm (1 in.) diameter aperture and the larger has a 63.5 mm (2 1/2 in.) diameter aperture. Fabric holders machined during the final reporting period are modified such that they may be used in any position, and at angles between horizontal to vertical positions. Additional locators were made to be used for positioning the fabric holder as well as adjusting the inclination.

The fabric sample holder is held in position for exposure of the fabric to the burner flame through the sample holder support, details of which are shown in Figure B.31. The fabric sample holder is slipped into the slots provided in the support legs and it is then secured in position by four hex

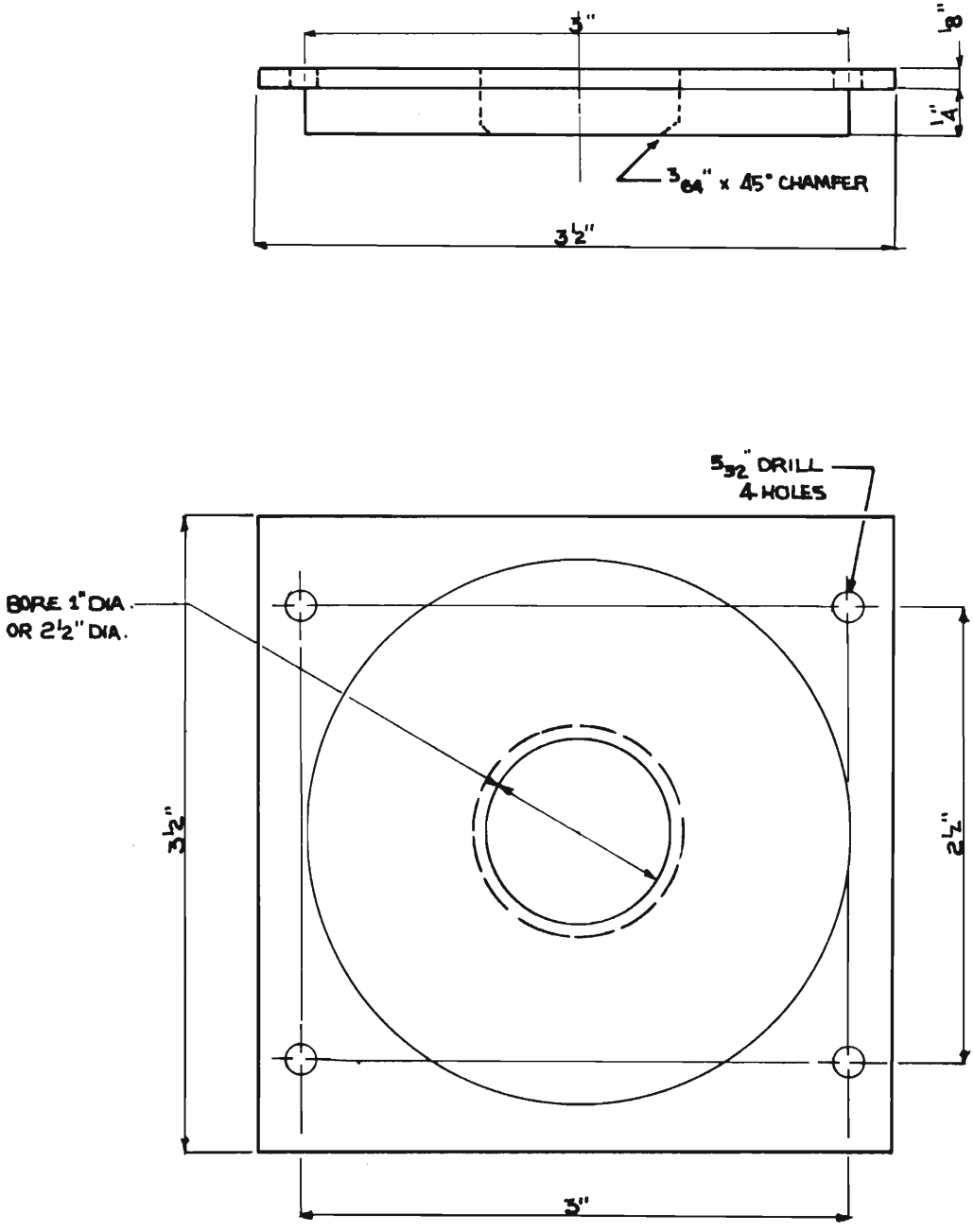

Figure B.29. Fabric Holder, Upper Body.

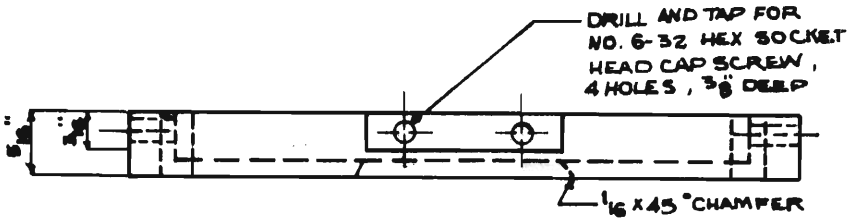

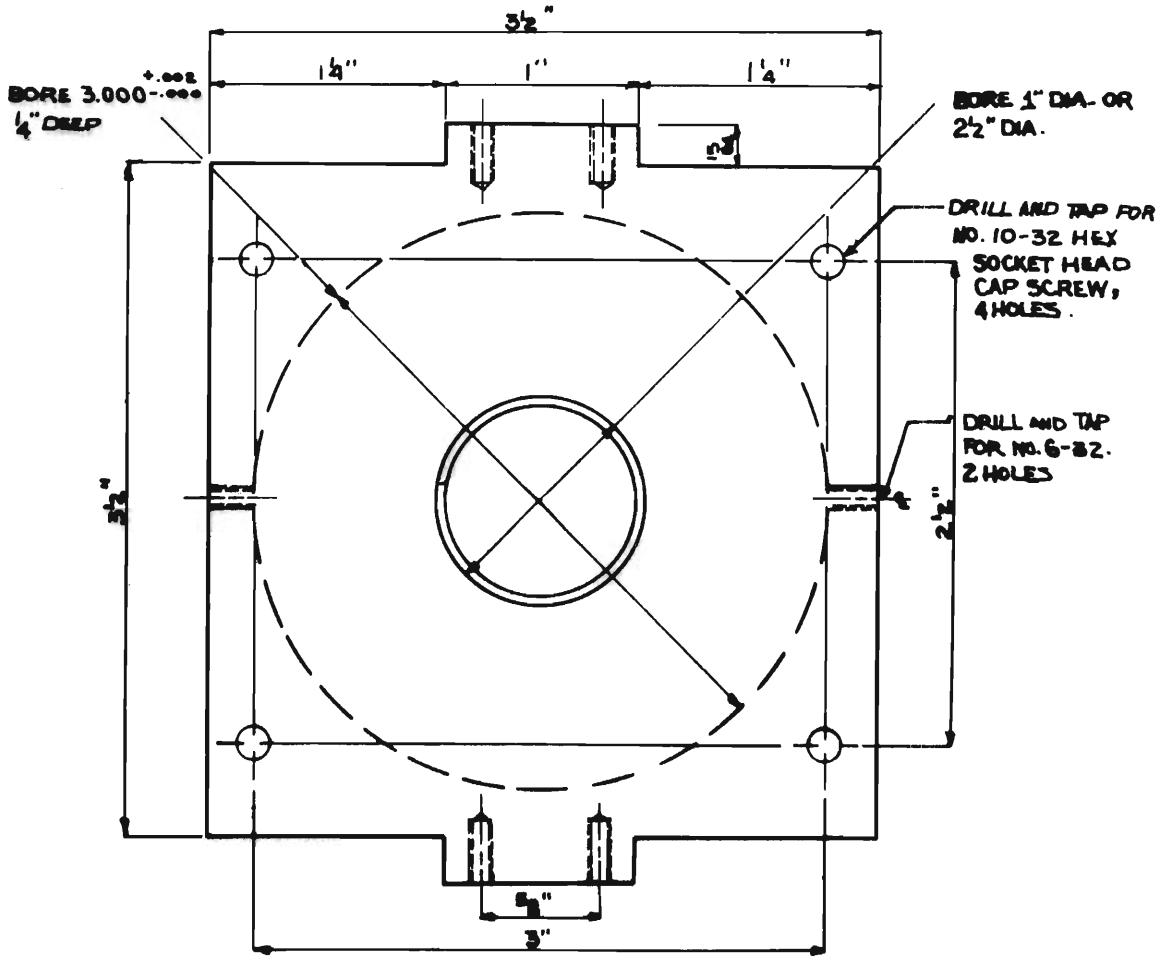

Figure B.30. Fabric Holder, Lower Body.

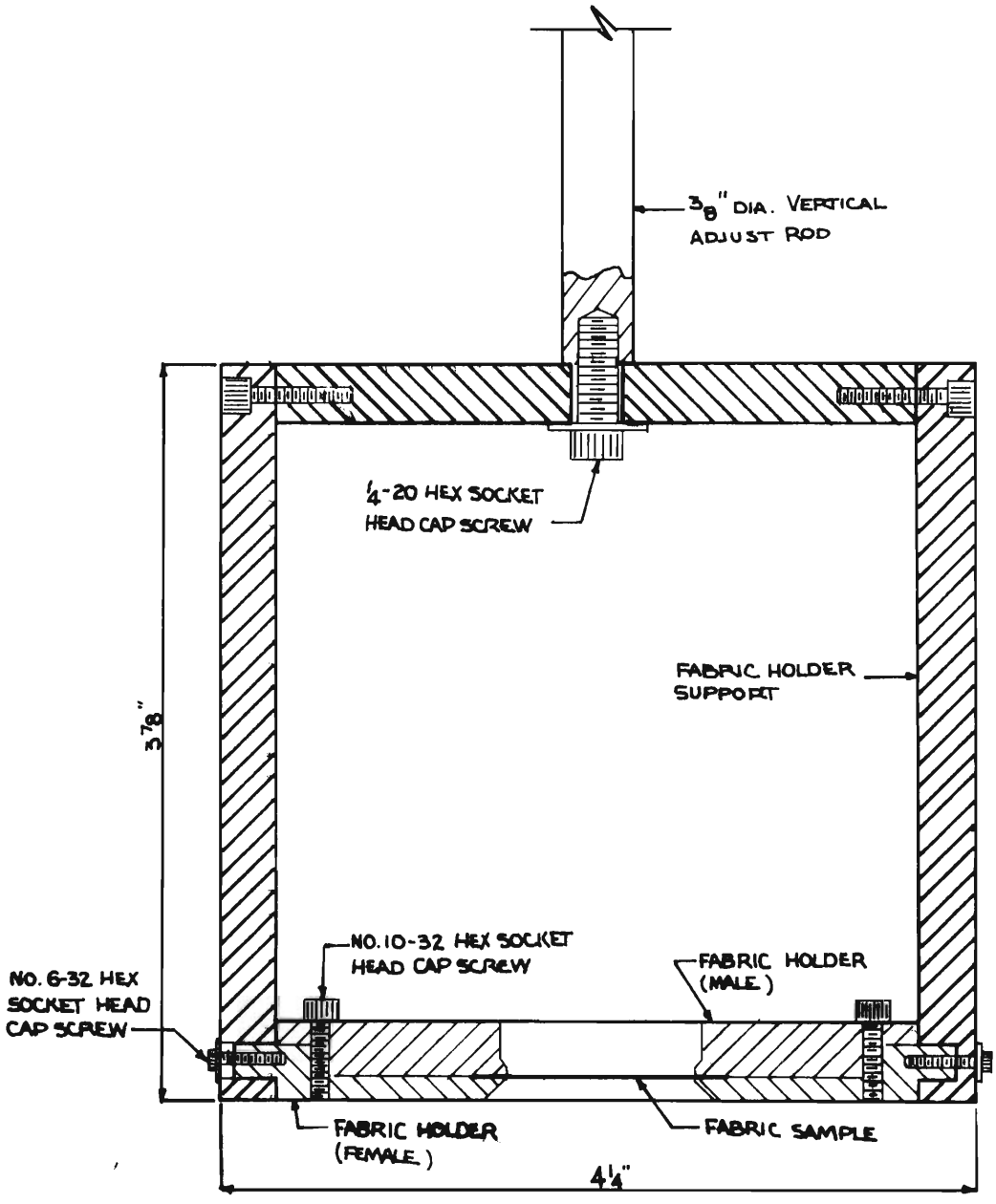

Figure B.31. Sample Holder Support with Sample Holder Position.

socket head cap screws.

The vertical adjusting rod, shown in part in Figure B.31, of the sample holder support is clamped in any desired vertical position above the burner by an aluminum clamp (Figure B.27). The supporting cradle is also shown in Figure B.27.

The components of the 25 mm and the 63.5 mm fabric holders are shown in Figure B.32. Also shown in the same figure are the assembled fabric holders and a 63.5 mm holder with the stainless steel screen in place.

Measurement of Convective Film Coefficient

It was discussed in Chapter II, Section C, Parts 2.a.iv and 3.a.iv that the 200 mesh stainless steel screen was used to measure the temperature history of the screen during flame heating and, through an inert heating model analysis, to evaluate the convective heat transfer film coefficient. Two wires are spot welded on the stainless steel screen. One wire is pulled out of the same wire mesh material as was used to cut the screen. The other wire is a 0.125 mm diameter constantan wire. The screen was used as one leg of a thermocouple while the constantan wire made up the other leg. One of the screens formed in this manner was placed in an oven and calibrated using an iron-constantan thermocouple as a reference. The calibration curve of the stainless steel screen is given in Section d of this Appendix.

The stainless steel screen, with the two wires attached to it, is clamped into a fabric holder using a thin ring of asbestos insulation on each side of the screen to thermally and electrically insulate the screen from the fabric holder. The two wires, each inserted in insulating spagetti are clamped into a thermocouple clamp as shown in Figure B.32.

To move the fabric holder assembly along the track of the superstructure a transport mechanism was designed to meet the requirements as stated in Chapter II, Section C and shown in Figures B.26 and B.27. Basically the system consists of a 28V DC, 0.01 hp motor, a variable voltage source, and assorted pulleys with belts for positive drive in either direction.

(iii) The Burner

In order to provide adjustment for the flow rates of both the fuel and the air, the 37 mm (1.5 in.) blast type burner of Fisher Scientific No. 3-910-5 was selected. The ports of the air are totally blocked and all air to the burner is provided from the compressed air supply in the laboratory. The lower structure of CITA with the burner in position is shown in Figure B.33.

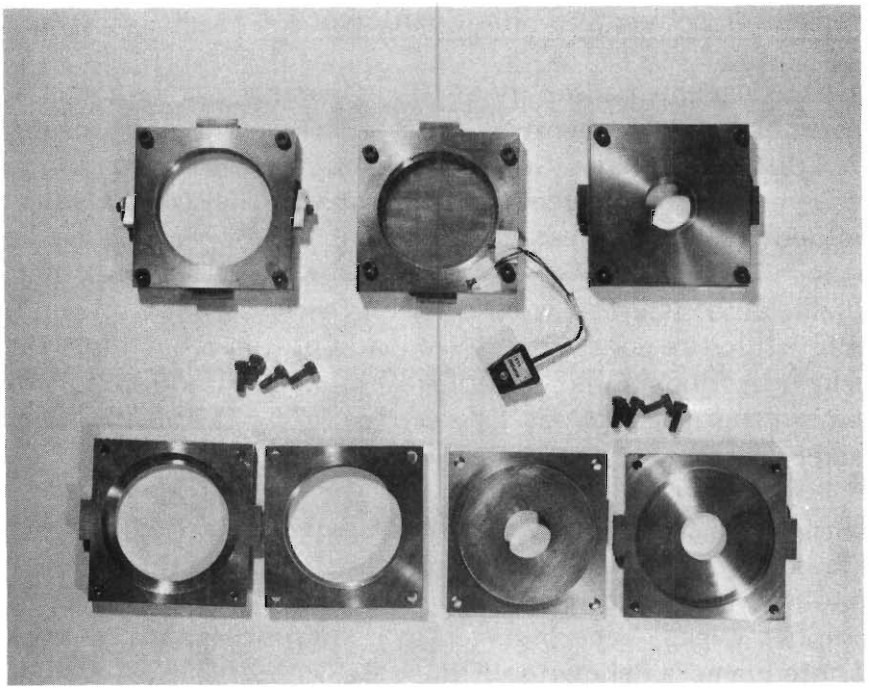

Figure B.32. One-inch and 2.5 inch Fabric Holders; Fabric Holder with SS Screen

c. Instrumentation

The instrumentation used with the Convective Ignition Time Apparatus consists of groups used for (i) flame characterization, (ii) auxiliary functions, and (iii) fabric destruction detection and destruction time measurement. Pictorial views of these groups are shown in Figures B.27 and B.28, and in Figures B.33, B.34 and B.35.

(i) Flame Characterization

The instrumentation used for the measurement of air and fuel flow rates is shown in Figure B.34 and schematically in Figure B.36. From pressure, temperature and volumetric flow rate data recorded with these instruments, calculations are carried out for the mass flow rates of air and fuel, the air-fuel ratio of the reacting mixture and the stoichiometric equivalence ratio. A mapping of the burner characteristics is given in Figures II - C.1, II - C.2 and II - C.3. Calibration curves of the two flowmeters are included in Section d of this Appendix.

The bottled methane gas for the burner is controlled by a two stage pressure regulator, Air Products No. E11-K-N5150, and a needle-valve on the upstream side of the flowmeter (see Figures B.34 and B.35). The flow of the fuel is measured by a variable area flowmeter, Brooks Sho-Rate Flowmeter Model 1355, Tube Number R-2-15-B and a Tantalum or glass float. Use of the particular float depends on the range of flows to be used during a series of tests. Downstream of the flowmeter a u-tube mercury manometer and an iron-constantan thermocouple is used to measure the pressure and temperature of the fuel, respectively.

The laboratory compressed air is filtered first through a Sears Model No. 382-1601 filter and dried by passing it through a Wilkerson Corporation Model No. 4001-2 dryer. The air pressure is controlled by a single stage pressure regulator, Air Products No. E11-I-N510B. The flow is regulated by a needle valve and measured by a variable area flowmeter, Metco Company, with a glass or stainless steel float. Downstream of the flowmeter a u-tube mercury manometer and an iron-constantan thermocouple are used to measure the pressure and temperature of the air, respectively.

A Disa Type 52-HOI Traversing Mechanism is used to carry the thermocouple or the quartz sampling probes during flame characterization tests. The Traversing Mechanisms is operated by a Disa Type 52C01 External Stepper Motor and controlled by a Type 52B01 Sweep Drive Unit. The position of the probe is related to a digital read-out on the Sweep Drive Unit where at the same time a DC voltage output is used to drive one of the coordinates of a Hewlett-Packard, Mosley 7005B X-Y Recorder. The output of a Chromel-Alumel or a Platinum-Platinum/13% Rhodium thermocouple drives the other coordinate of the X-Y recorder.

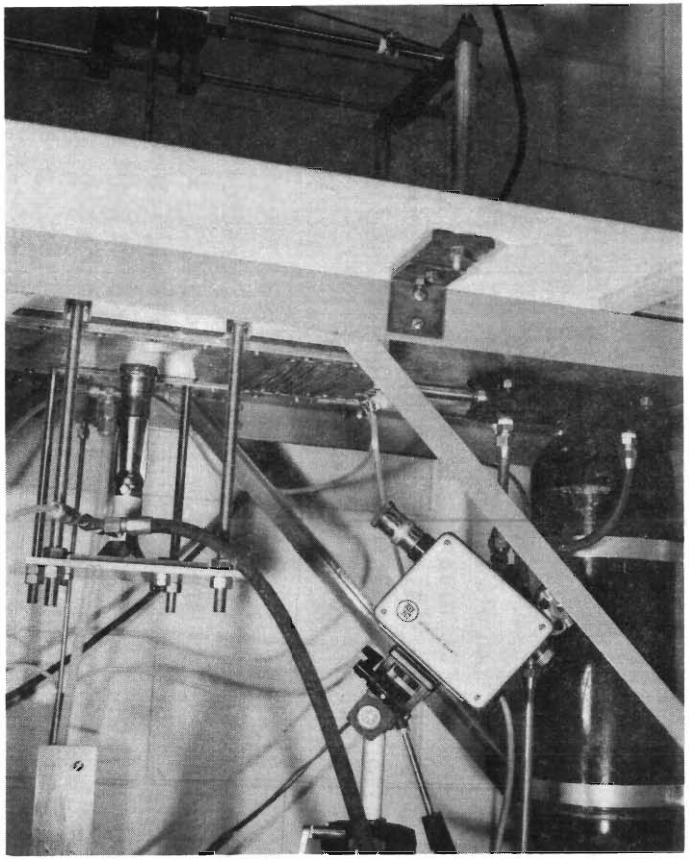

Figure B.33. Lower Structure of CITA with Burner in Position and Infrared Detector

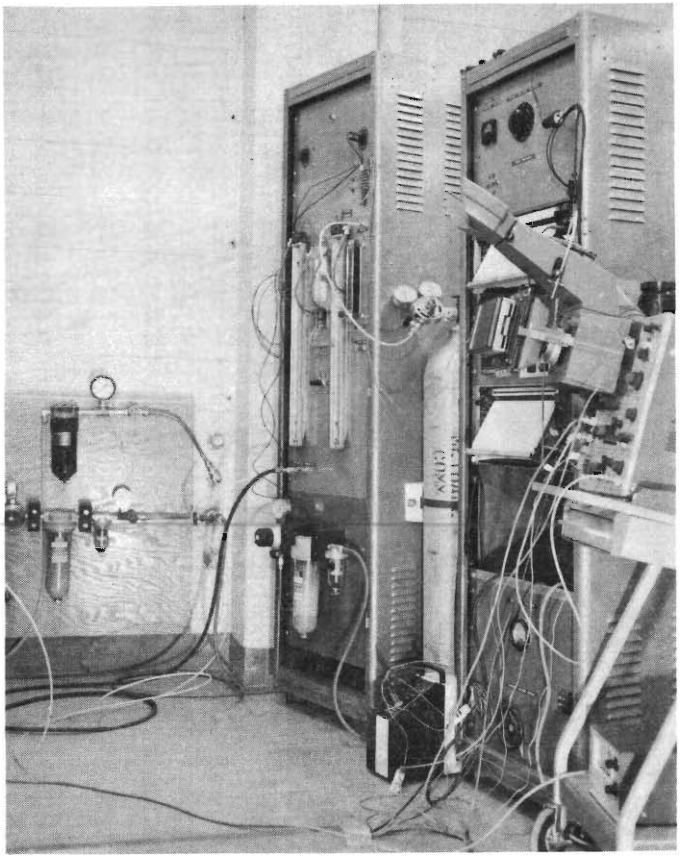

Figure B.34. Recording Instrumentation; Flow Control and Flow Measuring Devices

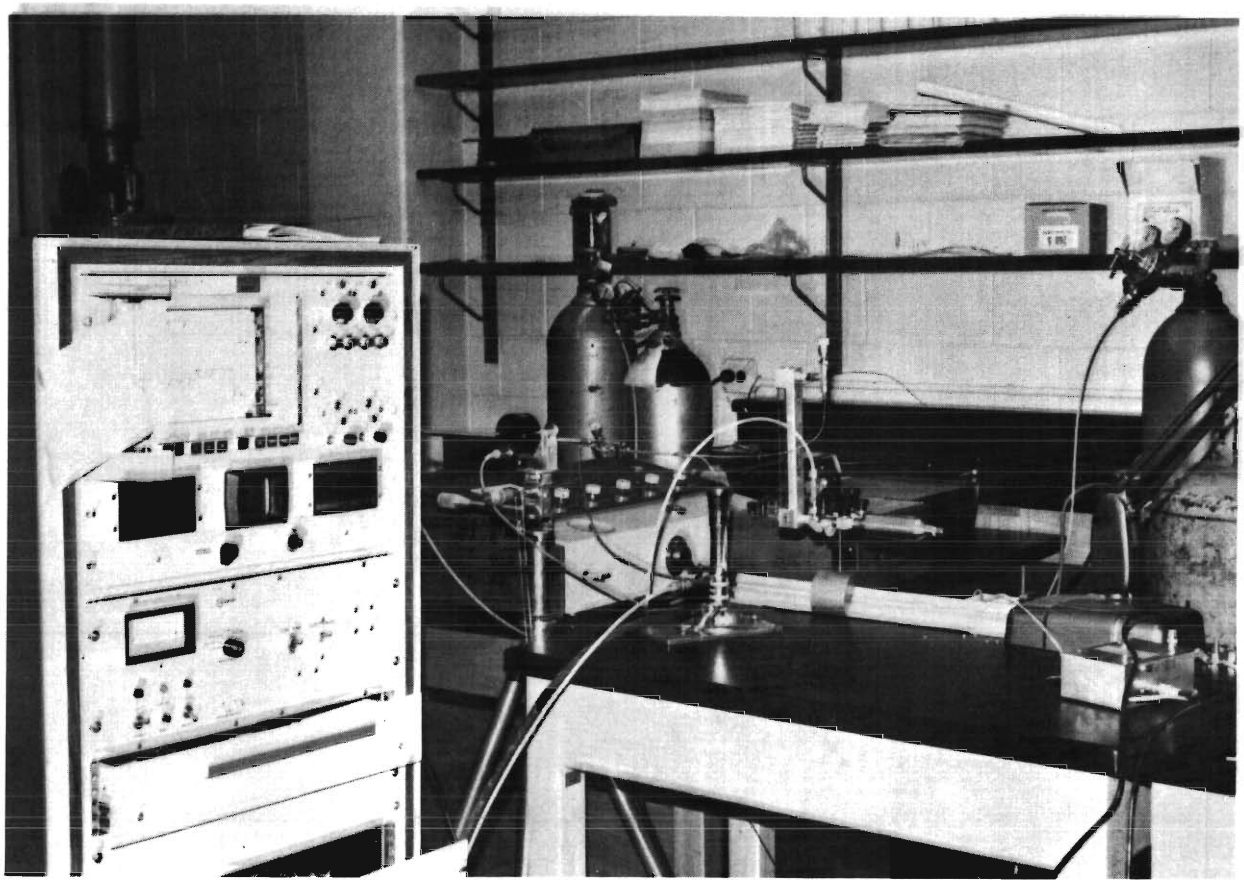

Figure B.35. Composition Analysis Instrumentation with Gas Chromatograph and Mass Spectrometer

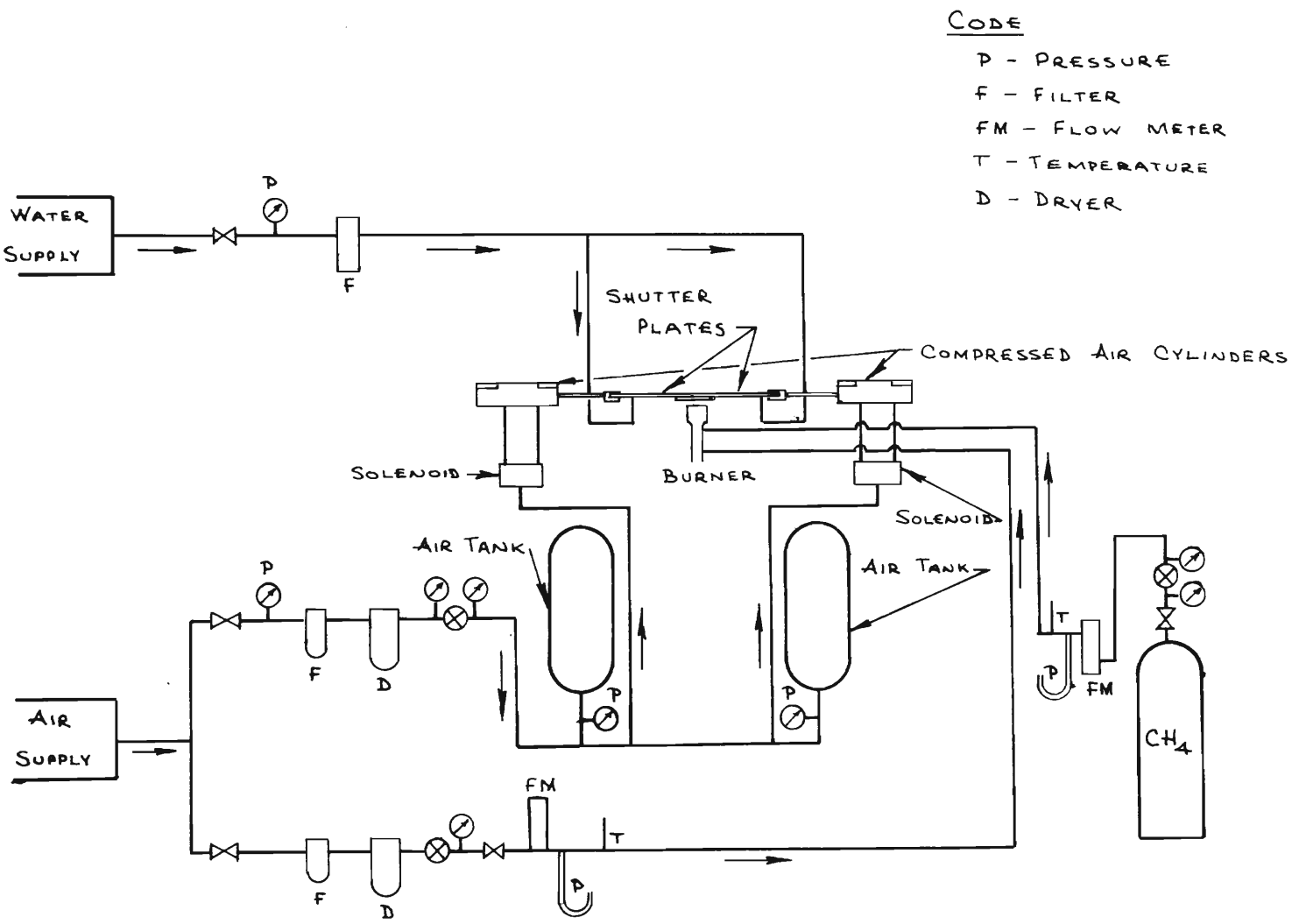

Figure B.36. Schematic of Convective Ignition Time Apparatus with Air, Fuel and Water Flow Paths.

Gas samples drawn through the quartz sampling probe are taken through a T-valve where the direct flow of the sample can be channeled through a Beckman GC-2A gas chromatograph for analysis. The output of the chromatograph is recorded on a Beckman 10 inch Potentiometric Recorder outfitted with a disk integrator. A fraction of the sample is allowed to leak through the leg of the T-valve and into the mass spectrometer. The mass spectromoter is instrumented to carry out a continuous sampling and detection of one or two species. The mass spectrometer is a Varian SI-150 Quadrupole Gas Analyzer with an axial cross beam ionizer, quadrupole filter assembly and an EAI-ESA-75 Electrometer Amplifier. The signal is further amplified by a Hewlett-Packard Signal Amplifier 8809A. The amplified output of the mass spectrometer, coupled with the Disa Traversing Mechanism and Sweep Drive Unit is used to drive the coordinates of a Hewlett-Packard Mosley 7005B X-Y Recorder. A pictorial view of the composition analysis instrumentation is shown in Figure B.35. A schematic diagram in Figure B.37 depicts the way the temperature and composition detection and recording instrumentation are coupled to produce the profiles presented in Chapter II, Section C.

The flame temperature at the fabric plane is measured by a chromel-alumel thermocouple and recorded on a strip chart pen-recorder. During the fabric destruction tests this thermocouple is used to monitor the back-side temperature of the fabric and when its output is made to drive one channel of a dual-beam oscilloscope it can be used to detect fabric destruction time. This function will be discussed in Part (iii) that will follow in this section. When total fabric destruction occurs this thermocouple is capable of recording the flame temperature as noted above. The recorded flame temperature is corrected for radiation [B.61] .

(ii) Auxiliary Instrumentation

Compressed air is used to open the CITA shutters through use of two air cylinders. The flow diagram for the air and the schematic of the shutter operating system is shown in Figure B.36.The air cylinders in turn are activated through two solenoid valves, also shown in Figure B.36. The schematic of the electrical circuit for the solenoid valves is shown in Figure B.38.

(iii) Fabric Destruction Detection and Destruction Time Measurement

Gas flame ignition of the fabric and the occurrence of the flame is sensed by an infrared detector (Mark 1 Infrascope by Barnes Engineering) focused on the front side of the fabric (the side exposed to the flame), through the gas flame (optically thin in infrared spectrum). A chromel-alumel thermocouple is placed adjacent and behind the fabric monitoring the temperature and sensing the fabric destruction (see Figures B.28, B.33 and B.38).

For the static tests, a voltage source (6v lantern battery) and a

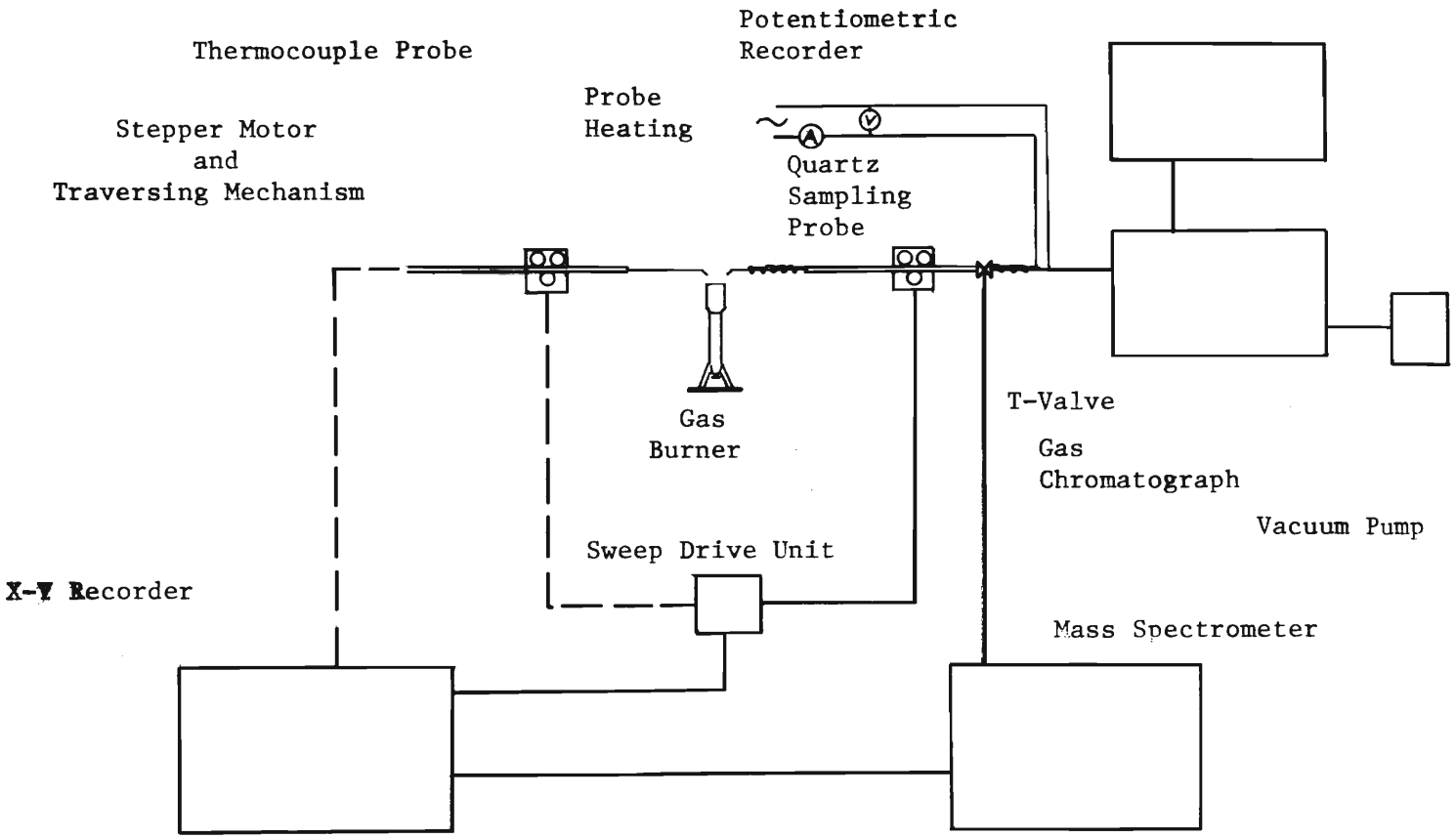

Figure B.37. Schematic of Instrumentation for Flame Characterization.

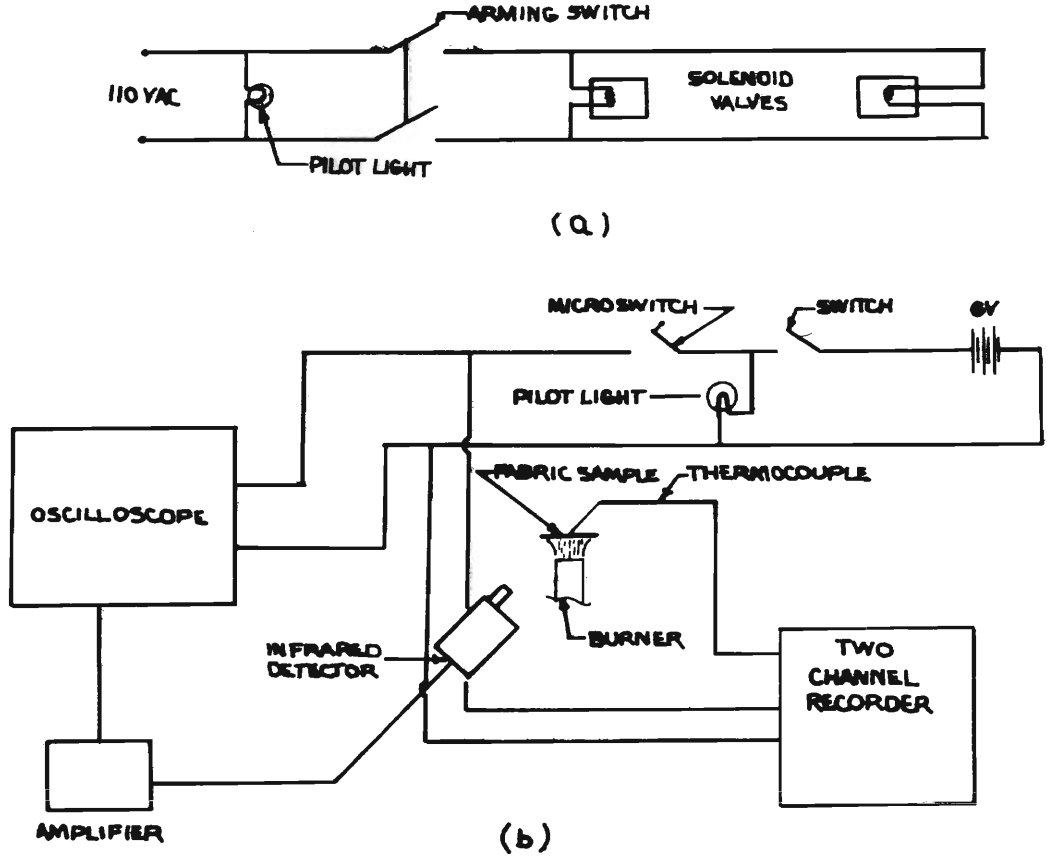

Figure B.38. (a) Schematic of Shutter Activation Electrical Circuit
(b) Schematic of Fabric Destruction Detection and Destruction Time Measuring Instrumentation, Static Tests.

microswitch, which is actuated by one of the moving shutters, is used to detect the instant when separation occurs in the two shutters and the fabric sample is exposed to the burner flame. The signal from the microswitch is used to produce a spike on one of the traces of the two channel Hewlett-Packard Type 7100B strip chart recorder, as well as on one or two dual-beam oscilloscopes as needed. The thermocouple output is recorded by the second trace of the pen-recorder or the oscilloscope. The switch which actuates the solenoid valves is used to trigger one or both dual-beam type 502A Tektronix oscilloscopes. One beam of one oscilloscope is sensing the amplified signal of the infrared detector and one beam of the second oscilloscope senses the thermocouple. The traces of the two oscilloscope beams are recorded on Polaroid film.

Fabric ignition or destruction time is measured from the time the microswitch is actuated by the moving shutter to the time where a sharp rise is detected on the infrared detector signal and/or on the thermocouple signal.

The chromel-alumel thermocouple placed behind the fabric, is allowed to continue recording the temperature after total destruction of the fabric has occured. In this manner the flame temperature is measured at that point. The schematic of the instrumentation is shown in Figure B.38.

It was found that for certain fabrics, such as the polyester, acetate, nylon, and blends that detection of fabric destruction was difficult due to melting and very little burning. The problem was solved when a high intensity lamp was placed a distance no less than 25 cm behind the fabric sample. The infrascope was focused on the lamp filament. When a break in the fabric occured the infrascope immediately sensed the intensity of the light and displayed it on the oscilloscope. The tungsten lamp is turned on only seconds before the shutters are triggered. Sample records of the infrared detector sensing fabric destruction have been included in Section d of this Appendix along with thermocouple records recorded on the oscilloscopes.

In the dynamic test, the dual-beam type 502A Tektronix oscilloscope is triggered at the start of motion of the sample transport system. Position of the traversing mechanism is known from the deflection of one of the oscilloscope beams, the relation between distance traveled on the apparatus and movement of the oscilloscope beam being known from previous calibration. The other trace records the output of the chromel-alumel thermocouple located on back of the fabric sample.

Fabric ignition or destruction time is measured from the time the fabric sample crosses the flame boundary to the time when a sharp rise is detected on the thermocouple signal. A schematic of the instrumentation for the dynamic fabric destruction tests is shown in Figure B.39.

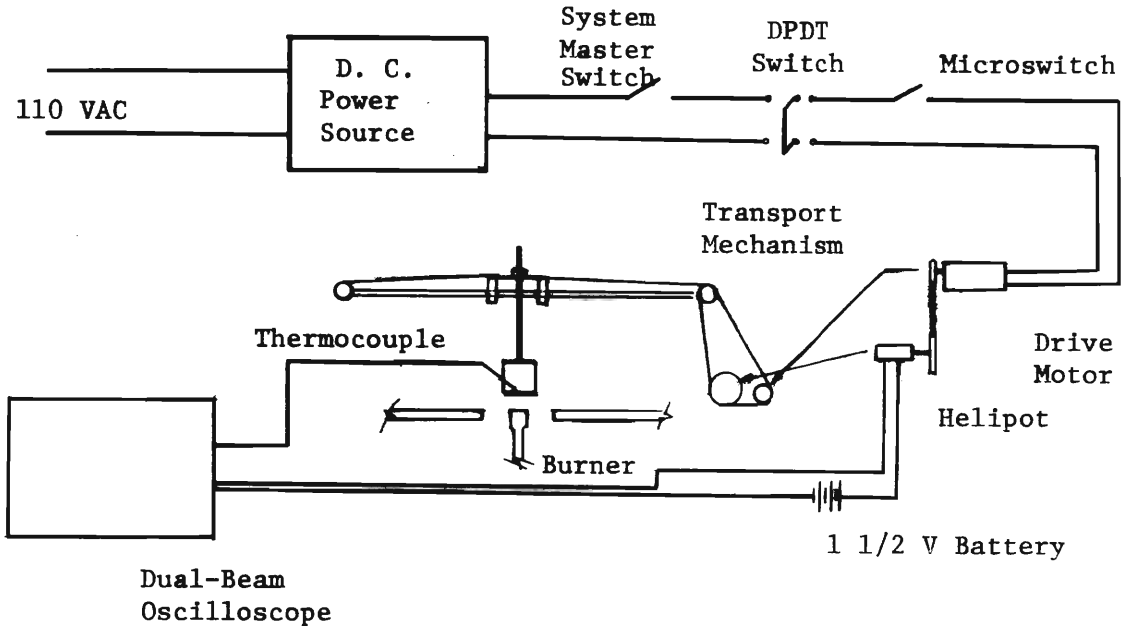

Figure B. 39. Schematic of Fabric Destruction Detection and Destruction Time Instrumentation, Dynamic Tests.

d. Calibration Curves and Sample Data Sheets

The calibration curve of the stainless steel screen used in the convective inert film coefficient determination is given on Figure B.40. The two figures that follow, Figures B.41 and B.42, are the calibration curves of the air and fuel flowmeters each with two floats.

The four pages after the calibration curves are sample data sheets for fabric destruction measurements.

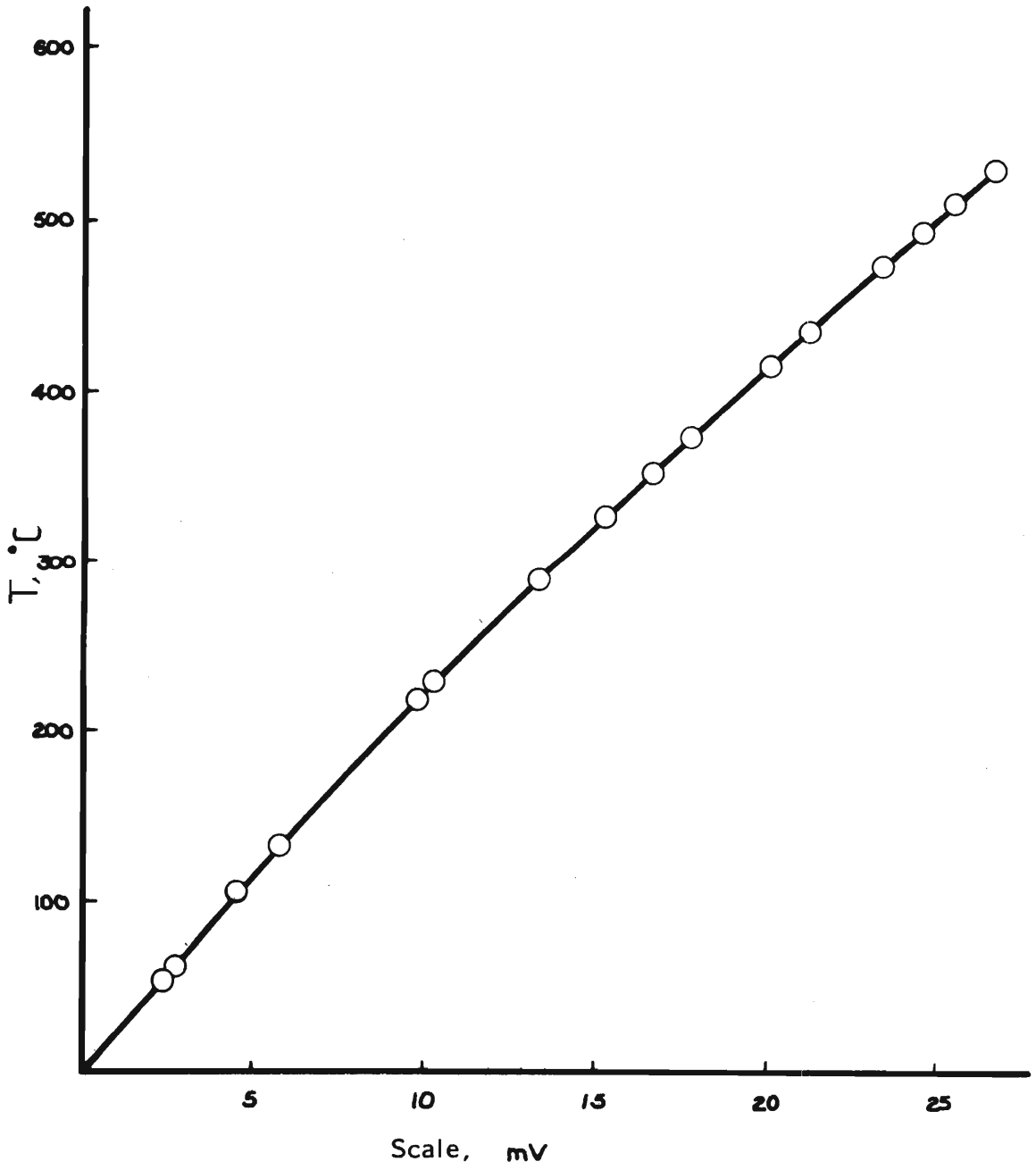

Figure B.40. SS Screen Calibration Curve.

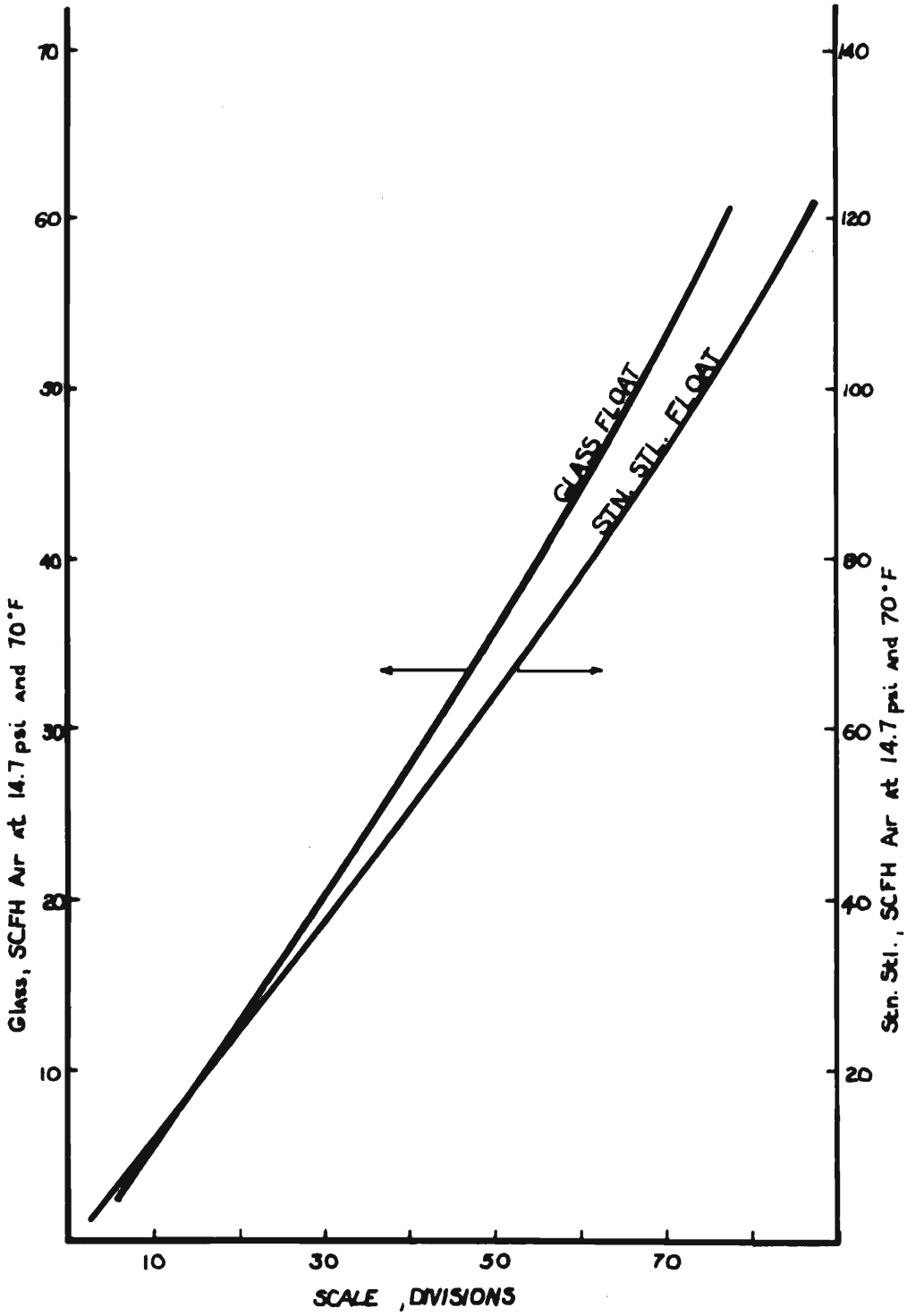

Figure B.41. Calibration Curve for Metco Flowmeter.

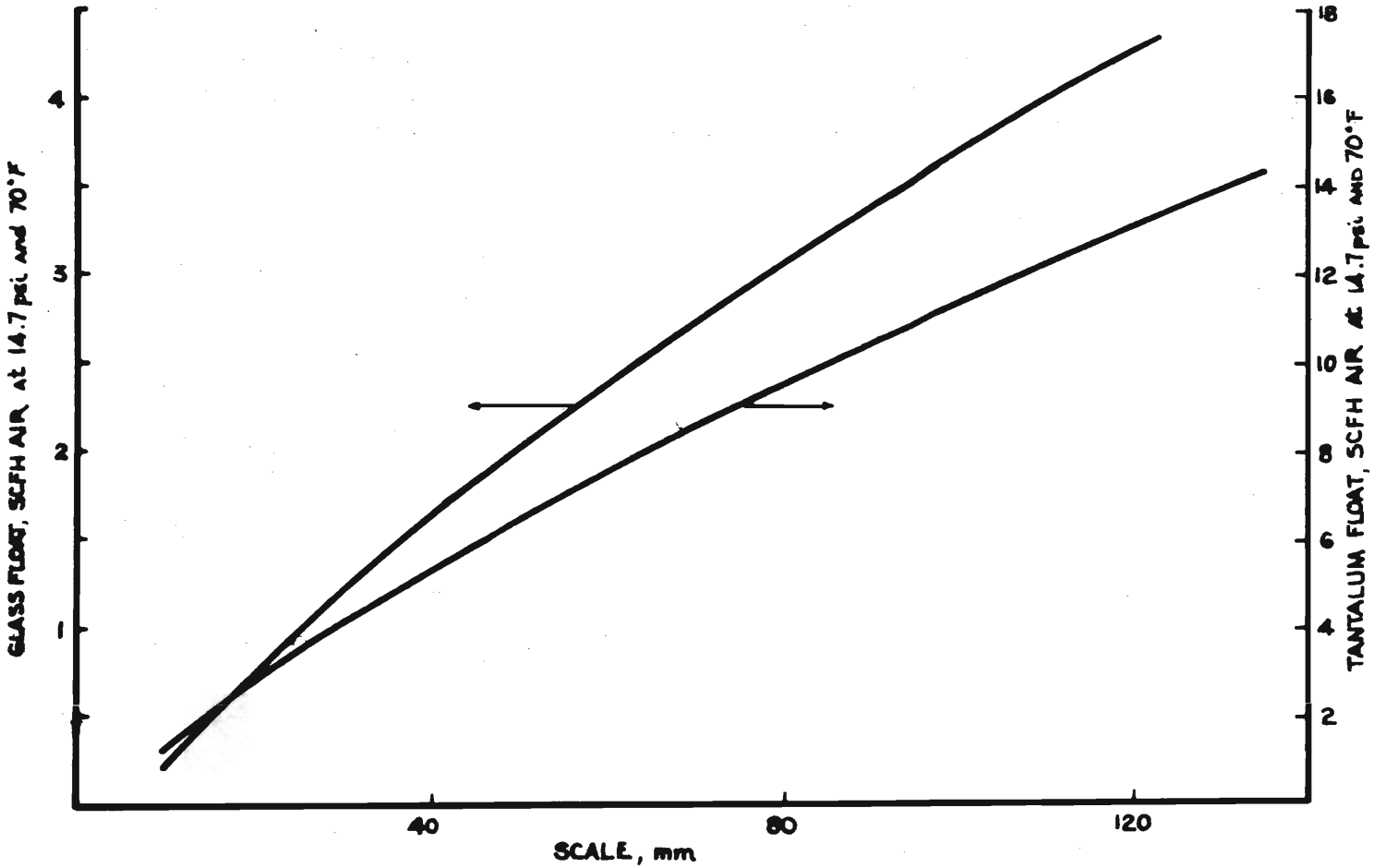

Figure B.42. Calibration Curve for Brooks Flowmeter, Tube R-2-15-B.

GEORGIA INSTITUTE OF TECHNOLOGY-MECHANICAL ENGINEERING
FABRIC FLAMMABILITY PROJECT
IGNITION TIME OF FABRICS

Date: 12-1-72 Experiment No.: 84 Experimentor: EC, RW

Fabric No.: 18 Fabric Holder Aperture: 2½"

Fabric Inclination Angle: 0° Fabric Height Above Burner: 3"

Room Temperature: 73.5°F Barometric Pressure: 29.183 "Hg.

Relative Humidity: 35%

Thermocouple Type: Air: J-C Methane: J-C Flame: C-A

Gas	P Reg. Del. psi	Flow Meter P(" Hg)	T (mV)	T (°F)	R(Div)	R(CFH)
Methane	6	12.22	1.200	74.3	95 L	3.53
Air	20	13.22	1.184	73.7	68 L	51.2

Flame Temperature: _____ mV 1315 °C

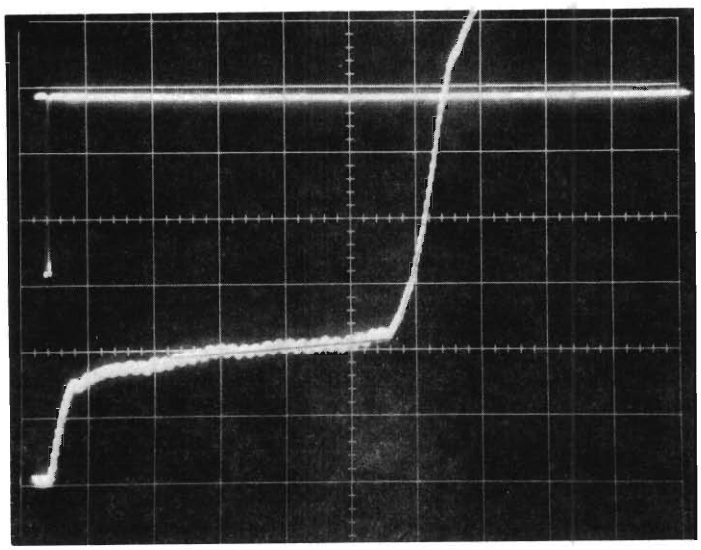

Oscilloscope Settings

Upper Beam

Sensitivity: 2 V/cm

Lower Beam

Sensitivity: 10 mV/cm

Sweep Rate: 0.5 sec/cm

Infrascope

Scale: A

Emissivity: 1.0

Ignition Time:

5.30 cm; 2.65 sec.

Thermocouple Ignition Time :

—— sec.

GEORGIA INSTITUTE OF TECHNOLOGY-MECHANICAL ENGINEERING
FABRIC FLAMMABILITY PROJECT
IGNITION TIME OF FABRICS

Date: 12-11-72 Experiment No.: 122 Experimentor: EC PD
Fabric No.: 10 Fabric Holder Aperture: 2½"
Fabric Inclination Angle: 0° Fabric Height Above Burner: ¾"
Room Temperature: 72.5°F Barometric Pressure: 29.210 "Hg.
Relative Humidity: 49%
Thermocouple Type: Air: I-C Methane: I-C Flame: C-A

Gas	P Reg. psi	Flow Meter P(" Hg)	T (mV)	T (°F)	R(Div)	R(CFH)
Metnane	6	12.16	1.164	73.069	142.5 ∠	4.75
Air	20	21.21	1.160	72.929	82 ∠	63.9

Flame Temperature: _____ mV 1357 °C

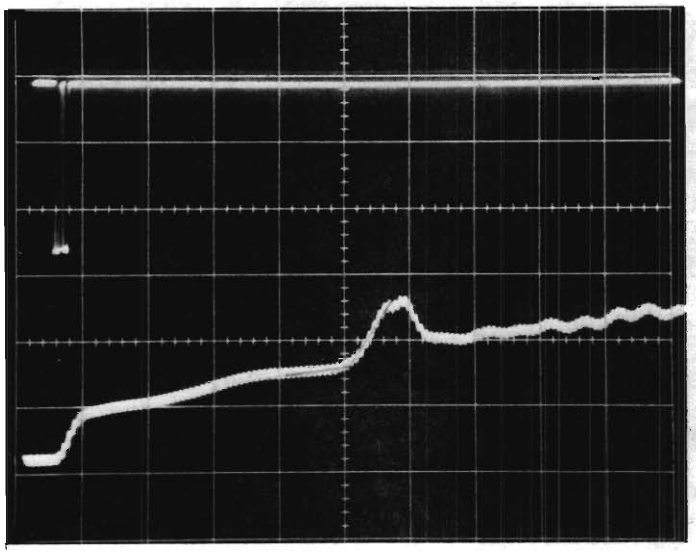

Oscilloscope Settings

Upper Beam
Sensitivity: 2 V/cm

Lower Beam
Sensitivity: 10 mV/cm
Sweep Rate: .2 sec/cm

Infrascope
Scale: A
Emissivity: 1.0
Ignition Time:
4.5 cm; 0.90 sec.
Thermocouple Ignition Time :
0.89 sec.

GEORGIA INSTITUTE OF TECHNOLOGY-MECHANICAL ENGINEERING
FABRIC FLAMMABILITY PROJECT
IGNITION TIME OF FABRICS

Date: 12-11-72 Experiment No.: 124 Experimentor: EC, PD
Fabric No.: 2 Fabric Holder Aperture: 2½"
Fabric Inclination Angle: 0° Fabric Height Above Burner: ¾"
Room Temperature: 73°F Barometric Pressure: 29.210 "Hg.
Relative Humidity: 49%
Thermocouple Type: Air: J-C Methane: J-C Flame: C-A

Gas	P Reg. Del. psi	Flow Meter P(" Hg)	T (mV)	T (°F)	R(Div)	R(CFH)
Methane	6	12.11	1.160	72.929	142.5 L	4.75
Air	20	20.52	1.152	72.643	82 L	63.9

Flame Temperature: _____ mV 1364 °C

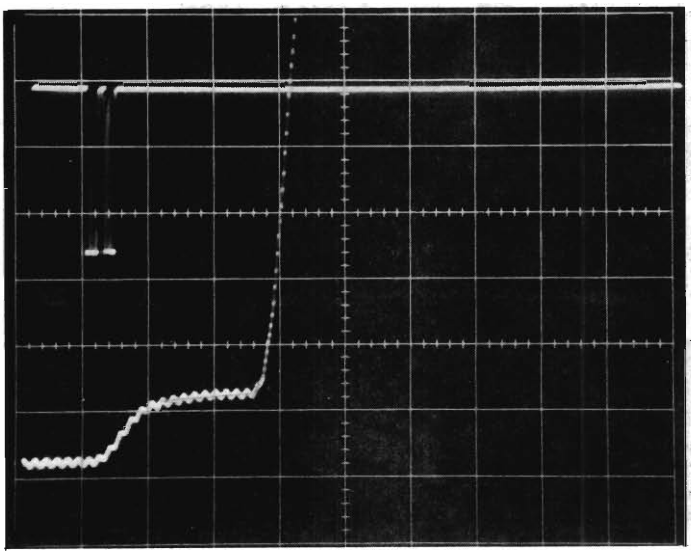

Oscilloscope Settings

Upper Beam
Sensitivity: 2 V/cm

Lower Beam
Sensitivity: 10 mV/cm
Sweep Rate: .1 sec/cm

Infrascope
Scale: A
Emissivity: 1.0
Ignition Time:
2.60 cm; 0.26 sec.

Thermocouple Ignition Time :
0.245 sec.

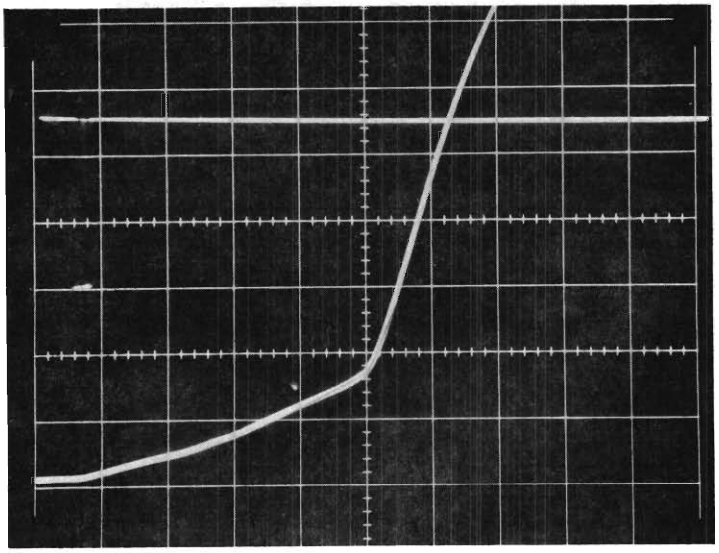

THERMOCOUPLE TRACE FOR EXPERIMENT 122

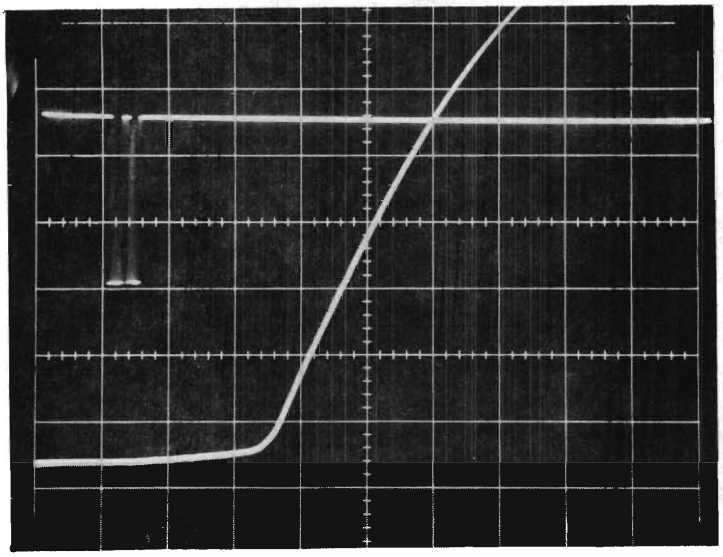

THERMOCOUPLE TRACE FOR EXPERIMENT 124

Appendix B.4

Setchkin Furnace Modification

Ignition and melting temperatures were measured as described in Appendix B.4 of Reference [1-2] but two improvements in the test apparatus design were made to achieve reliably uniform furnace temperatures.

Firstly, the inner ceramic tube of the Setchkin Furnace was replaced by a steel mantle, equipped with proper air flow passages. The 3 mm thick steel tube serves to equalize the interior furnace temperature due to its high thermal conductivity. High-temperature air flow connections to the furnace were also installed.

Secondly, a new purge air preheater was designed, constructed and installed as shown in Figure B.43. This heater affords air inlet temperatures of up to 500^{o}C, measured at the furnace inlet port. The air flows first through the outer annulus, reverses itself and passes through the 1.3 mm wide inner annulus along the 300 mm long, 16 mm-diameter Watlow heater element of 1 KW heating capacity (Type LI2A21). The outer flow passage is insulated by fiber glass and the preheater exit temperature is monitored by a thermocouple in the exit elbow (not shown in sketch).

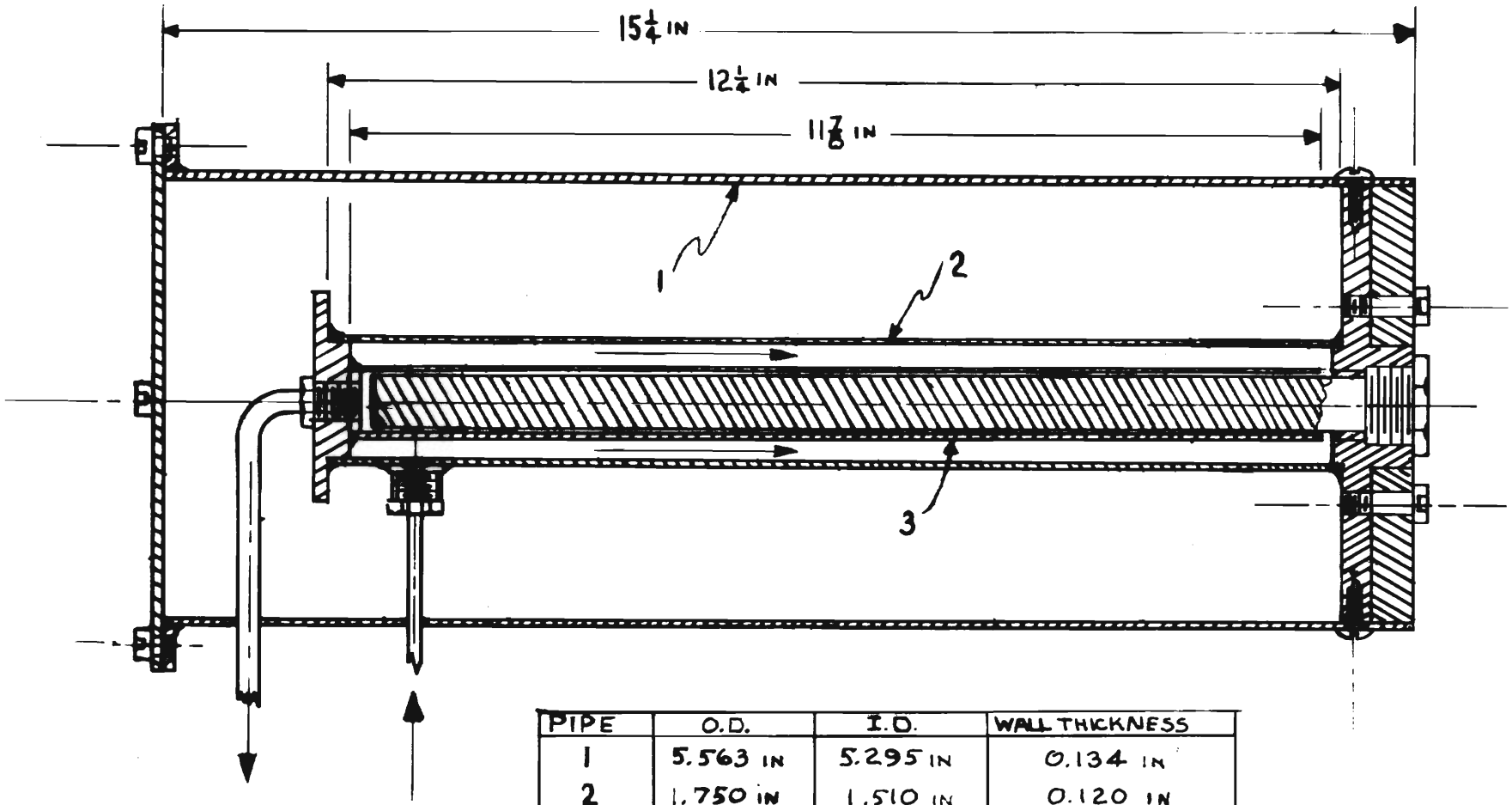

PIPE	O.D.	I.D.	WALL THICKNESS
1	5.563 IN	5.295 IN	0.134 IN
2	1.750 IN	1.510 IN	0.120 IN
3	0.865 IN	—	0.072 IN

B.43 Crossectional View of New Purge Air Preheater

Appendix C.

Literature Survey on Reaction Kinetics Of Fabrics

The reaction kinetic parameters found in the literature are listed in Table C-1 according to generic fabric type. Also listed for each fabric are the heating rate, atmosphere, the reaction temperature interval, and the reference.

The values found for heats of reaction, heats of fusion, and melting temperatures are found in Table C-2 according to generic fabric type and type of reaction.

A more complete literature survey is found in the Master Thesis prepared by Mr. William Edgar Giddens with the title "Reaction Kinetics of Textiles", Georgia Institute of Technology, School of Mechanical Engineering, March 1972.

Table C. 1 Kinetic Parameters Found in Literature Survey

Fabric Description	Atmosphere	Heating Rate °C/mn.	Temp. Range °C	Order of Reaction	Activation Energy kcal./mole	Pre-exponential Factor Sec^{-1}	Source*
α-Cellulose**	Vacuum	1	160-280	1	32	1.67×10^{10}	B.10
Cellulose R	Vacuum	4	258-282	1	36		23
ICR-1 Cellulose	Vacuum	4	300-361	1	46		23
ICR-3 Cellulose	Vacuum	4	282-361	1	47		23
α-Cellulose**	Vacuum	3	285-345	1	50.7-54.0		27
α-Cellulose	Vacuum	0.23-2.4	300-350	1	53.5	1.45×10^{17}	10
α-Cellulose	Vacuum	3	310-360	1	53.1-55.7		27
Avicel Cellulose	Vacuum	4	285-320	1	60	5.27×10^{13}	23

*Source numbers refer to Bibliography, Section B.
**Indicates fabric treated with flame retardent.

Table C. 1 (continued)

Fabric Description	Atmosphere	Heating Rate °C/mm.	Temp. Range °C	Order of Reaction	Activation Energy kcal./mole	Pre-exponential Factor Sec^{-1}	Source*
Cotton Yarn	Helium	3	251-354	1	48-54		B. 54
Cotton Yarn**	Helium	3	289-348	1	54-55		54
Cotton Cellulose	Air	5	320-380		56		9
Absorbent Cotton (ball milled)	Helium	3	245-337	1	80-86		54
Absorbent Cotton	Helium	3	265-357	1	82-86		54
Nylon 6.6	Air	5 + 10	380-480		50		9
Acetate	Vacuum	Static	180-465	1	46		55
Polyester***	Air	5	260-450	1.2	35		44
Polyester***	Air	5	450-550	1	79		44
Polyester***	Argon	5	200-450	1	20		44

***Laminac 4116 synthetic styrenated polyester

Table C. 2. Reaction Enthalpies Found in Literature Survey

Fabric Description	Heat of Pyrolysis cal/g.	Heat of Combustion cal/g.	Heat of Fusion cal/g.	Melting Temperature °C	Method of Evaluation	Source*
α Cellulose	88	-3540			DTA	B,27
α Cellulose**	72	-3550			DTA	27
Cotton (before laundry)	100				DSC***	40
Cotton (after laundry)	108				DSC	40
Nylon 6.6			22,20.3			58,59
Nylon 12			20			60
Polyester			11 - 16			58
Nylon 6				228		22
Nylon 6.6				258		22
Polyester				263		22

* Source numbers refer to Biblography
** Indicates fire retardant finish
*** Differential Scanning Calorimetry

BIBLIOGRAPHY

I-1. Government-Industry Research Committee on Fabric Flammability, "Study of Hazards from Burning Apparel and the Relation of Hazards to Test Methods." A work statement prepared by the Research Committee, Dr. E. Passaglia, Chairman, National Bureau of Standards, June 5, 1970.

I-2. Wulff, W., Zuber, N. et al, "Study of Hazards From Burning Apparel and the Relation of Hazards to Test Methods." Final Report, Georgia Institute of Technology, December 31, 1972.

I-3. Durbetaki, P., and Wulff, W. "The Study of Hazards from Burning Apparel and the Relation of Hazard to Test Methods." Research Proposal submitted to NSF by the School of Mechanical Engineering, Georgia Institute of Technology, Atlanta, Georgia 30332, September 21, 1972.

II-1. Wulff, W. et al. "Study of Hazards from Burning Apparel and the Relation of Hazards to Test Methods." Progress Report No. 5, Georgia Institute of Technology, School of Mechanical Engineering, Atlanta, Georgia, July 1, 1972.

II-2. Wulff, W. et al. "Study of Hazards from Burning Apparel and the Relation of Hazards to Test Methods." Progress Report No. 6, Georgia Institute of Technology, School of Mechanical Engineering, Atlanta, Georgia, October 1, 1972.

II-3 Hearle, J. W. S. and Peters, R. H., editors, "Moisture in Textiles", Textile Book Publishers, Inc. (Interscience Publishers, Inc.), The Textile Institute, Butterworths Scientific Publications, Manchester and London, 1960.

II-4. Eckert, E. R. G. and Drake, R. M., Analysis of Heat and Mass Transfer, McGraw-Hill, New York, 1972, pages 445-450.

II-5. Natrella, M. G., Experimental Statistics, Handbook 91, United States Department of Commerce, National Bureau of Standards (Portion of AMC Handbook).

III-1. Wulff, W. et al, Fabric Ignition, Submitted to Textile Research Journal, 1972.

III-2. Hodgman, C. D., Editor in Chief, Mathematical Tables From Handbook of Chemistry and Physics, Chemical Rubber Publishing Co., Cleveland Ohio, Third Printing, 1961, pg. 211.

B.1. Information Council on Fabric Flammability, Proceedings of the Third Annual Meeting, New York City, (1969).

B.2. Government-Industry Research Committee on Fabric Flammability, "Study of Hazards from Burning Apparel and the Relation of Hazards to Test Methods." A work statement prepared by the Research Committee, Dr. E. Passaglia, Chairman, National Bureau of Standards, June 5, 1970.

B.3. Tribus, M., "Decision Analysis Approach to Satisfying the Requirements of the Flammable Fabrics Act." Paper Presented at the Textile and Needle Trades Division, American Society of Quality Control, Greensboro, North Carolina, February 12, 1970.

B.4. Evans, R. B., Wulff, W. and Zuber, N., "The Study of Hazards from Burning Apparel and the Relation of Hazards to Test Methods", Research Proposal submitted by the School of Mechanical Engineering, Georgia Institute of Technology, to the Government-Industry Research Committee on Fabric Flammability, July 1970.

B.5. Wulff, W., Zuber, N. et al, "Study of Hazards From Burning Apparel and the Relation of Hazards to Test Methods." Final Report, Georgia Institute of Technology, December 31, 1972.

B.6. Madorsky, S. L., "Rates of Thermal Degradation of Polystyrene and Polyethylene in a Vacuum," J. Polymer Sci., 9, 133-156 (1952).

B.7. Mackenzie, R. C., Differential Thermal Analysis Vol. 1, Academic Press, London and New York (1970).

B.8. Borchardt, H. J. and Daniels, F., "The Application of Differential Thermal Analysis to the Study of Reaction Kinetics," J. Am. Chem. Soc., 79, 41-46 (1957).

B.9. Schwenker, R. F., Beck, L. R., and Zuccarello, R. K., "Applications of Differential Thermal Analysis and Dynamic Thermogravimetric Analysis in Textile Research," Am. Dyestuff Rept., 53, 817-827 (1964).

B.10. Akita, K. and Kase, M., "Determination of Kinetic Parameters for Pyrolysis of Cellulose and Cellulose Treated with Amononium Phosphate by Differential Thermal Analysis and Thermogravimetric Analysis," J. Polymer Sci.: Part A-1, 5, 833-848 (1967).

B.11. Freeman, E. S. and Carroll, B., "The Application of Thermoanalytical Techniques to Reaction Kinetics. The Thermogravimetric Evaluation of the Kinetics of the Decomposition of Calcium Oxalate Monohydrate," J. Phy. Chem. 62, 394-397 (1958).

B.12. Coats, A. W. and Redfern, J. P., "Kinetic Parameters from Thermogravimetric Data," Nature, 201, 68-69 (1964).

B.13. LeChatelier, H., "The Action of Heat on Clay," Bull. Soc. Franc. Mineral, 10, 204-11 (1887).

B.14. Roberts - Austen, W. C., "Fifth Report to the Alloys Research Committee," Proc. Inst. Mech. Engrs. (London), 1, 35-102 (1899).

B.15. Carpenter, H. C. H. and Keeling, B. F. E., "The Range of Solidification and Critical Ranges of Iron-Carbon Alloys," J. Iron Steel Inst. (London), 65(1), 224-42 (1904).

B.16. Carpenter, H. C. H., The Types of Structure and the Critical Ranges of High-Speed Tool Steels Under Varying Thermal Treatment," Collected Researches, Nat'l. Phys. Lab. (London), 2, 52-89 (1907).

B.17. Burgess, G. K., "On Methods of Obtaining Cooling Curves," Electrochem. Metal. Ind., 6, 366-71 (1908).

B.18. Burgess, G. K. and LeChatelier, H., "The Measurement of High Temperatures, John Wiley & Sons, New York (1912).

B.19. Smothers, W. J. and Chiang, Y., Handbook of Differential Thermal Analysis, Chemical Publishing Co., Inc., New York (1966).

B.20. Grimshaw, R. W., Heaton, E., and Roberts, A. L., "The Constitution of Refractory Clays, Part II," Trans. Brit. Ceram. Soc., 44, 76-92 (1945).

B.21. Godfrey, L. E. A., "Differential Thermal Analysis (DTA) and Thermogravimetric Analysis (TGA) Studies of Flame Retardent Rayon Fibers," Text. Res. J., February 1970, 116-126.

B.22. Loughlin, J. et al., "Differential Thermal Analysis in Predicting Fiber Blend and Probing Fiber Properties," Am. Dyestuff Rept., Feb. 1965, 25-38.

B.23. Ramiah, M. V., "Thermogravimetric and Differential Thermal Analysis of Cellulose, Hemicellulose, and Lignin," J. Appl. Polymer Sci., 14, 1323-1337 (1970).

B.24. Schwenker, R. F. and Zuccarello, R. K., "Differential Thermal Analysis of Synthetic Fibers," J. Polymer Sci.: Part C, 6, 1-16 (1964).

B.25. Hendrix, J. E. et al., "Pyrolysis and Combustion of Cellulose. I. Effects of Triphenyl Phosphate in the Presence of Nitrogenous Bases," J. Appl. Polymer Sci., 14, 1701-1723 (1970).

B.26. Perkins, R. M., Drake, G. L. and Reeves, W. A., "DTA and TGA Studies of Flame-Resistant Fabrics," J. Appl. Polymer Sci., 10, 1041-1066 (1966).

B.27. Tang, W. K. and Neill, W. K., "Effect of Flame Retardents on Pyrolysis and Combustion of α - Cellulose," J. Polymer Sci.: Part C, 6, 65-81 (1964).

B.28. Arens, P. L., A Study of the Differential Thermal Analysis of Clays and Clay Minerals, Gravenhage, Wageningen, Netherlands (1951).

B.29. Grimshaw, R. W. and Roberts, A. L., "Quantitative Determination of Some Minerals in Ceramic Materials by Thermal Means," Trans. Brit. Ceram. Soc., 52, 50-67 (1953).

B.30. Sabatier, I. G., "Measure of the Heats of Transformation by Differential Thermal Analysis," Bull. Soc. franc. mineral, 77, 953-68 (1954).

B.31. Speil, S. et al., "Differential Thermal Analysis. Its Application to Clays and Other Aluminous Minerals," Tech. Pap. Bur. Mines, Wash., No. 664, 1-37, (1945).

B.32. Nagusawa, K., "Differential Thermal Analysis Studies on the High-Low Inversion of Vein Quartz in Japan," J. Earth Sci., Nagoya Univ., 1, 156-76 (1953).

B.33. Berg, L. G., "Introduction to Thermal Analysis," Izd. Akad. Nauk SSSR, Moscow, 1961.

B.34. Bollin, E. M. and Kerr, P. F., "Differential Thermal Pyrosynthesis," Am. Mineralogist, 46, 823-58 (1961).

B.35. American Association of Textile Chemists and Colorists Monograph Number 3, Analytical Methods for a Textile Laboratory, AATCC, Research Triangle Park, North Carolina (1968).

B.36. Vold, M. J., "Differential Thermal Analysis," Anal. Chem., 21, 683-8 (1949).

B.37. Soule', J. L., "Quantitative Interpretation of Differential Thermal Analysis," J. Phys. Radium, 13, 516-20 (1952).

B.38. Kissinger, H. E., "Reaction Kinetics in Differential Thermal Analysis," Anal. Chem., 29, 1702-6 (1957).

B.39. Turner, W. N. and Johnson, F. C., "The Pyrolysis of Acrylic Fiber in Inert Atmosphere," J. Appl. Polymer Sci., 13, 2073-84 (1969).

B.40. Gilliland, B. F. and Smith, B. F., "Flame-Retardent Properties and Thermal Behavior of Selected Flame-Retardent Cotton Fabrics," J. Appl. Polymer Sci., 16, 1801-16 (1972).

B.41. Honda, K., "A Thermobalance," Sci. Rept. Tohoka Imp. Univ., 4, 97-103 (1915).

B.42. Guichard, M., "The Rate of Dehydration at Increasing Temperature," Bull. soc. chim. France, 37, 62-7 (1925).

B.43. Duval, C., "Sur la Thermogravimétric des Précipités Analytiques." Anal. Chim. Acta, 1, 341-4 (1947).

B.44. Anderson, D. A. and Freeman, E. S., "The Kinetics of the Thermal Degradation of the Synthetic Styrenated Polyester, Laminac 4116," J. Appl. Polymer Sci., 1, 192-199 (1959).

B.45. Slade, P. E. and Jenkins, L. T., Techniques and Methods of Polymer Evaluation, Vol. I, Marcel Dekker, Inc., New York, 1966.

B.46. Newkirk, A. E., "Thermal Methods of Analysis," Anal. Chem., 32, 1558-63 (1960).

B.47. McCarter, R. J., "Apparatus for Rate Studies of Vapor Producing Reactions," NBS Special Publication 338, 137-149.

B.48. McCarter, R. J., "Report on the Thermal Analysis of GIRCFF Fabrics," NBS Report 10846, May 11, 1972.

B.49. Chatterjee, P. K., "Application of Thermogravimetric Techniques to Reaction Kinetics," J. Polymer Sci.: Part A-1, 6, 3217-33 (1968).

B.50. Doyle, C. D., "Kinetic Analysis of Thermogravimetric Data," J. Appl. Polymer Sci., 5, 285-292 (1961).

B.51. Farmer, R. W., "Thermogravimetry of Plastics: Part 1: Empirical Homogeneous Kinetics," ASD-TDR-62-1043, Part 1.

B.52. Reich, L., "Estimation of Kinetic Parameters from Thermogravimetric Traces," J. Appl. Polymer Sci., 9, 3033-39 (1965).

B.53. Sharp, J. H. and Wentworth, S. A., "Kinetic Analysis of Thermogravimetric Data," Anal. Chem., 41, 2060-2 (1969).

B.54. Chatterjee, P. K., "Thermogravimetric Analysis of Cellulose," J. Polymer Sci.: Part A-1, 6, 3217-33 (1968).

B.55. Madorsky, S. L., Hart, V. E., and Strauss, S., "Thermal Degradation of Cellulose Materials," J. Res. NBS, 60, 343-9 (1958).

B.56. Bolz, R. E., and Tuve, G. L., editors, Handbook of Tables for Applied Engineering Science, Chemical Rubber Co., Cleveland, 1970.

B.57. Hamby, D. S., ed., American Cotton Handbook, Vol. 1, Interscience Pub., New York, 1965.

B.58. Cook, J. G., ed., Handbook of Textile Fibers, Merrow Pub. Co., Herts, England, 1968.

B.59. Ke, B. and Sisko, A. W., "Differential Thermal Analysis of High Polymers. III. Polyamicles," J. Polymer Sci., 50, 87-98 (1961).

B.60. The Plastics Manual, 5th Edition, 1971.

B.61. Fishenden, M. and Saunders, O. A., "The Errors in Gas Temperature Measurement and Their Calculation," Journal of the Institute of Fuel, 12, S5-S14 (1939).